ABSTRACT

DICHLOROMETHANE PYROLYSIS AND OXIDATION: FORMATION OF CHLORINATED AROMATIC PRECURSORS TO PCDD/F

by
Hong-Ming Chiang

The pyrolysis and oxidation of dichloromethane is studied in a tubular reactor at 1 atmosphere pressure, residence time between 0.3 to 2.0 seconds and in the temperature range 680 - 840 °C. Four reactant concentration ratios are:

I. $CH_2Cl_2 : Ar = 1 : 99$ II. $CH_2Cl_2 : CH_4 : Ar = 1 : 1 : 98$

III. $CH_2Cl_2 : O_2 : Ar = 1 : 4 : 95$ IV. $CH_2Cl_2 : CH_4 : O_2 : Ar = 1 : 1 : 4 : 94$

The degradation of dichloromethane, intermediate product formation and decomposition, and final products are studied in both pyrolytic and oxidative reaction environments. Chlorinated intermediate products: CH_3Cl, C_2HCl, C_2H_3Cl, CH_2CCl_2, CHClCHCl, and C_2HCl_3 are shown to be important in all systems but more difficult to destroy in the pyrolysis than in the oxidation. The conversion of these chloro-methyl radicals to corresponding chloro-formaldehydes, CO and CO_2 is observed to be slow by this reaction sequence. The demonstration of this bottleneck is another important result of this thesis. Results show that conversion primarily occurs through combination of 2 chloro-methyl radicals to chloro-ethanes, then ethylenes, then chloro-vinyl radicals. The major chloro-methyl radical conversion path under combustion condition is the chloro-

vinyl radical + O_2. Thermodynamic parameters: ΔH_{298}, S_{298} and $C_p(T)$ for all species in the reaction mechanism are evaluated and illustrated.

A reaction mechanism consisting of 635 elementary reactions and 215 species, to C_6 compounds, has been developed to simulate the thermal decomposition of dichloromethane and for use in predicting the formation of aromatics and intermediate molecular weight growth species in C_1 and C_2 chlorocarbon combustion. All reactions in the mechanism are elementary or derived from analysis of reaction systems encompassing elementary reaction steps. All reactions are thermochemically consistent and follow principles of Thermochemical Kinetics. Model data show good agreement for reagent decay and major product distribution in both pyrolytic and oxidative environments.

Unimolecular dissociation of CH_2Cl_2 and of chlorinated ethylenes is analyzed by unimolecular quantum RRK. Combination and addition reactions such as: $CH_2Cl + O_2$, $CHCl_2 + O_2$, $CH_3 + CH_2Cl$, $CH_3 + CHCl_2$, $CH_2Cl + CH_2Cl$, $CH_2Cl + CHCl_2$, $CHCl_2 + CHCl_2$, $C_2H_3 + O_2$, $CH_2CCl + O_2$, $CHClCH + O_2$, $CHClCCl + O_2$, $CCl_2CH + O_2$, and $C_2Cl_3 + O_2$ are treated with bimolecular quantum RRK analysis for k(E), combined with modified strong collision approach and/or Master equation analysis for fall-off effects.

Hydrocarbon and chlorocarbon radical addition to unsaturated species is responsible for molecular weight growth and ultimate formation of precursors to polychlorinated dibenzo dioxins and furans.

Reactions of $HSO + O$, $SO + OH$, $H + SO_2$, $OH + SO_2$, $H + SO_3$, $OH + HSO$, and $H + HOSO$ are analyzed as functions of pressure and temperature.

DICHLOROMETHANE PYROLYSIS AND OXIDATION: FORMATION OF CHLORINATED AROMATIC PRECURSORS TO PCDD/F

by
Hong-Ming Chiang

A Dissertation
Submitted to the Faculty of
New Jersey Institute of Technology
in Partial Fulfillment of the Requirements for the Degree of
Doctor of Philosophy

Department of Chemical Engineering,
Chemistry, and Environmental Science

May 1995

APPROVAL PAGE

DICHLOROMETHANE PYROLYSIS AND OXIDATION: FORMATION OF CHLORINATED AROMATIC PRECURSORS TO PCDD/F

Hong-Ming Chiang

Dr. Joseph W. Bozzelli, Dissertation Advisor — Date
Distinguished Professor of Chemical Engineering, Chemistry, and Environmental Science, NJIT

Dr. Richard B. Trattner, Committee Member — Date
Associate Chairperson for Environmental Science and Professor of Chemical Engineering, Chemistry, and Environmental Science, NJIT

Dr. Basil C. Baltzis, Committee Member — Date
Professor of Chemical Engineering, Chemistry, and Environmental Science, NJIT

Dr. Lev N. Krasnoperov, Committee Member — Date
Professor of Chemical Engineering, Chemistry, and Environmental Science, NJIT

Dr. Elmar R. Altwicker, Committee Member — Date
Professor of Chemical Engineering, Rensselaer Polytech. Institute

BIOGRAPHICAL SKETCH

Author: Hong-Ming Chiang

Degree: Doctor of Philosophy in Environmental Science

Date: May 1995

Undergraduate and Graduate Education:

- Doctor of Philosophy in Environmental Science,
  New Jersey Institute of Technology, Newark, NJ, 1995

- Master of Science in Environmental Science,
  New Jersey Institute of Technology, Newark, NJ, 1992

- Bachelor of Science in Chemical Engineering,
  Chinese Cultural University, Taipei, Taiwan, R.O.C., 1984

Major: Environmental Science

Presentations and Publications:

Chiang, Hong-Ming, Ritter, Edward R., and Kydd, Paul H. "Trace Organic Emissions from the One Gallon Technology Development Unit." *Medical Waste Disposal Steering Committee Meeting*, Newark, NJ, May **1990**.

Chaing, Hong-Ming, and Bozzelli, Joseph W. "Thermal Decomposition of Dichloro methane in Absence and Presence of added and/or CH_4." *Combustion Fundamentals and Applications*, p.322, **1993**, Proceeding of 1993 Joint Technical Meeting at New Orleans, Louisiana, The Central and Eastern States Sections of The Combustion Institute, March 15-17, **1993**.

Chaing, Hong-Ming, Wu, Yo-Ping, Ho, Wen-Ping, Won, Yang-Soo, Park, Byung-Ik, and Bozzelli, Joseph W. "A Reaction Mechanism and its Validation for Oxidation of CH_3Cl, CH_2Cl_2, C_2H_3Cl, $C_2H_2Cl_2$'s, C_2HCl_3 in Methane / Oxygen." *AIChE Annual Meeting*, St. Louis, Missouri, November 7-12, **1993**.

Chiang, Hong-Ming, and Kydd, Paul H. "Emissions Data from a Pyroxidizer Operating on Regulated Medical Waste." *Hazardous Waste Management Handbook*, p.90, PTR Prentice Hall, Englewood Cliffs, NJ, **1994**.

Chaing, Hong-Ming, and Bozzelli, Joseph W. "Pyrolysis and Oxidation of Dichloro methane and 1,2-Dichloroethylene in Absence and Presence of Methane." *Twenty fifth International Symposium on Combustion, the Combustion Institute*, Work In Progress Posters, The University of California, Irvine, CA, July , **1994**.

Chiang, Hong-Ming, Wu, Yo-Ping, Won, Yang-Soo, and Bozzelli, Joseph W. "Chemically Activation Analysis of CH_2Cl and $CHCl_2$ Combination Reaction." *208th ACS National Meeting*, Washington, DC, August 21-25, **1994**.

Chaing, Hong-Ming, and Bozzelli, Joseph W. "Formation of Chlorinated Ethylene Inter mediates in Pyrolysis of CH_2Cl_2 and CH_2Cl_2/CH_4" *208th ACS National Meeting*, Washington, DC, August 21-25, **1994**.

Chaing, Hong-Ming, and Bozzelli, Joseph W. "Mechanism for Oxidation and Molecular Weight Growth - to chlorinated benzenes and phenols, from high temperature reactions of C_1 and C_2 chlorocarbons" *AIChE Annual Meeting*, San Francisco, CA, November 13-19, **1994**.

Chaing, Hong-Ming, and Bozzelli, Joseph W. "Experiment and Detailed Reaction Mechanism of Chlorinated Ethylene Formation and Destruction in Pyrolysis of CH_2Cl_2 and CH_2Cl_2/CH_4" *Chemical and Physical Process in Combustion*, **1994**, page 278, Proceeding of 1994 Technical Meeting at Clearwater, Florida, The Eastern States Section of The Combustion Institute, December 5-7, **1994**.

This dessertation is dedicated to
my wife, Chang Shuchen Chiang

ACKNOWLEDGMENT

I wish to express my appreciation to Prof. Joseph W. Bozzelli, my advisor, not only for his professional advice but also his encouragement, patience, and kindness. I am deeply indebted to him for the opportunities which he made available to me.

I would also like to thank to my dissertation committee members, Dr. Richard B. Trattner, Dr. Basil C. Baltzis, Dr. Lev N. Krasnoperov and Dr. Elmar R. Altwicker for their helpful corrections and productive comments.

It is my pleasure to thank Dr. Edward Ritter, Dr. Yang Soo Won, Dr. Yo Ping Wu, Dr. Wen Pin Ho, who shared their experiences with me and helped me with GC/MS analysis. In addition, I like to thank my coworkers at NJIT, Dr. Tsan-Horng Lay, Wen-Chiun Ing, and Samuel Chern, for having dealt with me as a colleague, which has made my time at NJIT much more enjoyable and productive.

For love and inspiration I shall be eternally grateful to my wife, Shu-Chen, my parents and parents in law. Without their constant support and encouragement, I truly believe all of this would not have been possible.

TABLE OF CONTENTS

TABLE OF CONTENTS
(Continued)

Chapter **Page**

TABLE OF CONTENTS
(Continued)

TABLE OF CONTENTS
(Continued)

TABLE OF CONTENTS
(Continued)

Chapter **Page**

TABLE OF CONTENTS
(Continued)

Chapter **Page**

LIST OF TABLES

LIST OF TABLES
(Continued)

LIST OF TABLES
(Continued)

LIST OF FIGURES

LIST OF FIGURES
(Continued)

LIST OF FIGURES
(Continued)

LIST OF FIGURES
(Continued)

LIST OF FIGURES
(Continued)

LIST OF FIGURES
(Continued)

LIST OF FIGURES
(Continued)

LIST OF FIGURES
(Continued)

LIST OF FIGURES
(Continued)

CHAPTER 1

INTRODUCTION

In theory incineration can affect the total conversion of hazardous organic compounds to safe, innocuous, thermodynamically controlled, end-products, such as carbon dioxide and water, plus compounds like HCl, which maybe easily scrubbed with existing pollution control equipment. In practice, total conversion to innocuous materials is not easily achieved without considerable effort, and with an incinerator of less than optimum design or operating conditions, stable components in the waste feed may not be totally decomposed.(1) POHC (Principal Organic Hydrocarbon) and PIC (Product of Incomplete Combustion) emissions are due to a number of factors which include chemistry, operating conditions, uniformity of feed and mixing. The overall incineration process is complex and involves interactions of chemistry, heat transfer, and fluid dynamic phenomena. Louw et. al.,(2) for example, note that operating conditions of 1000 K and several minutes are needed to limit incinerators with certain hazardous feeds from emitting intolerable amounts of polychlorinated dibenzodioxins (PCDD).

The emission of hazardous organic compounds from poorly designed or inadequately controlled incinerators presents a significant concern to the environment. Hazardous organic compounds are also subject to thermal (pyrolytic) degradation in droplets or in solids feed to incinerators and in other sources not specifically designed or regulated for their disposal. It is important to understand the fundamental processes in

both oxidative and pyrolytic thermal decomposition kinetics. This will permit development of an optimum combustion process at an ideal level, that can then be utilized for improvements in commercial scale units.

One important family of hazardous wastes is the halogenated hydrocarbons. Such wastes include chlorinated methanes and ethanes, vinyl chloride, polychlorinated biphenyls (PCB's) and DDT (dichlorodiphenyltrichloroethylene) and others. In order to utilize incineration more effectively, and to better assess the applicability and limitation of the incineration process, the chemical kinetic steps involved in chlorinated hydrocarbon combustion must be understood in more detail. In addition, the manufacture of useful chemicals by the controlled oxidation and pyrolysis of chlorinated hydrocarbons may be possible through the detailed knowledge of their reaction pathways. It is also important to discern if combustion of one and two carbon chlorinated species, which are common solvents can result in formation of higher molecular weight chlorinated aromatic species. These chloro-aromatics could serve as precursors to polychlorinated dibenzofurans (PCDF) and polychlorinated dibenzodioxins (PCDD).

These chlorinated compounds are known to inhibit hydrocarbon combustion processes, increase the levels of carbon monoxide (higher CO to CO_2 ratios), and form high molecular weight compounds and soot in flames.(3,4) Results presented in this study show that chlorocarbons can facilitate or accelerate the initial rate of hydrocarbon breakdown as well as inhibit it. Chlorocarbons can interact differently with hydrocarbon combustion in each of two stages of the combustion process. They can serve to accelerate the first pyrolysis and initiation stages by providing a very active chlorine atom (radical

accelerates propagation). Chlorocarbons also inhibit oxidation of CO to CO_2 in the later - burnout combustion phase.

This dissertation reports on experiments and detailed model development, which focuses on methylene chloride, CH_2Cl_2, in reaction environments relevant to combustion. Appropriate previous literature is reviewed and experimental studies, which are performed over wide range of conditions are presented. The experimental data of this study and data in the literature are used to test (validate) a model which is developed to emulate CH_2Cl_2 combustion and incineration. The model is specifically not an empirical one, but a detailed reaction mechanism based on fundamental thermochemical and kinetic principles. It, can be used to characterize reactant loss, intermediate product formation and subsequent decay, and final product formations processes as function of both time and temperature. Interim stages of this thesis extend the model to account for molecular weight growth including chlorinated aromatic species. The 4 and 6 carbon products of molecular weight growth reactions are in effect trace species, under normal combustion conditions, but can be formed in somewhat higher concentrations when incinerator upset occurs.

The following sections in this introduction serve as summary descriptions of the thesis chapters. Relevant introductory and literature background material are in the beginning of each respective chapter. This is necessary because of the detail in each section and the associated problem of having this introductory material presented away from the detailed relevant descriptions and discussions. Previous literature studies on methylene chloride pyrolysis and oxidation are presented in the early parts of chapter 2.

The remainder of chapter 2 describes the experimental procedures in detail and presents results of the experiments.

Investigation into the thermal decomposition of chlorinated hydrocarbons has received significant attention in recent years, due to concern for the environmental impact from results of burning these materials. Specifically, there is a consistent observation of known or suspected toxic / carcinogenic chlorocarbons or chloro-oxy carbon species in the effluent from waste and resource recovery incinerators.(5) A number of studies on the high temperature reaction of chlorinated hydrocarbons have been performed, and are discussed in chapter 2.

Data are presented in chapter 2 on pyrolysis and oxidation of dichloromethane in the presence or absence of methane in a tubular reactor. The thermal reactions of dichloromethane are studied at 1 atmosphere pressure with six different residence times from 0.3 to 2.0 seconds in the range of temperature 680 - 840 °C. Four reactant concentration ratios are:

Table 1.1 Reactant Mole Fraction (%)

I.	$CH_2Cl_2 : Ar$	=	1 : 99
II.	$CH_2Cl_2 : CH_4 : Ar$	=	1 : 1 : 98
III.	$CH_2Cl_2 : O_2 : Ar$	=	1 : 4 : 95
IV.	$CH_2Cl_2 : CH_4 : O_2 : Ar$	=	1 : 1 : 4 : 94

The degradation of dichloromethane, the intermediate product formation and decomposition, and the final products are studied in both pyrolytic and oxidative reaction environments. The slowest decay of dichloromethane occurs in pyrolysis with CH_4

present. Chlorinated products, such as CH_3Cl, C_2HCl, C_2H_3Cl, CH_2CCl_2, CHClCHCl, and C_2HCl_3 etc. are shown to be more stable in pyrolysis than in oxidation. When oxygen is present, the concentration of chlorinated products decreases rapidly above 780 °C. Poor carbon mass balance in the CH_2Cl_2/Ar pyrolysis reaction environment at temperatures above 780 °C, implies that the formation of higher molecular weight species and soot are occurring at the higher temperatures in the absence of oxygen. The observation of soot which is not incorporated into the mass balance further supports this.

Chapter 3 describes and compares the results of the model to the experimental data on pyrolysis from chapter 2. A mechanism which contains 157 reactions and 51 species is developed and utilized to simulate the pyrolysis of CH_2Cl_2 and CH_2Cl_2/CH_4 mixtures. An important result is the barrier for HCl elimination from chlorinated ethylenes (C_2H_3Cl, CH_2CCl_2, CHClCHCl and C_2HCl_3) is determined to be ΔH_{rxn} + 40(±1) kcal/mol. Model show good fit for reagent decay and major product distribution in the pyrolytic reaction environments.

Importance of the chlorinated methyl radicals reactions with O_2 relative to conversion of chloro-methanes and chloro-methyl radicals is analyzed in chapter 3. These reaction systems are analyzed using QRRK for k(E) and with modified strong collision approach for fall-off, because formation of an energized adduct is involved. Predictions are compared to data of Fenter et al.(6) and show good agreement with the data of Fenter et al. for reactions $CH_2Cl + O_2 \rightarrow CH_2ClOO$ and $CHCl_2 + O_2 \rightarrow CHCl_2OO$. The conversion of these chloro-methyl radicals to corresponding chloro-formaldehydes, CO and CO_2 is observed to be slow by this reaction sequence. The demonstration of this

bottleneck is another important result of this thesis. Results show that conversion primarily occurs through combination of 2 chloro-methyl radicals to chloro-ethanes, then ethylenes, then chloro-vinyl radicals. The major chloro-methyl radical conversion path under combustion condition is the chloro-vinyl radical + O_2 (see chapter 5 and 6).

Extending the pyrolysis reaction steps, a detailed reaction mechanism consisting of 120 species and 433 elementary reactions is developed to model the experiments in the oxidative reaction systems of CH_2Cl_2 and CH_2Cl_2/CH_4. Comparison between model and experimental data for $CH_2Cl_2 : O_2 : Ar = 1 : 4 : 95$ ratio of concentrations shows good fits for CH_2Cl_2, C_2H_3Cl and CH_2CCl_2, while over-predicting CH_3Cl above 700 °C, and CHClCHCl, and C_2HCl_3 above 760 °C. In $CH_2Cl_2 : CH_4 : O_2 : Ar = 1 : 1 : 4 : 94$ reaction environments, the model shows good fits to the data for CH_4 and CH_2Cl_2 decay, as well as for chlorinated ethylene (C_2H_3Cl, CH_2CCl_2, CHClCHCl and C_2HCl_3) product distributions.

Chapter 4 describes the unimolecular dissociation of CH_2Cl_2 to CHCl + HCl and Cl + CH_2Cl analyzed using QRRK for k(E) with modified strong collision approach, and with multi-channel Master Equation analysis for fall-off effects. The high pressure limit rate constants for the primary reaction channels are determined over a wide range of temperature and pressure, shown as Table 1.2:

Table 1.2 High Pressure Limit Rate Constant, $k = AT^n\exp(-\alpha T)\exp(-E_a/RT)$

Reaction	$A(s^{-1})$	n	α	E_a(kcal/mol)
$CH_2Cl_2 \rightarrow CHCl + HCl$	2.25E11	1.0	0.0	74.2
$CH_2Cl_2 \rightarrow CH_2Cl + Cl$	8.22E15	0.34	1.09E-3	77.0

The calculations of QRRK with Master Equation analysis show good agreement with the experimental data of Lim and Michael(7) in their temperature range of 1400 - 2300 K and pressures of 6 to 16 torr. The results of modified strong collision approach also show reasonable agreement, but under predict the CHCl + HCl products under the experimental conditions of Lim and Michael.

Chapter 5 describes the chemically activated combination reaction of methyl and chloro-methyl radicals. The bimolecular combination of chloro-methyl radicals results in formation of activated chlorinated ethane adducts, which can be stabilized, further dissociate to lower energy products (chloro-ethyl radicals + Cl or chloroethylenes + HCl), or dissociate back to reactants before stabilization occurs. The overall reaction process is complex and is a strong function of both temperature and pressure. The reactions are, in addition, of importance and key to formation of C_2 species and to higher molecular weight growth in chlorocarbon pyrolysis and oxidation. Thermodynamic properties, high pressure limit rate constants, vibration frequencies, Lennard-Jones parameters, β and ΔE_{avg} are evaluated and presented. Rate constants for each channel in the reaction systems are estimated using a chemical activation quantum Rice-Ramsperger-Kassel (QRRK) calculation for k(E), combined with a modified strong collision approach and separately with multi-channel Master Equation analysis for comparison of fall-off analysis. Rate constants are calculated for the temperature range 300 - 2500 K and bath gas (Ar) in the pressure range 0.001 - 100 atm with comparison to experimental data where available.

Results at 1 atm indicate the formation of chlorinated ethanes are most important in low temperature range (below ~ 650 K) for the reaction systems in this study. Production of HCl + chlorinated ethylenes dominate at temperature between 700 to 1300 K. A decrease of these rates is observed above 1350 K as a result of increased dissociation to chloro-ethyl radical + Cl and to reactants (two chloro-methyl radicals) at the higher temperatures. Effect of pressure on the reaction channels at 300 K shows that stabilization of chloro-ethane dominates at pressures above 0.1 atm, with production of HCl + chlorinated ethylenes most important below 0.08 atm.

Master Equation and modified strong (beta) collision calculations on dissociation rate constants for CH_2ClCH_2Cl and $CHCl_2CHCl_2$ are observed near the high pressure limits at 1 atm for the lower temperatures and the agreement is very good for both over the temperatures 300 - 2500 K.

Chapter 6 describes reaction pathway analysis, thermodynamics and kinetic calculations for vinyl, and chloro-vinyl radical addition to O_2. This is a critically important reaction in prevention of higher molecular weight product and soot formation (see chapter 3). This is because the addition reaction of alkyl radicals to unsaturated hydrocarbons species is considered to the key step to formation of aromatics, soot, and higher molecular weight species in hydrocarbon pyrolysis.(8-13) Analogous molecular weight growth (MGW) reaction pathways for chlorinated hydrocarbon systems, C_1 and C_2 radical addition to chlorinated ethylenes, have been studied theoretically by Shi and Senkan.(14) Their analysis shows production of MWG species containing 3 to 4 carbons. These C_3 and C_4 species can subsequently result in the production of potential toxic chlorinated

benzenes, phenols, dibenzofurans and dioxins.(15) The molecular weight growth processes can be suppressed in the presence the O_2 by the fast reaction of alkyl radicals with oxygen. These reactions, furthermore, represent the principal pathways of the chloro-methyl and chloro-vinyl radical conversion in many hydrocarbon and chlorinated hydrocarbon oxidation and combustion processes.(16)

The high pressure limit A factors are evaluated from literature for the reactions $C_2H_3 + O_2$ to $C_2Cl_3 + O_2$ range from: $(4.0\pm0.8) \times 10^{12}$ to $(1.2\pm0.24) \times 10^{12}$ cm^3 mol^{-1} s^{-1}. The A factors decrease with increasing chlorine substitution. Energies of activation, E_a's are -(0.25±0.1) to -(0.83±0.23) kcal/mol and show a trend in negative activation energy (< 1 kcal/mol) with increasing chlorine substitution. The well depth (40±2 kcal/mol) to the peroxy adduct does not change significantly.

Calculations indicate that stabilization of the initially formed adducts (vinyl peroxy and chloro-vinyl peroxy radicals) is important at lower temperatures (below 400 K) and higher pressures (above 1 atm). Formation of the product sets: CH_2O (CHClO or CCl_2O) + C•HO (C•ClO) and vinoxy (chloro-vinoxy) + O dominate at high temperatures. They also increase in importance at lower pressures. Calculation results show very good agreement with experimental data, where available.

In chapter 7 the analysis of molecular weight growth is continued - to formation of chlorinated aromatics. Specifically described is the formation of chlorinated aromatic (dioxin precursors) from high temperature combustion reactions of C_1 and C_2 chlorocarbons. Polychlorinated dibenzodioxins (PCDDs) and dibenzofurans (PCDFs) are thought to be possible cancer hazards and known to have non-cancer health effects on

humans. Emissions of these compounds from incinerators to the atmosphere are the dominant source in the United States.(17-21) The reaction mechanisms for production of single ring aromatic compounds, chlorinated benzenes and phenols, from lower molecular weight species may be important initial steps for formation of PCDDs, PCDFs, polycyclic aromatics, soot and higher molecular weight compounds in combustion processes.(7,22-24) Specifically the precursors to PCDD/F species can be formed in these homogeneous processed.

A reaction mechanism consisting of 635 elementary reactions and 215 species is developed to describe the formation of single ring aromatics, chlorobenzenes, and intermediate molecular weight growth species in C_1 and C_2 chlorocarbon and hydrocarbon combustion. All reactions in the mechanism are elementary or are derived from analysis of reaction systems encompassing elementary reaction steps. All reactions are thermochemically consistent and follow principles of Thermochemical Kinetics(25). Quantum RRK theory is used for calculation of k(E) and the modified strong collision approach is used for fall-off effects in combination, addition, and insertion reactions and in unimolecular dissociations or isomerizations.

The mechanism is calibrated against laboratory and literature chlorocarbon oxidation and pyrolysis data over a range of fuel equivalence ratios, ϕ, from 0.5 to 2.0. The data is primarily reactant loss, intermediate product formation/loss, and final product concentrations.

The mechanism is then used in predicting levels of dioxin precursors (chlorinated aromatics) from various high temperature reactions of C_1 and C_2 chlorocarbons. Model

results show that the concentration of benzene and chlorinated benzenes increase with the ratio of CH_2Cl_2/fuel, and with increasing fuel equivalence ratios (higher levels formed in fuel rich conditions). Little quantitative data is available in the literature on formation of these PICs from well defined laboratory combustion or oxidation experiments. Additional quantitative data from controlled experiments would be useful for testing this mechanism.

SOx is a major pollutant from both petroleum and coal fired combustion operations and it is well known to contribute to acid rain.(26) Sulfur, in addition, is known to exist in a range of oxidation states from -2 to +6 (H_2S - SO_3),(27) its reactions with OH and H on surfaces are important to aerosol formation, with these sulfate aerosols strongly implicated in global climate change effects.(28) Radicals of sulfur compounds can catalytically destroy ozone, with mechanisms operative in both the troposphere and in the stratosphere.(29-31) The chemistry of formation and reactions of sulfur oxides in combustion and energy generation processes is important to understand, in order to develop methods for its minimization and removal.

The inclusion of reactions of sulfur and nitrogen oxides into our chloro and hydrocarbon oxidation mechanisms would make the kinetic models more useful for actual applications. Sulfur oxides are chosen for inclusion first. Chapter 8 presents results on our analysis of sulfur oxide species reactions. Here we perform quantum Rice-Ramsperger-Kassel (QRRK) analysis on several reaction systems of sulfur / oxygen species.

The thermodynamic properties related to these reaction systems have been evaluated. The addition reactions of HSO + O, H + SO_2 and the combination reaction of OH + SO have been treated by using quantum Rice-Ramsperger-Kassel theory for

determination of rate constants over 300 - 2000 K, and 0.001 - 100 atm. Thermodynamic analysis shows that H + SO_2 and OH + SO are the low energy bimolecular products, while HOSO is the lowest enthalpy adduct.

HSO_2 - Results of HSO + O reactions at 1 atm show that production of H + SO_2 is the dominate channel over 300 - 2000 K; the OH + SO product channel is next in importance. At temperatures above 800 K, the rate constant to H + SO_2 falls off, while reaction to OH + SO and dissociation of the complex to HSO + O increase in importance. Effectively no pressure dependence is observed for reaction at 1500 K, 10^{-3} - 10^{2} atm. Calculation results for H + SO_2 at 1 atm show that reverse reaction H + SO_2 is most important above 650 K, while HOSO stabilization and H + SO_2 rates are comparable at lower temperatures. The production of OH + SO increases in importance above 400 K, and is second in dominance above 700 K. The HOSO* complex from OH + SO dissociates back to OH + SO as the dominant channel at 1 atm, while dissociation to H + SO_2 is next in importance. H + SO_2 is observed to be most important product in the unimolecular dissociation of HSO_2 and HOSO at 300 -2000 K over the pressures 10^{-3} - 10^{2} atm.

HSO_3 - Calculation results of OH + SO_2 predict that stabilization is most important below 650 K, with dissociation back to OH + SO_2 next in importance, above that OH + SO_2 is observed to dominate. In H + SO_3 reactions, . OH + SO_2 is predicted to be the dominant channel over the temperature range 300 - 2000 K. Stabilization is second in importance below 1400 K. Dissociation back to H + SO_3 increases with temperature, and competes with stabilization near 1400 K.

H_2SO_2 - Results of OH + HSO indicate that reverse reaction; dissociation to OH + HSO, dominates at 300 - 2000 K, and stabilization is predicted next in importance below 750 K. H_2O elimination plus SO increases with temperature, and becomes second in importance above 750 K. In the H + HOSO reaction system, OH + HSO is most important between 300 to 2000 K, with stabilization next in importance below 600 K. H_2O + SO increases in importance with temperature, and becomes second in importance above 650 K. Reverse dissociation to H + HOSO is also observed to increase with temperature, and competes with H_2O + SO above 850 K.

Apparent rate constants for the reactions to various product channels and the dissociation of the stabilized adducts in argon bath gas are calculated. The calculations serve as useful estimates for rate constants and reaction paths in combustion and atmospheric kinetic modeling, where experimental data are not available.

CHAPTER 2

PYROLYSIS AND OXIDATION OF CH_2Cl_2 AND CH_2Cl_2/CH_4

2.1 Introduction

Controlled high-temperature incineration, in spite of the associated high cost, is an attractive waste reduction methodology because it leads to complete treatment and permanent disposal of both municipal and hazardous wastes.(32) The destruction of organic compounds in high temperature environments involves the combination of pyrolytic and oxidative processes. The pyrolysis process is initially one of continuous degradation to smaller and unsaturated species. At some stage of the decomposition process, the radical and unsaturated molecules reach a level where the combination rates become significant, leading ultimately to soot and/or higher molecular weight species. Under oxidation, the breakdown process is enhanced. Carbon-containing radicals combine with or add to oxygen, and further react to thermodynamically favored carbon oxides. They therefore have little chance to form high molecular weight species where well mixed excess oxygen. The oxidation process is highly exothermic in nature, and there are significant increases in temperature. As a result, more radicals are created and the reaction is driven to completion.(33-37)

Investigation of the thermal decomposition of chlorinated hydrocarbons has received significant attention over the past decade, due to the environmental impact from

burning these materials. A number of studies on the high temperature reaction of chlorinated hydrocarbons have been performed.

Weissman and Benson(22) studied the high temperature (1200 -1300 K) decomposition of CH_3Cl and CH_3Cl/CH_4 mixtures. They reported C_2 hydrocarbons as the major products of their experiments, and that CH_3Cl was a sort of catalyst for C_2 formation from CH_4.

Senser et al.(38,39) investigated PIC (Products of Incomplete Combustion) formation during the thermal reaction of CH_2Cl_2/CH_4/Air in a laminar flat flame at 1 atmosphere pressure and in the temperature range 1500-2000 K. They observed that a large number of stable intermediates (C_2H_2, C_2H_4, CH_3Cl, C_2H_3Cl, CH_2CCl_2, CHClCHCl and C_2HCl_3) are produced early in the flame, but at a critical region of flame they are rapidly decomposed. They also reported the presence of chlorine promotes ethane and CH_4 consumption. The author postulated that the oxidation of CH_4/CH_2Cl_2 mixtures is dominated by CH_3 and $CHCl_2$ radicals, and that the combination reaction of these radicals results in the formation of C_2 compounds.

The research group of Senkan(4,40,41) investigated the oxidative pyrolysis of CH_3Cl and CH_3Cl/CH_4 in a flow reactor at 0.68 atm and made a comparative study of the chemical structures of $CH_3Cl/CH_4/O_2/Ar$ and $CH_4/O_2/Ar$ flames at atmospheric pressure effecting soot formation. In the presence of chlorine, ample amounts of C_2H_2 and C_2H_4 were formed rapidly in comparison to the "no chlorine" reaction system. They concluded that the presence of oxygen in the system decreased the formation of carbonaceous

deposits (soot) and showed the important formation of C_2H_2 and C_2H_4, at combined yields as high as 60% when conversion of CH_3Cl was only 30%.

Taylor et al.(32,42) conducted oxidative pyrolysis of CH_3Cl, CH_2Cl_2, $CHCl_3$, and CCl_4 in a tubular reactor operating under laminar flow conditions over the temperature range 573 - 1273 K at 1.15 atm. Taylor indicated that under near pyrolytic conditions, PICs become more numerous, yields of chloroethylene compounds increase, and PIC stability increases with decreasing oxygen concentration. They also proposed that the combination of chloro-methyl radicals (chemical activation reaction) is the important pathway to the formation of C_2 chlorinated compounds.

The Thermochemical Kinetics Research group in NJIT has done a number of studies on both the thermal reaction of chlorinated methanes in tubular reactors and the kinetic reaction mechanism analysis. Huang(43) studied the reaction of hydrogen atom with methylene chloride in a flow system at pressure of 2.1 to 2.7 torr and room temperature. The major products observed were HCl and methane. The conversion of methylene chloride increases first to a maximum and then decreases with increasing concentration of methylene chloride. Tsao(44) examined the thermal reaction of dichloromethane with hydrogen over the temperature range of 700 - 900 °C, at 1 atm in a tubular reactor. The major products in this reaction system were methane and methyl chloride. The minor products were ethylene, acetylene and HCl. Trace amounts of: ethane, chloroethylene, 1,2-dichloroethylene, trichloroethylene, and benzene were also observed. No chlorocarbons were found at temperatures over 950 °C at 1.0 second residence time.

Under these conditions, the only products were methane, HCl, acetylene, ethane and benzene.

Tavakoli(45) investigated the reaction of $CH_2Cl_2/CH_4/Ar$ and $CH_2Cl_2/C_2HCl_3/CH_4/Ar$ at 1 atm in a tubular reactor over the temperature range of 750 - 1000 °C. Acetylene, ethylene, benzene, chloromethane, and HCl were observed as the major products, for temperatures above 750 °C and residence times of 0.08 to 2.0 seconds. Won(46) investigated the thermal reaction of CH_2Cl_2/CH_3CCl_3 mixtures in a hydrogen bath gas in a tubular reactor over the temperature range of 475 - 810 °C at 1 atm pressure. Won demonstrated that selective formation of HCl can result from the thermal reaction of chlorocarbon mixtures with H_2. He also showed that the decomposition of 1,1,1-trichloroethane accelerates the rate of dichloromethane decomposition, and that there is significant interaction between the decay products of 1,1,1-trichloroethane with the parent dichloromethane.

Ho(47) studied the thermal decomposition of dichloromethane in H_2/O_2 mixtures and argon bath gas. The reaction was carried out in a tubular reactor at 1 atmosphere total pressure over the temperature range from 610 to 820 °C with average residence times from 0.1 to 2.0 seconds. The major products observed in this study were methyl chloride, methane, CO, and HCl. It was found that oxygen almost has no effect on the decay of dichloromethane when the conversion is below 50% and/or the initial oxygen concentration is below 5%. When conversion is above 90%, the major products are HCl and non-chlorinated hydrocarbons such as CH_4, C_2H_2, C_2H_4. It was also shown that the

higher the ratio of O_2 to H_2, the lower the temperature needed to observe the formation of CO and CO_2.

Won(48) examined the thermal decomposition of chloroform in absence and presence of added O_2 and/or CH_4. The reactions were studied in a tubular reactor at a 1 atm with residence times of 0.3 - 2.0 seconds, 535 - 800 °C. Increases in O_2 were observed to speed chloroform decay. Won demonstrated that almost all major chlorinated products (C_2Cl_4, CH_2CCl_2, and C_2HCl_3 etc.) are C_2 compounds. Qing-Rui Yu(49) studied the thermal reaction of $CH_3Cl/CH_4/O_2$ and $CH_3Cl/H_2/O_2$ in tubular reactor at 1 atm and in the temperature range from 825 to 950 °C. All major intermediates were observed to be C_2 compounds.

This chapter presents experimental data on the reagent (CH_2Cl_2 and/or CH_4) decay, intermediate product formation and loss, and final product formation as functions of both temperature and residence time. The experiments are conducted to investigate the CH_2Cl_2 pyrolytic reaction environment, then the effects of adding CH_4 to CH_2Cl_2, then the effects of added O_2, and finally the effects of O_2 added to the CH_2Cl_2/CH_4 system. The experimental data are needed for comparison with the model (chapter 3) *i.e.* to improve or validate the kinetic reaction data in the mechanism.

2.2 Experiment

2.2.1 Experimental Apparatus

A diagram of the experimental apparatus is shown in Figure A1. The thermal reaction of CH_2Cl_2 is studied in a 10.5 mm I.D. tubular reactor at one atmospheric pressure. The

tubular reactor is housed within a three zone electric tube furnace of 45.7 cm length, each zone equipped with one independent temperature controller (Omega Engineering, Inc.). Nine temperatures between 680 °C (CH_2Cl_2 begin to decay) to 840 °C (more than 99% CH_2Cl_2 decay), and six residence times in the range from 0.3 to 2.0 seconds were studied. Four reactant concentration ratio are studied:

I.	$CH_2Cl_2 : Ar$	=	1 : 99
II.	$CH_2Cl_2 : CH_4 : Ar$	=	1 : 1 : 98
III.	$CH_2Cl_2 : O_2 : Ar$	=	1 : 4 : 95
IV.	$CH_2Cl_2 : CH_4 : O_2 : Ar$	=	1 : 1 : 4 : 94

Argon carrier is passed through dual saturation bubblers held at 0 °C using an ice bath. A second argon flow stream is used as make-up, to achieve the desired ratios of reagents. Methane and oxygen are then added to the CH_2Cl_2/Ar stream as required. The feed mixture can be transferred directly to the GC sampling valve via a by-pass line before entering the reactor. This is necessary in order to determine the GC peak areas that corresponded to the input concentration of the reagents. The inlet gas mixtures are preheated to about 150 °C to insure mixing and improve the reactor temperature control. The reactor effluent gas passes to the GC gas sampling valve through a heated line (~120 °C) in order to limit condensation. The gas mixtures are passed from the reactor exit to the GC inlet, through a pyrex tube which is packed with glass wool to trap carbon particles in order to prevent contamination of the GC system. The effluent of the reactor is passed

through a pyrex tube packed with glass wool to trap carbon particle and/or soot, and then through a sodium bicarbonate ($NaHCO_3$) flask for neutralization before it is released to a fume hood.

2.2.2 Temperature Control and Measurement

The quartz reactor tube is housed within a three zone furnace, each zone equipped with an independent temperature controller in order to adjust the operation condition to isothermal. The actual temperature profile of the tubular reactor is obtained using type K thermocouple probe, moved coaxially within the reactor, under a steady flow of argon gas. The temperature profiles obtained, as shown in Figure A2, are isothermal to within ±5 °C for the central 30 cm (over 70%) of the furnace length for several residence times at 700 °C. Temperature profiles at varied temperatures but only at 1 second residence time are also illustrated.

An energy balance calculation was done by Won(46) for the reaction system using the reactant concentration, the experimentally observed conversion, the observed products, and the known thermodynamic properties. It was determined that the thermal reactions can increase the temperature by a maximum of 1.5 °C. The temperature profiles obtained with no reactant flow (only inert), are therefore considered accurate.

2.2.3 Qualitative and Quantitative Analysis of Reagents and Reaction Products

An on-line HP-5890 gas chromatograph (GC) with two flame ionization detectors is used to determine the concentration of the reactants and products. Based on the smallest peak

area that can be routinely and repeatedly recorded, 500 μV-s (microvolt-seconds) for CH_4 and the response to 1 mole % standard of CH_4 (470,000 μV-s). The detection limit is estimated as 10 ppm_v. The GC uses a 2 m length by 2.16 mm I.D. stainless steel column packed with 1% Alltech AT-1000 on graphpac GB to separate reactants and products. Carbon monoxide, and carbon dioxide from the reactor effluent stream were separated using 1.67 m length by 2.16 mm I.D. stainless steel column packed with carbosphere 80/100 mesh, which is held at 70 °C in a Varian 1400 GC oven in order to obtain optimum resolution of CO and CO_2.

The GCs used six port sampling valves with 1.0 ml volume loop maintained at 170 °C and 1 atm pressure. Chromatogram peak integration was performed with a Varian 4270 integrator/plotter. A representative chromatogram is shown Figure A3, and Table A1 including average retention time and peak identification.

In order to increase the accuracy of quantitative analysis, a catalytic converter, 5% ruthenium on alumina (30/40 mesh) catalyst, was used to reduce CO and CO_2 with H_2 (10 ml/min) - conversion of CO and CO_2 to methane. The results show the product peaks at corresponding retention times, because the converter is at the exit of the carbosphere column. Quantitative analysis of CO and CO_2 (after reduction to CH_4) is performed using the second flame ionization detector.

The gas chromatogram (GC) is run with relatively high H_2 flow (≥ 30 ml/min) to optimize sensitivity of the flame ionization detector (FID) to CCl_4 and other chlorinated hydrocarbons. I routinely find the responses under this flow configuration for chlorinated hydrocarbons to be similar to hydrocarbons. Calibration of the flame ionization detector

to obtain appropriate molar response factors was done by injecting a known quantity of the relevant compound such as CH_4, C_2H_4, C_2H_6 etc. Liquid compounds such as CH_2CCl_2, C_2HCl_3 etc. were bubbled through a dual stage impinger, to form a saturated Ar-chlorocarbon mixture at ice point (0 °C), to the six port sampling valve, and the corresponding response area measured. The relative response factor determined for compounds is shown in Table A2. Sensitivity of the flame ionization detector in general, corresponds with the number of carbon atoms in the species. The relative response factor for C_1 compounds are all similar, and the relative response of C_2 compounds is nearly twice the response of the C_1 compounds. Thus, the effect of chlorine on the relative response factor is negligible for this flame ionization detector. Analysis of larger chlorohydrocarbons is based on the verified relative response factors, where the specific component peak area was converted to the equivalent number of moles of each compound.

Product identification was also performed in GC/MS (Finnigan 4000 series) with a 50 m length by 0.22 mm I.D. methyl silicone stationary phase capillary column.

2.2.4 Hydrochloric Acid Analysis

Quantitative analysis of HCl product was performed for experiments at each reaction condition. Samples for HCl are collected independently from the GC sampling as illustrated in Figure A1. In this HCl analysis, the reactor effluent is passed through a two stage bubbler before being exhausted to the fume hood. Each stage contains 20 ml of 0.005 M NaOH plus three drops of phenolphthalein indicator. The effluent gas is passed

through the two bubblers until the first stage solution reached the indicator end point. The time required for this to occur is recorded. At this point the bubbling is stopped, the aliquots are combined and then titrated to their end point with standardized 0.01 M HCl. Several titration are performed using buffer solution (pH 4.7) to discern if CO_2 was effecting the acidity. No significant effect was observed due to the relatively low CO_2 levels and the K_a of CO_2.

2.3 Experimental Results and Discussion

The pyrolytic and oxidative reaction of CH_2Cl_2 and CH_2Cl_2/CH_4 mixture in argon bath gas is carried out at atmospheric pressure in a tubular reactor. Reagent concentration ratio sets and temperature ranges shown as Table 2.3 are studied to investigate the reagent decay, product formation and loss for use in development and validating of the detailed reaction mechanism.

Table 2.3 Reactant Concentration Ratio and Temperature Range

	Reagent Mole Fraction (%)			Temperature Range (°C)
I.	CH_2Cl_2 : Ar	=	1 : 99	680 - 840
II.	CH_2Cl_2 : CH_4 : Ar	=	1 : 1 : 98	680 - 840
III.	CH_2Cl_2 : O_2 : Ar	=	1 : 4 : 95	680 - 820
IV.	CH_2Cl_2 : CH_4 : O_2 : Ar	=	1 : 1 : 4 : 94	680 - 840

Duplicate analysis is necessary to determine the reproducibility and systematic error of the experiments. Duplicated analysis is done at least 3 times for each by-pass run and once for every 2 to 3 reaction time.

2.3.1 Reagent Conversion

Experimental results on decomposition of dichloromethane are shown in Figure A4a and A4b as functions of residence time and temperature in four reaction environments. We see more CH_2Cl_2 conversion at higher temperature and longer residence time.

Figure A5 compares dichloromethane decay as a function of temperature at 1.0 second reaction time in four different reaction environments. Each experiment is run at constant temperature for 6 to 8 residence times. Runs at different temperature are on different days; thus data in this figure are obtained over a time period of several weeks. The uniformity and consistency of the data is a good test of the thoroughness of the experimental procedures. Oxygen has positive effect on the decomposition of dichloromethane in this study. Same result was observed by Ho et al.(47,50) for $CH_2Cl_2/H_2/O_2$ systems. The accelerated decomposition of dichloromethane, when O_2 is added, results in part, from the bimolecular reaction of O_2 with CH_2Cl_2 to HO_2 + $CHCl_2$ products. This reaction occurs in parallel with the unimolecular dissociation of dichloromethane under initiation conditions. The subsequent reactions involving combination of methyl and chloro-methyl radicals with O_2 are believed(51-54) to play a significant role in decomposition of chlorine-containing polymeric materials.

The slowest dichloromethane decay occurs in the presence of CH_4 and absence of O_2. Some of the reactive atoms and radicals which are produced from CH_2Cl_2 unimolecular dissociation (Cl, CH_2Cl, :CHCl), react with CH_4 (instead with CH_2Cl_2), which was added to serve as a fuel and as a hydrogen source to improve HCl production. When O_2 is added to the CH_2Cl_2 + CH_4 reaction system, CH_4 decay accelerates. This is also observed in the chloroform reaction systems(48) and illustrates that active intermediates react with O_2 to accelerate the chlorocarbon conversion. Chapter 6 will illustrates that the active intermediates are primarily vinyl radicals and to a much lesser extent, chloro-methyl radicals.

2.3.2 Product Distribution and Material Balance for Each Reaction Environments

HCl and CO, CO_2 are the major products under the oxygen reaction conditions. Carbon mass balance in the pyrolytic reaction environment is only 20 - 80% but it is near 100% when oxygen is present.

2.3.2.1 Product Distribution in CH_2Cl_2/Ar (Pyrolysis) - The decays of CH_2Cl_2, along with the formation and loss of stable intermediate products, at 1.0 second residence time as a function temperature are shown in Figure A6a and A6b. In this pyrolysis only reaction system, we can exclude the effects of oxygen and methane on CH_2Cl_2 decomposition and product distribution. The major products are C_2HCl_3, CH_3Cl, and CHClCHCl. Minor products observed are C_2H_4, C_2H_3Cl, and CH_2CCl_2. Chloro-acetylene, C_2HCl, appears

more stable and is higher in concentration for this reaction system relative to the other systems in this study.

2.3.2.2 Product Distribution in $CH_2Cl_2/CH_4/Ar$ - Figure A7a and A7b show observed product distributions as a function of temperature at 1.0 second residence time. Relatively high concentrations of CH_3Cl, C_2H_3Cl, CHClCHCl C_2HCl_3, and C_2H_2 are produced under this pyrolysis condition. Minor products are C_2H_4, C_2HCl, CH_2CCl_2. The product distribution for $CH_2Cl_2/CH_4/Ar$ reaction is qualitatively similar to the reaction of $CH_2Cl_2/CH_4/O_2/Ar$.

A trace amount of benzene is observed above 740 °C. The production of benzene in this pyrolysis condition is higher than that for $CH_2Cl_2/CH_4/O_2$ oxidation conditions. Higher levels of C_2H_2 C_2HCl, and C_2H_4 suggest that these species are intermediates to form benzene. This implies that the formation of single ring aromatics which are precursors of soot and higher molecular weight species in the pyrolytic reaction environment, is more probable that in the oxidative reaction environment.

2.3.2.3 Product Distribution in $CH_2Cl_2/O_2/Ar$ (No CH_4/Hydrogen Supply) - The main products over the range of temperatures are C_2HCl_3, CHClCHCl, CH_3Cl, C_2H_2, CO, and CO_2 as presented in Figure A8. Minor products observed are C_2H_3Cl, CH_2CCl_2, C_2HCl, with trace levels of C_2H_4, $CHCl_3$. More than 99% conversion of CH_2Cl_2 is observed at 800 °C, 1.0 second residence time. Similar results are shown in the previous study of Ho(50),

where complete decay (> 99%) of CH_2Cl_2 occurs at temperature ~ 800 °C over the range of equivalence ratio (ϕ) from 0.5 to 2.5.

2.3.2.4 Product Distribution in $CH_2Cl_2/CH_4/O_2/Ar$ - Figure A9a and A9b illustrate the distributions for the reagents (CH_2Cl_2 and CH_4), major products CO and CO_2, and minor products CH_3Cl, C_2H_3Cl, CH_2CCl_2, CHClCHCl, C_2HCl_3, C_2H_2, C_2H_4 as a function of temperature at 1.0 second residence time. Trace products $CHCl_3$, C_2HCl, C_2Cl_2 and benzene are also detected at levels below 0.005%. Formation of chlorinated hydrocarbons (CHClCHCl, C_2HCl_3, CH_3Cl and C_2H_3Cl etc.) initially increases with increasing temperature, then a maximum exists near 780 °C (for 1.0 residence time). The formation of C_2H_2 increases rapidly when the parent chlorinated hydrocarbon and CH_4 decreases, then drops above 820 °C. The major end product CO rises as the temperature increases to 740 °C where reagents and chlorinated products begins to decrease. Above 840 °C at 1.0 second residence time, no hydrocarbon or chlorinated hydrocarbon products are observed.

Benzene formation is observed in trace amount above 800 °C. Benzene can be formed from smaller, non-aromatic hydrocarbons (C_2H_2, C_2H_4, C_3H_4, and C_3H_6 etc.), and the mechanism for this formation is shown in chapter 7. To form an aromatic ring from smaller C_1 or C_2 species, there must be molecular weight growth, cyclization, and aromatization reactions. In the present experiment, it is difficult to obtain sufficient information to quantitatively validate the mechanism of benzene and chlorinated benzene formation. The trace levels observed are consistent with the prediction (chapter 7) but more data is needed.

2.3.2.5 Material Balance - Material balance gives important information about higher molecular weight species, soot and oxy-chlorinated compounds which were not detected quantitatively. The carbon material balances for the reaction systems of $CH_2Cl_2/CH_4/O_2/Ar$, $CH_2Cl_2/O_2/Ar$, $CH_2Cl_2/CH_4/Ar$, and CH_2Cl_2/Ar are listed in Tables A3 - A6, respectively. The oxidation reaction systems ($CH_2Cl_2/CH_4/O_2/Ar$ and $CH_2Cl_2/O_2/Ar$) show relatively good material balance over wide temperature range of 680 °C - 840 °C at 1.0 second residence time.

In reaction environments without oxygen ($CH_2Cl_2/CH_4/Ar$ and CH_2Cl_2/Ar), the material balance is low, 20 - 80%, at the higher temperatures. Brown flakes are also observed in the post-reactor zone and on the quartz fiber filter. This implies that the formation of high molecular weight species and soot is occurring at higher temperature in the absence of oxygen. When oxygen is present, the overall CH_2Cl_2 breakdown process is enhanced and soot formation is not observed.

2.4 Comparison of Main Product Distribution in the Four Reaction Environments

Figure A10 to Figure A13 show the comparison of major chlorinated intermediates as a function of temperature at 1.0 second residence time for each reaction environment.

2.4.1 CH_3Cl Product Distribution

The comparison of CH_3Cl product distribution in the four reaction systems is shown in Figure A10. In the $CH_2Cl_2/O_2/Ar$ reaction, the concentration of CH_3Cl is relatively low. The formation paths of CH_3Cl can be described as:

$$CH_3 + Cl_2 \rightarrow CH_3Cl + Cl$$

$$CH_2Cl + HCl \rightarrow CH_3Cl + Cl$$

$$CH_3 + Cl \rightarrow CH_3Cl$$

$$CH_3 + HCl \rightarrow CH_3Cl + H$$

$$CH_3 + CH_2Cl_2 \rightarrow CH_3Cl + CH_2Cl$$

In the presence of O_2, reactions of $CH_3 + O_2$ and $CH_2Cl + O_2$ will compete with above reactions, which decrease the formation of CH_3Cl.

The concentrations of CH_3Cl are relatively high in the CH_2Cl_2/CH_4 pyrolysis reaction system. They are higher here in all experiments where O_2 is present.

2.4.2 C_2HCl_3 Product Distribution

Figure A11 shows the comparison of C_2HCl_3 production in four reaction systems. The formation of C_2HCl_3 (trichloroethylene) is higher in CH_2Cl_2/Ar than for all other condition sets. When O_2 is added in the CH_2Cl_2/Ar system, the O_2 increase the C_2HCl_3 formation rate but also increases its decomposition. We see in Figure A11 that C_2HCl_3 shows more stability in the absence of O_2. The major formation paths of C_2HCl_3 can be described as:

$$CHCl_2 + CHCl_2 \rightarrow C_2HCl_3 + HCl$$

$$CHCl_2CHCl_2 \rightarrow C_2HCl_3 + HCl$$

$$CHCl_2CCl_2 \rightarrow C_2HCl_3 + Cl$$

Combination of two $CHCl_2$ radicals results in the formation of an energized $CHCl_2CHCl_2$* adduct, (see below) which can be stabilized, further dissociate to low energy product channels, or dissociate back to the two $CHCl_2$ radicals. The stabilized adduct can then unimolecular dissociate to C_2HCl_3 + HCl. Details of bimolecular QRRK analysis for this bimolecular reaction are presented in chapter 5.

$$\begin{array}{lcccl} CHCl_2 + CHCl_2 & \leftrightarrow & [CHCl_2CHCl_2]^* & \rightarrow & CHCl_2CHCl + Cl \\ & & \downarrow & \rightarrow & C_2HCl_3 + HCl \\ & & CHCl_2CHCl_2 & & \end{array}$$

When CH_4 is present ($CH_2Cl_2/CH_4/Ar$ and $CH_2Cl_2/CH_4/O_2/Ar$ reaction systems), the concentration of C_2HCl_3 is relatively low. This is a result of more conversion of chlorine to HCl and higher levels of CH_3, CH_2Cl radicals relative to $CHCl_2$ radicals. The resulting increase in the CH_3 and CH_2Cl combination reactions decreases the $CHCl_2$ + $CHCl_2$ combination to trichloroethylene. HCl levels and the number of species with one Cl are however increased.

2.4.3 C_2H_3Cl Product Distribution

Figure A12 shows that significant levels of C_2H_3Cl are observed in the presence of CH_4, with the reasons for this presented above. Formation of C_2H_3Cl increases with increasing temperature to a maximum near 800 °C. Vinyl chloride, C_2H_3Cl, levels are higher in the $CH_2Cl_2/CH_4/O_2/Ar$ and $CH_2Cl_2/CH_4/Ar$ cases, this is because higher levels of CH_3 combination with $CHCl_2$. Formation of C_2H_3Cl in both reaction systems shows similar trends. However, C_2H_3Cl in $CH_2Cl_2/CH_4/O_2/Ar$ decreases more rapidly than in $CH_2Cl_2/CH_4/Ar$ when the temperature increases above 780 °C. This implies that bimolecular reactions of hydrophilic radicals (OH, O and HO_2) and O_2 are responsible for acceleration of the C_2H_3Cl decay.

The vinyl chloride formation pathways can be described as:

$$CH_2Cl + CH_2Cl \rightarrow C_2H_3Cl + HCl$$

$$CH_3 + CHCl_2 \rightarrow C_2HCl_3 + HCl$$

$$CH_2ClCH_2Cl \rightarrow C_2H_3Cl + HCl$$

$$CH_3CHCl_2 \rightarrow C_2HCl_3 + HCl$$

$$CH_2ClCHCl \rightarrow C_2HCl_3 + Cl$$

$$CHCl_2CH_2 \rightarrow C_2HCl_3 + Cl$$

2.4.4 CHClCHCl (1,2-Dichloroethylene) Product Distribution

Figure A13 illustrates that O_2 has significant effect on the formation of CHClCHCl. The concentration of CHClCHCl in presence of CH_4 is relatively low. The reason is that

CH_2Cl, $CHCl_2$ and CHCl, which are produced from the parent compound CH_2Cl_2, react with CH_4, and other H containing species formed from reactions of CH_4.

The formation pathways of CHClCHCl are shown as below:

$$CH_2Cl + CHCl_2 \rightarrow CHClCHCl + HCl$$

$$CH_2ClCHCl_2 \rightarrow CHClCHCl + HCl$$

$$CHCl_2CHCl \rightarrow CHClCHCl + Cl$$

$$CHCl + CHCl \rightarrow CHClCHCl$$

The bimolecular reactions of hydrophilic radicals (OH, O and HO_2) and O_2 are responsible for acceleration of the 1,2-dichloroethylene.

2.5 Conclusions

The pyrolysis and oxidation of methylene chloride both with and without added methane mixture in argon bath gas is studied in a tubular reactor. The thermal reactions are studied at 1 atmosphere pressure with six different residence times from 0.3 to 2.0 seconds in the range of temperatures 680 - 840 °C. The degradation of dichloromethane, the intermediate product formation and decomposition, and final products are studied in both pyrolytic and oxidative reaction environments. The slowest decay of dichloromethane occurs when CH_4 is present and O_2 is absent. The chlorinated products, such as CH_3Cl, C_2HCl, C_2H_3Cl, CH_2CCl_2, CHClCHCl, and C_2HCl_3 etc. are shown to be more stable in the pyrolysis than in the oxidation. When oxygen is present, the concentration of

chlorinated products decreases more rapidly above 780 °C than when no oxygen is present. Carbon mass balance in the CH_2Cl_2/Ar reaction environment is less than 60% at temperatures above 780 °C, and less than 20% at temperatures above 840 °C. This implies that the formation of higher molecular weight species and soot occurs at higher temperatures in the absence of oxygen.

The conversion of these chloro-methyl radicals to corresponding chloro-formaldehydes, CO and CO_2 is observed to be slow by this reaction sequence. The demonstration of this bottleneck is another important result of this thesis. Results show that conversion primarily occurs through combination of 2 chloro-methyl radicals to chloro-ethanes, then ethylenes, then chloro-vinyl radicals. The major chloro-methyl radical conversion path under combustion condition is the chloro-vinyl radical + O_2 (see chapter 5 and 6).

CHAPTER 3

MODELING THE THERMAL DECOMPOSITION OF CH_2Cl_2 BY DETAILED REACTION MECHANISM

$$CH_2Cl + O_2 \leftrightarrow [CH_2ClOO]^* \rightarrow \text{PRODUCTS}$$
$$CHCl_2 + O_2 \leftrightarrow [CHCl_2OO]^* \rightarrow \text{PRODUCTS}$$

3.1 Introduction

The use of a detailed kinetic mechanism to simulate the combustion processes of hydrocarbons and chlorinated hydrocarbons is a developed research area. But validation is often requested for specific reaction systems. The use of a mechanism can greatly facilitate evaluation and optimization of a combustion process. However, by showing trends on improvements in emission levels as input concentrations or operating condition are varied. This technology also help evaluation of important chemical species, what key reactions are involved, and how the kinetics can be controlled to limit or promote the production of a given species during combustion.(55) Won and Bozzelli(56) used a detailed kinetic reaction mechanism consisting of 31 species and 67 elementary reactions to simulate thermal decomposition of 1% $CHCl_3$ in argon bath gas. The reaction were studied in tubular reactors at 1 atm with residence time 0.3 - 2.0 seconds in the temperature range of 535 - 800 °C. The modeling results showed good quantitative agreement with experiments. They reported that the C_2Cl_4 is primarily formed from combination of two $^1CCl_2$, and the formation of CCl_4 occurs by formation of CCl_3 and then combination of CCl_3 with Cl or reaction with Cl_2. The C_2Cl_4 and CCl_4 are non-desirable intermediates that need to be further reacted.

Ho et al.(57) used a 167 reaction mechanism to model the thermal reactions of $CH_2Cl_2/H_2/O_2$ mixtures, and (via reaction mechanism analysis) to investigate the implication for chlorine inhibition of CO conversion to CO_2. Their results indicated that the reaction $OH + HCl \rightarrow H_2O + Cl$ is a major cause of OH loss. This decrease in OH effectively stops CO burnout until equilibrium of OH, HCl, H_2O and Cl are achieved. The lower temperatures resulting from decreased CO conversion caused the $Cl + HO_2 \rightarrow HCl + O_2$ termination reaction to become an important contributor to inhibition in some cases. The model shows good agreement with experimental results on the thermal reaction of CH_2Cl_2. Ho et al.(58) later modified the reaction mechanism(57) and used it to simulate the pyrolysis/oxidation of CH_3Cl in $H_2/O_2/Ar$ mixtures. The model results show good fits to methyl chloride, intermediate, and final product specie profiles with both temperature and time of reaction.

A number of experiments and simulations of flat flames burning chlorinated C_1 and C_2 hydrocarbon have been studied by the research group of Senkan,(3,4,40,41,59,60) Where SANDIA flat program, PREMIX, was using. Chang and Senkan(60) used a 147 reaction mechanism that contained C_1 - C_4 and C_6 species to model a fuel-rich $C_2HCl_3/O_2/Ar$ flat flame at 1 atmosphere pressure. Comparisons between model and experiment were made and which showed good agreement for the major products. Karra et al.(4) simulated $CH_3Cl/O_2/Ar$ atmospheric flat flame using a detailed reaction mechanism consisting of 184 elementary reactions. The agreement between model and experimental data is general satisfactory, but the mechanism regard to the $C_1 \rightarrow C_2$ chemistry needed improvement. They also indicated that the chemically activated

recombination processes of C_1 radicals and reactions of molecular oxygen with chlorinated radicals must be described more precisely.

Lee et al.(61) employed a detailed reaction mechanism consisting of 38 species and 358 elementary reaction steps to simulate premixed flames burning CH_3Cl/CH_4/Air mixtures at atmospheric pressure. Lee et al.(62) later reduced the detailed reaction mechanism to short reaction mechanism containing 25 species, 63 elementary reactions for premixed CH_3Cl/Air flames. The results of reduced kinetic mechanism calculations conducted for experiments are in good agreement with the predictions of the full mechanism.

Miller et al.(55) used a reaction mechanism containing 52 species and 190 elementary reactions to model a CH_2Cl_2/CH_4/Air flat flame. The model showed good agreement with the experimental data of Senser.(63) Analysis of the results showed that the flame occurred in three stages, the first one dominated by chlorine chemistry with oxidation occurring in the second stage and CO conversion to CO_2 in third. They indicated that the depletion reactions for chlorinated C_2 compounds, and the reaction pathways for C_2HCl and C_2Cl_2 should be included in the reaction mechanism, due to their significant impact on the model.

There is less data in the literature on detailed reaction mechanism which model the thermal reaction of C_2 chlorinated hydrocarbons. Thomson et al.(64) used a 324 reaction mechanism to simulate the high temperature oxidation of CH_3CCl_3 in the post flame region of a turbulent combustor. Numeric modeling of chemical processes in the flow reactor was performed using the CHEMKIN package(65) with the PFR driver program.(66) The

model and the experimental data show reasonable agreement for all temperatures. They indicated that CH_3CCl_3 mainly undergoes unimolecular decomposition to form CH_2CCl_2 (loss of HCl). Reacting with either Cl or OH, CH_2CCl_2 then forms the CCl_2CH vinyl radical. This radical reacts via two routes, $CCl_2CH \rightarrow C_2HCl + Cl$ and $CCl_2CH + O_2 \rightarrow COCl_2 + CHO$, to form chloroacetylene (C_2HCl) and Phosgene ($COCl_2$).

In this chapter, a detailed reaction mechanism is developed based on fundamental thermodynamic and kinetic principles to model the experimental results discussed in chapter 2. Development of the reaction mechanism started from the simpler reaction system (CH_2Cl_2 pyrolysis) and progressed to the more complicated reaction system (CH_2Cl_2/CH_4 oxidation). In the CH_2Cl_2 pyrolytic reaction system, we can exclude the effect of CH_4 and O_2. This allows a simpler mechanism to be developed and most importantly validated for the pyrolysis. The reactions relative to CH_4 were then added to the validated CH_2Cl_2 pyrolysis reaction mechanism. The last, oxidation reaction steps were combined with the CH_2Cl_2/CH_4 pyrolysis reaction mechanism.

3.2 Computer Codes Used to Develop the Kinetic Model

Model requirements include:

- Accurate thermodynamic properties of all species in the reaction mechanism.
- Forward and reverse rate constants to be consistent with thermochemical principles - microscopic reversibility for all fundamental reactions.
- Isomerization rate constants to follow Transition State Theory (TST).

- Quantum Rice-Ramsperger-Kassel Theory(67,68) for k(E) combined with modified strong collision analysis for temperature and pressure compensation in chemical activation reactions (combination, addition, insertion) and in unimolecular dissociation reactions (simple, beta scission, isomerization).
- Abstraction Arrhenius A factors from literature evaluation or generically derived. Abstraction energies of activation (E_a's) from literature evaluation or from thermodynamics and Evans-Polanyi relationships.
- Model to be tested against data in the literature when data is available.

The following computer codes are helpful tools in mechanism validation and development.

3.2.1 THERM

THERM(69) is the computer code which can be used to calculate, edit, or enter thermodynamic property data for gas phase radicals and molecules using Benson Group Additivity method.(25) Properties of radicals are based on Bond Dissociation (BD) groups which is developed by Thermodynamic Kinetic Laboratory in NJIT. BD groups consist of enthalpy (ΔH_f), entropy (S_f), and heat capacity ($C_p(T)$) terms, which are added to the corresponding properties of the parent molecule to yield thermodynamic properties of the radical (parent molecule - H atom). All group contributions considered for a species are recorded and thermodynamic properties are generated in NASA polynomial format (for compatibility with CHEMKIN)(65) in addition to listing which are more convenient for thermodynamic, kinetic presentation and evaluation.

A thermodynamic data base up to C_6 for the species with C/H/Cl/O elements is developed and used for modeling the kinetic scheme of elementary reactions input to the program.

3.2.2 RADICALC

RADICALC(70) is a computer code that calculates the entropies and heat capacities of radicals and transition state structures for estimation of Arrhenius A factors as a function of temperature. Calculation of RADICALC is performed using a data base of vibrational frequencies, moments of inertia and barriers to internal rotations and principles of statistical mechanics.(71)

3.2.3 CPFIT

CPFIT(72,73) is a computer code that determine geometric mean frequency as well as a reduced three frequency set to describe the vibration frequencies of a molecule. It accepts input in the form of heat capacities at various temperatures in addition to the number of atoms and the number of internal rotors in the molecule. This code fits the heat capacity data in the above range to a reduced set of 3 frequencies. This comprises a 5 parameter set 3 frequencies plus degeneracies for 2 of the frequencies. Third degeneracy is determined from the number of atoms, N, and the total number of vibrations "3N - 6" for a nonlinear molecule or "3N - 5" for a linear molecule. The code also extends the temperature range to 5000 K.

3.2.4 CHEMACT

Quantum Rice-Ramsperger-Kassel analysis, as initially published by Dean,(67,68) and recently modified by Chang et. al.(74) is used to compute apparent rate constants over a wide range of temperature and pressure. Branching ratios of bimolecular combinations at different temperatures and pressures are calculated using modified computer code "CHEMACT".(68) This code uses the quantum version of RRK theory (QRRK) to evaluate the rate constants, k(E) as functions of temperature. The modified strong collision theory of Gilbert, Luther, and Troe(75) is used to calculate the fall-off pressure dependencies.

Modifications to the quantum RRK(74) calculation of ref. 68 include:

- Use of reduced set of 3 vibrational frequencies for describing the energy distribution and the 3 frequencies plus one external rotation to calculate the density of states, $\rho(E)/Q$.
- The F_E factor is now calculated for use in determining the collision efficiency β_c,(75) in place of the previously assigned 1.15 value.
- β_c is now calculated by : $\beta_c = (\alpha_c /(\alpha_c + F_E*k*T))^2/\Delta$ from Gilbert et. al. Eqn. 4.7,(75) $\Delta = \Delta_1 - (F_E*k*T)/(\alpha_c + F_E*k*T)*\Delta_2$. Where Δ_1 and Δ_2 are temperature-dependent integrals involving the density of states, and α_c is the average energy of down-collisions.
- The Lennard-Jones collision frequency Z_{LJ} is now calculated by $Z_{LJ} \equiv Z\ \Omega^{(2,2)}$ integral.,(76-78) Ω is obtained from fit of Reid et al.(78)

A bimolecular combination, addition or insertion reaction, can form an energized (chemically activated) adduct which can: be stabilized through collisions with the bath gas, or dissociate to products, isomerize, or dissociate back to reactants before stabilization occurs. The effect of pressure can be understood by realizing that the stabilization rate is a function of bath gas pressure. Increased pressure, results in increased stabilization rates and this can consequently decrease reaction of the energized adduct to products or back to reactants. In general one can expect adduct stabilization to dominate at high pressures and dissociation of the adduct to be more important at low pressure and/or high temperatures. Decrease of stabilization with temperature increase is understood by realizing that rates of dissociation of the adduct are often highly energy dependent (E_a) and increase exponentially with temperature. Stabilization rates can also decrease at high temperatures because the bath gas molecules have more internal energy and thus remove less energy from the adduct per collision.

An energy level diagram for formation of a chemically-activated adduct with illustration of product, reversible isomerization (BCDA*), reaction back to reactants, and stabilization ($ABCD^{o}$ and $BCDA^{o}$) channels is illustrated as Figure 3.2.4:

ABCD* is the activated complex formed by the reactants, and $ABCD^{o}$ is its stabilized adduct. The ABCD* can dissociate to products or react back to reactants, isomerize to BCDA* and other complexes, or be stabilized. The BCDA* adduct can also dissociate to products, isomerize back to ABCD* or be collisionally stabilized.

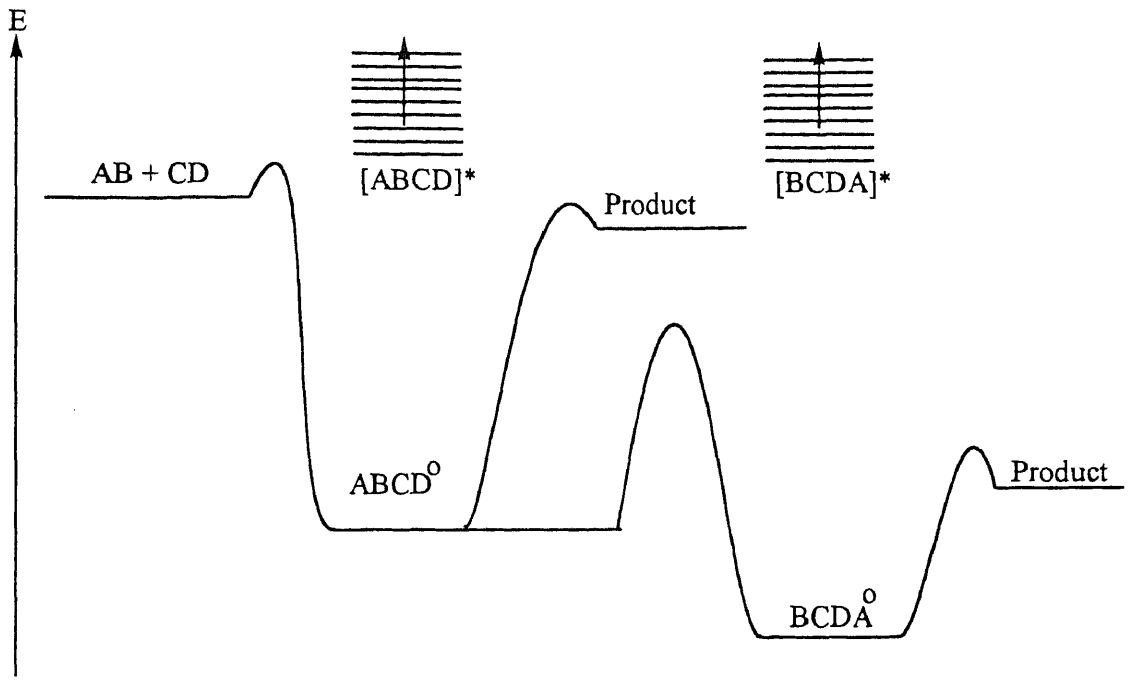

Figure 3.2.4 Energy Level Diagram for Bimolecular Chemical Activation Reaction

Input Data needed for CHEMACT(68): (QRRK for k(E) and modified strong collision for fall-off)

- Thermodynamic parameters: Enthalpy (ΔH_f), entropy (S_f) and heat capacities (C_p) as a function of temperature for reactants, adducts and products of the reaction system are important.
- Molecular parameters describing the size, collisional energy transfer and energy levels of the adduct formed by the initial reaction are also needed. These include the mass, vibrational frequency set of each adduct, and Lennard-Jones parameters. Vibrational frequencies include: reduced of 3 vibrational frequencies and respective degenercies.
- The bath gas molecule collision diameter (σ), well depth (e/k) and average energy transferred $(\Delta E)_{avg}$.

- High pressure limit rate constants for adduct formation and various isomerization and dissociation product channels of the adduct are also needed.

3.3 Kinetic Mechanism and Modeling

A 157 reaction mechanism which contains 51 species is utilized to simulate the pyrolysis of CH_2Cl_2 and CH_2Cl_2/CH_4 mixture. Expending the pyrolysis reaction steps, a detailed reaction mechanism consisting of 120 species and 433 elementary reactions is used to model the experiments in the oxidative reaction systems of CH_2Cl_2 and CH_2Cl_2/CH_4. This kinetic reaction mechanism is shown in Table B1 together with the rate parameters for the forward reaction paths. The CHEMKIN computer program package(65) is used in interpreting and integrating the reaction mechanism.

Specifics on Reaction Rate constants in the mechanism:

Abstraction Reactions - Abstraction reaction rate constants are not pressure dependent and therefore do not incorporate any quantum RRK analysis. When estimation is required for an abstraction rate constant, we use a generic reaction as a model and adjust for steric effects as best as I can. An example of the generic type of Arrhenius A factor analysis is Cl atom abstracting a H atom from 1,1-dichloethylene, where experiments can not discern whether the measures values are for the abstraction or the addition reaction. Here I would take the abstraction of H atom by Cl from 1,1,1-trichloroethane where both the mass and the reaction degeneracy are similar.

Evans Polanyi analysis is used on the reaction in the exothermic direction to estimate the energy of activation (E_a) for the rate constant. An Evan Polanyi plot, E_a

versus ΔH_{rxn}, allows use of a known ΔH_{rxn} to obtain E_a for these reactions. Clearly the abstraction reaction in an endothermic reaction must incorporate the ΔH_{rxn} or it ,the reaction rate constant, will violate thermodynamics.

Addition Reactions - Addition reactions are treated with the quantum RRK formalism described above. The reaction involve addition of an atom or radical to an unsaturated species and typically form an energized adduct with ca. 20 to 50 kcal/mol of energy above the ground state. This is sometimes sufficient to allow the adduct to react to other reaction products (lower energy) before stabilization occurs. An example would be a H atom addition to vinyl chloride, an olefin, forming one of two chloro-ethyl adducts with ca. 40 kcal/mol energy above the ground state. In the case of H atom addition to the carbon containing the Cl atom, the chloro-ethyl adduct formed $\bullet CH_2CH_2Cl$ could rapidly eliminate (beta scission) to form the lower energy products Cl atom plus ethylene. Some examples of the quantum RRK analysis for this reaction are fully described in chapter 7. It is important to note that reaction to other channels as well as isomerization, in addition to stabilization and reverse reaction are included in these calculations.

Elimination Reactions - Beta Scission - These reactions utilize the quantum RRK formalism and are treated in one of two ways. We use a unimolecualr quantum RRK formalism, where we determine the reverse reaction (addition) parameters for the high pressure case, then calculate the corresponding high pressure unimolecular beta scission rate constants using microscopic reversibility <MR>. The high pressure unimolecular elimination parameters are then input to the quantum RRK formalism to determine the high pressure limit and to calculate the apparent rate constants at the appropriate pressure.

The second method is simple use of the reverse rate constants from the CHEMACT addition reaction calculations, see above.

Elimination Reactions - Simple Unimolecular - Simple unimolecular (elimination) rate constants are determined by two methods similar to beta scission reactions. We use the unimolecular quantum RRK formalism, where we determine the reverse reaction (combination) parameters for the high pressure case, then calculate the corresponding high pressure unimolecular dissociation rate constants using microscopic reversibility <MR>. The high pressure unimolecular dissociation parameters are then input to the quantum RRK formalism to determine the high pressure limit and to calculate the apparent rate constants at the appropriate pressure. The second method is simple use of the reverse rate constants from CHEMACT combination reaction calculations.

Combination and Insertion Reactions - These reactions involve the combination of two radicals or an atom with a radicals. The energy of the adduct formed before stabilization is equal to the bond energy of the new bond(s) formed and typically on the order of 80 to 120 kcal/mol. This is usually sufficient for an adduct, with this initial energy above it's ground state energy, to react to lower energy products before stabilization occurs. The high pressure limit rate constant for combination is obtained from literature or estimated from known generic combinations. The quantum RRK chemical activation formalism is then used to determine the high pressure limit and to calculate the apparent rate constants at the appropriate pressure to all the recognized available channels.

Again, reaction to other channels as well as isomerization, in addition to stabilization and reverse reaction are included in this calculation. This is an important

aspect of the reaction analysis for both combination as well as insertion and addition reactions that other modelers do not incorporate. This leads to a more correct treatment of fall-off and pressure dependence for these non-elementary reaction systems. Rate constants for the model are obtained which incorporate these pressure dependency therefore make the model more fundamentally correct.

All reactions are thermochemically consistent and follow principles of Thermochemical Kinetics.(25) The thermodynamic data base, listed in Table B2 uses : evaluated literature data, THERM,(69) calculations of entropies S(T) and heat capacities $C_p(T)$ from changes of specific vibrations and internal rotations by use of statistical mechanical principles applied to the Thermodynamic Properties,(70) Hydrogen Bond Increment groups for radicals(79) as well as semi-empirical molecular orbital calculations.(80)

3.4 Results and Discussion

3.4.1 Pyrolysis of CH_2Cl_2 and CH_2Cl_2/CH_4

The initial reaction channels for CH_2Cl_2 pyrolysis and their high pressure limit rate constants include:

	A (1/sec)	n	E_a (kcal/mol)	
$CH_2Cl_2 \rightarrow CH_2Cl + Cl$	3.14E16	0.0	77.0 (ΔH_{rxn} - RT_m)	[I]
$CH_2Cl_2 \rightarrow {}^1CHCl + HCl$	3.25E11	1.0	74.2 (ΔH_{rxn} + 1.5)	[II]

The high pressure limit of A factor for reaction [I] is obtained from the high pressure limit A factor of the reverse reaction, Cl + CH_2Cl, Ho et al.(57) and microscopic reversibility. The E_a of reaction [II] is an average of $^1CH_2$ insertion, and $^1CCl_2$ insertion into HCl, $E_a = 0$ and 3 kcal/mol,(56) respectively. We discuss the calculation and comparison to the data of Lim et al.(7) for CH_2Cl_2 unimolecular dissociation in detail in chapter 4.

The chlorine radical has high activity(22,81) : it abstracts H from CH_2Cl_2 rapidly because it abstracts H with high A factors and low energies of activation. Here the Cl rapidly converts to HCl + $CHCl_2$ radicals. The $CHCl_2$ and CH_2Cl radicals abstract H from HCl to convert to CH_3Cl. The results is a high level of CH_2Cl and $CHCl_2$ radicals in the reaction system early relative to hydrocarbon systems. Combination reactions of these methyl and chloro-methyl radicals are the important formation paths for C_2 compounds as their rates grow quadratically with the radical concentrations. This combination reaction forms an energized chloroethane adduct, which can be stabilized, react to products or dissociate back to reactants before be collisionally stabilized. A kinetic on relative degrees of analysis stabilization and dissociation of the adduct is therefore needed as a function of temperature and pressure. The reactions are showed as below and the QRRK analysis are described in chapter 5.

$$
\begin{array}{lcll}
CH_3 + CH_2Cl & \leftrightarrow & (C_2H_5Cl)^* & \rightarrow \; C_2H_4 + HCl \\
 & & \downarrow & \rightarrow \; C_2H_5 + Cl \\
 & & C_2H_5Cl &
\end{array}
$$

$$
\begin{array}{lcccl}
CH_3 + CHCl_2 & \leftrightarrow & (CH_3CHCl_2)^* & \rightarrow & C_2H_3Cl + HCl \\
 & & \downarrow & \rightarrow & CH_3CHCl + Cl \\
 & & CH_3CHCl_2 & & \\
CH_2Cl + CH_2Cl & \leftrightarrow & (CH_2ClCH_2Cl)^* & \rightarrow & C_2H_3Cl + HCl \\
 & & \downarrow & \rightarrow & CH_2ClCH_2 + Cl \\
 & & CH_2ClCH_2Cl & & \\
CH_2Cl + CHCl_2 & \leftrightarrow & (CH_2ClCHCl_2)^* & \rightarrow & CH_2CCl_2 + HCl \\
 & & \downarrow & \rightarrow & CHClCHCl + HCl \\
 & & & \rightarrow & CH_2ClCHCl + Cl \\
 & & & \rightarrow & CHCl_2CH_2 + Cl \\
 & & CH_2ClCHCl_2 & & \\
CHCl_2 + CHCl_2 & \leftrightarrow & (CHCl_2CHCl_2)^* & \rightarrow & C_2HCl_3 + HCl \\
 & & \downarrow & \rightarrow & CHCl_2CHCl + Cl \\
 & & CHCl_2CHCl_2 & &
\end{array}
$$

The barrier for HCl elimination reaction from chlorinated ethylenes is very important to fit the experimental chlorinated ethylene product distribution. Additional experimental data are needed to further validate the barrier for HCl elimination from the chlorinated ethylenes. The evaluation of literature data on these reactions results in suggested values of $E_a = \Delta H_{rxn} + (42 - 45)$ kcal/mol.(82,83) These E_a's were consistently unsuccessful in matching our experimental chlorinated ethylene profiles. The E_a's of ΔH_{rxn} + 40(±1) kcal/mol for HCl loss, with A factors from Transition State Theory, yield the

results illustrated in Figure B2 and B3. The reaction mechanism includes abstraction of H by Cl, with Cl elimination from the chlorinated species also playing important rules.

Figure B1 is a comparison between model calculation and experimental results on reagent (CH_2Cl_2) decay and major product (CH_3Cl) profiles between 680 - 840 ^oC at 1.0 second residence time in CH_2Cl_2/Ar pyrolysis. The model results of CH_2Cl_2 and CH_3Cl, match experiments is excellent. Comparisons between model and experiment for chlorinated ethylene product distribution as a function of temperature at 1.0 second residence time in CH_2Cl_2/Ar pyrolysis are illustrated in Figure B2. Model results show good agreement with experimental data for the formation and decay of C_2HCl_3, CHClCHCl and CH_2CCl_2 in this amplified scale, while slightly over predicts the

further react to aldehydes, carbon monoxide and carbon dioxide. The kinetics of chlorinated carbon radicals has not been widely studied, particularly at relatively high temperatures above 1000 K. Methyl and chlorinated methyl radical combination with O_2 competes with the combination of chloro-methyl radicals to form C_2 compounds,(84) while reaction of vinyl and chloro-vinyl radicals with O_2 converts these active radicals rapidly and serves suppress the formation of higher molecular weight species.(85) The kinetic analysis on vinyl and chloro-vinyl radicals addition to oxygen, using QRRK analysis will be discussed in chapter 6.

Very little kinetic information on the reactions of chlorinated methyl radicals with O_2 is available. Only $CCl_3 + O_2 \rightarrow CCl_3OO$ has been well studied with the high pressure limit rate constant (1.51E12 ~ 3.09E12 $cm^3\ mol^{-1}\ s^{-1}$) for $CCl_3 + O_2 \rightarrow CCl_3OO$ determined over a range of temperatures 295 - 461 K and pressures 0.8 - 760 torr.(52,54,86,87) For the partially chlorinated methyl radicals (CH_2Cl and $CHCl_2$), only one kinetic study has been reported. Fenter et al.(6) investigated the rate constants for the addition of CH_2Cl and $CHCl_2$ to oxygen over the temperature range of 298 - 448 K with pressure range 1 - 760 torr in nitrogen bath gas. The following high pressure limit rate constants were determined:

$CH_2Cl + O_2 \rightarrow CH_2ClOO$ $\quad k_\infty(T) = (1.75\pm0.2) \times 10^{12}(T/300)^{-1.2\pm0.4}\ cm^3\ mol^{-1}\ s^{-1}$

$CHCl_2 + O_2 \rightarrow CHCl_2OO$ $\quad k_\infty(T) = (1.68\pm0.2) \times 10^{12}(T/300)^{-1.4\pm0.3}\ cm^3\ mol^{-1}\ s^{-1}$

In the next section, QRRK theory for k(E) and with modified strong collision approach for fall-off analysis is used to treat these two chemical activated reaction systems at different temperatures and pressures, and compare to the experimental data where available.

3.4.2.1 Reaction of $CH_2Cl + O_2$ - Potential energy diagram and QRRK input parameters for $CH_2Cl + O_2$ reaction are illustrated in Figure B5 and Table B3, respectively. Chloromethyl radical combines with O_2 to form the chemically activated CH_2ClOO^* adduct. The reaction channels of this energized adduct include stabilization, dissociation to CH_2ClO + O, CH_2O + ClO, dissociation back to reactants, or isomerization via H-shifts to a hydroperoxide which can subsequently β-scission before being collisionally stabilized. The absence of low-energy product channels; low barriers relative to dissociation back to reactants, suggests that significant stabilization of the initially formed adduct or dissociation back to reactants ($CH_2Cl + O_2$) occurs. The relatively low energy level (~ -31 kcal/mol relative to $CH_2Cl + O_2$) of ClO elimination to CH_2O + ClO caused this reaction may be important at higher temperatures, even the barrier is higher than that dissociation back to reactants. The rate constant for O_2 addition to CH_2Cl is taken from Fenter et al.,(6) with no barrier. The parameters for the energized CH_2ClOO^* adduct dissociation to CH_2ClO + O were obtained using as estimation of 1.51E13 $cm^3\ mol^{-1}\ s^{-1}$ for the high-pressure combination rate constant of the reverse reaction. The A factor for ClO elimination + CH_2O was obtained via Transition State Theory (TST), four-member ring transition state, with E_a = 31 kcal/mol calculated by AM1/MOPAC.(80) The A factor and barrier for the initial energized adduct isomerization to CHClOOH was calculated via TST

intramolecular H-shift to form a four-member ring transition state. The rate constant for the second adduct CHClOOH* β-scission to CHClO + OH was based upon the reverse reaction, OH addition to CHClO and microscopic reversibility.

Figure B6 compares the predictions to experimental data of Fenter et al.(6) in the temperature range 298 - 448 K and in the pressures 20 - 760 torr for the stabilization channel $CH_2Cl + O_2 \rightarrow CH_2ClOO$ in N_2 bath gas. The QRRK calculations slightly under predict at relatively lower temperatures (298 K), but is somewhat higher than actually observed at higher temperatures.

The predicted rate constants versus temperature at one atmosphere pressure are shown in Figure B7. The energized adduct dissociation back to reactants dominates below 600 K, because the complex does not have enough energy to surmount the higher barriers to product channels. As expected, the stabilization of energized adduct is next most important below 700 K. The formation of CH_2O + ClO increases in importance above 800 K, and becomes predominant above 1000 K. This is a new reaction path. It is very important in our reaction mechanism and it needs to be further analyzed at high levels of theory and in elementary reaction experiments. CH_2ClO + O, CHClOOH and CHClO + OH are shown to be little importance over a wide range of temperatures (300 -2000 K).

3.4.2.2 Reaction of $CHCl_2 + O_2$ - Figure B8 illustrates the potential energy diagram for $CHCl_2 + O_2$. The relatively shallow well for this $CHCl_2OO^*$ adduct (~ 25 kcal/mol) puts all the product reaction channels at least 6 kcal/mol higher in energy than dissociation back to reactants. Similar to the above reaction system, the absence of low-energy exit channels

suggests that significant stabilization of the initially formed adduct or dissociation back to reactants ($CH_2Cl + O_2$) should dominate, with a small amount ca. < 1% of reaction over the lowest barrier to products. Table B4 lists the input parameters for QRRK calculation.

Predictions of QRRK analysis are compared to the observation results of Fenter et al.(6) as a function of pressure in N_2 bath gas at temperatures 298 - 383 K in Figure B9. The fit is good at room temperature, but shows over-estimate at 333 and 383 K. It is noted that QRRK calculations suggest that the stabilization is somewhat larger than actually observed at 333 and 383 K, the fall-off behavior and temperature dependence are in good agreement at 298 K. This is result of back reaction of the stabilized adduct out the low energy (25 kcal/mol) well. As an example, the high pressure rate constant for this dissociation is 6.72E14exp(-21.54/0.7) at 350 K, k = 30.7 s^{-1}. Life time for an unimolecular reaction, $t_{1/2}$ = 0.693/k is then 0.023 sec., and its life time to dissociate is short on the experimental time of Fenter's experiments (ca. 0.1 sec.) The results is that to correctly model the stabilization, a CHEMKIN type model needs to be run on the system as a function of reaction time.

Figure B10 illustrates the calculated rate constants of various reaction channels as a function of temperature at 1 atm. Below 1000 K, stabilization of the energized adduct is next most important. CHClO + ClO increases in importance with temperature increased, and dominates above 1000 K. $CHCl_2O$ + O, CCl_2OOH, and $COCl_2$ + OH are trace products over a wide temperature range (300 - 2000 K). Again, ClO + CHClO is an important predicted path, further research is suggested on this channel.

3.4.2.3 Comparison Between Model and Experiments - Extending the pyrolysis reaction steps, a detailed reaction mechanism consisting of 120 species and 433 elementary reactions is developed to model the experiments in the oxidative reaction systems of CH_2Cl_2 and CH_2Cl_2/CH_4. Figure B11 compares the CH_2Cl_2 decay and CH_3Cl product distribution as a function of temperature at 1.0 second residence time in the $CH_2Cl_2 : O_2 : Ar = 1 : 4 : 95$ reaction system. The model shows reasonable agreement for CH_2Cl_2 decay over the experimental temperature range (680 - 840 °C), while it over-predicts the product distribution of CH_3Cl above 700 °C.

The comparisons of model to experiments for chlorinated ethylene formation and loss as a function of temperature at 1.0 second residence time in $CH_2Cl_2 : O_2 : Ar = 1 : 4 : 95$ are illustrated in Figure B12. The fit is good for C_2H_3Cl and CH_2CCl_2 at temperatures 680 - 840 °C. The model fit is good for CHClCHCl and C_2HCl_3 below 760 °C, but it over-predicts these species above 760 °C.

Figure B13 and B14 illustrate the comparison of reagent decay (CH_2Cl_2 and CH_4) and product distribution (C_2H_3Cl, CH_2CCl_2, CHClCHCl, C_2HCl_3), respectively, as a function of temperature at 1.0 second residence in $CH_2Cl_2 : CH_4 : O_2 : Ar = 1 : 1 : 4 : 94$. The model fit is good for both CH_4 and CH_2Cl_2 decay, and for chlorinated ethylene (C_2H_3Cl, CH_2CCl_2, CHClCHCl and C_2HCl_3) product distribution.

3.5 Conclusions

A 157 reaction mechanism which contains 51 species is utilized to simulate the pyrolysis of CH_2Cl_2 and CH_2Cl_2/CH_4 mixture. The barrier for HCl elimination from chlorinated

ethylenes (C_2H_3Cl, CH_2CCl_2, CHClCHCl and C_2HCl_3) is important to their decay profiles and is determined to be ΔH_{rxn} + 40(±1) kcal/mol in order to fit the experimental results. The model show good fit for reagent decay and major product distribution in both pyrolysis reaction environments.

Importance of the chlorinated methyl radicals reactions with O_2 relative to conversion of chloro-methanes and chloro-methyl radicals is analyzed in chapter 3. These reaction systems are analyzed using QRRK for k(E) and with modified strong collision approach for fall-off, because formation of an energized adduct is involved. Predictions are compared to data of Fenter et al.(6) and show good agreement with the data of Fenter et al. for reactions $CH_2Cl + O_2 \rightarrow CH_2ClOO$ and $CHCl_2 + O_2 \rightarrow CHCl_2OO$. The conversion of these chloro-methyl radicals to corresponding chloro-formaldehydes, CO and CO_2 is observed to be slow by this reaction sequence. The demonstration of this bottleneck is another important result of this thesis. Results show that conversion primarily occurs through combination of 2 chloro-methyl radicals to chloro-ethanes, then ethylenes, then chloro-vinyl radicals. The major chloro-methyl radical conversion path under combustion condition is the chloro-vinyl radical + O_2 (see chapter 5 and 6).

A detailed reaction mechanism consisting of 120 species and 433 elementary reactions is used to model the experiments in the oxidative reaction systems of CH_2Cl_2 and CH_2Cl_2/CH_4, where this mechanism includes all pyrolysis reactions. Comparison between model and experimental data in $CH_2Cl_2 : O_2 : Ar = 1 : 4 : 95$ shows a good agreement for CH_2Cl_2, C_2H_3Cl and CH_2CCl_2, while the model over-predicts for CH_3Cl above 700 °C, and for CHClCHCl, and C_2HCl_3 above 760 °C. In $CH_2Cl_2 : CH_4 : O_2 : Ar = 1 : 1 : 4 : 94$

reaction environment, the model shows good fits to the data for CH_4 and CH_2Cl_2 decay, and the chlorinated ethylene (C_2H_3Cl, CH_2CCl_2, CHClCHCl and C_2HCl_3) product distributions.

CHAPTER 4

UNIMOLECULAR DISSOCIATION OF CH_2Cl_2 USING QRRK WITH MODIFIED STRONG COLLISION AND WITH MASTER EQUATION ANALYSIS

4.1 Introduction

There are relatively few studies on the unimolecular dissociation of $CH_2Cl_2 \rightarrow CH_2Cl + Cl$ and $CH_2Cl_2 \rightarrow CHCl + HCl$, which are important initiation paths in the pyrolysis and oxidation of CH_2Cl_2. Lim and Michael(7) investigated the unimolecular decomposition of CH_2Cl_2 in reflected shock waves in the temperature range 1400 - 2300 K, at three pressures 6, 11, and 16 torr with various initial CH_2Cl_2 concentrations in krypton bath gas. The resulting product, Cl atoms, are monitored by the atomic resonance absorption (ARAS). The best fits to the experimental data obtained with high pressure limit rate constants (A factor and E_a), threshold energy (E_0), and collisional energy transfer (ΔE_{down}) for two primary dissociation reactions are listed as Table 4.1.1:

Table 4.1.1 Data of Lim and Michael

	$A(s^{-1})$	E_a(kcal/mol)	E_0(kcal/mol)	$\Delta E_{down}(cm^{-1})$
$CH_2Cl_2 \rightarrow CH_2Cl + Cl$	1.33E16	77.6	73.0	394
$CH_2Cl_2 \rightarrow CHCl + HCl$	3.10E14	75.5	78.25	630

Bozzelli et al.(57,80) studied the thermal decomposition of CH_2Cl_2 in a tubular reactor at 1 atm in the temperature range 873 - 1093 K with argon bath gas. They used evaluated data for thermodynamic properties of the various species, and applied QRRK(67,89) theory with modified strong collision analysis for fall-off to calculate rate constants for use in the reaction mechanism. The comparisons between model and experiments show satisfactory results. They report the high pressure limit and apparent rate constants, shown as Table 4.1.2, at 1 atm for two initiation reactions of CH_2Cl_2 decomposition:

Table 4.1.2 Data of Ho and Bozzelli

	high pressure limit		Apparent rate constants (1 atm)		
	$A(s^{-1})$	E_a(kcal/mol)	$A(s^{-1})$	n	E_a(kcal/mol)
$CH_2Cl_2 \rightarrow CH_2Cl + Cl$	1.02E16	76.8	7.41E40	-8.02	84.2
$CH_2Cl_2 \rightarrow CHCl + HCl$	2.10E14	77.6	1.44E37	-7.60	86.2

In this chapter, we use quantum Rice-Ramsperger-Kassel (QRRK) calculation for k(E), combined with a modified strong collision approach and multi-channel Master Equation(74) analysis for comparison of fall-off as well as comparison to the experimental data of Lim and Michael.(7)

4.2 Calculations

QRRK analysis, as initially presented by Dean,(67) later published by Dean et al.,(68) which are combined with "modified strong collision approach" by Chang et. al.,(74) and

with multi-channel Master Equation analysis developed by Chang et al.(74) are used to compute apparent rate constants over a range of temperature and pressure. Details of the QRRK are discussed in chapter 4.

The thermodynamic properties related to the species in this calculation are shown in Table B2.

4.3 Results and Discussion

The initial reaction channels for CH_2Cl_2 decomposition include:

$$CH_2Cl_2 \rightarrow CHCl + HCl \qquad [I]$$

$$CH_2Cl_2 \rightarrow CH_2Cl + Cl \qquad [II]$$

The potential energy diagram for CH_2Cl_2 unimolecular dissociation is shown in Figure C1. Table C1 shows the input parameters of QRRK calculation which include high pressure limit rate constants, three frequencies and the associated degeneracies, Lennard-Jones parameters (σ, e/k), $<\Delta E>_{avg}$ for QRRK when using modified strong collision analysis, and $<\Delta E>_{down}$ for Master Equation calculation.

The E_a for reaction [I] is taken from reverse reaction ^1CHCl insertion to HCl, which is an average of $^1CH_2$ insertion, and $^1CCl_2$ insertion into HCl, E_a = 0 and 3 kcal/mol(56), respectively. The high pressure limit A factor for reaction [II] is obtained from the high pressure limit A factor of the reverse reaction, Cl + CH_2Cl thermodynamics and microscopic reversibility. $<\Delta E>_{avg}$ and $<\Delta E>_{down}$ in QRRK calculation with Kr bath

gas are taken from the calculation of Lim and Michael(7), while $<\Delta E>_{avg}$ with Ar bath gas is from Knyazev et al.(89)

Figures C2, C3, and C4 show the results of QRRK with both the modified strong collision approach and the Master Equation analysis along with the experimental data of Lim and Michael for CH_2Cl_2 unimolecular dissociation to the two primary product channels at pressures 6, 11, and 16 torr. The calculation results of Master Equation analysis show in good agreement with the experimental data at all three pressures for the reaction channel, $CH_2Cl_2 \rightarrow CHCl + HCl$, while the results of QRRK with modified strong collision approach under estimate the rates at 6 and 11 torr. Both analysis methods show excellent fit to the experimental data for the reaction channel $CH_2Cl_2 \rightarrow CH_2Cl + Cl$.

Figure C5 illustrates results of QRRK with Master Equation analysis on dissociation rate constants versus temperature (1000/T) at 1 atm. Both reaction channels are near high pressure limit at lower temperatures. Pressure effects at 300 and 1000 K are shown in Figure C6 and C7, respectively. Fall-off begins at 4 atm and below at 300 K for $CH_2Cl + Cl$, while the fall-off behavior for $CHCl + HCl$ is observed below 0.03 atm. At 1000 K, both reaction channels are in the fall-off regime in the pressure range 10^{-3} - 10^{2} atm.

The calculated apparent rate constants for reactions $CH_2Cl_2 \rightarrow CHCl + HCl$ and $CH_2Cl_2 \rightarrow CH_2Cl + Cl$ at pressures 0.1 - 10 atm with Ar bath gas are listed in Table C1.

4.4 Conclusions

The unimolecular dissociation of CH_2Cl_2 has been studied by using QRRK for k(E) plus modified strong collision approach, and separately with multi-channel Master Equation analysis for fall-off effects. The high pressure limit rate constants for the primary reaction channels in the form are:

$$k = AT^n \exp(-\alpha T)\exp(-E_a/RT)$$

Reaction	$A(s^{-1})$	n	α	E_a(kcal/mol)
$CH_2Cl_2 \rightarrow CHCl + HCl$	2.25E11	1.0	0.0	74.2
$CH_2Cl_2 \rightarrow CH_2Cl + Cl$	8.22E15	0.34	1.09E-3	77.0

The calculations of QRRK with Master Equation analysis show good agreement with the experimental data of Lim and Michael in the temperature range of 1400 - 2300 K at pressures 6, 11, and 16 torr, with the results of modified strong collision approach also in reasonable fit.

Results of Master Equation analysis indicates that fall-off begins at 4 atm and below at 300 K for $CH_2Cl + Cl$, while the fall-off behavior for CHCl + HCl is observed below 0.03 atm.

CHAPTER 5

CHEMICALLY ACTIVATED COMBINATION REACTION OF METHYL AND CHLORO-METHYL RADICALS

5.1 Introduction

Combination reactions of methyl and chloro-methyl radicals are the important formation pathways of chlorinated ethylenes (C_2H_3Cl, CH_2CCl_2, CHClCHCl, and C_2HCl_3). These combination reactions form an energized chloroethane adduct, which can be stabilized, react to products, or dissociate back to reactants. Analysis of stabilization and dissociation of the adduct is therefore a function of both temperature and pressure. The important reaction pathways for these chlorinated methyl radicals include:

$$
\begin{array}{lcccl}
CH_3 + CH_2Cl & \leftrightarrow & (C_2H_5Cl)^* & \rightarrow & C_2H_4 + HCl \\
 & & \downarrow & \rightarrow & C_2H_5 + Cl \\
 & & C_2H_5Cl & & \\
CH_3 + CHCl_2 & \leftrightarrow & (CH_3CHCl_2)^* & \rightarrow & C_2H_3Cl + HCl \\
 & & \downarrow & \rightarrow & CH_3CHCl + Cl \\
 & & CH_3CHCl_2 & & \\
CH_2Cl + CH_2Cl & \leftrightarrow & (CH_2ClCH_2Cl)^* & \rightarrow & C_2H_3Cl + HCl \\
 & & \downarrow & \rightarrow & CH_2ClCH_2 + Cl \\
 & & CH_2ClCH_2Cl & &
\end{array}
$$

$$
\begin{array}{lcccl}
CH_2Cl + CHCl_2 & \leftrightarrow & (CH_2ClCHCl_2)^* & \rightarrow & CH_2CCl_2 + HCl \\
 & & \downarrow & \rightarrow & CHClCHCl + HCl \\
 & & \downarrow & \rightarrow & CH_2ClCHCl + Cl \\
 & & \downarrow & \rightarrow & CHCl_2CH_2 + Cl \\
 & & CH_2ClCHCl_2 & & \\
CHCl_2 + CHCl_2 & \leftrightarrow & (CHCl_2CHCl_2)^* & \rightarrow & C_2HCl_3 + HCl \\
 & & \downarrow & \rightarrow & CHCl_2CHCl + Cl \\
 & & CHCl_2CHCl_2 & &
\end{array}
$$

The relatively small adduct - 8 atoms and the availability of low energy product channels (relative to initial of the adduct) with a tight TST (HCl elimination) as well as mid energy products with loose TST's (Cl elimination) make fall-off analysis of this important reaction system both complex and interesting.(91-94)

H atom elimination from the energized adduct is higher in energy and less important, and therefore not included above. H atom addition to chloro-methyl radicals is however very important as it forms a C-H bond which is stronger than the existing C-Cl bond, and often results in fast decomposition of the adduct, loss of Cl or HCl plus the corresponding radical (di-radical).

Setser et al.(91-95) experimentally studied and performed RRKM calculations for unimolecular dissociation reactions of C_2H_5Cl, 1,1-$C_2H_4Cl_2$, 1,2-$C_2H_4Cl_2$, and 1,1,2-$C_2H_3Cl_3$ molecules. Setser reports that formation of HCl and chlorinated olefins from chloroethanes occurs primarily via α,β elimination (four-center) with three-center α,α

elimination having higher energy barriers. They recommend critical energies for HCl elimination from alkyl halide of about 55 or ΔH_{rxn} + (38 ~ 43) kcal/mol. Weissman and Benson(96) have also reported activation energies for the elimination of HCl from chloroethanes by four-center elimination where the barriers are 52 - 60 kcal/mol.

The C-C bond dissociation energies are relatively well known for ethane near 90 kcal/mol at 298 K. Increased chlorine substitution in the ethanes lowers the C-C bond dissociation energies; for example the C-C bond in 1,2-dichloroethane is 88.7 kcal/mol. While the E_a for dissociation to two C_1 radicals is much higher than for HCl elimination; the A factor for C-C bond cleavage is also about 100 times higher. This dissociation reaction can dominate at high temperatures.

Bozzelli et. al.(56,57,97) have reported in analysis of methyl and chloro-methyl combination (chemical activation) reactions at combustion conditions and report the HCl elimination to form chlorinated ethylenes to be the dominant reaction channel. Karra and Senkan(98) investigated combination reactions of CH_2Cl with CH_2Cl, and CH_3 with CH_2Cl using QRRK analysis in Ar and CH_4 bath gas for conditions of 500 - 1700 K and 0.5 - 10 atm. They report stabilization products are favored at temperatures below 1400 K, and that dissociation product channels become increasingly important at higher temperatures. Roussel et al.(99) and the research group of Setser(91-95) have further analyzed these reactions in some details, at temperature below 600 K where stabilization is shown to dominate.

Methyl and chlorine-substituted methyl radicals CH_2Cl, $CHCl_2$ and CCl_3 are the initial products from pyrolysis, oxidation, combustion, or photochemical reaction of

chlorinated methanes. The reactions of these radicals play a major role in the initial oxidation and pyrolysis chemistry of reaction systems in which they are participating. The chloro-methyl radical addition reactions with O_2 have low rate constants to products and thus , the combination reactions are the important formation pathways to C_2 compounds, chlorinated ethanes, ethylenes, and acetylenes. These chlorinated C_2 compounds are precursors to formation of higher molecular weight species, chlorinated-aromatics, dibenzo-furans, and dioxins and ultimately soot + Cl_2 in pyrolysis and fuel rich oxidation of chlorinated hydrocarbons (CHCs). An understanding of these combination and molecular weight growth (MWG) reactions is also important in combustion of chlorinated hydrocarbons, which has received significant attention due to the important role incineration plays in the treatment of hazardous chemical wastes.(99) The presence of known or suspected toxic/carcinogenic chlorocarbon or chloro-oxy carbon species in the effluent from waste and resource recovery incinerators may result from these chloro-methyl radical combination reactions in the combustion which persist due to the relatively low reactivity of the chloro-methyl peroxy radicals (see below).(5)

The importance of combination reactions for methyl and chloro-methyl radicals is further amplified by the relative slow abstraction reaction rates of these C_1 radicals relative to H, OH, and Cl combined with the low reactivity of their respective peroxy radicals. These C_1 radicals do not react rapidly with O_2 to form stable new products relative to higher carbon number hydrocarbon and chloro-hydrocarbon radicals. The C_1 radicals do react rapidly with O_2 to form peroxy species, but dissociation of the adduct back to reactants is its primary reaction under combustion conditions. Because for isomerization

or dissociation of the methyl or chloro-methyl peroxy radicals are 6 or more kcal/mol greater than dissociation of the adduct back to reactants. The low E_a and relatively high A ($\sim 10^{15}$ sec^{-1}) of the reverse reactions to dominate at even moderate temperature of 500 K and above.

Ho and Bozzelli(57) report that a much higher fraction of C_2 hydrocarbon and C_2 chlorocarbon formation occurs in CH_2Cl_2 and CH_3Cl systems than in CH_4 oxidation, and that this greater C_2 fraction results from the very high activity of Cl. The presence of chlorine in the system leads to rapid generation of Cl atoms, which results from the relative low C-Cl bond energies and ease (low E_a's) of HCl elimination reactions. Radicals like OH, H, CH_3, R• will rapidly abstract H from HCl. Cl then undergoes fast abstraction reactions with other parent chlorocarbons and hydrocarbons, as the reactions have high A factors and low (near zero) E_a's (above ΔH_{rxn}). This results in a more rapid formation of chlorocarbon radicals relative to when Cl is not present. The combination reaction is bimolecular and as the chlorohydrocarbon radical pool increases the combination reaction rates increase quadratically. Weissman and Benson,(22,100) Karra and Senkan,(41) Tavakoli et al.,(97) Won and Bozzelli,(56) Miller et al.,(55) Hung and Pfefferle,(101) Taylor et al.,(42) Lucas et al.(102) and Senser et al.(38,39) have also reported increased C_2 formation in C_1 chlorocarbon pyrolysis and oxidation.

Accurate temperature and pressure analysis of these reactions is critical to reliable modeling of the C_2 formation and further molecular weight growth in chlorohydrocarbon pyrolysis and oxidation. Accurate input parameters, and high pressure limit rate constants, are important for estimation of the apparent rate constants of the chemical activation and

dissociation reactions we analyze. The calculation results are compared to literature data and rate constants are determined for use over wide temperature and pressure ranges.

5.2 Thermodynamic Properties

Thermodynamic parameters - ΔH_{298}, S_{298} and $C_p(300)$ to $C_p(\infty)$ for species in the reaction schemes are listed in Table B2 along with appropriate references. Enthalpies of radials are from evaluated literature on C-H bond energies and ΔH_f of the stable molecule which corresponds to the radical with a H atom at the radical site. Entropies and $C_p(T)$ values are from use of Hydrogen Bond Increment (HBI).(79) The HBI group technique is based on known thermodynamic properties of the parent molecule and calculated changes that occur upon formation of a radical via loss of a H atom. The HBI incorporates changes that result from loss or changes in vibrational frequencies, internal rotation, and spin degeneracy. Symmetry is corrected for separately HBI groups, are described fully in Ref. 71, 103.

5.3 Kinetic Calculations

Branching ratios of methyl and chloro-methyl combination reactions at different temperatures and pressures are calculated using a quantum version of RRK theory (QRRK) to evaluate energy dependent rate constants, k(E), of the adduct to the various channels. QRRK analysis, as initially presented by Dean,(67,68) combined with "modified strong collision approach" of Gilbert et al.(74,75) and QRRK combined with a Master

Equation analysis(74) are used to compute rate constants over a range of temperature and pressure.

Modifications to the quantum RRK calculation(74) include :

- Use of a manifold of 3 frequencies plus incorporation of 1 external rotation for the density of states, $\rho(E)/Q$.
- Use of the reduced set of 3 vibrational frequencies and degeneracies are used in calculation of k(E) and of F(E).
- The F_E factor is calculated for use in determining the collision efficiency β_c,(75) in place of the previously assigned 1.15 value.
- β_c is now calculated by : $\beta_c = (\alpha_c /(\alpha_c + F_E*k*T))^2/\Delta$ from Gilbert et. al. Eqn. 4.7,(75) $\Delta = \Delta_1 - (F_E*k*T)/(\alpha_c + F_E*k*T)*\Delta_2$. Where Δ_1 and Δ_2 are temperature-dependent integrals involving the density of states, and α_c is the average energy of down-collisions.
- The Lennard-Jones collision frequency Z_{LJ} is now calculated by $Z_{LJ} \equiv Z\ \Omega^{(2,2)}$ integral.(76-78), Ω is obtained from fit of Reid et al.(78)

The QRRK analysis with the modified strong collision approach and constant F_E for fall-off has been used to analyze a variety of chemical activation reaction systems, Westmoreland et al.,(51,89,104) Dean et al.,(51,105-107) Bozzelli et al.(56,57,97,105-107) It is shown to yield reasonable results in these applications, and provides a simple framework by which the effects of temperature and pressure can be evaluated. Limitations affected by the QRRK assumptions are often over shadowed by uncertainties in high

pressure limit rate constants and thermodynamic properties for all species and TST's in the calculation systems.

Input information requirements for QRRK calculations :

Three frequencies and the associated degeneracies are computed from fits to heat capacity data, as described by Ritter.(72,73) These have been shown by Ritter to accurately reproduce molecular heat capacities, $C_p(T)$, and by Bozzelli et al.(108) to yield accurate vibrational state, $\rho(E)/Q$, to partition coefficient ratios. Frequencies are listed in Table D1.

Lennard-Jones parameters (σ, e/k) are obtained from tabulations(78) and from a calculation method based on molar volumes and compressibility.(109)

Arrhenius A factors for the bimolecular combination at the high pressure limit are obtained from literature, and from trends in homologous series of these type reactions. Figure D1 shows the high pressure limit A factors at 298 K from literature for combination reactions of methyl and chloro-methyl radicals versus total number of Cl's; the literature data for Figure D1 are listed in Table D2. Energies of activation, E_a for combination reactions is set to 0.0. These parameters are critical to accurate rate constant estimation by the QRRK formalism and are described in detail.

Literature data on rate constants for combination of chloro-methyl radicals show that they decrease with increasing Cl substitution. Figure D1 shows the trends at room temperature, rate constant 2.0E13 $cm^3\ mol^{-1}\ s^{-1}$ for $CH_2Cl + CH_2Cl$, 5.6E12 $cm^3\ mol^{-1}\ s^{-1}$ for $CHCl_2 + CHCl_2$, and 2.2E12 $cm^3\ mol^{-1}\ s^{-1}$ for $CCl_3 + CCl_3$.

Lesclaux et al.(99,110) studied the kinetics on the self-combination reactions of CH_2Cl, $CHCl_2$, and CCl_3 from 253 to 686 K at 760 torr. They further report the high pressure limit rate constants for all of these chloro-methyl combination reactions exhibit negative temperature dependence $(T/298)^n$ with n ranging from -0.74 to -1.0. Cobos and Troe(111) have also reported the high pressure limit rate constants of CCl_3 self-combination reaction, which also exhibit a slight temperature negative dependence with $k^\infty(300) = 6.0E12$ and $k^\infty(1500) = 5.0E12$ cm^3 mol^{-1} s^{-1}. A tabulation of recommended high pressure limit rate constants at 298 K for chloro-methyl combination is listed in Table 5.3. The high pressure limit A factors of k_1 in Table 5.5 - 5.9 are shown in the form of AT^n which are converted from that of $A(T/298)^n$ in Table D3.

Dissociation rate constants of the CH_2ClCH_2Cl and $CHCl_2CHCl_2$ to initial reactants (chloro-methyl radicals) is calculated from the combination rate constants, thermodynamic properties and microscopic reversibility. Dissociation of the chloroethanes to Cl plus chloro-ethyl radicals is calculated from the respective, reverse, combination rate constants of Cl + chloro-ethyl radical, using thermodynamic properties and microscopic reversibility. The Cl + chloro-ethyl combination rate constants are taken from the literature and are specified in Table D4. Table D4 shows the trend in k for Cl + chloro-alkyl radical is similar to that of chloro-methyl radical combination; the more Cl-substitution the lower rate constant. All reactions are thermochemically consistent and follow principles of Thermochemical Kinetics(25).

5.4 Results and Discussion

5.4.1 Combination of CH_3 with CH_2Cl

The potential energy diagram and input parameters for the chemical activated combination reaction of CH_3 + CH_2Cl are in Figure D2 and Table D5, respectively. The parameters in Table D5 - D9 are referenced to the ground (stabilized) state of the complex because this is the formalism used in QRRK Theory. The use of a more complicated for k(T), $k = AT^n\exp(-\alpha T)\exp(-E_a/RT)$, was chosen to more accurately fit the rate constant over a wide range of temperature.

Combination of CH_3 + CH_2Cl form an energized $C_2H_5Cl^*$ adduct, which can be stabilized, dissociate to low energy products, or dissociate back to reactants (CH_3 and CH_2Cl radicals). We have considered and choose to omit H + CH_3CHCl and $^1CH_2$ + CH_3Cl reaction channels, owing to the higher barriers. The HCl elimination channel is lower in energy than Cl dissociation or reverse reaction. The HCl elimination channel is lower in energy than Cl dissociation or reverse reaction. The higher A factors for C-Cl or C-C bond cleavage, require that these channels also need to be considered in the analysis at higher temperatures.

Figure D3 shows the rate constants versus temperature at 1 atm. Stabilization of C_2H_5Cl is most important at temperatures below 650 K, with the production of HCl + C_2H_4 next in importance. Between 700 and 1300K, HCl elimination + C_2H_4 is most important. Above 1000 K Cl + C_2H_5 increases in importance and dominates above 1400 K. The pressure effect for the production of various channels at 300 and 1000 K are illustrated in Figure D4. Stabilization of C_2H_5Cl is important at low temperatures and high

pressures. Product channel HCl + C_2H_4 dominates in the lower pressure range ($p < 0.02$ atm) at 300 K, and over wide pressure range ($p < 8$ atm) at 1000 K.

5.4.2 Combination of CH_3 + $CHCl_2$

The potential energy diagram and QRRK input parameters for CH_3 + $CHCl_2$ combination are shown in Figure D5 and Table D6, respectively. Figure D6 shows rate constants from QRRK calculation as a function of temperature at 1 atm. CH_3CHCl_2 stabilization is dominant below 650 K. The production of HCl + C_2H_3Cl is most important between 650 and 1350 K. Above 1400 K, Cl dissociation + CH_3CHCl becomes dominant. Figure D7 shows the pressure effect on the various channels. Production of C_2H_3Cl + HCl is most important, with Cl dissociation + CH_3CHCl next in importance at pressures below 0.08 atm, 300 K, and over a wide pressures (0.001 - 10 atm) at 1000 K.

5.4.3 Combination of CH_2Cl with CH_2Cl

The potential level energy diagram and input parameters of chemical activated calculation are illustrated in Figure D8 and Table D7, respectively. Figure D9 shows the results of QRRK calculations with modified strong collision and the Master Equation analysis at 1 atmosphere pressure for CH_2Cl + CH_2Cl. The results show some differences between the calculation with modified strong collision and Master Equation for fall-off analysis. This is because modified strong collision analysis does not allow reaction to lower energy product channels (HCl + C_2H_3Cl) when the adduct energy level is below the ground state energy of the initial reactants, while Master Equation analysis does.

The calculation shows that below 650 K, stabilization of CH_2ClCH_2Cl is most important, with the HCl elimination channel next in importance. Between 700 and 1400 K, CH_2ClCH_2Cl dissociation to C_2H_3Cl + HCl dominates. Above 1000 K, dissociation of Cl + CH_2ClCH_2 radicals becomes important; above 1400 K, Cl dissociation channel is similar in rate to HCl elimination. The turn over of both these rates above 1400 K is a result of the reverse dissociation (back to 2 chloro-methyl radicals) increasing in importance. Rate constants of the specific reaction channels as a function of pressure (log P) are illustrated in Figure D10. We see near pressure independence in the total, overall rate constant in both temperature ranges, but a dramatic change in products. At 300 K, the stabilization of CH_2ClCH_2Cl dominates at pressures above 0.1 atm with HCl + C_2H_3Cl the dominant product below 0.1 atm. Rate constants for HCl + C_2H_3Cl, Cl + CH_2ClCH_2 and dissociation back to reactants are near pressure independent at pressures below 0.01 atm, and show negative pressure dependence above 0.03 atm at 300 K. At 1000 K, higher pressures are needed to observe significant stabilization. We also note that the 300 K data indicates higher reaction rates to products than the 1000 K data. This is a result of the higher reverse reaction rate ($CH_2ClCH_2Cl \rightarrow CH_2Cl + CH_2Cl$) at the higher temperature.

Figure D11 compares calculation results of QRRK with modified strong collision and with Master Equation analysis to the experimental data of Roussel et al.(99) for CH_2Cl self-combination. Master Equation analysis is in good agreement with the experimental data, QRRK with modified strong collision analysis is also in reasonable agreement, but slightly over predicts stabilization at lower temperatures. Comparison of this study to the data of Karra and Senkan(98) on the CH_2Cl + CH_2Cl reaction at 1 atm

are presented in Figure D12. Our estimations show less stabilization, and more HCl + vinyl chloride and Cl + CH_2ClCH_2 production at higher temperatures.

5.4.4 Combination of CH_2Cl + $CHCl_2$

The potential energy diagram and QRRK input data for CH_2Cl + $CHCl_2$ are illustrated in Figure D13 and Table D8, respectively. The HCl elimination channels are lower in energy than Cl dissociation or reverse reaction. The results from QRRK calculation are shown in D14 (log k vs 1000/T) at 1 atmosphere pressure for the various channels of CH_2Cl + $CHCl_2$ $\rightarrow$ products. Below 800 K, the stabilization of $CH_2ClCHCl_2$ is most important, with the HCl elimination + chloroethylene channels next in importance. Between 800 and 1000 K $CH_2ClCHCl_2$* dissociates primarily to CHClCHCl + HCl. Figure D14 shows the HCl + CHClCHCl channel is more important than the HCl + CH_2CCl_2 and this is consistent with the results observed in our experiments (see Chapter 2). Above 1000 K the Cl elimination + $C_2H_3Cl_2$ radicals product channels increase in importance. Logarithmic rate constants (log k) of the specific reaction channels as a function of log P at 300 K, and 1000 K are illustrated in Figure D15. The stabilized $CH_2ClCHCl_2$ becomes dominant as pressure increases in both temperature ranges. The HCl + CHClCHCl channel is always more important than HCl + CH_2CCl_2 over the pressure range 10^{-3} - 10^{2} atm. In the pressures < 1 atm at 1000 K, production of HCl + CHClCHCl is most important, with Cl + $CH_2ClCHCl$ channel next in importance.

5.4.5 Combination of $CHCl_2$ with $CHCl_2$

Figure D16 illustrates the potential energy diagram, with input parameters for the QRRK calculation and kinetic input data are listed in Table D9.

Comparison of QRRK with modified strong collision and with Master Equation analysis versus the experimental data of Roussel et al.(99) for this CH_2Cl self-combination is illustrated in Figure D11. Both calculation methods show excellent agreement with the experimental data.

Results of QRRK with modified strong collision and with Master Eqn. analysis are illustrated in Figure D17 at 1 atm pressure. The two fall-off calculation methods show nearly identical results. $CHCl_2CHCl_2$ stabilization is most important below 800 K. Above 800K, HCl elimination + C_2HCl_3 is predicted to be dominant. The reverse reaction to two $CHCl_2$ radicals competes with Cl + $CHCl_2CHCl$ channel above 800 K. Both show maximum rate constant near 1150 K, with HCl + trichloroethylene about a factor of 2 higher than the Cl elimination channel. Pressure effects at two temperatures are shown in Figure D18. The overall rate constant show little change over the pressures 10^{-3} - 10^{2} at 500 K. $CHCl_2CHCl_2$ stabilization in the most important above 0.01 atm, and is observed to be near the high pressure limit at 1 atmosphere pressure. At 1000 K, stabilization of $CHCl_2CHCl_2$ is dominant above 1.0 atm, while HCl elimination + C_2HCl_3 becomes most important below 0.2 atm.

5.4.6 Dissociation of CH_2ClCH_2Cl and $CHCl_2CHCl_2$

Master Equation and modified strong (beta) collision calculations on dissociation rate constants for 1,2-dichloro and 1,1,2,2-tetrachloroethane are illustrated in Figure D19 and D20 respectively for 1 atm pressure, 300 to 2500 K. Input data are identical to that used in the chemical activation system, Table D7 and D9. Both reaction systems are near the high pressure limits at 1 atm for the lower temperatures and the agreement is very good for both over the entire temperature range. The dichloroethane (DCE) has a lower density of states and is in the fall-off at higher temperature, thus the difference between the calculations via Master Equation vs beta collision techniques are more apparent for DCE. Amplification of these curves 1000 - 2000 K are illustrated in Figures D21 - D22. Observation of the DCE dissociation data demonstrates that the beta collision calculations overestimate the higher dissociation energy channels and underestimate the lowest energy reaction. This is because they fail to correctly incorporate bleed of the energized species out the lower energy channel when in the fall-off regime.

Table D10 lists the rate constants by QRRK with modified strong collision analysis for methyl and chloro-methyl radical combinations, and by Master Equation analysis for stabilized complex unimolecular dissociation to various channels in Ar and N_2 bath gases at temperatures 300 - 2500 K.

5.5 Conclusions

The bimolecular combination reactions of chloro-methyl radicals result in formation of activated chlorinated ethane adducts, which can be stabilized, further dissociate to lower

energy products (chloro-ethyl radicals + Cl or chloroethylenes + HCl), or dissociate back to reactants before stabilization occurs. The overall reaction process is complex and is a strong function of both temperature and pressure. The reactions are, in addition, of key importance to formation of C_2 species and to higher molecular weight growth in chlorocarbon pyrolysis and oxidation. Rate constants for each channel in the reaction systems are estimated using a chemical activation quantum Rice-Ramsperger-Kassel (QRRK) calculation for k(E), combined with a modified strong collision approach and separately with multi-channel Master Equation analysis for comparison of fall-off analysis.

Rate constants are calculated for the temperature range 300 - 2500 K and bath gas (Ar and N_2) in the pressure range 0.001 - 100 atm with comparison to experimental data where available.

Results at 1 atm indicate the formation of chlorinated ethanes are most important in low temperature ranges (below ~ 650 K) for the reaction systems in this study. Production of HCl + chlorinated ethylenes become dominant at temperature between 700 - 1300 K. A decrease of these rates is observed above 1350 K as a result of dissociation to chloro-ethyl radical + Cl and back to reactants (two chloro-methyl radicals) become increasing in importance. Analysis the effects of pressure on the rates of various channels at 300 K shows that stabilization of chloroethane dominate at pressures above 0.1 atm, with production of HCl + chlorinated ethylenes (except HCl + CH_2CCl_2) most important at pressures below 0.08 atm.

Master Equation and modified strong (beta) collision calculations on dissociation rate constants for CH_2ClCH_2Cl and $CHCl_2CHCl_2$ are observed near the high pressure

limits at 1 atm for the lower temperatures and the agreement is very good for both over the temperatures 300 - 2500 K.

CHAPTER 6

REACTION PATHWAY ANALYSIS FOR VINYL, CHLORO-VINYL RADICALS WITH O_2

6.1 Introduction

The addition reaction of alkyl radical to unsaturated hydrocarbons species is considered to be a key step to the formation of aromatics, soot, and higher molecular weight species in hydrocarbon pyrolysis.(8-13) Analogous reaction pathways in chlorinated hydrocarbon reaction systems: C_1 and C_2 radical additions to chlorinated ethylenes has been studied theoretically by Shi and Senkan.(14) These additions can undergo further molecular weight growth reaction and subsequently result in production of potential toxic chlorinated benzenes, phenols, dibenzofurans and dioxins.(15) In the presence the O_2, the molecular weight growth processes can be suppressed by fast reactions of alkyl radicals with oxygen. These oxygen reactions, furthermore, represent the principal pathways of the radical conversion in many hydrocarbon and chlorinated hydrocarbon oxidation and combustion processes.(8,16) They are nearly solely responsible for suppression of soot formation and additionally : they are important for soot burnout.

Ethyl radical is a precursor to ethylene through the beta scission reaction ($C_2H_5 \rightarrow C_2H_4 + H$) and the reaction with O_2 ($C_2H_5 + O_2 \rightarrow C_2H_4 + H_2O$). Both of which readily occur at combustion conditions. This is however not a simple H transfer reaction, but an addition, H-isomerization and then beta scission.

$$C_2H_5 + O_2 \rightarrow C_2H_5OO\bullet$$

$$C_2H_5OO\bullet \rightarrow \bullet CH_2CH_2OOH$$

$$\bullet CH_2CH_2OOH \rightarrow CH_2{=}CH_2 + HO_2$$

The addition reaction of ethyl radical to molecular oxygen has been experimentally studied at pressures from 1 to 6000 Torr and temperatures from 300 to 900 K, which exhibit that the production of C_2H_4 + HO_2 by a process involving a stable, long-lived cyclic intermediate unrelated to the ethyl-peroxy radical and perform a significant negative pressure dependence.(117,120,122) The negative pressure dependence of the C_2H_4 yield from the reaction C_2H_5 + O_2 has also been investigated at 298 K for pressures from 1 to 6000 Torr in air diluent and 3 - 1500 Torr in He diluent by Kaiser et al.(123) and at pressures from 50 to 1500 Torr in the temperature range 260 - 530 K by Kaiser.(124) Kaiser(124) also confirmed that at lower temperature (260 - 400 K) formation of C_2H_4 from C_2H_5 + O_2 does not proceed by the direct abstraction reaction $C_2H_5 + O_2 \rightarrow C_2H_4 + HO_2$ as this would be expected to have a substantial activation energy: it proceeds through the $C_2H_5OO\bullet$ peroxy adduct as above.

Walker and coworkers(125) have also report similar pressure dependence for reactions of isopropyl radicals with O_2 to produce propene + HO_2. The observed pressure and temperature dependence for olefin formation in these reaction is not, however, consistent with a direct hydrogen-transfer mechanism, although that is often invoked in combustion modeling.(126,127) This is an important issue to resolve, since the rate

constants one would use for combustion models under engine or turbine conditions could change by orders of magnitude, due to the higher pressures.

The theoretical study for $C_2H_5 + O_2$ reaction to C_2H_4 yield and ethyl radical loss at pressures and temperatures has been done by Bozzelli and Dean(105) using QRRK theory of Dean(67) and by Wagner et al.(128) using RRKM theory for C_2H_5OO dissociation. These analyses postulate the formation of a chemically activated $C_2H_5O_2$* adduct, which can be stabilized, dissociate back to reactants ($C_2H_5 + O_2$) before collisionally stabilization, or react through a cyclic five-member ring intermediate to form a primary hydroperoxy alkyl radical (H shift), which can be stabilized or further react to $C_2H_4 + HO_2$. Wagner only considered direct reaction of C_2H_5OO to $C_2H_4 + HO_2$, while Bozzelli and Dean considered the isomer ($\bullet CH_2CH_2OOH$) formation and its subsequent reactions. The formation of $\bullet CH_2CH_2OOH$ adduct and of epoxide + OH from $\bullet CH_2CH_2OOH$ in this system is limited by a low Arrhenius A factor due to the tight transition states and a slightly high barriers. The modeling results of Wagner et al.(128) for ethyl radical loss and production of ethylene show good agreement with experimental data. The results of Bozzelli and Dean(105) show excellent agreement with the experimental data of Gutman's research group(120,122) and of Kaiser et al.(123,124) over a wide pressure range for He and N_2 bath gases.

There have been several recent studies on the reactions of unsaturated free radicals with molecular oxygen. Slagle et al.(129) investigated the gaseous reaction of vinyl radicals with O_2 at relative low pressure range 0.4 - 4 Torr and temperatures between 297 and 602 K. The overall rate constant ($k = 4.0E12e^{0.28/RT}$ cm^3 $mole^{-1}$ s^{-1}) is pressure

independence and is slightly decrease with increasing temperature in this experimental condition. The pressure independence of rate constant suggests that the addition complex formed in the $C_2H_3 + O_2$ reaction decomposing preferentially by the channel leading to the observed products rather than dissociation back to the original reactants. The products formed in this reaction are CHO and CH_2O. Fahr and Laufer(130) later measure the rate constant for C_2H_3 loss at 298 K show good agreement with Slagle rate constant. These data also agree with the room-temperature study of Krueger and Weitz.(131) Analogous reaction of methylvinyl radicals ($CH_3CH{=}CH$) with molecular oxygen has also been studied between 296 and 600 K by Slagle et al.(132) The rate constant is essentially constant throughout this temperature range, k = 4.50E12 cm^3 $mole^{-1}$ s^{-1}. The only products observed are CH_3CHO + CHO.

The reaction of vinyl radical with molecular oxygen has been analyzed by Westmoreland,(104) Bozzelli and Dean(106) using QRRK theory. The vinyl radical combines with O_2 to form the chemically activated $C_2H_3OO^*$ adduct. The reaction channels of $C_2H_3OO^*$ include dissociation back to reactants, collisionally stabilization, isomerization via hydrogen shifts with subsequent β-scission/stabilization, cyclization to form four-member ring cyclic peroxides with subsequent β-scission/stabilization, and C_2H_3O-O bond fission to form vinoxy + O. The results of both modeling show good agreement with experimental data, CH_2O and CHO are major products at lower temperatures.(129-131) The analysis of Westmoreland(104) also predicts that H + glyoxal and $C_2H_2 + HO_2$ are important product channels at relative high temperatures. The analysis of Bozzelli and Dean(106) indicates that the well depth for the vinyl peroxy

adduct is ~ 40 kcal/mol, *i.e.* more than 22 and 8 kcal/mol deeper than the allyl and ethyl additions respectively. The deeper well allow the initially formed adduct to undergo reactions such as isomerization or dissociation to other products even at lower temperatures. Bozzelli and Dean(106) predict that vinoxy + O channel becomes more important at higher temperatures.

Recent theoretical study for vinyl radical with O_2 has been analyzed by Carpenter(133) using semiempirical and *ab initio* molecular orbital calculations. Carpenter(133) suggests that formation of the three-member ring, dioxiranylmethyl radical has a lower barrier (23.5 kcal/mol) than that (46.9 kcal/mol) does formation of four-member ring, cyclic peroxides. The three-member ring intermediate can rapidly rearrange to an epoxy radical with a negligible activation barrier and highly exothermic, ΔH_{rxn} ~ -44 kcal/mol. The formation of CH_3 + CO_2 is predicted by the PM3 model to have a substantially higher activation enthalpy and presumably a less favorable activation entropy than the formation of the observed products, CHO + CH_2O.

Senkan et al.(134) investigated the kinetics of the reaction $CH_3CHCl + O_2 \leftrightarrow CH_3CHClO_2 \rightarrow$ products at temperatures 296 - 839 K and He densities of (3 - 49) x 10^{16} molecule cm^{-3} by laser photolysis/photoionization mass spectrometry. At low temperature (298 - 400 K) the rate constants are in the falloff region under the conditions of the experiments. The high pressure limit rate constant at 298 K, k^{∞} = 6.2E12 cm^3 mol^{-1} s^{-1} was estimated. The bond energy ΔH^o_{298} = -31.3 kcal/mol for $CH_3CHCl\text{-}O_2$, the entropy S^o_{298} = 81.5 cal mol^{-1} K^{-1} and the heat of formation ΔH^o_{298} = -13.1 kcal/mol of the CH_3CHClO_2 were obtained. The bond energies of $CH_3CHCl\text{-}O_2$ (ΔH^o_{298} = -31.3 kcal/mol) and $C_2H_5\text{-}O_2$

(ΔH^{o}_{298} = -35.0 kcal/mol)(16) shows that bond strength decrease 3.7 kcal/mol with one α-C-Cl substitution.

The reactions of chlorinated vinyl radicals CH_2CCl and C_2Cl_3 with molecular oxygen have been studied by Russell et al.(85) in a tubular reactor coupled to a photoionization mass spectrometer in the temperature range 298 - 648 K. The measured rate constants are $3.0E12e^{0.33/RT}$ cm^3 mol^{-1} s^{-1} for $CH_2CCl + O_2$ reaction and $1.3E12e^{0.83/RT}$ cm^3 mol^{-1} s^{-1} for $C_2Cl_3 + O_2$ reaction, respectively. They suggested that both of these reactions analogous vinyl + O_2 proceed via the formation of a short-lived bound RO_2 intermediate, that can dissociate back to reactants or form new oxygen-containing products following intramolecular rearrangement of the adduct. The only product detected was CH_2O in $CH_2CCl + O_2$ reaction system. The CH_2O ion signal rises exponentially, mirroring the observed exponential decay of CH_2CCl.

In this chapter, we extend the analysis of vinyl radical with oxygen to chlorinated vinyl radicals, CH_2CCl, CHClCH, CHClCCl, CCl_2CH, and C_2Cl_3 with oxygen. The lower barrier of the three-member ring transition structure, dioxiranylmethyl radical which postulated by Carpenter(133) from initial chemically activated adduct in vinyl + O_2, is presented as major pathway to compete with the other product channels. A chemical activation analysis is performed on addition reactions of vinyl, chlorinated vinyl radicals with O_2 and the predictions compared to the limited literature data. It is difficult to measure each of the products and the specific rate constants to the products of these important reactions over a wide range of both temperature and pressure. Our attempt is to use the experimental data where available, along with QRRK analysis incorporating

generic rate constants, evaluated thermodynamic properties and transition-state theory, to predict the reaction paths as a function of temperature and pressure. The deeper well in vinyl and chlorinated vinyl reaction with oxygen provide additional energy, *i.e.*, the initially formed adduct had higher energy relative to the barriers for unimolecular reactions. This leads to the faster rate constants and opens possibilities for new channels.

6.2 Calculations

The addition reactions of O_2 to vinyl and chlorinated vinyl radicals at different temperatures and pressures are calculated using a quantum version of RRK theory (QRRK) to evaluate energy dependent rate constants, k(E), for the various channels, and with modified strong collision approach to analyze fall-off effect. QRRK theory as initially presented by Dean(67), later published by Dean et al.(68), and used with "modified strong collision approach" by Chang et. al.(74) are used to compute apparent rate constants over a wide range of temperature and pressure.

The modifications to the quantum RRK calculation(74) include:

- A 3 frequency model for energy distribution and the 3 frequency model plus incorporation of 1 external rotation for the density of states, $\rho(E)/Q$.
- The F_E factor is now calculated for use in determining the collision efficiency β_c,(75) in place of the previously assigned 1.15 value.
- β_c is now calculated by : $\beta_c = (\alpha_c /(\alpha_c + F_E*k*T))^2/\Delta$ from Gilbert et. al. Eqn. 4.7,(75) $\Delta = \Delta_1 - (F_E*k*T)/(\alpha_c + F_E*k*T)*\Delta_2$. Where Δ_1 and Δ_2 are temperature-dependent

integrals involving the density of states, and α_c is the average energy of down-collisions.

- The Lennard-Jones collision frequency Z_{LJ} is now calculated by $Z_{LJ} \equiv Z\ \Omega^{(2,2)}$ integral.,(76-78) Ω is obtained from fit of Reid et al.(78)

QRRK analysis with the modified strong collision approach for fall-off has been used to analyze a variety of chemical activation reaction systems.(10,51,56,57,73,97,107) It is shown to yield reasonable results in these applications, and provides a simple framework by which the effects of temperature and pressure can be readily understood and evaluated by non-physics students. Limitations affected by the QRRK assumptions are likely over showed by uncertainties in high pressure limit rate constants and thermodynamic properties for all species and TST's in the calculation systems.

Input information requirements for QRRK calculations :

Three frequencies and the associated degeneracies are computed from fits to heat capacity data, as described by Ritter.(72,73) These have been shown by Ritter to accurately reproduce molecular heat capacities, $C_p(T)$, and by Bozzelli et al.(108) to yield accurate vibrational state, $\rho(E)/Q$, to partition coefficient ratios. This approach offers the advantage of avoiding the specification of the complete frequency distribution of the adduct.

Lennard-Jones parameters (σ, e/k) are obtained from tabulations(78) and from a calculation method based on molar volumes and compressibility.(109)

Arrhenius A-factors for vinyl and chlorinated vinyl radicals addition to O_2 at the high pressure limit are obtained from literature, and from trends in homologous series of

these type reactions. Slagle et al.(129) reported that overall rate constants for $C_2H_3 + O_2$ to be $(4.0\pm0.8) \times 10^{12} \exp(0.25\pm0.1 \text{ kcal/RT})$ $cm^3 mol^{-1} s^{-1}$, later Knyazev and Slagle(135) also determined this overall rate constants to be $(4.16\pm0.1) \times 10^{12} \exp(0.24\pm0.024 \text{ kcal/RT})$ $cm^3 mol^{-1} s^{-1}$. The overall rate constants for $CH_2CCl + O_2$ and $C_2Cl_3 + O_2$ were reported by Russell et al.(85) to be $(3.0\pm0.4) \times 10^{12} \exp(0.33\pm0.2 \text{ kcal/RT})$ $cm^3 mol^{-1} s^{-1}$ and $(1.2\pm0.24) \times 10^{12} \exp(0.83\pm0.23 \text{ kcal/RT})$ $cm^3 mol^{-1} s^{-1}$, respectively. From the above information, we can see that A factors for reactions $C_2H_3 + O_2$ to $C_2Cl_3 + O_2$ range from $(4.0\pm0.8) \times 10^{12}$ to $(1.2\pm0.24) \times 10^{12}$ $cm^3 mol^{-1} s^{-1}$, which increases with increasing chlorine substitution; energies of activation (E_a) for these reactions are shown from -(0.25±0.1) to -(0.83±0.23) kcal/mol. The trend of negative activation energy also increases with increasing chlorine substitution.

Dissociation of the energized (chloro) vinyl peroxy adducts to initial reactants (chloro-vinyl radicals + O_2) is calculated the Arrhenius parameters for the reverse addition, rate constants thermodynamics and microscopic reversibility. Dissociation of the energized adducts (as above) to products is also calculated from the combination rate constants of reverse reactions thermodynamic and microscopic reversibility. A and E_a for unimolecular isomerization reactions are determined using Transition State Theory(25) with the appropriate thermodynamic parameters

All reactions are thermochemically consistent and follow principles of Thermochemical Kinetics.(25) Thermodynamic properties related to these system as listed in Table B2 are from literature data. When no literature data are available, THERM,(69) calculations of entropies S(T) and heat capacities $C_p(T)$ changes of specific vibrations and

internal rotations that result when the respective H atom is lost from the parent (stable) molecule and use of statistical mechanics.(70) This technique is termed Hydrogen Bond Increment (HBI) groups for radicals.(79)

6.3 Results and Discussion

6.3.1 $C_2H_3 + O_2$

The potential energy level diagram and input parameters for the chemical activation calculations of vinyl radical + O_2 are shown in Figure E1 and Table E1, respectively. The vinyl radical combines with O_2 to form an energized $C_2H_3OO^*$ adduct, which can be stabilized, further dissociate to vinoxy radical + O, dissociate back to reactants, isomerize via H-shift with subsequent β-scission/stabilization, or further isomerize to form the three-member ring (dioxiranylmethyl radical) intermediate. This dioxiran intermediate can then rearrange to an epoxide-alkoxy radical (isomer) intermediate. The alkoxy radical intermediate can react via C-O or C-C bond cleavage (beta scission) to form two different intermediates, each of which then reacts to the same final product set CH_2O + CHO.

Bozzelli and Dean(106) mentioned the importance of vinoxy + O formation versus the initial cyclization, and suggested 35.4 kcal/mol as a lower limit for the vinoxy barrier and 26.4 kcal/mol barrier as an upper limit for the cyclization. In this study, we utilized the barriers 36.4 kcal/mol and 25.4 kcal/mol for vinoxy + O and initial cyclization, respectively. This gives a branching ratio of 75% at 450 K. This value represents a suitable compromise between the measurements of Gutman et al.(129) and the barrier inferred

from the molecular beam studies of Lee et al.(190,191) The data we selected are in accordance with Bozzelli and Dean.(106)

The overall rate constant for vinyl + O_2 has been reported(109,129,135) to slightly decline with increasing temperature at low pressures. Comparison of predicted values with literature for the total rate of vinyl + O_2 as a function of temperature at low pressures (0.4 to 4 torr) in He bath gas is shown in Figure E2. The predicted results show good agreement with the observations.

Figure E3 illustrates an important feature of this reaction system: that the product channels change dramatically with temperature. At 1 atmospheric pressure, C_2H_3OO stabilization is most important below 400 K with CH_2O + CHO next in importance. Above 400 K, CH_2O + CHO becomes dominant. The vinyl peroxy complex dissociation back to C_2H_3 + O_2 competes with the vinoxy + O channel over a wide temperature range (300 - 2500 K), and increases in importance with increasing temperature. The rate of vinoxy + O formation at ~ 1000 K is ca. one half of that predicted by Bozzelli and Dean,(106) where they reported the vinoxy + O is most important. This small decrease is because the average A factor for dissociation to vinoxy + O used by Bozzelli and Dean(106) was somewhat over-predicted at higher temperatures. In this study a more complex temperature dependence of on k(T), $k = AT^n\exp(-\alpha T)\exp(-E_a/RT)$, is utilized to more accurately fit the rate constant over a wide range of temperature.

The pressure effect on various reaction channels at 300 and 1500 K are illustrated in Figure E4 and E5, respectively. The total rate at 300 K is seen to be near constant over a wide pressure range (10^{-3} - 10^{2} atm), but this is owing to a tradeoff between the

C_2H_3OO stabilization and CH_2O + CHO product channel. A slightly lower overall rate constant is calculated at 1500 K relative to 300 K, due to an increases in the reverse dissociation rate. At 1500 K, we see participation of all the channels resulting from dissociation of the chemically activated adduct to the various products.

6.3.2 $CH_2CCl + O_2$

The potential energy diagram and input parameters for QRRK calculations are shown in Table E2 and Figure E6, respectively. The well depth of CH_2CClOO^* adduct in this system is estimated to be ~ 2 kcal/mol smaller than that in vinyl case, due to the Cl-substitution of CH_2CCl at α site (resonance). The reaction paths are similar to that in vinyl + O_2, with only one new reaction channel, ketene + ClO from CH_2CClOO^* adduct (ΔH_{rxn} = -8.5 kcal/mol). The barrier 31 kcal/mol for ClO elimination is from calibrated to AM1/PM3 calculations and taken as that of $CH_2ClOO^* \rightarrow CH_2O + ClO$.(136) The relatively lower A factor (tight transition state) of this ClO elimination combine with the lower barrier (~ 7 kcal/mol lower than chloro vinoxy + O and reverse dissociation to $CH_2CCl + O_2$) causes this channel to be more important at the relatively high temperature. The ClO elimination + ketene formation has not been reported previously as a product channel in this reaction system.

Figure E7 compares the predictions to the experimental data of Russell et al.(85) for overall rate constant of $CH_2CCl + O_2$. The fit shows good agreement with the observations.

The rate constants of various reaction channels versus temperature at 1 atm are shown in Figure E8. Stabilization of initially formed energized adduct is most important below 600 K, with CH_2O + CClO next in importance. Above 750 K, the C*CClO• + O reaction channel is predicted to be dominant. The formation of CH_2CO + ClO increases in importance above 1000 K, and becomes most important above 2000 K.

Figure E9 shows the effects of pressure on the rate constants to various reaction channels at 300 K. The total rate is predicted to have little pressure dependence over a wide pressure range, which is in agreement with the observations of Russell et al.,(85) where no measurable effect of pressure with a 2.5-fold change in pressure (1.47 - 6.74 torr) was observed. Production of CH_2O + CClO is predicted to be dominant at lower pressures (below 0.06 atm), which agrees with the observations of Russell et al.(85) which indicated CH_2O as the only product observed between 295 - 520 K at pressures below 0.01 atm. Figure E10 shows that at 1500 K, stabilization is unimportant even for pressures above 10 atm. At this temperature, the CH_2CO + ClO formation competes with C*CClO• + O over the pressure range of 10^{-3} - 10^{2} atm.

6.3.3 CHClCH + O_2

The potential energy diagram for CHClCH addition to O_2 is shown in Figure E11. We see the reaction paths are similar to those in vinyl + O_2 case. Table E3 lists the input parameters for the QRRK calculation.

Figure E12 shows the rate constants to various channels versus 1000/T at 1 atm. The total rate shows a slight decline below 1000 K, and it is near constant above 1000 K,

because dissociation back to reactants decreased a little above 1000 K. Stabilization of CHClCHOO is most important below 400 K, with CHClO + CHO next in importance. Above 400 K, CHClO + CHO becomes the dominant channel.

The effects of pressure on various reaction channels at 300 and 1500 K are illustrated in Figure E13 and E14, respectively. Results are similar to those in vinyl + O2 case. The total rate at 300 K is near constant over a wide pressure range (10^{-3} - 10^{2} atm), owing to a tradeoff between the CHClCHOO stabilization and CHClO + CHO product channel. At 1500 K, stabilization of energized adducts is seen to be unimportant, even at 100 atm.

All the channels resulting from dissociation of the chemically activated adduct to various products are observed with no pressure dependence at 1500 K, 10^{-3} - 10^{2} atm.

6.3.4 CHClCCl + O_2

The potential energy diagram and QRRK input parameters for CHClCCl + O_2 addition are shown in Figure E15 and Table E4, respectively. The consideration for each reaction path and ClO elimination from CHClCClOO are similar to those in the CH_2CCl + O_2 reaction.

The Arrhenius plot for various reaction channels at 1 atm is illustrated in Figure E16. Again, stabilization of CHClCClOO is most important in the lower temperatures (below 400 K), and it is second most important until 700 K. Above 400 K, the fastest channel calculated as CHClO + CClO, until 1800 K where it competes with dichloro vinoxy radical (CHClCClO•) + O. The formation of CHClCClO• + O becomes most important above 1800 K.

The effects of pressure on the reaction channels at 300 and 1500 K are shown in Figure E17 and E18, respectively. At 300 K, CHClCClOO stabilization affects the total rate at $P > 3$ atm, then falls off, and still remains most important until 0.3 atm. Formation of CHClO + CClO increases with pressure decrease, and becomes the dominant channel below 0.3 atm. At 1500 K, stabilization is seen to be unimportant, even at $P > 10$ atm. Reaction to all the channels resulting from dissociation of the chemically activated adduct to various products is observed, with little pressure dependence.

6.3.5 $CCl_2CH + O_2$

The potential energy diagram for $CCl_2CH + O_2$ addition is shown in Figure E19. The product set CCl_2CO + OH resulted from a four-member ring transition state of the energized CCl_2CHOO^* adduct. Although there is an expected high barrier (~ 40 kcal/mol) for this reaction, which causes it to be unimportant at lower temperatures, its highly exothermic (~ -30 kcal/mol) and needs to be included in the analysis. Input parameters for the QRRK calculation are listed in Table E5.

Figure E20 illustrates the predicted effect of temperature at atmospheric pressure. The total rate is seen to be similar to the other vinyl and chloro-vinyl radicals + O_2 cases. It shows a slight overall negative temperature dependence. Stabilization of CCl_2CHOO is most important below 400 K, with CCl_2O + CHO next in importance. CCl_2O + CHO is predicted to be dominant between 450 and 1400 K. $CCl_2CHO.$ + O as expected increasing in importance above 700 K, and competes with CCl_2O + CHO near 1400 K. Above 1400 K, $CCl_2CHO\bullet$ + O is dominant. The highly exothermic product set, CCl_2CO + OH is

predicted unimportant over the temperatures 300 - 2500 K, because the high barrier to the transition state.

The effects of pressure at 300 and 1500 K are illustrated in Figure E21 and E22, respectively. At 300 K, stabilization of CCl_2CHOO dominates above 0.2 atm, and is observed to be at the high pressure limit at 10 atm. Formation of CCl_2O + CHO increases with pressure decrease, and becomes most important below 0.15 atm at 300 K.

At high temperature (1500 K), stabilization is predicted to be unimportant until 10 atm. $CCl_2CHO\bullet$ + O is observed to be pressure independent and competes with CCl_2O + CHO over a wide pressure range, 10^{-3} - 10^{2} atm at 1500 K.

6.3.6 $C_2Cl_3 + O_2$

The potential energy diagram for $C_2Cl_3 + O_2$ is shown in Figure E23. The reaction paths are simpler than the other chloro-vinyl radicals + O_2 cases, because no intramolecular H-shift needs to be considered. Russell et al.(85) observed low levels for the CCl_2CO products. This observation suggests that there may be a significant reaction path $C_2Cl_3 + O_2 \rightarrow CCl_2CO + ClO$, which is also discussed for $CH_2CCl + O_2 \rightarrow CH_2CO + ClO$ and $CHClCCl + O_2 \rightarrow CHClCO + ClO$. Although there is no CCl_2O directly detected in the experimental results of Russell et al.,(85) they still reported that CCl_2O formation was considered significant. Table E6 lists the input parameters of QRRK calculation.

The Arrhenius plot for $C_2Cl_3 + O_2$ reaction to various reaction channels at 1 atm is illustrated in Figure E24. The total rate for $C_2Cl_3 + O_2$ is predicted to decrease with temperature increase, which is also observed by Russell et al.(85) at lower pressures 1.47 -

6.74 torr. Figure E7 shows the comparison between these prediction and the observations of Russell et al. for the overall rate constants versus 1000/T at pressures 1.47 - 6.74 torr in He bath gas. Our calculation fit the experimental data well, and clearly show the trend of negative temperature dependence. C_2Cl_3OO stabilization is most important below 400 K, with CCl_2O + CClO next in importance. Between 450 and 1400 K, CCl_2O + CClO dominates. $CCl_2CClO\bullet$ + O, CCl_2CO + ClO, and dissociation back to C_2Cl_3 + O_2 increase in importance above 700 K, and compete with CCl_2O + CClO above 1450 K.

Figure E25 illustrates the effects of pressure on the reaction channels at 300 K. The total rate at 300 K is seen to be near constant over a wide pressure range (10^{-3} - 10^{2} atm). As discussed previously, this is due to a tradeoff switch between the C_2Cl_3OO stabilization and CCl_2O + CClO product channel. A slightly lower overall rate constant is calculated at 1500 K relative to 300 K, as illustrated in Figure E26. This due to an increase in the reverse dissociation rate. At 1500 K, stabilization is predicted to be unimportant, and we see reaction to all channels resulting from dissociation of the chemically activated adduct various products.

Apparent rate constants for vinyl and chlorinated vinyl (CH_2CCl, CHClCH, CHClCHCl, CCl_2CH, and C_2Cl_3) radicals + O_2 in N_2 bath gas are listed in Table E7.

6.4 Conclusions

Thermodynamic properties for the molecules and radicals related to the reactions of vinyl and chloro-vinyl radicals addition to oxygen are evaluated. Reactions of vinyl and chlorinated vinyl radicals with O_2 are analyzed as bimolecular chemical activation systems

using quantum Rice-Ramsperger-Kassel theory for k(E) with modified strong collision approach for fall-off effects. Rate constants to the 10 possible channels are determined from 300 - 2500 K, and 0.001 - 100 atm. Agreement with experimental data in all cases is very good.

The high pressure limit A factors which have been evaluated from literature for reactions $C_2H_3 + O_2$ to $C_2Cl_3 + O_2$ range from $(4.0\pm0.8) \times 10^{12}$ to $(1.2\pm0.24) \times 10^{12}$ cm^3 mol^{-1} s^{-1}, which decrease with increasing chlorine substitution. Energies of activation (E_a) range from -(0.25±0.1) to -(0.83±0.23) kcal/mol, and show a trend to slightly higher negative activation energy (< 1 kcal/mol) with increasing chlorine substitution. The well depth (40±2 kcal/mol) to the peroxy does not change significantly.

Calculations indicate that stabilization of the initially formed adducts (vinyl peroxy and chloro-vinyl peroxy radicals) is important at low temperatures (below 400 K) and higher pressures (above 1 atm). Formation of the product sets: CH_2O (CHClO or CCl_2O) + C•HO (C•ClO) and vinoxy (chloro-vinoxy) + O dominate at high temperatures, and also increase in importance at lower pressures. Calculation results show very good agreement with experimental data, where available.

CHAPTER 7

FORMATION OF CHLORINATED AROMATICS (DIOXIN PRECURSORS) FROM HIGH TEMPERATURE COMBUSTION REACTIONS OF C_1 AND C_2 CHLOROCARBONS : REACTION MECHANISM ANALYSIS

7.1 Introduction

Polychlorinated dibenzodioxins (PCDDs) and polychlorinated dibenzofurans (PCDFs) are a probable carcinogen and a known noncancer health hazard to humans. The dominant source of these compounds in the United States is emission from incinerators into the atmosphere.(17-21) Formation of PCDDs and PCDFs during incineration is known to occur in the post combustion zone of incinerators at temperatures between 200 - 500 °C, (137-141) but the formation mechanism is still unclear. The reaction mechanisms for production of single ring aromatic compounds, chlorinated benzenes and phenols (precursors to multi-ring aromatics such as PCDDs), from lower molecular weight species are the important initial steps for formation of these polycyclic aromatics, soot and higher molecular weight compounds in combustion processes.(8,22-24) A number of researchers have provided experimental confirmation on a variety of high molecular weight polycyclic aromatics present in rich, hydrocarbon, flames(142-144), and proposed reaction paths and kinetics for formation of benzene and other higher molecular weight species, based on addition reactions of radicals to acetylene, Diels-Alder reactions, or combination reactions of propargyl radicals.(8,10,11,22-24,145,146)

Weissman and Benson(22) indicated addition reactions of saturated hydrocarbon radicals to C_2H_2 and C_2H_4 are of significance to high molecular weight growth; but they indicated that the addition of alkyl radicals to C_2H_4 appears to be of little importance. The addition of vinyl radical to C_2H_4 is however very important; it leads to the observed product of butadiene from butenyl radical. The addition of C_2H_3 to C_2H_2 results in formation of the butadienyl radical, then the butadienyl radical decomposes to vinylacetylene + H. Weissman and Benson proposed the formation pathways of benzene are C_2H_3 addition to butadiene through subsequent cyclizations and dehydrogenations, and the additions of C_4 radicals to C_2H_2 and C_2H_4.

Frenklach et al.(8) investigated the chemical reaction pathways to soot by experimenting with detailed kinetic models in shock-tube pyrolysis of acetylene. A reaction mechanism consisting of approximately 600 elementary, reversible reactions and 180 species were considered to explain the time scale of soot formation and soot yields obtained in this study. The mechanism development was based on the mechanism of Tanzawa and Gardiner,(146) and then modified according to physical organic chemistry principles to comprise the likely radical and atom reactions that could lead eventually to cyclization, molecular weight growth and aromatics. The formation reactions of polycyclic aromatics may be considered irreversible because of the ring's stabilization energy. Subsequent reactions to multi-ring aromatics also have this effect or near irreversible reactions. Frenklach et al. indicated that the main bottleneck for polycyclic aromatics and soot appears at the formation of the first aromatic ring.

Colket(23) investigated the pyrolysis of acetylene and vinylacetylene in a single-pulse shock tube as well as by using a detailed reaction mechanism. Colket suggested that early benzene formation (T < 1500 K) from acetylene arises principally from acetylene addition to the normal-butadienyl (n-C_4H_5) radical, not the n-C_4H_3 (vinyl-acetylene) radical, *i.e.*,

$$n\text{-}C_4H_5\ (+\ C_2H_2) \rightarrow L\text{-}C_6H_7 \rightarrow CyC_6H_7\ (\text{-}H) \rightarrow CyC_6H_6$$

Where L and Cy represent linear and cyclic, respectively. Colket's results for vinyl-acetylene at temperatures below 1500 K indicate that the major formation paths to benzene is through vinyl radical addition to the vinyl-acetylene.

Glassman(24) reviewed the literature for soot formation in combustion processes and indicated that the critical soot equivalence ratios of pre-mixed flames and the smoke heights of diffusion flames at a fixed temperature are excellent means of comparing the relative sooting tendencies of various fuels. Glassman also indicated that concentration of H atom, vinyl radicals and acetylene play a significant role in the rate processes leading to the aromatic ring formation, while the rate of formation of the first rings is the rate controlling step to soot emission.

Westmoreland et al.(10) indicated formation of benzene in $C_2H_2/O_2/Ar$ flames by bimolecular QRRK calculations(67) on addition of vinyl radical to acetylene, which forms a chemically energized adduct that can isomerize before stabilization. They concluded that

addition of 1-C_4H_3 and 1-C_4H_5 to acetylene have the following advantages over other paths:

1. Chemically activated isomerization is strongly favored because the cyclic isomers that can be formed, are much more stable than thermalized linear adducts. This stability inhibits chemically activated reverse isomerization and overcomes the entropy loss from cyclization.
2. The energy in the chemically activated adducts greatly exceeds the thermal barrier to isomerization. Cyclization can take place directly by low-activation energy, radical self-addition (intramolecular) within the adducts.
3. The conjugated π bonds of these linear adducts add to their thermal stability. This provides a deeper well or more energy for stabilization.
4. No bimolecular abstraction or addition of H is necessary to form an aromatic species.

Fahr and Stein(12) studied the kinetic reactions of vinyl and phenyl radicals with ethylene, acetylene and benzene in a Kundsen cell flow reactor at temperatures 1000 - 1330 K. They reported rate constants ($cm^3\ mol^{-1}\ s^{-1}$) at 1100 K are:

	k (R• = vinyl)	k (R• = phenyl)
$R\bullet + C_2H_2 \rightarrow R\text{-}C_2H + H$	$(2.0\pm0.4) \times 10^{11}$	$(2.6\pm0.6) \times 10^{11}$
$R\bullet + C_2H_4 \rightarrow R\text{-}C_2H_3 + H$	$(1.4\pm0.2) \times 10^{11}$	$(1.5\pm0.4) \times 10^{11}$
$R\bullet + C_6H_6 \rightarrow R\text{-}C_6H_5 + H$	$(4.5\pm1.2) \times 10^{10}$	$(6.0\pm2.0) \times 10^{10}$

When combined with room temperature addition rates from the literature, Fahr and Stein obtained the rate constants ($cm^3\ mol^{-1}\ s^{-1}$):

$k(\text{vinyl} + \text{ethyne} \rightarrow \text{vinylacetylene} + H) = 10^{12.3} \exp(-5.0\ \text{kcal/RT})$

$k(\text{phenyl} + \text{benzene} \rightarrow \text{biphenyl} + H) = 10^{11.6} \exp(-4.0\ \text{kcal/RT})$

Wang and Frenklach(13) used semiempirical quantum mechanical AM1 calculations for the chemically activated reactions of acetylene with vinyl, 1-buten-3-yn-1-yl, 1,3-butadien-1-yl, phenyl, 1-ethynylphenyl, 2-naphthyl, and 4-phenanthryl radicals. The reaction rate coefficients were then calculated on the RRKM level theory, using the AM1 molecular parameters with small corrections to match the available experimental data. Their results support the hypothesis that reactions of multi-ring aromatic species are similar to those of benzene and phenyl. The distribution of reaction channels and the rate coefficients computed for the addition of acetylene to larger aromatic radicals are similar to those of acetylene addition to the non-cyclic species, such as n-C_4H_3 and n-C_4H_5.

Stein et al.(145) investigated the formation paths from propargyl radicals to benzene where he used 1,5-hexadiyne as a source of propargyl. Two studies, one at atmospheric pressure with residence times near 30 seconds and the second under Kundsen flow conditions ($< 10^{-3}$ torr) with residence times of the order of 0.1 second. They reported that benzene formation from C_4 radical addition reactions may be significantly less than propargyl combination under their conditions. They also proposed that phenyl-

substituted propargyl radicals are involved in the formation of larger aromatic species. The reaction schemes are illustrated below:

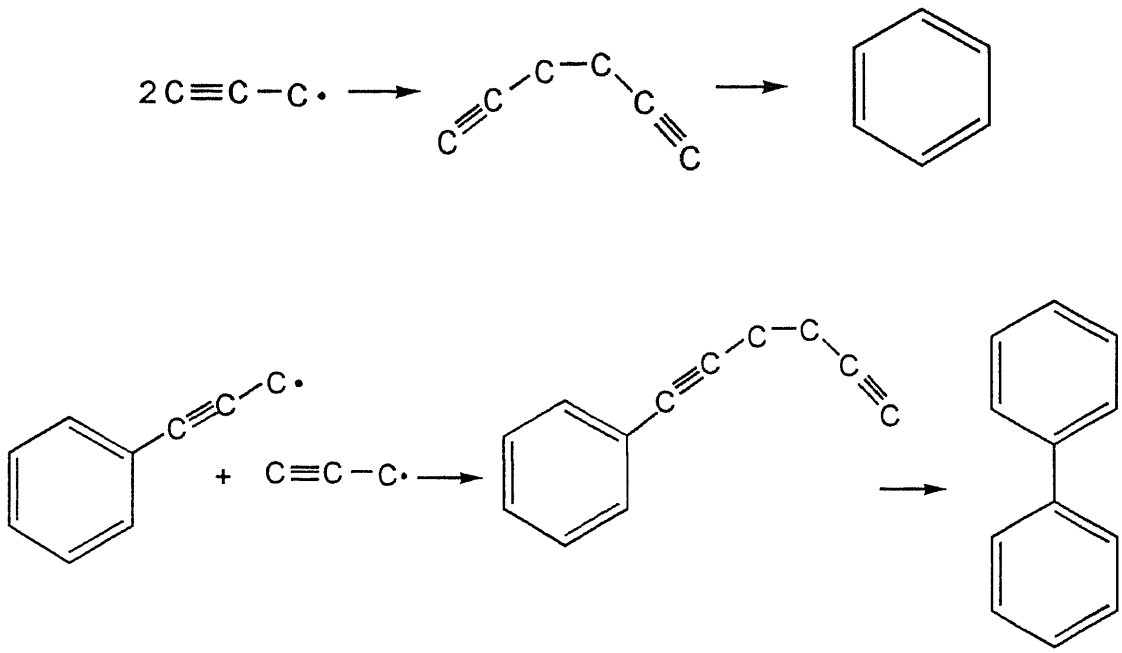

Very little has been published on the molecular weight growth reaction pathway for chlorinated species. Shi and Senkan(14) studied the activation energies for the addition of chlorinated C_1 and C_2 vinylic hydrocarbon radicals to chlorinated ethylenes and acetylenes using the semiempirical MNDO calculation with the PM3 set of parameters at the UHF level. They reported that calculated activation energies increased with increasing chlorine substitution of the species, and β sites (β carbon equal one carbon away from the chlorine substituted carbon) were determined to be the preferred addition sites.

There are no elementary reaction mechanisms for prediction of chlorinated single ring aromatics: chlorinated benzenes and phenols from oxidation of C_1 and C_2

hydrocarbons and/or chlorocarbons. Taylor et al.(147) investigated the pyrolysis of trichloroethylene (no oxygen present) using fused silica tubular reactors. They developed an elementary reaction mechanism consisting 39 species and 62 reactions to describe molecular growth up to CyC_8Cl_6 (hexachloroethynylbenzene or hexachloroethynylfulvene isomer) and CyC_8Cl_8 (Octachloroethenylbenzene or octachloroethenylfulvene isomer). Comparison of predicted versus observed reagent (C_2HCl_3) decay, major products (HCl, C_2Cl_2, and C_2Cl_4) and minor species (C_4Cl_4, CyC_6Cl_6, CyC_8Cl_6, and CyC_8Cl_8) were shown to be in good agreement.

C_4 radical addition to C_2 unsaturated molecules, C_2 radical addition to C_4 unsaturated compounds, and propargyl radical combinations are considered to be the major formation pathways of benzene and chlorinated benzenes. There is little chance for formation of propargyl or chloro-propargyl radicals in the combustion of CH_2Cl_2, while the formation of C_2 compounds is important.

This chapter presents the reaction pathway development and kinetic analysis for molecular weight growth by reactions of C_2 addition to C_2: C_2 addition to C_4; and C_4 addition to C_2 compounds. The reactions and their kinetic parameters are assembled into a mechanism and this reaction mechanism is used to predict the formation levels of chlorinated benzenes versus ratio of initial reagents ($[CH_2Cl_2]/[fuel]$) and fuel equivalence ratios (ϕ). The reaction pathways for benzene and chloro-benzene with OH radical are also illustrated.

7.2 Kinetic Reaction Mechanism

The reaction mechanism is based upon fundamental principles of thermochemical kinetics including Transition State Theory (TST) and on accurate molecular thermodynamic properties. The mechanism consists of elementary reactions with each reaction based on literature evaluation, or if it is estimated, on thermochemical and kinetic principles and in agreement with similar - generic reaction rates in the literature.

We incorporate corrections to experimentally determined rate constants(182,113) where the measurements were performed at low pressures, and where pressure changes may effect the rate; correction to adjust for atmospheric conditions. Here we utilize a technique (quantum RRK analysis) that calculates k(E) values and modified strong collision analysis(75) for calculation of fall-off effects in unimolecular reactions and in chemical activation processes such as addition or combination reactions. We apply this analysis to rate constants, which are pressure dependent that are reported in the literature from measurements at other pressures, as well as our estimated rate constants for these type reactions.

If fundamentally correct, the mechanism's applicability should extend beyond the bounds of the experimental calibrations it was developed under, because of the thermochemical and kinetic principles (theories) it is based on. The model is not just a mathematical or optimized fit to the experimental data over a limited parameter range. No rate constants are arbitrarily adjusted to obtain fits to experimental data for validations.

Model Requirements include:

- Accurate thermodynamic properties of all reacting species.

- Forward and reverse rate constants to be consistent with thermochemical principals - microscopic reversibility for all fundamental reactions.
- Isomerization rate constants to follow Transition State Theory.
- Quantum RRK theory(67,68) for k(E) combined with modified strong collision analysis for temperature and pressure compensation in chemical activation reactions (addition, combination, insertion) and for in unimolecular dissociation reactions (simple, beta scission and isomerization).
- Abstraction Arrhenius A factors from literature evaluation(113) or generically derived. Abstraction Ea's from literature evaluation(113) or from thermodynamics and Evans-Polanyi relationships.
- Model to be tested against data in the literature when data is available.

The following computer codes are helpful tools in mechanism validation and development.

THERM(69) - calculates thermodynamic parameters of radicals and molecular species based on the methods of Benson group additivity(25) and properties of radicals based on Bond Dissociation (BD) groups developed in these laboratories. BD groups consist of ΔH_f, S_f and heat capacity terms, $C_p(T)$, which are added to the corresponding properties of the parent molecule to yield thermodynamic properties of the radical (parent - H atom). THERM also converts the data in listing form into NASA format so that it can be used by the CHEMKIN (65) integration codes.

DISSOC(68) - performs calculations on unimolecular dissociation as a function of temperature and pressure, for pressure dependence.

CHEMACT(68) - calculates apparent bimolecular rate constants over a range of temperature and pressure on reactions which form a chemically activated adduct for combination, insertion and addition type reactions.

THERMRXN - which is part of THERM(69) utilizes thermodynamic parameters plus Arrhenius A's and E_a ratios of each reaction in the mechanism, in addition to evaluation of specific rate constants in both the forward and reverse directions over a range of temperatures. This data serves as a check in our mechanism generation to see if any typing (computer input data) or rate constant estimations are in error, through comparisons of listed forward and reverse rate constants and the thermodynamics.

TRANSCAL(149) - A technique to calculate transport properties of molecules and radicals - Lennard-Jones collision diameters and energy transfer well depth; boiling point, polarizability, and viscosity - using group additivity. This program uses the same groups, with a different data base, as THERM.(69) The parameters are then used as input transport properties to the flame code above.

RADICALC(70) - Calculation of the entropy and heat capacities of radicals and transition states for estimation of Arrhenius A factors as a function of temperature is performed using a data bases of vibrational frequencies, moments of inertia and barriers to internal rotations and principles of statistical mechanics.(71)

Specifics on Reaction Rate Constants:

Abstraction Reactions - Abstraction reaction rate constants are not pressure dependent and therefore do not incorporate any quantum RRK analysis. When estimation is required for an abstraction rate constant we use a generic reaction as a model and adjust for steric

effects as best we can. An example of the generic type of Arrhenius A factor analysis is Cl atom abstracting an H from 1,1-dichloro-ethylene, where experiments can not discern whether the measured values are for the abstraction or the addition reaction. Here we would take the abstraction by Cl or H from 1,1,1-trichlorethane where both the mass and the reaction degeneracy are similar. The Ea is calculated separately.

Evans Polanyi analysis is used on the reaction in the exothermic direction to estimate the energy of activation for the rate constant. An Evans Polanyi plot, E_a versus delta H reaction, allows use of a known ΔH_{rxn} to obtain E_a for these reactions. Clearly the abstraction reaction in an endothermic reaction must incorporate the ΔH_{rxn} or it, the reaction rate constant, will violate thermodynamics.

Addition Reactions - Addition reactions are treated with the quantum RRK formalism described above. The reactions involve addition of an atom or radical to an unsaturated species and typically form an energized adduct with ca. 20 to 50 kcal/mol of energy above the ground state. This is sometimes sufficient to allow the adduct to react to other reaction products (lower energy) before stabilization occurs). An example would be H atom addition to vinyl chloride, an olefin, forming one of two chloro-ethyl radicals with ca. 40 kcal/mol energy above the ground state. In the case of H Atom addition to the carbon containing the Cl atom, the chloro-ethyl adduct formed $\bullet CH_2CH_2Cl$ could rapidly eliminate Cl (beta scission) to form the lower energy products Cl atom plus ethylene. Some examples of the quantum RRK analysis for this reaction are described below.

It is important to note that reaction to other channels as well as isomerization, in addition to stabilization and reverse reaction are included in this calculation.

Elimination - Beta Scission Reactions - These reactions utilize the quantum RRK formalism and are treated in one of two ways. We use a unimolecular quantum RRK formalism, where we determine the reverse reaction (addition) parameters for the high pressure case, then calculate the corresponding high pressure unimolecular beta scission rate constants using microscopic reversibility <MR>. The high pressure unimolecular elimination parameters are then input to the quantum RRK formalism to determine the high pressure limit and to calculate the apparent rate constants at the appropriate pressure.

The second method is simple use of the reverse rate constants from the addition reaction and use of the CHEMACT calculations (see below).

Dissociation Reactions - Simple Unimolecular - Simple unimolecular (dissociation) rate constants are determined by two methods similar to the case of beta scission reactions. We use the unimolecular quantum RRK formalism. Here we determine the reverse reaction (combination) rate constant parameters for the high pressure case, then calculate the corresponding high pressure unimolecular dissociation rate constant using microscopic reversibility <MR>. The high pressure unimolecular elimination parameters are then input to the quantum RRK formalism to calculate the apparent dissociation rate constants at the appropriate pressure.

The second method is simple use of the reverse rate constants from the CHEMACT combination reaction calculations.

Combination and Insertion Reactions - These reactions involve the combination of two radical species, or an atom and a radical. The energy of the adduct formed before stabilization is equal to the bond energy of the new bond(s) formed and typically on the

order of 80 to 120 kcal/mol. This is usually sufficient for an adduct, with this initial energy above it's ground state energy, to react to lower energy products before stabilization occurs. The high pressure limit rate constant for combination is obtained from the literature or estimated from known generic combination rates. The combined quantum RRK chemical activation formalism(67,68) is then used to determine the high pressure limit and to calculate the apparent rate constants at the appropriate pressure to all the channels. This is an important aspect of our reaction analysis for both these combination as well as insertion and addition reactions that other modelers do not incorporate.

This leads to a more correct treatment of fall-off and pressure dependence for these non-elementary reaction systems. Rate constants for the model are obtained which incorporate these pressure dependency therefore make the model more fundamentally correct.

Thermodynamic Properties - Thermodynamic properties listed in Table F1 are calculated by the THERM(69) computer code. Enthalpies of radials are from evaluated literature C-H bond energies and ΔH_f of the stable molecule which corresponds to the radical with a H atom at the radical site. Entropies and $C_p(T)$ values are from use of Hydrogen Bond Increment (HBI).(71) The HBI group technique is based on known thermodynamic properties of the parent molecule and calculated changes that occur upon formation of a radical via loss of a H atom. The HBI approach incorporates (i) evaluated literature bond energies, (ii) calculated entropy and heat capacity increments resulting from loss and/or change in vibrational frequencies including frequencies corresponding to

inversion of the radical center, (iii) increments from changes in barriers to internal rotation, and (iv) spin degeneracy.(79,103)

Reaction Paths - The reaction scheme for molecular weight growth of methane and chloro-methane to C_6 chlorinated benzenes ($CyC_6H_4Cl_2$) is shown in Figure F1. The presence of chlorine in the system leads to rapid generation of Cl atoms, which results from the relative low C-Cl bond energies and low energies of activation (E_a's) for HCl elimination reactions. Radicals like OH, H, CH_3, R• will rapidly abstract H from HCl, generating a Cl atom. Cl then undergoes relatively fast abstraction reactions with other parent chlorocarbons and hydrocarbons, as the reactions have high A factors and low (near zero above ΔH_{rxn}) E_a's. This results in a more rapid formation of Cl, and chlorocarbon radicals relative to when Cl is not present. The additions of these chlorocarbon radicals to unsaturated compounds therefore play a critically important role in the molecular weight growth.

The addition reaction of radicals to ethylene is known(13,22) less important than to acetylene in the molecular weight growth, except for the vinyl radical addition to ethylene and acetylene, both reactions show similar in importance. We discuss the molecular weight growth up to single ring aromatic compounds by the chemically activated reactions of:

- C_2 radical addition to chlorinated ethylenes and acetylenes
- C_2 radical addition to chlorinated C_4 unsaturated compounds
- C_4 radical addition to C_2 unsaturated compounds

The above addition/combination reaction systems are analyzed by QRRK(67,68) theory for k(E) and with modified strong collision approach(74,75) for fall-off effects under combustion condition. One example of each type of reaction will be illustrated in detail in this chapter.

The overall reaction mechanism is a combination of several subset mechanisms in sequence of increasing complexity: first pyrolysis reactions of CH_2Cl_2, second pyrolysis in presence of CH_4 - a hydrocarbon, and third oxidation of CH_2Cl_2. These are then illustrated in Table B1. These are combined with reactions describing the formation of larger molecules and radicals and ultimately the formation of single ring aromatic molecules and radicals as shown in Table F2. Oxidation of C_4 intermediates primarily via paths similar to vinyl + O_2 are also included, in order to limit MWG in presence of O_2. The molecular weight growth reactions are basically considered as those in pyrolysis of C_2H_3Cl, CHClCHCl, and C_2HCl_3, which are sub-mechanisms to the CH_2Cl_2 pyrolysis and oxidation. The C_2HCl_3 reaction paths are based on the mechanism of Taylor et al.;(147) but the thermodynamic and kinetic analysis is original.

Table F3 lists the nomenclature and notation of the species, for example C_4H_4Cl(N1 means a linear primary C_4H_4Cl radical, C_4H_4Cl(I1 means a linear secondary C_4H_4Cl radical, $C_6H_3Cl_3$(L1 means a linear $C_6H_3Cl_3$ molecule, and $C_6H_3Cl_3$(Y1 means a cyclic $C_6H_3Cl_3$, while C_4H_4Cl(N1 and C_4H_4Cl(N2 mean the C_4H_4Cl isomers with different site of Cl-substitution, respectively.

The mechanism is calibrated against laboratory and literature C_1 and C_2 chlorocarbon oxidation and pyrolysis. The mechanism is then used in predicting levels of

dioxin precursors (chlorinated aromatics) from various high temperature reactions of C_1 and C_2 chlorocarbons.

Numerical calculation for the formation of chlorobenzenes from C_1 and C_2 chlorocarbons is performed using CHEMKIN(65) package.

7.3 Results and Discussion

7.3.1 Results of QRRK Calculation

The chemical activated reactions leading to molecular weight growth and C_6 aromatic species include: C_2 radical addition to C=C molecules, C_2 radical addition to C≡C molecules, and two types of C_4 radical addition to C≡C molecules. There are several isomers for these species due to the numbers and different substitution sites of Cl atom(s). In the next section, one example for each type of reaction is treated using QRRK formalism, and the calculation results are illustrated.

7.3.1.1 CH_2CCl addition to C_2HCl - The potential energy diagram and input parameters with corresponding references for the QRRK calculation are shown in Figure F2 and Table F4, respectively. Addition of CH_2CCl to the α-site of C_2HCl forms an energized $C_4H_3Cl_2$(N4* (2,3-butadienyl radical) adduct. Shi and Senkan(14) considered that β-site is the preferred addition site, but in this chemically activated reaction, addition to α-site leads to a rapid reaction through a low energy product channel. The chloro-vinyl acetylene (C=CClC≡C) + Cl product channel is 25 kcal/mol below the energy of the reactants and is important to formation of aromatics and MWG products in this mechanism.

QRRK calculation results at 1 atm are illustrated in Figure F3. C=CClC≡C + Cl is observed to be dominant channel and nearly equal to the total rate at temperatures 300 - 2500 K, with stabilization about 2 orders of magnitude lower than that of this C=CClC≡C + Cl channel.

7.3.1.2 CH_2CCl addition to C_2H_3Cl - Figure F4 shows the potential energy diagram for the addition reaction of CH_2CCl to C_2H_3Cl. It is similar to the CH_2CCl + C_2HCl reaction. The 2,3-dichlorobutenyl adduct rapidly β-scissions to Cl + 2-chlorobutadiene, which is the lowest energy product channel other than stabilization and is shown to be the dominant path. Input parameters for the QRRK calculation are shown in Table F5.

Figure F5 illustrates the Arrhenius plot at 1 atm. 2-chlorobutadiene + Cl is most important over the temperature range 300 - 2500 K.

7.3.1.3 C_4H_4Cl(N1 + C_2HCl - The potential energy diagram and input parameters for kinetic analysis on the chemically activated adduct, $C_6H_5Cl_2$(N1*, are shown in Figure F6 and Table F6, respectively. Chlorobutadienyl radical addition to C_2HCl results in formation of $C_6H_5Cl_2$(N1* adduct. The different reaction channels can be described as:

addition/stabilization:

C_4H_4Cl(N1 + C_2HCl ↔ C_6H_5Cl(N1* → $C_6H_5Cl_2$(N1

addition/dissociation:

C_4H_4Cl(N1 + C_2HCl ↔ C_6H_5Cl(N1* → $C_6H_4Cl_2$(L1 + H

addition/isomerization/stabilization:

$C_4H_4Cl(N1 + C_2HCl \leftrightarrow C_6H_5Cl(N1^* \leftrightarrow Cl12CHD.^* \rightarrow Cl12CHD.$

addition/isomerization/dissociation:

$C_4H_4Cl(N1 + C_2HCl \leftrightarrow C_6H_5Cl(N1^* \leftrightarrow Cl12CHD.^* \rightarrow Cl + CyC_6H_5Cl$

Calculated rate constants versus temperature (1000/T) for various products at 1 atm are illustrated in Figure F7. Stabilization of $C_6H_5Cl_2(N1$ is most important below 350 K, and second in importance between 350 and 1350 K. Cl + chlorobenzene is observed to dominate above 350 K. Cl + $C_6H_4Cl_2(L1$ increases in importance with temperature increase, and becomes second in importance above 1350 K.

7.3.1.4 $C_4H_2Cl(N2 + C_2HCl$ - The potential energy diagram for the addition of 1-chloro-1-buten-3-yn-1-yl to chloroacetylene is illustrated in Figure F8. The pathways for the energized adduct are:

stabilization:

$C_4H_2Cl(N2 + C_2HCl \leftrightarrow C_6H_3Cl_2(N1^* \rightarrow C_6H_3Cl_2(N1$

dissociation:

$C_4H_2Cl(N2 + C_2HCl \leftrightarrow C_6H_3Cl_2(N1^* \rightarrow C_6H_2Cl_2(L1 + H$

isomerization/stabilization:

$C_4H_2Cl(N2 + C_2HCl \leftrightarrow C_6H_3Cl_2(N1^* \leftrightarrow C_6H_3Cl_2(Y1^* \rightarrow C_6H_3Cl_2(Y1$

isomerization/dissociation:

$$C_4H_2Cl(N2 + C_2HCl \leftrightarrow C_6H_3Cl_2(N1^* \leftrightarrow C_6H_3Cl_2(Y1^* \rightarrow C_6H_2Cl_2(Y + H$$

Comparison between $C_4H_2Cl(N2 + C_2HCl$ and $C_4H_4Cl(N1 + C_2HCl$, shows that the relatively high barrier for $C_6H_3Cl_2(Y1$ adduct dissociation to $C_6H_2Cl_2(Y + H$ leads to significant stabilization of $C_6H_3Cl_2(Y1$.

Input parameters for the QRRK calculation are shown in Table F7 along with their corresponding references.

An Arrhenius plot at 1 atm for $C_4H_2Cl(N2 + C_2HCl \rightarrow$ products is presented in Figure F9. Stabilization of $C_6H_3Cl_2(N1$ is most important below 600 K, with $C_6H_3Cl_2(Y1$ (dichloro-phenyl) next in importance. $C_6H_3Cl_2(Y1$ is observed to be the dominant channel between 600 and 1250 K, with a maximum rate near 900 K. $H + C_6H_2Cl_2(L1$ increases in importance above 1250 K, and becomes the dominant channel above 1550 K.

7.3.2 Results of Model Prediction

A detailed kinetic reaction mechanism consisting of 635 elementary reactions and 215 species based upon fundamental thermochemical and kinetic principles, Transition State Theory and evaluated literature rate constant data is developed and utilized to predict the formation of benzene and chlorinated benzenes from high temperature combustion of CH_2Cl_2.

Figures F10 - F12 illustrate the predicted concentrations of benzene and chlorinated benzenes as a function of initial reactant ratio ($[CH_2Cl_2]/[fuel]$) at 1200 K and

stoichiometry (ϕ = 1.0). In our stoichiometric calculations, all Cl is assumed to react to HCl. In our model calculations, significant Cl_2 is formed for $\phi < 1$. All Cl does react to HCl when $\phi > 1$. Benzene and chlorobenzene are observed to have the maximum yields at the ratio of CH_2Cl_2/fuel = 1, while the concentrations of dichloro-, trichloro, and hexachloro-benzene continue to increase with increasing ratio of CH_2Cl_2/fuel.

Figure F13 - F15 show the product yields of benzene and chlorinated benzenes versus fuel equivalence ratio (ϕ) at 1200 K with the ratio of CH_2Cl_2/fuel held constant at 1.0. The model predicts the aromatic product levels increase as ϕ increases.

The model prediction at 800 K also shows a similar trend to that at 1200 K for benzene and chlorinated benzene formation.

7.3.3 Reaction Pathway Analysis for CyC_6H_6 + OH and CyC_6H_5Cl + OH

Figure F16 illustrates the potential energy diagram for CyC_6H_6 + OH and CyC_6H_5Cl + OH. The upper plot shows that OH addition to CyC_6H_6 forms an energized cyclohexadienyl adduct (CHD.) which can be stabilized, dissociate to phenol + H, or dissociate back to reactants. This reaction is in equilibrium and controlled by OH levels. The phenol will rapidly react - lose a weak bonded H from OH to form phenoxy which can further react to PCDD/F.

The reaction of OH addition to CyC_6H_5Cl, as shown in the lower plot of Figure F16, forms an energized chloro-cyclohexadienyl adduct which can rapidly dissociate to phenol + Cl. This reaction is exothermic and relatively fast. Its rate is controlled by concentration of reactants.

7.4 Conclusions

A reaction mechanism consisting of 635 elementary reactions and 215 species has been developed to describe the formation of single ring aromatics, chloro-benzenes, and intermediate molecular weight growth species in C_1 and C_2 chlorocarbon and hydrocarbon combustion.

All reactions in the mechanism are elementary or derived from analysis of reaction systems encompassing elementary reaction steps. All reactions are thermochemically consistent and follow principles of Thermochemical Kinetics. Quantum RRK theory is used for calculation of k(E) and modified strong collision approach is used for fall-off analysis of combination, addition, and insertion reactions and in unimolecular dissociations or isomerizations.

The mechanism is calibrated against laboratory and literature chlorocarbon oxidation and pyrolysis data for chloro-methane and chloro-ethane systems over the range of fuel equivalence ratios, ϕ, from 0.5 to 2.0. The data is primarily reactant loss, intermediate product formation/loss, and final product concentrations. The mechanism is then used in predicting levels of dioxin precursors (chlorinated aromatic) from high temperature reactions of C_1 and C_2 chlorocarbons.

Model results show that the concentration of benzene and chlorinated benzenes increase with the ratio of CH_2Cl_2 to fuel, and with increasing fuel equivalence ratios (higher levels formed in fuel rich conditions). Concentrations of chlorinated benzenes are on the order of 0.1 ppm for $\phi = 1$ and 4% CH_2Cl_2, 1% CH_4 in the combustion system.

Little quantitative data is available in the literature on formation of these PICs from well defined laboratory combustion or oxidation experiments. Additional quantitative data from controlled experiments would be useful for testing this mechanism.

CHAPTER 8

QUANTUM RICE-RAMSPERGER-KASSEL (QRRK) ANALYSIS ON THE REACTION SYSTEM OF SULFUR CONTAINING SPECIES

8.1 Introduction

Sulfur and sulfur compounds are present as pollutants in crude oil, natural gas and coal in the range 0.2 to 10%.(150) SOx is a major pollutant from both petroleum and coal fired combustion operations and it is well known to contribute to acid rain.(26) Sulfur, in addition, is known to exist in a range of oxidation states from -2 to +6 (H_2S - SO_3),(27) its reactions with OH and H on surfaces are important to aerosol formation, with these sulfate aerosols strongly implicated in global climate change effects.(28) Radicals of sulfur compounds can catalytically destroy ozone, with mechanisms operative in both the troposphere and in the stratosphere.(29-31) The chemistry of formation and reactions of sulfur oxides in combustion and energy generation processes is important to understand, in order to develop methods for its minimization and removal.

Reaction mechanisms that describe combustion of hydrocarbons (HCs) and chlorohydrocarbons (CHCs)(4,11,55,58,60,61,64,151) have been developed for use in modeling combustion processes, and while the models are always being improved, they are generally considered to be acceptable *i.e.* they achieve satisfactory results under testing. The current data base on sulfur compound reactions in combustion processes is less thoroughly developed, and only a few reaction mechanisms are available. These are in

addition rather limited in numbers of species and interactions with other molecules. Many sulfur oxide reaction pathways are still unstudied and/or unknown.

Cullis and Mulcahy(152) reviewed and interpreted kinetic behavior of organic and inorganic sulfur-containing compounds which either undergo combustion themselves or are present in gaseous combustion systems. They demonstrated how information regarding the kinetics of sulfur compound reactions, derived from laboratory experiments, is useful in interpreting the behavior of sulfur in practical combustion systems.

Frenklach et al.(153) reported an experimental and modeling study on the oxidation of the H_2S. The experiment was conducted in reflected shock waves from 950 to 1200 K at 1 atm. A reaction mechanism including 17 species, and 57 elementary reactions was developed to describe the observed ignition delays and their modeling results led to satisfactory agreement with the experimental data. The sulfur-containing species listed in the mechanism include: S, HS, SO, S_2, HSO, H_2S, SO_2 and SO_3. They reported that other oxides of sulfur and H-S-O species may play significant roles, especially under high-pressure, low-temperature conditions; but did not include reactions for them.

An experimental and numerical study of sulfur chemistry in an $H_2/O_2/SO_2$ flame was investigated by Zachariah and Smith.(154) The experiment was studied in low pressure (100-150 torr) premixed laminar $H_2/O_2/Ar$ flat flames doped with SO_2. The proposed chemical kinetic model contains 17 species (9 sulfur-containing species: S, HS, S_2, H_2S, SO, SO_2, S_2O, HSO, and HSO_2) and 44 reversible elementary reactions. The model provided good agreement with the experimental results. They reported that sulfur in

a flame lowers the propagation velocity, which they attribute to homogeneous catalytic effects of sulfur dioxide resulting in losses of the primary chain carrier (see below). HSO_2 was implicated as an important sulfur intermediate in the SO_2 catalytic cycle and the HSO_2 chemistry was reported to be very important in the resulting distribution of sulfur species. The deficiency in understanding the overall system was attributed to the lack of kinetics for several important reactions proposed.

Hydrogen sulfide is known(155) to inhibit the oxidation of hydrogen. The inhibition is reportedly caused by reactions (I), (II) and (III).(152)

			ΔH_{f298}(kcal/mol)	
$O + H_2S$	$\rightarrow$	$SO + H_2$	-53.3	(I)
$O + SO + M$	$\rightarrow$	$SO_2 + M$	-132.0	(II)
$SO + OH$	$\rightarrow$	$H + SO_2$	-29.9	(III)

The sum of (I) and (II) is loss of two O atoms: $2O + H_2S \rightarrow H_2 + SO_2$

Fair and Thrush(156) studied the reaction of hydrogen atoms with hydrogen sulfide in the presence of small amounts of oxygen and deduced a value of 7.0E13 cm^3 mol^{-1} s^{-1} for reaction (III) in the pressure range 1 - 4 torr at 298 K. Jourdain et al.(157) also studied reaction (III) in a discharge flow reactor at room temperature, they reported the rate constant, k = 5.0E13 cm^3 mol^{-1} s^{-1}. Wine and Hynes(158) have recently reviewed the literature on kinetics and mechanisms of gaseous sulfur. They recommended the rate

constant, k(T) = 8.4E12exp(1920/T), for the reverse reaction of reaction (III), but include no pressure dependence.

There is no kinetic information available on the reaction HSO + O. Several research groups have done reaction pathway analysis of H + SO_2 forming the activated complex, HSO_2*, which may also be formed from HSO + O.

Webster and Walsh,(159) investigated the influence of added sulfur compounds to the hydrogen-oxygen reaction system. They reported that the inhibiting effect SO_2 at partial pressures below 3 torr, on the second explosion limit could be attributed to formation of HSO_2, reaction (IV). Fenimore and Jones(160) proposed that reaction (IV), followed by the SO_2 regeneration reactions (V) and (VI), would serve as a catalytic loss mechanism for H and OH.

			ΔH_{f298}(kcal/mol)	
$H + SO_2 + M$	$\rightarrow$	$HSO_2 + M$	5.9	(IV)
$H + HSO_2$	$\rightarrow$	$H_2 + SO_2$	-110.1	(V)
$OH + HSO_2$	$\rightarrow$	$H_2O + SO_2$	-125.3	(VI)

Binns and Marshall(161) investigated the reaction H + SO_2 $\rightarrow$ products using an *ab initio* calculations, in order to study catalytic removal of atomic hydrogen in flames by sulfur oxide. Energies of two the adducts HOSO and HSO_2 were estimated at optimized geometries using spin-projected MP4/6-31G* calculations. The calculations indicate that planar *cis* HOSO is more stable than C_s HSO_2 by 32 kcal/mol and predict a H-OSO bond

energy of 26.0 kcal/mol. HSO_2 is 6.0 kcal/mol endothermic with respect to H + SO_2, and is therefore insufficiently stable to be significant in combustion chemistry. They also proposed an unusually large energy barrier for reaction (IV), of about 22.7 kcal/mol relative to H + SO_2.

Wheeler(162) later suggested that the addition of hydroxyl radical to sulfur dioxide, reaction (VII), which would be followed by reactions (VIII) and (IX), as a mechanism of catalytic loss of H and OH radicals.

			ΔH_{f298}(kcal/mol)	
$OH + SO_2 + M$	$\rightarrow$	$HOSO_2 + M$	-32.0	(VII)
$H + HOSO_2$	$\rightarrow$	$H_2O + SO_2$	-87.4	(VIII)
$OH + HOSO_2$	$\rightarrow$	$H_2O_2 + SO_2$	-19.5	(IX)

This H and OH radical addition-abstraction cycle has been generally accepted and subsequent work(163,164) has focused on the determination of the relative importance of the various elementary reactions, including reverse reactions of (IV) and (VII).

Gordon and Mulac,(165) David et al.,(166) Harris et al., (167,168) and Wine et al.(169) have investigated the kinetics of OH + SO_2 $\rightarrow$ products at 760 torr and temperature up to 420 K. The rate constant for OH + SO_2 $\rightarrow$ $HOSO_2$ are in reasonable agreement and range from 5.0E11 to 1.0E12 cm^3 mol^{-1} s^{-1}.

The research group of Marshall(161,170-172) has recently studied a number of HSO_x reaction paths and thermodynamic properties. These systems include: H + SO_2 $\rightarrow$

HSO_2, $H + SO_2 \rightarrow HOSO$, $HOSO \rightarrow HSO_2$; characterization of $O(^1D) + H_2S$ pathways involving H_2SO, HOSH, and H_2OS; theoretical studies of the RSOO, ROSO, RSO_2 and HOOS (R = H, CH_3) radicals; characterization of $O(^3P) + H_2S$ transition states, and the enthalpy of formation of HSO and HOS.

QRRK analysis has been used by Westmoreland et al., Dean et al., and Bozzelli et al.(51,56,57,89,97,105-107,173) to analyze a number of chemical activation reaction systems involving hydrocarbon, chlorohydrocarbon, and nitrogen reaction systems. It is shown to yield results in good agreement with experimental data for these systems, and it provides a framework by which the effects of both temperature and pressure on the rate processes can be understood and evaluated.

In this study, we:

- assemble and evaluate thermodynamic properties ($\Delta H_{f,298}$, S_{298}, and C_p) related to the sulfur compound reaction systems from literature. When no literature data are available, semi-empirical molecular orbital calculations(80) are utilized.
- use modified quantum RRK calculations for k(E) and modified strong collision analysis for fall-off to treat the chemical activation systems:

$$HSO + O \leftrightarrow (HSO_2)^* \leftrightarrow (HOSO)^* \rightarrow \text{ products}$$

$$\hookrightarrow \text{ products}$$

$$H + SO_2 \leftrightarrow (HOSO)^* \rightarrow \text{ products}$$

$$OH + SO \leftrightarrow (HOSO)^* \rightarrow \text{ products}$$

$$H + SO_3 \leftrightarrow (HOSO_2)^* \rightarrow \text{ products}$$

$OH + SO_2 \leftrightarrow (HOSO_2)^* \rightarrow$ products

$H + HOSO \leftrightarrow (HOSHO)^* \rightarrow$ products

$OH + HSO \leftrightarrow (HOSHO)^* \rightarrow$ products

This analysis provides rate constants to stabilized adducts and products as functions of pressure (0.001 - 100 atm) and temperature (300 to 2000 K).

8.2 Thermochemistry

Thermodynamic properties ($\Delta H_{f,298}$, S_{298}, and C_p) are critically important for estimation of kinetic processes. They provide lower limits to reaction barriers and important information on A factors. They also provide a convenient way to determine reverse reaction rate constants using the calculated equilibrium constant and the known forward rate. Literature data on thermodynamic properties of species listed in Table G1 are reviewed. MOPAC(80) calculations for equilibrium geometries, vibrational frequencies and moments of inertia at the AM1(174) and PM3(175) levels are performed for HSO, HOS, HSO_2, HOSO, HOSH, H_2SO, HOSOH, HOSHO, and $HOSO_2$. Vibrational frequencies for normal coordinate analysis are determined on these species. Principles of statistical mechanics and the RRHO approximation were used to calculate entropies, S(298) and heat capacities, $C_p(T)$ for these molecules.

Thermodynamic properties of sulfur-containing compounds relating to this study are summarized in Table G1, but precise ΔH_f of several compounds are not well known and require some comment.

The enthalpies of formation for HSO and HOS radicals are somewhat controversial. Published evaluations for heat formation for HSO are -3,(176) and -5 ± 4 kcal/mol.(177) Davidson et al.(178) analyzed the results of their crossed molecular bean experiments to obtained ΔH^0_{f298} (HSO) = -1.4 ± 1.9 kcal/mol. Luke and McLean(179) determined the heats of formation of HSO and HOS to be -0.4 and -2.9 respectively using two independent *ab initio* methods. They also predicted that the HOS isomer is more stable by 3.1 kcal/mol than the HSO radicals. Melius(180) calculated ΔH^0_{f298}(HOS) and ΔH^0_{f298}(HSO) by the BAC-MP4 method to be -5.0 and -1.1 kcal/mol, respectively.

This result on the ΔH^0_f between HSO and HOS contrasts the theoretical calculations of Xantheas and Dunning, Jr.(181,182) These authors estimate the enthalpy of formation of HSO is -5.4 ± 1.3 kcal/mol through a series of multireference configuration interaction (MR-CI) calculations. Their computed result show that the HSO isomer is 5.4 kcal/mol more stable than HOS radical. Volpi et al.(183) determined the enthalpy of formation of HSO to be -0.9 ± 0.7 kcal/mol from the analysis of high resolution crossed beam reactive scattering experiments on the reaction $O + H_2S \rightarrow HSO + H$. Espinosa-Garcia and Corchado(184) determined the enthalpy of formation of HSO is -2.1 ± 0.9 kcal/mol using GAUSSIAN 90 system of programs. The latest theoretical values proposed by Marshall et al.(172) for $\Delta H_{f,298}$ of HSO and HOS are -4.75 and -1.31 kcal/mol, respectively. They characterized the transition states on the $O(^3P) + H_2S$ potential energy surface at MP2=FULL/6-31G(*d*) level. The above literature values show ΔH^0_f of HSO from -5.4 to -0.9 kcal/mol and of HOS from -0.5 to 4.5, respectively.

8.3 Kinetic Calculations

Kineticists are becoming increasingly aware of the necessity to properly treat the pressure-dependence of simple dissociation and combination reactions in combustion systems. These reactions are not simple one-step processes. A bimolecular combination reaction, forms an energized (chemically activated) adduct which can: be stabilized through collisions with the bath gas, dissociate to products, isomerize, or dissociate back to reactants before stabilization occurs. The effect of pressure can be understood by realizing that the stabilization rate is a function of bath gas pressure. Increased pressure, results in increased stabilization rates and this can consequently decrease reaction of the energized adduct to product or back to reactant. In general one can expect adduct stabilization to dominate at high pressures and dissociation of the adduct to be more important at low pressure or high temperatures. Decrease of stabilization with temperature increase is understood by realizing that rates of dissociation of the adduct are often highly energy dependent (E_a) and increase exponentially with temperature. Stabilization rates decrease at high temperatures because the bath gas molecules have more internal energy and thus remove less energy from the adduct per collision.

The scheme of bimolecular chemically activated reactions is illustrated as Figure 8.2. where ABCD* is an activated complex which formed directly by the reactants, and $ABCD^{o}$ is its stabilized adduct. The ABCD* can dissociate to products or react back to reactants, isomerize to BCDA* and other complexes, or be stabilized. The isomers can also be collisionally stabilized, or dissociate to products.

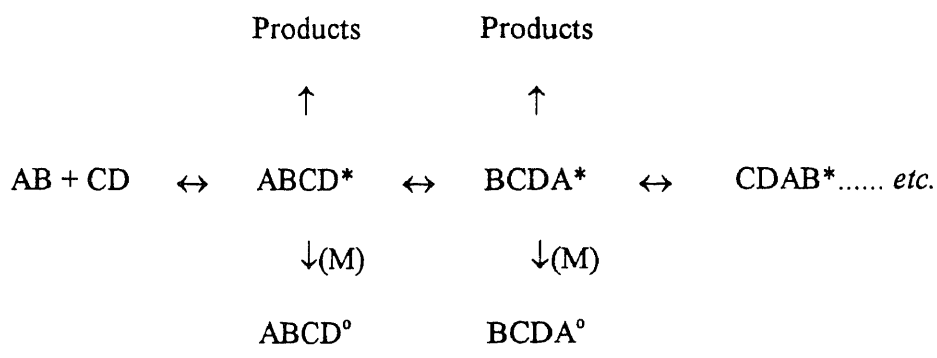

Figure 8.2 The Scheme of Bimolecular Chemically Activated Reactions

Quantum RRK analysis, as initially published by Dean,(67,68) and recently modified by Chang et. al.(74) is used to compute apparent rate constants over a wide range of temperature and pressure. Branching ratios of bimolecular combinations at different temperatures and pressures are calculated using modified computer code "CHEMACT".(68) This code uses the quantum version of RRK theory (QRRK) to evaluate the rate constants, k(E) as functions of temperature. The modified strong collision theory of Gilbert, Luther, and Troe(75) is used to calculate the fall-off pressure dependencies.

Modifications to the quantum RRK(74) calculation of ref. 67 include:

- Use of reduced set of 3 vibrational frequencies for describing the energy distribution and the 3 frequencies plus one external rotation to calculate the density of states, $\rho(E)/Q$.
- The F_E factor is now calculated for use in determining the collision efficiency β_c,(75) in place of the previously assigned 1.15 value.

- β_c is now calculated by : $\beta_c = (\alpha_c /(\alpha_c + F_E*k*T))^2/\Delta$ from Gilbert et. al. Eqn. 4.7,(75) $\Delta = \Delta_1 - (F_E*k*T)/(\alpha_c + F_E*k*T)*\Delta_2$. Where Δ_1 and Δ_2 are temperature-dependent integrals involving the density of states, and α_c is the average energy of down-collisions.
- The Lennard-Jones collision frequency Z_{LJ} is now calculated by $Z_{LJ} \equiv Z\ \Omega^{(2,2)}$ integral.,(76-78) Ω is obtained from fit of Reid et al.(78)

Input information requirements for QRRK calculations :

Three frequencies and the associated degeneracies are computed from fits to the temperature-dependent heat capacity data, as described by Ritter,(72,73) and Bozzelli et al.(108) These have been shown by Ritter to accurately reproduce molecular heat capacities and vibrational state densities. This approach represents an improvement over the single geometric mean frequency used earlier(67) and offers the advantage of avoiding the specification of the complete frequency distribution of the adduct. We believe that this three-frequency model provides a suitable approach to analyze both unimolecular fall-off and bimolecular chemical activation reactions. Lennard-Jones parameters (σ, e/k) were obtained from tabulations(78) and from a calculation method based on molar volumes and compressibility.(109)

Arrhenius A-factors for the bimolecular combination and addition reactions at the high pressure limit are obtained from literature, or estimated from well studied generic reactions of iso-electronic species. Activation energy (E_a) for combination reactions is set to 0.0. E_a's for addition reactions are evaluated from literature. A and E_a for unimolecular isomerization reactions are determined using Transition State theory(25) with the

appropriate thermodynamic parameters. Kinetic parameters for dissociation to reactants and products are obtained from application of microscopic reversibility. The input parameters listed in Table 8.2 - 8.4 use the form $k(T) = AT^n \exp(-\alpha T) \exp(-E_a/RT)$; this was chosen to more accurately fit the A factor component of the rate constant over the wide temperature range.

Complete details of the high pressure limit rate constants, vibration frequencies, Lennard-Jones parameters, β and ΔE_{avg}, literature references for the systems in this study are included in Table G2 - G4. Accurate high pressure limit rate constants and thermodynamic property parameters are very important to accuracy of the calculated rate constants.

8.4 Results and Discussion

8.4.1 HSO + O, H + SO_2, and OH + SO Reactions

Input parameters for the QRRK calculations and a potential energy diagram of HSO + O , H + SO_2, and OH + SO reactions are illustrated in Table G2 and Figure G1, respectively. The input parameters for dissociation of the complexes, see Table G2, are referenced to the ground state of the complexes. The input high pressure limit rate constant for O + HSO $\rightarrow$ HSO_2 is considered as the same as O atm combination to a large hydrocarbon radical, A ~ 6.0E13 cm^3 mol^{-1} s^{-1}, Ea = 0.0 kcal/mol.(148) The high pressure limit A factor for $HSO_2 \rightarrow H + SO_2$ is from the reverse reaction H + SO_2 and microscopic reversibility (MR). We estimate the A factor of H + SO_2 as H atom addition to unsaturated bond of an olefin hydrocarbon, A = 1.3E13 cm^3 mol^{-1} s^{-1}.(148) E_a for $HSO_2 \rightarrow H + SO_2$ is 9.5

kcal/mol from the *ab initio* calculations of Binns and Marshall.(161) HSO_2 intramolecular isomerization to HOSO is calculated via the reverse reaction HOSO $\rightarrow$ HSO_2 and (MR). A for HOSO isomerization to HSO_2 is from transition state theory(25) (three-member cyclic intermediate) loss of 1 rotor, $\Delta S^{\ddagger} = -4.3$ cal mol^{-1} K^{-1}. The energy barrier relative to HOSO is from calculations of Binns and Marshall,(161) 55.0 kcal/mol. This is similar to that predicted for the isomerization of HSO to HOS from Plummer.(185) The rate constant of HOSO $\rightarrow$ O + HOS is evaluated from the reverse reaction O + HOS and microscopic reversibility, where the A factor for O + HOS is assigned as O + HSO. The A factor for OH + SO $\rightarrow$ HOSO is taken one half of OH addition to C_2H_4, due to degeneracy of 2 for OH + C_2H_4. An unusual large energy barrier of 22.7 kcal/mol for H + SO_2 $\rightarrow$ HOSO is proposed by Binns and Marshall(161) from MP2/3-21G(*) level calculations. They checked the transition state geometry at level, PMP4/6-31G*, to support that the geometry is indeed reliable. In our calculations we allow the barriers for $HSO_2 \rightarrow H + SO_2$ and HOSO $\rightarrow$ H + SO_2 to vary over the range 5.0 - 9.5 and 10.5 - 22.7 kcal/mol, respectively. The results of these calculations at 1 atm show that total rate and the rate constants for the major channels, H + SO_2 and OH + SO, change less than $\pm 1.0\%$ over these range of barrier heights.

8.4.1.1 HSO + O - The oxygen atom bonds to the sulfur atom of the HSO radical to form an energized adduct HSO_2*, which can be collisionally stabilized, dissociate to H + SO_2 product, react back to reactants (O + HSO), or undergo intramolecular isomerization via H atom shift before stabilization to a second energized adduct HOSO*. HOSO* can be

stabilized, dissociate to O + HOS, OH + SO and H + SO_2 product channels, or isomerize back to HSO_2. Thermodynamic analysis shows that H + SO_2 and OH + SO are the lower energy bimolecular products while HOSO is the lowest enthalpy adduct.

We calculate that the major reaction pathway of HSO + O is to H + SO_2 via HSO_2 adduct. The fractional of HSO_2* that isomerizes to HOSO* also decomposes to H + SO_2. This H + SO_2 is the major product channel for O + HSO, because it is lower in energy than other bimolecular products, and its formation has a lower barrier than HOSO along with a higher A factor (looser transition state).

Figure G2 shows the rate constants for HSO + O $\rightarrow$ products as a function of 1000/T at 1 atmosphere pressure. H + SO_2 is the primary channel over a wide temperature range, 300 - 2000 K; OH + SO is second in importance. At temperatures above 800 K, the rate constant of H + SO_2 channel falls off slightly, while OH + SO and the dissociation of the complex back to reactants, HSO + O, increase in importance. OH + SO and reverse reaction HSO + O compete with the H + SO_2 product channel at temperatures near 2000 K. The stabilization channels HSO_2, HOSO, as well as the HOS + O product set, are lower in significance under these conditions.

Plots of rate constants versus pressure at 300 K and 1500 K for the major product channels H + SO_2, OH + SO and the reverse reaction HSO + O are shown in Figure G3. In this Figure, effectively no pressure dependence is observed for reaction at 1500 K in the pressures 10^{-3} - 10^{2} atm, while shows slightly negative pressure dependence in the pressures above 10 atm at 300K.

8.4.1.2 H + SO_2 - There are two sites for H addition to SO_2, addition to the S atom and to the O atom. Figure G1 shows that H atom addition to the O atom of SO_2 results in an adduct (HOSO) with a lower energy than addition to the S atom. The isomerization of HSO_2 to HOSO is 13.5 kcal/mol higher than dissociation of $HSO_2 \rightarrow H + SO_2$, while the barrier of HOSO $\rightarrow HSO_2$ is 6.3 kcal/mol higher than HOSO dissociation to H + SO_2. This isomerization between HSO_2* and HOSO* is therefore less important than dissociation back to the reactants (H + SO_2). Calculation results at 1 atm are illustrated in Figure 8.4 and show that reverse reaction H + SO_2 is most important above 650 K, while HOSO stabilization and H + SO_2 rates are comparable at lower temperatures. The production of OH + SO increases in importance above 400 K, and is second in dominance above 700 K. The product channels O + HOS and O + HSO are less important.

Figure G5 shows the rate constants as a function of pressure for important product channels, HOSO, OH + SO, and reverse reaction to H + SO_2 at 300 and 1000 K. Dissociation back to reactants (H + SO_2) is most important and independent of pressure below 1 atm at 300 K and independent on pressure over a wide pressure range (10^{-3} - 10^{2} atm) at 1000 K. HOSO stabilization is next in importance and is near high pressure limit at 10 atm, 300 K, but it is still in the falloff regime at 100 atm and 1000 K.

8.4.1.3 OH + SO - OH addition to SO forms the HOSO* adduct. An Arrhenius plot for the reaction channels of OH + SO at 1 atm is shown in Figure G6. Dissociation to HOS + O and HSO + O are low in importance over a wide temperature range 300 - 2000 K, due to their high dissociation barriers relative to the reaction channels OH + SO and H + SO_2.

Reverse reaction to OH + SO is the dominant channel in all temperature, while dissociation to H + SO_2 is next in importance.

Figure G7 shows the apparent rate constants versus pressure for HOSO stabilization, H + SO_2, and OH + SO at 300 and 1000 K. HOSO* dissociation back to OH + SO is most important and shows no pressure dependence above 1 atm at 300 K and over the pressure range 10^{-3} - 10^{2} atm at 1000 K. Stabilization of HOSO is next in importance above 10 atm at 300 K, and it is still in fall-off regime at 100 atm in the temperatures of 300 and 1000 K. H + SO_2 is next in importance below 1 atm at 300 K, and below 0.03 atm at 1000 K.

8.4.1.4 HSO_2 - The product channels of HSO_2 unimolecular dissociation are H + SO_2, HSO + O, and HOSO. We treat the isomerization to HOSO as a product channel, because we do not consider multi-wells in our analysis for unimolecular dissociation. Figure G8 illustrates an Arrhenius plot at 1 atm for HSO_2 unimolecular dissociation. H + SO_2 is most important in the temperatures 300 -2000 K, with isomerization to HOSO next in importance.

Figure G9 shows the rate constants versus pressure for H + SO_2 and HOSO at 300 and 1500 K. Rate constants of both channels are observed to increase with pressure. H + SO_2 is predicted to be dominant at 300 and 1500 K over the pressures 10^{-3} - 10^{2} atm.

8.4.1.5 HOSO - The Arrhenius plot at 1 atm for HOSO unimolecular dissociation is shown in Figure G10. H + SO_2 still dominates at temperatures 300 -2000 K, with OH + SO next in importance.

Figure G11 illustrates the effect of pressure for H + SO_2, OH + SO, and HSO_2 at 300 and 1500 K. H + SO_2 is observed to be most important.

8.4.2 H + SO_3 and OH + SO_2 Reactions

A potential energy diagram and input parameters for chemically activated reactions, H + SO_3 and OH + SO_2, are illustrated in Figure G12 and Table G3, respectively. The high pressure limit A factor for bimolecular reaction, OH + SO_2 → $HOSO_2$, is taken from the recommended data of Atkinson et al.,(188) with E_a ~ 0.0 kcal/mol. The high pressure limit A factor for $HOSO_2$ → O + HOSO is from the reverse reaction O + HOSO, thermodynamics and microscopic reversibility <MR>. We estimate the A factor of O + HOSO as O atm combination to a large hydrocarbon radical, A ~ 9.6E13 cm^3 mol^{-1} s^{-1}, Ea = 0.0 kcal/mol.(148) The high pressure limit A factor for $HOSO_2$ → H + SO_3 is from the reverse reaction H + SO_3, thermodynamics and microscopic reversibility <MR>. We estimate the A factor of H + SO_3 as H atom addition to unsaturated bond of hydrocarbon, A = 3.0E13 cm^3 mol^{-1} s^{-1}.(148) E_a for H + SO_3 is estimated to be 3.0 kcal/mol.(189)

8.4.2.1 OH + SO_2 - The relative shallow well for this HO-SO_2 adduct (~ 31 kcal/mol) makes all of the channels to products at least 20 kcal/mol higher in energy than dissociation back to reactants. An Arrhenius plot for OH addition to SO_2 at 1 atm is

shown in Figure G13. Stabilization is most important below 650 K, with dissociation back to OH + SO_2 next in importance, above that OH + SO_2 is observed to dominate. Dissociation to H + SO_3 and O + HOSO is low in importance.

Figure G14 illustrates the pressure effect for $HOSO_2$ and OH + SO_2 at 300 and 1000 K. Stabilization is the dominant channel above 0.03 atm, and is near the high pressure limit at 3 atm. Dissociation back to OH + SO_2 increases in importance with temperature increase and pressure decrease. At 1000 K, OH + SO_2 is predicted to be most important below 12.5 atm.

8.4.2.2 H + SO_3 - H addition to SO_3 forms an energized $HOSO_2$* adduct. The initial H-OSO_2 adduct energy is about 20 kcal/mol higher in energy than in the OH + SO_2 case. This causes higher fractions of the energized adduct to dissociate into OH + SO_2 rather than to reactants. Figure G15 shows rate constants versus temperature at 1 atmosphere pressure. OH + SO_2 is predicted to dominance over the temperature range 300 - 2000 K. Stabilization is second in importance below 1400 K. Dissociation back to H + SO_3 increases with temperature, and competes with stabilization near 1400 K.

The pressure effect for $HOSO_2$, H + SO_3, and OH + SO_2 at 300 and 1000 K is illustrated in Figure G16. OH + SO_2 is most important at pressures 10^{-3} - 10^{2} atm, and little pressure dependence is observed below 10 atm in both temperatures.

8.4.3 H + HOSO and OH + HSO Reactions

Input parameters on H + HOSO and OH + HSO for QRRK calculations and a potential energy diagram are illustrated in Table G4 and Figure G17, respectively. The high pressure limit rate constant for H + HOSO is considered as that H atom combination with large radicals, A = 1.0E14 cm^3 mol^{-1} s^{-1}, Ea = 0.0 kcal/mol.(148) The high pressure limit rate constant for HOSHO → OH + HSO is from the reverse reaction OH + HSO and microscopic reversibility <MR>. We estimate the A factor of OH + HSO as OH combination with a large radical, A ~ 2.7E13 cm^3 mol^{-1} s^{-1}, E_a = 0.0 kcal/mol.(148) The high pressure limit A factor for HOSHO → H_2O + SO is calculated from Transition State Theory, $\Delta S^{\ddagger}$ = -4.3 cal mol^{-1} K^{-1}. The energy barrier is considered as that of H_2O elimination from alcohol, $E_a = \Delta H_{rxn}$ + 47 kcal/mol, see Table G4.

8.4.3.1 OH + HSO - Figure G18 shows the rate constants versus temperature for the various reaction channels at 1 atm. Dissociation back to OH + HSO dominates from 300 to 2000 K, and stabilization is next in importance below 750 K. H_2O elimination plus SO increases with temperature, and becomes second in importance above 750 K.

Figure G19 shows the rate constants as a function of pressure for HOSHO, H_2O + SO, H + HOSO, and reverse reaction to OH + HSO at 300 and 1000 K. At 300 K, stabilization is most important above 2.5 atm, with dissociation back to OH + HSO next in importance. Below 2.5 atm, OH + HSO is observed to be the dominant channel. At 1000 K, dissociation back to OH + HSO dominates at pressures 10^{-3} - 10^{2} atm, with H_2O + SO next in importance.

8.4.3.2 H + HOSO - Figure G20 shows rate constants versus temperature at 1 atm. OH + HSO is most important at temperatures 300 - 2000 K, with stabilization next in importance below 600 K. H_2O + SO increases in importance with increasing temperature, and becomes second in importance above 650 K. Reverse dissociation to H + HOSO is also observed to increase in importance with temperature, and competes with H_2O + SO above 850 K.

Figure G21 illustrates the rate constants of the reaction channels versus pressure at 300 and 1500 K. At 300 K, stabilization is most important at relatively high pressure, $P >$ 35 atm, with OH + HSO next in importance. Below 35 atm, OH + HSO is predicted to be the dominant channel at 300 K, and observed to be near constant and similar to the 1000 K data below 6 atm.

Apparent rate constants for reactions : HSO + O, H + SO_2, OH + SO, H + SO_3, OH + SO_2, H + HOSO, OH + HSO to product channels and the dissociation of the stabilized adducts in N_2 bath gas are calculated and listed in Table G5. The calculations serve as useful estimates for rate constants and reaction paths in combustion and atmospheric kinetic modeling, where the experimental data are not available.

8.4 Conclusions

The various reaction channels of reaction : HSO + O, H + SO_2, OH + SO, H + SO_3, OH + SO_2, H + HOSO, and OH + HSO have been treated by using quantum Rice-Ramsperger-Kassel theory for k(E) and with modified strong collision approach for fall-off in

temperature range 300 - 2000 K and in pressure range 0.001 - 100 atm. The thermodynamic properties related to this reaction system have been evaluated and tabulated. The input high pressure limit rate constants for the reaction channels are obtained from literature, or estimated from well studied generic reactions.

The thermodynamic properties related to these reaction systems have been evaluated. The addition reactions of HSO + O, H + SO_2 and the combination reaction of OH + SO have been treated by using quantum Rice-Ramsperger-Kassel theory for determination of rate constants over 300 - 2000 K, and 0.001 - 100 atm. Thermodynamic analysis shows that H + SO_2 and OH + SO are the low energy bimolecular products, while HOSO is the lowest enthalpy adduct.

HSO_2 - Results of HSO + O reactions at 1 atm show that production of H + SO_2 is the dominate channel over 300 - 2000 K; the OH + SO product channel is next in importance. At temperatures above 800 K, the rate constant to H + SO_2 falls off, while reaction to OH + SO and dissociation of the complex to HSO + O increase in importance. Effectively no pressure dependence is observed for reaction at 1500 K, 10^{-3} - 10^{2} atm. Calculation results for H + SO_2 at 1 atm show that reverse reaction H + SO_2 is most important above 650 K, while HOSO stabilization and H + SO_2 rates are comparable at lower temperatures. The production of OH + SO increases in importance above 400 K, and is second in dominance above 700 K. The HOSO* complex from OH + SO dissociates back to OH + SO as the dominant channel at 1 atm, while dissociation to H + SO_2 is next in importance. H + SO_2 is observed to be most important product in the

unimolecular dissociation of HSO_2 and HOSO at 300 -2000 K over the pressures 10^{-3} - 10^2 atm.

HSO_3 - Calculation results of OH + SO_2 predict that stabilization is most important below 650 K, with dissociation back to OH + SO_2 next in importance, above that OH + SO_2 is observed to dominate. In H + SO_3 reactions, . OH + SO_2 is predicted to be the dominant channel over the temperature range 300 - 2000 K. Stabilization is second in importance below 1400 K. Dissociation back to H + SO_3 increases with temperature, and competes with stabilization near 1400 K.

H_2SO_2 - Results of OH + HSO indicate that reverse reaction; dissociation to OH + HSO, dominates at 300 - 2000 K, and stabilization is predicted next in importance below 750 K. H_2O elimination plus SO increases with temperature, and becomes second in importance above 750 K. In the H + HOSO reaction system, OH + HSO is most important between 300 to 2000 K, with stabilization next in importance below 600 K. H_2O + SO increases in importance with temperature, and becomes second in importance above 650 K. Reverse dissociation to H + HOSO is also observed to increase with temperature, and competes with H_2O + SO above 850 K.

Apparent rate constants for the reactions to various product channels and the dissociation of the stabilized adducts in argon bath gas are calculated. The calculations serve as useful estimates for rate constants and reaction paths in combustion and atmospheric kinetic modeling, where experimental data are not available.

APPENDIX I

TABLES

Table A1 Average Retention Time
Column 1: 1.5 m length x 2.16 mm I.D.; 1% AT-1000 on Graphpac GB
Detector: Flame Ionization Detector (270 °C)
Oven Temperature : 45 °C (hold 5 min.), 15 °C/min. to 220 °C (hold 22 min.)
Carrier Gas : Helium (35 ml/min.)

Compound	Average Retention Time (min.)
CH_4	1.32
C_2H_2	1.88
C_2H_4	2.22
C_2H_6	2.68
CH_3Cl	4.32
C_2HCl	7.02
C_3H_6 or C_3H_8	7.55
C_2H_3Cl	9.02
C_2H_5Cl	10.20
CH_2Cl_2	11.35
C_4H_{10}	13.16
CH_2CCl_2	13.90
CH_3CHCl_2	14.10
CHClCHCl	15.35
$CHCl_3$	17.09
CH_3CCl_3	17.42
CCl_4	17.90
C_2HCl_3	19.60
C_6H_6	20.86

Column 2: 1.7 m length x 2.16 mm I.D.; Carbosphere 80/100 mesh
Detector: Flame Ionization Detector (270 °C); Oven Temperature: 70 °C
Carrier Gas: Helium (30 ml/min.)

Compound	Average Retention Time (min.)
CO	1.62
CH_4	2.98
CO_2	6.95

Table A2 Relative Response Factor of Several Compounds
First Flame Ionization Detector

Compound	Relative Response Factor (RRF)
Methane	1.00
Acethylene	1.85
Ethylene	2.00
Ethane	2.15
Chloromethane	1.02
Propyne	3.33
Propene	3.45
Vinyl Chloride	1.93
Dichloromethane	0.98
1,1-Dichloroethylene	1.88
1,1,1-Trichloroethane	1.85
Chloroform	0.97
Tetrachlorocarbon	0.90
1,1,2-Trichloroethane	2.10

Second Flame Ionization Detector

Compound	Relative Response Factor (RRF)
Methane	1.00
Carbon monoxide	1.01
Carbon dioxide	0.96

Table A3 Material Balance for 100 Moles Carbon
Residence Time : 1.0 second
in CH_2Cl_2 : CH_4 : O_2 : Ar = 1 : 1 : 4 : 94

	Temperature (°C)								
Species	680	700	720	740	760	780	800	820	840
CH_4	49.13	49.01	48.92	46.47	45.21	41.45	35.54	29.83	21.53
C_2H_2	0.01	0.03	0.08	0.19	0.52	1.27	2.78	3.92	0.39
C_2H_4	0.02	0.03	0.07	0.11	0.21	0.37	0.50	0.55	0.03
CH_3Cl	0.15	0.21	0.48	0.72	1.53	2.29	2.36	1.49	-
CHCCl	-	-	-	-	0.15	0.25	0.40	0.23	-
C_2H_3Cl	0.11	0.17	0.39	0.68	1.21	1.73	1.64	0.82	-
CH_2Cl_2	47.70	46.53	44.42	37.38	26.67	14.44	3.44	0.51	0.11
CH_2CCl_2	-	-	-	-	0.12	0.25	0.58	0.65	-
CHClCHCl	0.12	0.23	0.53	0.78	1.30	1.70	1.42	0.51	-
C_2HCl_3	0.23	0.50	1.06	1.63	2.76	3.34	2.19	0.70	-
CO	0.73	0.87	1.85	3.64	8.15	15.00	27.25	39.17	71.06
CO_2	0	0.05	0.08	0.18	0.64	1.41	2.21	4.05	10.97
Total	98.21	97.66	97.89	91.83	88.51	83.53	80.34	82.49	104.10

Table A4 Material Balance for 100 Moles Carbon
Residence Time : 1.0 second
in CH_2Cl_2 : O_2 : Ar = 1 : 4 : 95

	Temperature (°C)							
Species	680	700	720	740	760	780	800	820
C_2H_2	-	-	0.04	0.11	0.35	0.85	0.37	0.04
C_2H_4	0.03	-	-	-	-	-	-	-
CH_3Cl	0.16	0.32	0.61	1.08	1.80	-	-	-
CHCCl	-	-	-	0.16	0.43	-	-	-
C_2H_3Cl	-	-	-	0.14	0.26	-	-	-
CH_2Cl_2	93.33	91.44	89.08	69.82	39.56	3.42	0.23	-
CH_2CCl_2	-	-	-	0.33	0.18	-	-	-
CHClCHCl	0.55	2.02	2.49	4.03	7.22	-	-	-
C_2HCl_3	0.54	1.40	3.20	5.47	9.75	1.53	-	-
CO	1.09	1.92	4.24	8.70	20.93	63.91	70.88	72.55
CO_2	-	-	0.37	0.48	1.99	7.96	8.77	13.54
Total	95.72	97.11	100.06	90.31	82.48	77.69	80.25	86.14

Table A5 Material Balance for 100 Moles Carbon
Residence Time : 1.0 second
in CH_2Cl_2 : CH_4 : Ar = 1 : 1 : 98

	Temperature (°C)								
Species	680	700	720	740	760	780	800	820	840
CH_4	49.79	50.11	49.79	48.30	47.73	45.78	44.14	39.25	37.32
C_2H_2	-	0.02	0.05	0.11	0.30	0.76	1.87	3.25	5.26
C_2H_4	0.06	0.12	0.20	0.34	0.52	0.80	1.18	1.45	1.79
CH_3Cl	0.34	0.45	0.75	1.29	2.25	3.35	4.29	4.27	4.10
CHCCl	-	-	-	-	0.13	0.25	0.41	0.64	0.85
C_2H_3Cl	0.07	0.12	0.25	0.46	0.88	1.30	1.60	1.36	0.75
CH_2Cl_2	47.37	47.70	43.85	40.91	35.43	26.16	14.08	7.51	3.13
CH_2CCl_2	-	-	-	0.06	0.10	0.14	0.22	0.27	0.36
CHClCHCl	0.18	0.29	0.54	0.91	1.42	1.89	2.17	2.00	1.41
C_2HCl_3	0.12	0.25	0.52	0.85	1.64	2.36	2.65	2.29	1.52
Total	48.97	49.53	47.98	46.61	45.22	41.46	36.37	31.46	28.69

Table A6 Material Balance for 100 Moles Carbon
Residence Time : 1.0 second
in CH_2Cl_2 : Ar = 1 : 99

	Temperature (°C)								
Species	680	700	720	740	760	780	800	820	840
C_2H_2	-	0.02	-	0.11	0.23	0.53	1.34	2.44	3.44
C_2H_4	-	0.02	-	0.05	0.02	0.07	0.09	0.03	0.00
CH_3Cl	0.51	0.79	1.33	2.25	3.65	4.53	5.82	5.20	3.70
CHCCl	-	-	-	-	0.23	0.52	1.72	4.71	5.71
C_2H_3Cl	-	0.13	0.24	0.41	0.60	0.77	0.76	0.19	-
CH_2Cl_2	94.49	93.93	87.32	77.93	62.47	33.94	10.00	2.00	-
CH_2CCl_2	-	-	-	0.08	0.21	0.19	0.42	0.47	0.33
CHClCHCl	0.40	0.76	1.41	2.42	3.96	5.24	5.03	1.54	0.30
C_2HCl_3	0.38	0.71	1.44	2.88	5.33	8.06	8.73	6.52	4.18
Total	95.78	96.37	91.73	86.12	76.71	53.86	33.93	23.11	17.65

Table B1 Detailed Mechanism for $CH_2Cl_2/CH_4/O_2/Ar$ Reaction System

Pyrolysis

Reactions	A[a]	n	E_a[b]	source
1. CH3Cl = CH3 + Cl	4.52E30	-14.86	85930	1
2. CH3Cl = [1]CH2 + HCl	1.17E20	-2.68	107000	1
3. CH3Cl + H = CH3 + HCl	3.72E13	0.00	7600	2
4. CH3Cl + Cl = CH2Cl + HCl	3.20E13	0.00	3100	3
5. CH3Cl + Cl = CH3 + Cl2	1.00E14	0.00	25000	2
6. CH3Cl + CH3 = CH4 + CH2Cl	3.31E11	0.00	9400	2
7. CH2Cl2 = [1]CHCl + HCl	2.64E32	-5.67	77930	1
8. CH2Cl2 = CH2Cl + Cl	4.71E35	-6.31	83580	1
9. CH2Cl2 + H = CH2Cl + HCl	1.08E13	0.00	6100	2
10. CH2Cl2 + Cl = CHCl2 + HCl	5.00E13	0.00	2900	2
11. CH2Cl2 + Cl = CH2Cl + Cl2	1.00E14	0.00	21400	2
12. CH2Cl2 + CH3 = CH4 + CHCl2	6.76E10	0.00	7200	2
13. CH2Cl2 + CH3 = CH3Cl + CH2Cl	6.30E11	0.00	15500	4
14. CHCl3 = CHCl2 + Cl	1.03E34	-6.19	78820	1
15. CHCl3 = [1]CCl2 + HCl	7.95E32	-5.96	60060	1
16. CHCl3 + CH3 = CH3Cl + CHCl2	9.45E11	0.00	13000	5
17. CHCl3 + H = CHCl2 + HCl	8.34E12	0.00	5600	6
18. CHCl3 + CH3 = CCl3 + CH4	1.90E10	0.00	5800	2
19. CHCl3 + Cl = CCl3 + HCl	1.60E13	0.00	3300	7
20. CHCl3 + Cl = Cl2 + CHCl2	1.00E14	0.00	21000	2
21. CH2Cl + CH2Cl = CH2ClCH2Cl	5.74E42	-9.77	7242	8
22. CH2Cl + CH2Cl = CH2ClCH2 + Cl	7.69E13	-0.33	2313	8
23. CH2Cl + CH2Cl = C2H3Cl + HCl	4.21E22	-3.02	3780	8
24. CH2Cl + CHCl2 = CH2ClCHCl2	7.64E44	-10.57	8059	8
25. CH2Cl + CHCl2 = CH2ClCHCl + Cl	1.24E18	-1.80	3418	8
26. CH2Cl + CHCl2 = CHClCHCl + HCl	7.40E20	-2.57	4594	8
27. CH2Cl + CHCl2 = CHCl2CH2 + Cl	1.78E15	-0.88	3753	8

Table B1 (cont'd)

Reactions	A[a]	n	E_a[b]	source
28. CH2Cl + CHCl2 = CH2CCl2 + HCl	6.10E18	-2.20	4375	8
29. CH2Cl + CH3 = C2H5Cl	1.62E43	-9.89	7545	8
30. CH2Cl + CH3 = C2H4 + HCl	4.26E19	-2.02	3623	8
31. CH2Cl + CH3 = C2H5 + Cl	2.68E14	-0.57	2395	8
32. CHCl2 + CH3 = CH3CHCl2	7.64E42	-9.99	6858	8
33. CHCl2 + CH3 = C2H3Cl + HCl	3.98E19	-2.08	3256	8
34. CHCl2 + CH3 = CH3CHCl + Cl	1.31E16	-1.08	2172	8
35. CHCl2 + CHCl2 = CHCl2CHCl2	8.01E42	-9.80	8453	8
36. CHCl2 + CHCl2 = CHCl2CHCl + Cl	5.57E19	-2.23	7239	8
37. CHCl2 + CHCl2 = C2HCl3 + HCl	2.17E17	-1.45	6409	8
38. CHCl + CHCl = CHClCHCl	2.68E26	-5.51	3000	8
39. CHCl + CHCl = C2HCl + HCl	1.33E14	-0.56	470	8
40. CHCl + CHCl = CHCHCl + Cl	9.03E10	0.41	-240	8
41. CHCl + CH4 = C2H5Cl	1.09E36	-7.75	7555	8
42. CHCl + CH4 = C2H5 + Cl	6.82E08	1.07	6880	8
43. CHCl + CH4 = C2H4 + HCl	1.82E14	-0.62	3910	8
44. CHCl + CH2Cl2 = CH2ClCHCl2	1.18E36	-7.95	8089	8
45. CHCl + CH2Cl2 = CH2CCl2 + HCl	4.26E13	-0.71	4680	8
46. CHCl + CH2Cl2 = CHCl2CH2 + Cl	1.25E06	1.85	4420	8
47. CHCl + CH2Cl2 = CHClCHCl + HCl	1.91E14	-0.72	4690	8
48. CHCl + CH2Cl2 = CH2ClCHCl + Cl	5.32E08	0.99	3782	8
49. C2H5Cl = C2H4 + HCl	6.03E27	-4.49	61920	1
50. C2H5Cl = C2H5 + Cl	7.62E49	-10.97	91555	1
51. CH3CHCl2 = C2H3Cl + HCl	5.45E33	-6.28	61500	1
52. CH3CHCl2 = CH3CHCl + Cl	5.59E49	-10.98	84643	1
53. CH2ClCH2Cl = C2H3Cl + HCl	1.61E20	-2.20	57512	1
54. CH2ClCH2Cl = CH2ClCH2 + Cl	1.36E39	-7.59	84586	1
55. CH2ClCHCl2 = CH2ClCHCl + Cl	9.45E51	-11.62	82821	1

Table B1 (cont'd)

Reactions	A[a]	n	E_a[b]	source
56. CH2ClCHCl2 = CHClCHCl + HCl	1.36E30	-5.19	59759	1
57. CH2ClCHCl2 = CH2CCl2 + HCl	6.75E31	-5.91	63367	1
58. CH2ClCHCl2 = CHCl2CH2 + Cl	5.81E53	-12.05	88114	1
59. CHCl2CHCl2 = C2HCl3 + HCl	9.81E15	-0.82	59854	1
60. CHCl2CHCl2 = CHCl2CHCl + Cl	1.92E36	-6.81	77946	1
61. CH3CHCl = C2H3Cl + H	2.54E13	0.00	46360	1
62. CH2ClCH2 = C2H4 + Cl	1.90E35	-7.56	24900	1
63. CH2ClCHCl = C2H3Cl + Cl	5.36E37	-8.30	27077	1
64. CHCl2CH2 = C2H3Cl + Cl	1.48E25	-4.67	20717	1
65. CH3CCl2 = CH2CCl2 + H	2.08E13	0.0	40900	1
66. CHCl2CHCl = CHClCHCl + Cl	3.84E35	-7.66	23308	1
67. CH2ClCCl2 = CH2CCl2 + Cl	3.13E37	-8.13	27055	1
68. C2H3Cl = C2H2 + HCl	7.64E33	-6.30	72516	1
69. C2H3Cl = C2H3 + Cl	5.15E45	10.01	100436	1
70. C2H3Cl + CH3 = C2H3 + CH3Cl	3.15E11	0.00	24800	9
71. C2H3Cl + Cl = CHCHCl + HCl	5.00E13	0.0	7000	10
72. C2H3Cl + Cl = CH2CCl + HCl	3.00E13	0.00	5500	10
73. C2H3Cl + H = C2H3 + HCl	1.00E13	0.0	6500	11
74. C2H3Cl + H = CH2ClCH2	8.25E09	-0.10	3524	8
75. C2H3Cl + H = C2H4 + Cl	2.92E13	-0.09	5900	8
76. CH2CCl2 = C2HCl + HCl	2.62E30	-5.13	76515	1
77. CH2CCl2 = CH2CCl + Cl	4.41E49	-10.88	95808	1
78. CH2CCl2 + H = CH2CCl + HCl	1.20E13	0.00	5500	12
79. CH2CCl2 + H = CHCl2CH2	7.43E14	-1.19	6087	12
80. CH2CCl2 + H = C2H3Cl + Cl	4.63E14	-0.56	7257	12
81. CH2CCl2 + H = CCl2CH + H2	1.58E13	0.00	6000	13
82. CH2CCl2 + CH3 = CH2CCl + CH3Cl	6.30E11	0.00	21500	14
83. CH2CCl2 + Cl = CCl2CH + HCl	2.00E13	0.00	7000	15

Table B1 (cont'd)

Reactions	A[a]	n	E_a[b]	source
84. CHClCHCl = C2HCl + HCl	4.79E27	-4.27	74528	1
85. CHClCHCl = CHCHCl + Cl	2.81E48	-10.79	97688	1
86. CHClCHCl + HCl = CH2CCl2 + HCl	1.45E03	2.71	49060	8
87. CHClCHCl + HCl = CHCl2CH2 + Cl	7.78E20	-1.93	69776	8
88. CHClCHCl + HCl = CH2ClCHCl + Cl	6.77E18	-1.45	64960	8
89. CHClCHCl + H = CHCHCl + HCl	1.20E13	0.00	6000	15
90. CHClCHCl + H = CH2ClCHCl	2.78E17	-2.59	5455	8
91. CHClCHCl + H = C2H3Cl + Cl	3.64E13	-0.03	5831	8
92. CHClCHCl + Cl = CHClCCl + HCl	2.50E13	0.00	7000	15
93. CHClCHCl + CH3 = CHCHCl + CH3Cl	6.30E11	0.00	23000	16
94. C2HCl3 = CHClCCl + Cl	2.81E46	-10.04	92118	1
95. C2HCl3 = CCl2CH + Cl	2.76E49	-11.26	95358	1
96. C2HCl3 = C2Cl2 + HCl	8.28E26	-4.14	74822	1
97. C2HCl3 + Cl = C2Cl3 + HCl	1.70E13	0.0	7000	15
98. C2HCl3 + H = CH2ClCCl2	5.70E16	-2.25	5325	8
99. C2HCl3 + H = CHCl2CHCl	1.76E15	-2.23	5950	8
100. C2HCl3 + H = CH2CCl2 + Cl	1.63E13	-0.01	5814	8
101. C2HCl3 + H = CHClCHCl + Cl	7.16E12	0.00	6504	8
102. C2HCl3 + H = CHClCCl + HCl	1.20E13	0.00	4500	15
103. C2HCl3 + H = CCl2CH + HCl	1.00E13	0.00	5500	15
104. C2HCl3 + CH3 = CHClCCl + CH3Cl	6.30E11	0.00	19500	17
105. C2HCl3 + CH3 = CCl2CH + CH3Cl	3.15E11	0.00	23500	18
106. C2HCl + H = HCl + C2H	1.00E13	0.00	17030	12
107. C2HCl + H = C2H2 + Cl	2.00E13	0.00	2100	12
108. C2HCl + Cl = HCl + C2Cl	8.00E13	0.00	23800	12
109. CH2CCl = C2HCl + H	8.03E39	-8.49	53853	1
110. CHClCCl = C2HCl + Cl	4.23E33	-7.10	26965	1
111. CCl2CH = C2HCl + Cl	5.03E30	-6.32	21780	1

Table B1 (cont'd)

Reactions	A^a	n	E_a^b	source
112. CHCHCl = C2H2 + Cl	7.50E28	-5.83	21471	1
113. C2Cl3 = C2Cl2 + Cl	1.72E32	-6.70	25456	1
114. CH4 = CH3 + H	7.43E13	0.00	101000	13
115. CH4 + Cl = CH3 + HCl	5.00E13	0.00	3900	2
116. CH4 + H = CH3 + H2	1.55E14	0.00	11000	2
117. CH3 + H = CH2 + H2	9.00E13	0.00	15100	19
118. CH3 + CH3 = C2H6	1.13E12	0.00	-4270	20
119. CH3 + CH3 = C2H5 + H	4.51E13	0.00	15900	20
120. CH3 + C2H3 = CH4 + C2H2	3.92E11	0.00	0	21
121. CH3 + C2H5 = CH4 + C2H4	1.15E12	0.00	0	22
122. CH2 + CH2 = C2H2 + H2	4.00E13	0.00	0	19
123. CH2 + CH4 = CH3 + CH3	1.81E05	0.00	0	21
124. ^{1}CH2 + M = CH2 + M	1.00E13	0.00	0	19
125. ^{1}CH2 + CH4 = C2H5 + H	9.43E12	-0.13	6620	23
126. ^{1}CH2 + CH4 = CH3 + CH3	3.45E22	-2.48	7460	23
127. ^{1}CH2 + CH4 = C2H6	5.78E46	-10.31	12830	23
128. ^{1}CH2 + C2H6 = CH3 + C2H5	1.20E14	0.00	0	19
129. CH + H2 = CH2 + H	1.45E14	0.00	3497	22
130. CH + H2 = CH3	1.45E14	0.00	3497	22
131. C2H6 = C2H5 + H	3.64E16	0.00	89500	23
132. C2H6 + CH3 = C2H5 + CH4	1.51E-7	6.00	6047	22
133. C2H6 + H = C2H5 + H2	1.44E09	1.50	7412	2
134. C2H6 + Cl = C2H5 + HCl	4.64E13	0.00	170	24
135. C2H5 + C2H4 = C2H3 + C2H6	1.68E13	0.00	22160	25
136. C2H5 + C2H5 = C2H4 + C2H6	1.40E12	0.00	0	21
137. C2H5 + Cl2 = C2H5Cl + Cl	7.58E12	0.00	-240	26
138. C2H5 = C2H4 + H	3.80E43	-9.54	51000	27
139. C2H4 = C2H3 + H	2.82E15	0.00	108000	25

Table B1 (cont'd)

Reactions	A[a]	n	E_a[b]	source
140. C2H4 = C2H2 + H2	8.52E43	-8.32	121240	28
141. C2H4 + CH3 = CH4 + C2H3	0.36	4.00	11113	25
142. C2H4 + H = C2H3 + H2	1.50E14	0.0	10200	28
143. C2H4 + Cl = C2H3 + HCl	1.00E14	0.00	7000	3
144. C2H4 + H2 = C2H5 + H	1.02E13	0.00	68154	21
145. C2H3 = C2H2 + H	6.24E29	-5.29	46500	25
146. C2H3 + H = C2H2 + H2	9.64E13	0.00	0	21
147. C2H3 + Cl2 = C2H3Cl + Cl	5.25E12	0.00	-480	26
148. C2H2 = C2H + H	1.16E13	0.00	124000	25
149. C2H2 + Cl = C2H + HCl	1.58E14	0.00	26900	3
150. C2H + H2 = C2H2 + H	3.50E12	0.00	2100	3
151. C2H + CH4 = C2H2 + CH3	1.20E13	0.00	0	25
152. C2H + C2H4 = C2H2 + C2H3	1.20E13	0.00	0	25
153. H + Cl + M = HCl + M	7.20E21	-2.00	0	29
154. H + H + M = H2 + M	6.52E17	-1.0	0	22
155. H + HCl = H2 + Cl	2.30E13	0.00	3500	21
156. H + Cl2 = HCl + Cl	8.59E13	0.00	1170	2
157. Cl + Cl + M = Cl2 + M	2.34E14	0.00	-1800	22
Oxidation				
158. CH3Cl + O = CH2Cl + OH	1.56E13	0.31	11266	30
159. CH3Cl + OH = CH2Cl + H2O	1.74E10	0.89	2890	31
160. CH3Cl + O2 = CH2Cl + HO2	3.00E13	0.00	52600	32
161. CH3Cl + HO2 = CH2Cl + H2O2	9.00E10	0.00	8500	13
162. CH2Cl2 + O = CHCl2 + OH	6.62E06	1.99	5710	33
163. CH2Cl2 + OH = CHCl2 + H2O	2.64E09	1.09	1526	31
164. CH2Cl2 + O2 = CHCl2 + HO2	4.00E13	0.00	50800	34
165. CH2Cl2 + HO2 = CHCl2 + H2O2	6.00E10	0.00	15300	13
166. CHCl3 + O = CCl3 + OH	1.14E13	0.22	9400	33

Table B1 (cont'd)

Reactions	A[a]	n	E_a[b]	source
167. CHCl3 + OH = CCl3 + H2O	3.00E07	1.52	516	31
168. CHCl3 + O2 = CCl3 + HO2	2.00E13	0.00	46700	35
169. CHCl3 + HO2 = CCl3 + H2O2	2.25E12	0.00	14700	13
170. CH2Cl + O2 = CH2ClOO	1.03E37	-8.28	6232	8
171. CH2Cl + O2 = CH2ClO + O	5.67E29	-5.12	33898	8
172. CH2Cl + O2 = CH2O + ClO	2.79E17	-1.60	8402	8
173. CH2Cl + O2 = CHClO + OH	1.23E20	-2.26	24537	8
174. CH2Cl + HO2 = CH2ClO + OH	1.14E13	-0.07	74	8
175. CH2Cl + HO2 = CHClO + H2O	1.35E04	2.08	-532	8
176. CH2Cl + HO2 = CH2ClOOH	3.33E22	-4.15	2230	8
177. CH2Cl + ClO = CH2ClO + Cl	1.34E11	0.40	-672	8
178. CH2Cl + ClO = CHClO + HCl	4.60E14	-0.66	1053	8
179. CH2Cl + O = CH2O + Cl	3.49E16	-1.04	914	8
180. CH2Cl + O = CHO + HCl	2.77E09	1.11	-724	8
181. CH2Cl + OH = CH2O + HCl	3.38E14	-0.50	444	8
182. CH2Cl + OH = CH2OH + Cl	7.31E05	1.98	-386	8
183. CH2Cl + CH2O = CH3Cl + CHO	5.50E03	2.81	5860	2
184. CHCl2 + O2 = CHClO + ClO	1.43E23	-3.17	15020	8
185. CHCl2 + O2 = CHCl2OO	1.18E32	-6.78	4551	8
186. CHCl2 + O2 = CHCl2O + O	2.50E34	-6.75	42024	8
187. CHCl2 + O2 = COCl2 + OH	2.66E24	-3.64	31407	8
188. CHCl2 + HO2 = CHCl2O + OH	2.02E13	-0.18	200	8
189. CHCl2 + HO2 = COCl2 + H2O	6.51E05	1.56	-350	8
190. CHCl2 + ClO = CHCl2O + Cl	9.68E10	0.40	-400	8
191. CHCl2 + ClO = COCl2 + HCl	1.65E15	-0.92	900	8
192. CHCl2 + O = CHClO + Cl	3.63E13	-0.11	98	8
193. CHCl2 + O = CClO + HCl	2.03E06	1.74	-1032	8
194. CHCl2 + OH = CHClO + HCl	8.39E14	-0.68	616	8

Table B1 (cont'd)

Reactions	A[a]	n	E_a[b]	source
195. CHCl2 + OH = CHClOH + Cl	2.09E05	2.13	-316	8
196. CHCl + O = CO + HCl	7.65E08	0.86	-500	8
197. CHCl + O = CHO + Cl	4.95E13	-0.01	10	8
198. CHCl + OH = CH2O + Cl	1.10E09	0.30	-89	8
199. CHCl + OH = CHO + HCl	3.20E09	0.55	-422	8
200. CHCl + OH = CHClO + H	6.35E12	-0.35	307	8
201. CHCl + O2 = CHClO + O	3.21E11	0.00	4	8
202. C2H3Cl + OH = CHCHCl + H2O	1.20E13	0.00	5800	35
203. C2H3Cl + OH = CH2CCL + H2O	6.00E13	0.00	5300	35
204. C2H3Cl + OH = CH2CHOH + Cl	1.44E22	-2.7	5210	12
205. C2H3Cl + OH = CH3 + CHClO	3.13E07	0.91	9390	12
206. C2H3Cl + OH = CH3CHO + Cl	3.91E13	-0.98	10370	12
207. C2H3Cl + O = CH2CHClO	2.65E32	-7.14	5960	12
208. C2H3Cl + O = CH2 + CHClO	5.01E12	-0.23	1650	12
209. C2H3Cl + O = CHCHCl + OH	6.02E07	1.57	7190	37
210. C2H3Cl + O = CH2CCl + OH	3.00E07	1.57	6190	37
211. C2H3Cl + ClO = CH2Cl + CHClO	1.00E12	0.0	0	15
212. CH2CCl2 + OH = CH2CCl2OH	1.41E30	-6.46	5020	12
213. CH2CCl2 + OH = CH2CClOH + Cl	2.56E13	-0.5	2000	12
214. CH2CCl2 + OH = CH3CClO + Cl	1.21E05	1.15	11800	12
215. CH2CCl2 + OH = CH3 + COCl2	4.23E03	1.75	11690	12
216. CH2CCl2 + OH = CH2OHCCl2	6.79E09	0.00	-6100	13
217. CH2CCl2 + OH = CHCl2CH2O	1.64E05	0.00	5800	13
218. CH2CCl2 + OH = CHCl2 + CH2O	1.72E10	0.00	12100	13
219. CH2CCl2 + OH = CCl2CH + H2O	1.00E13	0.00	5800	13
220. CH2CCl2 + O = CH2CCl2O	1.58E15	-2.89	2910	12
221. CH2CCl2 + O = CH2 + COCl2	5.04E11	0.00	2000	12
222. CH2CCl2 + O = CCl2CH + OH	6.02E07	1.57	7190	37

Table B1 (cont'd)

Reactions	A[a]	n	E_a[b]	source
223. CHClCHCl + O = CHClCCl + OH	4.58E14	0.00	14610	37
224. CHClCHCl + O = CHCl2 + CHO	8.50E11	0.00	1950	15
225. CHClCHCl + O = Cl + CHClCHO	8.50E11	0.00	1950	15
226. CHClCHCl + OH = CHClCHClOH	5.56E16	-2.98	-1053	8
227. CHClCHCl + OH = CHClCHOH + Cl	1.43E12	-0.02	-111	8
228. CHClCHCl + OH = H2O + CHClCCl	1.00E13	0.0	5300	8
229. C2HCl3 + OH = CHClCCl2OH	2.01E07	0.00	-6200	13
230. C2HCl3 + OH = CHClCClOH + Cl	2.89E12	0.00	2400	13
231. C2HCl3 + OH = CH2Cl + COCl2	5.96E07	0.00	14100	13
232. C2HCl3 + OH = CHClOHCCl2	1.12E07	0.00	-6000	13
233. C2HCl3 + OH = CCl2CHOH + Cl	2.71E12	0.00	2200	13
234. C2HCl3 + OH = CHCl2 + CHClO	1.78E08	0.00	15900	13
235. C2HCl3 + OH = C2Cl3 + H2O	3.0E12	0.0	5800	13
236. C2HCl3 + O = CHClCCl2O	9.27E09	0.00	600	13
237. C2HCl3 + O = CHCl + COCl2	3.83E11	0.00	4900	13
238. C2HCl3 + O = CHClOCCl2	1.08E10	0.00	-3000	13
239. C2HCl3 + O = CHClO + CCl2	6.46E11	0.00	1000	13
240. C2HCl3 + O = C2Cl3 + OH	3.10E12	0.00	7000	13
241. C2HCl + OH = CH2Cl + CO	2.40E-3	4.00	-2000	12
242. C2HCl + O = CHCl + CO	5.10E06	2.00	1900	12
243. C2HCl + O = CHCO + Cl	5.10E06	2.00	1900	12
244. CH2CCl + O2 = C*CClOO	8.07E30	-6.39	3153	8
245. CH2CCl + O2 = CH2CO + ClO	4.73E05	1.83	4423	8
246. CH2CCl + O2 = C*CClO. + O	9.60E16	-1.31	4015	8
247. CH2CCl + O2 = C2HCl + HO2	1.86E10	0.61	3627	8
248. CH2CCl + O2 = CH2O + CClO	4.56E20	-2.59	3917	8
249. CHCHCl + O2 = CCl*COO	3.51E28	-5.94	1483	8
250. CHCHCl + O2 = ClC*CO. + O	1.77E13	-0.32	3606	8

Table B1 (cont'd)

Reactions	A^a	n	E_a^b	source
251. CHCHCl + O2 = C2HCl + HO2	1.26E12	0.02	3546	8
252. CHCHCl + O2 = CHClO + CHO	2.61E16	-1.22	1776	8
253. CHClCCl + O2 = ClC*CClOO	9.13E28	-6.03	1729	8
254. CHClCCl + O2 = CHClCO + ClO	7.03E04	1.93	5461	8
255. CHClCCl + O2 = ClC*CClO. + O	1.01E12	0.10	3674	8
256. CHClCCl + O2 = C2Cl2 + HO2	6.56E12	-0.20	9911	8
257. CHClCCl + O2 = CHClO + CClO	1.84E19	-2.11	3122	8
258. CCl2CH + O2 = Cl2C*COO	6.11E25	-5.13	443	8
259. CCl2CH + O2 = CCl2CO + OH	1.46E03	2.43	2492	8
260. CCl2CH + O2 = Cl2C*CO. + O	1.03E13	-0.26	2720	8
261. CCl2CH + O2 = COCl2 + CHO	4.37E16	-1.39	1956	8
262. C2Cl3 + O2 = Cl2C*CClOO	1.22E26	-5.22	520	8
263. C2Cl3 + O2 = CCl2CO + ClO	6.20E02	2.44	3309	8
264. C2Cl3 + O2 = Cl2C*CClO. + O	1.51E13	-0.38	2796	8
265. C2Cl3 + O2 = COCl2 + CClO	9.39E17	-1.82	2407	8
266. CH4 + O2 = CH3 + HO2	7.90E13	0.00	56000	19
267. CH4 + O = CH3 + OH	1.02E09	1.5	8604	19
268. CH4 + HO2 = CH3 + H2O2	1.80E11	0.00	18700	19
269. CH4 + OH = CH3 + H2O	1.60E06	2.10	2460	19
270. CH4 + CH3O = CH3 + CH3OH	1.57E11	0.00	8842	21
271. CH3 + O = CH2O + H	1.34E14	-0.08	79	38
272. CH3 + O = CH2OH	6.57E12	0.04	-24	38
273. CH3 + O2 = CH3OO	3.36E34	-7.43	5960	38
274. CH3 + O2 = O + CH3O	7.89E14	-0.46	31150	38
275. CH3 + O2 = OH + CH2O	1.58E11	0.03	10420	38
276. CH3 + OH = ^{1}CH2 + H2O	9.08E15	-0.99	2909	38
277. CH3 + OH = CH2O + H2	4.04E12	-0.51	2839	38
278. CH3 + OH = CH2OH + H	6.55E13	-0.31	4619	38

Table B1 (cont'd)

Reactions	A[a]	n	E_a[b]	source
279. CH3 + OH = CH3O + H	5.61E12	-0.23	12444	38
280. CH3 + HO2= CH3O + OH	2.00E13	0.00	0	19
281. CH3 + ClO = CH3O + Cl	3.33E11	0.46	30	23
282. CH3 + ClO = CH2O + HCl	3.47E18	-1.80	2070	23
283. [1]CH2 + O2 = CO + OH + H	3.00E13	0.00	0	19
284. CH + O2 = CO + OH	3.31E13	0.0	0	22
285. CH + O2 = CHO + O	3.31E13	0.0	0	22
286. C2H6 + O = C2H5 + OH	9.99E08	1.50	5803	22
287. C2H6 + OH = H2O + C2H5	7.22E06	2.00	864	22
288. C2H6 + O2 = C2H5 + HO2	6.03E13	0.00	51866	22
289. C2H5 + O2 = C2H4 + HO2	1.00E27	-4.826	9468	27
290. C2H5 + O2 = C2H5O + O	1.10E13	-0.21	27934	27
291. C2H5 + O2 = C2H5OO	4.85E12	0.0	0	27
292. C2H5 + O = C2H4 + OH	5.00E13	0.0	0	39
293. C2H4 + OH = C2H3 + H2O	2.02E13	0.00	5955	19
294. C2H4 + OH = CH3 + CH2O	1.00E13	0.00	0	40
295. C2H4 + O2 = C2H3 + HO2	4.22E13	0.00	57623	21
296. C2H4 + O = CH3 + CHO	3.50E06	2.08	0	41
297. C2H4 + O = CH2O + CH2	2.50E13	0.00	5000	22
298. C2H4 + HO2 = CH3CHO + OH	6.03E09	0.00	15800	21
299. C2H4 + ClO = CH2Cl + CH2O	1.00E12	0.00	0	15
300. C2H3 + OH = C2H2 + H2O	3.01E13	0.00	0	21
301. C2H3 + H2O2 = C2H4 + HO2	1.21E10	0.00	-596	21
302. C2H3 + CH2O = C2H4 + CHO	5.42E03	2.81	5862	21
303. C2H3 + O2 = C2H3OO	3.53E26	-5.22	1141	8
304. C2H3 + O2 = CH2CHO + O	1.28E12	0.01	1035	8
305. C2H3 + O2 = C2H2 + HO2	1.51E08	1.12	823	8
306. C2H3 + O2 = CH2O + CHO	1.67E16	-1.21	1611	8

Table B1 (cont'd)

Reactions	A^a	n	E_a^b	source
307. C2H2 + O2 = C2H + HO2	1.20E13	0.0	74500	21
308. C2H2 + O2 = CHO + CHO	1.20E11	0.00	44500	12
309. C2H2 + O = CO + CH2	7.94E13	0.00	15000	13
310. C2H2 + O = CH2CO	1.70E11	0.00	0	42
311. C2H2 + O = CHCO + H	3.50E04	2.70	1400	43
312. C2H2 + OH = C2H + H2O	1.45E04	2.68	12040	21
313. C2H2 + OH = CH2CO + H	3.20E11	0.00	201	44
314. C2H2 + HO2 = CH2CO + OH	6.02E09	0.00	7984	21
315. C2H + O2 = CO + CHO	5.00E13	0.00	1500	45
316. C2H + O = CH + CO	1.00E13	0.0	0	45
317. CH3CHO = CH3 + CHO	7.00E15	0.00	81674	22
318. CH3CHO + OH = CH3CO + H2O	3.40E12	0.00	-600	22
319. CH3CHO + O = CH3CO + OH	5.00E12	0.00	1800	28
320. CH3CHO + HO2 = CH3CO + H2O2	1.50E11	0.00	9000	46
321. CH3CHO + O2 = CH3CO + HO2	1.00E13	0.00	38900	46
322. CH3CHO + CH3 = CH3CO + CH4	8.50E10	0.00	6000	28
323. CH2CO = CH2 + CO	3.00E14	0.00	70900	28
324. CH2CO + O = CH2 + CO2	1.74E12	0.00	1350	19
325. CH2CO + H = CH3 + CO	1.80E13	0.00	3378	22
326. CH2CO + O = CHCO + OH	1.00E12	0.00	8000	19
327. CH2CO + OH = CHCO + H2O	7.50E12	0.00	2000	19
328. CH2CO + OH = CH2O + CHO	3.00E12	0.00	1500	15
329. CHCO + H = CH2S + CO	3.00E13	0.00	0	28
330. CH3O + O2 = CH2O + HO2	1.00E13	0.00	7165	28
331. CH3O + M = CH2O + H + M	1.96E14	0.00	25070	28
332. CH3O + CO = CO2 + CH3	1.57E13	0.00	11800	21
333. CH3O + HO2 = CH2O + H2O2	3.01E11	0.00	0	21
334. CH3O + CH3 = CH4 + CH2O	2.41E13	0.00	0	21

Table B1 (cont'd)

Reactions	A[a]	n	E_a[b]	source
335. CH3O + O = OH + CH2O	6.03E12	0.00	0	21
336. CH3O + OH = H2O + CH2O	1.81E13	0.00	0	21
337. CH3O + H = CH2O + H2	1.99E13	0.0	0	21
338. CH3O + CH2 = CH3 + CH2O	1.81E13	0.0	0	21
339. CH3O + C2H5 = C2H6 + CH2O	2.41E13	0.0	0	21
340. CH3O + ClO = HOCl + CH2O	2.41E13	0.0	0	13
341. CH3O + Cl = HCl + CH2O	4.00E14	0.0	0	13
342. CH2O + ClO = CHO + HOCl	6.03E11	0.00	4200	47
343. CH2O + CH3 = CH4 + CHO	5.54E03	2.81	5862	21
344. CH2O + O = CHO + OH	4.16E11	0.57	2762	22
345. CH2O + OH= CHO + H2O	3.44E09	1.18	-447	22
346. CH2O + HO2= CHO+ H2O2	1.99E12	0.00	11665	21
347. CH2O + Cl = CHO + HCl	4.40E13	0.00	0	24
348. CH2O = CHO+H	2.54E28	-5.16	71501	38
349. CH2O = H2+CO	2.26E25	-4.65	81990	38
350. CH2O + O2 = CHO + HO2	2.00E13	0.00	38900	46
351. CH2O + H = CHO + H2	2.29E10	1.05	3279	22
352. CHO + M = H + CO + M	1.87E17	-1.00	17000	48
353. CHO + H = CO + H2	9.04E13	0.00	0	22
354. CHO + O2 = CO2 + OH	5.45E14	-1.15	2018	49
355. CHO + O2 = CO + HO2	6.25E15	-1.15	2018	49
356. CHO + O = CO + OH	3.00E13	0.00	0	22
357. CHO + OH = CO + H2O	5.00E13	0.00	0	22
358. CHO + CH3 = CH4 + CO	1.21E14	0.00	0	21
359. CHO + HO2 = CO + H2O2	5.00E12	0.00	0	21
360. CHO + Cl = CO + HCl	1.50E13	0.00	0	13
361. CO + OH = CO2 + H	6.32E06	1.50	-497	22
362. CO + HO2 = CO2+OH	1.51E14	0.00	23648	21

Table B1 (cont'd)

Reactions	A[a]	n	E_a[b]	source
363. CO + O2 = CO2 +O	2.53E12	0.00	47600	21
364. CO + O + M = CO2 + M	5.30E13	0.00	-45400	21
365. H + O2 = O + OH	1.99E14	0.00	16802	22
366. H + O2 + M = HO2 + M	6.16E17	-0.80	0	22
367. H + H2O = H2 + OH	6.19E07	1.90	18411	22
368. H + OH + M = H2O + M	8.34E21	-2.0	0	22
369. H + O + M = OH + M	4.71E18	-1.00	0	21
370. H + HO2 = OH + OH	1.69E14	0.00	874	21
371. H + HO2 = H2 + O2	6.62E13	0.00	2126	21
372. H + HOCl = HCl + OH	9.55E13	0.00	7620	23
373. H + H2O2 = OH + H2O	2.41E13	0.00	3974	21
374. H + H2O2 = H2 + HO2	4.82E13	0.00	7950	21
375. O + O + M = O2 + M	1.88E13	0.00	-1788	21
376. O + H2 = H + OH	5.12E04	2.67	6285	22
377. O + H2O = OH + OH	4.58E09	1.30	17100	21
378. O + HO2 = OH + O2	1.75E13	0.00	-397	21
379. O + H2O2 = HO2 + OH	9.63E06	2.00	3974	21
380. O + HCl = OH + Cl	6.03E12	0.00	6600	47
381. O + HOCl = OH + ClO	6.03E12	0.00	4370	47
382. OH + HO2 = H2O + O2	1.45E16	-1.00	0	21
383. OH + H2O2 = HO2 + H2O	1.75E12	0.0	318	21
384. O2 + H2O2 = HO2 + HO2	5.42E13	0.0	39740	21
385. H2O2 + M = OH + OH + M	1.29E33	-4.86	53247	21
386. H2O2 + Cl = HCl + HO2	6.62E12	0.00	1950	47
387. Cl + HO2= HCl + O2	1.08E13	0.00	100	47
388. Cl + HOCl = Cl2 + OH	1.81E12	0.00	260	47
389. Cl + HOCl = HCl + ClO	1.81E12	0.00	258	13
390. Cl + CO = CClO	1.19E24	-3.80	0	47

Table B1 (cont'd)

Reactions	A^a	n	E_a^b	source
391. Cl + HO2 = ClO + OH	2.47E13	0.00	894	47
392. HOCl = Cl + OH	1.76E20	-3.01	56720	23
393. HOCl = H + ClO	8.12E14	-2.09	93690	23
394. ClO + CO = Cl + CO2	6.03E11	0.00	7352	23
395. ClO + CH3 = CH3Cl + O	6.00E12	0.00	4000	13
396. ClO + Cl = O + Cl2	1.05E12	0.00	9200	47
397 ClO + CH4 = CH3 + HOCl	6.03E11	0.00	7353	47
398. ClO + CH3Cl = CH2Cl + HOCl	3.03E11	0.00	10700	13
399. ClO + H2 = HOCl + H	6.03E11	0.00	9539	47
400. CClO + OH = CO + HOCl	3.30E12	0.00	0	13
401. CClO + OH = CO2 + HCl	7.17E11	-0.02	-117	23
402. CClO + O = CO2 + Cl	1.00E13	0.00	0	50
403. CClO + O2 = CO2 + ClO	1.00E13	0.0	0	15
404. CClO + H = CO + HCl	3.50E16	-0.79	5000	50
405. CClO + H = CHO + Cl	3.90E09	1.15	-200	50
406. CClO + CH3 = CO + CH3Cl	3.30E12	0.00	0	2
407. CClO + Cl = CO + Cl2	1.50E19	-2.17	1500	51
408. COCl2 = CClO + Cl	1.30E12	0.00	68000	13
409. COCl2 + OH = CClO + HOCl	1.00E13	0.00	15000	15
410. COCl2 + OH = HCl + Cl + CO2	1.0E13	0.00	15000	15
411. COCl2 + O = CClO + ClO	2.0E13	0.00	17000	15
412. COCl2 + H = CClO + HCl	1.20E14	0.00	10400	15
413. COCl2 + CH3 = CClO + CH3Cl	1.9E13	0.00	12900	13
414. COCl2 + Cl = CClO + Cl2	3.20E14	0.00	23500	2
415. CHClO + H = CHO + HCl	8.33E13	0.00	7400	23
416. CHClO + H = CH2O + Cl	6.99E14	-0.58	6360	23
417. CHClO = CHO + Cl	8.86E29	-5.15	92920	23
418. CHClO = CO + HCl	1.10E30	-5.19	92960	23

Table B1 (cont'd)

Reactions	A[a]	n	E_a[b]	source
419. CHClO + OH = CClO + H2O	7.50E12	0.00	1200	13
420. CHClO + OH = HCO2 + HCl	1.98E07	1.20	-1516	23
421. CHClO + O = CClO + OH	8.80E12	0.00	3500	13
422. CHClO + O2 = CClO + HO2	4.50E12	0.00	41800	13
423. CHClO + Cl = CClO + HCl	1.25E13	0.00	500	13
424. CHClO + CH3 = CClO + CH4	2.50E10	0.00	6000	13
425. CHClO + CH3 = CHO + CH3Cl	1.50E13	0.00	8800	13
426. CHClO + ClO = CClO + HOCl	3.00E11	0.00	7000	47
427. CH2ClO = CHClO + H	1.83E27	-5.13	21170	23
428. CH2ClO = CH2O + Cl	4.53E31	-6.41	22560	23
429. C2Cl2 + OH = Cl + ClCCOH	1.20E12	0.00	-140	23
430. ClCCOH + OH = H2O + ClCCO	5.00E12	0.00	0	23
431. ClCCOH + O = OH + ClCCO	1.00E13	0.00	0	23
432. ClCCOH + Cl = HCl + ClCCO	1.00E13	0.00	0	23
433. ClCCO + O2 = CClO + CO2	1.00E12	0.00	5000	23

a : Unit of A factor, $cm^3\ mol^{-1}\ s^{-1}$
b : Unit of E_a , cal/mol

SOURCES of Reaction Mechanism

1 Apparent rate constant by DISSOC computer code analysis.
2 Kerr, J. A. ; Moss, S. J. "Handbook of Bimolecular and Termolecular Gas Reaction, Vol.I & II", CRC Press Inc., **1981**.
3 Weissman, M.; Benson, S. W. *Int. J. Chem. Kinet.* 1984, 16, 307.
4 A taken 1/2 as that of $CCl_4 + CH_3 \rightarrow CCl_3 + CH_3Cl$, A = 1.26E12, Ea = 15500, from Evans Polanyi analysis. Ref: Matheson, I.; Tedder, J. *Intl. J. of Chem. Kinet.* **1982**, 14, 1033.
5 A taken 3/4 as that of $CCl_4 + CH_3 \rightarrow CCl_3 + CH_3Cl$, A = 1.26E12, Ea = 13000 (Ref: source 4).
6 Estimated from $H + CH_3Cl \rightarrow CH_3 + HCl$, $H + CH_2Cl_2 \rightarrow CH_2Cl + HCl$, and $H + CCl_4 \rightarrow CCl_3 + HCl$.
7 Parmar, S. M.; Benson, J. W. *J. Phys. Chem.* **1988**, 92, 2652.
8 Apparent rate constant by CHEMACT computer code analysis.
9 A taken 1/4 as that of $CCl_4 + CH_3 \rightarrow CCl_3 + CH_3Cl$, A = 3.15E11, Ea = 24800, (Ref: source 4).
10 Monion, J. A.; Louw, R. *J. Chem. Perk. Trans. 2*, **1988**, 1547.
11 Barrat, R. B.; Bozzelli, J. W. *J. Phys. Chem.* **1992**, 96, 2494.
12 Wu, Y. P., Ph.D. Dissertation, NJIT, Newark, **1992**.
13 Won, Y. S., Ph.D. Dissertation, NJIT, Newark, **1991**.
14 A taken 1/2 as that of $CCl_4 + CH_3 \rightarrow CCl_3 + CH_3Cl$, A = 6.30E11, Ea = 21500, (Ref: source 4).

15 Bozzelli, J. W. estimated in this work.
16 A taken 1/2 as that of $CCl_4 + CH_3 \rightarrow CCl_3 + CH_3Cl$, A = 6.30E11, Ea = 23000, (Ref: source 4).
17 A taken 1/2 as that of $CCl_4 + CH_3 \rightarrow CCl_3 + CH_3Cl$, A = 6.30E11, Ea = 19500, (Ref: source 4).
18 A taken 1/4 as that of $CCl_4 + CH_3 \rightarrow CCl_3 + CH_3Cl$, A = 3.15E11, Ea = 23500, (Ref: source 4).
19 Miller, J. A.; Bowman, C. T. *Pro. Ener. Comb. Sci.* **1989**, 15, 287.
20 Zhong, X.; Bozzelli, J. W. Eastern States Section Meeting of Combustion Institute: Princeton, **1993**.
21 Tsang, W.; Hampson, R. F. *J. Phys. Chem. Ref. Data* **1986**, 15, 1087.
22 Baulch, D. L.; Cobos, C. J.; Cox, R. A.; Esser, C.; Frank, P.; Just, Th.; Kerr, J. A.; Pilling, M. J.; Troe, J; Walker, R. W.; Warnatz, J. *J. Phys. Chem. Ref. Data* **1992**, 21, 665.
23 Ho, W. P.; Barat, R. B.; Bozzelli, J. W. *Combust. and Flame* **1992**, 88, 265.
24 Atkinson, R.; Baulch, D. L.; Cox, R. A.; Hampson, R. F.; Kerr, J. A.; Troe, J; *J. Phys. Chem. Ref. Data* **1989**, 18, 881.
25 Dean, A. M. *J. Phys. Chem.* 1985, 89, 4600.
26 Timonen, R. S.; Russell, J. J.; Sarzynski, D.; Gutman, D. *J. Phys. Chem.* **1987**, 91, 1873.
27 Bozzelli, J. W.; Dean, A. M. *J. Phys. Chem.* **1990**, 94, 3313.
28 Warnatz, J. *Combustion Chemistry* (W.C. Gardiner, Jr., Ed.) Springer-Verlag, New York, **1984**.
29 Pitz, W.; Westbrook, C. K. Western States Section Meeting of Combustion Institute, **1990**.
30 Ko, T.; Fontijn, A.; Lim, K. P.; Michael, J. V. *Twenty-fourth Symposium (International) on Combustion*; The Combustion Institute: Pittsburgh, **1992**, 735.
31 Taylor, P. H.; Jiang, Z.; Dellinger, B. *Intl. J. of Chem. Kinet.* **1993**, 25, 9.
32 A taken 3/4 as that of $CH_4 + O_2 \rightarrow CH_3 + HO_2$, A = 3.0E13, Ea = ΔH_{rxn}, (Ref: source 21).
33 Su, M-C; Lim, K. P.; Michael, J. V.; Hranisavljevic, J.; Xun, Y. M.; Fontijn, A. *J. Phys. Chem.* **1994**, 98, 8411.
34 A taken 1/2 as that of $CH_4 + O_2 \rightarrow CH_3 + HO_2$, A = 2.0E13, Ea = ΔH_{rxn}, (Ref: source 21).
35 A taken 1/4 as that of $CH_4 + O_2 \rightarrow CH_3 + HO_2$, A = 1.0E13, Ea = ΔH_{rxn}, (Ref: source 21).
36 Liu, A.-D.; Mulac, W. A.; Jonah, C.D. *Intl. J. of Chem. Kinet.* **1987**, 19, 25.
37 Hranisavljevic, J.; Adusei, G. Y.; Xun, Yanmei; Fontijn, A. accepted by *Combust. Sci. and Tech.* September, **1993**.
38 Ing, W. C. reaction mechanism of Methenol Pyrolisis and Oxidation. **1995**
39 Hennessy, R. J.; Robison, C.; Smith, D. B. *Twenty-first Symposium (International) on ombustion*; The Combustion Institute: Pittsburgh, **1986**, 761.
40 Olson, D. B.; Gardiner, W. C. Jr. *Combust. and Flame*, **1978**, 32, 151.
41 Karra, S. B.; Gutman, D.; Senkan, S. M. *Combust. Sci. and Tech.* **1988**, 60, 45.
42 Gaedtke, H.; Glaenzer, K.; Hippler, H.; Luther, K.; Troe, J. *Symp. Intl. Combust. Proc.* **1973**, 14, 295.
43 Axelsson, E. I.; Brezinsky, K.; Westbrook, C. K. The Canadian and Western State Sections Meeting of Combust. Inst.: Banff, Alberta, Canada, **1986**.
44 Vandooren, J.; Van Tiggelen, P. J. *Symp. Inst. Combust. Proc.* **1977**, 16, 1133.
45 Warnatz, J. *Combust. Sci. and Tech.* **1983**, 34, 177.
46 Dean, A. M. reaction mechanism of Hydrocarbon, **1987**.
47 Demore, W. B.; Molina, M. J.; Waston, R. T.; Golden, D. M.; Hampson, R. F.; Kurylo, M. J.; Howard, C. J.; Ravishankara, A. R.; Sander, S. P. *JPL Publication* **1987**, 8, 87.
48 Timonen, R. S.; Ratajczak, E.; Gutman, D.; Wagner, A. F. *J. Phys. Chem.* **1987**, 91, 5325.
49 Bozzelli, J. W.; Dean, A. M. *J. Phys. Chem.* **1993**, 97, 4427.
50 Barat, R. B.; Sarofim, A. F.; Longwell, J. P.; Bozzelli, J. W. *Combust. Sci. and Tech.* **1990**, 74, 361.
51 Baulch, D. L.; Duxbury, J.; Grant, S. J.; Montague, D. C. *J. Phys. Chem. Ref. Data* **1981**, 1, 10.

Table B2 Thermodynamic Properties

Species	$H_{f,298}$	S_{298}	C_p300	C_p400	C_p500	C_p600	C_p800	C_p1000	C_p1500	source
H	52.10	27.36	4.97	4.97	4.97	4.97	4.97	4.97	4.97	a
H2	0.00	31.21	6.90	6.95	6.99	7.02	7.10	7.21	7.72	a
CL	28.90	39.50	5.20	5.34	5.40	5.41	5.35	5.30	5.24	b
HCL	-22.07	44.60	6.96	6.95	6.99	7.07	7.29	7.56	8.10	c
CL2	0.00	53.30	8.10	8.38	8.59	8.74	8.91	8.99	9.10	b
AR	0.00	36.98	4.97	4.97	4.97	4.97	4.97	4.97	4.97	a
O	59.55	38.47	5.23	5.14	5.08	5.04	5.01	5.01	4.98	a
OH	9.49	43.88	7.15	7.10	7.07	7.06	7.13	7.33	7.87	a
O2	0.00	49.01	7.02	7.23	7.44	7.65	8.04	8.35	8.73	a
CO	-26.42	47.21	6.96	7.02	7.13	7.27	7.61	7.94	8.41	a
CLO	24.20	54.10	7.50	7.91	8.21	8.43	8.69	8.81	9.00	b
CLOCL	19.70	63.60	11.10	11.90	12.50	12.90	13.30	13.50	13.70	d
OCLO	25.00	61.50	9.90	10.90	11.70	12.20	12.90	13.30	13.80	b
CLOO	23.00	63.00	11.60	12.10	12.70	13.10	14.00	14.60	15.70	b
HOCL	-17.80	56.50	8.90	9.50	10.00	10.50	11.10	11.50	12.40	b
HO2	3.50	54.70	8.30	8.90	9.40	9.90	10.70	11.40	12.40	a
H2O	-57.80	45.10	8.00	8.10	8.40	8.60	9.20	9.80	11.20	b
H2O2	-32.50	55.60	10.40	11.40	12.30	13.10	14.20	15.10	16.80	a
^{1}CCL2	52.00	63.40	11.10	11.80	12.40	12.90	13.60	14.00	14.50	e
CCL3	19.00	72.00	15.90	17.00	17.90	18.40	19.00	19.20	19.50	b,f
CCL4	-22.90	74.20	19.90	21.70	22.90	23.20	24.60	24.90	25.50	c
CCLO	-4.00	63.50	10.80	11.20	11.60	12.00	12.50	12.80	13.40	b
COCL2	-52.60	67.80	13.80	15.20	16.20	17.00	17.90	18.40	19.20	c
CCL3O	-0.81	77.19	19.98	21.42	23.04	23.93	24.91	25.15		g
CO2	-94.00	51.00	8.90	9.80	10.60	11.30	12.30	12.90	13.90	a
CCL3OO	-.90	86.30	24.30	26.40	28.60	29.70	31.00	31.50		h
CH	142.00	43.72	6.97	6.97	7.03	7.12	7.41	7.77	8.74	a
^{1}CHCL	72.00	56.10	8.80	9.40	10.10	10.80	12.10	13.20	14.70	i,j
CHCL2	23.50	66.70	12.30	13.90	14.90	15.40	16.70	17.40	18.40	k,f
CHCL3	-24.20	70.60	15.70	17.70	19.30	20.40	21.90	22.80	24.20	c
CHO	10.40	53.60	8.20	8.70	9.20	9.70	10.70	11.50	12.50	i
CHCLO	-39.30	61.80	11.10	12.40	13.50	14.40	15.70	16.50	18.10	b
CHCL2O	-1.00	70.10	13.90	16.30	18.00	19.30	21.20	22.20		g
CCL2OH	-7.60	70.40	16.30	18.70	20.10	21.20	22.40	23.00		g
CHCL2OCL	-19.00	80.50	19.60	22.40	24.30	25.50	26.90	27.60		g
CCL3OH	-52.70	79.60	21.00	22.70	24.60	25.70	27.20	27.90		g
HCO2	-38.24	57.75	8.89	10.79	12.36	13.55	15.64	16.92		g
CHCLOO	46.50	69.80	16.30	19.20	21.10	22.10	23.60	24.60		g
COHCLO	-99.89	66.51	13.93	16.03	17.61	18.82	20.53	21.97		g
CHCL2OO	-1.50	82.61	19.10	22.10	24.20	25.80	27.70	28.90		h
CCL2OOH	10.20	79.10	21.10	24.30	26.20	27.50	28.90	29.70		g
CCL3OOH	-35.90	89.20	25.80	28.30	30.60	32.00	33.70	34.60		g
^{1}CH2	101.40	44.10	8.30	8.70	9.20	9.60	10.40	11.10	12.40	i
CH2	92.30	46.30	8.30	8.70	9.20	9.60	10.40	11.10	12.40	a

Table B2 (cont'd)

Species	H_{f298}	S_{298}	C_p300	C_p400	C_p500	C_p600	C_p800	C_p1000	C_p1500	source
CH2CL	29.10	58.50	9.90	11.10	12.30	13.40	14.50	15.60	16.70	k,f
CH2CL2	-22.80	64.60	12.20	14.20	15.80	17.20	19.30	20.80	23.00	c
CH2O	-26.00	50.90	8.40	9.30	10.40	11.50	13.30	14.80	16.20	g
CHCLOH	-7.40	65.80	13.10	15.40	17.00	18.10	19.00	21.00		g
CH2CLO	-.80	64.20	10.70	13.00	14.90	16.20	18.60	20.20		g
CH2CLOCL	-18.80	74.60	16.40	19.10	21.20	22.40	24.30	25.60		g
CHCL2OH	-53.00	73.10	15.80	18.40	20.20	21.80	23.90	25.30		g
CH2OO	51.30	60.60	14.10	16.50	18.10	19.40	21.30	22.70	24.20	g
CH2CLOO	.00	75.10	15.90	18.80	21.10	22.70	25.10	26.90		h
CHCLOOH	10.40	74.50	17.90	21.00	23.10	24.40	26.30	27.70		g
CHOHCLO	-41.09	71.64	15.20	16.88	18.49	19.46	22.35	23.81		g
CHCL2OOH	-36.10	82.70	20.60	24.00	26.30	28.10	30.40	31.90		g
CH3	35.20	46.30	9.20	10.00	10.80	11.50	12.90	14.00	16.20	a
CH3CL	-19.50	56.00	9.70	11.50	13.20	14.60	17.00	18.80	21.80	l
CH2OH	-2.60	56.70	10.90	12.60	14.10	15.40	17.50	19.10	20.60	g
CH3O	3.90	54.20	8.55	10.20	11.90	13.50	16.20	18.30	20.30	g
CH2CLOH	-52.80	67.20	12.60	15.10	17.10	18.70	21.30	23.30		g
CH3OCL	-14.00	64.60	14.20	16.40	18.20	19.70	22.00	23.70	25.40	d,f
CH3OO	4.90	62.00	13.70	16.10	18.20	20.00	22.80	25.00	27.20	g
CH2OOH	15.20	65.40	15.70	18.30	20.20	21.70	24.00	25.80	27.50	g
CH3OOCL	-13.70	78.90	18.00	21.10	24.00	28.80	29.20	31.60		g
CH2CLOOH	-35.90	76.80	17.40	20.70	23.20	25.00	27.80	29.90		g
CH4	-17.90	44.40	8.50	9.70	11.10	12.40	15.00	17.20	20.60	a
CH3OH	-48.00	57.30	10.40	12.30	14.20	16.00	19.00	21.30	25.00	g
CH3OOH	-31.10	66.80	15.20	17.90	20.30	22.30	25.50	28.00	30.50	g
C2CL2	50.10	65.00	15.80	16.90	17.70	18.30	19.10	19.60	20.20	a
C2CL3	53.00	79.10	18.60	20.40	21.60	22.50	23.70	25.30		i,f
C2CL4	-3.40	81.40	22.70	24.90	26.60	27.90	29.30	30.00	30.50	c
C2CL5	7.50	92.20	27.60	30.20	32.10	33.60	35.30	36.10	37.00	m
C2CL6	-33.80	95.10	32.60	35.60	38.10	39.60	41.30	41.80	42.50	c
CLCCO	69.63	65.76	13.90	15.11	16.11	17.43	18.32	18.86		g
CCL2CO	-23.76	72.36	18.57	20.71	22.55	23.22	24.06	24.72		g
CL2C*CCLO.	-12.73	80.96	21.68	24.39	26.03	27.41	28.90	29.74		g
CL2C*CCLOO	11.48	90.50	25.22	28.23	30.08	31.61	33.36	34.40		g
CL2C.COOCL	15.65	83.30	27.40	30.17	32.24	33.73	36.05	37.91		g
CL2CCOCLO.	-19.52	81.20	24.57	29.75	32.41	34.10	36.34	37.09		g
CL2C.OCCLO	-61.58	95.24	25.40	28.17	30.10	31.49	33.38	34.82		g
CO.CL2CCLO	-49.54	88.37	25.65	29.94	31.75	32.70	34.18	34.55		g
C2H	132.00	49.50	9.00	9.60	10.10	10.60	11.40	12.10	12.90	a
C2HCL	51.10	58.10	13.10	14.20	15.10	15.80	16.80	17.50	18.80	i
HCLC2	91.10	64.37	9.40	10.56	11.91	13.06	14.99	16.29		i
CCL2CH	58.20	69.50	15.60	17.70	19.20	20.30	21.70	22.60	23.60	i,f
CHCLCCL	55.30	70.50	15.10	17.00	18.50	19.60	21.40	22.30	23.60	i,f

Table B2 (cont'd)

Species	H_{f298}	S_{298}	C_p300	C_p400	C_p500	C_p600	C_p800	C_p1000	C_p1500	source
CHCL2CCL2	5.80	87.80	24.20	26.60	28.50	29.90	31.80	32.90	34.50	i,f
C2HCL5	-34.00	91.00	28.30	31.70	34.30	36.20	38.50	39.80	41.70	c
CHCO	41.30	60.30	11.80	12.90	14.30	14.80	15.70	16.80	18.10	g
CHCLCO	-19.20	66.99	15.50	17.49	19.52	20.50	21.73	22.81		g
CLCCOH	17.67	67.41	15.84	17.19	18.37	19.86	21.08	21.94		g
CHCLCCLO	-20.30	77.60	19.10	21.60	23.60	25.10	27.10	28.30	30.20	d
CL2C*CO.	-7.73	74.96	18.68	21.39	23.31	24.71	26.62	27.85		g
CLC*CCLO.	-8.17	75.59	18.61	21.17	23.00	24.69	26.57	27.83		g
CHCLCCL2O	23.00	90.90	21.80	26.20	28.50	30.00	32.00	33.00	37.40	g
CHCLOCCL2	29.50	88.50	22.50	26.30	29.00	30.80	32.60	33.20	34.90	g
CCL2CCLOH	-36.90	89.90	24.00	26.40	27.80	28.60	29.10	29.30	32.50	g
CCL2CCL2OH	-31.50	94.10	27.80	31.90	33.90	35.30	37.00	38.00		g
CHCL2CCL2O	-20.50	92.10	26.20	31.10	33.80	35.70	37.90	39.10		g
CLC*CCLOO	16.04	85.13	22.15	25.01	27.05	28.89	31.03	32.49		g
CLC.CO2CL	23.25	77.77	24.74	27.51	29.91	31.33	33.94	36.11		g
CLC2OCLO.	-17.02	74.38	20.59	24.14	26.82	28.37	31.98	33.43		g
CCL2*C.Q	38.51	88.80	24.48	27.78	29.75	31.29	32.91	33.96		g
CL2C*COO	16.48	84.50	22.22	25.23	27.36	28.91	31.08	32.51		g
CL2C.CYCOO	18.15	77.31	24.56	27.12	29.36	30.63	32.89	35.43		g
CL2CYCOCO.	-17.02	75.21	21.73	26.70	29.53	31.00	33.18	34.61		g
CO.CL2C*O	-30.64	83.17	22.50	26.63	28.66	29.93	32.15	33.05		g
CO.CLCCL*O	-48.80	82.67	21.08	23.56	25.58	26.68	29.56	30.90		g
CL2C.OC*O	-51.89	88.13	22.30	25.01	27.11	28.65	31.25	32.85		g
CLC.OCCL*O	-57.88	90.60	23.01	25.65	27.86	29.04	31.20	33.13		g
CLC.*CCLQ	36.54	86.76	24.63	27.62	29.65	31.39	33.16	33.94		g
CYCO2C.*O	5.97	67.87	28.78	20.65	22.71	23.98	26.47	29.16		g
O*C*COO.	5.47	77.74	18.87	20.62	22.45	23.32	24.94	26.48		g
C2H2	54.10	48.00	10.60	11.90	13.00	13.90	15.30	16.30	18.20	a
CH2CCL	60.40	63.00	11.60	13.90	15.70	17.10	19.20	20.40	22.10	i,f
CHCHCL	63.30	62.30	11.80	14.30	16.10	17.50	19.50	20.60	22.30	i,f
CHCLCHCL	.70	69.20	16.00	18.50	20.70	22.50	25.30	27.10	29.30	i
Z_CHCLCHCL	.45	69.20	15.61	18.41	20.57	22.23	24.60	26.23		c
CH2CCL2	.60	69.20	16.00	18.50	20.70	22.50	25.30	27.10	29.30	i
CH2CLCCL2	7.00	81.30	20.80	23.40	25.40	27.00	29.40	30.90	33.80	i,f
CHCL2CHCL	9.80	82.10	20.90	23.70	25.70	27.30	29.60	31.10	33.90	i,f
CCL3CH2	14.80	81.40	22.00	24.70	26.70	28.20	30.40	31.90	34.10	i,f
C2H2CL3	8.50	83.10	22.00	24.70	26.70	28.20	30.40	31.90	34.10	i,f
CH2CLCCL3	-37.20	86.00	26.10	29.50	32.20	34.20	36.90	38.50	40.60	c
CHCL2CHCL2	-37.20	86.00	26.10	29.50	32.20	34.20	36.90	38.50	40.60	c
CH2CO	-11.70	57.80	12.70	14.60	16.70	17.80	19.50	20.90	23.00	g
CLC*CO.	-0.17	67.80	15.81	18.33	20.21	21.99	24.34	26.00		g
C*CCLO.	-3.17	69.59	15.61	18.17	20.28	21.99	24.29	25.94		g
CHCLCCLOH	-43.50	76.40	20.20	23.40	25.80	27.60	29.90	31.40	33.70	d
CHCL2CHO	-46.90	78.60	18.80	22.00	24.40	26.30	28.60	30.10	33.00	g

Table B2 (cont'd)

Species	H_{f298}	S_{298}	C_p300	C_p400	C_p500	C_p600	C_p800	C_p1000	C_p1500	source
CH2CCL2O	33.70	80.00	19.90	23.60	26.30	28.20	30.40	31.50	33.90	g
CHCLCHO	-6.00	70.10	15.80	18.50	20.60	22.30	24.80	26.50	29.00	d
CHCLCCLOH	-34.80	81.50	20.50	23.10	24.80	25.90	26.80	27.40	31.30	d
CH2OCCL2	35.60	80.30	19.90	23.60	26.30	28.20	30.40	31.50	33.90	g
CCL2CHOH	-41.60	77.80	19.40	21.90	23.90	25.60	28.30	30.00		g
CHCLCHCLO	24.50	84.60	17.00	19.50	21.80	23.70	26.60	28.40	31.10	g
CH2CLCCLO	-59.00	80.00	18.80	22.00	24.40	26.30	28.60	30.10	33.00	d
CHCLCCL2OH	-24.90	90.90	24.00	28.40	30.80	32.50	34.80	36.10		g
CH2CLCCL2O	-17.40	86.80	22.70	27.70	30.60	32.60	35.40	37.00		g
CHCLOHCCL2	-30.00	90.10	23.80	26.30	28.30	29.60	32.70	34.30		g
CHCL2CHCLO	-19.00	88.10	22.20	25.50	28.20	29.90	33.50	35.40		g
CHCL2CCLOH	-28.10	90.70	22.20	24.80	27.10	28.60	31.80	33.50		g
CHOCHO	-50.60	65.40	14.90	17.50	19.60	21.40	24.20	25.80	28.40	g
C*CCLOO	21.04	79.15	19.15	22.01	24.33	26.19	28.75	30.60		g
C.*CCLQ	46.50	78.51	21.21	24.26	26.45	28.36	30.70	32.14		g
C.CYCO2CL	34.35	69.38	20.84	23.74	26.22	28.21	31.45	34.20		g
CYCOCCL(O)	-8.92	68.22	17.87	21.82	24.17	26.97	30.45	32.41		g
CCL*COO	23.05	77.34	19.35	22.17	24.26	26.19	28.80	30.66		g
CLC.CYCOO	25.75	71.79	21.90	24.46	27.03	28.23	30.78	33.63		g
CLCYCOC(O)	-14.52	68.39	17.75	21.09	23.94	25.27	28.82	30.95		g
CO.CLC*O	-29.90	77.47	17.93	20.25	22.49	23.91	27.53	29.40		g
CO.CCL*O	-40.70	76.51	18.49	21.25	23.49	25.34	28.14	30.03		g
CLC.OC*O	-48.19	82.82	19.85	22.70	24.97	26.55	29.37	31.42		g
C.OCCL*O	-48.58	82.05	19.46	21.82	23.90	25.75	28.52	31.00		g
C.CL*CQ	41.54	80.76	21.63	24.62	26.93	28.69	30.88	32.05		g
C2H3	71.00	56.20	10.80	12.40	13.80	15.10	17.10	18.70	21.30	n
C2H3CL	5.00	63.00	12.30	15.30	17.70	19.60	22.40	24.20	26.80	o
CH3CCL2	11.30	73.60	17.20	20.30	22.90	25.20	28.50	30.80	33.80	i,f
CHCL2CH2	16.00	77.30	17.90	20.90	23.30	25.20	28.00	29.90	33.10	i,f
CH2CLCHCL	11.40	75.70	17.70	20.30	22.50	24.30	27.00	29.10	33.90	i,f
CH2CLCHCL2	-34.70	81.40	21.30	24.80	27.60	29.80	33.00	35.00	38.90	i
CH3CCL3	-33.80	76.50	22.00	25.70	28.50	30.80	34.00	35.90	38.90	i
CH3CO	-2.20	62.70	11.70	13.80	15.90	17.80	20.80	23.10	25.30	g
CH2CHO	3.12	61.78	12.92	15.31	17.44	19.24	22.10	24.12		g
C*CO.	4.29	61.80	12.81	15.33	17.31	19.29	22.06	24.11		g
CH2CLCHO	-43.30	70.90	16.20	18.80	21.10	23.10	26.30	28.50	32.00	g
CH2CHCLO	36.60	74.10	15.40	18.20	20.70	22.30	25.90	27.80		g
CH2OCHCL	37.70	75.80	16.60	18.60	20.70	22.80	26.70	29.50	32.20	g
CH2CCLOH	-37.90	71.11	16.90	19.60	22.03	23.87	26.62	26.83		g
CH3CCLO	-58.30	70.40	16.20	18.80	21.10	23.10	26.30	28.50	32.00	c
CH2CLCHO	-41.60	74.00	14.90	17.90	20.50	22.70	26.00	28.40	32.10	d
CHCLCHOH	-33.10	72.50	16.40	18.70	20.90	22.90	25.90	28.10	31.50	g
CH2CCL2OH	-17.80	82.60	21.40	25.90	28.60	30.40	33.00	34.50		g
CHCL2CHOH	-24.00	83.20	19.50	22.50	25.00	27.20	30.30	32.50		g

Table B2 (cont'd)

Species	H_{f298}	S_{298}	C_p300	C_p400	C_p500	C_p600	C_p800	C_p1000	C_p1500	source
CHCLCHCLOH	-23.40	85.40	20.00	22.80	25.20	26.80	30.40	32.50		g
CH2CLCHCLO	-15.90	81.40	18.80	22.10	25.00	26.90	31.00	33.30		g
CH3CCL2O	-14.80	77.00	20.20	25.00	27.90	30.10	33.20	35.30		g
CHCL2CH2O	-14.90	80.60	19.50	23.20	26.10	28.50	32.00	34.40		g
CH2OHCCL2	-25.90	82.60	21.10	24.00	26.20	28.20	31.10	33.30		g
C.CYCO2	36.85	64.77	18.00	20.69	23.34	25.11	28.29	31.72		g
CYC2O(O.)	-6.42	62.24	15.03	18.77	21.83	23.87	27.29	29.93		g
C.OCHO	-38.99	73.67	17.65	19.94	22.02	23.86	27.05	29.50		g
O.CCHO	-21.80	71.31	15.34	17.94	20.40	22.57	26.11	28.53		g
C.*COOH	51.03	76.70	18.24	20.87	23.06	24.90	27.72	29.73	32.89	g
C2H3OO	29.20	72.20	16.80	19.60	22.10	24.20	27.50	29.90	32.20	g
C2H4	12.50	52.30	10.20	12.70	14.90	16.80	20.00	22.40	26.20	a
CH2CLCH2	20.70	68.50	13.90	16.80	19.40	21.70	25.50	28.40	32.60	k
CH3CHCL	18.00	67.30	14.10	17.10	19.70	21.90	25.40	28.10	32.30	k
C2H4CL	17.50	67.30	14.10	17.10	19.70	21.90	25.40	28.10	32.30	k
CH3CHCL2	-31.10	73.00	18.10	21.80	24.90	27.40	31.10	33.50	37.80	i
CH2CLCH2CL	-30.60	74.10	18.20	21.50	24.30	26.70	30.20	32.80	38.70	i
C2H4CL2	-30.60	74.10	18.20	21.50	24.30	26.70	30.20	32.80	38.70	i
CH3CHO	-39.10	63.10	13.20	15.70	18.20	20.40	24.20	26.90	29.70	g
CH2CHOH	-29.60	62.91	14.15	17.32	19.97	22.08	25.19	27.44	31.09	g
CH2OHCHCL	-18.30	77.90	17.30	20.40	23.10	25.40	28.90	31.50		g
CH2CHCLOH	-15.30	77.10	17.40	20.30	23.00	24.70	28.60	30.90		g
CH3CHCLO	-12.30	71.60	16.20	19.40	22.30	24.40	28.90	31.60		g
CH2CLCH2O	-10.80	73.80	16.00	19.80	22.90	25.50	29.50	32.30		g
CHCL2CH2OH	-66.90	83.60	21.50	25.30	28.60	31.00	34.80	37.50		g
C2H5	28.30	57.90	12.20	14.80	17.10	19.20	22.80	25.70	30.50	p
C2H5CL	-26.80	66.00	15.00	18.60	21.60	24.20	28.40	31.40	36.20	a
C2H5O	-4.20	64.00	13.50	17.10	20.20	23.00	27.30	30.60	33.80	g
CH2CH2OOH	7.80	79.10	19.50	23.60	26.90	29.60	33.60	36.60	39.50	g
C2H5OO	-4.50	73.20	18.60	22.90	26.50	29.40	33.90	37.30	40.70	g
C2H6	-20.20	54.80	12.50	15.80	18.70	21.30	25.80	29.30	34.90	a
C2H5OOH	-40.60	76.60	20.20	24.80	28.60	31.70	36.60	40.40	44.10	g

Unit: ΔH_f, kcal/mol; S and C_p, cal mol^{-1} K^{-1}

SOURCES of Thermodynamic Properties

a. *JANAF Thermochemical Tables 3rd ed.* NSRDS-NBS, **1986**, 37.

b. Benson, S. W. *Thermochemical Kinetics*, 2nd ed., Wiley, New York, **1976**.

c. Stull, D. R.; Westrum, E. F.; Sinke, G. C. *The Chemical Thermodynamics Organic Compounds*, Robert E. Kreger Publishing Co., **1987**.

d. Melius, C. F., Sandia National Laboratories, BAC-MP4 Heats of Formation and Free Energies, **1991**.

e. Kohn, D. W.; Robles, E. S. J.; Logan, C. F.; Chen, P. *J. Phys. Chem.* **1993**, 97, 4936.

f. Ritter, E. R.; Bozzelli J. W. The Eastern States Section of The Combuion Institute, Princeton University, New Jersey, **1993**, 459.
g. THERM: Computer Code for Thermodynamic Properties Estimation, Ritter, E. R.; Bozzelli, J. W. *Intl. J. Chem. Kinet.* **1991**, 23, 767.
h. Russell, J. J.; Seetula, J. A., Gutman, D.; Melius, C. F., twenty- *Symposium (International) on Combustion*; The Combustion Institute, **1990**, 163.
i. Estimated by Bozzelli, J. W. from literature review and evaluated bond energies.
j. Lias, S. G.; Karpas, Z.; Liebman, J. F. *J. American Chem. Soc.* **1985**, 107, 6087.
k. Tschuikow-Roux, E.; Paddison, S. *Intl. J. Chem. Kinet.* **1987**, 19, 15.
l. Rodgers, A. S. Selected Values for Thermodynamic Properties of Chemical Compounds, Thermodynamic Research Center, Texas A&M University, **1982**.
m. Orlov, Y. D.; Lebedev, Y. A.; Korsunskii, B. L. *Russ. J. Chem. Phys.* **1985**, 1424.
n. McMillen, D. F.; Golden, D. M. *ann. Rev. Phys. Chem.* **1982**, 33, 493.
o. Monion, J. A.; Louw, R. *J. Chem. Perk. Trans. 2*, **1988**, 1547.
p. Brouard, M.; Lightfoot, P. D.; Pilling, M. J. *J. Phys. Chem.* **1986**, 90, 445.

Table B3 QRRK Input Data for $CH_2Cl + O_2 \leftrightarrow [CH_2ClOO]^* \rightarrow$ Products

	Reaction	A^a	n	α	E_a^b
k_1	$CH_2Cl + O_2 \rightarrow CH_2ClOO$	3.32E15	-1.3	0.0	0.0
k_{-1}	$CH_2ClOO \rightarrow CH_2Cl + O_2$	1.38E23	-3.38	9.598E-4	26.1
k_2	$CH_2ClOO \rightarrow CH_2ClO + O$	1.15E23	-2.92	-6.633E-4	56.2
k_3	$CH_2ClOO \rightarrow CH_2O + ClO$	6.41E09	1.0	0.0	31.0
k_4	$CH_2ClOO \rightarrow C.HClOOH$	2.57E10	1.0	0.0	46.7
k_{-4}	$C.HClOOH \rightarrow CH_2ClOO$	4.12E09	1.0	0.0	36.3
k_5	$C.HClOOH \rightarrow CHClO + OH$	1.94E24	-3.76	-9.815E-5	1.0

a: A's in sec^{-1} and $cm^3\ mol^{-1}\ s^{-1}$
b: Ea in kcal/mol
<ν> 3 Frequencies: 599.1 606.7 1755.6
Degeneracy: 4.374 3.193 3.932
L.J. Parameters: σ = 4.774 Å; e/k = 505.573 K
$\langle\Delta E\rangle_{avg}$ for Ar = 450 cm^{-1}
β as function of Temperature:

T(K)	300	500	900	1200	1500	1800	2100	2500
β	0.317	0.168	0.054	0.027	0.017	0.013	0.012	0.013

k_1 A = 3.32E15, n = -1.3, Ea = 0.0, from $k = 2.0E12(T/300)^{-1.3}$
Ref: Fenter et al. and Gutman et al., *J. Phys. Chem.* **1993**, 97, 4695.

k_{-1} Via k_1 and Microscopic-Reversibility <MR>, $Ea = \Delta H - RT_m$

k_2 Via k_2 and <MR>

k_{-2} A_{-2} taken as that for $CH_3O + O$, A = 1.51E13, Ea = 0.0,
Ref: Baulch et al., *J. Phys. Chem. Ref. Data* **1992**, 21, 411.

k_3 TST, $k = AT^n e^{(-Ea/RT)}$, loss of one rotor, $A = 10^{10.75} * 10^{-4.3/4.56} = 6.41E09$, n = 1.0
Ea = 31, Ref: AM1/UHF.

k_4 TST, $k = AT^n e^{(-Ea/RT)}$, loss of one rotor, gain one Optical Isomer and degeneracy,
$A = 10^{10.75} * 10^{(-4.3+1.38)/4.6} * 2 = 2.57E10$, n = 1.0,
$Ea = 27(RS) + 10.4(\Delta H_{rxn}) + 9.03(E_{abs}) = 46.7$

k_{-4} Via k_4 and <MR>

k_5 Via k_{-5} and <MR>, Ea = 1.0

k_{-5} A_{-5} taken as that of $CH_3CHO + OH \rightarrow CC.OOH$, A = 8.0E12,
Ref: Bozzelli, J. W.; Dean, A. M., *J. Phys. Chem.* **1990**, 94, 3313.

<ν> From "CPFIT" Computer Code (Ref: Ritter, E. R., *J. Chem. Inf. Computat. Sci.*, **1991**, 31, 400) and Cp data for CH_2ClOO

σ, e/k Calculated from critical properties for CH_2ClOO (Ref: Reid, R. C.; Prausnitz, J. M.; Sherwood, T. K. *The Properties of Gases and Liquids*, 3rd Ed. McGraw-Hill Co., New York, **1977**).

Table B4 QRRK Input Data for $CHCl_2 + O_2 \leftrightarrow [CHCl_2OO]^* \rightarrow$ Products

	Reaction	A[a]	n	α	E_a[b]
k_1	$CHCl_2 + O_2 \rightarrow CHCl_2OO$	8.78E15	-1.5	0.0	0.0
k_{-1}	$CHCl_2OO \rightarrow CHCl_2 + O_2$	7.69E26	-4.92	-1.201E-4	21.5
k_2	$CHCl_2OO \rightarrow CHCl_2O + O$	1.95E22	-2.95	-7.18E-4	57.5
k_3	$CHCl_2OO \rightarrow CHClO + ClO$	1.28E10	1.0	0.0	31.0
k_4	$CHCl_2OO \rightarrow C.Cl_2OOH$	1.28E10	1.0	0.0	47.3
k_{-4}	$C.Cl_2OOH \rightarrow CHCl_2OO$	4.13E09	1.0	0.0	35.6
k_5	$C.Cl_2OOH \rightarrow CCl_2O + OH$	9.92E24	-3.93	-2.838e-4	1.00

a: A's in sec^{-1} and $cm^3\ mol^{-1}\ s^{-1}$
b: E_a in kcal/mol
<ν> 3 Frequencies: 312.3 705.7 1023.1
Degeneracy: 5.013 1.153 5.335
L.J. Parameters: σ = 5.0862 Å; e/k = 542.243 K
$\langle\Delta E\rangle_{avg}$ for Ar = 450 cm^{-1}
β as function of Temperature:

T(K) :	300	500	900	1200	1500	1800	2100	2500
β :	0.305	0.149	0.041	0.025	0.021	0.022	0.025	0.029

k_1 A = 8.78E15, n = -1.5, Ea = 0.0, from $k = 1.7E12(T/300)^{-1.5}$
Ref: Fenter et al. and Gutman et al., *J. Phys. Chem.* **1993**, 97, 4695.

k_{-1} Via k_1 and Microscopic-Reversibility <MR>, $Ea = \Delta H - RT_m$

k_2 Via k_2 and <MR>

k_{-2} A_{-2} taken as that for $CH_3O + O$, A = 1.51E13, Ea = 0.0,
Ref: Baulch et al., *J. Phys. Chem. Ref. Data* **1992**, 21, 411.

k_3 TST, $k = AT^n e^{(-Ea/RT)}$, loss of one rotor and degeneracy,
$A = 10^{10.75} * 10^{-4.3/4.56} * 2 = 1.28E10$, n = 1.0, Ea = 31, Ref: AM1/UHF.

k_4 TST, $k = AT^n e^{(-Ea/RT)}$, loss of one rotor, gain one Optical Isomer,
$A = 10^{10.75} * 10^{(-4.3+1.38)/4.6} = 1.28E10$, n = 1.0,
$Ea = 27(RS) + 11.7(\Delta H_{rxn}) + 8.60(E_{abs}) = 47.3$

k_{-4} Via k_4 and <MR>

k_5 Via k_{-5} and <MR>, Ea = 1.0

k_{-5} A_{-5} taken as that of $CH_3CHO + OH \rightarrow CC.OOH$, A = 8.0E12,
Ref: Bozzelli, J. W.; Dean, A. M., *J. Phys. Chem.* **1990**, 94, 3313.

<ν> From "CPFIT" Computer (Ref: Ritter, E. R., *J. Chem. Inf. Computat. Sci.*, **1991**, 31, 400) and Cp data for Cp data for $CHCl_2OO$

σ, e/k Calculated from critical properties for $CHCl_2OO$ (Ref: Reid, R. C.; Prausnitz, J. M.; Sherwood, T. K. *The Properties of Gases and Liquids*, 3rd Ed. McGraw-Hill Co., New York, **1977**).

Table C1 Quantum RRK Input Data for $CH_2Cl_2 \leftrightarrow [CH_2Cl_2]^* \rightarrow$ Products

	Reaction	A[a]	n	α	E_a[b]	ΔH_{298}
k_1	$CH_2Cl_2 \rightarrow CHCl + HCl$	2.25E11	1.0	0.0	74.2	72.7
k_2	$CH_2Cl_2 \rightarrow CH_2Cl + Cl$	7.13E15	0.34	1.09E-3	77.0	80.5

a: A's in s^{-1}
b: E_a in kcal/mol

<ν> 3 Frequencies: 538.6 1240.3 2710.7
Degeneracy: 3.071 3.662 2.267
L.J. Parameters: σ = 4.898 Å; e/k = 356.3 K
$\langle\Delta E\rangle_{avg}$ for Ar = 450 cm^{-1}, for Kr = 630 cm^{-1}
$\langle\Delta E\rangle_{down}$ for Kr = 1470 cal

β as function of Temperature:	T(K) :	400	500	600	900	1200	1500	1800	2100
in Ar Bath Gas	β :	0.234	0.18	0.14	0.075	0.044	0.028	0.018	0.012

k_1 Transition State Theory: loss of no rotor, degeneracy, $k = AT^n e^{(-Ea/RT)}$
$A_3 = 10^{10.75} * 4 =$ 2.25E11, n = 1, $E_a = \Delta H_{rxn} + 1.5$, (Ref: Lim, K. P.; Michael, J. V. J. *Twenty-fifth Symposium (International) on Combustion*; The Combustion Institute: Pittsburgh. **1994**)

k_2 Via k_{-2} and <MR>, E_a = 77.0, (Ref. as k_1)

k_{-2} A_{-2} = 1.30E14, from the trend of A factor for Cl + Radical combination reaction, Ea = 0.0

<ν> From "CPFIT" Computer Code (Ref: Ritter, E. R. *J. Chem. Inf. Computat. Sci.*, **1991**, 31, 400.) and Cp data for CH_2Cl_2

σ, e/k Calculated from critical properties for CH_2Cl_2 (Ref: Reid, R. C.; Prausnitz, J. M.; and Sherwood, T. K. *The Properties of Gases and Liquids*, 3rd Ed. McGraw-Hill Co., New York, **1977**).

Calculated Apparent Rate Constants in Ar bath Gas

Reactions	A(cm^3 mol^{-1} s^{-1})	n	E(cal/mol)	P(atm)	T(K)
$CH_2Cl_2 \rightarrow CHCl + HCl$	7.54E+34	-6.54	78320	0.1	300-1500
$CH_2Cl_2 \rightarrow CHCl + HCl$	2.64E+32	-5.67	77930	1	300-1500
$CH_2Cl_2 \rightarrow CHCl + HCl$	2.47E+28	-4.35	76830	10	300-1500
$CH_2Cl_2 \rightarrow CH_2Cl + Cl$	1.70E+35	-6.48	83220	0.1	300-1500
$CH_2Cl_2 \rightarrow CH_2Cl + Cl$	4.71E+35	-6.31	83580	1	300-1500
$CH_2Cl_2 \rightarrow CH_2Cl + Cl$	6.70E+33	-5.50	83700	10	300-1500

Table D1 Reduced vibrational frequencies, geo-mean frequency, number of internal rotors and $C_p(0)$ and $C_p(\infty)$

$CHCl_2$ --------- HARMONIC OSCIL FIT ----------
vibration 1: modes = 2.581 frequency = 628.2 cm^{-1}
vibration 2: modes = 1.857 frequency = 622.9 cm^{-1}
vibration 3: modes = 1.562 frequency = 2498.3 cm^{-1}
geometric mean vibration: modes = 6.000 frequency = 897.5 cm^{-1}
calculations for a non-linear molecule with 6 int modes (0 internal rotors)
$C_p(0)$: 7.948 $C_p(inf)$: 19.870

CH_2Cl --------- HARMONIC OSCIL FIT ----------
vibration 1: modes = 1.827 frequency = 697.0 cm^{-1}
vibration 2: modes = 2.848 frequency = 1281.6 cm^{-1}
vibration 3: modes = 1.325 frequency = 4000.0 cm^{-1}
geometric mean vibration: modes = 6.000 frequency = 1368.7 cm^{-1}
calculations for a non-linear molecule with 6 int modes (0 internal rotors)
$C_p(0)$: 7.948 $C_p(inf)$: 19.870

CH_3 --------- HARMONIC OSCIL FIT ----------
vibration 1: modes = 1.223 frequency = 666.0 cm^{-1}
vibration 2: modes = 2.045 frequency = 1518.9 cm^{-1}
vibration 3: modes = 2.733 frequency = 3328.2 cm^{-1}
geometric mean vibration: modes = 6.000 frequency = 1835.4 cm^{-1}
calculations for a non-linear molecule with 6 int modes (0 internal rotors)
$C_p(0)$: 7.948 $C_p(inf)$: 19.870

C_2HCl_3 --------- HARMONIC OSCIL FIT ----------
vibration 1: modes = 6.197 frequency = 319.1 cm^{-1}
vibration 2: modes = 5.284 frequency = 1122.5 cm^{-1}
vibration 3: modes = 0.519 frequency = 3991.4 cm^{-1}
geometric mean vibration: modes = 12.000 frequency = 619.3 cm^{-1}
calculations for a non-linear molecule with 12 int modes (0 internal rotors)
$C_p(0)$: 7.948 $C_p(inf)$: 31.792

CHClCHCl --------- HARMONIC OSCIL FIT ----------
vibration 1: modes = 4.655 frequency = 379.3 cm^{-1}
vibration 2: modes = 5.677 frequency = 1261.1 cm^{-1}
vibration 3: modes = 1.668 frequency = 2269.7 cm^{-1}
geometric mean vibration: modes = 12.000 frequency = 858.7 cm^{-1}
calculations for a non-linear molecule with 12 int modes (0 internal rotors)
$C_p(0)$: 7.948 $C_p(inf)$: 31.792

Table D1 (cont'd)

CH_2CCl_2 --------- HARMONIC OSCIL FIT ----------
vibration 1: modes = 4.655 frequency = 379.3 cm^{-1}
vibration 2: modes = 5.677 frequency = 1261.1 cm^{-1}
vibration 3: modes = 1.668 frequency = 2269.7 cm^{-1}
geometric mean vibration: modes = 12.000 frequency = 858.7 cm^{-1}
calculations for a non-linear molecule with 12 int modes (0 internal rotors)
$C_p(0)$: 7.948 $C_p(inf)$: 31.792

$CHCl_2CHCl$ --------- HARMONIC OSCIL FIT ----------
vibration 1: modes = 3.424 frequency = 100.1 cm^{-1}
vibration 2: modes = 7.386 frequency = 695.9 cm^{-1}
vibration 3: modes = 3.689 frequency = 2365.2 cm^{-1}
geometric mean vibration: modes = 14.50 frequency = 601.0 cm^{-1}
calculations for a non-linear molecule with 15 int modes(1 internal rotors)
$C_p(0)$: 7.948 $C_p(inf)$: 36.759

$CHCl_2CHCl_2$ --------- HARMONIC OSCIL FIT ----------
vibration 1: modes = 8.181 frequency = 100.1 cm^{-1}
vibration 2: modes = 7.280 frequency = 951.6 cm^{-1}
vibration 3: modes = 2.040 frequency = 1999.5 cm^{-1}
geometric mean vibration: modes = 17.50 frequency = 362.1 cm^{-1}
calculations for a non-linear molecule with 18 int modes(1 internal rotors)
$C_p(0)$: 7.948 $C_p(inf)$: 42.720

C_2H_3Cl --------- HARMONIC OSCIL FIT ----------
vibration 1: modes = 4.570 frequency = 656.5 cm^{-1}
vibration 2: modes = 5.237 frequency = 1405.2 cm^{-1}
vibration 3: modes = 2.193 frequency = 3998.8 cm^{-1}
geometric mean vibration: modes = 12.00 frequency = 1273.1 cm^{-1}
calculations for a non-linear molecule with 12 int modes(0 internal rotors)
$C_p(0)$: 7.948 $C_p(inf)$: 31.792

$CHCl_2CH_2$ --------- HARMONIC OSCIL FIT ----------
vibration 1: modes = 3.690 frequency = 250.2 cm^{-1}
vibration 2: modes = 7.025 frequency = 916.9 cm^{-1}
vibration 3: modes = 3.785 frequency = 2552.4 cm^{-1}
geometric mean vibration: modes = 14.500 frequency = 860.7 cm^{-1}
calculations for a non-linear molecule with 15 int modes(1 internal rotors)
$C_p(0)$: 7.948 $C_p(inf)$: 36.759

Table D1 (cont'd)

$CH_2ClCHCl$ --------- HARMONIC OSCIL FIT ----------
vibration 1: modes = 5.490 frequency = 466.9 cm^{-1}
vibration 2: modes = 2.281 frequency = 594.8 cm^{-1}
vibration 3: modes = 6.729 frequency = 2027.9 cm^{-1}
geometric mean vibration: modes = 14.500 frequency = 958.9 cm^{-1}
calculations for a non-linear molecule with 15 int modes(1 internal rotors)
$C_p(0)$: 7.948 $C_p(inf)$: 36.759

$CH_2ClCHCl_2$ --------- HARMONIC OSCIL FIT ----------
vibration 1: modes = 5.108 frequency = 250.2 cm^{-1}
vibration 2: modes = 7.620 frequency = 824.1 cm^{-1}
vibration 3: modes = 4.772 frequency = 2384.9 cm^{-1}
geometric mean vibration: modes = 17.500 frequency = 777.6 cm^{-1}
calculations for a non-linear molecule with 18 int modes(1 internal rotors)
$C_p(0)$: 7.948 $C_p(inf)$: 42.720

CH_2ClCH_2 --------- HARMONIC OSCIL FIT ----------
vibration 1: modes = 4.143 frequency = 601.7 cm^{-1}
vibration 2: modes = 2.315 frequency = 801.3 cm^{-1}
vibration 3: modes = 8.042 frequency = 1910.7 cm^{-1}
geometric mean vibration: modes = 14.50 frequency = 1195.6 cm^{-1}
calculations for a non-linear molecule with 15 int modes(1 internal rotors)
$C_p(0)$: 7.948 $C_p(inf)$: 36.759

CH_3CHCl --------- HARMONIC OSCIL FIT ----------
vibration 1: modes = 3.998 frequency = 641.6 cm^{-1}
vibration 2: modes = 3.532 frequency = 800.1 cm^{-1}
vibration 3: modes = 6.971 frequency = 2159.7 cm^{-1}
geometric mean vibration: modes = 14.50 frequency = 1213.5 cm^{-1}
calculations for a non-linear molecule with 15 int modes(1 internal rotors)
$C_p(0)$: 7.948 $C_p(inf)$: 36.759

CH_3CHCl_2 --------- HARMONIC OSCIL FIT ----------
vibration 1: modes = 3.610 frequency = 250.3 cm^{-1}
vibration 2: modes = 9.222 frequency = 980.7 cm^{-1}
vibration 3: modes = 4.668 frequency = 2659.7 cm^{-1}
geometric mean vibration: modes = 17.500 frequency = 965.5 cm^{-1}
calculations for a non-linear molecule with 18 int modes(1 internal rotors)
$C_p(0)$: 7.948 $C_p(inf)$: 42.720

Table D1 (cont'd)

CH_2ClCH_2Cl --------- HARMONIC OSCIL FIT ----------

vibration 1: modes = 5.890 frequency = 609.8 cm^{-1}
vibration 2: modes = 3.366 frequency = 501.6 cm^{-1}
vibration 3: modes = 8.243 frequency = 2091.5 cm^{-1}
geometric mean vibration: modes = 17.50 frequency = 1049.5 cm^{-1}
calculations for a non-linear molecule with 18 int modes(1 internal rotors)
$C_p(0)$: 7.948 $C_p(inf)$: 42.720

C_2H_5 --------- HARMONIC OSCIL FIT ----------

vibration 1: modes = 3.872 frequency = 676.0 cm^{-1}
vibration 2: modes = 3.686 frequency = 1178.7 cm^{-1}
vibration 3: modes = 6.941 frequency = 2572.5 cm^{-1}
geometric mean vibration: modes = 14.500 frequency = 1476.3 cm^{-1}
calculations for a non-linear molecule with 15 int modes(1 internal rotors)
$C_p(0)$: 7.948 $C_p(inf)$: 36.759

C_2H_5Cl --------- HARMONIC OSCIL FIT ----------

vibration 1: modes = 6.161 frequency = 607.0 cm^{-1}
vibration 2: modes = 6.582 frequency = 1387.1 cm^{-1}
vibration 3: modes = 4.757 frequency = 2950.3 cm^{-1}
geometric mean vibration: modes = 17.500 frequency = 1273.1 cm^{-1}
calculations for a non-linear molecule with 18 int modes(1 internal rotors)
$C_p(0)$: 7.948 $C_p(inf)$: 42.720

Table D2 Arrhenius Parameters for Chloro-Methyl Radical Combination Reactions

Reaction	No. of Cl	k in $cm^3\ mol^{-1}\ s^{-1}$	Reference
$CH_3 + CH_3$	(0 + 0)	2.40E13	112 (Baulch)
		2.50E13	113
		5.00E13	100 (Weis & BSN)
		3.60E13	114 (Wagner)
		2.83E13	111 (Cobos)
$CH_3 + CH_2Cl$	(0 + 1)	2.00E13	113
		5.00E13	100
		1.20E13	91 (Setser)
$CH_3 + CHCl_2$	(0 + 2)	1.58E13	113
		2.30E13	100
$CH_2Cl + CH_2Cl$	(1 + 1)	3.98E12	113
		1.00E13	100
		$1.7E13(T/298)^{-0.85}$	99 (Lesclaux)
		2.10E13	91
$CH_3 + CCl_3$	(0 + 3)	1.99E13	113
$CH_2Cl + CHCl_2$	(1 + 2)	7.94E12	113
$CH_2Cl + CCl_3$	(1 + 3)	7.94E12	113
$CHCl_2 + CHCl_2$	(2 + 2)	3.98E12	112
		$5.6E12*(T/298)^{-0.74}$	99
$CHCl_2 + CCl_3$	(2 + 3)	7.07E12	113
		1.14E12	100
$CCl_3 + CCl_3$	(3 + 3)	4.46E12	113
		$2.0E12*(T/298)^{-1.0}$	110 (Danis)
		6.00E12	111
		3.98E12	115 (Huybrechts)

Table D3 Recommended High Pressure Limit A Factors for Chloro-Methyl Combination Reactions from Evaluation of Literature (see Fig. D1 and Table D2)
$k = A * (T/298)^{-(0.80\pm0.20)}$ cm^3 mol^{-1} s^{-1}

	CH_3	CH_2Cl	$CHCl_2$	CCl_3
CH_3	3.2×10^{13}	2.8×10^{13}	2.5×10^{13}	9.8×10^{12}
CH_2Cl		2.4×10^{13}	9.8×10^{12}	6.1×10^{12}
$CHCl_2$			5.6×10^{12}	4.2×10^{12}
CCl_3				2.2×10^{12}

Table D4 Literature Rate Constants for Cl + (Chloro) Methyl Radical

Reaction	A (cm^3 mol^{-1} sec^{-1})	Sources
$Cl + CH_3$	1.54E14	116
$Cl + C_2H_5$	1.45E14	117
$Cl + CCl_3$	3.92E13	118
$Cl + CCl_3CHCl$	7.08E13	119
$Cl + C_2Cl_5$	7.94E12	100

Table D5 QRRK Input Data for $CH_3 + CH_2Cl \leftrightarrow [C_2H_5Cl]^* \rightarrow$ Products

	Reaction	A^a	n	α	E_a^b
k_1	$CH_3 + CH_2Cl \rightarrow C_2H_5Cl$	1.79E15	-0.75	0.0	0.00
k_{-1}	$C_2H_5Cl \rightarrow CH_3 + CH_2Cl$	7.40E16	0.22	0.002389	89.01
k_2	$C_2H_5Cl \rightarrow C_2H_5 + Cl$	7.81E16	-0.23	0.000787	82.34
k_3	$C_2H_5Cl \rightarrow C_2H_4 + HCl$	1.92E10	1.0	0.0	56.23

a: A's in sec^{-1} and $cm^3\ mol^{-1}\ s^{-1}$
b: Ea in kcal/mol
<ν> 3 Frequencies: 607.0 1387.1 2950.3
Degeneracy: 6.161 6.582 4.757
L.J. Parameters: $\sigma = 4.898$ Å e/k = 300.0 K
$\langle\Delta E\rangle_{avg}$ for Ar = 450 cm^{-1}
β as function of T, T(K) : 450 600 750 900 1200 1500 1800 2100
β : 0.242 0.164 0.113 0.079 0.04 0.021 0.012 0.008

k_1 $A_1 = 2.5E13(T/298)^{-0.75}$, from Figure 4.1 and Table 4.2, literature review: Arrhenius A Factor for Combination Reaction of Chloro-Methyl Radicals vs. No. of Cl's. Ea = 0.0

k_{-1} Via k_1 and Microscopic-Reversibility <MR>, Ea = $\Delta H - RT_m$

k_2 Via k_{-2} and <MR>, Ea = $\Delta H - RT_m$

k_{-2} A_{-2} = 1.40E14, from the trend of A factor for Cl + Radical Combination after literature review, see Table 3. Ea = 0.0

k_3 Transition State Theory: loss of one rotor and degeneracy, $k = AT^n e^{(-Ea/RT)}$
$A_3 = 10^{10.75} * 10^{-4.3/4.56} * 3 = 1.92E10$, n = 1, Ea = $\Delta H + 39$, Ref: Weissman, M.; Benson, S. W. *Intl. J. of Chem. Kinet.* 1984, 16, 307. and Dai, H-L; Specht, E.; Berman, M. R.; *J. Chem. Phys.* **1982**, 77, 4494.

<ν> From "CPFIT" Computer Code (Ref: Ritter, E. R. *J. Chem. Inf. Computat. Sci.* **1991**, 31, 400) and C_p data for C_2H_5Cl

σ, e/k Calculated from critical properties for C_2H_5Cl (Ref: Reid, R. C.; Prausnitz, J. M.; Sherwood, T. K. *The Properties of Gases and Liquids* 3rd Ed. McGraw-Hill Co., New York, **1977**.)

Table D6 QRRK Input Data for $CH_3 + CHCl_2 \leftrightarrow [CH_3CHCl_2]^* \rightarrow$ Products

	Reaction	A[a]	n	α	E_a[b]
k_1	$CH_3 + CHCl_2 \rightarrow CH_3CHCl_2$	1.36E15	-0.75	0.0	0.00
k_{-1}	$CH_3CHCl_2 \rightarrow CH_3 + CHCl_2$	4.05E18	-0.43	0.002101	87.25
k_2	$CH_3CHCl_2 \rightarrow CH_3CHCl + Cl$	2.20E18	-0.76	0.000296	75.87
k_3	$CH_3CHCl_2 \rightarrow C_2H_3Cl + HCl$	3.84E10	1.0	0.0	54.03

a: A's in sec^{-1} and $cm^3\ mol^{-1}\ s^{-1}$
b: Ea in kcal/mol
<ν> 3 Frequencies: 250.3 980.7 2659.7
Degeneracy: 3.61 9.222 4.668
L.J. Parameters: σ = 5.103 Å e/k = 415.31 K
$\langle\Delta E\rangle_{avg}$ for Ar = 450 cm^{-1}
β as function of T, T(K) : 450 600 750 900 1200 1500 1800 2100
β : 0.238 0.159 0.108 0.075 0.036 0.018 0.011 0.008

k_1 $A_1 = 1.90E13(T/298)^{-0.75}$, from Figure 4.1 and Table 4.2, literature review: Arrhenius A Factor for Combination Reaction of Chloro-Methyl Radicals vs. No. of Cl's. Ea = 0.0

k_{-1} Via k_1 and Microscopic-Reversibility <MR>, $Ea = \Delta H - RT_m$

k_2 Via k_{-2} and <MR>, $Ea = \Delta H - RT_m$

k_{-2} A_{-2} = 6.70E13, from the trend of A factor for Cl + Radical Combination after literature review, see Table 3. Ea = 0.0

k_3 Transition State Theory: loss of one rotor, degeneracy, $k = AT^n e^{(-Ea/RT)}$
$A_3 = 10^{10.75} * 10^{-4.3/4.56} * 6 =$ 1.92E10, n = 1, Ea = ΔH + 40, Ref: Weissman, M.; Benson, S. W. *Intl. J. of Chem. Kinet.* 1984, 16, 307. and Dai, H-L; Specht, E.; Berman, M. R.; *J. Chem. Phys.* **1982, 77,** 4494.

<ν> From "CPFIT" Computer Code (Ref: Ritter, E. R. *J. Chem. Inf. Computat. Sci.* **1991**, 31, 400) and C_p data for CH_3CHCl_2.

σ, e/k Calculated from critical properties for CH_3CHCl_2 (Ref: Reid, R. C.; Prausnitz, J. M.; Sherwood, T. K. *The Properties of Gases and Liquids* 3rd Ed. McGraw-Hill Co., New York, **1977**.)

Table D7 QRRK Input Data for $CH_2Cl + CH_2Cl \leftrightarrow [CH_2ClCH_2Cl]^* \rightarrow$ Products

	Reaction	A^a	n	α	E_a^b
k_1	$CH_2Cl + CH_2Cl \rightarrow CH_2ClCH_2Cl$	1.22E15	-0.75	0.0	0.00
k_{-1}	$CH_2ClCH_2Cl \rightarrow CH_2Cl + CH_2Cl$	7.95E18	-0.34	0.002008	86.45
k_2	$CH_2ClCH_2Cl \rightarrow CH_2ClCH_2 + Cl$	4.99E17	-0.51	0.000265	79.10
k_3	$CH_2ClCH_2Cl \rightarrow C_2H_3Cl + HCl$	2.56E10	1.0	0.0	54.53

a: A's in sec^{-1} and $cm^3\ mol^{-1}\ s^{-1}$
b: Ea in kcal/mol
<ν> 3 Frequencies: 609.8 501.6 2091.5
Degeneracy: 5.89 3.366 8.243
L.J. Parameters: σ = 5.116 Å e/k = 445.49 K
$\langle\Delta E\rangle_{avg}$ for Ar = 450 cm^{-1}
β as function of T, T(K) : 500 600 750 900 1000 1200 1500 1800
β : 0.153 0.134 0.09 0.062 0.049 0.03 0.016 0.009

k_1 Roussel P.B., et al., *J. Chem. Soc. Faraday Trans.*, **87**, 2367-2377, (1991)

k_{-1} Via k_1 and Microscopic-Reversibility <MR>, Ea = $\Delta H - RT_m$

k_2 Via k_{-2} and <MR>, Ea = $\Delta H - RT_m$

k_{-2} A_{-2} = 6.55E13, from the trend of A factor for Cl + Radical Combination after literature review, see Table 3. Ea = 0.0

k_3 Transition State Theory: loss of one rotor, degeneracy, $k = AT^n e^{(-Ea/RT)}$
$A_3 = 10^{10.75} * 10^{-4.3/4.56} * 4 =$ 2.56E10, n = 1, Ea = ΔH + 41, Ref: Weissman, M.; Benson, S. W. *Intl. J. of Chem. Kinet.* 1984, 16, 307. and Dai, H-L; Specht, E.; Berman, M. R.; *J. Chem. Phys.* **1982**, 77, 4494.

<ν> From "CPFIT" Computer Code (Ref: Ritter, E. R. *J. Chem. Inf. Computat. Sci.* **1991**, 31, 400) and C_p data for CH_2ClCH_2Cl

σ, e/k Calculated from critical properties for CH_2ClCH_2Cl (Ref: Reid, R. C.; Prausnitz, J. M.; Sherwood, T. K. *The Properties of Gases and Liquids* 3rd Ed. McGraw-Hill Co., New York, **1977**.)

Table D8 QRRK Input Data for $CH_2Cl + CHCl_2 \leftrightarrow [CH_2ClCHCl_2]^* \rightarrow$ Products

	Reaction	A[a]	n	α	E_a[b]
k_1	$CH_2Cl + CHCl_2 \rightarrow CH_2ClCHCl_2$	7.02E14	-0.75	0.0	0.00
k_{-1}	$CH_2ClCHCl_2 \rightarrow CH_2Cl + CHCl_2$	1.78E21	-1.34	0.001293	84.56
k_2	$CH_2ClCHCl_2 \rightarrow CH_2ClCHCl + Cl$	2.78E18	-0.89	0.000285	73.05
k_3	$CH_2ClCHCl_2 \rightarrow CHClCHCl + HCl$	2.56E10	1.0	0.0	55.33
k_4	$CH_2ClCHCl_2 \rightarrow CHCl_2CH_2 + Cl$	2.37E17	-0.30	0.000621	77.81
k_5	$CH_2ClCHCl_2 \rightarrow CH_2CCl_2 + HCl$	6.41E09	1.0	0.0	55.43

a: A's in sec^{-1} and $cm^3\ mol^{-1}\ s^{-1}$
b: Ea in kcal/mol
<ν> 3 Frequencies: 350.7 1117.0 2796.0
Degeneracy: 5.830 8.806 4.083
L.J. Parameters: σ = 5.397 Å e/k = 478.04 K
$\langle\Delta E\rangle_{avg}$ for Ar = 450 cm^{-1}
β as function of T, T(K) : 450 600 750 900 1200 1500 1800 2100
β : 0.236 0.156 0.105 0.072 0.034 0.017 0.011 0.008

k_1 $A_1 = 9.80E12(T/298)^{-0.75}$, from Figure 4.1 and Table 4.2, literature review: Arrhenius A Factor for Combination Reaction of Chloro-Methyl Radicals vs. No. of Cl's. Ea = 0.0

k_{-1} Via k_1 and Microscopic-Reversibility <MR>, Ea = ΔH - RT_m

k_2 Via k_{-2} and <MR>, Ea = ΔH - RT_m

k_{-2} A_{-2} = 4.15E13, from the trend of A factor for Cl + Radical Combination after literature review, see Table 3. Ea = 0.0

k_3 Transition State Theory: loss of one rotor, degeneracy, $k = AT^n e^{(-Ea/RT)}$
$A_3 = 10^{10.75} * 10^{-4.3/4.56} * 4 =$ 2.56E10, n = 1, Ea = ΔH + 42, Ref: Weissman, M.; Benson, S. W. *Intl. J. of Chem. Kinet.* 1984, 16, 307. and Dai, H-L; Specht, E.; Berman, M. R.; *J. Chem. Phys.* **1982**, **77**, 4494.

k_4 Via k_{-4} and <MR>, Ea = ΔH - RT_m

k_{-4} A_{-4} = 4.30E13, from the trend of A factor for Cl + Radical Combination after literature review, see Table 3. Ea = 0.0

k_5 Transition State Theory: loss of one rotor, degeneracy, $k = AT^n e^{(-Ea/RT)}$
$A_3 = 10^{10.75} * 10^{-4.3/4.56} =$ 6.41E09, n = 1, Ea = ΔH + 42, Ref: as k_3

<ν> From "CPFIT" Computer Code (Ref: Ritter, E. R. *J. Chem. Inf. Computat. Sci.* **1991**, 31, 400) and C_p data for $CH_2ClCHCl_2$.

σ, e/k Calculated from critical properties for $CH_2ClCHCl_2$ (Ref: Reid, R. C.; Prausnitz, J. M.; Sherwood, T. K. *The Properties of Gases and Liquids* 3rd Ed. McGraw-Hill Co., New York, **1977**.)

Table D9 QRRK Input Data for $CHCl_2 + CHCl_2 \leftrightarrow [CHCl_2CHCl_2]^* \rightarrow$ Products

	Reaction	A[a]	n	α	E_a[b]
k_1	$CHCl_2 + CHCl_2 \rightarrow CHCl_2CHCl_2$	4.01E14	-0.75	0.0	0.00
k_{-1}	$CHCl_2CHCl_2 \rightarrow CHCl_2 + CHCl_2$	1.01E26	-3.09	0.0004769	80.26
k_2	$CHCl_2CHCl_2 \rightarrow CHCl_2CHCl + Cl$	7.21E20	-1.78	0.000132	73.81
k_3	$CHCl_2CHCl_2 \rightarrow C_2HCl_3 + HCl$	2.56E10	1.0	0.0	56.33

a: A's in sec^{-1} and $cm^3\ mol^{-1}\ s^{-1}$
b: Ea in kcal/mol
<ν> 3 Frequencies: 100.1 951.6 1999.5
Degeneracy: 8.181 7.28 2.040
L.J. Parameters: σ = 5.91 Å e/k = 525.9 K
$\langle\Delta E\rangle_{avg}$ for Ar = 450 cm^{-1}
β as function of T, T(K): 500 600 750 900 1000 1200 1500 1800
β : 0.145 0.125 0.081 0.054 0.041 0.024 0.012 0.008

k_1 Roussel P.B., et al., *J. Chem. Soc. Faraday Trans.*, **87**, 2367-2377, (1991)

k_{-1} Via k_1 and Microscopic-Reversibility <MR>, Ea = $\Delta H - RT_m$

k_2 Via k_{-2} and <MR>, Ea = $\Delta H - RT_m$

k_{-2} A_{-2} = 2.80E13, from the trend of A factor for Cl + Radical Combination after literature review, see Table 3. Ea = 0.0

k_3 Transition State Theory: loss of one rotor, degeneracy, $k = AT^n e^{(-Ea/RT)}$
$A_3 = 10^{10.75} * 10^{-4.3/4.56} * 4 =$ 2.56E10, n = 1, Ea = ΔH + 43, Ref: Weissman, M.; Benson, S. W. *Intl. J. of Chem. Kinet.* 1984, 16, 307. and Dai, H-L; Specht, E.; Berman, M. R.; *J. Chem. Phys.* **1982**, 77, 4494.

<ν> From "CPFIT" Computer Code (Ref: Ritter, E. R. *J. Chem. Inf. Computat. Sci.* **1991**, 31, 400) and C_p data for $CHCl_2CHCl_2$.

σ, e/k Calculated from critical properties for $CHCl_2CHCl_2$ (Ref: Reid, R. C.; Prausnitz, J. M.; Sherwood, T. K. *The Properties of Gases and Liquids* 3rd Ed. McGraw-Hill Co., New York, **1977**.)

Table D10 Apparent rate constants, $k = AT^n \exp(-E/RT)$

Reactions	A($cm^3\ mol^{-1}\ s^{-1}$)	n	E(cal/mol)	P(atm)	T(K)
$CH_3 + CH_2Cl \rightarrow C_2H_5Cl$	8.07E+38	-9.29	4653	0.01	300-2500
$CH_3 + CH_2Cl \rightarrow C_2H_5Cl$	2.57E+41	-9.71	5806	0.1	300-2500
$CH_3 + CH_2Cl \rightarrow C_2H_5Cl$	1.62E+43	-9.89	7545	1.0	300-2500
$CH_3 + CH_2Cl \rightarrow C_2H_5Cl$	1.54E+42	-9.42	7780	3.0	300-2500
$CH_3 + CH_2Cl \rightarrow C_2H_5Cl$	2.77E+39	-8.45	7370	10.0	300-2500
$CH_3 + CH_2Cl \rightarrow C_2H_5 + Cl$	7.91E+10	0.39	-869	0.01	300-2500
$CH_3 + CH_2Cl \rightarrow C_2H_5 + Cl$	3.22E+12	-0.06	274	0.1	300-2500
$CH_3 + CH_2Cl \rightarrow C_2H_5 + Cl$	2.68E+14	-0.57	2395	1.0	300-2500
$CH_3 + CH_2Cl \rightarrow C_2H_5 + Cl$	1.07E+14	-0.42	3079	3.0	300-2500
$CH_3 + CH_2Cl \rightarrow C_2H_5 + Cl$	1.47E+12	0.16	3292	10.0	300-2500
$CH_3 + CH_2Cl \rightarrow C_2H_4 + HCl$	7.86E+16	-1.30	587	0.01	300-2500
$CH_3 + CH_2Cl \rightarrow C_2H_4 + HCl$	2.78E+18	-1.73	1743	0.1	300-2500
$CH_3 + CH_2Cl \rightarrow C_2H_4 + HCl$	4.26E+19	-2.02	3623	1.0	300-2500
$CH_3 + CH_2Cl \rightarrow C_2H_4 + HCl$	3.19E+18	-1.66	4016	3.0	300-2500
$CH_3 + CH_2Cl \rightarrow C_2H_4 + HCl$	5.08E+15	-0.82	3823	10.0	300-2500
$CH_3 + CHCl_2 \rightarrow CH_3CHCl_2$	1.45E+38	-9.25	4244	0.01	300-2500
$CH_3 + CHCl_2 \rightarrow CH_3CHCl_2$	1.69E+40	-9.55	5020	0.1	300-2500
$CH_3 + CHCl_2 \rightarrow CH_3CHCl_2$	7.64E+42	-9.99	6858	1.0	300-2500
$CH_3 + CHCl_2 \rightarrow CH_3CHCl_2$	8.37E+42	-9.83	7488	3.0	300-2500
$CH_3 + CHCl_2 \rightarrow CH_3CHCl_2$	2.53E+41	-9.20	7597	10.0	300-2500
$CH_3 + CHCl_2 \rightarrow CH_3CHCl + Cl$	4.58E+12	-0.12	-587	0.01	300-2500
$CH_3 + CHCl_2 \rightarrow CH_3CHCl + Cl$	5.54E+13	-0.43	151	0.1	300-2500
$CH_3 + CHCl_2 \rightarrow CH_3CHCl + Cl$	1.31E+16	-1.08	2172	1.0	300-2500
$CH_3 + CHCl_2 \rightarrow CH_3CHCl + Cl$	4.04E+16	-1.19	3145	3.0	300-2500
$CH_3 + CHCl_2 \rightarrow CH_3CHCl + Cl$	8.35E+15	-0.95	3812	10.0	300-2500

Table D10 (cont'd)

Reactions	A($cm^3 mol^{-1} s^{-1}$)	n	E(cal/mol)	P(atm)	T(K)
$CH_3 + CHCl_2 \rightarrow C_2H_3Cl + HCl$	3.60E+16	-1.25	560	0.01	300-2500
$CH_3 + CHCl_2 \rightarrow C_2H_3Cl + HCl$	4.35E+17	-1.55	1327	0.1	300-2500
$CH_3 + CHCl_2 \rightarrow C_2H_3Cl + HCl$	3.98E+19	-2.08	3256	1.0	300-2500
$CH_3 + CHCl_2 \rightarrow C_2H_3Cl + HCl$	3.49E+19	-2.03	4033	3.0	300-2500
$CH_3 + CHCl_2 \rightarrow C_2H_3Cl + HCl$	1.15E+18	-1.57	4382	10.0	300-2500
$CH_2Cl + CH_2Cl \rightarrow CH_2ClCH_2Cl$	1.26E+39	-9.34	3786	0.01	300-2500
$CH_2Cl + CH_2Cl \rightarrow CH_2ClCH_2Cl$	9.42E+40	-9.59	5731	0.1	300-2500
$CH_2Cl + CH_2Cl \rightarrow CH_2ClCH_2Cl$	5.74E+42	-9.77	7242	1.0	300-2500
$CH_2Cl + CH_2Cl \rightarrow CH_2ClCH_2Cl$	1.18E+42	-9.40	7565	3.0	300-2500
$CH_2Cl + CH_2Cl \rightarrow CH_2ClCH_2Cl$	5.65E+39	-8.56	7304	10.0	300-2500
$CH_2Cl + CH_2Cl \rightarrow CH_2ClCH_2 + Cl$	1.03E+11	0.45	-240	0.01	300-2500
$CH_2Cl + CH_2Cl \rightarrow CH_2ClCH_2 + Cl$	9.75E+11	0.18	460	0.1	300-2500
$CH_2Cl + CH_2Cl \rightarrow CH_2ClCH_2 + Cl$	7.69E+13	-0.33	2313	1.0	300-2500
$CH_2Cl + CH_2Cl \rightarrow CH_2ClCH_2 + Cl$	8.68E+13	-0.31	3114	3.0	300-2500
$CH_2Cl + CH_2Cl \rightarrow CH_2ClCH_2 + Cl$	5.11E+12	0.08	3550	10.0	300-2500
$CH_2Cl + CH_2Cl \rightarrow C_2H_3Cl + HCl$	2.80E+20	-2.44	1393	0.01	300-2500
$CH_2Cl + CH_2Cl \rightarrow C_2H_3Cl + HCl$	2.38E+21	-2.70	2109	0.1	300-2500
$CH_2Cl + CH_2Cl \rightarrow C_2H_3Cl + HCl$	4.21E+22	-3.02	3780	1.0	300-2500
$CH_2Cl + CH_2Cl \rightarrow C_2H_3Cl + HCl$	8.76E+21	-2.79	4301	3.0	300-2500
$CH_2Cl + CH_2Cl \rightarrow C_2H_3Cl + HCl$	5.13E+19	-2.12	4318	10.0	300-2500
$CH_2Cl + CHCl_2 \rightarrow CH_2ClCHCl_2$	5.75E+40	-10.04	4954	0.01	300-2500
$CH_2Cl + CHCl_2 \rightarrow CH_2ClCHCl_2$	3.31E+43	-10.52	6379	0.1	300-2500
$CH_2Cl + CHCl_2 \rightarrow CH_2ClCHCl_2$	7.64E+44	-10.57	8059	1.0	300-2500
$CH_2Cl + CHCl_2 \rightarrow CH_2ClCHCl_2$	5.07E+43	-10.06	8244	3.0	300-2500

Table D10 (cont'd)

Reactions	A($cm^3 mol^{-1} s^{-1}$)	n	E(cal/mol)	P(atm)	T(K)
$CH_2Cl + CHCl_2 \rightarrow CH_2ClCHCl_2$	9.46E+40	-9.09	7849	10.0	300-2500
$CH_2Cl + CHCl_2 \rightarrow CH_2ClCHCl + Cl$	1.84E+14	-0.77	-169	0.01	300-2500
$CH_2Cl + CHCl_2 \rightarrow CH_2ClCHCl + Cl$	1.61E+16	-1.31	1233	0.1	300-2500
$CH_2Cl + CHCl_2 \rightarrow CH_2ClCHCl + Cl$	1.24E+18	-1.80	3418	1.0	300-2500
$CH_2Cl + CHCl_2 \rightarrow CH_2ClCHCl + Cl$	5.30E+17	-1.66	4121	3.0	300-2500
$CH_2Cl + CHCl_2 \rightarrow CH_2ClCHCl + Cl$	1.06E+16	-1.13	4404	10.0	300-2500
$CH_2Cl + CHCl_2 \rightarrow CHClCHCl + HCl$	7.95E+17	-1.79	1225	0.01	300-2500
$CH_2Cl + CHCl_2 \rightarrow CHClCHCl + HCl$	5.86E+19	-2.30	2655	0.1	300-2500
$CH_2Cl + CHCl_2 \rightarrow CHClCHCl + HCl$	7.40E+20	-2.57	4594	1.0	300-2500
$CH_2Cl + CHCl_2 \rightarrow CHClCHCl + HCl$	6.57E+19	-2.23	5029	3.0	300-2500
$CH_2Cl + CHCl_2 \rightarrow CHClCHCl + HCl$	1.89E+17	-1.46	4954	10.0	300-2500
$CH_2Cl + CHCl_2 \rightarrow CHCl_2CH_2 + Cl$	1.56E+11	0.22	166	0.01	300-2500
$CH_2Cl + CHCl_2 \rightarrow CHCl_2CH_2 + Cl$	1.26E+13	-0.31	1512	0.1	300-2500
$CH_2Cl + CHCl_2 \rightarrow CHCl_2CH_2 + Cl$	1.78E+15	-0.88	3753	1.0	300-2500
$CH_2Cl + CHCl_2 \rightarrow CHCl_2CH_2 + Cl$	1.37E+15	-0.82	4550	3.0	300-2500
$CH_2Cl + CHCl_2 \rightarrow CHCl_2CH_2 + Cl$	5.79E+13	-0.38	4964	10.0	300-2500
$CH_2Cl + CHCl_2 \rightarrow CH_2CCl_2 + HCl$	5.24E+15	-1.39	980	0.01	300-2500
$CH_2Cl + CHCl_2 \rightarrow CH_2CCl_2 + HCl$	3.96E+17	-1.91	2408	0.1	300-2500
$CH_2Cl + CHCl_2 \rightarrow CH_2CCl_2 + HCl$	6.10E+18	-2.20	4375	1.0	300-2500
$CH_2Cl + CHCl_2 \rightarrow CH_2CCl_2 + HCl$	6.39E+17	-1.88	4840	3.0	300-2500
$CH_2Cl + CHCl_2 \rightarrow CH_2CCl_2 + HCl$	2.24E+15	-1.13	4803	10.0	300-2500
$CHCl_2 + CHCl_2 \rightarrow CHCl_2CHCl_2$	1.07E+48	-11.99	7746	0.01	300-2500
$CHCl_2 + CHCl_2 \rightarrow CHCl_2CHCl_2$	5.39E+47	-11.55	9015	0.1	300-2500
$CHCl_2 + CHCl_2 \rightarrow CHCl_2CHCl_2$	8.01E+42	-9.80	8453	1.0	300-2500
$CHCl_2 + CHCl_2 \rightarrow CHCl_2CHCl_2$	2.48E+39	-8.63	7631	3.0	300-2500

Table D10 (cont'd)

Reactions	A($cm^3 mol^{-1} s^{-1}$)	n	E(cal/mol)	P(atm)	T(K)
$CHCl_2 + CHCl_2 \rightarrow CHCl_2CHCl_2$	1.16E+35	-7.22	6464	10.0	300-2500
$CHCl_2 + CHCl_2 \rightarrow CHCl_2CHCl + Cl$	5.66E+18	-2.07	3474	0.01	300-2500
$CHCl_2 + CHCl_2 \rightarrow CHCl_2CHCl + Cl$	7.26E+20	-2.62	5872	0.1	300-2500
$CHCl_2 + CHCl_2 \rightarrow CHCl_2CHCl + Cl$	5.57E+19	-2.23	7239	1.0	300-2500
$CHCl_2 + CHCl_2 \rightarrow CHCl_2CHCl + Cl$	6.62E+17	-1.64	7345	3.0	300-2500
$CHCl_2 + CHCl_2 \rightarrow CHCl_2CHCl + Cl$	5.30E+14	-0.71	7037	10.0	300-2500
$CHCl_2 + CHCl_2 \rightarrow C_2HCl_3 + HCl$	7.85E+19	-2.32	3873	0.01	300-2500
$CHCl_2 + CHCl_2 \rightarrow C_2HCl_3 + HCl$	3.94E+20	-2.46	5871	0.1	300-2500
$CHCl_2 + CHCl_2 \rightarrow C_2HCl_3 + HCl$	2.17E+17	-1.45	6409	1.0	300-2500
$CHCl_2 + CHCl_2 \rightarrow C_2HCl_3 + HCl$	2.57E+14	-0.57	6088	3.0	300-2500
$CHCl_2 + CHCl_2 \rightarrow C_2HCl_3 + HCl$	2.38E+10	0.62	5358	10.0	300-2500
$C_2H_5Cl \rightarrow C_2H_5 + Cl$	2.44E+72	-20.10	92526	0.01	300-2500
$C_2H_5Cl \rightarrow C_2H_5 + Cl$	2.74E+76	-20.08	97132	0.1	300-2500
$C_2H_5Cl \rightarrow C_2H_5 + Cl$	1.41E+64	-15.52	95731	1.0	300-2500
$C_2H_5Cl \rightarrow C_2H_5 + Cl$	4.29E+56	-13.00	93977	3.0	300-2500
$C_2H_5Cl \rightarrow C_2H_5 + Cl$	2.68E+48	-10.32	91775	10.0	300-2500
$C_2H_5Cl \rightarrow C_2H_4 + HCl$	7.18E+40	-8.76	65283	0.01	300-2500
$C_2H_5Cl \rightarrow C_2H_4 + HCl$	2.04E+34	-6.60	63645	0.1	300-2500
$C_2H_5Cl \rightarrow C_2H_4 + HCl$	1.48E+27	-4.31	61592	1.0	300-2500
$C_2H_5Cl \rightarrow C_2H_4 + HCl$	7.17E+23	-3.25	60584	3.0	300-2500
$C_2H_5Cl \rightarrow C_2H_4 + HCl$	2.62E+20	-2.17	59508	10.0	300-2500
$CH_3CHCl_2 \rightarrow CH_3CHCl + Cl$	1.51E+74	-20.27	86999	0.01	300-2500
$CH_3CHCl_2 \rightarrow CH_3CHCl + Cl$	2.40E+74	-19.31	90090	0.1	300-2500
$CH_3CHCl_2 \rightarrow CH_3CHCl + Cl$	3.80E+63	-15.34	88793	1.0	300-2500

Table D10 (cont'd)

Reactions	A(cm^3 mol^{-1} s^{-1})	n	E(cal/mol)	P(atm)	T(K)
$CH_3CHCl_2 \rightarrow CH_3CHCl + Cl$	8.72E+56	-13.11	87282	3.0	300-2500
$CH_3CHCl_2 \rightarrow CH_3CHCl + Cl$	2.58E+49	-10.64	85309	10.0	300-2500
$CH_3CHCl_2 \rightarrow C_2H_3Cl + HCl$	1.60E+44	-9.76	63926	0.01	300-2500
$CH_3CHCl_2 \rightarrow C_2H_3Cl + HCl$	6.10E+37	-7.62	62390	0.1	300-2500
$CH_3CHCl_2 \rightarrow C_2H_3Cl + HCl$	4.67E+30	-5.32	60419	1.0	300-2500
$CH_3CHCl_2 \rightarrow C_2H_3Cl + HCl$	1.75E+27	-4.22	59405	3.0	300-2500
$CH_3CHCl_2 \rightarrow C_2H_3Cl + HCl$	4.21E+23	-3.08	58300	10.0	300-2500
$CH_2ClCH_2Cl \rightarrow CH_2ClCH_2 + Cl$	2.14E+72	-19.88	89384	0.01	300-2500
$CH_2ClCH_2Cl \rightarrow CH_2ClCH_2 + Cl$	1.52E+75	-19.59	93595	0.1	300-2500
$CH_2ClCH_2Cl \rightarrow CH_2ClCH_2 + Cl$	2.75E+63	-15.24	92282	1.0	300-2500
$CH_2ClCH_2Cl \rightarrow CH_2ClCH_2 + Cl$	1.22E+56	-12.77	90585	3.0	300-2500
$CH_2ClCH_2Cl \rightarrow CH_2ClCH_2 + Cl$	7.60E+47	-10.09	88395	10.0	300-2500
$CH_2ClCH_2Cl \rightarrow C_2H_3Cl + HCl$	3.88E+42	-9.28	64069	0.01	300-2500
$CH_2ClCH_2Cl \rightarrow C_2H_3Cl + HCl$	1.20E+36	-7.13	62474	0.1	300-2500
$CH_2ClCH_2Cl \rightarrow C_2H_3Cl + HCl$	8.33E+28	-4.82	60457	1.0	300-2500
$CH_2ClCH_2Cl \rightarrow C_2H_3Cl + HCl$	3.25E+25	-3.73	59436	3.0	300-2500
$CH_2ClCH_2Cl \rightarrow C_2H_3Cl + HCl$	7.74E+21	-2.58	58311	10.0	300-2500
$CH_2ClCHCl_2 \rightarrow CH_2ClCHCl + Cl$	7.74E+76	-20.50	87028	0.01	300-2500
$CH_2ClCHCl_2 \rightarrow CH_2ClCHCl + Cl$	7.37E+69	-17.59	87303	0.1	300-2500
$CH_2ClCHCl_2 \rightarrow CH_2ClCHCl + Cl$	3.66E+57	-13.38	84770	1.0	300-2500
$CH_2ClCHCl_2 \rightarrow CH_2ClCHCl + Cl$	2.10E+51	-11.34	83135	3.0	300-2500
$CH_2ClCHCl_2 \rightarrow CH_2ClCHCl + Cl$	4.32E+44	-9.18	81239	10.0	300-2500
$CH_2ClCHCl_2 \rightarrow CHClCHCl + HCl$	1.66E+43	-9.46	63359	0.01	300-2500
$CH_2ClCHCl_2 \rightarrow CHClCHCl + HCl$	3.21E+36	-7.25	61659	0.1	300-2500

Table D10 (cont'd)

Reactions	A($cm^3\ mol^{-1}\ s^{-1}$)	n	E(cal/mol)	P(atm)	T(K)
$CH_2ClCHCl_2 \rightarrow CHClCHCl + HCl$	1.74E+29	-4.91	59579	1.0	300-2500
$CH_2ClCHCl_2 \rightarrow CHClCHCl + HCl$	6.83E+25	-3.83	58548	3.0	300-2500
$CH_2ClCHCl_2 \rightarrow CHClCHCl + HCl$	1.94E+22	-2.71	57444	10.0	300-2500
$CH_2ClCHCl_2 \rightarrow CHCl_2CH_2 + Cl$	3.00E+79	-21.68	91126	0.01	300-2500
$CH_2ClCHCl_2 \rightarrow CHCl_2CH_2 + Cl$	3.42E+76	-19.76	93364	0.1	300-2500
$CH_2ClCHCl_2 \rightarrow CHCl_2CH_2 + Cl$	6.22E+63	-15.24	91285	1.0	300-2500
$CH_2ClCHCl_2 \rightarrow CHCl_2CH_2 + Cl$	6.94E+56	-12.93	89588	3.0	300-2500
$CH_2ClCHCl_2 \rightarrow CHCl_2CH_2 + Cl$	2.05E+49	-10.49	87539	10.0	300-2500
$CH_2ClCHCl_2 \rightarrow CH_2CCl_2 + HCl$	9.61E+45	-10.59	66971	0.01	300-2500
$CH_2ClCHCl_2 \rightarrow CH_2CCl_2 + HCl$	4.40E+38	-8.15	65224	0.1	300-2500
$CH_2ClCHCl_2 \rightarrow CH_2CCl_2 + HCl$	4.28E+30	-5.56	62985	1.0	300-2500
$CH_2ClCHCl_2 \rightarrow CH_2CCl_2 + HCl$	7.05E+26	-4.35	61854	3.0	300-2500
$CH_2ClCHCl_2 \rightarrow CH_2CCl_2 + HCl$	7.87E+22	-3.10	60636	10.0	300-2500
$CHCl_2CHCl_2 \rightarrow CHCl_2CHCl + Cl$	8.76E+71	-18.27	88298	0.01	300-2500
$CHCl_2CHCl_2 \rightarrow CHCl_2CHCl + Cl$	1.94E+61	-14.67	85986	0.1	300-2500
$CHCl_2CHCl_2 \rightarrow CHCl_2CHCl + Cl$	3.62E+49	-10.85	82821	1.0	300-2500
$CHCl_2CHCl_2 \rightarrow CHCl_2CHCl + Cl$	1.51E+44	-9.13	81246	3.0	300-2500
$CHCl_2CHCl_2 \rightarrow CHCl_2CHCl + Cl$	4.27E+38	-7.37	79559	10.0	300-2500
$CHCl_2CHCl_2 \rightarrow C_2HCl_3 + HCl$	1.15E+41	-8.71	67821	0.01	300-2500
$CHCl_2CHCl_2 \rightarrow C_2HCl_3 + HCl$	5.47E+33	-6.34	65780	0.1	300-2500
$CHCl_2CHCl_2 \rightarrow C_2HCl_3 + HCl$	2.85E+26	-4.02	63595	1.0	300-2500
$CHCl_2CHCl_2 \rightarrow C_2HCl_3 + HCl$	1.56E+23	-2.99	62576	3.0	300-2500
$CHCl_2CHCl_2 \rightarrow C_2HCl_3 + HCl$	7.26E+19	-1.94	61511	10.0	300-2500

Table E1 QRRK Input Data for $C_2H_3 + O_2 \leftrightarrow [C_2H_3OO]^* \rightarrow$ Products

	Reaction	A[a]	n	α	E_a[b]	ΔH_{Rxn298}
k_1	$C_2H_3 + O_2 \rightarrow C_2H_3OO$	4.20E12	0.0	0.0	-0.2	-41.8
k_{-1}	$C_2H_3OO \rightarrow C_2H_3 + O_2$	1.15E17	-0.73	1.43E-3	38.7	
k_2	$C_2H_3OO \rightarrow CH_2CHO + O$	2.39E15	-0.38	8.399E-4	36.4	33.4
k_3	$C_2H_3OO \rightarrow C.{=}COOH$	2.57E10	1.0	0.0	33.0	21.8
k_{-3}	$C.{=}COOH \rightarrow C_2H_3OO$	2.19E09	1.0	0.0	11.2	
k_4	$C.{=}COOH \rightarrow C_2H_2 + HO_2$	8.30E11	0.0	0.0	11.6	6.6
k_5	$C_2H_3OO \rightarrow C.CyCO_2$	6.41E09	1.0	0.0	23.5	7.6
k_{-5}	$C.CyCO_2 \rightarrow C_2H_3OO$	1.73E11	1.0	0.0	15.9	
k_6	$C.CyCO_2 \rightarrow CyC_2O(O.)$	6.41E09	1.0	0.0	5.0	-43.3
k_{-6}	$CyC_2O(O.) \rightarrow C.CyCO_2$	4.20E10	1.0	0.0	48.3	
k_7	$CyC_2O(O.) \rightarrow C.OCHO$	2.50E11	1.0	0.0	4.0	-32.6
k_{-7}	$C.OCHO \rightarrow CyC_2O(O.)$	7.31E08	1.0	0.0	36.6	
k_8	$C.OCHO \rightarrow CH_2O + CHO$	4.81E12	0.0	0.0	29.9	23.4
k_9	$CyC_2O(O.) \rightarrow O.CCHO$	4.02E11	1.0	0.0	4.0	-15.4
k_{-9}	$O.CCHO \rightarrow CyC_2O(O.)$	6.41E09	1.0	0.0	19.4	
k_{10}	$O.CCHO \rightarrow CH_2O + CHO$	2.63E13	0.0	0.0	12.7	6.2

a: A's in sec^{-1} and $cm^3\ mol^{-1}\ s^{-1}$
b: E_a in kcal/mol
<ν> 3 Frequencies: 331.9 1541.8 3997.7
Degeneracy: 5.240 8.839 0.421
L.J. Parameters: σ = 4.36 Å; e/k = 451.0 K
$\langle\Delta E\rangle_{avg}$ for Ar = 450 cm^{-1}
β as function of T, T(K) : 300 500 900 1200 1500 1800 2100 2500
β : 0.306 0.151 0.04 0.021 0.016 0.016 0.018 0.022

k_1 Slagle, I. R.; Park, J-Y; Heaven, M. C.; Gutman, D. *J. Am. Chem. Soc.* **1984**, 106, 4356.

k_{-1} Via k_1 and Microscopic-Reversibility <MR>, $E_a = \Delta H - RT_m$

k_2 Via k_{-2} and <MR>

k_{-2} A taken as that of $O + CH_3O$, A = 2.0E13, Ref: Herron, J. T. *J. Phys. Chem. Ref. Data* **1988**, 17, 967. E_a = 3.0, Ref: Bozzelli, J. W.; Dean, A. M. *J. Phys. Chem.* **1993**, 97, 4427.

k_3 TST, loss of one rotor, degeneracy and gain of Optical Isomer, $k = AT^n e^{(-Ea/RT)}$
$A = 10^{10.75} * 10^{(-4.3+1.38)/4.56} * 2 =$ 2.57E10, n = 1,
$E_a = 6.0(RS) + 21.8(\Delta H_{rxn}) + 5.2(E_{abs}) = 33.0$

k_{-3} Via k_3 and <MR>

Table E1 (cont'd)

k_4	Via k_{-4} and <MR>
k_{-4}	A taken as that of $HO_2 + C_2H_4$, A = 5.60E11, E_a = 5.0, Ref: Bozzelli, J. W.; Dean, A. M. *J. Phys. Chem.* **1990**, 94, 3313.
k_5	Transition State Theory (TST), loss of one rotor, $k = AT^n e^{(-Ea/RT)}$ $A = 10^{10.75} * 10^{-4.3/4.56} = 6.41E09$, n = 1, E_a = 23.5, Ref: Carpenter, B. K. *J. Am. Chem. Soc.* **1993**, 115, 9806.
k_{-5}	Via k_5 and <MR>
k_6	TST, loss of one rotor, $k = AT^n e^{(-Ea/RT)}$ $A = 10^{10.75} * 10^{-4.3/4.56} = 6.41E09$, n = 1, E_a = 5.0
k_{-6}	Via k_6 and <MR>
k_7	Via k_{-7} and <MR>, E_a = 4.0
k_{-7}	TST, loss of 2 rotors, $k = AT^n e^{(-Ea/RT)}$ $A = 10^{10.75} * 10^{-8.6/4.56} = 7.31E08$, n = 1, E_a via k_7 and <MR>
k_8	Via k_{-8} and <MR>
k_{-8}	A taken as that of $CH_3 + CO$, A = 5.2E11, E_a = 6.5, Ref: Anastasi, C.; Maw, P. R. *J. Chem. Soc. Faraday Trans. 1*, **1982**, 78, 2423.
k_9	Via k_{-10} and <MR>, E_a = 4.0, (Ref. as k_5)
k_{-9}	TST, loss of one rotor, $k = AT^n e^{(-Ea/RT)}$ $A = 10^{10.75} * 10^{-4.3/4.56} = 6.41E09$, n = 1, E_a via k_9 and <MR>
k_{10}	Via k_{-10} and <MR>
k_{-10}	A taken as that of $CH_3 + CO$, A = 5.2E11, E_a = 6.5, (Ref. as k_{-8})
<v>	From "CPFIT" Computer Code (Ref: Ritter, E. R. *J. Chem. Inf. Computat. Sci.* **1991**, 31, 400) and C_p data for C_2H_3OO
σ, e/k	Calculated from critical properties for C_2H_3OO (Ref: Reid, R. C.; Prausnitz, J. M.; Sherwood, T. K. *The Properties of Gases and Liquids* 3rd Ed. McGraw-Hill Co., New York, **1977**.)

Table E2 QRRK Input Data for $CH_2CCl + O_2 \leftrightarrow [CH_2CClOO]^* \rightarrow$ Products

	Reaction	A[a]	n	α	E_a[b]	ΔH_{Rxn298}
k_1	$CH_2CCl + O_2 \rightarrow C^*CClOO$	3.20E12	0.0	0.0	-0.33	-39.4
k_{-1}	$C^*CClOO \rightarrow CH_2CCl + O_2$	7.36E20	-2.40	2.992E-4	38.4	
k_2	$C^*CClOO \rightarrow CH_2CO + ClO$	6.41E09	1.0	0.0	31.0	-8.5
k_3	$C^*CClOO \rightarrow C^*CClO. + O$	5.37E16	-0.74	5.564E-4	38.3	35.3
k_4	$C^*CClOO \rightarrow C.^*CClQ$[c]	2.57E10	1.0	0.0	35.5	25.5
k_{-4}	$C.^*CClQ \rightarrow C^*CClOO$	1.75E10	1.0	0.0	10.0	
k_5	$C.^*CClQ \rightarrow C_2HCl + HO_2$	3.21E13	0.0	0.0	13.1	8.1
k_6	$C^*CClOO \rightarrow C.CyCO_2Cl$	6.41E09	1.0	0.0	23.5	13.3
k_{-6}	$C.CyCO_2Cl \rightarrow C^*CClOO$	3.10E11	1.0	0.0	10.2	
k_7	$C.CyCO_2Cl \rightarrow CyCOCCl(O)$	6.41E09	1.0	0.0	5.0	-43.3
k_{-7}	$CyCOCCl(O) \rightarrow C.CyCO_2Cl$	2.46E10	1.0	0.0	48.3	
k_8	$CyCOCCl(O) \rightarrow C.OCCl^*O$	5.13E11	1.0	0.0	4.0	-39.7
k_{-8}	$C.OCCl^*O \rightarrow CyCOCCl(O)$	7.31E08	1.0	0.0	43.7	
k_9	$C.OCCl^*O \rightarrow CH_2O + CClO$	1.17E13	0.0	0.0	25.1	18.6
k_{10}	$CyCOCCl(O) \rightarrow CO.CCl^*O$	2.18E11	1.0	0.0	4.00	-31.8
k_{-10}	$CO.CCl^*O \rightarrow CyCOCCl(O)$	6.41E09	1.0	0.0	35.8	
k_{11}	$CO.CCl^*O \rightarrow CH_2O + CClO$	2.41E14	0.0	0.0	17.2	10.7

a: A's in sec^{-1} and $cm^3\ mol^{-1}\ s^{-1}$
b: E_a in kcal/mol
c: -Q = -OOH
<ν> 3 Frequencies: 250.2 1084.8 2820.5
Degeneracy: 5.162 7.122 2.216
L.J. Parameters: σ = 4.7113 Å; e/k = 460.77 K
$\langle\Delta E\rangle_{avg}$ for Ar = 450 cm^{-1}

β as function of T, T(K)	300	500	900	1200	1500	1800	2100	2500
β	0.304	0.148	0.038	0.021	0.018	0.019	0.022	0.027

k_1 A = 3.2E12, E_a = -0.33, Ref: Russell, J. J.; Seetula, J. A.; Gutman, D.; Senkan, S. M. *J. Phys. Chem.* **1989**, 93, 1934.

k_{-1} Via k_1 and Microscopic-Reversibility <MR>, $E_a = \Delta H - RT_m$

k_2 TST, loss of one rotor, $k = AT^n e^{(-Ea/RT)}$
$A = 10^{10.75} * 10^{-4.3/4.56} = 6.41E09$, n = 1.0, E_a = 31.0 (AM1/PM3).

k_3 Via k_{-3} and <MR>

k_{-3} A taken as that of O + CH_3O, A = 2.0E13, Ref: Herron, J. T. *J. Phys. Chem. Ref. Data* **1988**, 17, 967. E_a = 3.0, Ref: Bozzelli, J. W.; Dean, A. M. *J. Phys. Chem.* **1993**, 97, 4427.

Table E2 (cont'd)

k_4	TST, loss of one rotor, degeneracy and gain of Optical Isomer, $k = AT^n e^{(-Ea/RT)}$ $A = 10^{10.75} * 10^{(-4.3+1.38)/4.56} * 2 = 2.57E10$, n = 1.0, $E_a = 6.0(RS) + 25.5(\Delta H_{rxn}) + 4.0(E_{abs}) = 35.5$
k_{-4}	Via k_4 and <MR>
k_5	Via k_{-5} and <MR>
k_{-5}	A taken as that of $HO_2 + C_2H_4$, A = 5.60E11, E_a = 5.0, Ref: Bozzelli, J. W.; Dean, A. M. *J. Phys. Chem.* **1990**, 94, 3313.
k_6	Transition State Theory (TST), loss of one rotor, $k = AT^n e^{(-Ea/RT)}$ $A = 10^{10.75} * 10^{-4.3/4.56} = 6.41E09$, n = 1, E_a = 23.5, Ref: Carpenter, B. K. *J. Am. Chem. Soc.* **1993**, 115, 9806.
k_{-6}	Via k_6 and <MR>
k_7	TST, loss of one rotor, $k = AT^n e^{(-Ea/RT)}$ $A = 10^{10.75} * 10^{-4.3/4.56} = 6.41E09$, n = 1.0, E_a = 5.0
k_{-7}	Via k_7 and <MR>
k_8	Via k_{-8} and <MR>, E_a = 4.0 (Ref. as k_6)
k_{-8}	TST, loss of 2 rotors, $k = AT^n e^{(-Ea/RT)}$ $A = 10^{10.75} * 10^{-8.6/4.56} = 7.31E08$, n = 1, E_a via k_8 and <MR>
k_9	Via k_{-9} and <MR>
k_{-9}	A taken as that of $CH_3 + CO$, A = 5.2E11, E_a = 6.5, Ref: Anastasi, C.; Maw, P. R. *J. Chem. Soc. Faraday Trans. 1*, **1982**, 78, 2423.
k_{10}	Via k_{-10} and <MR>, Ea = 4.0
k_{-10}	TST, loss of one rotor, $k = AT^n e^{(-Ea/RT)}$ $A = 10^{10.75} * 10^{-4.3/4.56} = 6.41E09$, n = 1.0, E_a via k_{10} and <MR>
k_{11}	Via k_{-11} and <MR>
k_{-11}	A taken as that of $CH_3 + CO$, A = 5.2E11, E_a = 6.5, (Ref. as k_{-9})
<ν>	From "CPFIT" Computer Code (Ref: Ritter, E. R. *J. Chem. Inf. Computat. Sci.* **1991**, 31, 400) and C_p data for C*CClOO
σ, e/k	Calculated from critical properties for C*CClOO (Ref: Reid, R. C.; Prausnitz, J. M.; Sherwood, T. K. *The Properties of Gases and Liquids* 3rd Ed. McGraw-Hill Co., New York, **1977**.)

Table E3 QRRK Input Data for CHClCH + O_2 ↔ [CHClCHOO]* → Products

	Reaction	A[a]	n	α	E_a[b]	ΔH_{Rxn298}
k_1	CHClCH + O_2 → CCl*COO	3.20E12	0.0	0.0	-0.33	-40.2
k_{-1}	CCl*COO → CHClCH + O_2	4.92E19	-1.83	5.273E-4	37.4	
k_2	CCl*COO → ClC*CO. + O	1.95E16	-0.57	5.127E-4	39.3	36.3
k_3	CCl*COO → C.Cl*CQ[c]	1.29E10	1.0	0.0	30.8	18.5
k_{-3}	C.Cl*CQ → CCl*COO	1.02E09	1.0	0.0	12.3	
k_4	C.Cl*CQ → C_2HCl + HO_2	1.01e13	0.0	0.0	18.1	13.1
k_5	CCl*COO → ClC.CyCOO	6.41E09	1.0	0.0	23.5	2.7
k_{-5}	ClC.CyCOO → CCl*COO	3.76E10	1.0	0.0	20.8	
k_6	ClC.CyCOO → ClCyCOC(O)	6.41E09	1.0	0.0	5.0	-40.3
k_{-6}	ClCyCOC(O) → ClC.CyCOO	1.13E11	1.0	0.0	45.3	
k_7	ClCyCOC(O) → ClC.OC*O	1.48E12	1.0	0.0	4.0	-33.7
k_{-7}	ClC.OC*O → ClCyCOC(O)	7.31E08	1.0	0.0	37.7	
k_8	ClC.OC*O → CHClO + CHO	1.28E13	0.0	0.0	25.8	19.3
k_9	ClCyCOC(O) → CO.ClC*O	3.88E11	1.0	0.0	4.00	-15.4
k_{-9}	CO.ClC*O → ClCyCOC(O)	6.41E09	1.0	0.0	19.4	
k_{10}	CO.ClC*O → CHClO + CHO	4.29E14	0.0	0.0	7.5	1.0

a: A's in sec^{-1} and $cm^3\ mol^{-1}\ s^{-1}$
b: E_a in kcal/mol
c : -Q = -OOH
<ν> 3 Frequencies: 450.6 1569.1 3612.9
Degeneracy: 8.130 5.088 1.282
L.J. Parameters: σ = 4.774 Å; e/k = 461.44 K
$\langle\Delta E\rangle_{avg}$ for Ar = 450 cm^{-1}

β as function of T, T(K) :	300	500	900	1200	1500	1800	2100	2500
β :	0.305	0.149	0.039	0.021	0.017	0.018	0.020	0.025

k_1 A = 3.2E12, E_a = -0.33, taken as that of CH_2CCl + O_2, Ref: Russell, J. J.; Seetula, J. A.; Gutman, D.; Senkan, S. M. *J. Phys. Chem.* **1989**, 93, 1934.

k_{-1} Via k_1 and Microscopic-Reversibility <MR>, $E_a = \Delta H - RT_m$

k_2 Via k_{-2} and <MR>

k_{-2} A taken as that of O + CH_3O, A = 2.0E13, Ref: Herron, J. T. *J. Phys. Chem. Ref. Data* **1988**, 17, 967. E_a = 3.0, Ref: Bozzelli, J. W.; Dean, A. M. *J. Phys. Chem.* **1993**, 97, 4427.

k_3 TST, loss of one rotor, and gain a Optical Isomer, $k = AT^n e^{(-Ea/RT)}$
$A = 10^{10.75} * 10^{(-4.3+1.38)/4.56} = 1.29E10$, n = 1.0,
$E_a = 6.0(RS) + 18.5(\Delta H_{rxn}) + 6.3(E_{abs}) = 30.8$

k_{-3} Via k_3 and <MR>

Table E3 (cont'd)

k_4	Via k_{-4} and <MR>
k_{-4}	A taken as that of $HO_2 + C_2H_4$, A = 5.60E11, E_a = 5.0, Ref: Bozzelli, J. W.; Dean, A. M. *J. Phys. Chem.* **1990**, 94, 3313.
k_5	Transition State Theory (TST), loss of one rotor, $k = AT^n e^{(-Ea/RT)}$ $A = 10^{10.75} * 10^{-4.3/4.56} = 6.41E09$, n = 1, E_a = 23.5, Ref: Carpenter, B. K. *J. Am. Chem. Soc.* **1993**, 115, 9806.
k_{-5}	Via k_5 and <MR>
k_6	TST, loss of one rotor, $k = AT^n e^{(-Ea/RT)}$ $A = 10^{10.75} * 10^{-4.3/4.56} = 6.41E09$, n = 1.0, E_a = 5.0
k_{-6}	Via k_6 and <MR>
k_7	Via k_{-7} and <MR>, E_a = 4.0 (Ref. as k_5)
k_{-7}	TST, loss of 2 rotors, $k = AT^n e^{(-Ea/RT)}$ $A = 10^{10.75} * 10^{-8.6/4.56} = 7.31E08$, n = 1, E_a via k_7 and <MR>
k_8	Via k_{-8} and <MR>
k_{-8}	A taken as that of $CH_3 + CO$, A = 5.2E11, E_a = 6.5, Ref: Anastasi, C.; Maw, P. R. *J. Chem. Soc. Faraday Trans. 1*, **1982**, 78, 2423.
k_9	Via k_{-9} and <MR>, E_a = 4.0 (Ref. as k_5)
k_{-9}	TST, loss of one rotor, $k = AT^n e^{(-Ea/RT)}$ $A = 10^{10.75} * 10^{-4.3/4.56} = 6.41E09$, E_a via k_9 and <MR>
k_{10}	Via k_{-10} and <MR>
k_{-10}	A taken as that of $CH_3 + CO$, A = 5.2E11, E_a = 6.5, (Ref. as k_{-8})
<v>	From "CPFIT" Computer Code (Ref: Ritter, E. R. *J. Chem. Inf. Computat. Sci.* **1991**, 31, 400) and C_p data for ClC*COO
σ, e/k	Calculated from critical properties for ClC*COO (Ref: Reid, R. C.; Prausnitz, J. M.; Sherwood, T. K. *The Properties of Gases and Liquids* 3rd Ed. McGraw-Hill Co., New York, **1977**.)

Table E4 QRRK Input Data for CHClCCl + O_2 ↔ [CHClCClOO]* → Products

	Reaction	A[a]	n	α	E_a[b]	ΔH_{Rxn298}
k_1	CHClCCl + O_2 → ClC*CClOO	2.00E12	0.0	0.0	-0.5	-39.3
k_{-1}	ClC*CClOO → CHClCCl + O_2	1.54E20	-2.07	2.806E-4	36.8	
k_2	ClC*CClOO → CHClCO + ClO	6.41E09	1.0	0.0	41.0	-11.0
k_3	ClC*CClOO → ClC*CClO. + O	6.95E16	-0.84	-9.975E-5	38.3	35.3
k_4	ClC*CClOO → ClC.*CClQ[c]	1.29E10	1.0	0.0	32.2	20.5
k_{-4}	ClC.*CClQ → ClC*CClOO	2.48E09	1.0	0.0	11.7	
k_5	ClC.*CClQ → C_2Cl_2 + HO_2	1.67E13	0.0	0.0	22.1	17.1
k_6	ClC*CClOO → ClC.CO_2Cl	6.41E09	1.0	0.0	23.5	7.2
k_{-6}	ClC.CO_2Cl → ClC*CClOO	8.20E10	1.0	0.0	16.3	
k_7	ClC.CO_2Cl → ClC_2OClO.	6.41E09	1.0	0.0	5.0	-40.3
k_{-7}	ClC_2OClO. → ClC.CO_2Cl	1.07E11	1.0	0.0	45.3	
k_8	ClC_2OClO. → ClC.OCCl*O	2.93E12	1.0	0.0	4.0	-40.9
k_{-8}	ClC.OCCl*O → ClC_2OClO.	7.31E08	1.0	0.0	44.9	
k_9	ClC.OCCl*O → CHClO + CClO	3.30E13	0.0	0.0	21.1	14.6
k_{10}	ClC_2OClO. → CO.ClCCl*O	2.17E11	1.0	0.0	4.00	-31.8
k_{-10}	CO.ClCCl*O → ClC_2OClO.	6.41E09	1.0	0.0	35.8	
k_{11}	CO.ClCCl*O → CHClO + CClO	9.72E14	0.0	0.0	12.0	5.5

a: A's in sec^{-1} and $cm^3\ mol^{-1}\ s^{-1}$
b: E_a in kcal/mol
c : -Q = -OOH
<ν> 3 Frequencies: 377.0 1346.3 3991.4
Degeneracy: 8.911 4.842 0.747
L.J. Parameters: σ = 5.1335 Å; e/k = 499.36 K
$\langle\Delta E\rangle_{avg}$ for Ar = 450 cm^{-1}
β as function of T, T(K) : 300 500 900 1200 1500 1800 2100 2500
β : 0.30 0.142 0.036 0.022 0.021 0.023 0.028 0.034

k_1 A = 2.0E12, E_a = -0.5, estimated from CH_2CCl + O_2 and C_2Cl_3 + O_2, Ref: Russell, J. J.; Seetula, J. A.; Gutman, D.; Senkan, S. M. *J. Phys. Chem.* **1989**, 93, 1934.

k_{-1} Via k_1 and Microscopic-Reversibility <MR>, $E_a = \Delta H - RT_m$

k_2 TST, loss of one rotor, $k = AT^n e^{(-Ea/RT)}$
$A = 10^{10.75} * 10^{-4.3/4.56}$ = 6.41E09, n = 1.0, E_a = 31.0, (AM1/PM3)

k_3 Via k_{-3} and <MR>

k_{-3} A taken as that of O + CH_3O, A = 2.0E13, Ref: Herron, J. T. *J. Phys. Chem. Ref. Data* **1988**, 17, 967. E_a = 3.0, Ref: Bozzelli, J. W.; Dean, A. M. *J. Phys. Chem.* **1993**, 97, 4427.

Table E4 (cont'd)

k_4	TST, loss of one rotor, and gain a Optical Isomer, $k = AT^n e^{(-Ea/RT)}$ $A = 10^{10.75} * 10^{(-4.3+1.38)/4.56} = 1.29E10$, $n = 1.0$, $E_a = 6.0(RS) + 20.5(\Delta H_{rxn}) + 5.7(E_{abs}) = 32.2$
k_{-4}	Via k_4 and <MR>
k_5	Via k_{-5} and <MR>
k_{-5}	A taken as that of $HO_2 + C_2H_4$, A = 5.60E11, $E_a = 5.0$, Ref: Bozzelli, J. W.; Dean, A. M. *J. Phys. Chem.* **1990**, 94, 3313.
k_6	Transition State Theory (TST), loss of one rotor, $k = AT^n e^{(-Ea/RT)}$ $A = 10^{10.75} * 10^{-4.3/4.56} = 6.41E09$, $n = 1$, $E_a = 23.5$, Ref: Carpenter, B. K. *J. Am. Chem. Soc.* **1993**, 115, 9806.
k_{-6}	Via k_6 and <MR>
k_7	TST, loss of one rotor, $k = AT^n e^{(-Ea/RT)}$ $A = 10^{10.75} * 10^{-4.3/4.56} = 6.41E09$, $n = 1.0$, $E_a = 5.0$
k_{-7}	Via k_7 and <MR>
k_8	Via k_{-8} and <MR>, $E_a = 4.0$
k_{-8}	TST, loss of 2 rotors, $k = AT^n e^{(-Ea/RT)}$ $A = 10^{10.75} * 10^{-8.6/4.56} = 7.31E08$, $n = 1$, E_a via k_8 and <MR>
k_9	Via k_{-9} and <MR>
k_{-9}	A taken as that of $CH_3 + CO$, A = 5.2E11, $E_a = 6.5$, Ref: Anastasi, C.; Maw, P. R. *J. Chem. Soc. Faraday Trans. 1*, **1982**, 78, 2423.
k_{10}	Via k_{-10} and <MR>, $E_a = 4.0$ (Ref. as k_6)
k_{-10}	TST, loss of one rotor, $k = AT^n e^{(-Ea/RT)}$ $A = 10^{10.75} * 10^{-4.3/4.56} = 6.41E09$, E_a via k_{10} and <MR>
k_{11}	Via k_{-11} and <MR>
k_{-11}	A taken as that of $CH_3 + CO$, A = 5.2E11, $E_a = 6.5$, (Ref. as k_{-9})
<ν>	From "CPFIT" Computer Code (Ref: Ritter, E. R. *J. Chem. Inf. Computat. Sci.* **1991**, 31, 400) and C_p data for ClC*CClOO
σ, e/k	Calculated from critical properties for ClC*CClOO (Ref: Reid, R. C.; Prausnitz, J. M.; Sherwood, T. K. *The Properties of Gases and Liquids* 3rd Ed. McGraw-Hill Co., New York, **1977**.)

Table E5 QRRK Input Data for $CCl_2CH + O_2 \leftrightarrow [CCl_2CHOO]^* \rightarrow$ Products

	Reaction	A[a]	n	α	E_a[b]	ΔH_{Rxn298}
k_1	$CCl_2CH + O_2 \rightarrow Cl_2C^*COO$	2.00E12	0.0	0.0	-0.5	-41.7
k_{-1}	$Cl_2C^*COO \rightarrow CCl_2CH + O_2$	9.88E19	-1.87	6.797E-4	39.1	
k_2	$Cl_2C^*COO \rightarrow Cl_2C^*CO. + O$	2.18E16	-0.59	4.966E-4	38.3	35.3
k_3	$Cl_2C^*COO \rightarrow CCl_2CO + OH$	6.41E09	1.0	0.0	39.5	-30.7
k_4	$Cl_2C^*COO \rightarrow Cl_2C.CyCOO$	6.41E09	1.0	0.0	23.5	1.7
k_{-4}	$Cl_2C.CyCOO \rightarrow Cl_2C^*COO$	9.90E10	1.0	0.0	21.8	
k_5	$Cl_2C.CyCOO \rightarrow Cl_2CyCOCO.$	6.41E09	1.0	0.0	5.0	-35.2
k_{-5}	$Cl_2CyCOCO. \rightarrow Cl_2C.CyCOO$	2.29E10	1.0	0.0	40.2	
k_6	$Cl_2CyCOCO. \rightarrow Cl_2C.OC^*O$	2.64E11	1.0	0.0	4.0	-34.8
k_{-6}	$Cl_2C.OC^*O \rightarrow Cl_2CyCOCO.$	7.31E08	1.0	0.0	38.8	
k_7	$Cl_2C.OC^*O \rightarrow CCl_2O + CHO$	2.16E13	0.0	0.0	16.2	9.7
k_8	$Cl_2CyCOCO. \rightarrow CO.Cl_2C^*O$	2.44E11	1.0	0.0	4.0	-13.6
k_{-8}	$CO.Cl_2C^*O \rightarrow Cl_2CyCOCO.$	6.41E09	1.0	0.0	17.6	
k_9	$CO.Cl_2C^*O \rightarrow CCl_2O + CHO$	2.04E14	0.0	0.0	1.0	-11.5

a: A's in sec^{-1} and $cm^3\ mol^{-1}\ s^{-1}$
b: E_a in kcal/mol
<ν> 3 Frequencies: 288.6 882.7 2445.0
Degeneracy: 6.606 5.728 2.166
L.J. Parameters: σ = 5.1335 Å; e/k = 499.36 K
$\langle\Delta E\rangle_{avg}$ for Ar = 450 cm^{-1}

β as function of T, T(K)	300	500	900	1200	1500	1800	2100	2500
β	0.30	0.141	0.036	0.022	0.021	0.024	0.029	0.035

k_1 A = 2.0E12, E_a = -0.5, estimated from $CH_2CCl + O_2$ and $C_2Cl_3 + O_2$, Ref: Russell, J. J.; Seetula, J. A.; Gutman, D.; Senkan, S. M. *J. Phys. Chem.* **1989**, 93, 1934.

k_{-1} Via k_1 and Microscopic-Reversibility <MR>, $E_a = \Delta H - RT_m$

k_2 Via k_{-2} and <MR>

k_{-2} A taken as that of $O + CH_3O$, A = 2.0E13, Ref: Herron, J. T. *J. Phys. Chem. Ref. Data* **1988**, 17, 967. E_a = 3.0, Ref: Bozzelli, J. W.; Dean, A. M. *J. Phys. Chem.* **1993**, 97, 4427.

k_3 TST, loss of one rotor, $k = AT^n e^{(-Ea/RT)}$
$A = 10^{10.75} * 10^{-4.3/4.56}$ = 6.41E09, n = 1.0, $E_a = 27(RS) + 12.5(E_{abs})$.

k_4 Transition State Theory (TST), loss of one rotor, $k = AT^n e^{(-Ea/RT)}$
$A = 10^{10.75} * 10^{-4.3/4.56}$ = 6.41E09, n = 1, E_a = 23.5, Ref: Carpenter, B. K. *J. Am. Chem. Soc.* **1993**, 115, 9806.

k_{-4} Via k_4 and <MR>

Table E5 (cont'd)

k_5	TST, loss of one rotor, $k = AT^n e^{(-Ea/RT)}$ $A = 10^{10.75} * 10^{-4.3/4.56} = 6.41E09$, $n = 1.0$, $E_a = 5.0$
k_{-5}	Via k_5 and <MR>
k_6	Via k_{-6} and <MR>, $E_a = 4.0$
k_{-6}	TST, loss of 2 rotors, $k = AT^n e^{(-Ea/RT)}$ $A = 10^{10.75} * 10^{-8.6/4.56} = 7.31E08$, $n = 1$, E_a via k_6 and <MR>
k_7	Via k_{-7} and <MR>
k_{-7}	A taken as that of $CH_3 + CO$, $A = 5.2E11$, $E_a = 6.5$, Ref: Anastasi, C.; Maw, P. R. *J. Chem. Soc. Faraday Trans. 1*, **1982**, 78, 2423.
k_8	Via k_{-8} and <MR>, Ea = 4.0 (Ref. as k_4)
k_{-8}	TST, loss of one rotor, $k = AT^n e^{(-Ea/RT)}$ $A = 10^{10.75} * 10^{-4.3/4.56} = 6.41E09$, E_a via k_8 and <MR>
k_9	Via k_{-9} and <MR>
k_{-9}	A taken as that of $CH_3 + CO$, $A = 5.2E11$, $E_a = 6.5$, (Ref. as k_{-7})
<v>	From "CPFIT" Computer Code (Ref: Ritter, E. R. *J. Chem. Inf. Computat. Sci.* **1991**, 31, 400) and C_p data for Cl_2C^*COO
σ, e/k	Calculated from critical properties for Cl_2C^*COO (Ref: Reid, R. C.; Prausnitz, J. M.; Sherwood, T. K. *The Properties of Gases and Liquids* 3rd Ed. McGraw-Hill Co., New York, **1977**.)

Table E6 QRRK Input Data for $C_2Cl_3 + O_2 \leftrightarrow [CCl_2CClOO]^* \rightarrow$ Products

	Reaction	A^a	n	α	E_a^b	ΔH_{Rxn298}
k_1	$C_2Cl_3 + O_2 \rightarrow Cl_2C^*CClOO$	1.55E12	0.0	0.0	-0.65	-39.4
k_{-1}	$Cl_2C^*CClOO \rightarrow C_2Cl_3 + O_2$	5.29E22	-2.81	-6.445E-4	38.2	
k_2	$Cl_2C^*CClOO \rightarrow CCl_2CO + ClO$	6.41E09	1.0	0.0	31.0	-11.0
k_3	$Cl_2C^*CClOO \rightarrow Cl_2C^*CClO. + O$	2.47E16	-0.61	4.456E-4	38.3	35.3
k_4	$Cl_2C^*CClOO \rightarrow Cl_2C.COOCl$	6.41E09	1.0	0.0	23.5	4.2
k_{-4}	$Cl_2C.COOCl \rightarrow Cl_2C^*CClOO$	7.47E10	1.0	0.0	19.3	
k_5	$Cl_2C.COOCl \rightarrow Cl_2CCOClO.$	6.41E09	1.0	0.0	5.0	-35.2
k_{-5}	$Cl_2CCOClO. \rightarrow Cl_2C.COOCl$	2.54E10	1.0	0.0	40.2	
k_6	$Cl_2CCOClO. \rightarrow Cl_2C.OCClO$	3.31E11	1.0	0.0	4.0	-42.1
k_{-6}	$Cl_2C.OCClO \rightarrow Cl_2CCOClO.$	7.31E08	1.0	0.0	46.1	
k_7	$Cl_2C.OCClO \rightarrow CCl_2O + CClO$	8.62E13	0.0	0.0	11.5	5.0
k_8	$Cl_2CCOClO. \rightarrow CO.Cl_2CClO$	1.77E11	1.0	0.0	4.0	-30.0
k_{-8}	$CO.Cl_2CClO \rightarrow Cl_2CCOClO.$	6.41E09	1.0	0.0	34.0	
k_9	$CO.Cl_2CClO \rightarrow CCl_2O + CClO$	8.98E14	0.0	0.0	1.0	-7.1

a: A's in s^{-1} and $cm^3\ mol^{-1}\ s^{-1}$
b: E_a in kcal/mol

<ν> 3 Frequencies: 389.1 437.3 1464.3
Degeneracy: 7.63 4.012 2.859

L.J. Parameters: σ = 5.6547 Å; e/k = 604.0259 K

$\langle\Delta E\rangle_{avg}$ for Ar = 450 cm^{-1}

β as function of T, T(K) :	300	500	900	1200	1500	1800	2100	2500
β :	0.295	0.134	0.034	0.025	0.027	0.033	0.039	0.048

k_1 A = 1.55E12, Ea = -0.65, Ref: Russell, J. J.; Seetula, J. A.; Gutman, D.; Senkan, S. M. *J. Phys. Chem.* **1989**, 93, 1934.

k_{-1} Via k_1 and Microscopic-Reversibility <MR>, $E_a = \Delta H - RT_m$

k_2 TST, loss of one rotor, $k = AT^n e^{(-Ea/RT)}$
$A = 10^{10.75} * 10^{-4.3/4.56} = 6.41E09$, n = 1.0, E_a = 31.0, (AM1/PM3)

k_3 Via k_{-3} and <MR>

k_{-3} A taken as that of O + CH_3O, A = 2.0E13, Ref: Herron, J. T. *J. Phys. Chem. Ref. Data* **1988**, 17, 967. E_a = 3.0, Ref: Bozzelli, J. W.; Dean, A. M. *J. Phys. Chem.* **1993**, 97, 4427.

k_4 Transition State Theory (TST), loss of one rotor, $k = AT^n e^{(-Ea/RT)}$
$A = 10^{10.75} * 10^{-4.3/4.56} = 6.41E09$, n = 1, E_a = 23.5, Ref: Carpenter, B. K. *J. Am. Chem. Soc.* **1993**, 115, 9806.

k_{-4} Via k_4 and <MR>

Table E6 (cont'd)

k_5	TST, loss of one rotor, $k = AT^n e^{(-Ea/RT)}$ $A = 10^{10.75} * 10^{-4.3/4.56} = 6.41E09$, $n = 1.0$, $E_a = 5.0$
k_{-5}	Via k_5 and <MR>
k_6	Via k_{-6} and <MR>, $E_a = 4.0$
k_{-6}	TST, loss of 2 rotors, $k = AT^n e^{(-Ea/RT)}$ $A = 10^{10.75} * 10^{-8.6/4.56} = 7.31E08$, $n = 1$, E_a via k_6 and <MR>
k_7	Via k_{-7} and <MR>
k_{-7}	A taken as that of $CH_3 + CO$, $A = 5.2E11$, $E_a = 6.5$, Ref: Anastasi, C.; Maw, P. R. *J. Chem. Soc. Faraday Trans. 1*, **1982**, 78, 2423.
k_8	Via k_{-8} and <MR>, Ea = 4.0 (Ref. as k_4)
k_{-8}	TST, loss of one rotor, $k = AT^n e^{(-Ea/RT)}$ $A = 10^{10.75} * 10^{-4.3/4.56} = 6.41E09$, E_a via k_8 and <MR>
k_9	Via k_{-9} and <MR>
k_{-9}	A taken as that of $CH_3 + CO$, $A = 5.2E11$, Ea = 6.5, (Ref. as k_{-7})
<v>	From "CPFIT" Computer (Ref: Ritter, E. R. *J. Chem. Inf. Computat. Sci.* **1991**, 31, 400) and C_p data for Cl_2C^*CClOO
σ, e/k	Calculated from critical properties for Cl_2C^*CClOO (Ref: Reid, R. C.; Prausnitz, J. M.; Sherwood, T. K. *The Properties of Gases and Liquids* 3rd Ed. McGraw-Hill Co., New York, **1977**.)

Table E7 Apparent rate constants, $k = AT^n \exp(-E/RT)$, in N_2 bath gas, at Temperatures 300 - 2500 K

Reactions	$A(cm^3\ mol^{-1}\ s^{-1})$	n	E_a(cal/mol)	P(atm)
$C_2H_3 + O_2 \rightarrow C_2H_3OO$	1.99E+21	-4.59	-446	0.001
$C_2H_3 + O_2 \rightarrow C_2H_3OO$	2.20E+22	-4.61	-419	0.01
$C_2H_3 + O_2 \rightarrow C_2H_3OO$	5.32E+23	-4.72	-169	0.1
$C_2H_3 + O_2 \rightarrow C_2H_3OO$	3.53E+26	-5.22	1141	1.0
$C_2H_3 + O_2 \rightarrow C_2H_3OO$	1.28E+28	-5.52	2176	3.0
$C_2H_3 + O_2 \rightarrow C_2H_3OO$	7.92E+28	-5.56	3134	10.0
$C_2H_3 + O_2 \rightarrow CH_2CHO + O$	7.97E+09	0.63	-426	0.001
$C_2H_3 + O_2 \rightarrow CH_2CHO + O$	8.70E+09	0.62	-403	0.01
$C_2H_3 + O_2 \rightarrow CH_2CHO + O$	1.93E+10	0.52	-185	0.1
$C_2H_3 + O_2 \rightarrow CH_2CHO + O$	1.28E+12	0.01	1035	1.0
$C_2H_3 + O_2 \rightarrow CH_2CHO + O$	3.20E+13	-0.37	2131	3.0
$C_2H_3 + O_2 \rightarrow CH_2CHO + O$	3.97E+14	-0.66	3363	10.0
$C_2H_3 + O_2 \rightarrow C_2H_2 + HO_2$	9.65E+04	2.02	-1300	0.001
$C_2H_3 + O_2 \rightarrow C_2H_2 + HO_2$	1.09E+05	2.00	-1267	0.01
$C_2H_3 + O_2 \rightarrow C_2H_2 + HO_2$	3.24E+05	1.87	-967	0.1
$C_2H_3 + O_2 \rightarrow C_2H_2 + HO_2$	1.51E+08	1.12	823	1.0
$C_2H_3 + O_2 \rightarrow C_2H_2 + HO_2$	3.52E+10	0.46	2619	3.0
$C_2H_3 + O_2 \rightarrow C_2H_2 + HO_2$	8.66E+12	-0.18	4941	10.0
$C_2H_3 + O_2 \rightarrow CH_2O + CHO$	9.11E+13	-0.57	38	0.001
$C_2H_3 + O_2 \rightarrow CH_2O + CHO$	1.00E+14	-0.59	65	0.01
$C_2H_3 + O_2 \rightarrow CH_2O + CHO$	2.40E+14	-0.69	309	0.1
$C_2H_3 + O_2 \rightarrow CH_2O + CHO$	1.67E+16	-1.21	1611	1.0
$C_2H_3 + O_2 \rightarrow CH_2O + CHO$	2.53E+17	-1.53	2677	3.0
$C_2H_3 + O_2 \rightarrow CH_2O + CHO$	8.46E+17	-1.65	3743	10.0
$CH_2CCl + O_2 \rightarrow C^*CClOO$	1.04E+24	-5.32	-76	0.001

Table E7 (cont'd)

Reactions	A(cm^3 mol^{-1} s^{-1})	n	E_a(cal/mol)	P(atm)
$CH_2CCl + O_2 \rightarrow C^*CClOO$	1.81E+25	-5.39	76	0.01
$CH_2CCl + O_2 \rightarrow C^*CClOO$	4.84E+27	-5.79	1042	0.1
$CH_2CCl + O_2 \rightarrow C^*CClOO$	8.07E+30	-6.39	3153	1.0
$CH_2CCl + O_2 \rightarrow C^*CClOO$	1.81E+31	-6.32	3915	3.0
$CH_2CCl + O_2 \rightarrow C^*CClOO$	1.55E+30	-5.83	4207	10.0
$CH_2CCl + O_2 \rightarrow CH_2CO + ClO$	8.36E+02	2.60	2470	0.001
$CH_2CCl + O_2 \rightarrow CH_2CO + ClO$	1.00E+03	2.58	2520	0.01
$CH_2CCl + O_2 \rightarrow CH_2CO + ClO$	4.08E+03	2.41	2913	0.1
$CH_2CCl + O_2 \rightarrow CH_2CO + ClO$	4.73E+05	1.83	4423	1.0
$CH_2CCl + O_2 \rightarrow CH_2CO + ClO$	5.57E+06	1.55	5462	3.0
$CH_2CCl + O_2 \rightarrow CH_2CO + ClO$	1.71E+07	1.44	6492	10.0
$CH_2CCl + O_2 \rightarrow C^*CClO. + O$	1.76E+13	-0.26	1355	0.001
$CH_2CCl + O_2 \rightarrow C^*CClO. + O$	2.50E+13	-0.31	1449	0.01
$CH_2CCl + O_2 \rightarrow C^*CClO. + O$	2.65E+14	-0.60	2101	0.1
$CH_2CCl + O_2 \rightarrow C^*CClO. + O$	9.60E+16	-1.31	4015	1.0
$CH_2CCl + O_2 \rightarrow C^*CClO. + O$	9.00E+17	-1.56	5097	3.0
$CH_2CCl + O_2 \rightarrow C^*CClO. + O$	1.28E+18	-1.58	6045	10.0
$CH_2CCl + O_2 \rightarrow C_2HCl + HO_2$	1.06E+06	1.80	671	0.001
$CH_2CCl + O_2 \rightarrow C_2HCl + HO_2$	1.51E+06	1.75	766	0.01
$CH_2CCl + O_2 \rightarrow C_2HCl + HO_2$	1.75E+07	1.45	1441	0.1
$CH_2CCl + O_2 \rightarrow C_2HCl + HO_2$	1.86E+10	0.61	3627	1.0
$CH_2CCl + O_2 \rightarrow C_2HCl + HO_2$	8.53E+11	0.16	5117	3.0
$CH_2CCl + O_2 \rightarrow C_2HCl + HO_2$	2.63E+13	-0.23	6883	10.0
$CH_2CCl + O_2 \rightarrow CH_2O + CClO$	4.10E+16	-1.47	679	0.001
$CH_2CCl + O_2 \rightarrow CH_2O + CClO$	6.98E+16	-1.54	826	0.01
$CH_2CCl + O_2 \rightarrow CH_2O + CClO$	1.79E+18	-1.93	1766	0.1

Table E7 (cont'd)

Reactions	A(cm^3 mol^{-1} s^{-1})	n	E_a(cal/mol)	P(atm)
$CH_2CCl + O_2 \rightarrow CH_2O + CClO$	4.56E+20	-2.59	3917	1.0
$CH_2CCl + O_2 \rightarrow CH_2O + CClO$	6.37E+20	-2.60	4783	3.0
$CH_2CCl + O_2 \rightarrow CH_2O + CClO$	4.40E+19	-2.23	5277	10.0
$CHClCH + O_2 \rightarrow CCl^*COO$	8.13E+22	-5.21	-348	0.001
$CHClCH + O_2 \rightarrow CCl^*COO$	9.33E+23	-5.22	-310	0.01
$CHClCH + O_2 \rightarrow CCl^*COO$	2.94E+25	-5.36	9	0.1
$CHClCH + O_2 \rightarrow CCl^*COO$	3.51E+28	-5.94	1483	1.0
$CHClCH + O_2 \rightarrow CCl^*COO$	1.60E+30	-6.26	2578	3.0
$CHClCH + O_2 \rightarrow CCl^*COO$	1.45E+31	-6.36	3611	10.0
$CHClCH + O_2 \rightarrow ClC^*CO. + O$	3.32E+11	0.16	2497	0.001
$CHClCH + O_2 \rightarrow ClC^*CO. + O$	3.53E+11	0.16	2514	0.01
$CHClCH + O_2 \rightarrow ClC^*CO. + O$	6.29E+11	0.09	2669	0.1
$CHClCH + O_2 \rightarrow ClC^*CO. + O$	1.77E+13	-0.32	3606	1.0
$CHClCH + O_2 \rightarrow ClC^*CO. + O$	4.01E+14	-0.70	4573	3.0
$CHClCH + O_2 \rightarrow ClC^*CO. + O$	1.16E+16	-1.10	5845	10.0
$CHClCH + O_2 \rightarrow C_2HCl + HO_2$	3.68E+06	1.58	-6	0.001
$CHClCH + O_2 \rightarrow C_2HCl + HO_2$	5.04E+06	1.54	76	0.01
$CHClCH + O_2 \rightarrow C_2HCl + HO_2$	6.15E+07	1.23	735	0.1
$CHClCH + O_2 \rightarrow C_2HCl + HO_2$	1.26E+12	0.02	3546	1.0
$CHClCH + O_2 \rightarrow C_2HCl + HO_2$	1.21E+15	-0.81	5780	3.0
$CHClCH + O_2 \rightarrow C_2HCl + HO_2$	5.69E+17	-1.53	8357	10.0
$CHClCH + O_2 \rightarrow CHClO + CHO$	5.79E+13	-0.47	-18	0.001
$CHClCH + O_2 \rightarrow CHClO + CHO$	6.60E+13	-0.49	18	0.01
$CHClCH + O_2 \rightarrow CHClO + CHO$	2.01E+14	-0.63	322	0.1
$CHClCH + O_2 \rightarrow CHClO + CHO$	2.61E+16	-1.22	1776	1.0

Table E7 (cont'd)

Reactions	A(cm^3 mol^{-1} s^{-1})	n	E_a(cal/mol)	P(atm)
CHClCH + O_2 → CHClO + CHO	6.13E+17	-1.60	2930	3.0
CHClCH + O_2 → CHClO + CHO	5.05E+18	-1.83	4171	10.0
CHClCCl + O_2 → ClC*CClOO	8.93E+21	-4.91	-1184	0.001
CHClCCl + O_2 → ClC*CClOO	1.28E+23	-4.95	-1087	0.01
CHClCCl + O_2 → ClC*CClOO	1.60E+25	-5.26	-381	0.1
CHClCCl + O_2 → ClC*CClOO	9.13E+28	-6.03	1729	1.0
CHClCCl + O_2 → ClC*CClOO	1.74E+30	-6.23	2811	3.0
CHClCCl + O_2 → ClC*CClOO	2.50E+30	-6.09	3601	10.0
CHClCCl + O_2 → CHClCO + ClO	5.59E+02	2.52	4099	0.001
CHClCCl + O_2 → CHClCO + ClO	6.08E+02	2.51	4121	0.01
CHClCCl + O_2 → CHClCO + ClO	1.30E+03	2.42	4326	0.1
CHClCCl + O_2 → CHClCO + ClO	7.03E+04	1.93	5461	1.0
CHClCCl + O_2 → CHClCO + ClO	1.93E+06	1.53	6524	3.0
CHClCCl + O_2 → CHClCO + ClO	4.63E+07	1.16	7822	10.0
CHClCCl + O_2 → ClC*CClO. + O	1.08E+09	0.94	1748	0.001
CHClCCl + O_2 → ClC*CClO. + O	1.27E+09	0.92	1790	0.01
CHClCCl + O_2 → ClC*CClO. + O	4.77E+09	0.76	2140	0.1
CHClCCl + O_2 → ClC*CClO. + O	1.01E+12	0.10	3674	1.0
CHClCCl + O_2 → ClC*CClO. + O	3.47E+13	-0.32	4861	3.0
CHClCCl + O_2 → ClC*CClO. + O	5.74E+14	-0.64	6158	10.0
CHClCCl + O_2 → C_2Cl_2 + HO_2	3.06E+09	0.74	7840	0.001
CHClCCl + O_2 → C_2Cl_2 + HO_2	3.41E+09	0.73	7868	0.01
CHClCCl + O_2 → C_2Cl_2 + HO_2	9.45E+09	0.61	8136	0.1
CHClCCl + O_2 → C_2Cl_2 + HO_2	6.56E+12	-0.20	9911	1.0
CHClCCl + O_2 → C_2Cl_2 + HO_2	5.87E+15	-1.03	11893	3.0

Table E7 (cont'd)

Reactions	A(cm^3 mol^{-1} s^{-1})	n	E_a(cal/mol)	P(atm)
$CHClCCl + O_2 \rightarrow C_2Cl_2 + HO_2$	1.92E+19	-2.00	14628	10.0
$CHClCCl + O_2 \rightarrow CHClO + CClO$	1.49E+15	-0.97	276	0.001
$CHClCCl + O_2 \rightarrow CHClO + CClO$	2.08E+15	-1.01	365	0.01
$CHClCCl + O_2 \rightarrow CHClO + CClO$	2.32E+16	-1.30	1024	0.1
$CHClCCl + O_2 \rightarrow CHClO + CClO$	1.84E+19	-2.11	3122	1.0
$CHClCCl + O_2 \rightarrow CHClO + CClO$	2.63E+20	-2.42	4322	3.0
$CHClCCl + O_2 \rightarrow CHClO + CClO$	4.85E+20	-2.46	5375	10.0
$CCl_2CH + O_2 \rightarrow Cl_2C^*COO$	3.27E+19	-4.21	-1799	0.001
$CCl_2CH + O_2 \rightarrow Cl_2C^*COO$	3.95E+20	-4.23	-1748	0.01
$CCl_2CH + O_2 \rightarrow Cl_2C^*COO$	1.87E+22	-4.42	-1324	0.1
$CCl_2CH + O_2 \rightarrow Cl_2C^*COO$	6.11E+25	-5.13	443	1.0
$CCl_2CH + O_2 \rightarrow Cl_2C^*COO$	3.31E+27	-5.47	1623	3.0
$CCl_2CH + O_2 \rightarrow Cl_2C^*COO$	2.69E+28	-5.55	2675	10.0
$CCl_2CH + O_2 \rightarrow CCl_2CO + OH$	4.79E+00	3.13	924	0.001
$CCl_2CH + O_2 \rightarrow CCl_2CO + OH$	5.32E+00	3.12	951	0.01
$CCl_2CH + O_2 \rightarrow CCl_2CO + OH$	1.34E+01	3.00	1194	0.1
$CCl_2CH + O_2 \rightarrow CCl_2CO + OH$	1.46E+03	2.43	2492	1.0
$CCl_2CH + O_2 \rightarrow CCl_2CO + OH$	6.27E+04	1.97	3659	3.0
$CCl_2CH + O_2 \rightarrow CCl_2CO + OH$	2.15E+06	1.55	5045	10.0
$CCl_2CH + O_2 \rightarrow Cl_2C^*CO. + O$	2.20E+10	0.50	1029	0.001
$CCl_2CH + O_2 \rightarrow Cl_2C^*CO. + O$	2.47E+10	0.48	1060	0.01
$CCl_2CH + O_2 \rightarrow Cl_2C^*CO. + O$	6.98E+10	0.36	1332	0.1
$CCl_2CH + O_2 \rightarrow Cl_2C^*CO. + O$	1.03E+13	-0.26	2720	1.0
$CCl_2CH + O_2 \rightarrow Cl_2C^*CO. + O$	4.59E+14	-0.72	3917	3.0
$CCl_2CH + O_2 \rightarrow Cl_2C^*CO. + O$	1.38E+16	-1.12	5298	10.0

Table E7 (cont'd)

Reactions	A(cm^3 mol^{-1} s^{-1})	n	E_a(cal/mol)	P(atm)
$CCl_2CH + O_2 \rightarrow CCl_2O + CHO$	2.40E+13	-0.47	-215	0.001
$CCl_2CH + O_2 \rightarrow CCl_2O + CHO$	2.86E+13	-0.50	-168	0.01
$CCl_2CH + O_2 \rightarrow CCl_2O + CHO$	1.25E+14	-0.68	229	0.1
$CCl_2CH + O_2 \rightarrow CCl_2O + CHO$	4.37E+16	-1.39	1956	1.0
$CCl_2CH + O_2 \rightarrow CCl_2O + CHO$	1.29E+18	-1.79	3198	3.0
$CCl_2CH + O_2 \rightarrow CCl_2O + CHO$	9.30E+18	-2.01	4438	10.0
$C_2Cl_3 + O_2 \rightarrow Cl_2C^*CClOO$	1.86E+19	-4.15	-2135	0.001
$C_2Cl_3 + O_2 \rightarrow Cl_2C^*CClOO$	2.46E+20	-4.18	-2061	0.01
$C_2Cl_3 + O_2 \rightarrow Cl_2C^*CClOO$	2.04E+22	-4.44	-1482	0.1
$C_2Cl_3 + O_2 \rightarrow Cl_2C^*CClOO$	1.22E+26	-5.22	520	1.0
$C_2Cl_3 + O_2 \rightarrow Cl_2C^*CClOO$	4.68E+27	-5.51	1684	3.0
$C_2Cl_3 + O_2 \rightarrow Cl_2C^*CClOO$	1.97E+28	-5.51	2640	10.0
$C_2Cl_3 + O_2 \rightarrow CCl_2CO + ClO$	2.92E+00	3.10	1827	0.001
$C_2Cl_3 + O_2 \rightarrow CCl_2CO + ClO$	3.24E+00	3.08	1854	0.01
$C_2Cl_3 + O_2 \rightarrow CCl_2CO + ClO$	7.98E+00	2.97	2092	0.1
$C_2Cl_3 + O_2 \rightarrow CCl_2CO + ClO$	6.20E+02	2.44	3309	1.0
$C_2Cl_3 + O_2 \rightarrow CCl_2CO + ClO$	1.95E+04	2.02	4392	3.0
$C_2Cl_3 + O_2 \rightarrow CCl_2CO + ClO$	5.86E+05	1.62	5717	10.0
$C_2Cl_3 + O_2 \rightarrow Cl_2C^*CClO. + O$	1.57E+10	0.47	887	0.001
$C_2Cl_3 + O_2 \rightarrow Cl_2C^*CClO. + O$	1.84E+10	0.45	929	0.01
$C_2Cl_3 + O_2 \rightarrow Cl_2C^*CClO. + O$	6.88E+10	0.28	1275	0.1
$C_2Cl_3 + O_2 \rightarrow Cl_2C^*CClO. + O$	1.51E+13	-0.38	2796	1.0
$C_2Cl_3 + O_2 \rightarrow Cl_2C^*CClO. + O$	5.84E+14	-0.82	3987	3.0
$C_2Cl_3 + O_2 \rightarrow Cl_2C^*CClO. + O$	1.32E+16	-1.18	5322	10.0
$C_2Cl_3 + O_2 \rightarrow CCl_2O + CClO$	1.48E+14	-0.75	-155	0.001

Table E7 (cont'd)

Reactions	A(cm^3 mol^{-1} s^{-1})	n	E_a(cal/mol)	P(atm)
$C_2Cl_3 + O_2 \rightarrow CCl_2O + CClO$	1.92E+14	-0.78	-86	0.01
$C_2Cl_3 + O_2 \rightarrow CCl_2O + CClO$	1.41E+15	-1.03	451	0.1
$C_2Cl_3 + O_2 \rightarrow CCl_2O + CClO$	9.39E+17	-1.82	2407	1.0
$C_2Cl_3 + O_2 \rightarrow CCl_2O + CClO$	2.22E+19	-2.19	3649	3.0
$C_2Cl_3 + O_2 \rightarrow CCl_2O + CClO$	9.94E+19	-2.35	4825	10.0

Table F1 Thermodynamic Properties

Species	H_{f298}	S_{298}	C_p300	C_p400	C_p500	C_p600	C_p800	C_p1000	C_p1500	source
C4CL2	103.40	78.10	22.10	23.80	25.00	26.20	28.00	29.00		a
C4CL3(N	101.40	90.20	25.70	28.00	29.80	31.20	33.10	34.20		a
C4CL3(I1	101.40	90.20	25.70	28.00	29.80	31.20	33.10	34.20		a
C4CL3(I2	128.20	86.10	25.50	27.70	29.10	31.50	32.20	33.20		b
C4CL4	46.40	93.30	30.30	33.50	35.20	36.90	38.50	39.40		a
C4CL5(N	43.40	108.80	34.00	36.20	38.20	39.90	42.40	43.80		a
C4CL5(I1	43.40	108.80	34.00	36.20	38.20	39.90	42.40	43.80		a
C4CL5(I2	17.80	83.00	35.50	39.60	41.80	43.50	45.00	45.90		b
C4CL6	-7.70	110.20	37.90	41.60	43.70	45.80	47.70	48.80		a
C4CL7(N	5.40	123.10	44.50	48.20	51.40	53.40	56.10	57.30		a
C4CL8	-41.60	124.50	48.40	53.70	56.90	59.20	61.40	62.40		a
C4HCL(L	108.10	69.80	20.20	22.50	23.90	25.10	26.80	28.00		b
C4HCL2(N1	106.90	81.10	24.40	27.70	28.70	31.30	32.40	32.90		b
C4HCL3(L	47.61	88.03	26.67	30.34	31.90	35.02	36.94	38.10		b
C4HCL4(N	52.40	100.90	31.40	35.10	37.70	39.70	42.10	43.50		a
C4HCL4(N1	52.40	100.90	31.40	35.10	37.70	39.70	42.10	43.50		a
C4HCL4(I	52.40	100.90	31.40	35.10	37.70	39.70	42.10	43.50		a
C4HCL4(I1	53.16	97.88	31.14	35.62	38.19	40.32	42.22	43.54		b
C4HCL5	-.60	103.00	35.60	39.80	42.90	45.10	47.90	49.40		a
C4HCL6(N	12.40	119.80	40.20	43.90	46.80	49.00	52.00	53.80		a
C4HCL6(I	12.40	119.80	40.20	43.90	46.80	49.00	52.00	53.80		a
C#CC#C	110.80	59.70	17.60	20.10	21.70	23.00	24.90	26.30	28.80	b
C4H2CL(N1	116.90	73.30	21.60	24.80	25.90	28.60	30.10	31.10		b
C4H2CL(N2	117.30	76.40	20.60	24.20	26.00	28.80	30.80	32.10		b
C4H2CL(I1	111.10	77.00	19.70	23.50	25.40	28.20	30.50	32.00		b
C4H2CL2(L	50.30	79.30	24.00	27.90	29.60	32.80	35.00	36.40		b
C4H2CL2(L2	55.07	80.24	23.87	27.50	29.11	32.32	34.71	36.27		b
C4H2CL2(L3	57.95	83.26	22.83	26.93	29.25	32.54	35.29	37.31		b
C4H2CL3(N1	57.00	90.40	30.00	33.70	35.60	37.90	39.50	40.60		b
C4H2CL3(N2	57.40	91.80	28.90	33.10	35.80	38.10	40.20	41.60		b
C4H2CL3(N3	57.40	91.80	28.90	33.10	35.80	38.10	40.20	41.60		b
C4H2CL3(I1	51.20	92.50	28.00	32.40	35.10	37.60	39.80	41.60		b
C4H2CL4(L1	-3.70	95.30	31.60	36.60	39.70	42.40	45.10	47.10		b
C4H2CL4(L2	2.00	92.90	30.80	36.40	40.10	42.60	45.90	48.20		b
C4H2CL4(L3	-9.50	95.00	32.40	36.80	39.40	42.20	44.40	46.00		b
C4H2CL5(N1	11.00	114.70	35.80	40.00	42.40	45.10	49.50	51.70		b
C4H2CL5(N2	13.10	113.00	35.00	39.90	42.80	45.30	50.20	52.60		b
C4H2CL5(N3	11.50	113.60	35.70	41.50	44.80	47.50	50.40	52.20		b
C4H2CL5(N4	12.70	111.90	34.90	41.30	45.10	47.70	51.10	53.10		b
C.*CC#C	127.27	68.62	17.84	21.45	23.30	26.12	28.64	30.32	33.50	b
C*C.C#C	125.07	69.30	16.92	20.69	22.66	25.59	28.27	30.26	33.37	b
C4H3CL(L1	60.70	74.50	20.20	24.50	27.00	30.40	33.40	35.60		b
CLC*CC#C	60.70	74.50	20.20	24.50	27.00	30.40	33.40	35.60		b
C4H3CL(L2	57.83	71.54	21.25	25.09	26.90	30.19	32.78	34.63		b

Table F1 (cont'd)

Species	H_{f298}	S_{298}	C_p300	C_p400	C_p500	C_p600	C_p800	C_p1000	C_p1500	source
C*CCLC#C	57.83	71.54	21.25	25.09	26.90	30.19	32.78	34.63		b
C*CC#CCL	65.41	75.47	20.03	24.09	26.46	29.84	33.16	35.48		b
C4H3CL2(N1	67.30	84.00	26.10	30.30	33.00	35.40	38.00	39.80		b
C4H3CL2(N2	64.80	84.00	26.10	30.30	33.00	35.40	38.00	39.80		b
C4H3CL2(N3	67.30	84.00	26.10	30.30	33.00	35.40	38.00	39.80		b
C4H3CL2(N4	64.50	82.67	27.23	30.89	32.87	35.21	37.35	38.82		b
C4H3CL2(N5	64.88	84.04	26.19	30.32	33.01	35.43	38.03	39.86		b
C4H3CL2(I1	68.06	86.09	24.23	28.99	32.51	35.12	38.34	40.84		b
C4H3CL2(I2	65.18	84.72	25.27	29.56	32.37	34.90	37.66	39.80		b
C4H3CL3(L1	.80	89.90	28.50	33.30	36.70	39.70	42.80	45.20		b
C4H3CL3(L2	6.60	88.90	27.70	33.20	37.10	39.90	43.60	46.30		b
C4H3CL4(N1	17.60	110.00	31.90	36.50	39.40	42.20	47.20	49.80		b
C4H3CL4(N2	19.70	108.40	31.10	36.30	39.70	42.50	48.00	50.80		b
C4H3CL4(N3	17.70	107.70	31.90	36.70	39.80	42.60	47.90	50.70		b
C4H3CL4(N4	17.20	106.60	31.90	38.10	42.10	45.00	48.80	51.20		b
C4H3CL5(L1	-29.90	114.40	36.10	41.30	44.60	47.90	53.10	55.80		b
C4H3CL5(L2	-27.80	112.70	35.30	41.20	44.90	48.10	53.90	56.80		b
C4H3CL5(L3	-32.90	111.20	36.40	42.90	46.90	50.10	53.70	56.10		b
C4H3CL5(L4	-31.80	109.50	35.60	42.70	47.20	50.30	54.50	57.00		b
C*CC#C	68.17	66.77	17.41	21.68	24.25	27.71	31.23	33.84	37.93	b
C4H4CL(N1	77.70	77.60	22.30	26.90	30.30	32.90	36.40	39.00		b
C4H4CL(N2	74.84	76.25	23.39	27.48	30.22	32.73	35.80	38.03		b
C4H4CL(N3	74.84	76.25	23.39	27.48	30.22	32.73	35.80	38.03		b
C4H4CL(N4	75.22	77.62	22.35	26.91	30.36	32.95	36.48	39.07		b
C4H4CL(I1	72.64	76.93	22.47	26.72	29.58	32.20	35.43	37.97		b
C4H4CL(I2	72.64	76.93	22.47	26.72	29.58	32.20	35.43	37.97		b
C4H4CL(I3	75.52	78.30	21.43	26.15	29.72	32.42	36.11	39.01		b
C4H4CL2(L1	11.10	82.10	24.70	29.90	34.10	37.20	41.30	44.40		b
C4H4CL2(L2	5.40	79.44	26.80	31.12	33.82	36.80	39.94	42.34		b
C4H4CL2(L3	8.28	82.19	25.76	30.55	33.96	37.02	40.62	43.38		b
C4H4CL3(N1	24.30	103.00	28.10	33.10	36.70	39.70	45.70	48.90		b
C4H4CL4(L1	-26.80	107.60	32.60	37.90	41.40	44.80	50.60	53.70		b
C4H4CL4(L2	-24.70	105.90	31.90	37.80	41.70	45.00	51.40	54.70		b
C4H4CL4(L3	-23.20	107.30	32.30	38.00	41.90	45.40	51.50	54.90		b
C4H4CL4(L4	-27.20	104.10	32.60	39.50	44.20	47.60	52.20	55.10		b
C*CC*C.	85.18	69.83	19.55	24.07	27.57	30.25	34.25	37.24	42.13	b
C*CC.*C	82.98	70.51	18.63	23.31	26.93	29.72	33.88	37.18	42.00	b
C4H5CL(L1	15.74	74.40	22.96	27.71	31.17	34.32	38.39	41.55		b
C4H5CL(L2	18.62	75.77	21.92	27.14	31.31	34.54	39.07	42.59		b
C4H5CL2(N1	30.19	92.57	26.55	31.22	34.36	37.54	43.25	46.45		b
C4H5CL2(N2	32.42	93.33	25.51	30.69	34.46	37.74	43.93	47.33		b
C*CC*C	26.08	66.60	19.12	24.30	28.52	31.84	36.84	40.76	46.56	b
C4H6CL(N1	39.88	85.54	22.71	27.85	31.67	35.04	41.70	45.50		b
C4H6CL(N2	39.20	83.17	23.63	28.27	32.11	35.69	40.50	44.12		b

Table F1 (cont'd)

Species	H_{f298}	S_{298}	C_p300	C_p400	C_p500	C_p600	C_p800	C_p1000	C_p1500	source
C4H6CL(N3	41.43	83.93	22.59	27.74	32.21	35.09	41.28	45.00		b
C4H6CL2(L1	-18.81	90.04	27.33	32.41	35.98	39.63	46.26	50.25		b
C4H6CL2(L2	-16.58	90.80	26.29	31.88	36.08	39.83	46.94	51.13		b
C*CCC.	48.89	76.14	19.79	24.90	29.42	33.19	38.95	43.17	50.06	b
C6CL2	163.50	92.20	28.30	30.70	32.60	34.40	37.20	38.90		a
C6CL3	160.30	105.70	37.10	40.50	43.00	44.80	46.80	47.60		a
C6CL4(L	101.20	109.50	38.10	40.60	42.00	44.20	46.40	47.80		a
C6CL5(L	91.90	124.40	41.50	44.80	47.30	49.20	51.70	53.30		a
C6CL5(Y	53.00	109.10	39.20	45.40	49.50	52.20	55.20	56.00		a
C6CL6(L	50.70	125.50	46.00	49.50	51.30	54.00	56.20	57.70		a
C6CL6(Y	-8.26	104.90	41.30	46.40	50.60	53.60	57.70	60.20		b
C6CL7(L	39.70	141.80	50.10	54.00	56.70	58.50	60.40	61.40		a
C6CL8(L	-5.90	138.80	53.90	58.40	60.70	63.80	66.10	67.60		a
C6HCL2(N1	183.70	88.50	30.50	34.90	35.80	41.00	41.70	42.60		b
C6HCL3(L1	100.38	96.56	34.92	39.87	40.99	45.51	47.35	48.36		b
C6HCL5(L1	46.27	114.23	42.50	48.55	51.08	55.06	57.52	59.02		b
C6H2CL(N1	194.00	83.70	26.60	31.50	33.10	38.50	40.10	41.80		b
C6H2CL2(L1	110.72	91.79	31.08	36.46	38.34	43.03	45.80	47.57		b
C6H2CL2(L2	110.72	91.79	31.08	36.46	38.34	43.03	45.80	47.57		b
C6H2CL2(L3	103.14	86.48	32.30	37.46	38.78	43.38	45.42	46.72		b
C6H2CL2(Y	85.32	80.74	26.29	31.15	34.49	38.15	42.00	44.39		b
C6H2CL3(N1	110.19	100.36	37.24	42.69	44.89	48.62	50.67	51.95		b
C6H2CL3(Y	59.12	91.72	30.82	37.19	41.93	45.34	49.89	52.79		b
C6H2CL4(L1	50.83	108.86	39.43	45.33	48.05	52.34	55.19	57.11		b
C6H2CL4(L2	50.83	107.21	39.43	45.33	48.05	52.34	55.19	57.11		b
C6H2CL4(L3	49.03	105.53	39.88	46.14	48.87	52.93	55.59	57.38		b
OMPCLBZ	-7.72	95.57	34.96	41.89	47.09	50.96	56.00	59.16		b
C6H2CL5(N1	50.60	118.11	44.67	50.80	53.96	57.40	59.69	61.43		b
CHD.5CL	-0.68	107.65	39.16	47.14	51.28	55.22	60.83	63.34		b
C6H3CL(L1	121.06	87.02	27.24	33.05	35.69	40.55	44.25	46.78		b
C6H3CL(L2	113.48	83.09	28.46	34.05	36.13	40.90	43.87	45.93		b
C6H3CL(Y1	95.66	75.97	22.45	27.74	31.84	35.67	40.45	43.60		b
C6H3CL(Y2	95.66	74.32	22.45	27.74	31.84	35.67	40.45	43.60		b
C6H3CL2(N1	120.53	95.59	33.40	39.28	42.24	46.14	49.12	51.16		b
C6H3CL2(N2	120.53	93.94	33.40	39.28	42.24	46.14	49.12	51.16		b
C6H3CL2(N3	120.15	92.11	33.82	39.33	41.69	45.59	48.21	50.15		b
C6H3CL2(Y1	66.53	83.32	26.89	33.28	38.23	41.93	47.09	50.52		b
C6H3CL2(Y2	66.53	83.32	26.89	33.28	38.23	41.93	47.09	50.52		b
C6H3CL2(Y3	66.53	83.32	26.89	33.28	38.23	41.93	47.09	50.52		b
C6H3CL(L1	121.06	87.02	27.24	33.05	35.69	40.55	44.25	46.78		b
C6H3CL(L2	113.48	83.09	28.46	34.05	36.13	40.90	43.87	45.93		b
C6H3CL(Y1	95.66	75.97	22.45	27.74	31.84	35.67	40.45	43.60		b
C6H3CL(Y2	95.66	74.32	22.45	27.74	31.84	35.67	40.45	43.60		b
C6H3CL2(N1	120.53	95.59	33.40	39.28	42.24	46.14	49.12	51.16		b

Table F1 (cont'd)

Species	H_{f298}	S_{298}	C_p300	C_p400	C_p500	C_p600	C_p800	C_p1000	C_p1500	source
C6H3CL2(N2	120.53	93.94	33.40	39.28	42.24	46.14	49.12	51.16		b
C6H3CL2(N3	120.15	92.11	33.82	39.33	41.69	45.59	48.21	50.15		b
C6H3CL2(Y1	66.53	83.32	26.89	33.28	38.23	41.93	47.09	50.52		b
C6H3CL2(Y2	66.53	83.32	26.89	33.28	38.23	41.93	47.09	50.52		b
C6H3CL2(Y3	66.53	83.32	26.89	33.28	38.23	41.93	47.09	50.52		b
C6H3CL3(L1	61.17	102.44	35.59	41.92	45.40	49.86	53.64	56.32		b
C6H3CL3(L2	58.29	101.07	36.63	42.49	45.26	49.64	52.96	55.28		b
C6H3CL3(L3	58.29	99.42	36.63	42.49	45.26	49.64	52.96	55.28		b
C6H3CL3(L4	61.17	102.44	35.59	41.92	45.40	49.86	53.64	56.32		b
C6H3CL3(L5	61.17	100.79	35.59	41.92	45.40	49.86	53.64	56.32		b
C6H3CL3(L6	53.59	100.16	36.81	42.92	45.84	50.21	53.26	55.47		b
C6H3CL3(L7	53.59	98.51	36.81	42.92	45.84	50.21	53.26	55.47		b
OPCLBZ	-0.31	88.55	31.03	37.98	43.39	47.55	53.20	56.89		b
DMCLBZ	0.90	89.30	30.33	37.30	42.70	46.55	52.30	56.10		b
OMCLBZ	-0.31	88.55	31.03	37.98	43.39	47.55	53.20	56.89		b
C6H3CL4(N1	60.64	111.01	41.75	48.15	51.95	55.45	58.51	60.70		b
C6H3CL4(N2	60.64	111.01	41.75	48.15	51.95	55.45	58.51	60.70		b
C6H3CL4(N3	66.04	108.13	41.40	48.01	51.78	55.14	58.38	60.81		b
CL1256CHD.	7.3	102.70	35.38	42.16	45.83	49.94	57.69	60.99		b
CL1245CHD.	6.73	102.09	35.38	42.20	45.79	49.92	57.69	60.83		b
CL1156CHD.	12.83	99.62	36.24	44.19	49.02	53.37	58.08	61.01		b
C6H4(L	123.82	76.94	24.62	30.64	33.48	38.42	42.32	45.14	49.48	b
BENZYNE	106.0	68.17	18.61	24.33	29.19	33.19	38.90	42.81		b
C6H4CL(N1	130.87	89.17	29.56	35.87	39.59	43.66	47.57	50.37		b
C6H4CL(N2	130.49	87.34	29.98	35.92	39.04	43.11	46.66	49.36		b
C6H4CL(N3	130.49	85.69	29.98	35.92	39.04	43.11	46.66	49.36		b
C6H4CL(Y1	73.94	77.68	22.96	29.37	34.53	38.52	44.29	48.25		b
C6H4CL(Y2	73.94	77.68	22.96	29.37	34.53	38.52	44.29	48.25		b
C6H4CL2(L1	71.51	96.02	31.75	38.51	42.75	47.38	52.09	55.53		b
C6H4CL2(L2	68.63	94.65	32.79	39.08	42.61	47.16	51.41	54.49		b
C6H4CL2(L3	68.63	94.65	32.79	39.08	42.61	47.16	51.41	54.49		b
C6H4CL2(L4	68.63	93.00	32.79	39.08	42.61	47.16	51.41	54.49		b
C6H4CL2(L5	63.93	93.74	32.97	39.51	43.19	47.73	51.71	54.68		b
C6H4CL2(L6	61.05	92.37	34.01	40.08	43.05	47.51	51.03	53.64		b
C6H4CL2(L7	61.05	90.72	34.01	40.08	43.05	47.51	51.03	53.64		b
C6H4CL2(L8	63.93	93.74	32.97	39.51	43.19	47.73	51.71	54.68		b
C6H4CL2(L9	63.93	92.09	32.97	39.51	43.19	47.73	51.71	54.68		b
C6H4CL2(Y1	5.30	81.70	27.20	34.10	39.70	44.20	50.40	54.60		b
C6H4CL2(Y2	6.10	83.30	27.10	34.10	39.70	44.10	50.40	54.60		b
C6H4CL2(Y3	7.18	83.22	27.30	34.46	40.16	44.62	50.84	55.00		b
C6H4CL3(N1	70.90	104.50	37.90	44.70	49.30	52.90	56.90	59.90		b
C6H4CL3(N2	68.10	103.22	38.95	45.31	49.16	52.75	56.28	58.87		b
C6H4CL3(N3	68.10	103.22	38.95	45.31	49.16	52.75	56.28	58.87		b
C6H4CL3(N4	70.98	104.59	37.91	44.74	49.30	52.90	56.90	59.90		b

Table F1 (cont'd)

Species	H_{f298}	S_{298}	C_p300	C_p400	C_p500	C_p600	C_p800	C_p1000	C_p1500	source
C6H4CL3(N5	70.98	104.59	37.91	44.74	49.30	52.90	56.90	59.90		b
C6H4CL3(N6	70.60	103.22	38.95	45.31	49.16	52.75	56.28	58.87		b
C6H4CL3(N7	70.60	103.22	38.95	45.31	49.16	52.75	56.28	58.87		b
C6H4CL3(I1	71.28	105.27	36.99	43.98	48.66	52.44	56.59	59.85		b
C6H4CL3(I2	68.40	103.90	38.03	44.55	48.52	52.22	55.91	58.81		b
C6H4CL3(I3	68.40	103.90	38.03	44.55	48.52	52.22	55.91	58.81		b
C6H4CL3(I4	65.62	102.53	39.07	45.12	48.38	52.00	55.23	57.77		b
CL125CHD.	17.07	95.67	31.54	38.79	43.14	47.44	56.14	60.04		b
CL256CHD.	16.49	94.67	32.46	39.21	43.58	48.09	54.94	58.66		b
CL246CHD.	16.49	94.67	32.46	39.21	43.58	48.09	54.94	58.66		b
CL126CHD.	17.72	96.28	31.54	38.75	43.18	47.46	56.14	60.20		b
CL124CHD.	17.07	95.67	31.54	38.79	43.14	47.44	56.14	60.04		b
CL156CHD.	20.89	94.67	32.46	39.21	43.58	48.09	54.94	58.66		b
CL145CHD.	20.24	94.06	32.46	39.25	43.54	48.07	54.94	58.50		b
C6H5(N	140.83	80.92	26.14	32.51	36.39	40.63	45.11	48.57	53.58	b
PHENYL	81.35	69.38	19.51	25.91	31.32	35.69	42.12	46.57	53.07	b
C6H5CL(L1	78.97	88.23	28.95	35.67	39.96	44.68	49.86	53.70		b
C6H5CL(L2	71.39	85.95	30.17	36.67	40.40	45.03	49.48	52.85		b
C6H5CL(L3	71.39	85.95	30.17	36.67	40.40	45.03	49.48	52.85		b
C6H5CL(L4	74.27	87.32	29.13	36.10	40.54	45.25	50.16	53.89		b
C6H5CL(L5	71.39	84.30	30.17	36.67	40.40	45.03	49.48	52.85		b
CYC6H5CL	12.30	74.80	23.30	30.50	36.40	41.20	48.00	52.70		b
C6H5CL2(N1	81.30	98.10	34.00	41.30	46.60	50.40	55.40	59.10		b
C6H5CL2(N2	78.44	96.80	35.11	41.90	46.51	50.27	54.73	58.08		b
C6H5CL2(N3	78.44	96.80	35.11	41.90	46.51	50.27	54.73	58.08		b
C6H5CL2(N4	78.44	96.80	35.11	41.90	46.51	50.27	54.73	58.08		b
C6H5CL2(N5	80.94	96.80	35.11	41.90	46.51	50.27	54.73	58.08		b
C6H5CL2(N6	78.06	95.43	36.15	42.47	46.37	50.05	54.05	57.04		b
C6H5CL2(N7	78.06	95.43	36.15	42.47	46.37	50.05	54.05	57.04		b
C6H5CL2(N8	80.94	96.80	35.11	41.90	46.51	50.27	54.73	58.08		b
C6H5CL2(N9	80.94	96.80	35.11	41.90	46.51	50.27	54.73	58.08		b
C6H5CL2(I1	78.74	97.48	34.19	41.14	45.87	49.74	54.36	58.02		b
C6H5CL2(I2	75.86	96.11	35.23	41.71	45.73	49.52	53.68	56.98		b
C6H5CL2(I3	81.62	98.85	33.15	40.57	46.01	49.96	55.04	59.06		b
C6H5CL2(I4	78.74	97.48	34.19	41.14	45.87	49.74	54.36	58.02		b
C6H5CL2(I5	78.74	97.48	34.19	41.14	45.87	49.74	54.36	58.02		b
C6H5CL2(I6	78.74	97.48	34.19	41.14	45.87	49.74	54.36	58.02		b
C6H5CL2(I7	75.86	96.11	35.23	41.71	45.73	49.52	53.68	56.98		b
C6H5CL2(I8	75.86	96.11	35.23	41.71	45.73	49.52	53.68	56.98		b
CL12CHD.	27.41	89.25	27.70	35.38	40.49	44.96	54.59	59.25		b
CL26CHD.	26.73	88.25	28.62	35.80	40.93	45.61	53.39	57.87		b
CL25CHD.	26.08	87.64	28.62	35.84	40.89	45.59	53.39	57.71		b
CL24CHD.	26.08	87.64	28.62	35.84	40.89	45.59	53.39	57.71		b
CL15CHD.	28.54	89.84	28.32	35.04	39.99	44.69	52.69	57.21		b

Table F1 (cont'd)

Species	H_{f298}	S_{298}	C_p300	C_p400	C_p500	C_p600	C_p800	C_p1000	C_p1500	source
CL56CHD.	25.40	86.64	29.54	36.26	41.33	46.24	52.19	56.33		b
CL46CHD.	25.40	86.64	29.54	36.26	41.33	46.24	52.19	56.33		b
CL16CHD.	31.23	88.25	28.62	35.80	40.93	45.61	53.39	57.87		b
CL14CHD.	30.58	87.64	28.62	35.84	40.89	45.59	53.39	57.71		b
C6H6	19.80	64.25	19.53	26.69	32.68	37.67	45.30	50.60	58.17	b
C6H6(L	81.73	79.53	26.33	33.26	37.75	42.55	47.93	52.06	58.11	b
C6H6CL(N1	88.78	90.38	31.27	38.49	43.86	47.79	53.18	57.29		b
C6H6CL(N2	88.40	89.01	32.31	39.06	43.72	47.57	52.50	56.25		b
C6H6CL(N3	88.40	89.01	32.31	39.06	43.72	47.57	52.50	56.25		b
C6H6CL(N4	91.28	90.38	31.27	38.49	43.86	47.79	53.18	57.29		b
C6H6CL(N5	88.40	89.01	32.31	39.06	43.72	47.57	52.50	56.25		b
C6H6CL(N6	88.40	89.01	32.31	39.06	43.72	47.57	52.50	56.25		b
C6H6CL(I1	89.08	91.06	30.35	37.73	43.22	47.26	52.81	57.23		b
C6H6CL(I2	86.20	89.69	31.39	38.30	43.08	47.04	52.13	56.19		b
C6H6CL(I3	86.20	89.69	31.39	38.30	43.08	47.04	52.13	56.19		b
C6H6CL(I4	89.08	91.06	30.35	37.73	43.22	47.26	52.81	57.23		b
C6H6CL(I5	86.20	89.69	31.39	38.30	43.08	47.04	52.13	56.19		b
CL1CHD.	40.92	81.22	24.78	32.43	38.24	43.11	51.84	56.92		b
CL2CHD.	36.42	81.22	24.78	32.43	38.24	43.11	51.84	56.92		b
CL3CHD.	40.24	80.22	25.70	32.85	38.68	43.76	50.64	55.54		b
CL4CHD.	39.59	79.61	25.70	32.89	38.64	43.74	50.64	55.38		b
C6H7(N1	98.74	82.59	28.47	35.65	41.07	45.09	50.95	55.46	62.31	b
CHD.	49.93	73.20	21.86	29.48	36.01	41.25	49.09	54.57	62.70	b
OHCHD.	10.79	81.36	25.51	33.94	40.94	46.17	54.13	59.52		b
CLOHCHD.	-0.35	87.66	29.16	37.92	44.80	50.04	57.23	62.09		b
CL4OHCHD.	-29.39	109.14	39.76	47.65	52.39	56.87	63.08	66.16		b
CL5OHCHD.	-40.41	114.56	44.52	51.48	55.48	60.00	63.43	65.57		b
CL6OHCHD.	-49.42	122.59	47.44	54.43	57.73	61.85	66.18	67.90		b
OPCLPH	-31.47	90.76	32.14	39.49	45.35	49.70	55.79	59.72		b
OMCLPH	-30.47	90.28	32.06	39.43	45.25	49.67	55.78	59.72		b
OMMCLPH	-44.14	97.30	35.99	43.34	48.95	53.08	58.58	61.99		b
TCLPH	-46.19	103.87	39.40	46.14	51.34	55.08	60.07	63.12		b
PCLPH	-45.83	109.37	43.01	49.33	54.20	57.56	62.00	64.63		b

Unit: ΔH_f, kcal/mol; S and C_p, cal mol^{-1} K^{-1}

SOURCES of Thermodynamic Properties

a. Taylor, P. H.; Tirey, D. A.; Rubey, W. A.; Dellinger, B. submitted to *Combust. Sci.and Tech.* **1993**.

b. THERM: Computer Code for Thermodynamic Properties Estimation, Ritter, E. R.; Bozzelli, J. W. *Intl. J. Chem. Kinet.* **1991**, 23, 767.

Table F2 Reaction Mechanism for Molecular Weight Growth from C_2 to C_6

C4 Reaction

Reactions	A[a]	n	E_a[b]	source
1. C2H3 + C2H3 = C2H4 + C2H2	2.16E13	-0.01	11	1
2. C2H3 + C2H3 = C*CC*C	2.63E11	-0.60	-217	1
3. C2H3 + CHCHCl = C4H5Cl(L2	1.06E44	-9.89	8760	1
4. C2H3 + CHCHCl = C*CC*C. + Cl	1.43E09	1.28	3860	1
5. C2H3 + CHCHCl = C*CC#C + HCl	1.35E20	-2.04	4880	1
6. C2H3 + CH2CCl = C4H5Cl(L1	5.70E46	-10.72	9740	1
7. C2H3 + CH2CCl = C*CC.*C + Cl	1.32E13	0.16	4950	1
8. C2H3 + CH2CCl = C*CC#C + HCl	9.35E22	-2.97	6970	1
9. CHCHCl + CHCHCl = C4H4Cl2(L1	1.27E44	-10.08	8630	1
10. CHCHCl + CHCHCl = C4H4Cl(N1 + Cl	4.11E07	1.64	3800	1
11. CHCHCl + CHCHCl = ClC*CC#C + HCl	3.86E19	-1.93	4780	1
12. CH2CCl + CH2CCl = C4H4Cl2(L2	1.53E46	-10.66	9500	1
13. CH2CCl + CH2CCl = C4H4Cl(I1 + Cl	4.12E12	0.23	5630	1
14. CH2CCl + CH2CCl = C*CClC#C + HCl	8.16E21	-2.67	5900	1
15. CH2CCl + CHCHCl = C4H4Cl2(L3	1.21E45	-10.42	8800	1
16. CH2CCl + CHCHCl = C4H4Cl(N2 + Cl	3.46E09	0.96	3700	1
17. CH2CCl + CHCHCl = C4H4Cl(I3 + Cl	1.14E11	0.57	3750	1
18. CH2CCl + CHCHCl = C*CClC#C + HCl	1.10E21	-2.48	4950	1
19. CH2CCl + CHCHCl = ClC*CC#C + HCl	8.03E19	-2.20	4810	1
20. CHCHCl + CHClCCl = C4H3Cl3(L1	2.22E44	-10.16	8860	1
21. CHCHCl + CHClCCl = C4H3Cl2(N1 + Cl	2.23E10	0.67	4980	1
22. CHCHCl + CHClCCl = C4H3Cl2(I1 + Cl	2.34E10	0.75	5000	1
23. CHCHCl + CHClCCl = C4H3Cl2(N3 + Cl	2.23E10	0.67	4980	1
24. CHCHCl + CHClCCl = C4H2Cl2(L + HCl	1.78E21	-2.52	5630	1
25. CHCHCl + CHClCCl = C4H2Cl2(L3 + HCl	1.23E18	-1.74	5300	1
26. CHClCCl + CHClCCl = C4H2Cl4(L3	4.57E46	-10.85	10030	1
27. CHClCCl + CHClCCl = C4H2Cl3(N1 + Cl	1.70E13	-0.25	6700	1

Table F2 (cont'd)

Reactions	A[a]	n	E_a[b]	source
28. CHClCCl + CHClCCl = C4H2Cl3(I1 + Cl	5.33E16	-1.06	6640	1
29. CHClCCl + CHClCCl = C4HCl3(L + HCl	6.89E20	-2.58	6850	1
30. C2H3 + C2H3Cl = Cl + C*CC*C	5.06E11	-0.06	5120	1
31. CH2CCl + C2H3Cl = Cl + C4H5Cl(L1	6.05E11	-0.08	5170	1
32. CHCHCl + C2H3Cl = Cl + C4H5Cl(L2	5.49E11	-0.07	5150	1
33. CHCHCl + CHClCHCl = Cl + C4H4Cl2(L1	2.57E13	-0.54	6270	1
34. CHClCCl + CHClCHCl = Cl + C4H3Cl3(L1	7.06E11	-0.10	5220	1
35. CCl2CH + CHClCHCl = Cl + C4H3Cl3(L2	3.27E12	-0.29	5660	1
36. CHCHCl + C2HCl3 = Cl + C4H3Cl3(L2	6.18E15	-1.22	7830	1
37. CHClCCl + C2HCl3 = Cl + C4H2Cl4(L1	1.76E12	-0.21	5460	1
38. CCl2CH + C2HCl3 = Cl + C4H2Cl4(L2	2.20E14	-0.81	6770	1
39. CHCHCl + C2HCl3 = Cl + C4H3Cl3(L1	4.82E11	-0.05	5110	1
40. CHClCCl + C2HCl3 = Cl + C4H2Cl4(L3	4.76E11	-0.05	5080	1
41. CCl2CH + C2HCl3 = Cl + C4H2Cl4(L1	5.84E11	-0.08	5150	1
42. C2H3 + C2H2 = C*CC*C.	4.92E40	-9.24	13310	1
43. C2H3 + C2H2 = H + C*CC#C	1.57E18	-1.79	11350	1
44. CH2CCl + C2H2 = C4H4Cl(N2	2.41E39	-8.77	13120	1
45. CH2CCl + C2H2 = H + C*CClC#C	2.51E19	-2.17	13030	1
46. CHCHCl + C2H2 = C4H4Cl(N1	1.73E39	-8.77	11910	1
47. CHCHCl + C2H2 = H + ClC*CC#C	3.20E18	-1.81	12400	1
48. C2H3 + C2HCl = C4H4Cl(N3	1.23E18	-3.70	4300	1
49. C2H3 + C2HCl = Cl + C*CC#C	3.39E11	-0.01	5010	1
50. CH2CCl + C2HCl = C4H3Cl2(N4	4.43E13	-2.21	2860	1
51. CH2CCl + C2HCl = Cl + C*CClC#C	3.50E11	-0.01	5000	1
52. CHCHCl + C2HCl = C4H3Cl2(N1	3.45E13	-2.33	3000	1
53. CHCHCl + C2HCl = Cl + ClC*CC#C	3.23E11	0.00	5000	1
54. CHClCCl + C2H2 = C4H3Cl2(N3	4.36E36	-7.91	12260	1
55. CHClCCl + C2H2 = H + C4H2Cl2(L3	9.65E19	-2.29	13500	1

Table F2 (cont'd)

Reactions	A[a]	n	E_a[b]	source
56. CHClCCl + C2HCl = C4H2Cl3(N1	5.79E11	-1.65	2350	1
57. CHClCCl + C2HCl = Cl + C4H2Cl2(L	3.41E11	-0.01	5000	1
58. C*CC*C. = H + C*CC#C	1.21E40	-8.51	46360	1
59. C4H4Cl(N2 = H + C*CClC#C	7.26E35	-7.33	45000	1
60. C4H4Cl(N1 = H + ClC*CC#C	6.11E37	-7.80	45580	1
61. C4H4Cl(N3 = Cl + C*CC#C	1.05E42	-9.54	27870	1
62. C4H3Cl2(N4 = Cl + C*CClC#C	2.78E40	-8.99	28300	1
63. C4H3Cl2(N1 = Cl + ClC*CC#C	3.62E41	-9.33	28000	1
64. C4H3Cl2(N3 = H + C4H2Cl2(L3	3.09E32	-6.28	44120	1
65. C4H2Cl3(N1 = Cl + C4H2Cl2(L	3.07E40	-8.95	28340	1
66. C*CC*C + Cl = C*CC*C. + HCl	5.00E13	0.00	10000	2
67. C*CC*C + Cl = C*CC.*C + HCl	5.00E13	0.00	8000	2
68. C4H5Cl(L1 + Cl = HCl + C4H4Cl(N2	5.00E13	0.00	10000	2
69. C4H5Cl(L1 + Cl = HCl + C4H4Cl(N3	2.50E13	0.00	8000	3
70. C4H5Cl(L1 + Cl = HCl + C4H4Cl(I1	2.50E13	0.00	8000	3
71. C4H5Cl(L2 + Cl = HCl + C4H4Cl(N1	5.00E13	0.00	10000	2
72. C4H5Cl(L2 + Cl = HCl + C4H4Cl(N4	2.50E13	0.00	7500	3
73. C4H5Cl(L2 + Cl = HCl + C4H4Cl(I2	2.50E13	0.00	5000	3
74. C4H4Cl2(L1 + Cl = C4H3Cl2(I1 + HCl	2.50E13	0.00	8000	3
75. C4H4Cl2(L2 + Cl = C4H3Cl2(N4 + HCl	5.00E13	0.00	10000	2
76. C4H4Cl2(L3 + Cl = C4H3Cl2(I2 + HCl	2.50E13	0.00	8000	3
77. C4H4Cl2(L3 + Cl = C4H3Cl2(N1 + HCl	5.00E13	0.00	10000	2
78. C*CC.*C = C*CC*C.	6.41E09	1.00	41900	4
79. C4H4Cl(I1 = C4H4Cl(N2	6.41E09	1.00	41900	4
80. C4H4Cl(I2 = C4H4Cl(N4	6.41E09	1.00	41900	4
81. C4H4Cl(I3 = C4H4Cl(N1	6.41E09	1.00	41900	4
82. C4H3Cl2(I1 = C4H3Cl2(N2	6.41E09	1.00	41900	4
83. C4H3Cl2(I2 = C4H3Cl2(N5	6.41E09	1.00	41900	4

Table F2 (cont'd)

Reactions	A[a]	n	E_a[b]	source
84. C2H2 + C2H2 = C*CC#C	5.89E13	0.00	44600	5
85. C2H2 + C2HCl = ClC*CC#C	4.00E13	0.00	40000	6
86. C2HCl + C2HCl = C4H2Cl2(L	3.00E13	0.00	35000	6
87. C*CC#C + Cl = C.*CC#C + HCl	2.50E13	0.00	10000	3
88. C*CC#C + Cl = C*C.C#C + HCl	2.50E13	0.00	8000	3
89. C4H2Cl2(l + Cl = C4HCl2(N1 + HCl	2.50E13	0.00	7500	3
90. ClC*CC#C + Cl = C4H2Cl(N2 + HCl	2.50E13	0.00	7500	3
91. ClC*CC#C + Cl = C4H2Cl(I1 + HCl	2.50E13	0.00	2000	3
92. C*C.C#C = C.*CC#C	6.41E09	1.00	42300	4
93. C4H2Cl(I1 = C4H2Cl(N1	6.41E09	1.00	42300	4
94. C4HCl2(N1 = C4HCl(L + Cl	4.06E14	0.00	31100	7
95. C4H2Cl(N2 = C4HCl(L + H	1.02E13	0.00	54000	8
96. C4H2Cl(I1 = C#CC#C + Cl	6.31E13	0.00	29600	7
97. C4H2Cl(N1 = C#CC#C + Cl	1.80E14	0.00	23800	7
98. C.*CC#C = C#CC#C + H	1.04E12	0.00	38130	8
99. C*C.C#C = C#CC#C + H	1.00E12	0.00	40000	8
100. C4H3Cl2(I1 = ClC*CC#C + Cl	5.96E14	0.00	22540	7
101. C4H2Cl3(I1 = C4H2Cl2(L + Cl	1.51E14	0.00	29000	7
102. C4HCl4(I1 = C4HCl3(L + Cl	6.09E14	0.00	24350	7
103. C4H4Cl2(L1 + Cl = C4H3Cl2(N2 + HCl	5.00E13	0.00	4500	2
104. C4H3Cl3(L1 + Cl = C4H2Cl3(N2 + HCl	5.00E13	0.00	7500	2
105. C4H3Cl3(L1 + Cl = C4H2Cl3(N3 + HCl	5.00E13	0.00	7500	2
106. C4H3Cl3(L1 + Cl = C4H2Cl3(I1 + HCl	2.50E13	0.00	2000	3
107. C4H2Cl4(L3 + Cl = C4HCl4(I1 + HCl	2.50E13	0.00	13000	3
108. C4H2Cl3(I1 = C4H2Cl3(N3	6.41E09	1.00	44500	4
109. C4HCl4(I1 = C4HCl4(N1	6.41E09	1.00	41000	4
110. C2HCl3 + Cl = CHClCCl + Cl2	1.00E14	0.00	33000	9
111. C2Cl4 + Cl = C2Cl3 + Cl2	1.00E14	0.00	37000	9

Table F2 (cont'd)

Reactions	A^a	n	E_a^b	source
112. C2Cl4 = C2Cl3 + Cl	1.00E15	0.00	81500	10
113. C2Cl3 + C2HCl3 = C4HCl6(N	6.00E11	0.00	4000	9
114. C2Cl3 + C2Cl2 = C4Cl5(N	5.00E11	0.00	7000	9
115. C2Cl3 + C2Cl4 = C4Cl7(N	5.00E11	0.00	7000	9
116. C2Cl3 + C2Cl3 = C4Cl6	6.12E13	-0.50	0	9
117. C2Cl2 + C2Cl2 = C4Cl4	2.00E13	0.00	30000	9
118. C4Cl4 + Cl = C4Cl3(I1 + Cl2	1.00E14	0.00	28000	9
119. C4Cl4 + Cl = C4Cl3(N + Cl2	1.00E14	0.00	30000	9
120. C4Cl3(I1 = C4Cl2 + Cl	2.50E13	0.00	35000	9
121. C4Cl3(N = C4Cl2 + Cl	2.50E13	0.00	33000	9
122. C4Cl4 = C4Cl3(I1 + Cl	1.00E16	0.00	82000	9
123. C4Cl4 = C4Cl3(N + Cl	1.00E16	0.00	84000	9
124. C4HCl5 = C4HCl4(N1 + Cl	1.00E16	0.00	82000	9
125. C4HCl5 = C4HCl4(I + Cl	1.00E16	0.00	80000	9
126. C4HCl5 + Cl = C4HCl4(N1 + Cl2	1.00E14	0.00	29000	9
127. C4HCl5 + Cl = C4HCl4(I + Cl2	1.00E14	0.00	27000	9
128. C4Cl5(N = C4Cl4 + Cl	1.75E13	0.00	36000	9
129. C4Cl5(I1 = C4Cl4 + Cl	1.75E13	0.00	38000	9
130. C4HCl5 + Cl = C4Cl5(I1 + HCl	1.70E13	0.00	4000	9
131. C4Cl6 = C4Cl5(N + Cl	1.20E16	0.00	80000	9
132. C4Cl6 = C4Cl5(I1 + Cl	1.20E16	0.00	78000	9
133. C4Cl6 + Cl = C4Cl5(N + Cl2	1.00E14	0.00	26000	9
134. C4Cl6 + Cl = C4Cl5(I1 + Cl2	1.00E14	0.00	24000	9
135. C4HCl6(N = C4HCl5 + Cl	2.50E13	0.00	16000	9
C6 Reaction				
136. C*CC*C. + C2H2 = C6H6 + H	3.65E13	-0.63	4550	1
137. C*CC*C. + C2HCl = CYC6H5Cl + H	4.02E12	-0.42	4400	1
138. C4H4Cl(N1 + C2H2 = C6H6 + Cl	2.41E13	-0.57	4460	1

Table F2 (cont'd)

Reactions	A[a]	n	E_a[b]	source
139. C4H4Cl(N2 + C2H2 = CYC6H5Cl + H	1.12E14	-0.77	4870	1
140. C4H4Cl(N3 + C2H2 = CYC6H5Cl + H	4.21E13	-0.65	4580	1
141. C4H4Cl(N4 + C2H2 = CYC6H5Cl + H	1.35E14	-0.80	4740	1
142. C4H4Cl(N1 + C2HCl = CYC6H5Cl + Cl	2.20E12	-0.35	4190	1
143. C4H4Cl(N2 + C2HCl = C6H4Cl2(Y2 + H	1.28E13	-0.56	4730	1
144. C4H4Cl(N3 + C2HCl = C6H4Cl2(Y1 + H	2.36E13	-0.64	4900	1
145. C4H4Cl(N4 + C2HCl = C6H4Cl2(Y2 + H	1.30E13	-0.57	4680	1
146. C4H3Cl2(N1 + C2H2 = CYC6H5Cl + Cl	6.15E13	-0.70	4600	1
147. C4H3Cl2(N4 + C2H2 = C6H4Cl2(Y3 + H	1.68E14	-0.83	4880	1
148. C4H3Cl2(N5 + C2H2 = C6H4Cl2(Y2 + H	2.21E14	-0.86	4890	1
149. C4H3Cl2(N3 + C2H2 = CYC6H5Cl + Cl	6.15E13	-0.70	4600	1
150. C4H3Cl2(N2 + C2H2 = CYC6H5Cl + Cl	6.09E13	-0.70	4600	1
151. C4H3Cl2(N1 + C2HCl = C6H4Cl2(Y1 + Cl	2.11E12	-0.34	4200	1
152. C4H3Cl2(N4 + C2HCl = OPClBZ + H	1.37E14	-0.85	5460	1
153. C4H3Cl2(N5 + C2HCl = DMClBZ + H	7.71E14	-1.06	5970	1
154. C4H3Cl2(N3 + C2HCl = C6H4Cl2(Y2 + Cl	3.49E12	-0.41	4270	1
155. C4H3Cl2(N2 + C2HCl = C6H4Cl2(Y2 + Cl	3.63E12	-0.41	4290	1
156. C4H2Cl3(N1 + C2H2 = C6H4Cl2(Y3 + Cl	1.11E13	-0.47	4380	1
157. C4H2Cl3(N2 + C2H2 = C6H4Cl2(Y3 + Cl	2.98E13	-0.60	4500	1
158. C4H2Cl3(N1 + C2HCl = DMClBZ + Cl	1.01E12	-0.25	4090	1
159. C4H2Cl3(N2 + C2HCl = DMClBZ + Cl	1.68E12	-0.32	4160	1
160. C4HCl4(N1 + C2H2 = OMClBZ + Cl	4.12E16	-1.58	5500	1
161. C4HCl4(N1 + C2HCl = OMPClBZ + Cl	2.79E12	-0.39	4180	1
162. C.*CC#C + C2H2 = PHENYL	2.74E40	-8.91	14674	1
163. C.*CC#C + C2HCl = C6H4Cl(Y1	1.72E41	-9.26	14770	1
164. C4H2Cl(N2 + C2H2 = C6H4Cl(Y1	3.60E39	-8.64	14483	1
165. C4H2Cl(N2 + C2HCl = C6H3Cl2(Y1	7.65E41	-9.47	15070	1
166. C4H2Cl(N1 + C2H2 = C6H4Cl(Y2	2.84E54	-13.72	17647	1

Table F2 (cont'd)

Reactions	A[a]	n	E_a[b]	source
167. C4H2Cl(N1 + C2HCl = C6H3Cl2(Y2	3.33E45	-11.37	13587	1
168. C4HCl2(N1 + C2H2 = C6H3Cl2(Y3	3.41E51	-12.88	16593	1
169. C4HCl2(N1 + C2HCl = C6H2Cl3(Y	2.10E45	-10.96	14662	1
170. PHENYL + Cl = CYC6H5Cl	9.00E12	0.00	0	11
171. C6H4Cl(Y1 + Cl = C6H4Cl2(Y2	9.00E12	0.00	0	11
172. C6H4Cl(Y2 + Cl = C6H4Cl2(Y3	9.00E12	0.00	0	11
173. C6H3Cl2(Y1 + Cl = DMClBZ	9.00E12	0.00	0	11
174. C6H3Cl2(Y2 + Cl = OPClBZ	9.00E12	0.00	0	11
175. C6H3Cl2(Y3 + Cl = OMClBZ	9.00E12	0.00	0	11
176. C6H2Cl3(Y + Cl = OMPClBZ	9.00E12	0.00	0	11
177. C4Cl3(I1 + C2Cl2 = C6Cl5(L	4.30E12	0.00	30000	9
178. C4Cl5(I1 + C2Cl2 = C6Cl7(L	3.20E12	0.00	30000	9
179. C4Cl3(N + C2Cl2 = C6Cl5(L	4.30E12	0.00	6000	9
180. C4Cl5(N + C2Cl2 = C6Cl7(L	3.20E12	0.00	6000	9
181. C6Cl5(L = C6Cl5(Y	1.00E10	0.00	0	9
182. C6Cl7(L = C6Cl6(Y + Cl	1.00E10	0.00	0	9
183. C6Cl5(Y + Cl = C6Cl6(Y	7.20E14	-0.50	0	9
184. C6Cl6(Y + Cl = C6Cl5(Y + Cl2	1.00E14	0.00	38000	9
185. C6Cl5(L + Cl = C6Cl6(L	7.20E14	-0.50	0	9
186. C6Cl6(L = C6Cl6(Y	1.00E10	0.00	0	9

a : Unit of A factor, $cm^3\ mol^{-1}\ s^{-1}$
b : Unit of E_a , cal/mol

SOURCES of Reaction Mechanism

1. Apparent rate constant by CHEMACT computer code analysis.
2. A taken as that of $C_2H_3Cl + Cl \rightarrow CHCHCl + HCl$, A=5.00E13, Ea = ΔH + (2.0±0.5), (Ref: Monion, J. A.; Louw, R. *J. Chem. Perk. Trans. 2*, **1988**, 1547.)
3. A taken as that of $C_2H_3Cl + Cl \rightarrow CH_2CCl + HCl$, A=2.50E13, Ea = ΔH + (2.0±0.5), (Ref: source 2).
4. Transition State Theory: loss of no rotor, $\Delta S^{\ddagger} = -4.3$, $A = 10^{(10.75 + (-4.3/4.56))}$, n = 1.0 Ea = 27.7(RS) + 2.2(ΔH_{rxn}) + 12.0(E_{abs}).
5. Kiefer, J. H.; Mitchell, K. I.; Kern, R. D.; Yong, J. N. *J. Phys. Chem.* **1988**, 92, 677.

6. Estimated from: $C_2H_2 + C_2H_2 \rightarrow$ C*CC#C, (Ref: source 5) and $C_2Cl_2 + C_2Cl_2 \rightarrow C_4Cl_4$, (Ref: source 9).
7. Reverse reaction taken 1/3 as that of Cl + C_2H_2, A=1/3(1.39E14), Ea=0.5, and <MR>. (Ref: Baulch, D. L.; Cobos, C. J.; Cox, R. A.; Esser, C.; Frank, P.; Just, Th.; Kerr, J. A.; Pilling, M. J.; Troe, J; Walker, R. W.; Warnatz, J. *J. Phys. Chem. Ref. Data* **1992**, 21, 665).
8. Reverse reaction taken 1/3 as that of H + C_2H_2, A=1/3(8.4E12), Ea=2.50, and <MR>. (Ref: source 7).
9. Taylor, P. H.; Tirey, D. A.; Rubey, W. A.; Dellinger, B. submitted to *Combust. Sci. and Tech.* **1993**.
10. Won, Y. S.; Bozzelli, J. W. *Combust. Sci. and Tech.* **1992**, 85, 345.
11. Ritter, E. R.; Bozzelli, J. W.; Dean, A. M. *J. Phys. Chem.* **1990**, 94, 2493.

Table F3 Notation of the species
The length of species can't more than 10 characters.
The symbol of species in this study are noted below:
(L : Linear molecule (N : Primary Radical
(I : Secondary Radical (Y : Cyclic compound

C4Cl2	ClC≡C-C≡CCl	C4Cl3(I1	Cl2C=C.-C≡CCl
C4Cl3(N	ClC.=CCl-C≡CCl	C4Cl4	Cl2C=CCl-C≡CCl
C4Cl5(N	Cl2C=CCl-CCl=C.Cl	C4Cl5(I1	Cl2C=C.-CCl=CCl2
C4Cl6	Cl2C=CCl-CCl=CCl2	C4Cl7	Cl2C=CCl-CCl2-C.Cl2
C4HCl(L	ClC≡C-C≡CH	C4HCl2(N1	ClC.=CCl-C≡CH
C4HCl3(L	HClC=CCl-C≡CCl	C4HCl4(I	Cl2C=CH-C.=CCl2
C4HCl4(N1	Cl2C=CH-CCl=C.Cl	C4HCl4(I1	HClC=CCl-C.=CCl2
C4HCl5	Cl2C.-CHCl-CCl=CCl2	C4HCl6(N	ClC=CH-CCl=CCl2
C#CC#C	HC≡C-C≡CH	C4H2Cl(N1	HC.=CCl-C≡CH
C4H2Cl(N2	ClC.=CH-C≡CH	C4H2Cl(I1	HClC=C.-C≡CH
C4H2Cl2(L	HClC=CCl-C≡CH	C4H2Cl2(L2	H2C=CClC≡CCl
C4H2Cl2(L3	ClHC=CHC≡CCl	C4H2Cl3(N1	HClC=CCl-CCl=C.H
C4H2Cl3(N2	HClC=CH-CCl=C.Cl	C4H2Cl3(N3	ClC.=CH-CCl=CHCl
C4H2Cl3(I1	HClC=CCl-C.=CHCl	C4H2Cl4(L1	HClC=CCl-CH=CCl2
C4H2Cl4(L2	Cl2C=CH-CH=CCl2	C4H2Cl4(L3	HClC=CCl-CCl=CHCl
C4H2Cl5(N1	HClC=CCl-CHCl-C.Cl2	C4H2Cl5(N2	Cl2C=CH-CHCl-C.Cl2
C4H2Cl5(N3	HClC=CCl-CCl2-C.HCl	C4H2Cl5(N4	Cl2C=CH-CCl2-C.HCl
C.*CC#C	HC.=CH-C≡CH	C*C.C#C	H2C=C.-C≡CH
ClC*CC#C	HClC=CH-C≡CH	C*CClC#C	H2C=CCl-C≡CH
C*CC#CCl	H2C=CHC≡CCl	C4H3Cl2(N1	HClC=CH-CCl=C.H
C4H3Cl2(N2	HClC=CH-CH=C.Cl	C4H3Cl2(N3	HC.=CH-CCl=CHCl
C4H3Cl2(N4	H2C=CCl-CCl=C.H	C4H3Cl2(N5	H2C=CCl-CH=C.Cl
C4H3Cl2(I1	HClC=CH-C.=CHCl	C4H3Cl2(I2	H2C=CCl-C.=CHCl
C4H3Cl3(L1	HClC=CCl-CH=CHCl	C4H3Cl3(L2	Cl2C=CH-CH=CHCl
C4H3Cl4(N1	HClC=CCl-CHCl-C.HCl	C4H3Cl4(N2	Cl2C=CH-CHCl-C.HCl
C4H3Cl4(N3	HClC=CH-CHCl-C.Cl2	C4H3Cl4(N4	HClC=CH-CCl2-C.HCl
C*CC#C	H2C=CH-C≡CH	C4H4Cl(N1	HClC=CH-CH=C.H
C4H4Cl(N2	H2C=CCl-CH=C.H	C4H4Cl(N3	H2C=CH-CCl=C.H

Table F3 (cont'd)

C4H4Cl(N4	H2C=CH-CH=C.Cl	C4H4Cl(I1	H2C=C.-CCl=CH2
C4H4Cl(I2	H2C=CH-C.=CHCl	C4H4Cl(I3	H2C=C.-CH=CHCl
C4H4Cl2(L1	HClC=CH-CH=CHCl	C4H4Cl2(L2	H2C=CCl-CCl=CH2
C4H4Cl2(L3	H2C=CCl-CH=CHCl	C4H4Cl3(N1	HClC=CH-CHCl-C.HCl
C*CC*C.	H2C=CH-CH=C.H	C*CC.*C	H2C=CH-C.=CH2
C4H5Cl(L1	H2C=CH-CCl=CH2	C4H5Cl(L2	H2C=CH-CH=CHCl
C4H5Cl2(N1	H2C=CCl-CHCl-C.H2	C4H5Cl2(N2	HClC=CH-CHCl-C.H2
C*CC*C	H2C=CH-CH=CH2	C4H6Cl(N1	H2C=CH-CHCl-C.H2
C6HCl3(L1	ClC≡C-CCl=CCl-C≡CH	C6H2Cl2(L1	ClC≡C-CCl=CH-C≡CH
C6H2Cl2(L2	ClC≡C-CH=CCl-C≡CH	C6H2Cl2(L3	HC≡C-CCl=CCl-C≡CH
C6H2Cl3(N1	ClC.=CH-CCl=CCl-C≡CH	C6H2Cl4(L1	HClC=CCl-CCl=CH-C≡CCl
C6H2Cl4(L2	HClC=CH-CCl=CHClC≡CCl	C6H2Cl4(L3	Cl2C=CCl-CCl=CH-C≡CH
C6H3Cl(L1	ClC≡C-CH=CH-C≡CH	C6H3Cl(L2	HC≡C-CH=CCl-C≡CH
C6H3Cl2(N1	ClC.=CH-CCl=CH-C≡CH	C6H3Cl2(N2	ClC.=CH-CH=CCl-C≡CH
C6H3Cl2(N3	HC.=CH-CCl=CCl-C≡CH	C6H3Cl3(L1	HCl=CH-CCl=CH-C≡CCl
C6H3Cl3(L2	H2=CCl-CCl=CH-C≡CCl	C6H3Cl3(L3	H2=CCl-CH=CCl-C≡CCl
C6H3Cl3(L4	HCl=CCl-CH=CH-C≡CCl	C6H3Cl3(L5	HCl=CH-CH=CCl-C≡CCl
C6H3Cl3(L6	HCl=CCl-CCl=CH-C≡CH	C6H3Cl3(L7	HCl=CH-CCl=CCl-C≡CH
C6H3Cl4(N1	HClC=CCl-CCl=CH-CH=C.Cl	C6H3Cl4(N2	HClC=CH-CCl=CCl-CH=C.Cl
C6H3Cl4(N3	Cl_2C=CCl-CCl=CH-CH=C.H	C6H4(L	HC≡C-CH=CH-C≡CH
C6H4Cl(N3	HC.=CH-CH=CCl-C≡CH	C6H4CL2(L1	HClC=CH-CH=CH-C≡CCl
C6H4CL2(L2	H2C=CCl-CH=CH-C≡CCl	C6H4CL2(L3	H2C=CH-CCl=CH-C≡CCl
C6H4CL2(L4	H2C=CH-CH=CCl-C≡CCl	C6H4CL2(L5	HClC=CH-CCl=CH-C≡CH
C6H4CL2(L6	H2C=CCl=CCl=CH-C≡CH	C6H4CL2(L7	H2C=CCl-CH=CCl-C≡CH
C6H4CL2(L8	HClC=CCl-CH=CH-C≡CH	C6H4CL2(L9	HClC=CH-CH=CCl-C≡CH
C6H4Cl3(N1	HClC=CH-CCl=CH-CH=C.Cl	C6H4Cl3(N2	H2C=CCl-CCl=CH-CH=C.Cl
C6H4Cl3(N3	H2C=CCl-CH=CCl-CH=C.Cl	C6H4Cl3(N4	HClC=CCl-CH=CH-CH=C.Cl
C6H4Cl3(N5	HClC=CH-CH=CCl-CH=C.Cl	C6H4Cl3(N6	HClC=CCl-CH=CH-CCl=C.H
C6H4Cl3(N7	H2C=CCl-CH=CCl-CCl=C.H	C6H4Cl3(I1	HClC=CCl-C.=CH-CH=CHCl
C6H4Cl3(I2	H2C=CCl-C.=CCl-CH=CHCl	C6H4Cl3(I3	HClC=CCl-C.=CH-CCl=CH2
C6H4Cl3(I4	H2C=CCl-C.=CCl-CCl=CH2	C6H5(N	HC≡C-CH=CH-CH=C.H

Table F3 (cont'd)

C6H5Cl(L1	H2C=CH-CH=CH-C≡CCl	C6H5Cl(L2	H2C=CCl-CH=CH-C≡CH
C6H5Cl(L3	H2C=CH-CCl=CH-C≡CH	C6H5Cl(L4	HClC=CH-CH=CH-C≡CH
C6H5Cl(L5	H2C=CH-CH=CCl-C≡CH	C6H5Cl2(N1	HClC=CH-CH=CH-CH=C.Cl
C6H5Cl2(N2	H2C=CCl-CH=CH-CH=C.Cl	C6H5Cl2(N3	H2C=CH-CCl=CH-CH=C.Cl
C6H5Cl2(N4	H2C=CH-CH=CCl-CH=C.Cl	C6H5Cl2(N5	HClC=CH-CCl=CH-CH=C.H
C6H5Cl2(N6	H2C=CCl-CCl=CH-CH=C.H	C6H5Cl2(N7	H2C=CCl-CH=CCl-CH=C.H
C6H5Cl2(N8	HClC=CCl-CH=CH-CH=C.H	C6H5Cl2(N9	HClC=CH-CH=CH-CCl=C.H
C6H5Cl2(N0	H2C=CCl-CH=CH-CCl=C.H	C6H5Cl2(NN	H2C=CH-CH=CCl-CCl=C.H
C6H5Cl2(I1	HClC=CCl-C.=CH-CH=CH2	C6H5Cl2(I2	H2C=CCl-C.=CCl-CH=CH2
C6H5Cl2(I3	HClC=CH-C.=CH-CH=CHCl	C6H5Cl2(I4	H2C=CCl-C.=CH-CH=CHCl
C6H5Cl2(I5	H2C=CH-C.=CCl-CH=CHCl	C6H5Cl2(I6	HClC=CH-C.=CH-CCl=CH2
C6H5Cl2(I7	H2C=CCl-C.=CH-CCl=CH2	C6H5Cl2(I8	H2C=CH-C.=CCl-CCl=CH2
C6H5Cl3(L1	HClC=CH-CH=CH-CH=CCl2	C6H6Cl(N1	H2C=CH-CH=CH-CH=C.Cl
C6H6Cl(N2	H2C=CCl-CH=CH-CH=C.H	C6H6Cl(N3	H2C=CH-CCl=CH-CH=C.H
C6H6Cl(N4	HClC=CH-CH=CH-CH=C.H	C6H6Cl(N5	H2C=CH-CH=CCl-CH=C.H
C6H6Cl(N6	H2C=CH-CH=CH-CCl=C.H	C6H6Cl(I1	HClC=CH-C.=CH-CH=CH2
C6H6Cl(I2	H2C=CCl-C.=CH-CH=CH2	C6H6Cl(I3	H2C=CH-C.=CCl-CH=CH2
C6H6Cl(I4	H2C=CH-C.=CH-CH=CHCl	C6H6Cl(I5	H2C=CH-C.=CH-CCl=CH2
C6H7(N1	H2C=CH-CH=CH-CH=C.H		
C6H2Cl2(Y	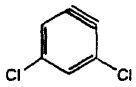	C6H2Cl3(Y	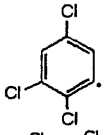
OMPClBZ	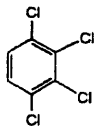	CHD.5Cl	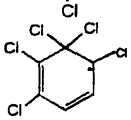
C6H3Cl(Y1		C6H3Cl(Y2	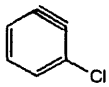
C6H3Cl2(Y1	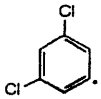	C6H3Cl2(Y2	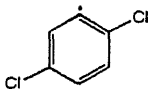
C6H3Cl2(Y3		OPClBZ	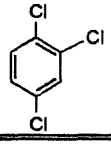

Table F3 (cont'd)

DMClBZ	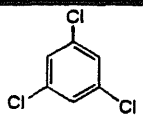	OMClBZ	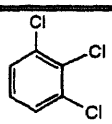
Cl1256CHD.	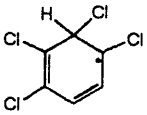	Cl1245CHD.	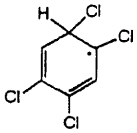
Cl1156CHD.	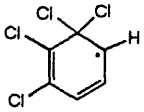	BENZYNE	
C6H4Cl(Y1		C6H4Cl(Y2	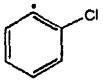
C6H4Cl2(Y1	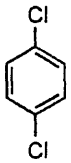	C6H4Cl2(Y2	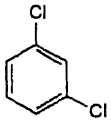
C6H4Cl2(Y3	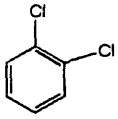	Cl125CHD.	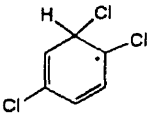
Cl256CHD.	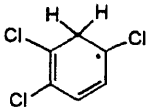	Cl246CHD.	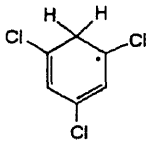
Cl126CHD.	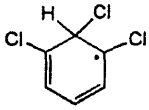	Cl124CHD.	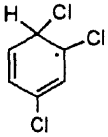
Cl156CHD.	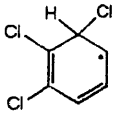	Cl145CHD.	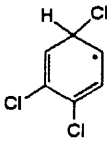
PHENYL		CYC6H5Cl	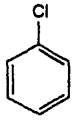
Cl12CHD.	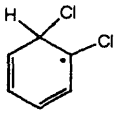	Cl26CHD.	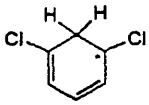
Cl25CHD.	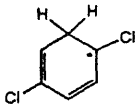	Cl24CHD.	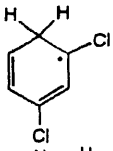
Cl15CHD.	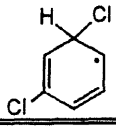	Cl56CHD.	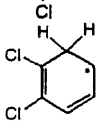

Table F3 (cont'd)

Cl46CHD.	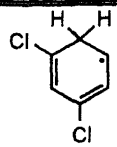	Cl16CHD.	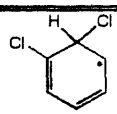
Cl14CHD.	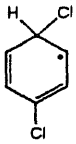	C6H6	
Cl1CHD.	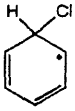	Cl2CHD.	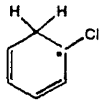
Cl3CHD.	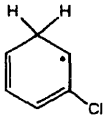	Cl4CHD.	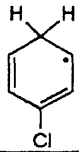

Table F4 QRRK Input Data for $CH_2CCl + C_2HCl \leftrightarrow [C_4H_3Cl_2(N4]^* \rightarrow$ Products

	Reaction	A[a]	n	α	E_a[b]
k_1	$CH_2CCl + C_2HCl \rightarrow C_4H_3Cl_2(N4$[c]	3.15E11	0.0	0.0	5.0
k_{-1}	$C_4H_3Cl_2(N4 \rightarrow CH_2CCl + C_2HCl$	2.40E27	-5.11	-2.157E-3	52.0
k_2	$C_4H_3Cl_2(N4 \rightarrow Cl + C{=}CClC{\equiv}C$[d]	6.14E22	-3.22	-1.46E-3	23.2

a: A's in sec^{-1} and $cm^3\ mol^{-1}\ s^{-1}$
b: Ea in kcal/mol
c: $C_4H_3Cl_2(N4$: $H_2C{=}CCl{-}CCl{=}C.H$
d: $C{=}CClC{\equiv}C$: $H_2C{=}CCl{-}C{\equiv}CH$
<ν> 3 Frequencies: 332.4 1167.9 3994.7
Degeneracy: 11.684 5.797 3.019
L.J. Parameters: σ = 5.327 Å e/k = 456.655 K
$\langle\Delta E\rangle_{avg}$ for Ar = 450 cm^{-1}
β as function of Temperature:

T(K)	300	500	900	1200	1500	1800	2100
β	0.292	0.129	0.028	0.020	0.023	0.030	0.038

k_1 A_1 taken as 1/2 that of $C_2H_3 + C_2H_2$, A = 1/2(6.30E11), Ea = 5.0, Ref: Dean, A.M., *J. Phys. Chem.* **1985**, 89, 4600.

k_{-1} Via k_1 and Microscopic-Reversibility <MR>

k_2 Via k_{-2} and <MR>

k_{-2} A_{-2} taken as 1/3 that of Cl + C≡C, A = 1/3(1.39E14), Ref: Atkinson et al., *J. Phys. Chem. Ref. Data* **1992**, 21, 1125. Ea = 1.0(EST)

<ν> From "CPFIT" Computer (Ref: Ritter, E. R., *J. Chem. Inf. Computat. Sci.*, **1991**, 31, 400) and Cp data for $C_4H_3Cl_2(N4$

σ, e/k Calculated from critical properties for $C_4H_3Cl_2(N4$ (Ref: Reid, R. C.; Prausnitz, J. M.; Sherwood, T. K. *The Properties of Gases and Liquids*, 3rd Ed. McGraw-Hill Co., New York, **1977**).

Table F5 QRRK Input Data for $CH_2CCl + C_2H_3Cl \leftrightarrow [C_4H_5Cl_2(N1]^* \rightarrow$ Products

	Reaction	A[a]	n	α	E_a[b]
k_1	$CH_2CCl + C_2H_3Cl \rightarrow C_4H_5Cl_2(N1$[c]	3.16E11	0.0	0.0	5.0
k_{-1}	$C_4H_5Cl_2(N1 \rightarrow CH_2CCl + C_2H_3Cl$	1.30E19	-2.08	4.867E-4	40.2
k_2	$C_4H_5Cl_2(N1 \rightarrow Cl + C_4H_5Cl(L1$[d]	1.15E12	0.59	1.77E-3	15.4

a: A's in sec^{-1} and $cm^3\ mol^{-1}\ s^{-1}$
b: Ea in kcal/mol
c: $C_4H_5Cl_2(N1$: $H_2C{=}CCl\text{-}CHCl\text{-}C.H_2$
d: $C_4H_5Cl(L1$: $H_2C{=}CH\text{-}CCl{=}CH_2$
<ν> 3 Frequencies: 465.2 1853.7 3979.2
Degeneracy: 13.82 10.548 1.632
L.J. Parameters: σ = 5.507 Å e/k = 448.94 K
$\langle\Delta E\rangle_{avg}$ for Ar = 450 cm^{-1}
β as function of Temperature:

T(K)	300	500	900	1200	1500	1800	2100
β	0.281	0.113	0.027	0.027	0.038	0.050	0.062

k_1 A_1 taken as twice that of $C_2H_3 + C_2H_4$, A = 3.16E11, Ea = 5.0, Ref: Dean, A.M., *J. Phys. Chem.* **1985**, 89, 4600.

k_{-1} Via k_1 and Microscopic-Reversibility <MR>

k_2 Via k_{-2} and <MR>

k_{-2} A_{-2} taken as 1/2 that of Cl + CHClCHCl, A_{-2} = 1/2(5.6E13), Ref: Wallington et al., *J. Atoms. Chem.* **1990**, 19, 1097. Ea = 1.0 (EST)

<ν> From "CPFIT" Computer Code (Ref: Ritter, E. R., *J. Chem. Inf. Computat. Sci.*, **1991**, 31, 400) and Cp data for $C_4H_5Cl_2(N1$

σ, e/k Calculated from critical properties for $C_4H_5Cl_2(N1$ (Ref: Reid, R. C.; Prausnitz, J. M.; Sherwood, T. K. *The Properties of Gases and Liquids*, 3rd Ed. McGraw-Hill Co., New York, **1977**).

Table F6 QRRK Input Data for $C_4H_4Cl(N1 + C_2HCl \leftrightarrow [C_6H_5Cl_2(N1]^* \rightarrow$ Products

	Reaction	A[a]	n	α	E_a[b]
k_1	$C_4H_4Cl(N1^c + C_2HCl \rightarrow C_6H_5Cl_2(N1^d$	1.58E11	0.0	0.0	3.7
k_{-1}	$C_6H_5Cl_2(N1 \rightarrow C_4H_4Cl(N1 + C_2HCl$	2.20E20	-2.24	7.469E-4	51.2
k_2	$C_6H_5Cl_2(N1 \rightarrow C_6H_4Cl_2(L1^e + H$	3.00E12	0.47	1.048E-3	45.4
k_3	$C_6H_5Cl_2(N1 \rightarrow Cl12CHD.^f$	1.70E11	0.0	0.0	12.0
k_{-3}	$Cl12CHD. \rightarrow C_6H_5Cl_2(N1$	4.74E13	0.0	0.0	65.9
k_4	$Cl12CHD. \rightarrow CyC_6H_5Cl^g + Cl$	1.34E15	-0.39	1.657E-3	14.3

a: A's in sec^{-1} and $cm^3\ mol^{-1}\ s^{-1}$
b: Ea in kcal/mol
c: $C_4H_4Cl(N1$: HClC=CH-CH=C.H
d: $C_6H_5Cl_2(N1$: HClC=CH-CH=CH-CH=C.Cl
e: $C_6H_4Cl_2(L1$: HClC=CH-CH=CH-C≡CCl

f: Cl12CHD. : 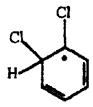
g: CyC_6H_5Cl : 

<ν> 3 Frequencies: 250.5 863.8 2968.2
Degeneracy: 9.363 16.983 5.654
L.J. Parameters: σ = 6.0076 Å e/k = 503.099 K
$\langle\Delta E\rangle_{avg}$ for Ar = 450 cm^{-1}
β as function of Temperature:

T(K)	300	500	900	1200	1500	1800	2100
β	0.249	0.077	0.055	0.093	0.127	0.153	0.167

k_1 A_1 taken as 1/2 that of C=CC=C. + C_2H_2, A = 1/2(3.16E11), Ea = 3.7, Ref: Dean, A.M., *J. Phys. Chem.* **1985**, 89, 4600.

k_{-1} Via k_1 and Microscopic-Reversibility <MR>

k_2 Via k_{-2} and <MR>

k_{-2} A_{-2} taken as that of H + CC≡C, A = 6.30E12, Ea = 3.1, Ref: Dean, A.M., *J. Phys. Chem.* **1985**, 89, 4600.

k_3 A = 1.70E11, Ref: Westmoreland et al., *J. Phys. Chem.* **1989**, 93, 8171.
Ea = 12.0, Ref: Wang, H.; Frenklach, M., *J. Phys. Chem.* **1994**, 98, 11465.

k_{-3} Via k_3 and <MR>

k_4 Via k_{-4} and <MR>

k_{-4} A_{-4} taken as 1/2 that of Cl + C_2H_2, A = 1/2(3.75E13), Ref: Kaiser, E.W., *Intl. J. Chem. Kinet.* **1992**, 64, 2129. Ea = 0.5(EST)

<ν> From "CPFIT" Computer Code Code (Ref: Ritter, E. R., *J. Chem. Inf. Computat. Sci.*, **1991**, 31, 400) and Cp data for $C_6H_5Cl_2(N1$

σ, e/k Calculated from critical properties for $C_6H_5Cl_2(N1$ (Ref: Reid, R. C.; Prausnitz, J. M.; Sherwood, T. K. *The Properties of Gases and Liquids*, 3rd Ed. McGraw-Hill Co., New York, **1977**).

Table F7 QRRK Input Data for $C_4H_2Cl(N2 + C_2HCl \leftrightarrow [C_6H_3Cl_2(N1]^* \rightarrow$ Products

	Reaction	A[a]	n	α	E_a[b]
k_1	$C_4H_2Cl(N2^c + C_2HCl \rightarrow C_6H_3Cl_2(N1^d$	1.58E11	0.0	0.0	3.1
k_{-1}	$C_6H_3Cl_2(N1 \rightarrow C_4H_2Cl(N2 + C_2HCl$	2.27E22	-3.0	-1.785E-4	50.9
k_2	$C_6H_3Cl_2(N1 \rightarrow C_6H_2Cl_2(L1^e + H$	5.94E14	-0.65	1.511E-4	45.3
k_3	$C_6H_3Cl_2(N1 \rightarrow C_6H_3Cl_2(Y1^f$	4.00E10	0.0	0.0	16.0
k_{-3}	$C_6H_3Cl_2(Y1 \rightarrow C_6H_3Cl_2(N1$	7.90E13	0.0	0.0	70.0
k_4	$C_6H_3Cl_2(Y1 \rightarrow C_6H_2Cl_2(Y^g + H$	3.02E13	0.08	1.496E-3	72.9

a: A's in sec^{-1} and $cm^3\ mol^{-1}\ s^{-1}$
b: Ea in kcal/mol
c: $C_4H_2Cl(N2$: HC≡C-CH=C.Cl
d: $C_6H_3Cl_2(N1$: HC≡C-CH=CCl-CH=C.Cl
e: $C_6H_2Cl_2(L1^e$: HC≡C-CH=CCl-C≡CCl

f: $C_6H_3Cl_2(Y1$: 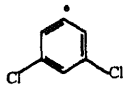
g: $C_6H_2Cl_2(Y$: 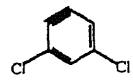

<ν> 3 Frequencies: 304.3 1067.0 3999.9
Degeneracy: 13.102 11.184 1.714
L.J. Parameters: σ = 5.9233 Å e/k = 499.4535 K
$\langle\Delta E\rangle_{avg}$ for Ar = 450 cm^{-1}
β as function of Temperature:

T(K)	300	500	900	1200	1500	1800	2100
β	0.262	0.087	0.039	0.061	0.087	0.109	0.126

k_1 A_1 taken as 1/2 that of C=CC=C. + C_2H_2, A = 1/2(3.16E11), Ref: Dean, A.M., *J. Phys. Chem.* **1985**, 89, 4600. Ea = 3.1, Ref: Wang, H.; Frenklach, M., *J. Phys. Chem.* **1994**, 98, 11465.

k_{-1} Via k_1 and Microscopic-Reversibility <MR>

k_2 Via k_{-2} and <MR>

k_{-2} A_{-2} taken as that of H + CC≡C, A = 6.30E12, Ea = 3.1, Ref: Dean, A.M., *J. Phys. Chem.* **1985**, 89, 4600.

k_3 A = 4.00E10, Ref: Westmoreland et al., *J. Phys. Chem.* **1989**, 93, 8171. Ea = 16.0, Ref: Wang, H.; Frenklach, M., *J. Phys. Chem.* **1994**, 98, 11465.

k_{-3} Via k_3 and <MR>

k_4 Via k_{-4} and <MR>

k_{-4} A_{-4} taken as that of H + CC≡C, A = 6.30E12, Ref: Dean, A.M., *J. Phys. Chem.* **1985**, 89, 4600.

<ν> From "CPFIT" Computer (Ref: Ritter, E. R., *J. Chem. Inf. Computat. Sci.*, **1991**, 31, 400) and Cp data for $C_6H_3Cl_2(N1$

σ, e/k Calculated from critical properties for $C_6H_3Cl_2(N1$ Ref: Reid, R. C.; Prausnitz, J. M.; Sherwood, T. K. *The Properties of Gases and Liquids*, 3rd Ed. McGraw-Hill Co., New York, **1977**).

Table G1 Thermodynamic Properties[a]

species	ΔH_{f298}	S_{298}	C_p 300	C_p400	C_p500	C_p600	C_p800	C_p1000	C_p1500	source
H	52.1	27.36	4.97	4.97	4.97	4.97	4.97	4.97	4.97	186
H_2	0.0	31.21	6.90	6.95	6.99	7.02	7.10	7.21	7.72	186
AR	0.0	36.98	4.97	4.97	4.97	4.97	4.97	4.97	4.97	186
O	59.5	38.47	5.23	5.14	5.08	5.04	5.01	5.01	4.98	186
OH	9.5	43.88	7.15	7.10	7.07	7.06	7.13	7.33	7.87	186
O_2	0.0	49.01	7.02	7.23	7.44	7.65	8.04	8.35	8.73	186
SO	1.5	53.02	7.22	7.55	7.84	8.08	8.43	8.62	8.95	25
SO_2	-71.0	59.30	9.54	10.41	11.12	11.71	12.55	13.03	13.61	25
SO_3	-94.6	61.35	12.17	13.76	15.05	16.07	17.45	18.16	19.02	25
SH	34.0	46.70	7.70	7.60	7.50	7.55	7.60	7.90	8.40	25
HSO	-5.4	57.80	9.02	9.93	10.73	11.36	12.22	12.73	13.34	182,80
HOS	0.0	57.15	8.71	9.42	10.00	10.45	11.08	11.53	12.33	182,80
HSO_2	-13.0	63.68	11.94	13.68	14.99	15.97	17.28	18.05	18.98	161,80
HOSO	-45.0	64.62	11.87	13.43	14.56	15.36	16.4	17.06	18.09	161,80
H_2S	-4.8	49.20	8.20	8.50	8.90	9.50	10.20	10.9	12.30	25
HOSH	-28.5	58.66	10.83	12.22	13.47	14.46	15.82	16.62	17.60	170,80
H_2SO	-11.3	57.26	9.53	11.13	12.66	13.95	15.82	17.00	18.44	170,80
HOSOH	-75.3	64.93	13.92	15.87	17.33	18.4	19.85	20.85	22.57	180,80
HOSHO	-64.5	64.48	13.58	15.84	17.65	19.01	20.82	21.95	23.54	180,80
$HOSO_2$	-93.5	70.72	16.74	18.76	20.13	21.07	22.22	22.94	24.02	187,80

[a] Units: ΔH_f: kcal/mol; S and C_p: cal/mol/K

Table G2 QRRK Input Data for $HSO + O \leftrightarrow [HSO_2]^* \rightarrow$ Products
$H + SO_2 \leftrightarrow [HOSO]^* \rightarrow$ Products
$OH + SO \leftrightarrow [HOSO]^* \rightarrow$ Products

	Reaction	A[a]	n	α	Ea[b]	$\Delta H_{rxn,298}$
k_1	$HSO + O \rightarrow HSO_2$	6.62E13	0.0	0.0	0.0	-67.1
k_{-1}	$HSO_2 \rightarrow HSO + O$	4.65E17	-0.55	0.001006	65.4	
k_2	$HSO_2 \rightarrow H + SO_2$	9.64E12	0.0	0.0	9.5	-6.0
k_3	$HSO_2 \rightarrow HOSO$	9.64E12	1.0	0.0	23.0	-32.0
k_{-3}	$HOSO \rightarrow HSO_2$	6.41E09	1.0	0.0	55.0	
k_4	$HOSO \rightarrow O + HOS$	1.09E18	-0.84	0.0009251	102.6	104.5
k_5	$HOSO \rightarrow OH + SO$	5.29E14	0.13	0.000264	54.0	56.0
k_6	$HOSO \rightarrow H + SO_2$	1.52E12	0.46	0.001291	48.7	26.1

a: A's in s^{-1} and $cm^3\ mol^{-1}\ s^{-1}$ b: Ea in kcal/mol

<ν> 3 Frequencies: 514.4 918.9 1732.2

Degeneracy: 2.199 2.618 1.183

Lennard-Jones Parameters: σ = 4.112 Å; e/k = 335.3 K

$\langle\Delta E\rangle_{avg}$ for Ar = 450 cm^{-1}

β as function of Temperature:

T(K)	300	500	700	900	1200	1500	1800
β	0.309	0.159	0.093	0.065	0.049	0.044	0.043

k_1 A is from evaluated literature rate constants on O atom combination with large radicals. An example is $O + C_2H_5$, A = 6.62E13, Ea = 0.0, (Ref: NIST data base, version 5.0, **1992**)

k_{-1} Via k_1 and Microscopic-Reversibility <MR>

k_2 Via k_{-2} and <MR>, Ea = 9.5, Ref: Binns, D.; Marshall, P. *J. Chem. Phys.* **1991**, 95, 4940.

k_{-2} A is from evaluated literature rate constants on H addition to unsaturated bonds. An example is $H + C_2H_4$, A = 1.32E13, (Ref: NIST data base, version 5.0, **1992**)

k_3 Via k_{-3} and <MR>

k_{-3} TST, $k = AT^n e^{(-Ea/RT)}$, loss of one rotor, $A_{-3} = 10^{10.75} * 10^{(-4.3/4.56)} = 6.41E09$, n =1, Ea = 55.0, Ref: Binns, D.; Marshall, P. *J. Chem. Phys.* **1991**, 95, 4940.

k_4 Via k_{-4} and <MR>

k_{-4} A is from evaluated literature rate constants on O atom combination with large radicals. An example is $O + C_2H_5$, A = 6.62E13, Ea = 0.0, (Ref: NIST data base, version 5.0, **1992**)

k_5 Via k_{-5} and <MR>

Table G2 (cont'd)

k_{-5}	A is from evaluated literature rate constants on OH addition to unsaturated bonds. An example is OH + C_2H_4, A = 2.70E12, Ea = 0.0, (Ref: NIST data base, version 5.0, **1992**)
k_6	Via k_{-6} and <MR>, Ea = 22.7, Ref: Binns, D.; Marshall, P. *J. Chem. Phys.* **1991**, 95, 4940.
k_{-6}	A is from evaluated literature rate constants on H addition to unsaturated bonds. An example is H + C_2H_4, A = 1.32E13, (Ref: NIST data base, version 5.0, **1992**)
<v>	From "CPFIT" Computer Code (Ref: Ritter, E. R., *J. Chem. Inf. Computat. Sci.* **1991**, 31, 400) and C_p data for HSO_2.
σ, e/k	Calculated from critical properties for HSO_2, (Ref: Reid, R. C.; Prusnitz, J. M.; Poling, B. E. *The properties of Gases and Liquids* 3nd ed., McGraw-Hill, Singapore, **1988**.)

Table G3 QRRK Input Data for $OH + SO_2 \leftrightarrow [HOSO_2]^* \rightarrow$ Products
$H + SO_3 \leftrightarrow [HOSO_2]^* \rightarrow$ Products

	Reaction	A^a	n	α	E_a^b	$\Delta H_{rxn,298}$
k_1	$OH + SO_2 \rightarrow HOSO_2$	1.21E12	0.0	0.0	0.0	-32.0
k_{-1}	$HOSO_2 \rightarrow OH + SO_2$	5.75E20	-2.53	0.0007962	28.9	
k_2	$HOSO_2 \rightarrow HOSO + O$	4.30E21	-2.19	-0.0002813	105.8	108.5
k_3	$HOSO_2 \rightarrow H + SO_3$	1.15E17	-1.84	-0.0005279	54.0	51.0

a: A's in s^{-1} and $cm^3\ mol^{-1}\ s^{-1}$
b: E_a in kcal/mol
<ν> 3 Frequencies: 292.0 991.5 4000.0
Degeneracy: 5.921 4.873 1.206
Lennard-Jones Parameters: σ = 4.39 Å; e/k = 384.5 K
$\langle\Delta E\rangle_{avg}$ for Ar = 450 cm^{-1}
β as function of Temperature:

T(K)	300	500	700	900	1200	1500	1800
β	0.314	0.163	0.089	0.05	0.024	0.016	0.0014

k_1 A = 1.21E12, Ea = 0.0, Ref: Atkinson, R., et al., *J. Phys. Chem. Ref. Data*, **1992**, 21, 1125.

k_{-1} Via k_1 and Microscopic-Reversibility <MR>

k_2 Via k_{-2} and <MR>

k_{-2} A is from evaluated literature rate constants (Ref: NIST data base, version 5.0, **1992**) on O atom combination with large radicals. An example is $O + C_3H_7$, A = 9.64E13, Ea = 0.0

k_3 Via k_{-3} and <MR>

k_{-3} A is from evaluated literature rate constants (Ref: NIST data base, version 5.0, **1992**) on H addition to unsaturated bonds. An example is $H + C_2H_4$, A = 3.0E13, Ea taken as that of $H + SO_2$, Ea = 3.0, Ref: Schofield et al., *J. Phys. Chem. Ref. Data*, **2**, 25, (1973).

<ν> From "CPFIT" Computer Code (Ref: Ritter, E. R., *J. Chem. Inf. Computat. Sci.* **1991**, 31, 400) and Cp data for $HOSO_2$

σ, e/k Patrick, R.; Golden, D. M. *Intl. J. of Chem. Kinet.* **1983**, 15, 1189.

Table G4 QRRK Input Data for HOSO + H ↔ [HOSHO]* → Products
HSO + OH ↔ [HOSHO]* → Products

	Reaction	A^a	n	α	E_a^b	$\Delta H_{rxn,298}$
k_1	H + HOSO → HOSHO	1.00E14	0.0	0.0	0.0	-71.6
k_{-1}	HOSHO → H + HOSO	1.48E14	0.54	0.001854	70.2	
k_2	HOSHO → OH + HSO	1.75E18	-0.44	0.0024	66.1	68.6
k_3	HOSHO → H_2O + SO	6.41E09	1.0	0.0	55.2	8.2

a: A's in s^{-1} and $cm^3\ mol^{-1}\ s^{-1}$
b: E_a in kcal/mol
<ν> 3 Frequencies: 435.2 1132.7 3770.8
Degeneracy: 3.137 4.804 1.059
Lennard-Jones Parameters : σ = 4.112 Å; e/k = 335.3 K
$\langle\Delta E\rangle_{avg}$ for Ar = 450 cm^{-1}
β as function of Temperature: T(K) : 300 500 700 900 1200 1500 1800
β : 0.332 0.191 0.119 0.078 0.045 0.027 0.0017

k_1 A is from evaluated literature rate constants (Ref: NIST data base, version 5.0, **1992**) on H atom combination with large radicals. An example is H + C_3H_7, A = 1.00E14, Ea = 0.0

k_{-1} Via k_1 and Microscopic-Reversibility <MR>

k_2 Via k_{-2} and <MR>

k_{-2} A is from evaluated literature rate constants (Ref: NIST data base, version 5.0, **1992**) on OH combination with large radicals. An example is OH + C_2H_5, A = 2.7E13, Ea = 0.0

k_3 TST, $k = AT^n e^{(-Ea/RT)}$, loss of one rotor, $A = 10^{10.75} * 10^{-4.3/4.56} = 6.41E09$, Ea = 47 + ΔH, Evaluated H_2O elimination:

- Melius et al., 20th Symposium (International) on Combustion, **1984**.
- Walch, S, P. *J. Chem. Phys.* 1993, **99**, 5295.
  Butkovskaya, N. I.; Zhao, Y.; Setser, D. W. *J. Chem. Phys.* **1994**, 98, 10779.
- and ring strains involving 3rd row (periodic table) elements, Benson, S. W. "Thermochemical Kinetics" John Wiley & sons, Inc., New York, **1976**.

<ν> From "CPFIT" Computer Code (Ref: Ritter, E. R., *J. Chem. Inf. Computat. Sci.* **1991**, 31, 400) and Cp data for HOSHO

σ, e/k Calculated from critical properties for HOSHO (Ref: Reid, R. C.; Prusnitz, J. M.; Poling, B. E. *The properties of Gases and Liquids* 3nd ed., McGraw-Hill, Singapore, **1988**.)

Table G5 Apparent rate constants at temperatures 300 - 2000 K, in N_2 bath gas

Reactions	A[a]	n	E_a(cal/mol)	P(atm)
$HSO + O + M \rightarrow HSO_2 + M$	5.86E+14	-0.28	-1120	low pressure limit
$HSO + O \rightarrow H + SO_2$	4.06E+14	-0.29	170	0.001 - 100
$HSO + O + M \rightarrow HOSO + M$	1.93E+19	-2.10	1310	low pressure limit
$HSO + O \rightarrow O + HOS$	1.16E+09	0.48	5129	0.001 - 100
$HSO + O \rightarrow OH + SO$	2.49E+12	0.21	257	0.001 - 100
$H + SO_2 \rightarrow OH + SO$	3.57E+18	-1.45	6281	0.001 - 100
$OH + SO + M \rightarrow HOSO + M$	1.26E+29	-4.64	2290	low pressure limit
$HOSO + M \rightarrow O + HOS + M$	4.14E+29	-4.80	105220	low pressure limit
$HOSO + M \rightarrow H + SO_2 + M$	8.83E+18	-1.87	40640	low pressure limit
$HSO_2 + M \rightarrow HOSO + M$	5.06E+12	1.07	23300	low pressure limit
$HSO_2 + M \rightarrow H + SO_2 + M$	5.06E+12	0.07	9800	low pressure limit
$OH + SO_2 + M \rightarrow HOSO_2 + M$	1.87E+31	-4.61	2050	low pressure limit
$OH + SO_2 \rightarrow O + HOSO$	3.86E+08	1.89	76000	0.001 - 100
$OH + SO_2 \rightarrow H + SO_3$	4.85E+02	2.69	23840	0.001 - 100
$HOSO_2 + M \rightarrow O + HOSO + M$	2.48E+17	-0.33	105250	low pressure limit
$HOSO_2 + M \rightarrow H + SO_3 + M$	3.20E+16	-0.81	53730	low pressure limit
$H + SO_3 \rightarrow O + HOSO$	2.53E05	2.92	50280	0.001 - 100
$HSO + OH + M \rightarrow HOSHO + M$	7.16E+31	-4.82	3260	low pressure limit
$HSO + OH \rightarrow H + HOSO$	5.31E+07	1.57	3750	0.001 - 100
$HSO + OH \rightarrow H_2O + SO$	1.66E+09	1.03	474	0.001 - 100
$HOSHO + M \rightarrow H + HOSO + M$	3.91E+34	-5.47	74420	low pressure limit
$HOSHO + M \rightarrow H_2O + SO + M$	3.72E+42	-7.64	59960	low pressure limit
$H + HOSO \rightarrow H_2O + SO$	1.06E+05	2.41	-675	0.001 - 100

a : Unit $cm^3\ mol^{-1}\ s^{-1}$ for bimolecular reaction
$cm^6\ mol^{-2}\ s^{-1}$ for tert-molecular reaction

APPENDIX II

FIGURES

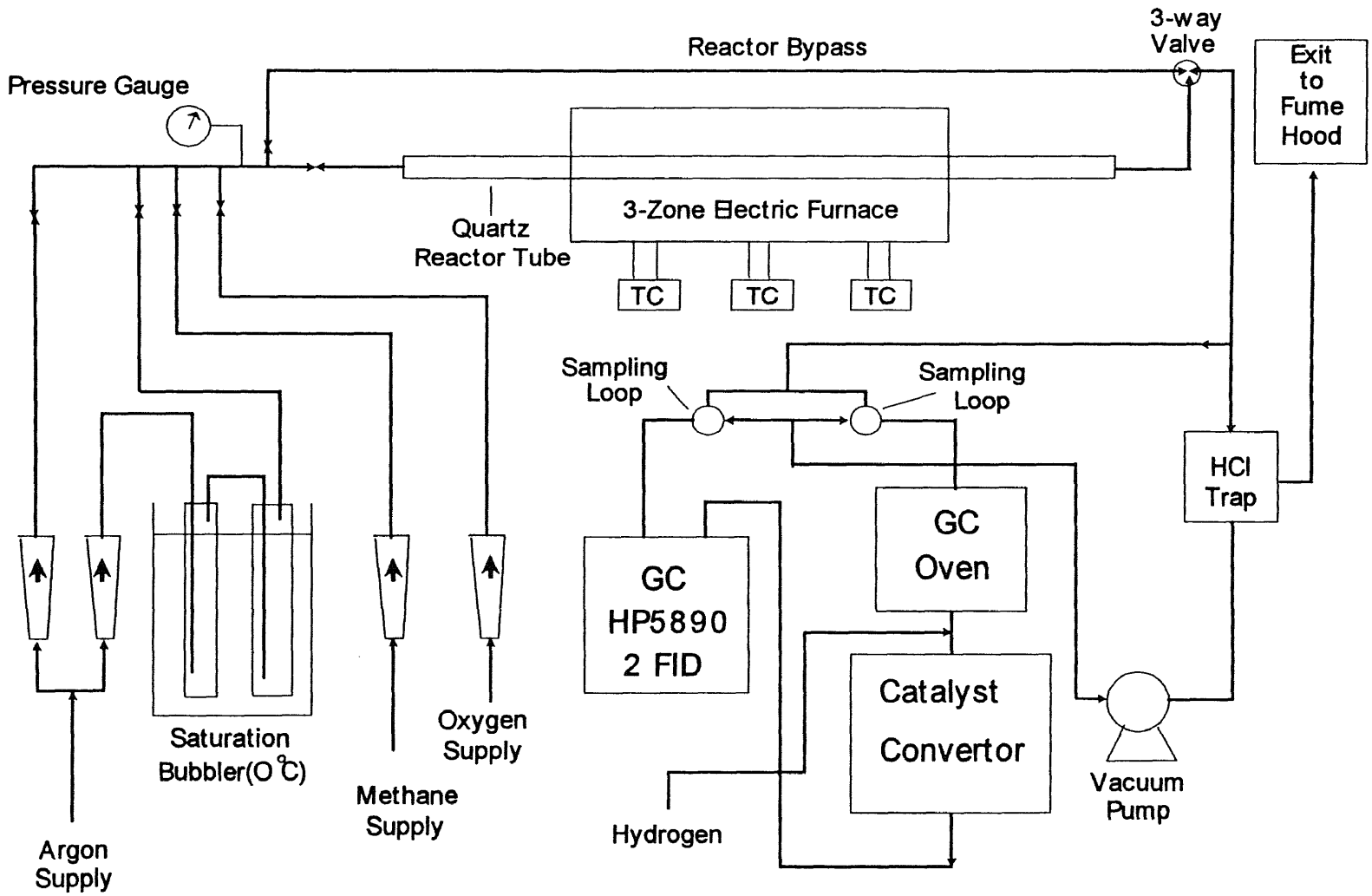

Figure A1 Experimental Apparatus

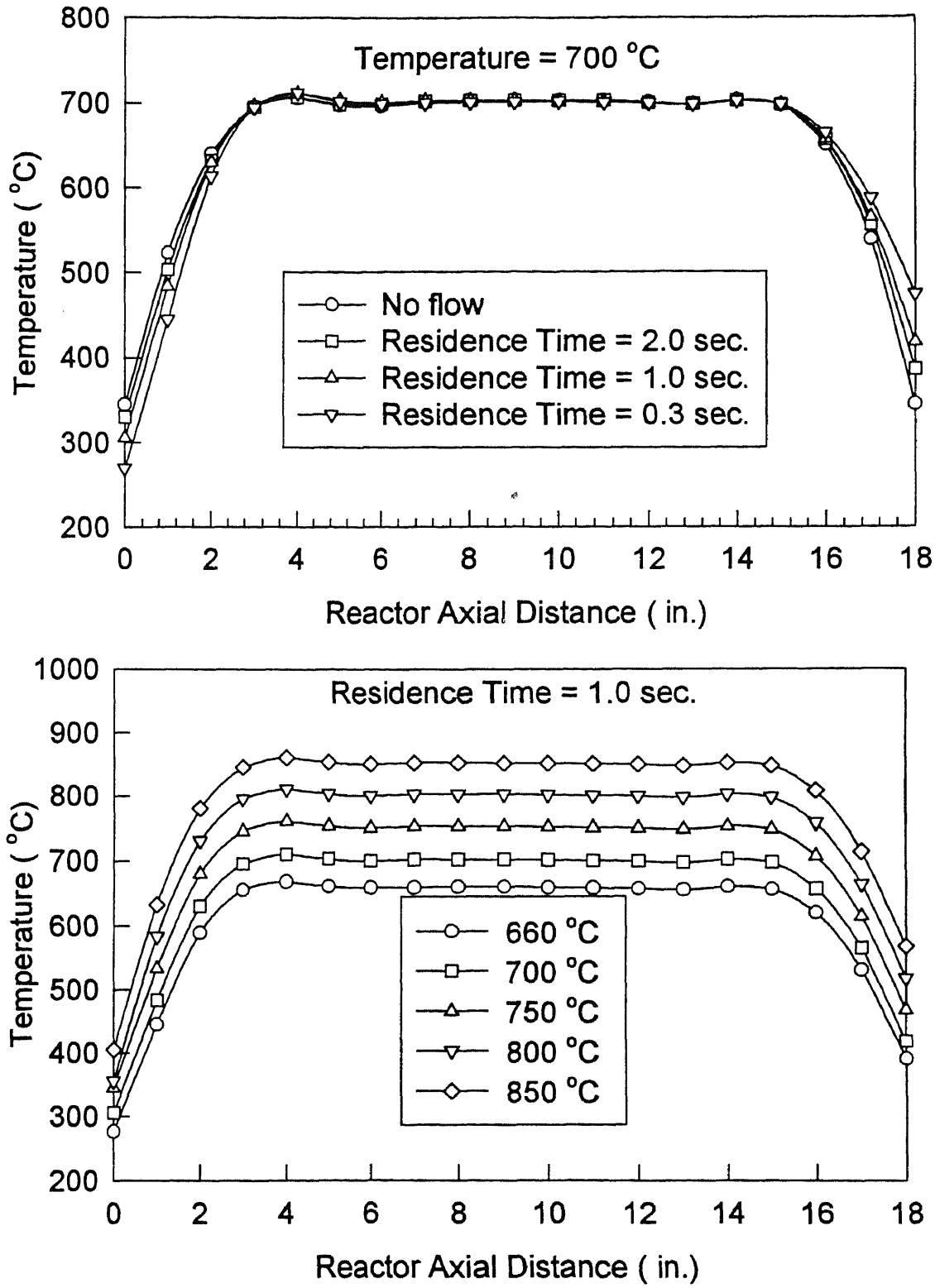

Figure A2 Reactor Temperature Profiles with Tight Control

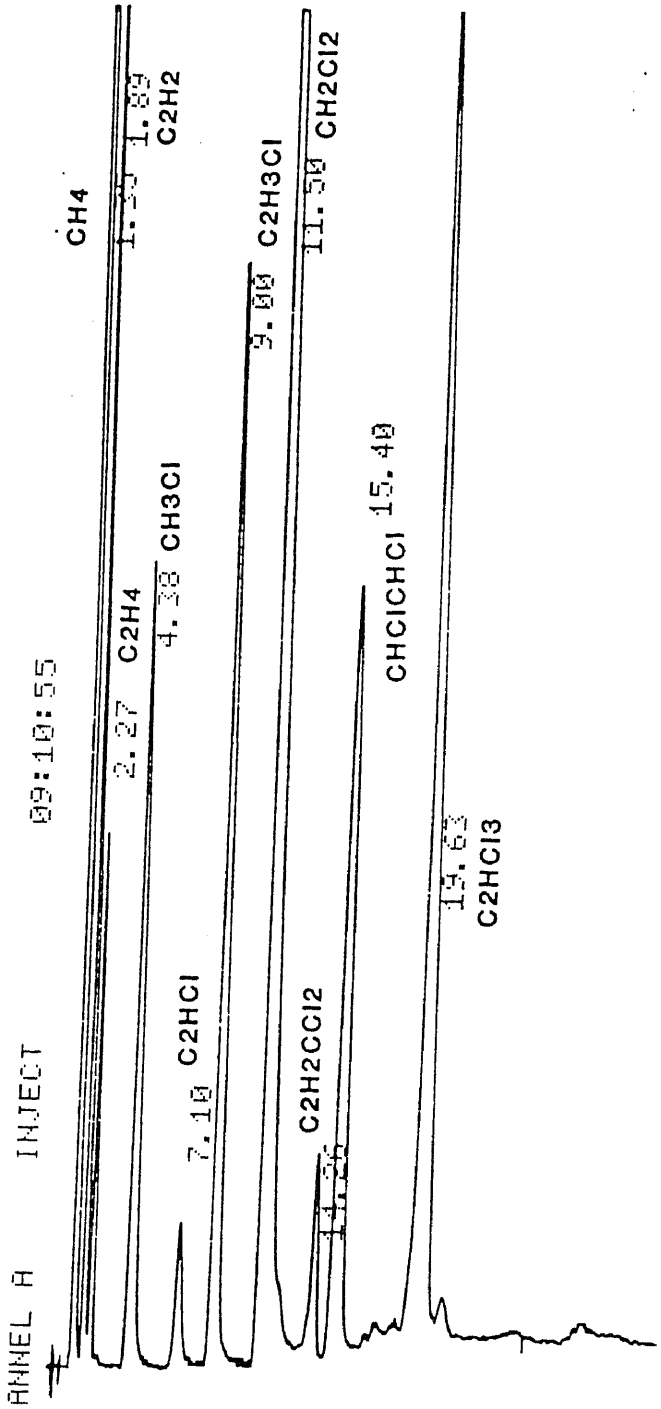

Figure A3 Sample Chromatogram $CH_2Cl_2/CH_4/O_2/Ar$ Reaction
Column : 1.5 m length x 2.16 mm I.D.; 1% AT-1000 on Graphpac GB
Detector : Flame Ionization Detector (270 °C)
Oven Temperature : 45 °C (hold 5 min.), 15 °C/min. to 220 °C (hold 22 min.)
Carrier Gas : Helium (35 ml/min.)
Reaction Conditions : 1 second residence, 780 °C

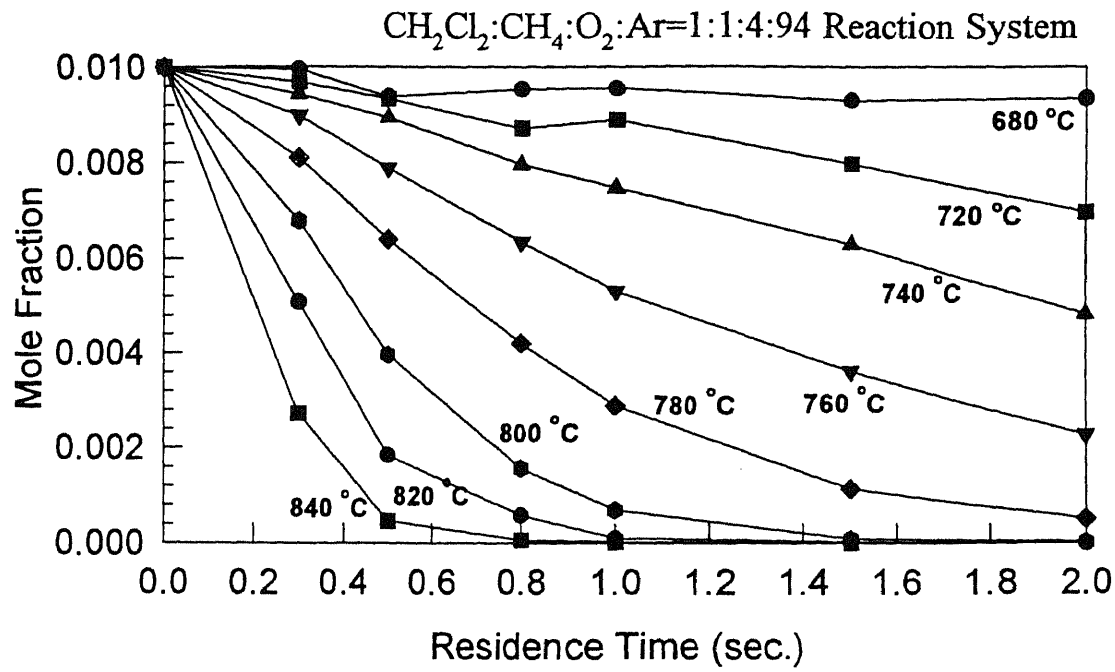

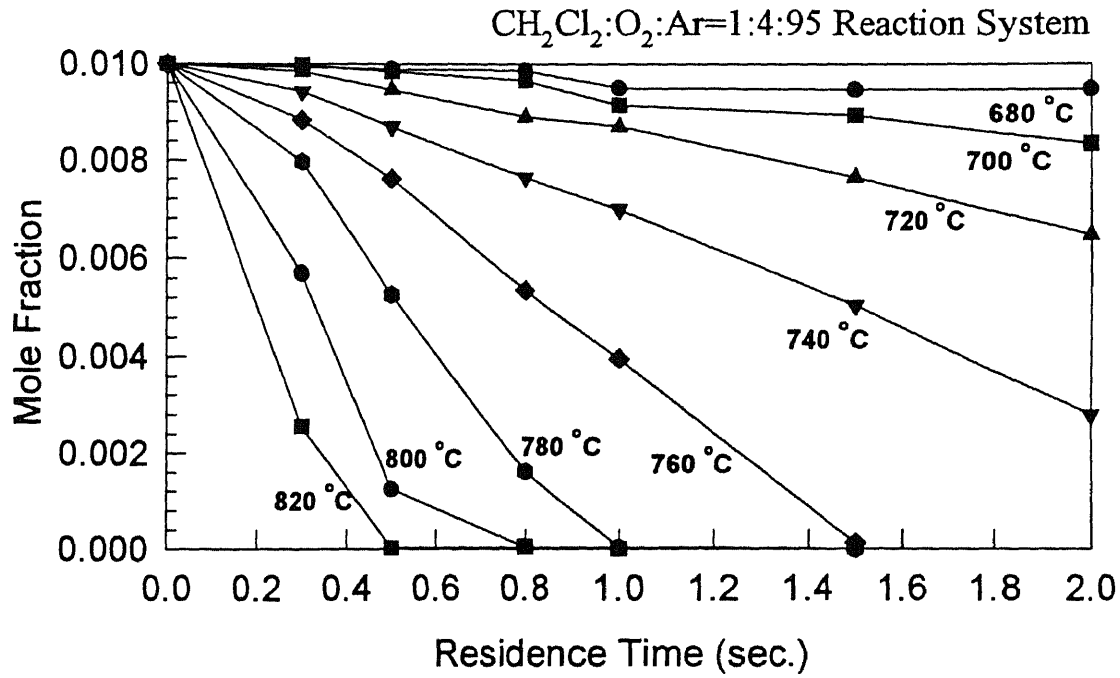

Figure A4 Experimental Results Decay of CH_2Cl_2 vs. Time/Temperature

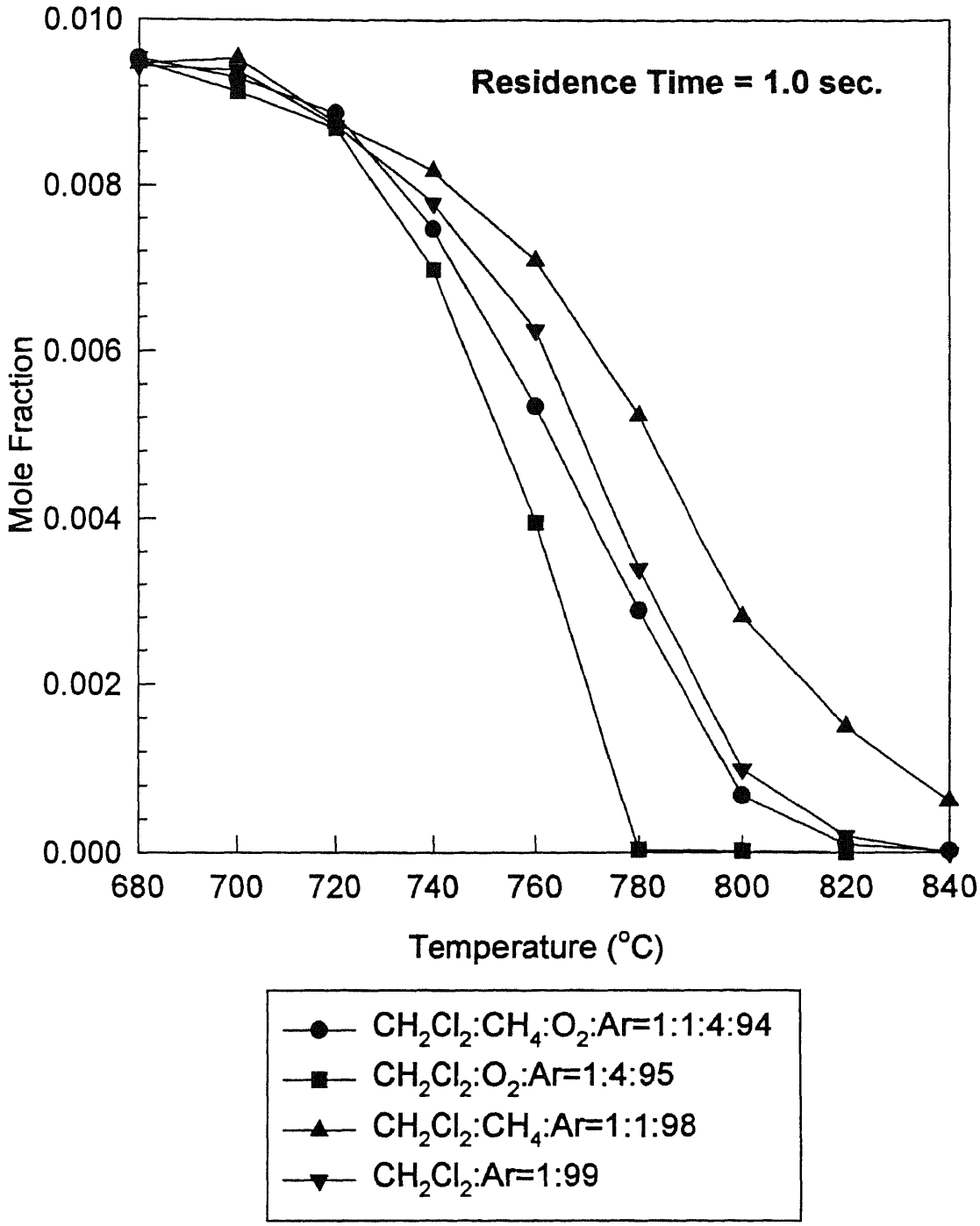

Figure A5 Decay of CH_2Cl_2 vs Temperature in different Reaction Environments

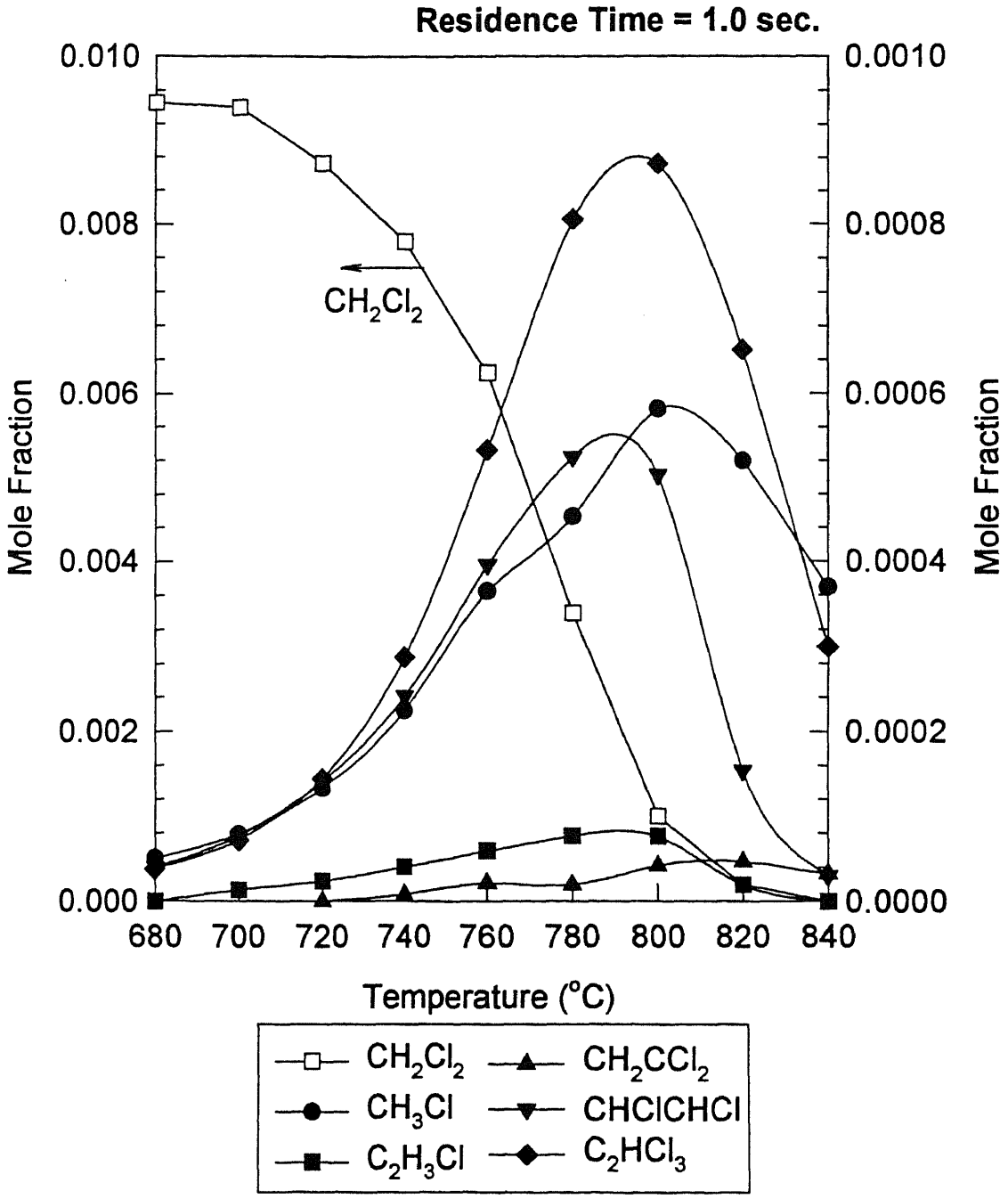

Figure A6a Product Distribution vs Temperature in CH_2Cl_2:Ar=1:99 Reaction System

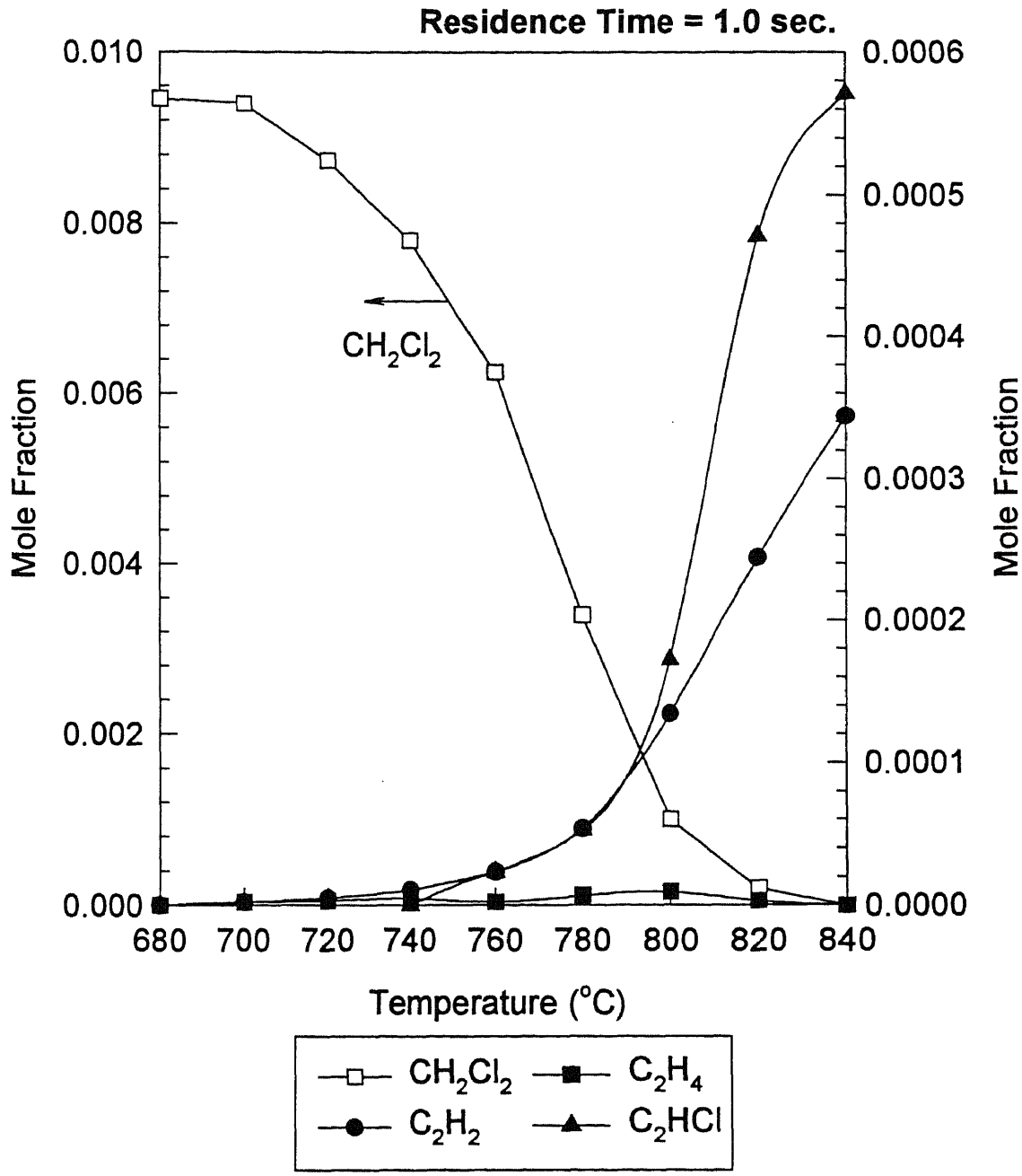

Figure A6b Product Distribution vs Temperature in CH_2Cl_2:Ar = 1:99 Reaction System

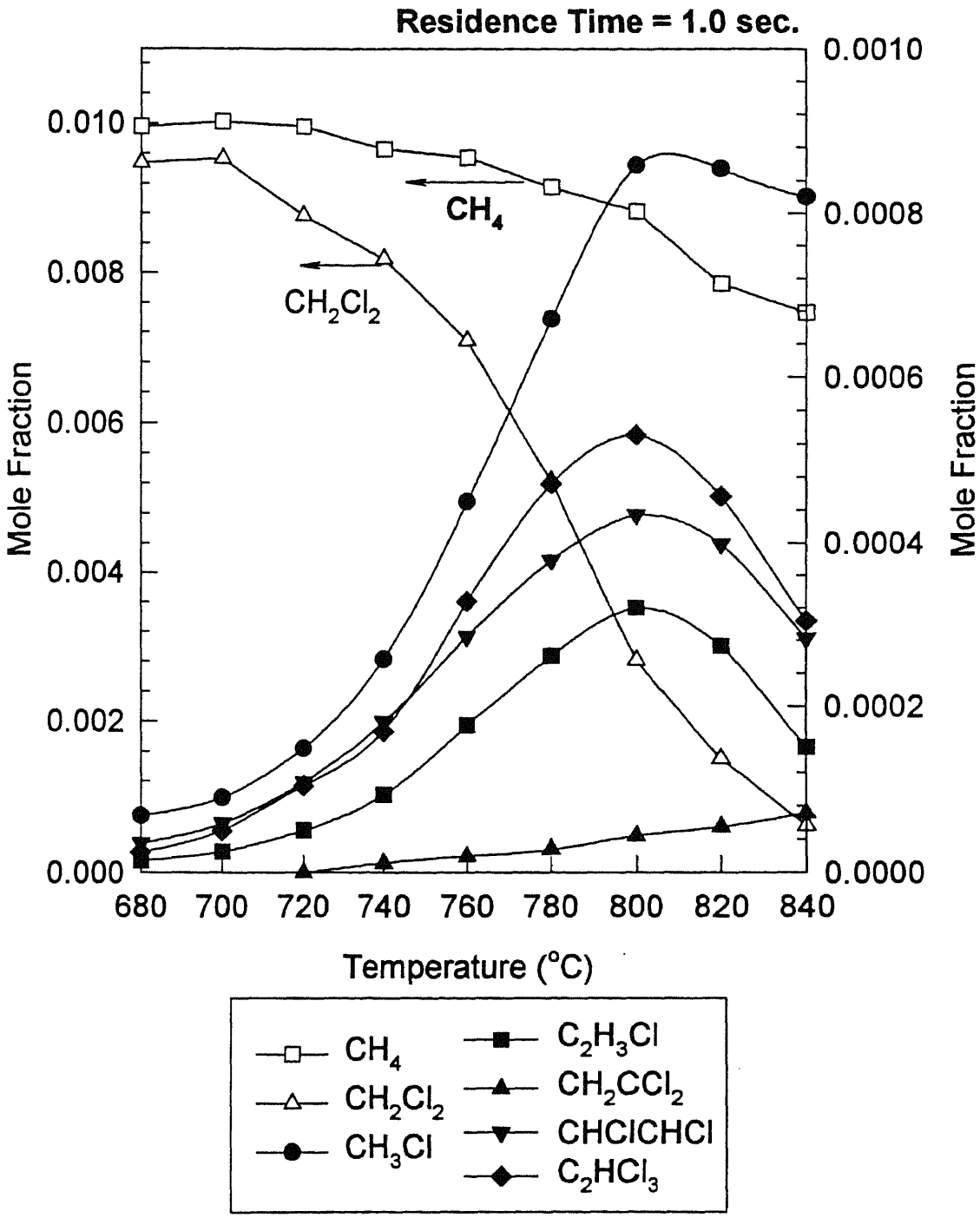

Figure A7a Product Distribution vs Temperature in CH_2Cl_2:CH_4:Ar=1:1:98 Reaction System

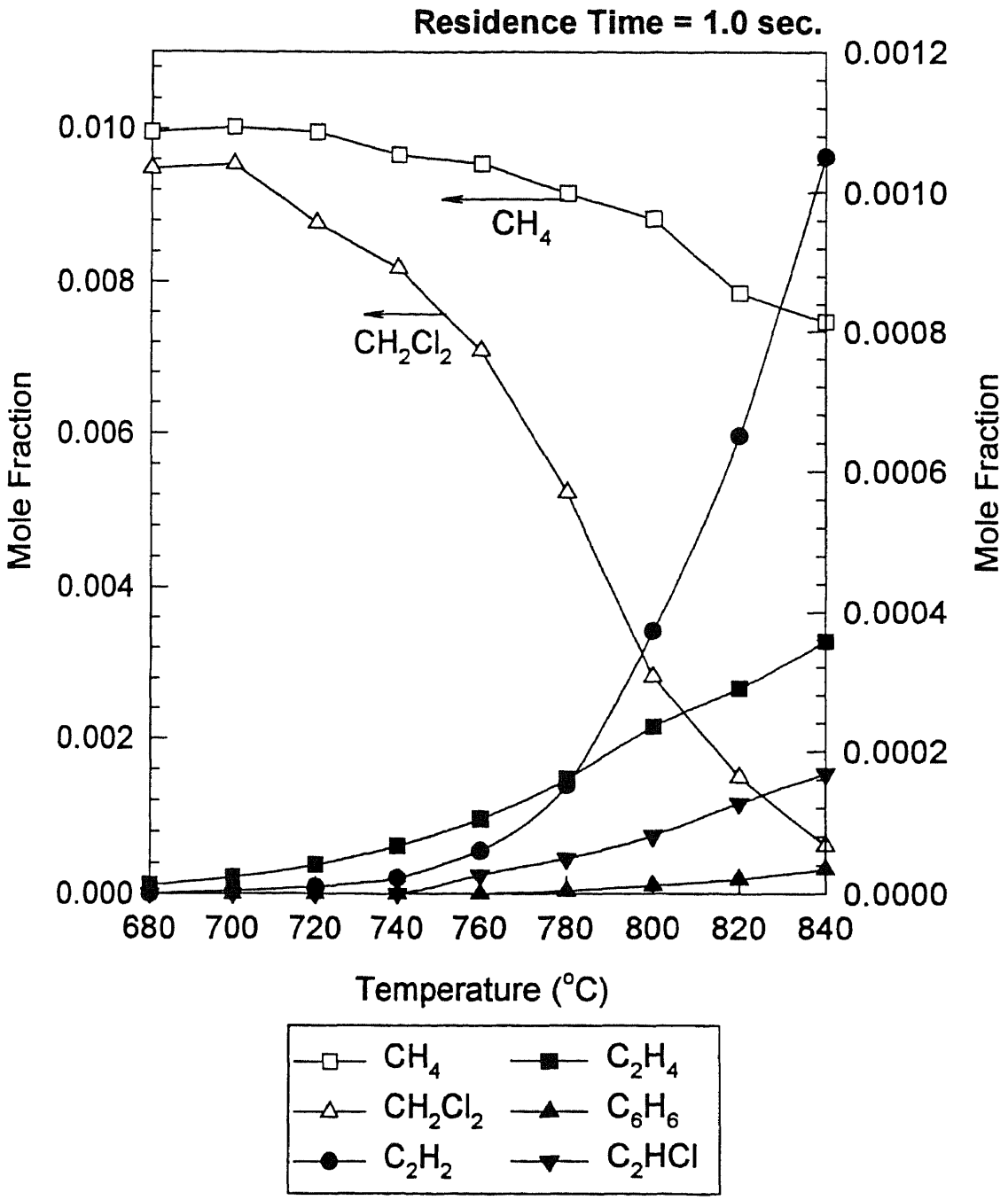

Figure A7b Product Distribution vs Temperature in CH_2Cl_2:CH_4:Ar=1:1:98 Reaction System

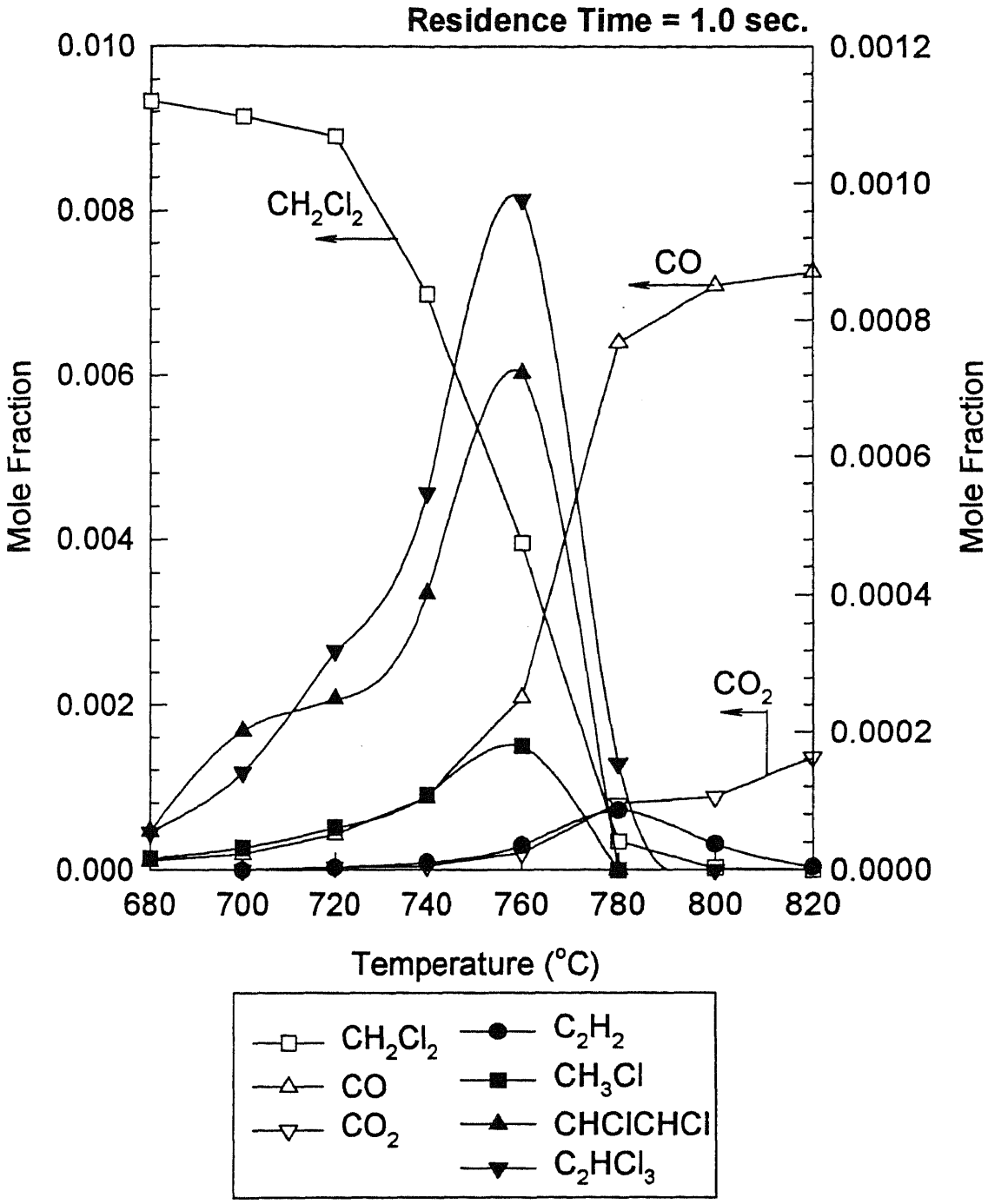

Figure A8 Product Distribution vs Temperature in CH_2Cl_2:O_2:Ar=1:4:95 Reaction System

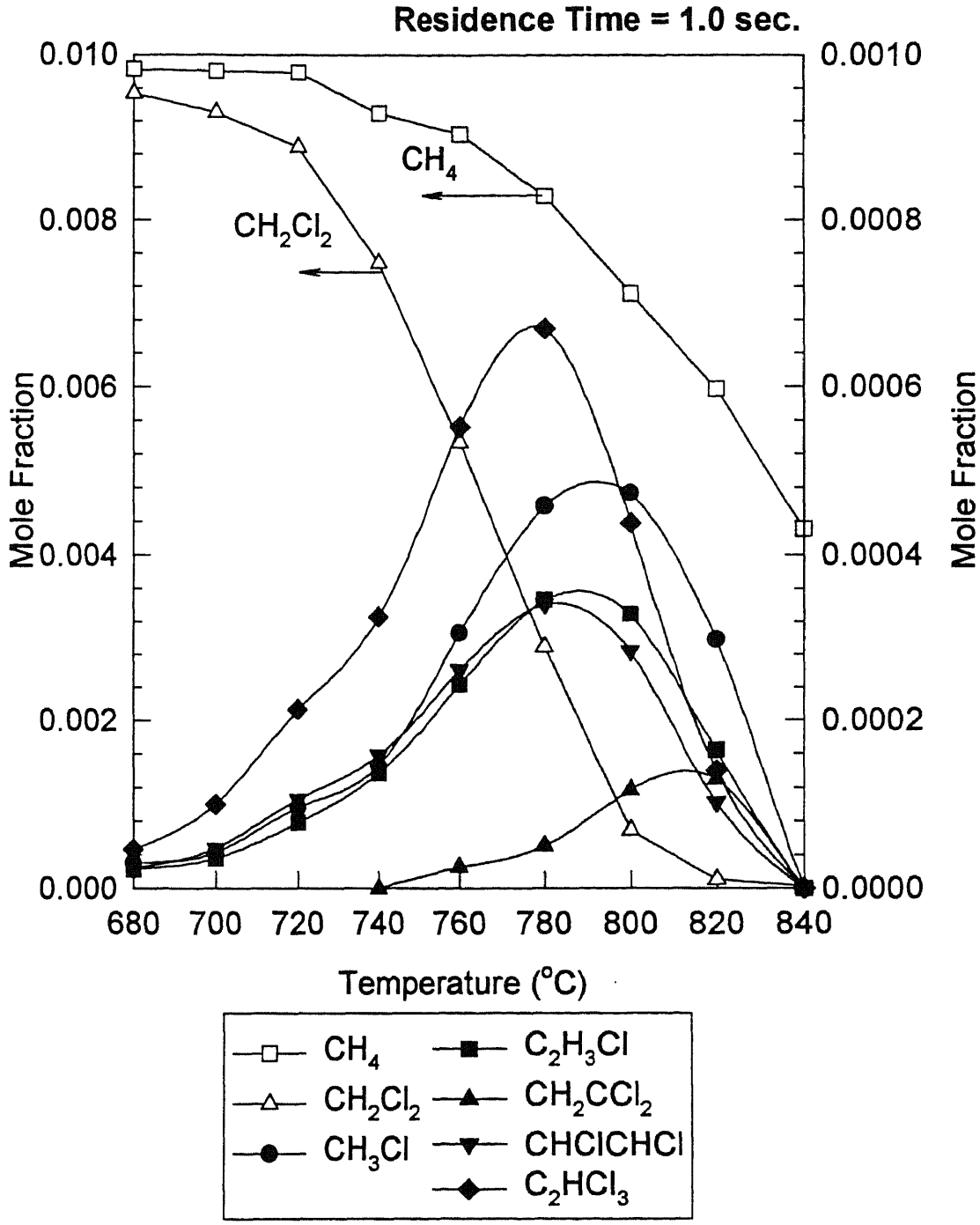

Figure A9a Product Distribution vs Temperature in CH_2Cl_2:CH_4:O_2:Ar=1:1:4:94 Reaction System

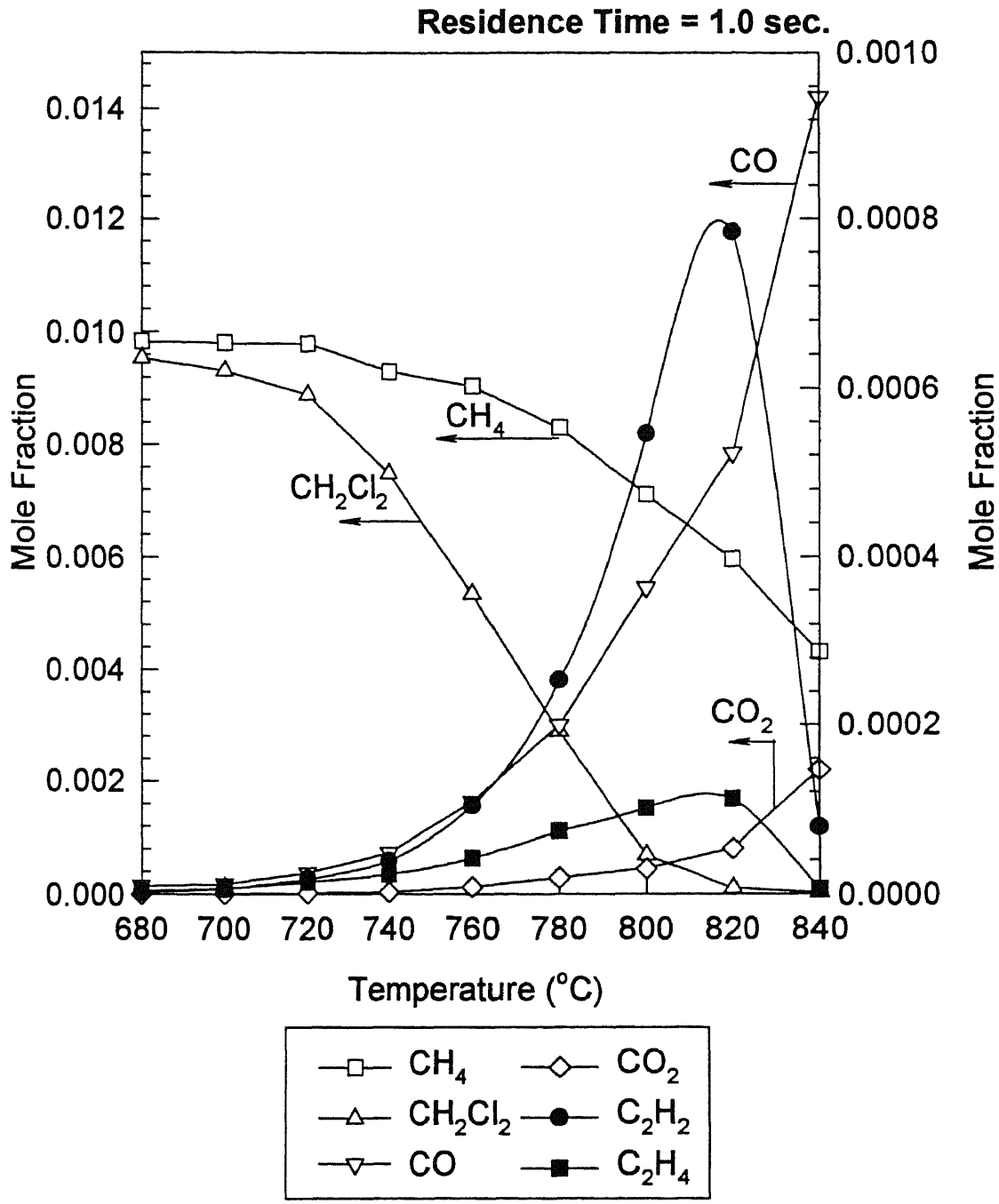

Figure A9b Product Distribution vs Temperature in CH_2Cl_2:CH_4:O_2:Ar=1:1:4:94 Reaction System

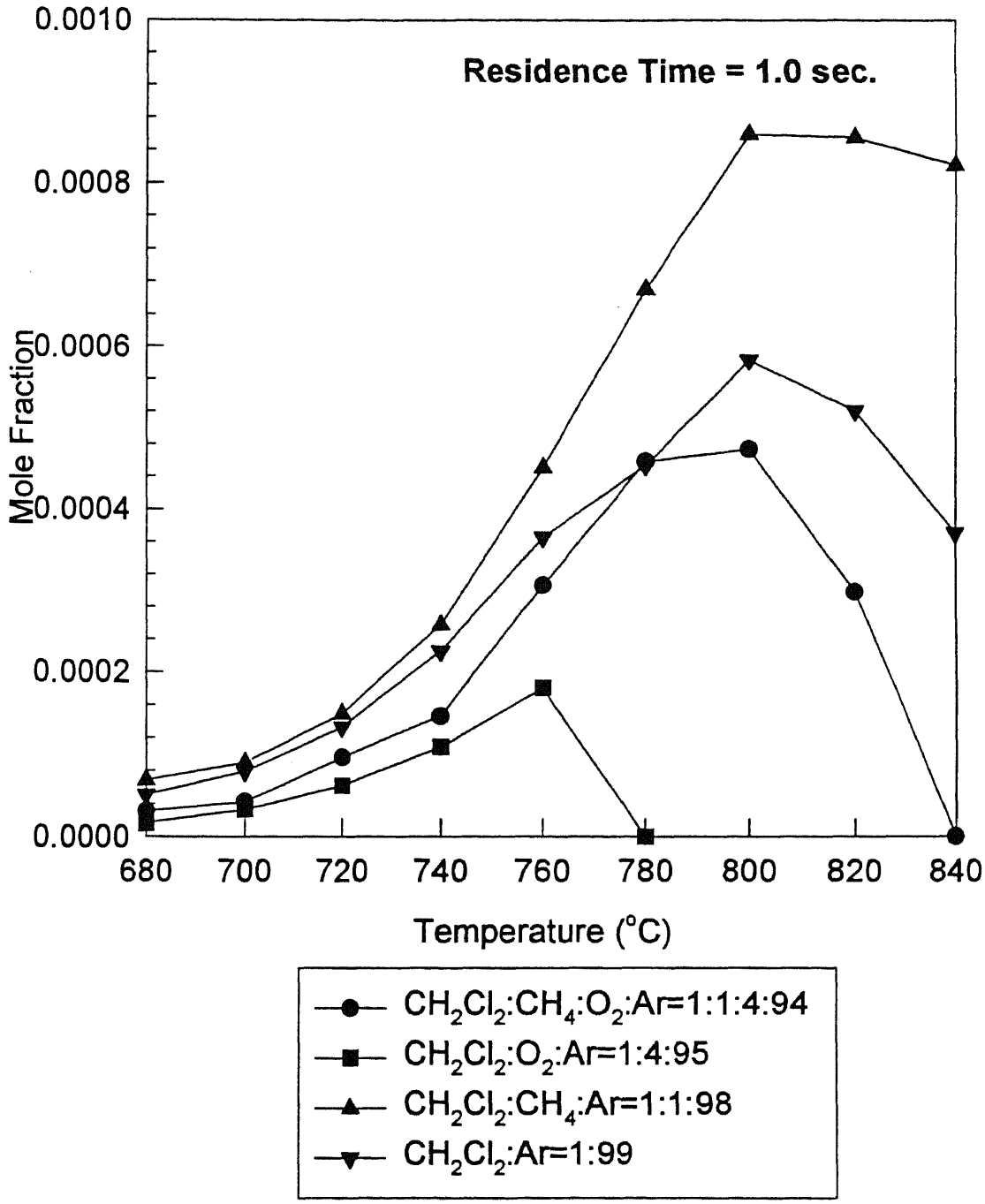

Figure A10 CH_3Cl Distribution vs Temperature in different Reaction Environments

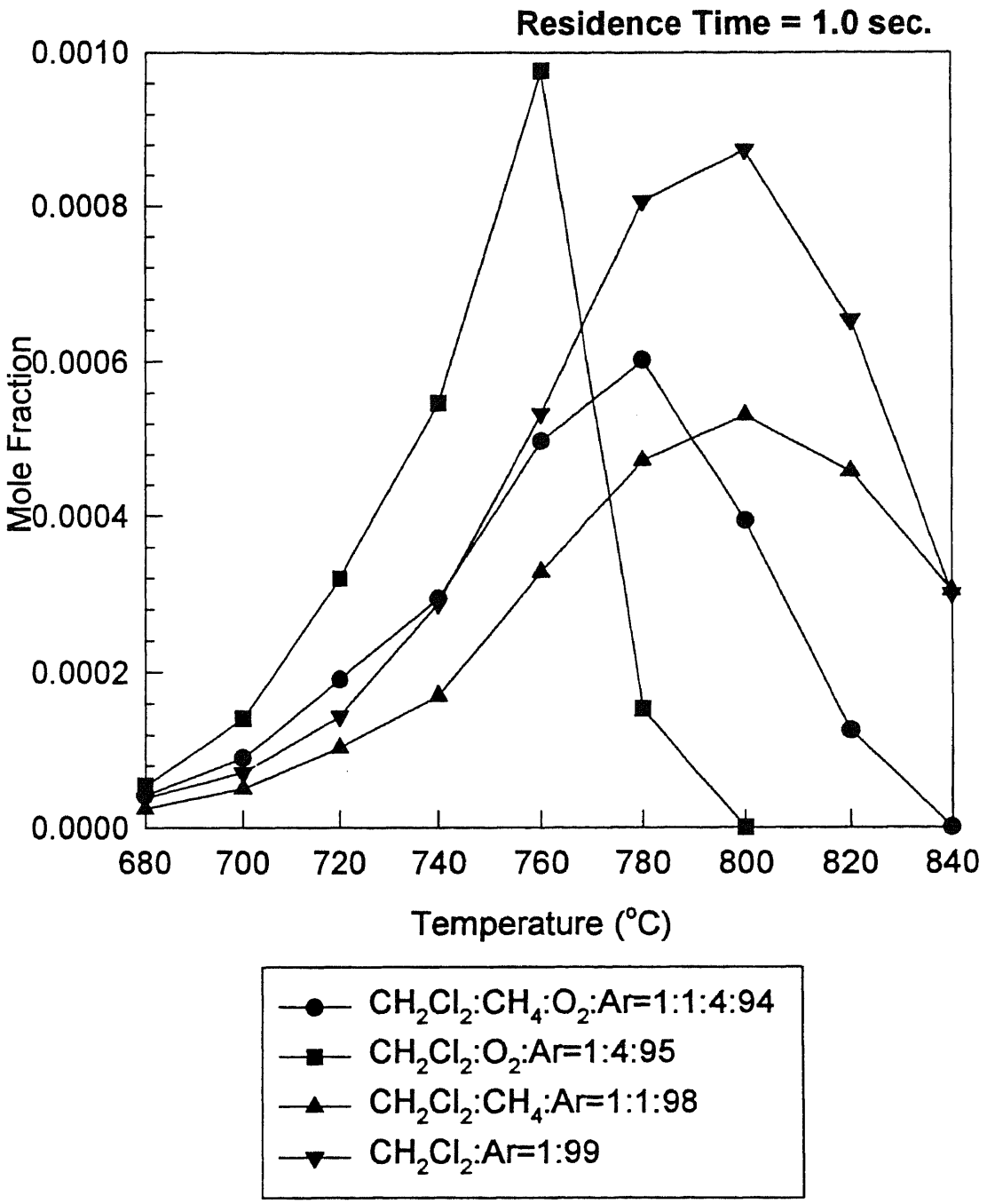

Figure A11 C_2HCl_3 Distribution vs Temperature in different Reaction Environments

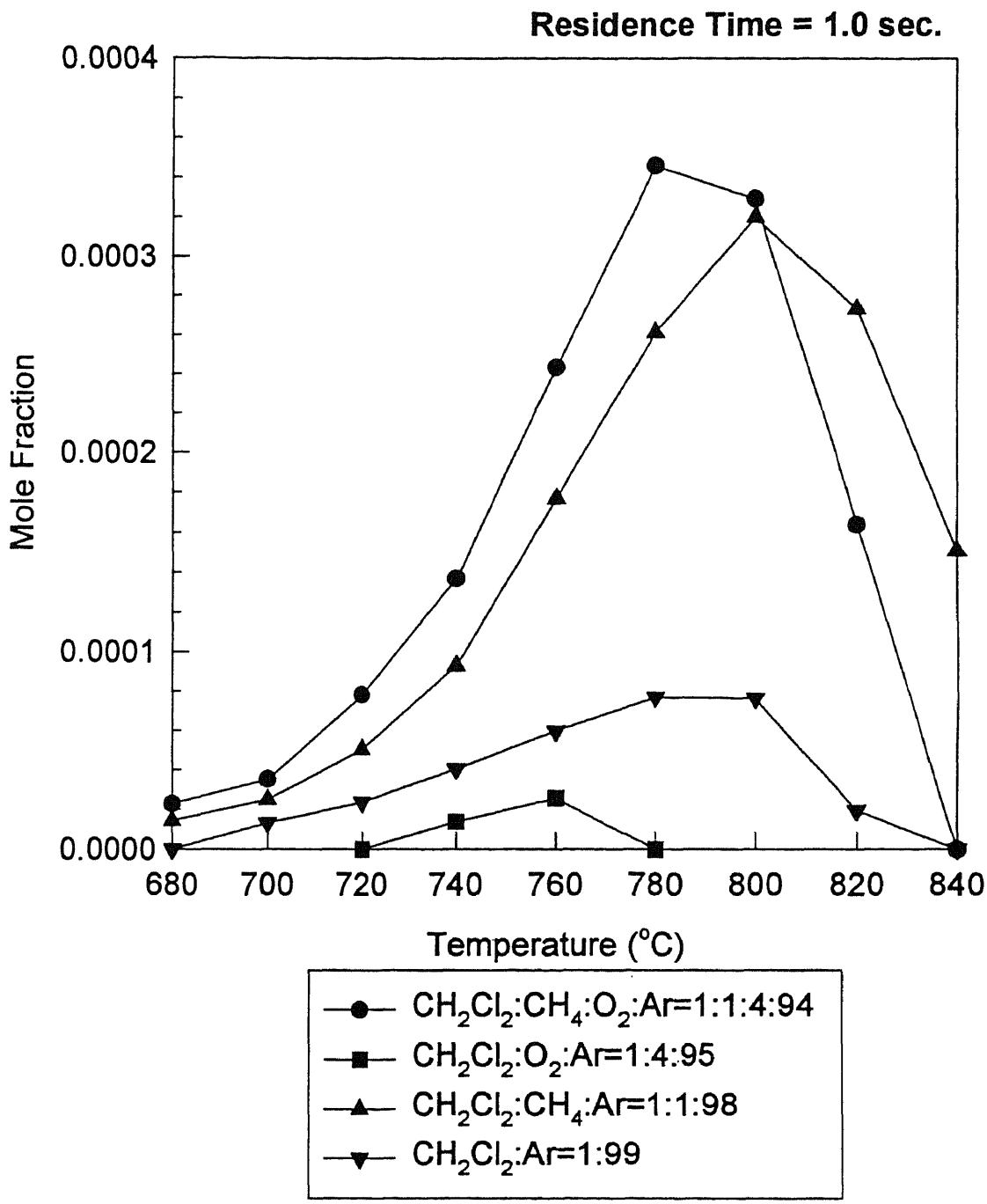

Figure A12 C_2H_3Cl Distribution vs Temperature in different Reaction Environments

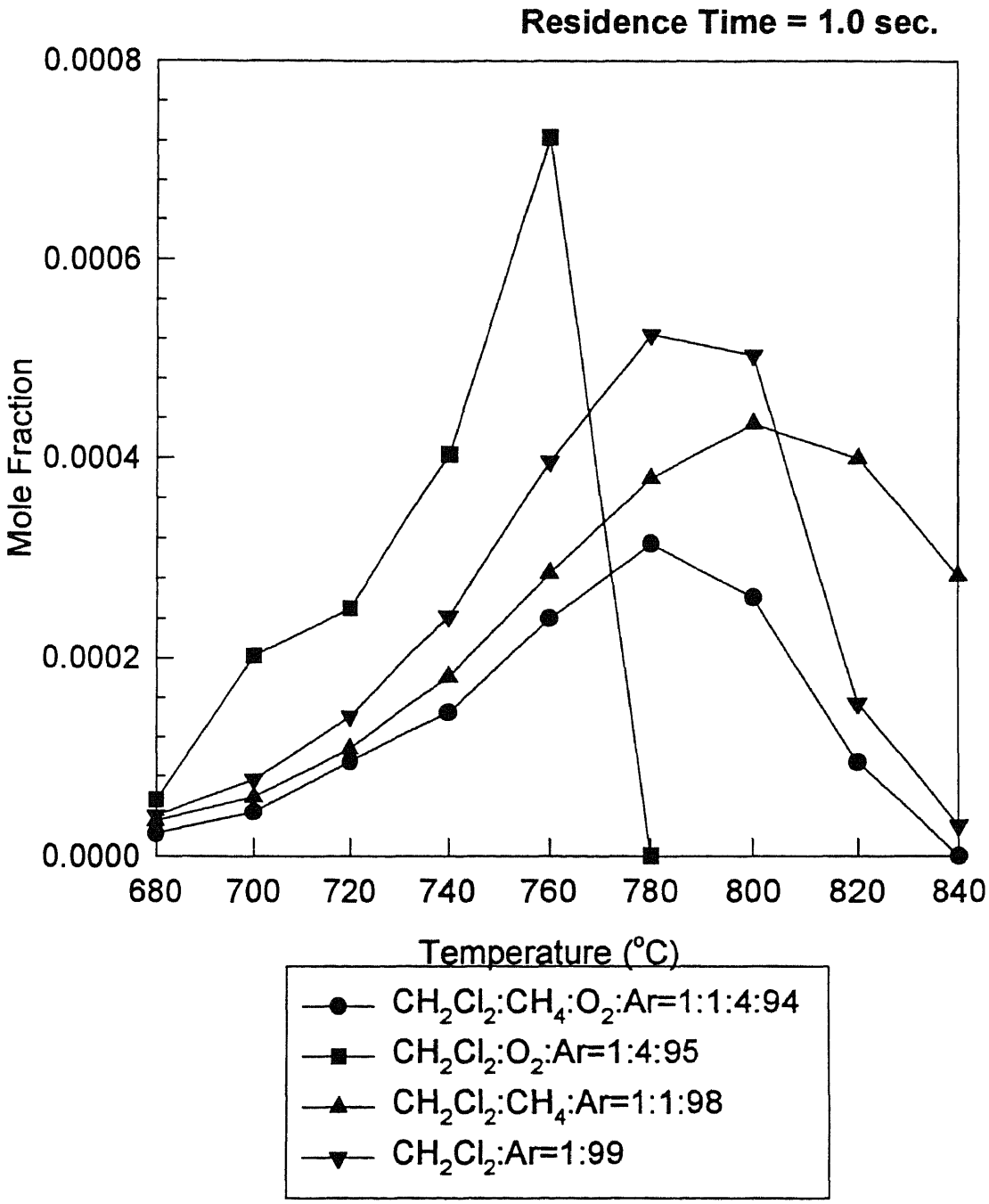

Figure A13 CHClCHCl Distribution vs Temperature in different Reaction Environments

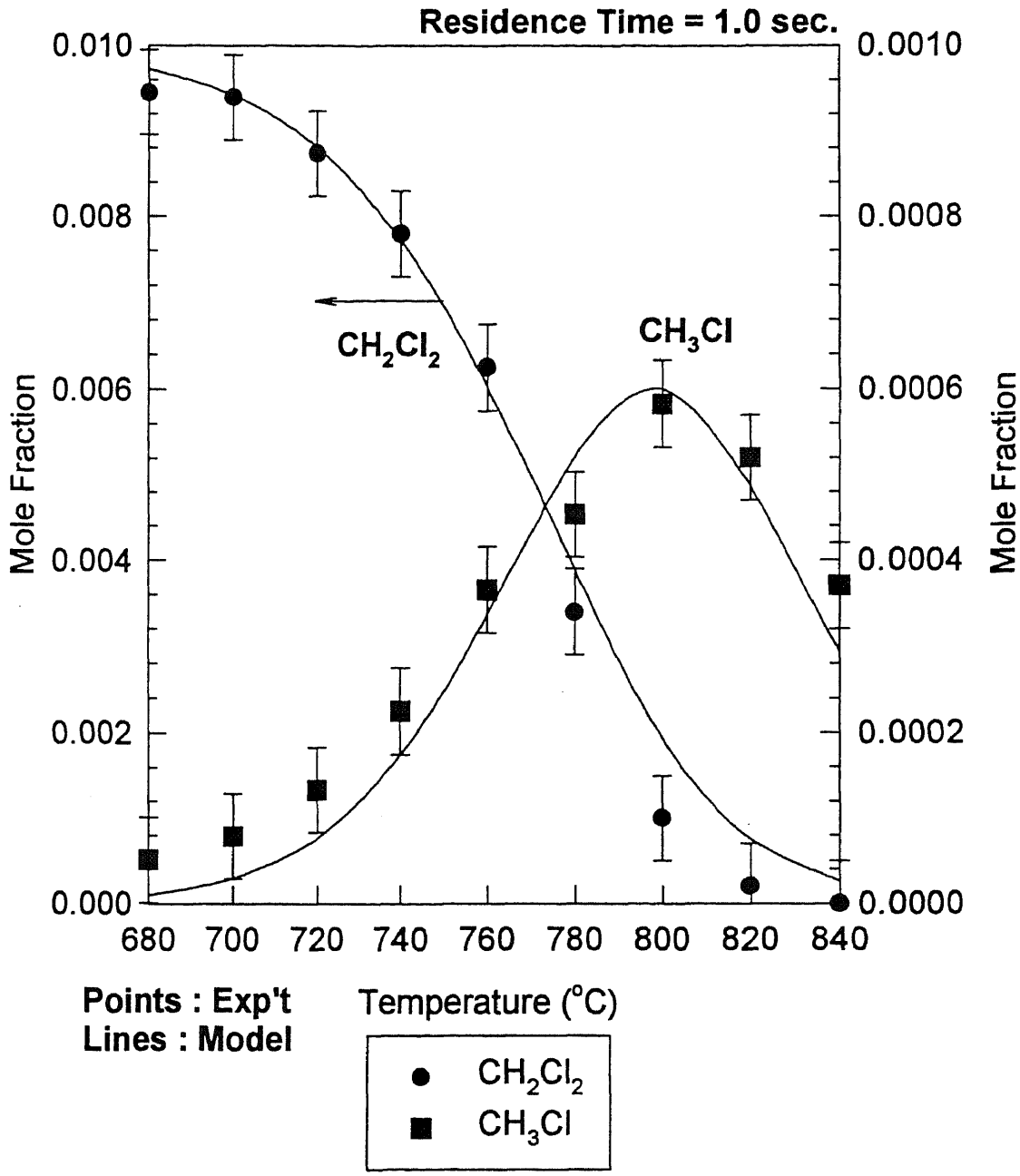

Figure B1 Model versus Experiment CH_2Cl_2 and CH_3Cl vs Temperature in CH_2Cl_2 : Ar = 1 : 99

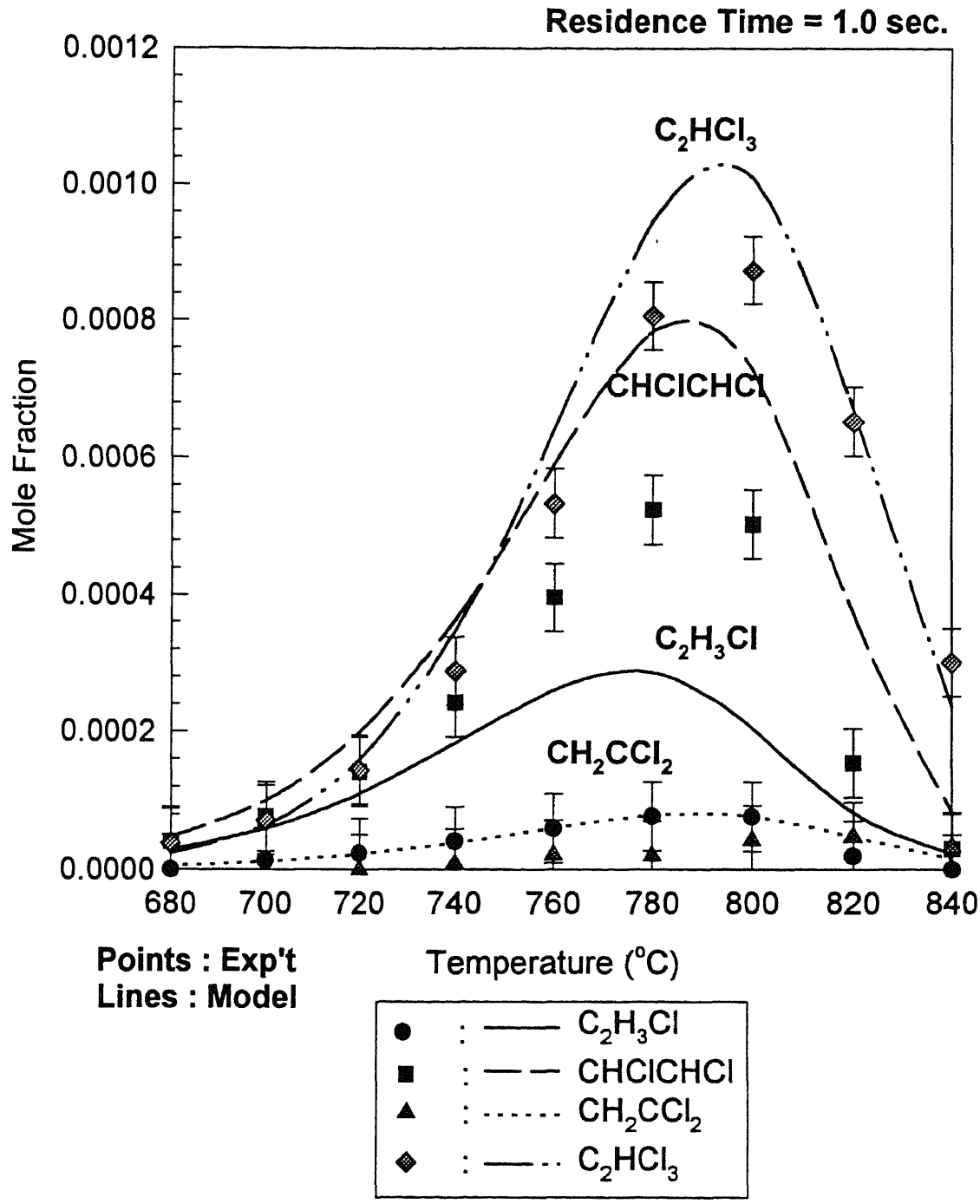

Figure B2 Model versus Experiment C_2H_3Cl, CH_2CCl_2, CHClCHCl and C_2HCl_3 vs Temperature in CH_2Cl_2 : Ar = 1 : 99

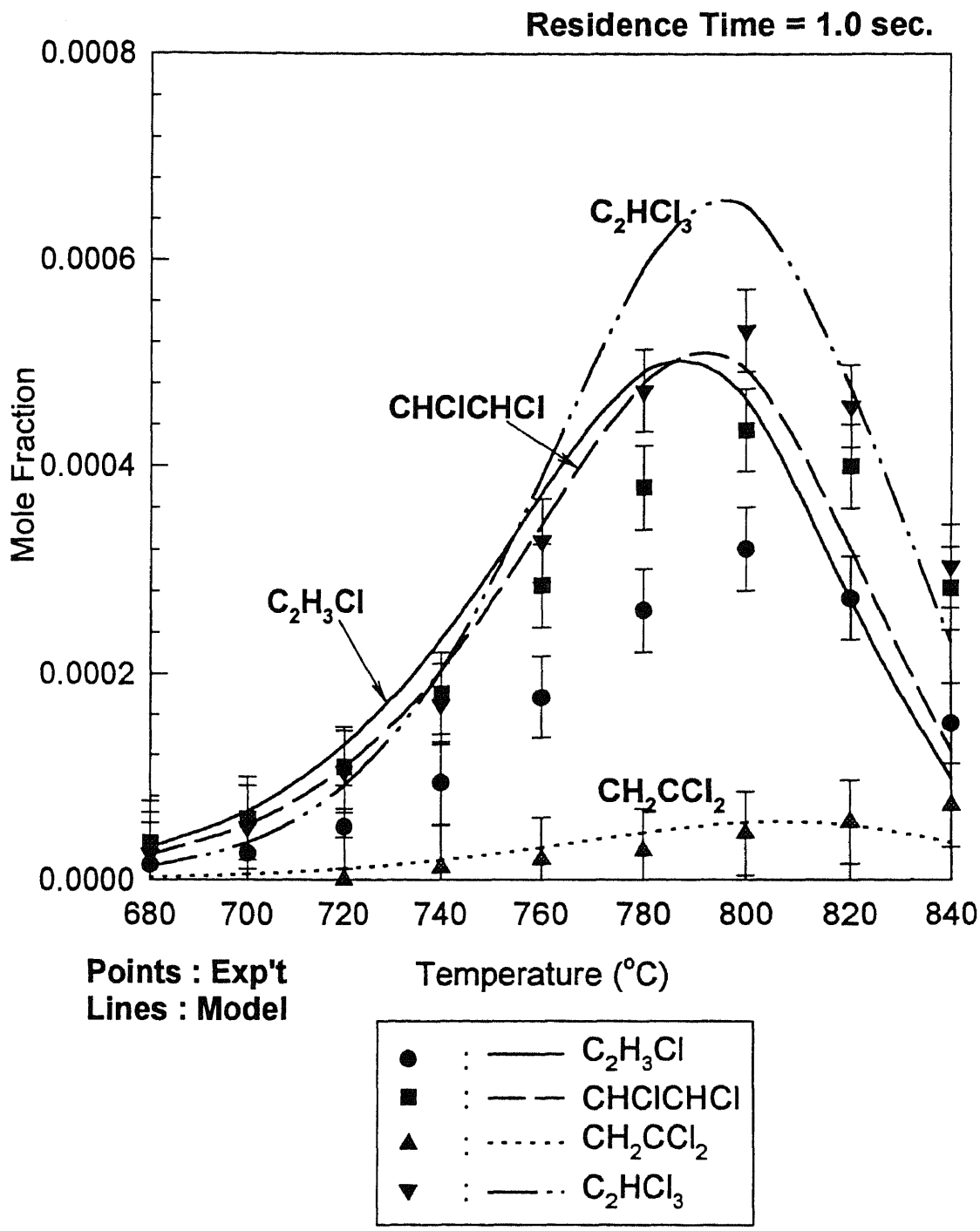

Figure B3 Model versus Experiment C_2H_3Cl, CH_2CCl_2, CHClCHCl and C_2HCl_3 vs Temperature in $CH_2Cl_2 : CH_4 : Ar = 1 : 1 : 98$

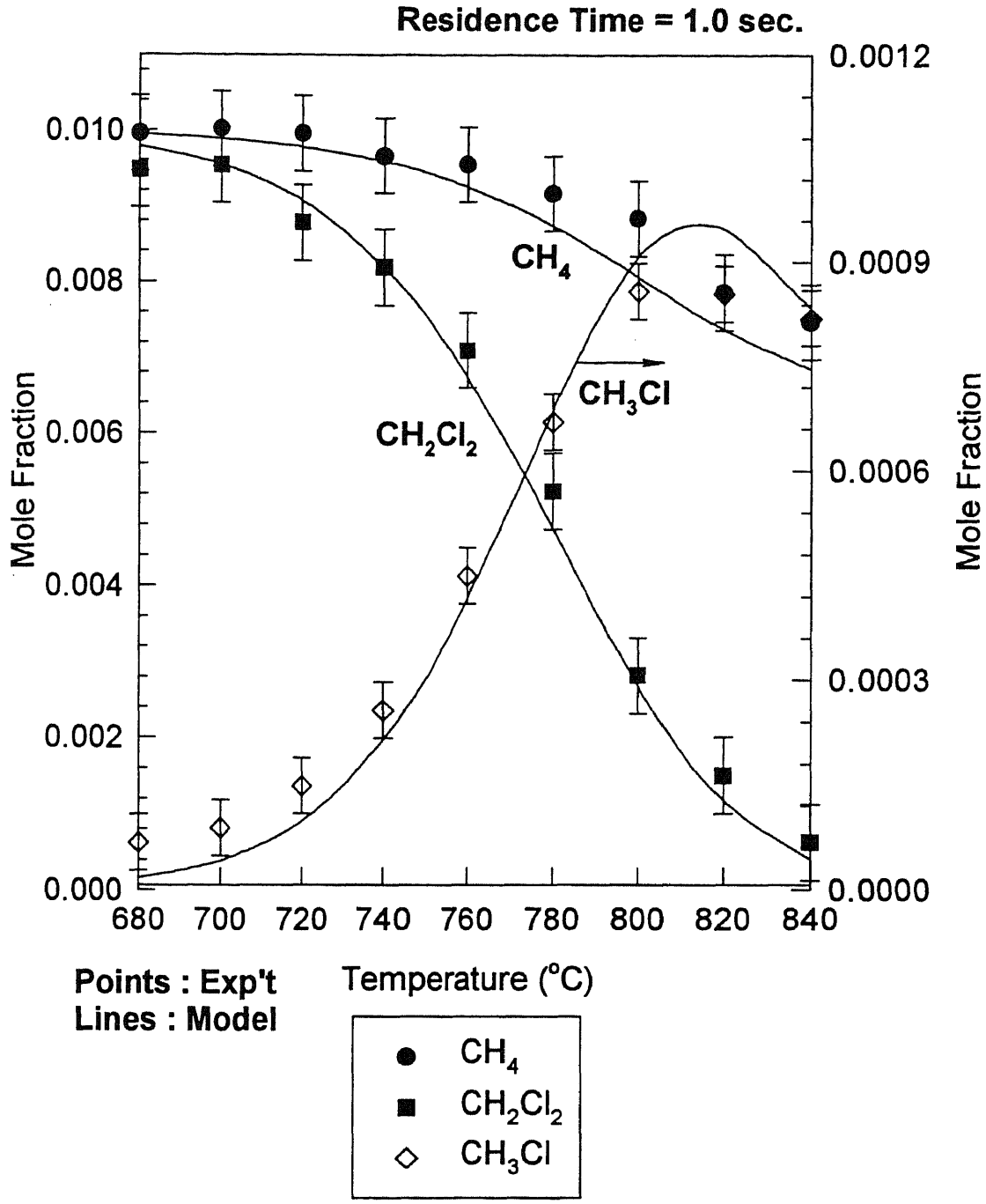

Figure B4 Model versus Experiment CH_2Cl_2, CH_4 and CH_3Cl vs Temperature in CH_2Cl_2 : CH_4 : Ar = 1 : 1 : 98

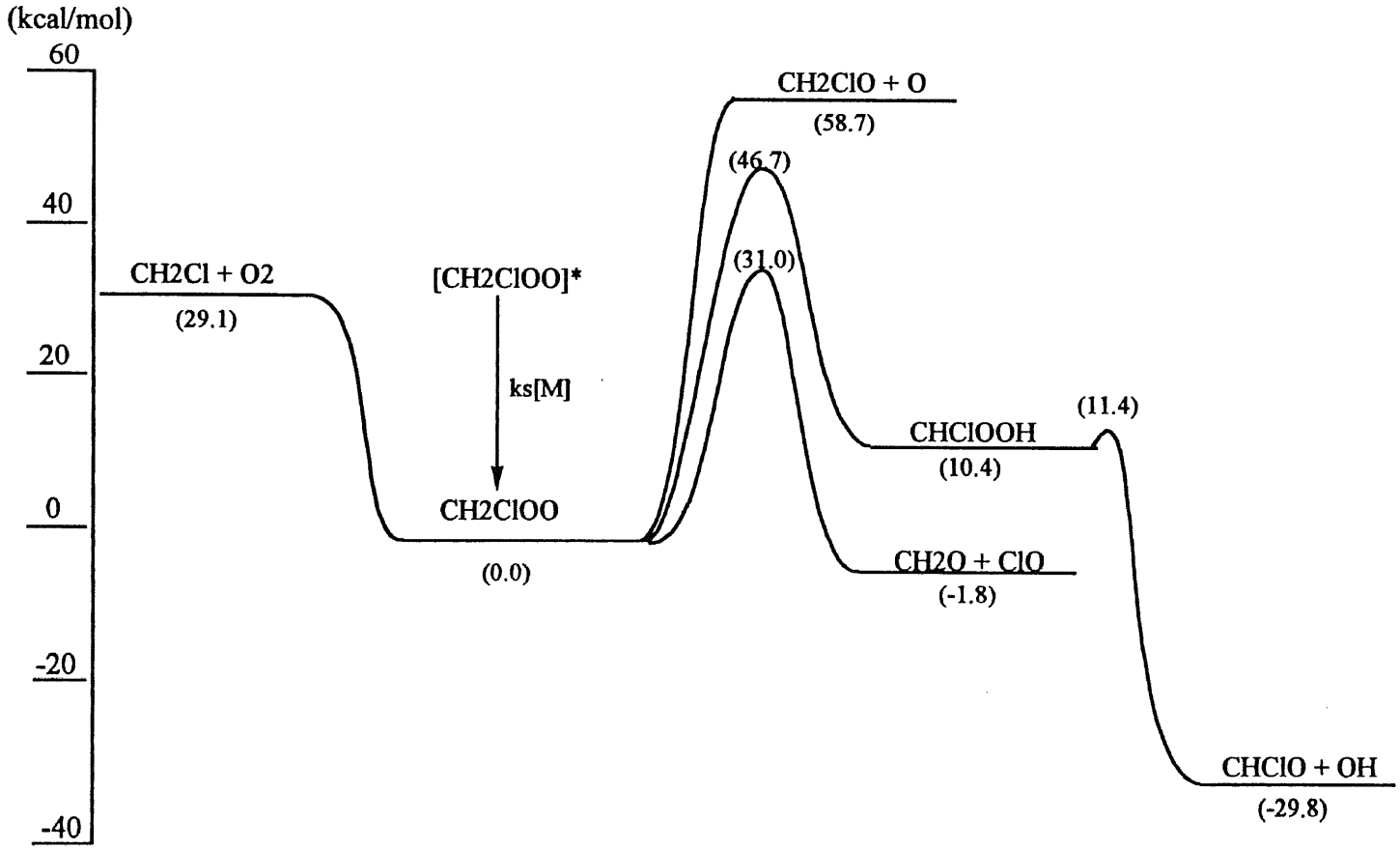

Figure B5 Potential Energy Digram for
CH2Cl + O2 ⟷ [CH2ClOO]* ⟶ Products

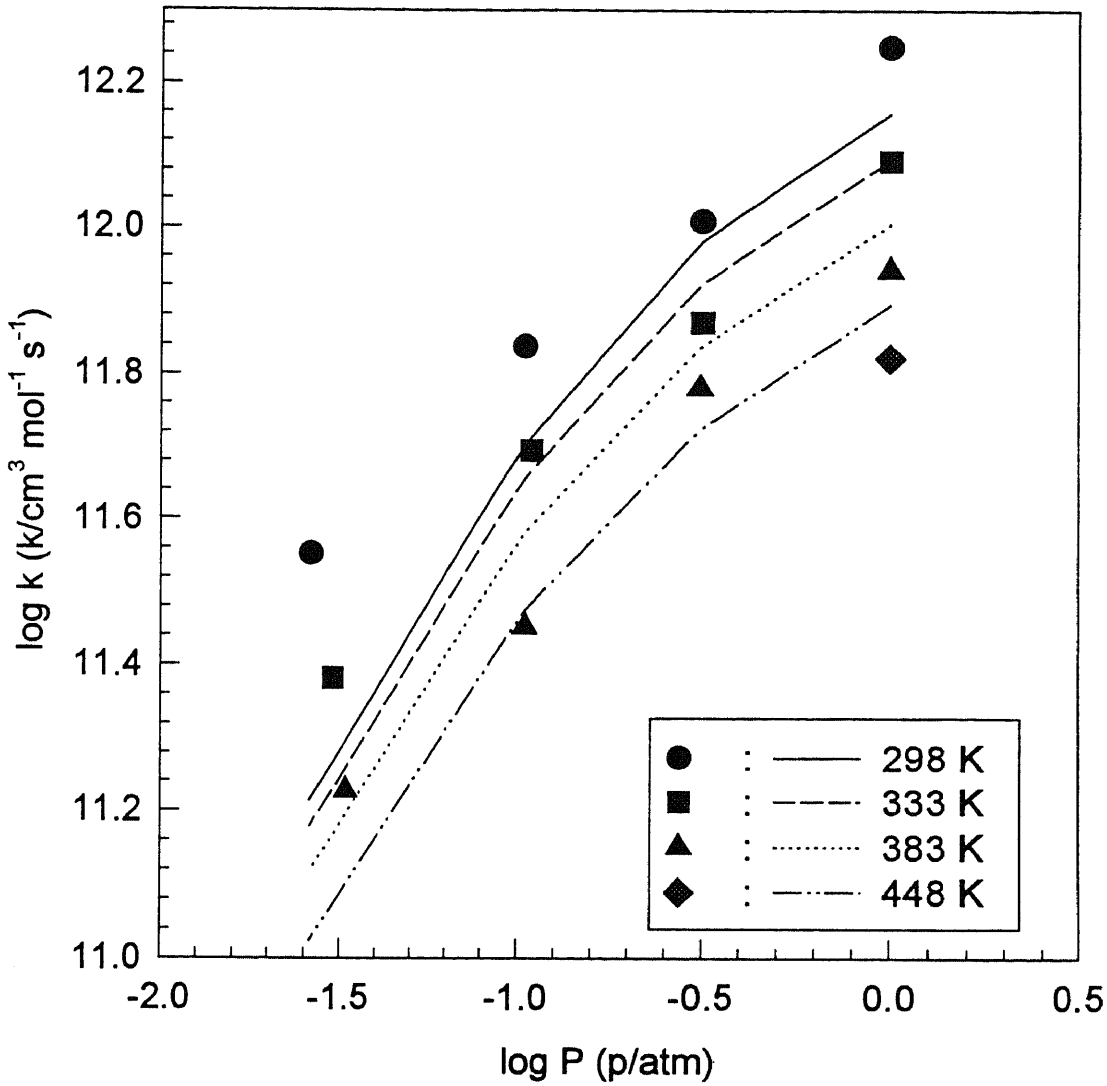

Bath gas : N_2
Symbols: Fenter et al. (1993)
lines: CHEMACT fit

Figure B6 Comparison of QRRK Calculation to Data of Fenter et al. for $CH_2Cl + O_2 \longrightarrow CH_2ClOO$

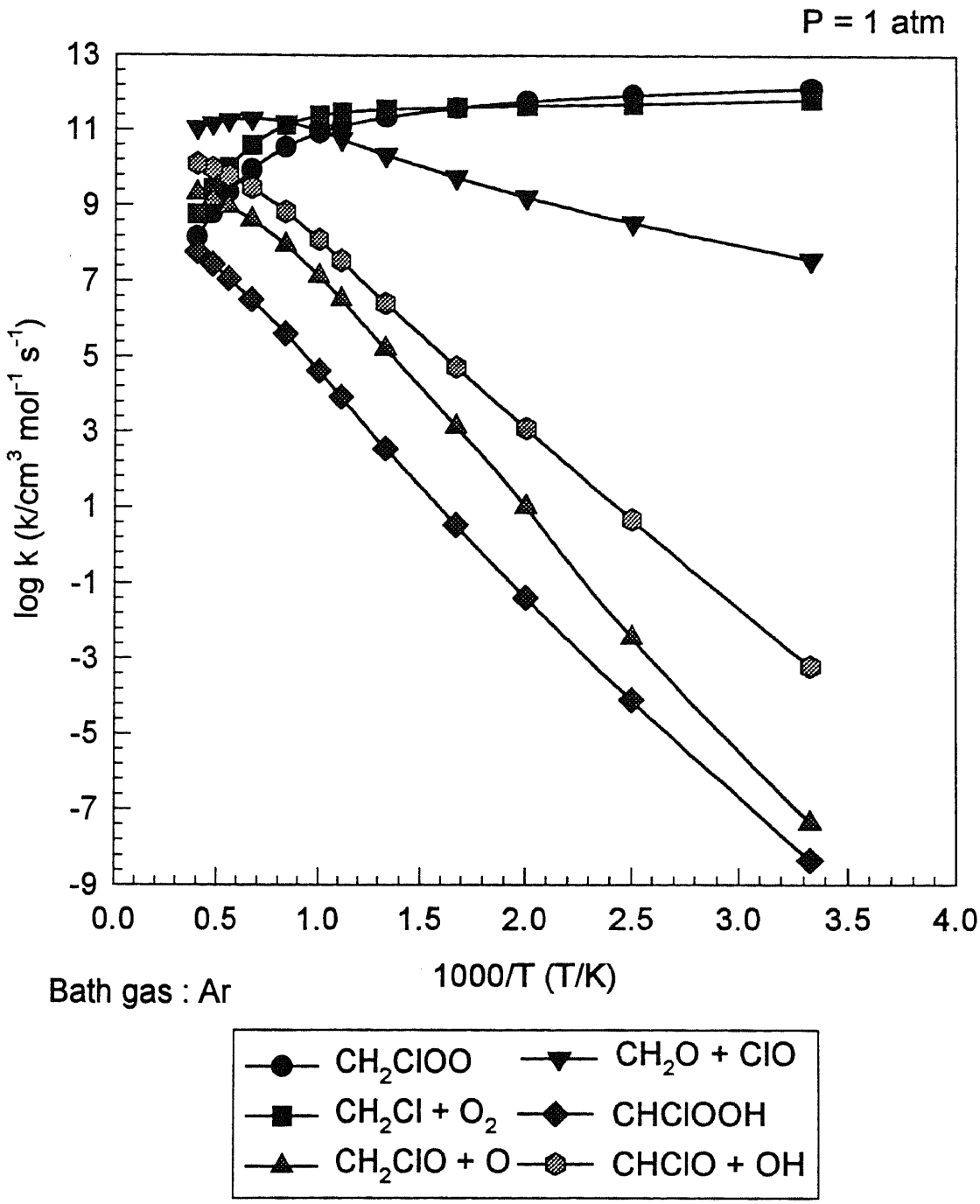

Figure B7 Results of QRRK Analysis
$CH_2Cl + O_2$ <=> $[CH_2ClOO]^*$ => Products

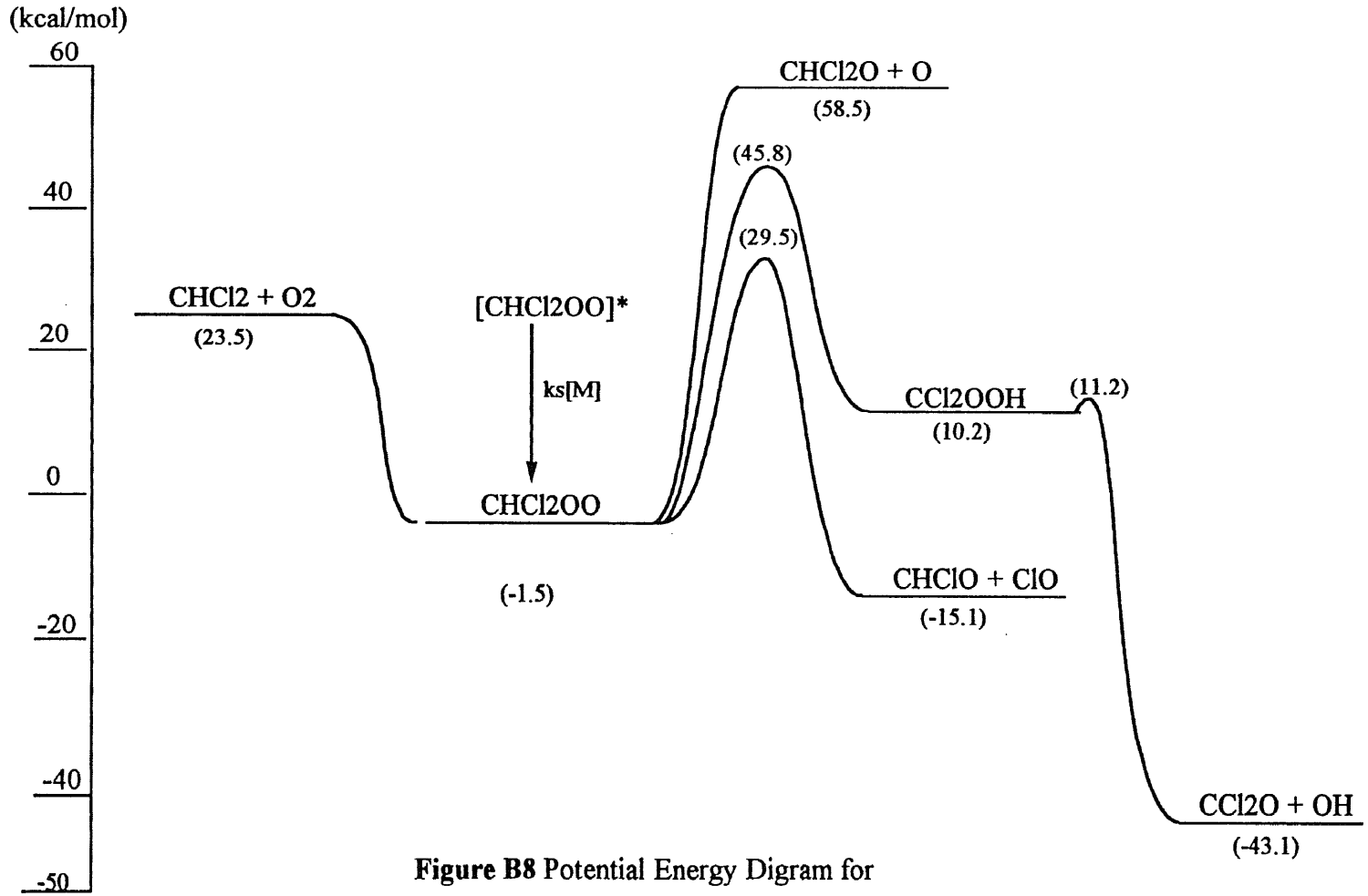

Figure B8 Potential Energy Digram for
CHCl2 + O2 ⟷ [CHCl2OO]* ⟶ Products

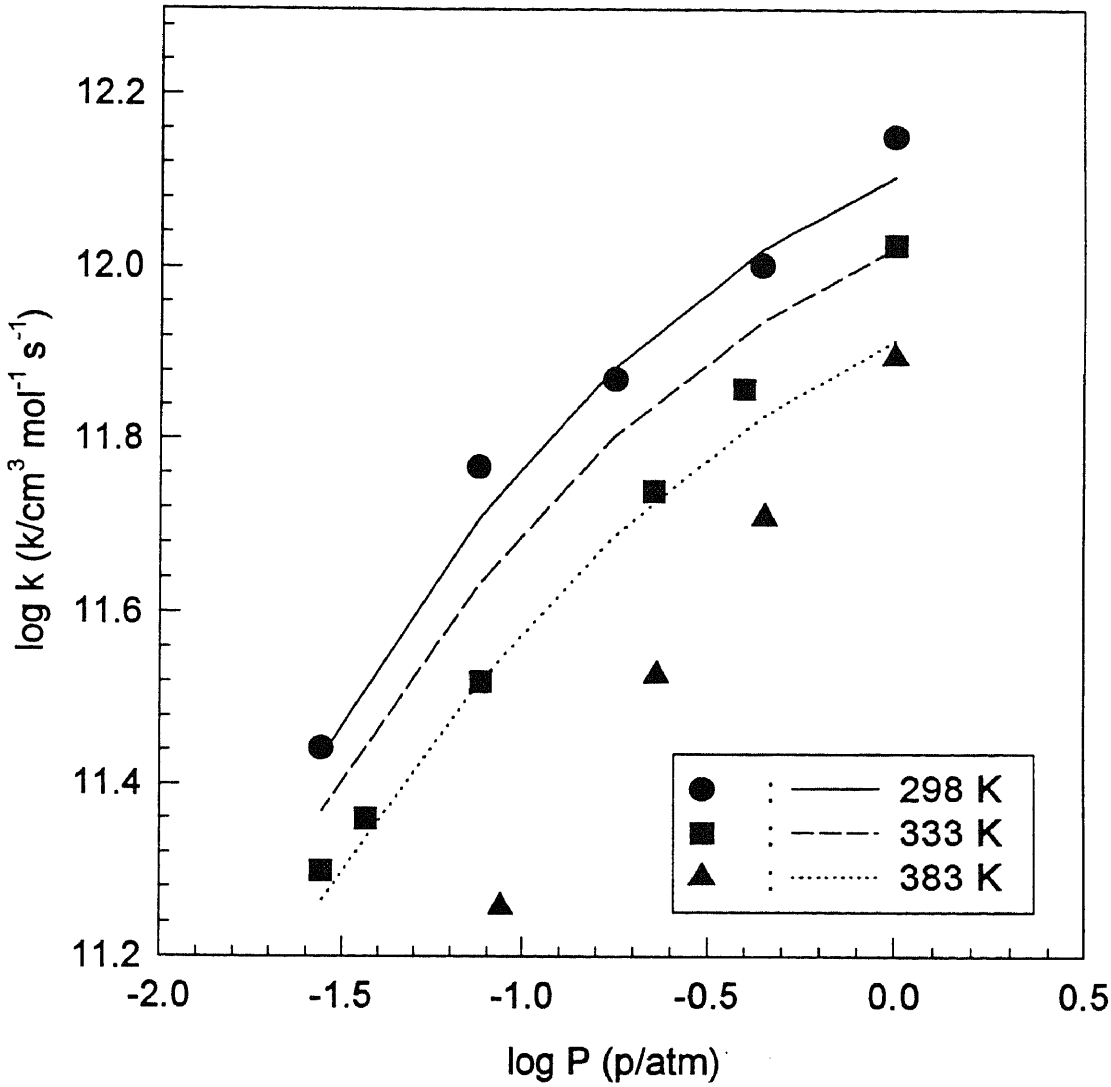

Bath gas : N_2
Symbols: Fenter et al. (1993)
lines: CHEMACT fit

Figure B9 Comparison of QRRK Calculation to Data of Fenter et al. for $CHCl_2 + O_2 \longrightarrow CHCl_2OO$

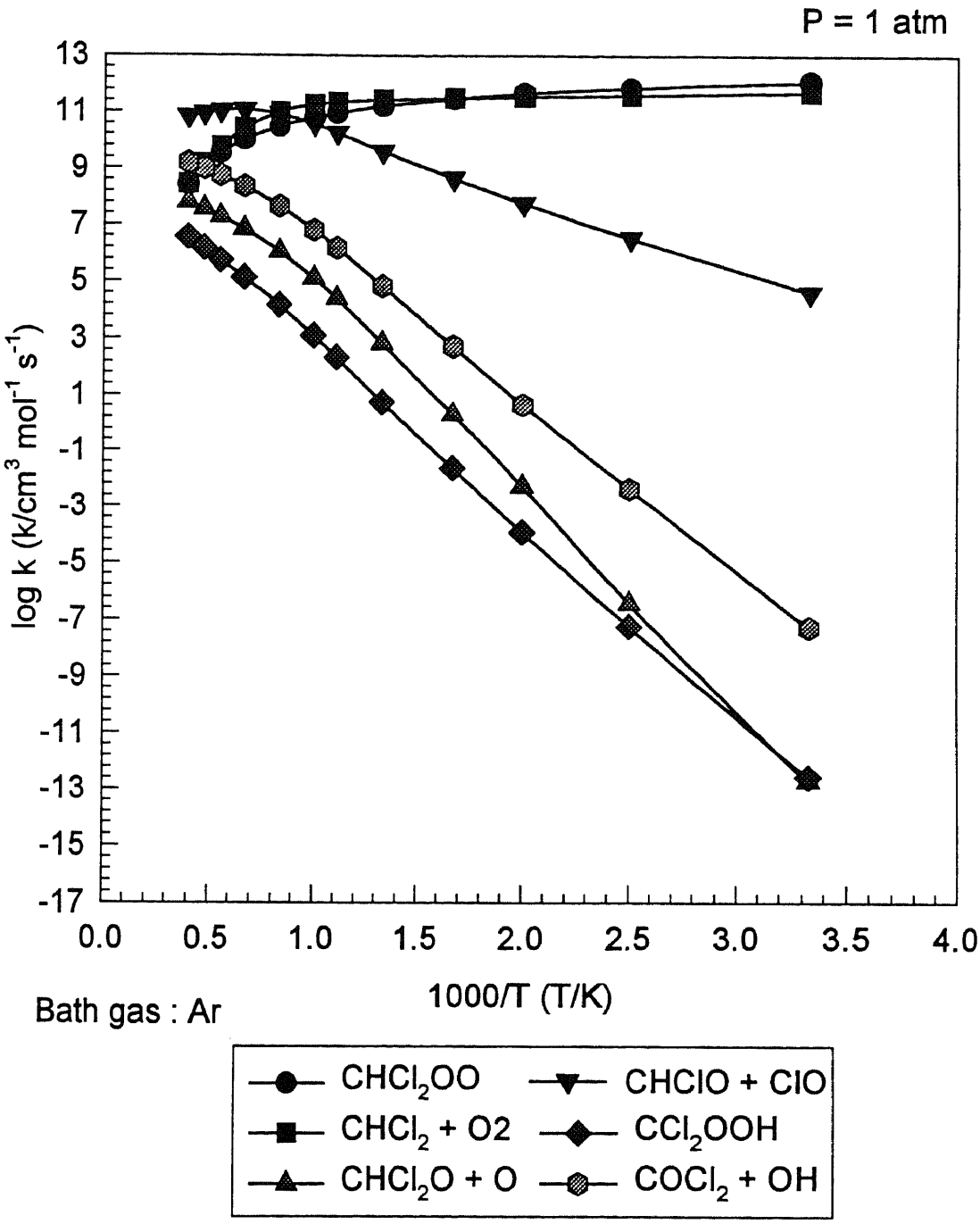

Figure B10 Results of QRRK Analysis
$CHCl_2 + O_2$ <=> $[CHCl_2OO]^*$ => Products

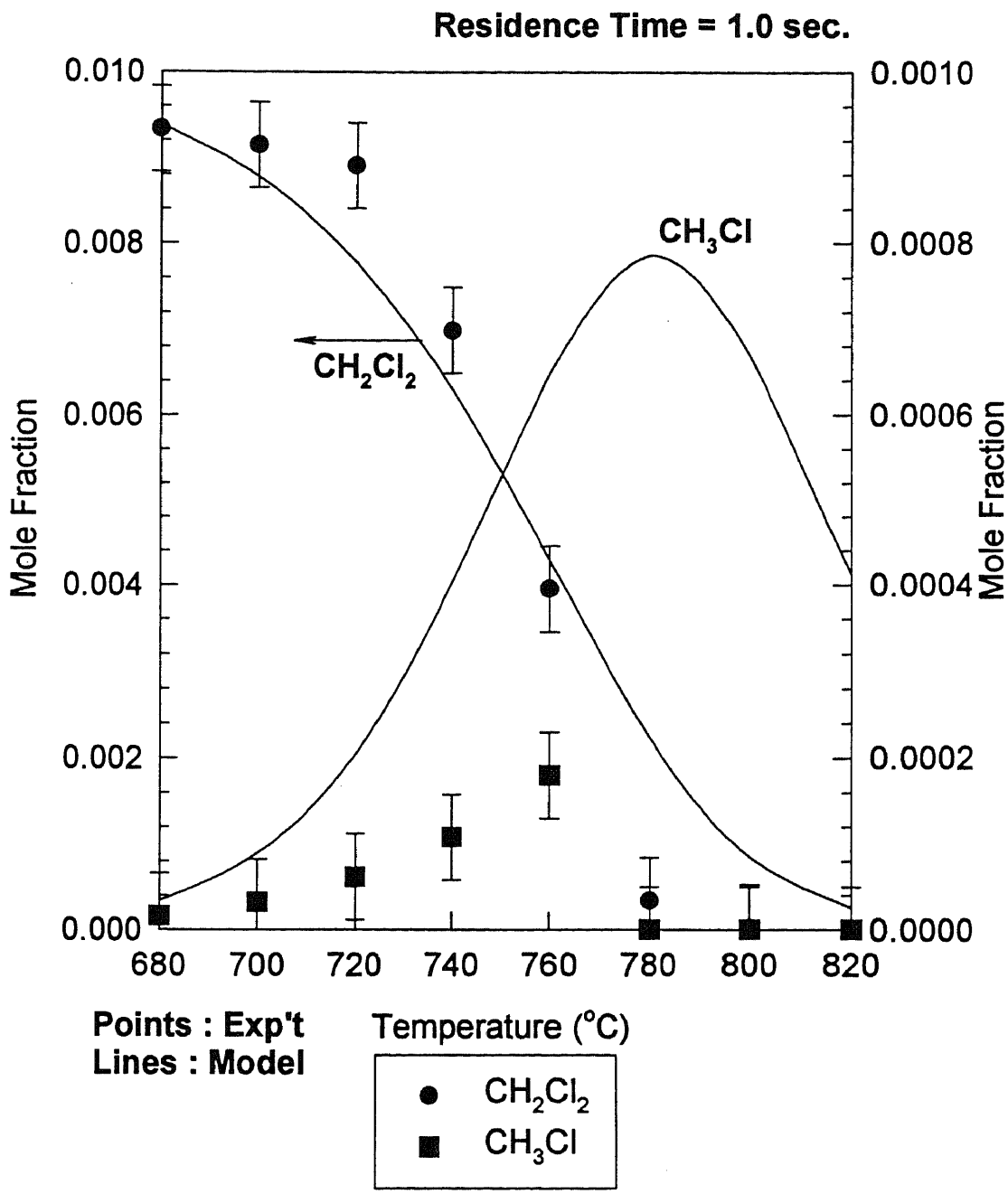

Figure B11 Model versus Experiment CH_2Cl_2 and CH_3Cl vs Temperature in $CH_2Cl_2 : O_2 : Ar = 1 : 4 : 95$

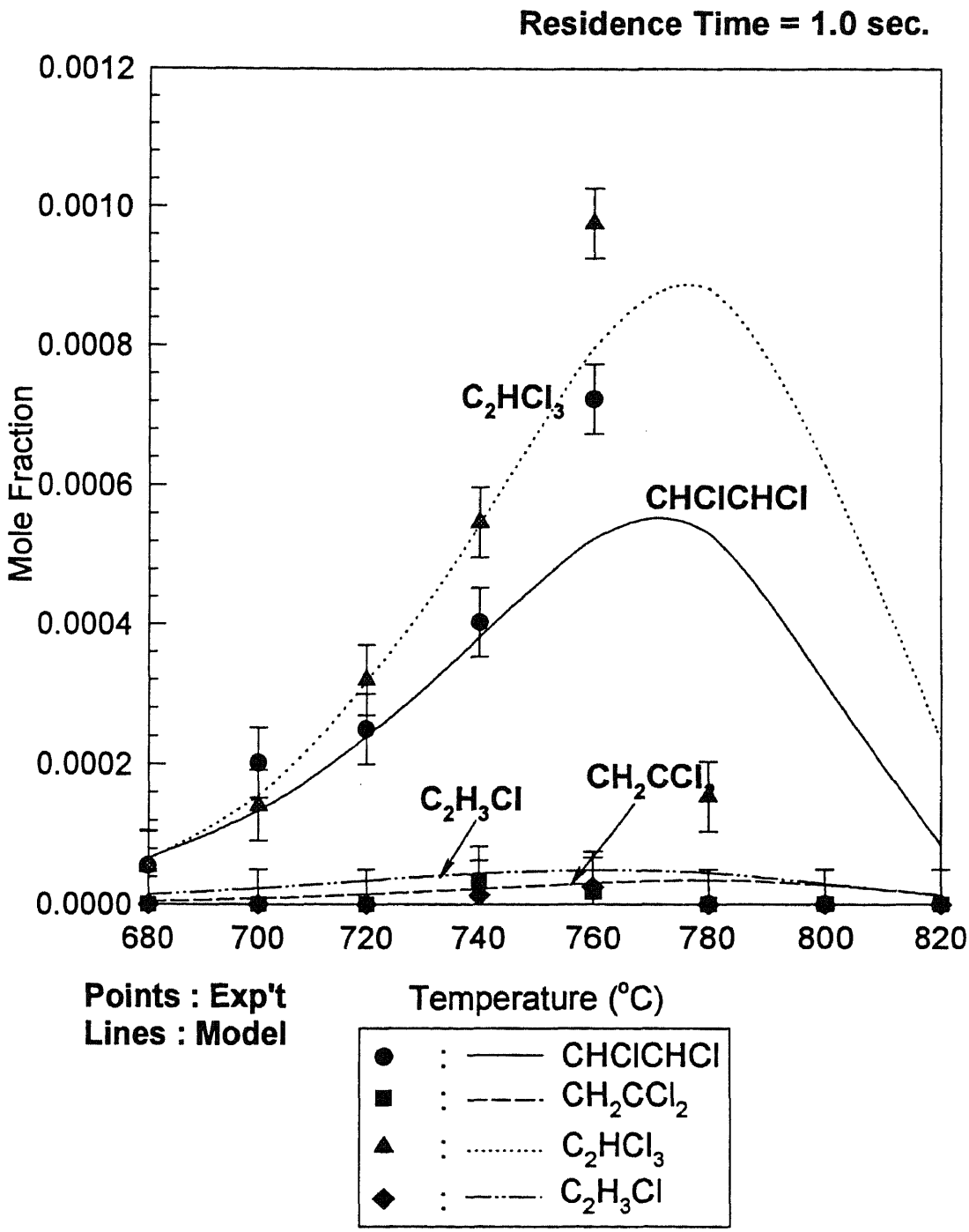

Figure B12 Model versus Experiment C_2H_3Cl, CH_2CCl_2, CHClCHCl and C_2HCl_3 vs Temperature in $CH_2Cl_2 : O_2 : Ar = 1 : 4 : 95$

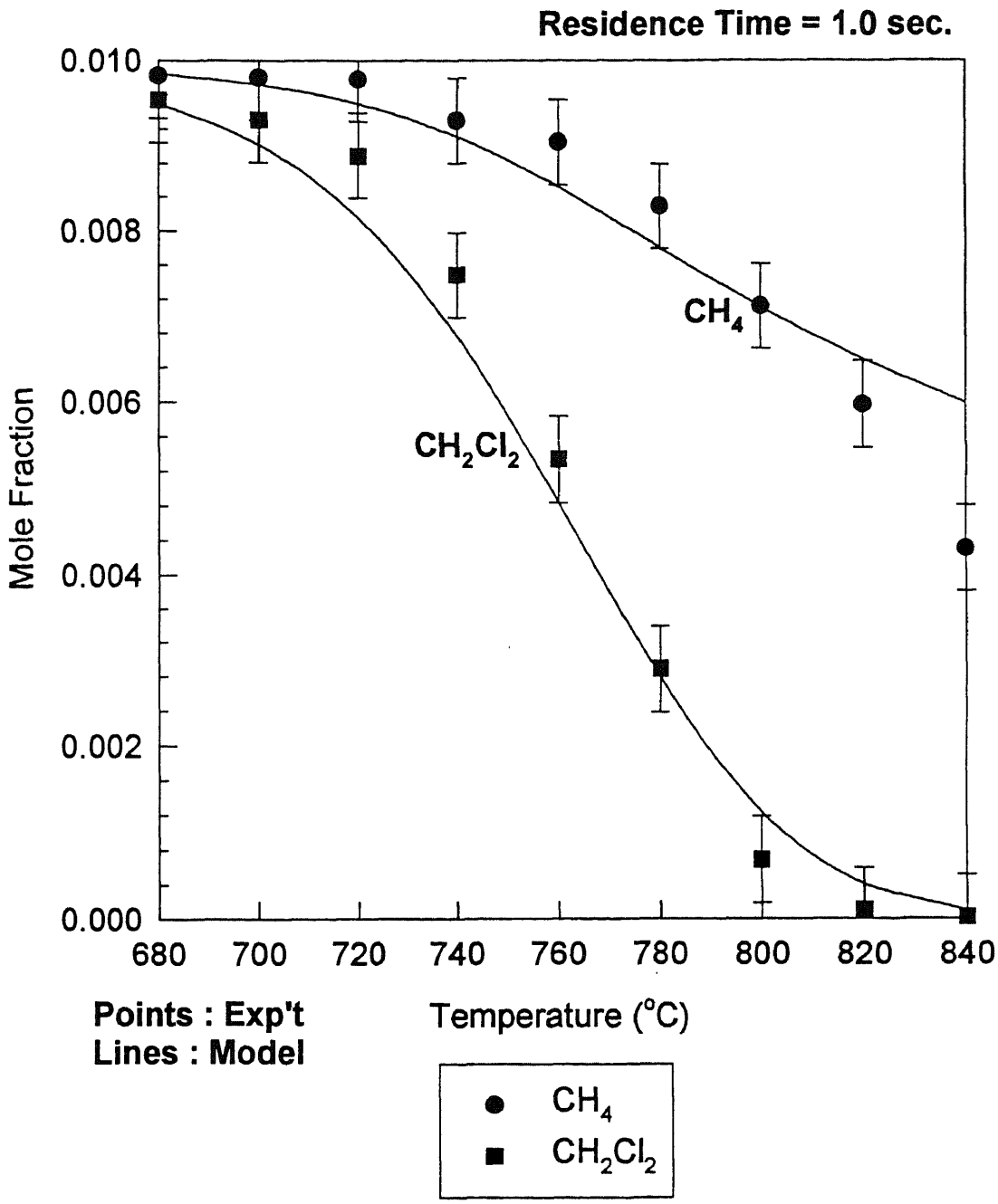

Figure B13 Model versus Experiment CH_2Cl_2 and CH_4 vs Temperature in $CH_2Cl_2 : CH_4 : O_2 : Ar = 1 : 1 : 4 : 94$

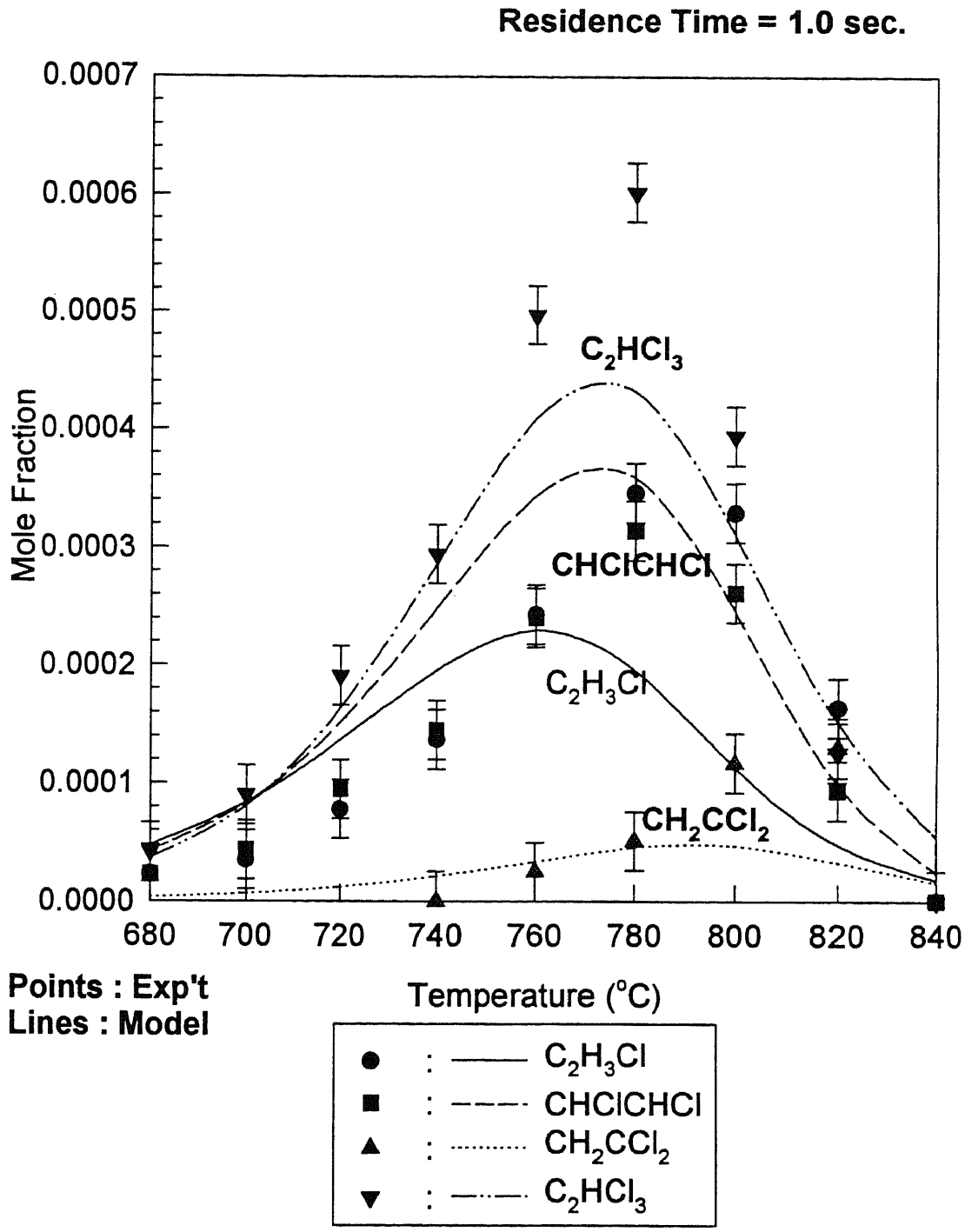

Figure B14 Model versus Experiment C_2H_3Cl, CH_2CCl_2, CHClCHCl and C_2HCl_3 vs Temperature in $CH_2Cl_2 : CH_4 : O_2 : Ar = 1 : 1 : 4 : 94$

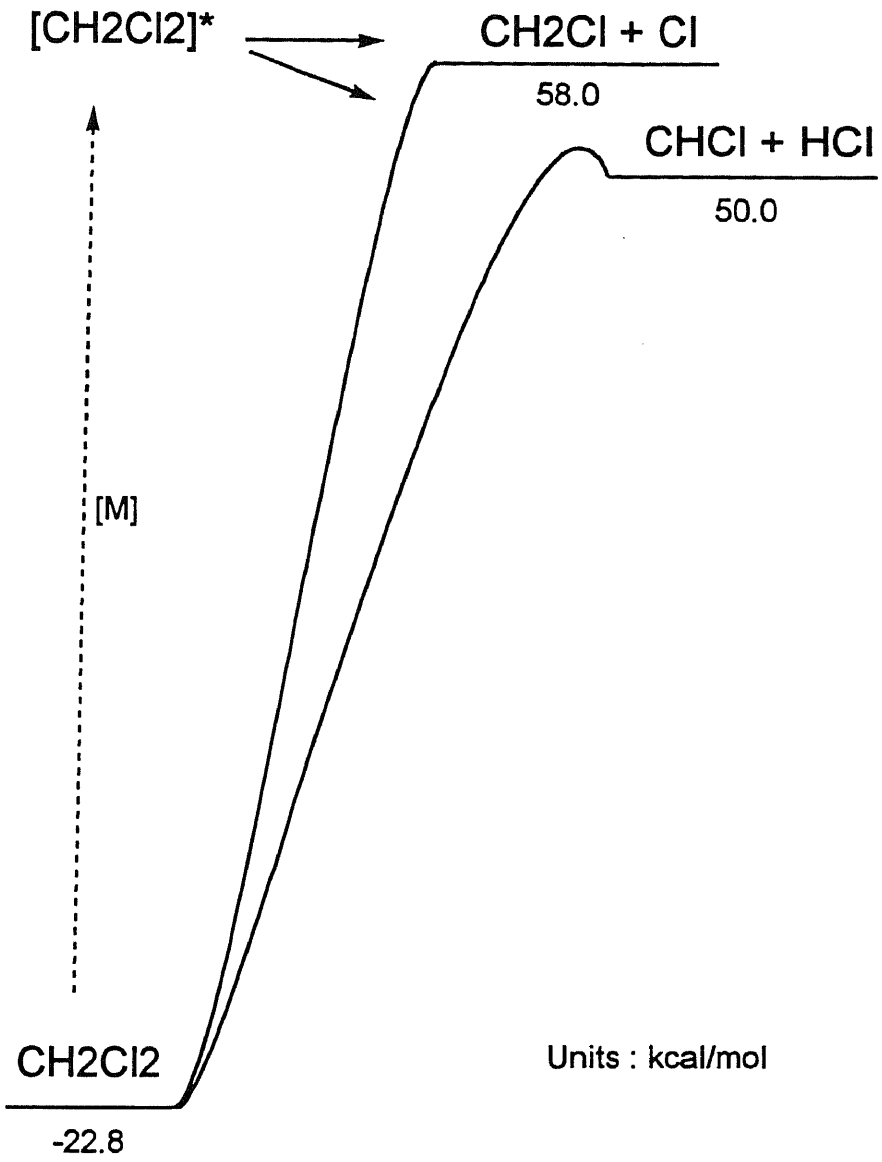

Figure C1 Potential Energy Diagram for
CH2Cl2 ⟷ [CH2Cl2]* ⟶ Products

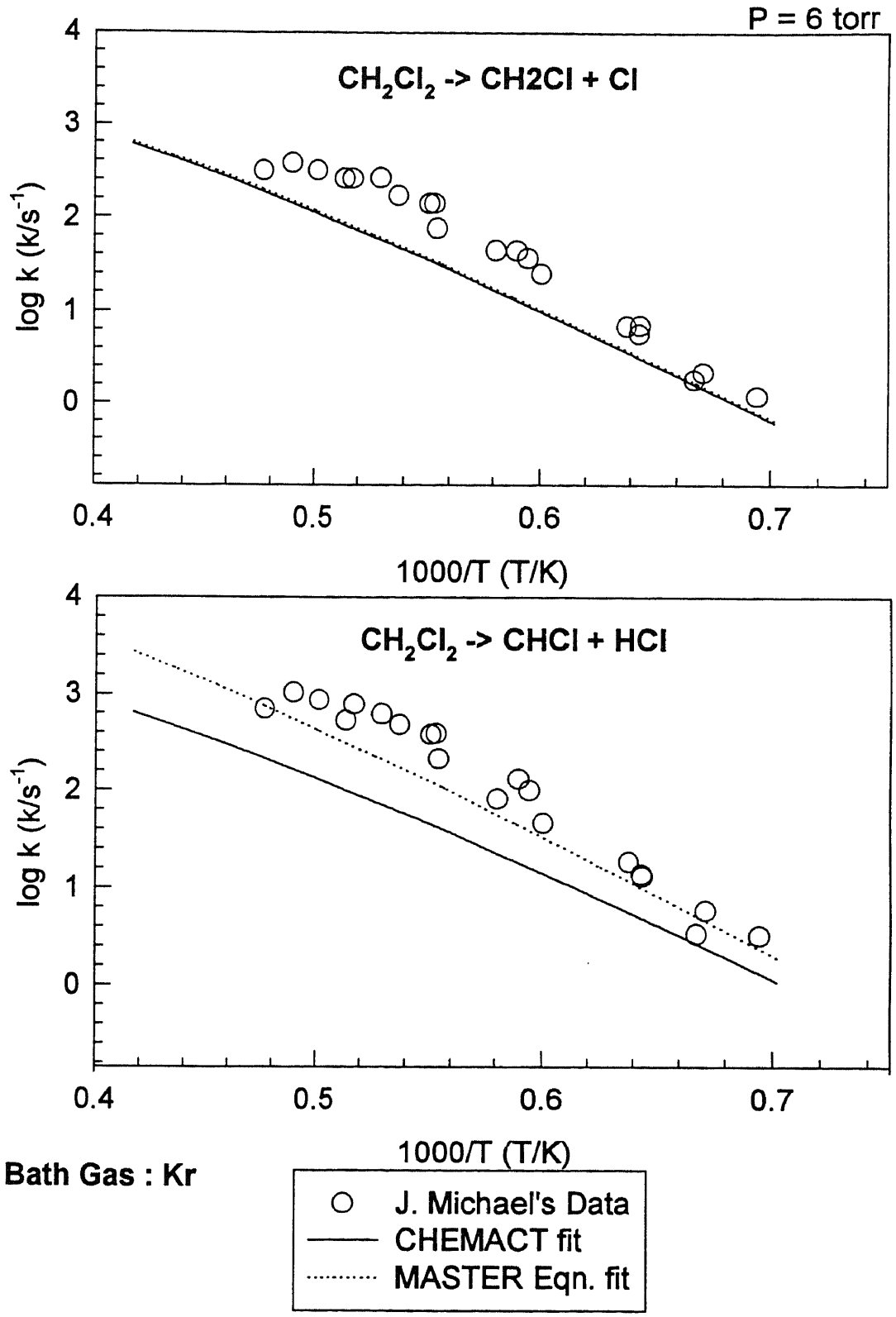

Figure C2 NJIT Analysis vs. Experimental Data of Lim et al.

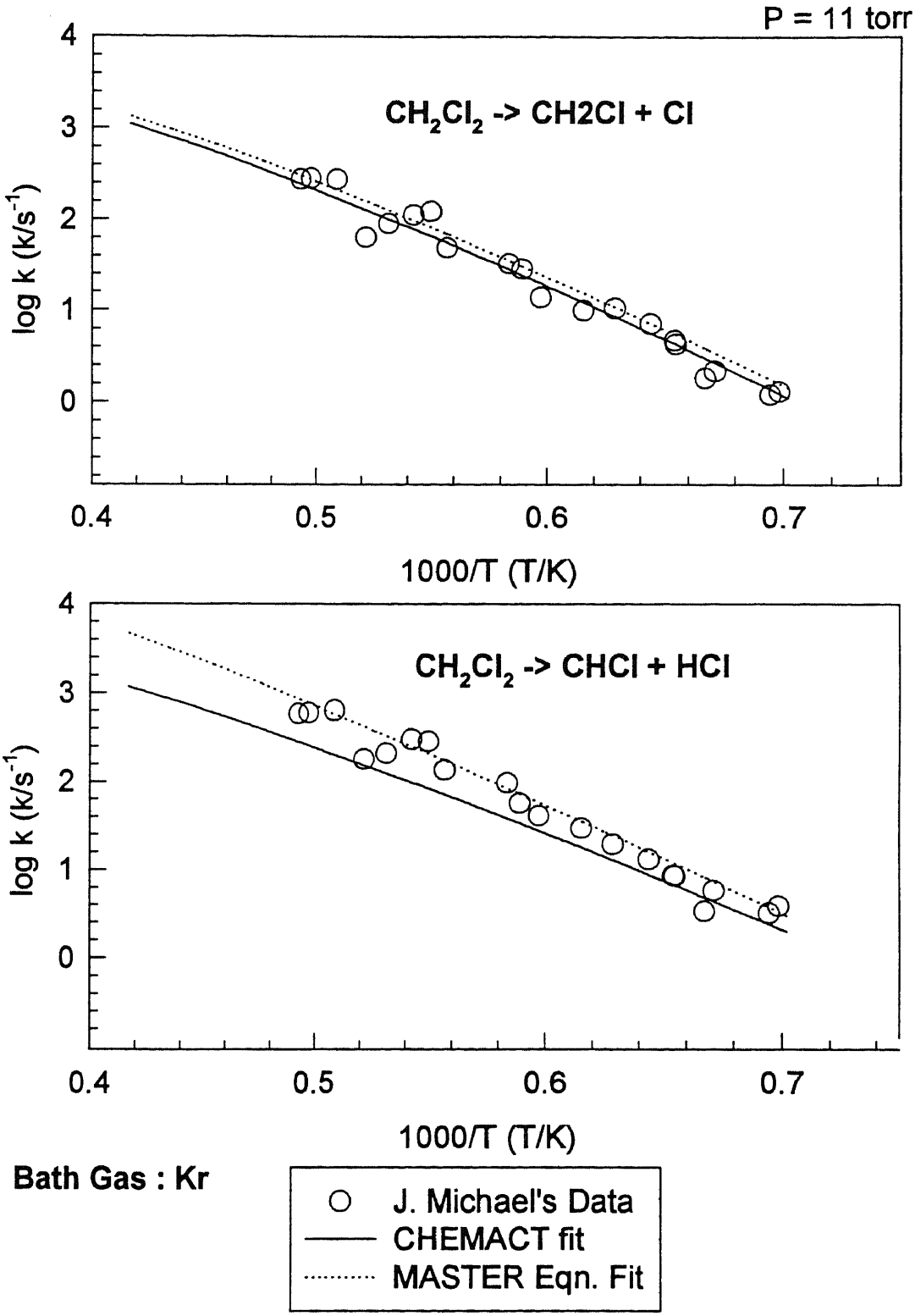

Figure C3 NJIT Analysis vs. Experimental Data of Lim et al.

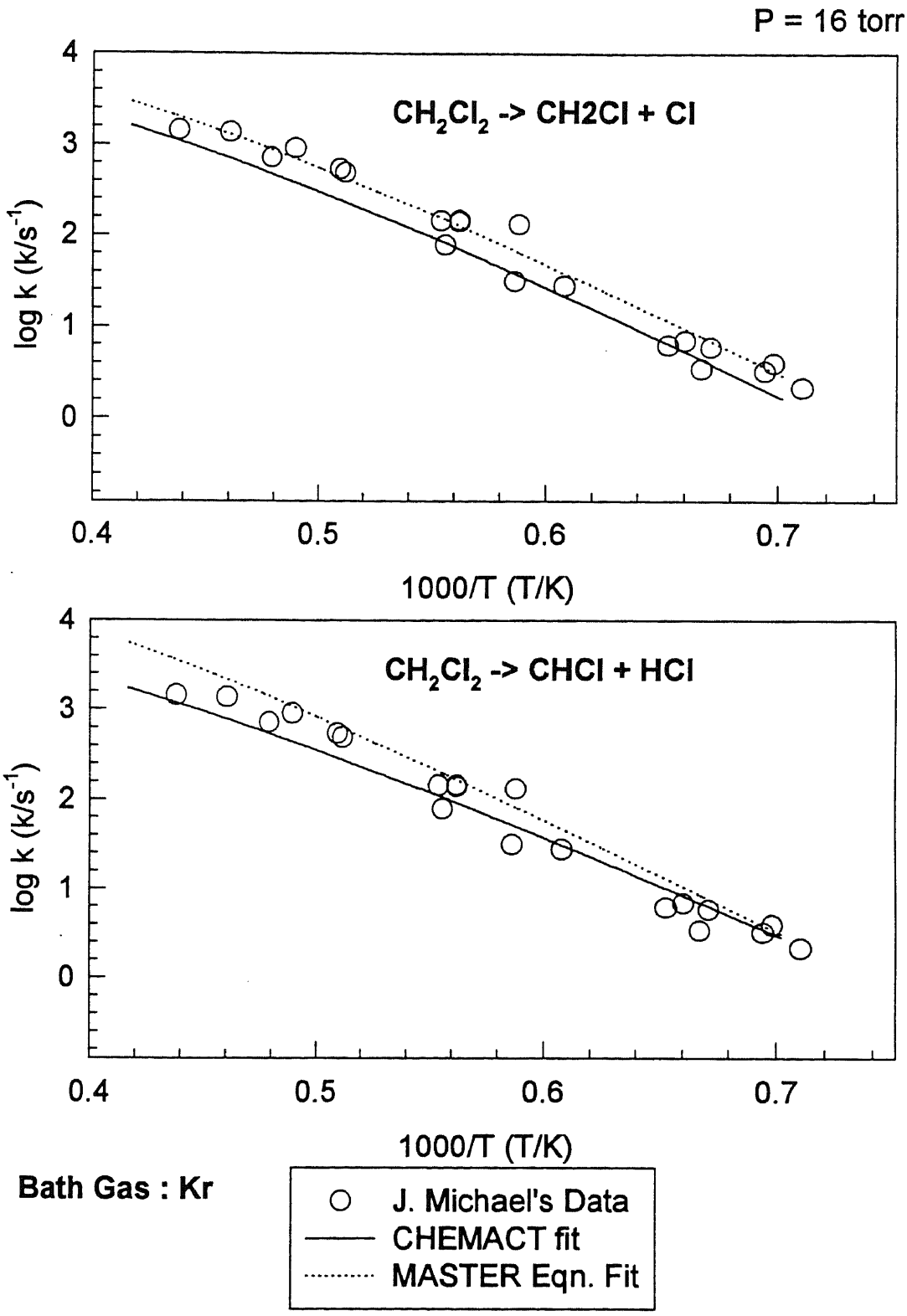

Figure C4 NJIT Analysis vs. Experimental Data of Lim et al.

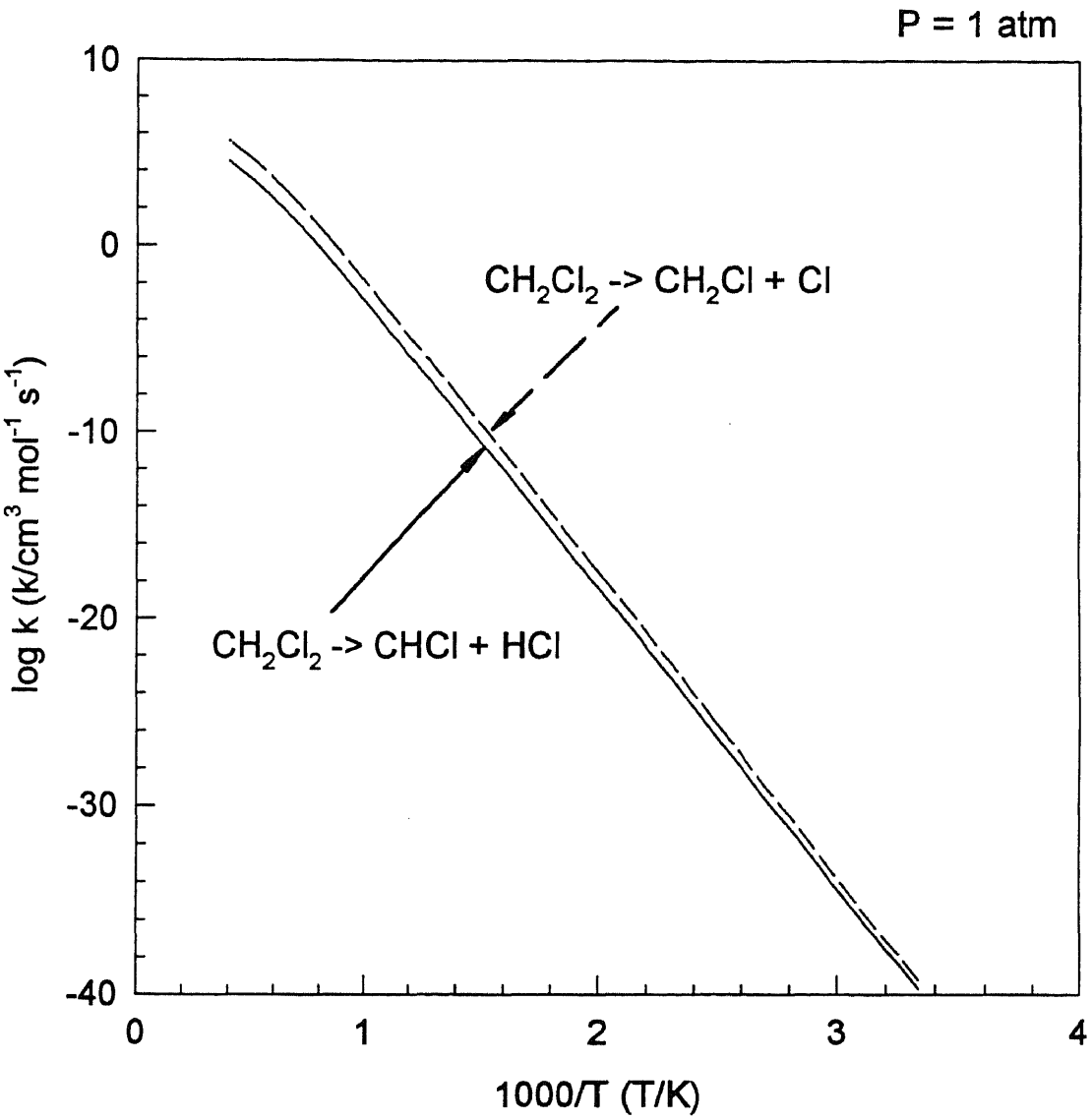

Figure C5 Results of Master Eqn. Analysis for CH_2Cl_2 Unimolecular Dissociation

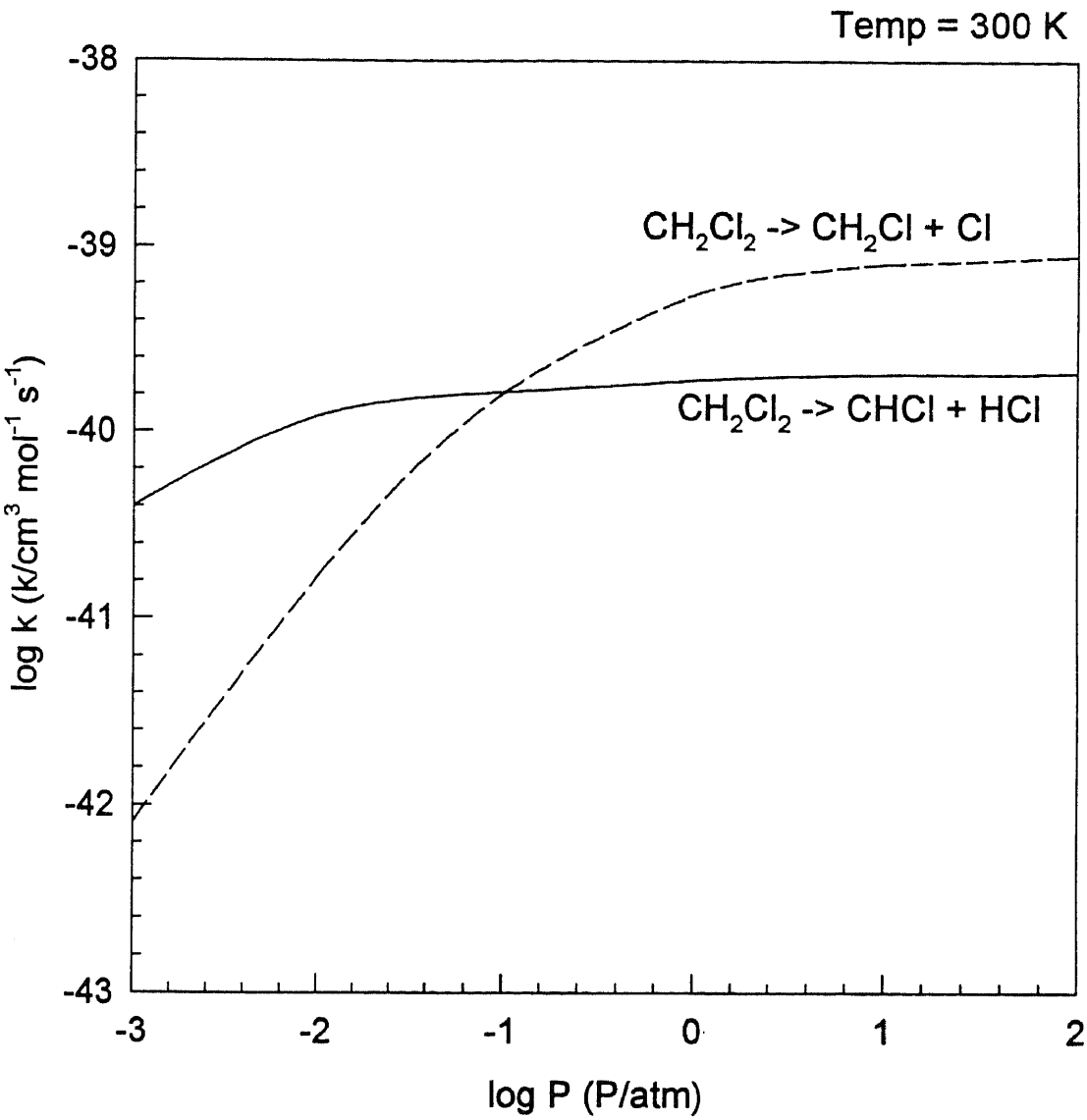

Figure C6 Results of Master Eqn. Analysis for CH_2Cl_2 Unimolecular Dissociation

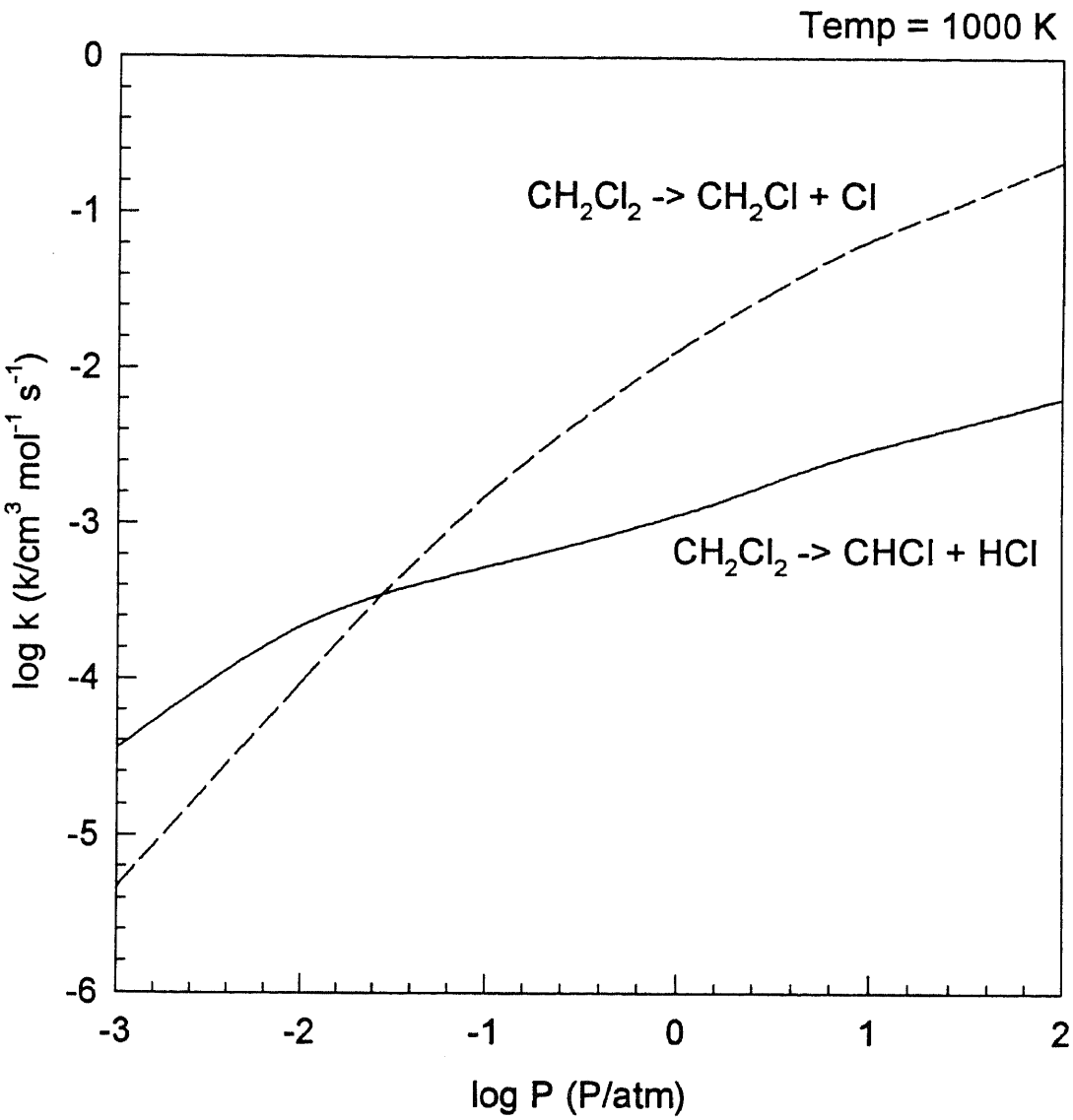

Figure C7 Results of Master Eqn. Analysis for CH_2Cl_2 Unimolecular Dissociation

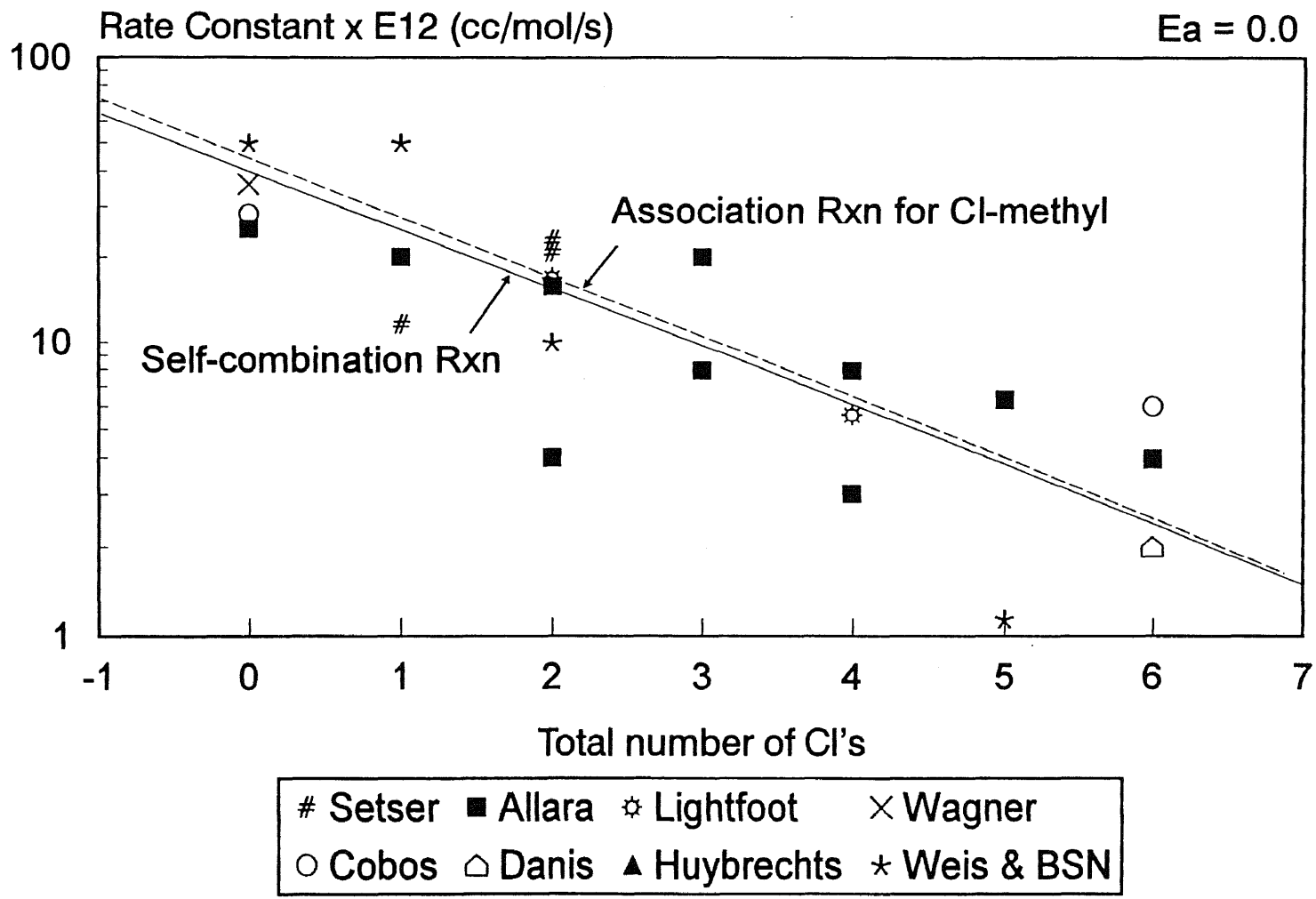

Figure D1 A Factor for Combination Reaction of Chloro-Methyl Radicals vs Number of Cl's

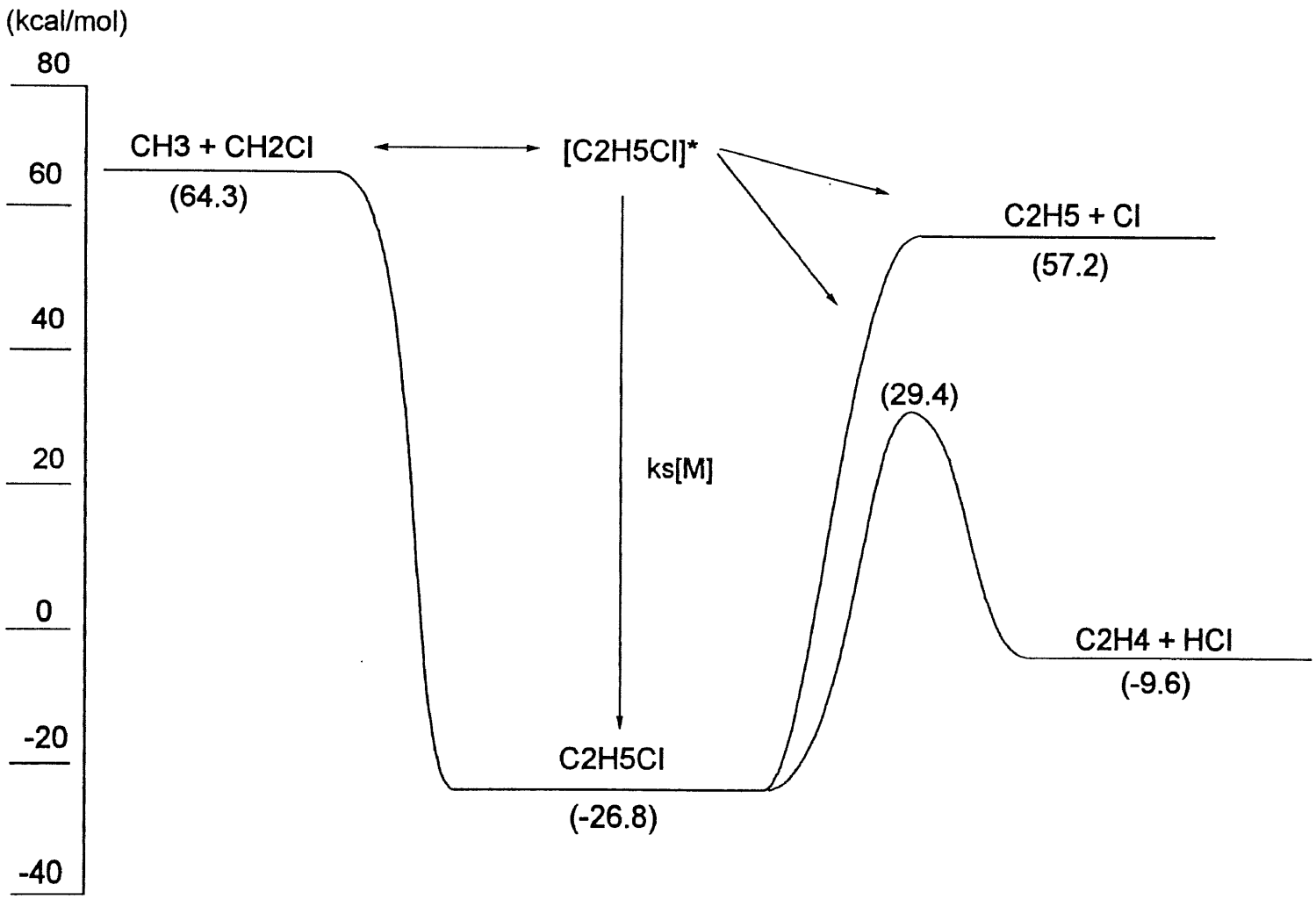

Figure D2 Potential Energy Diagram for
CH3 + CH2Cl ⟷ [C2H5Cl]* ⟶ Products

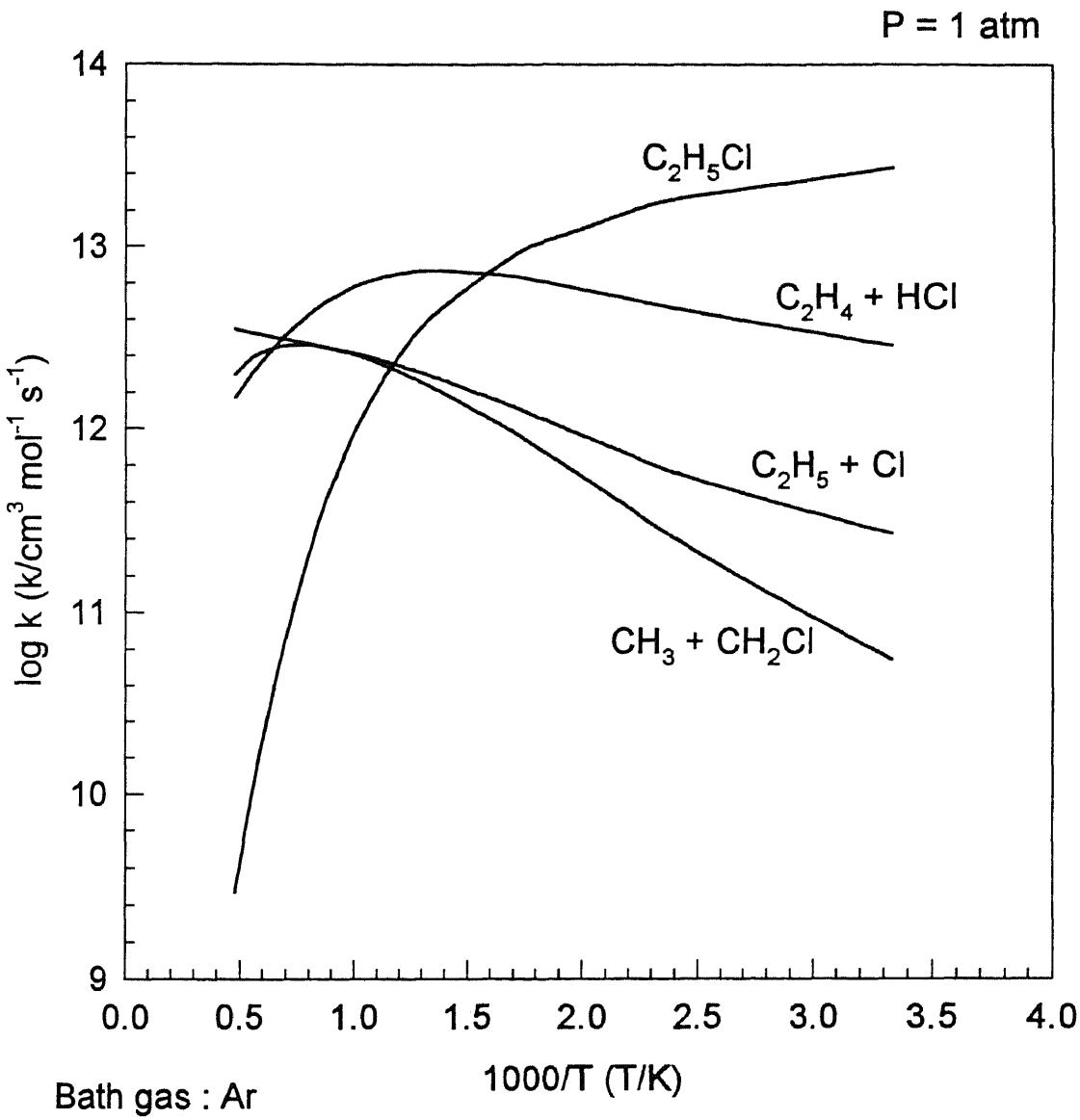

Figure D3 Results of QRRK Analysis
$CH_3 + CH_2Cl$ <=> $[C_2H_5Cl]^*$ => Products

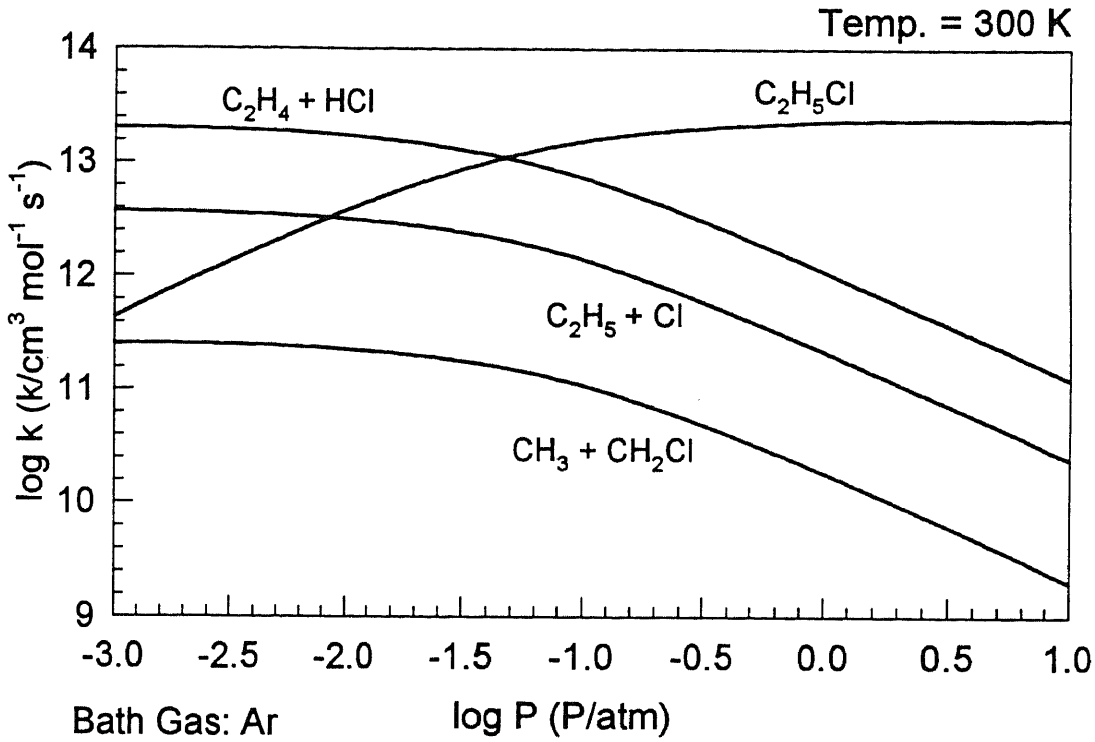

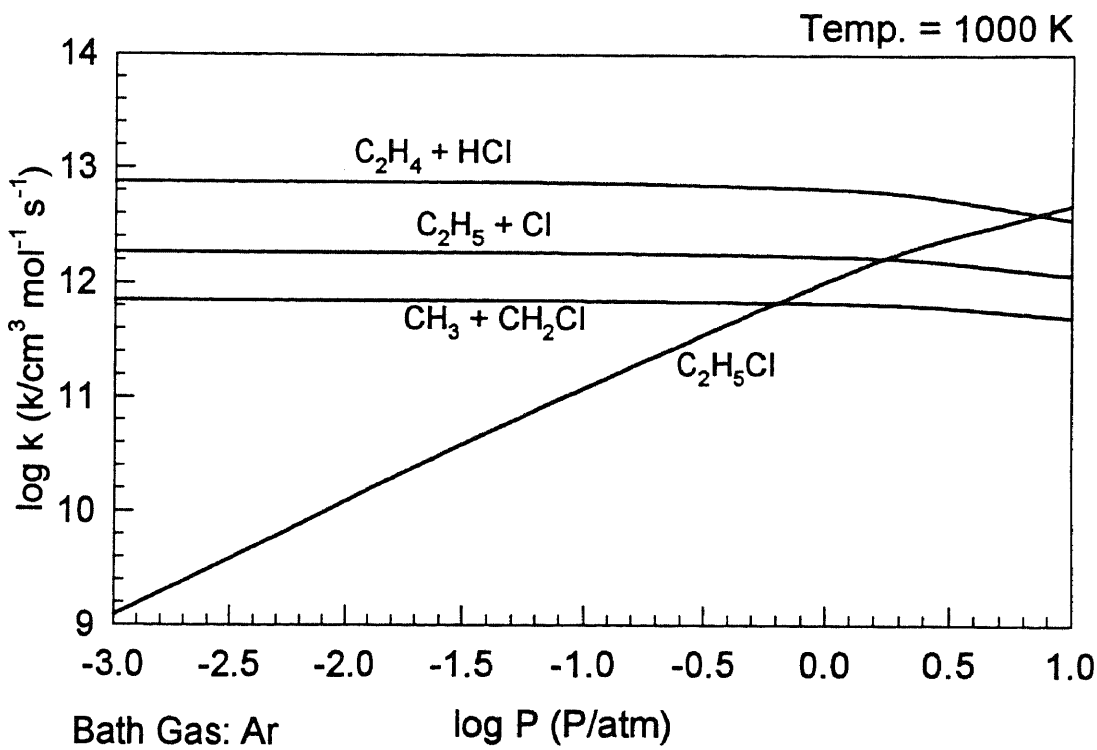

Figure D4 Results of QRRK Analysis
$CH_3 + CH_2Cl$ <=> $[C_2H_5Cl]^*$ => Products

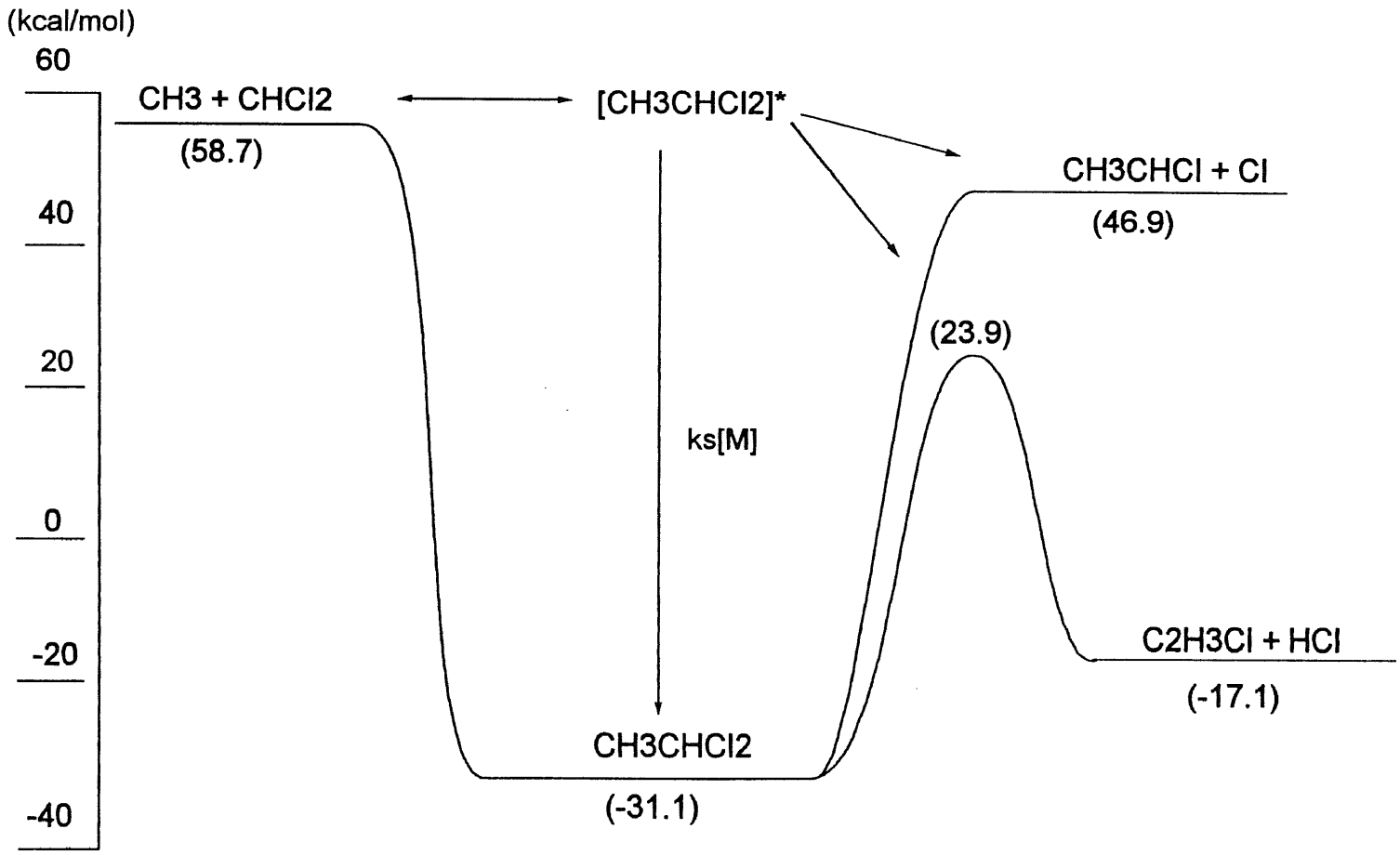

Figure D5 Potential Energy Diagram for
CH3 + CHCl2 ⟷ [CH3CHCl2]* ⟶ Products

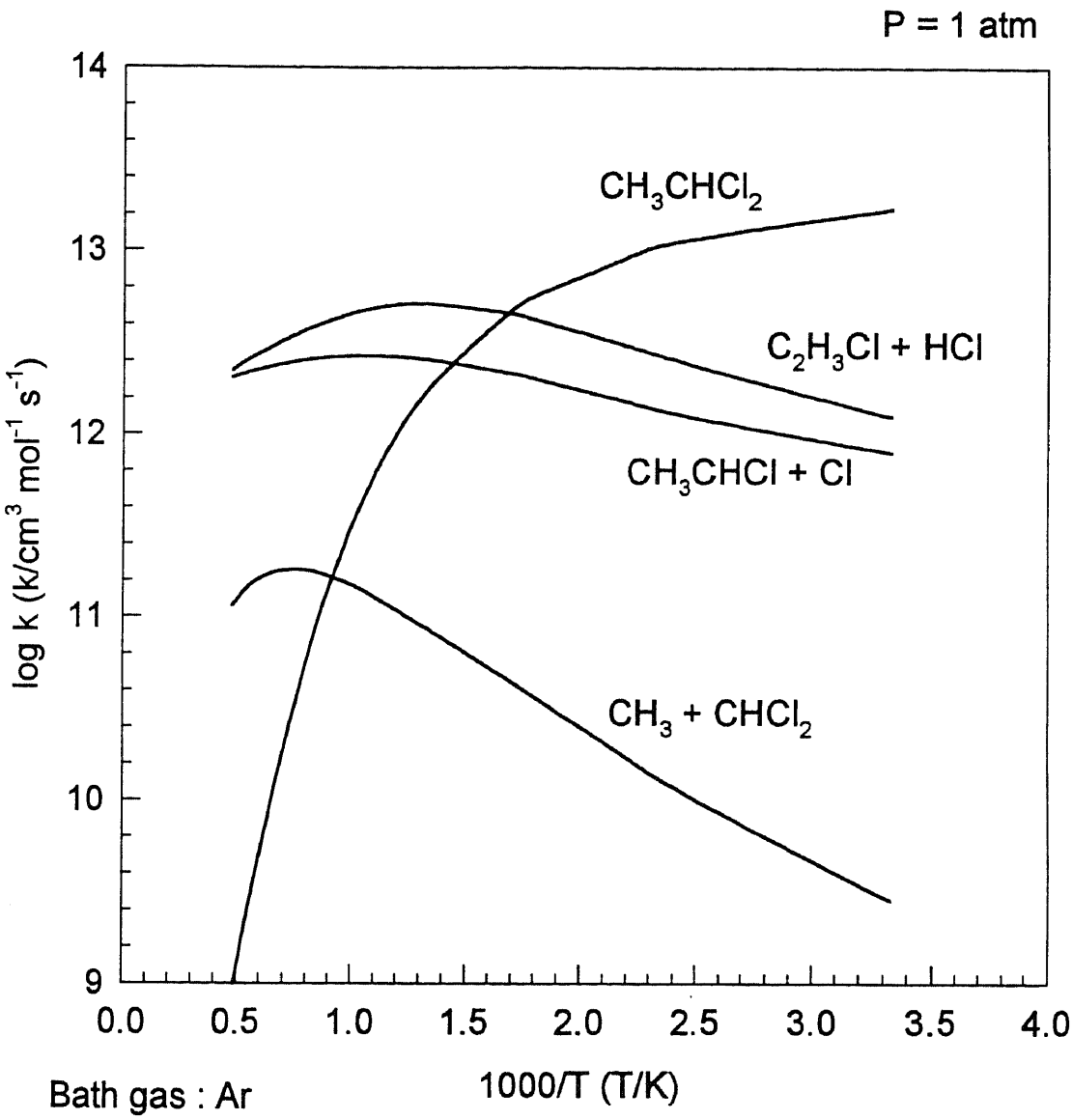

Figure D6 Results of QRRK Analysis
$CH_3 + CHCl_2$ <=> $[CH_3CHCl_2]^*$ => Products

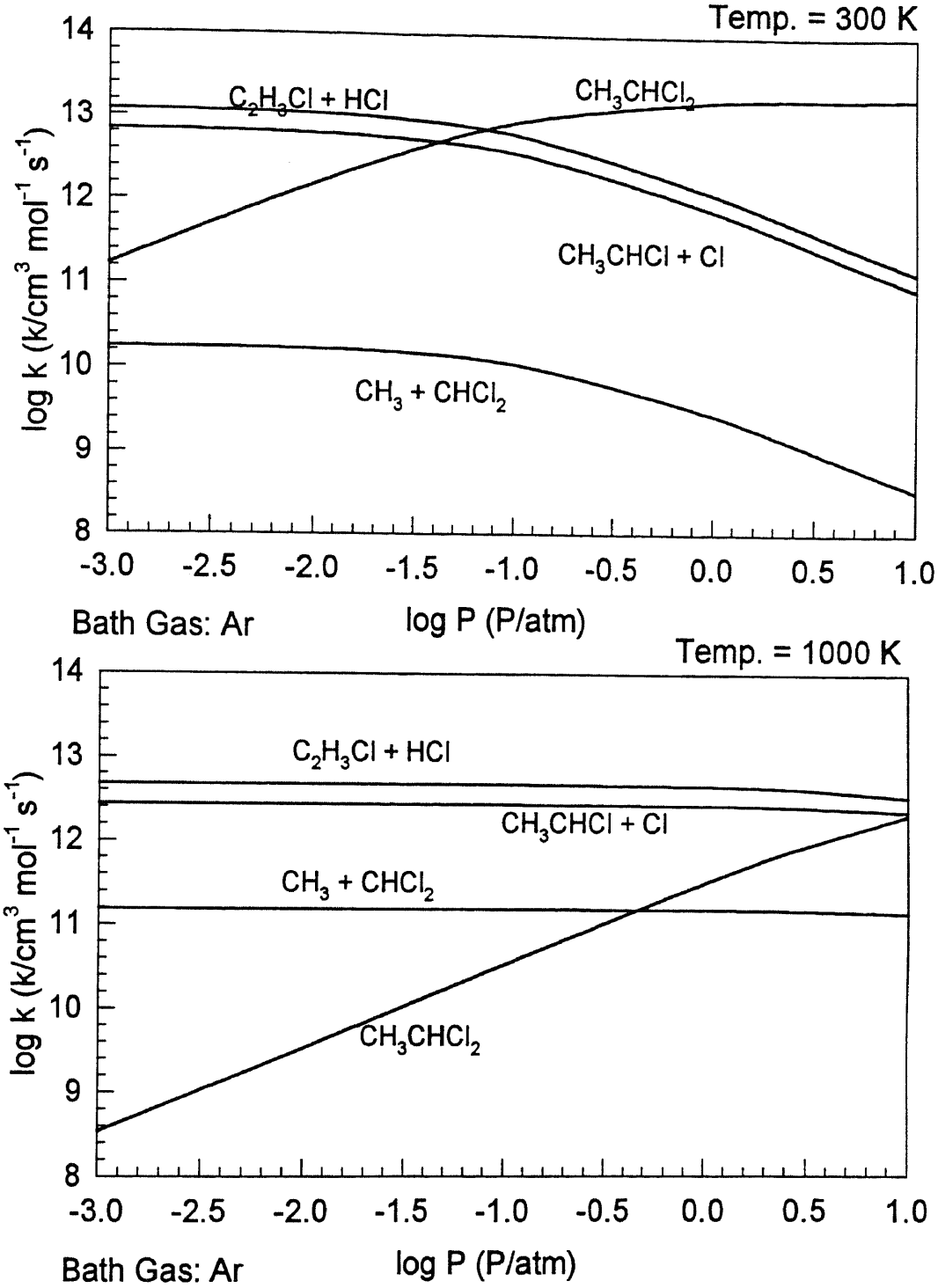

Figure D7 Results of QRRK Analysis
$CH_3 + CHCl_2 \Leftrightarrow [CH_3CHCl_2]^* \Rightarrow$ Products

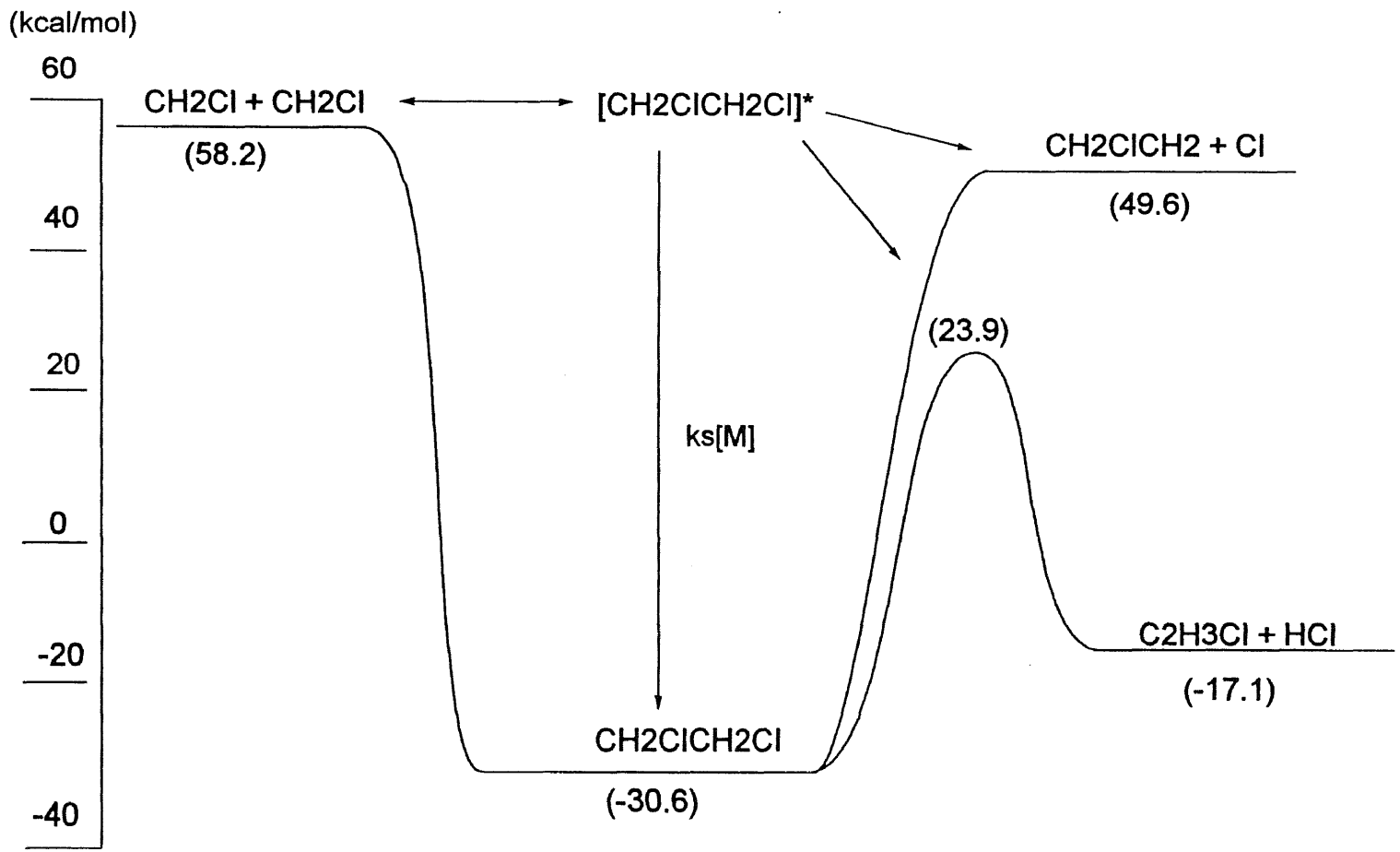

Figure D8 Potential Energy Diagram for
CH2Cl + CH2Cl ⟷ [CH2ClCH2Cl]* ⟶ Products

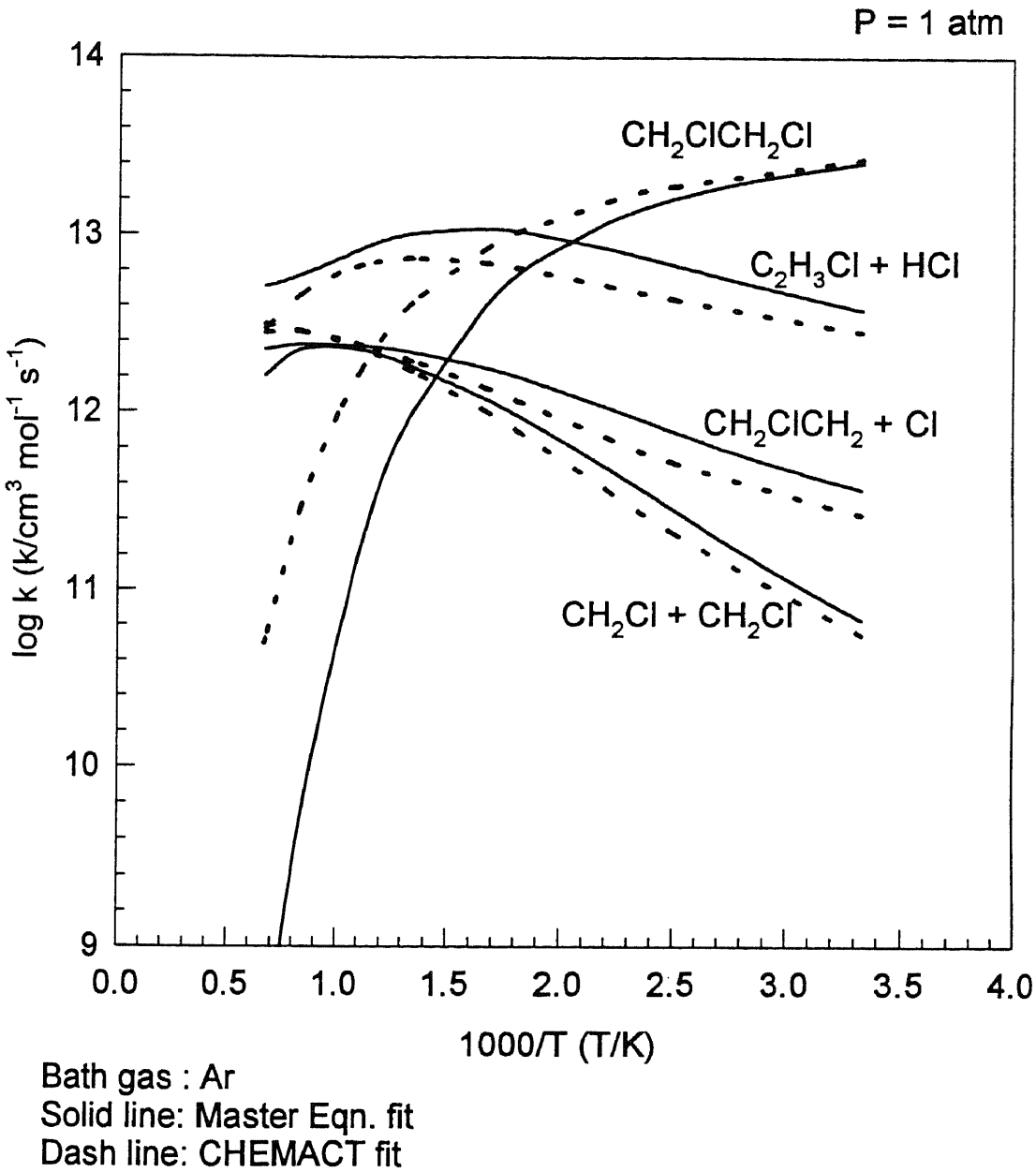

Bath gas : Ar
Solid line: Master Eqn. fit
Dash line: CHEMACT fit

Figure D9 Results of QRRK and Master Eqn. Analysis
$CH_2Cl + CH_2Cl$ <=> $[CH_2ClCH_2Cl]^*$ => Products

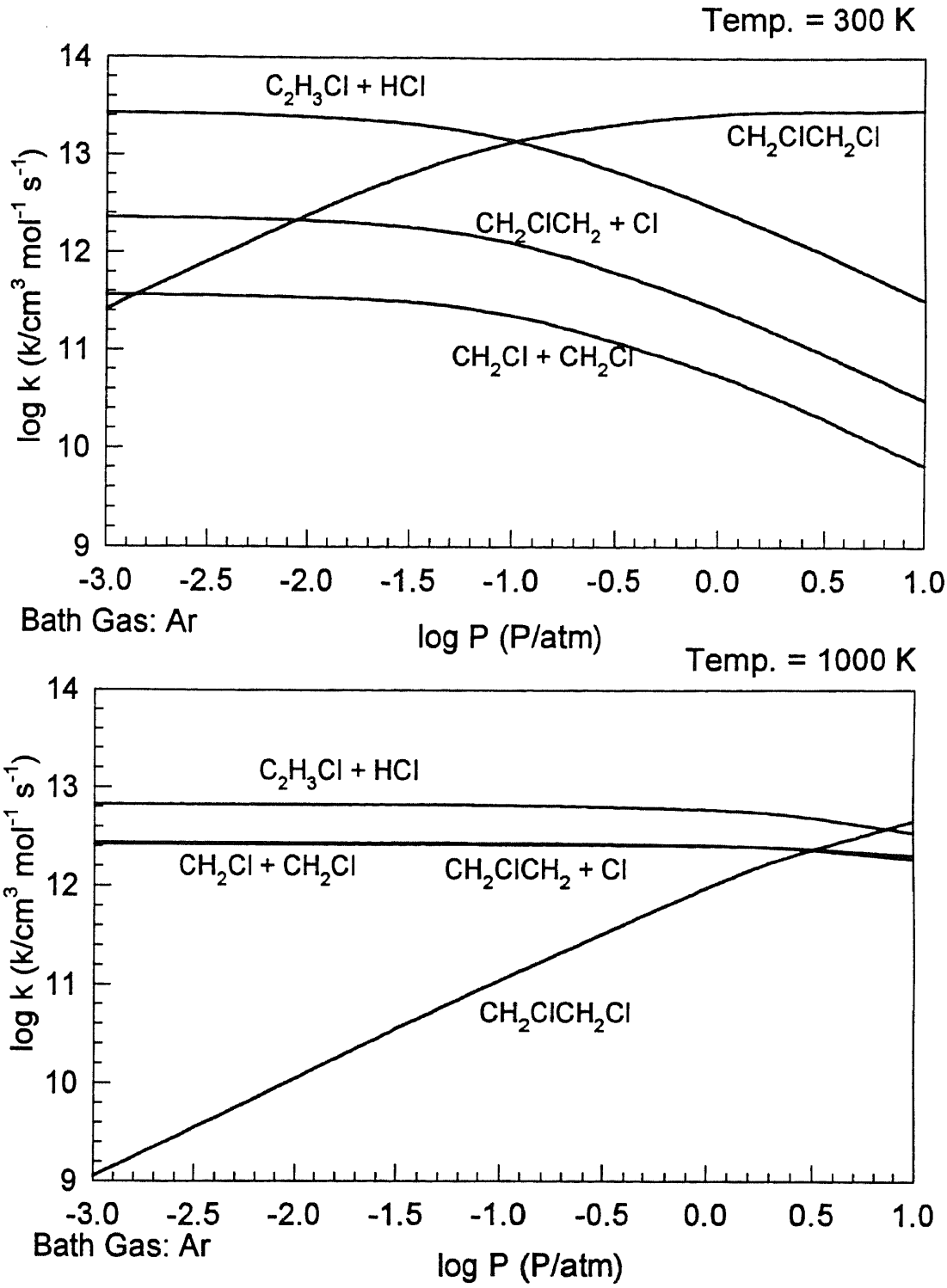

Figure D10 Results of QRRK Analysis
$CH_2Cl + CH_2Cl$ <=> $[CH_2ClCH_2Cl]^*$ => Products

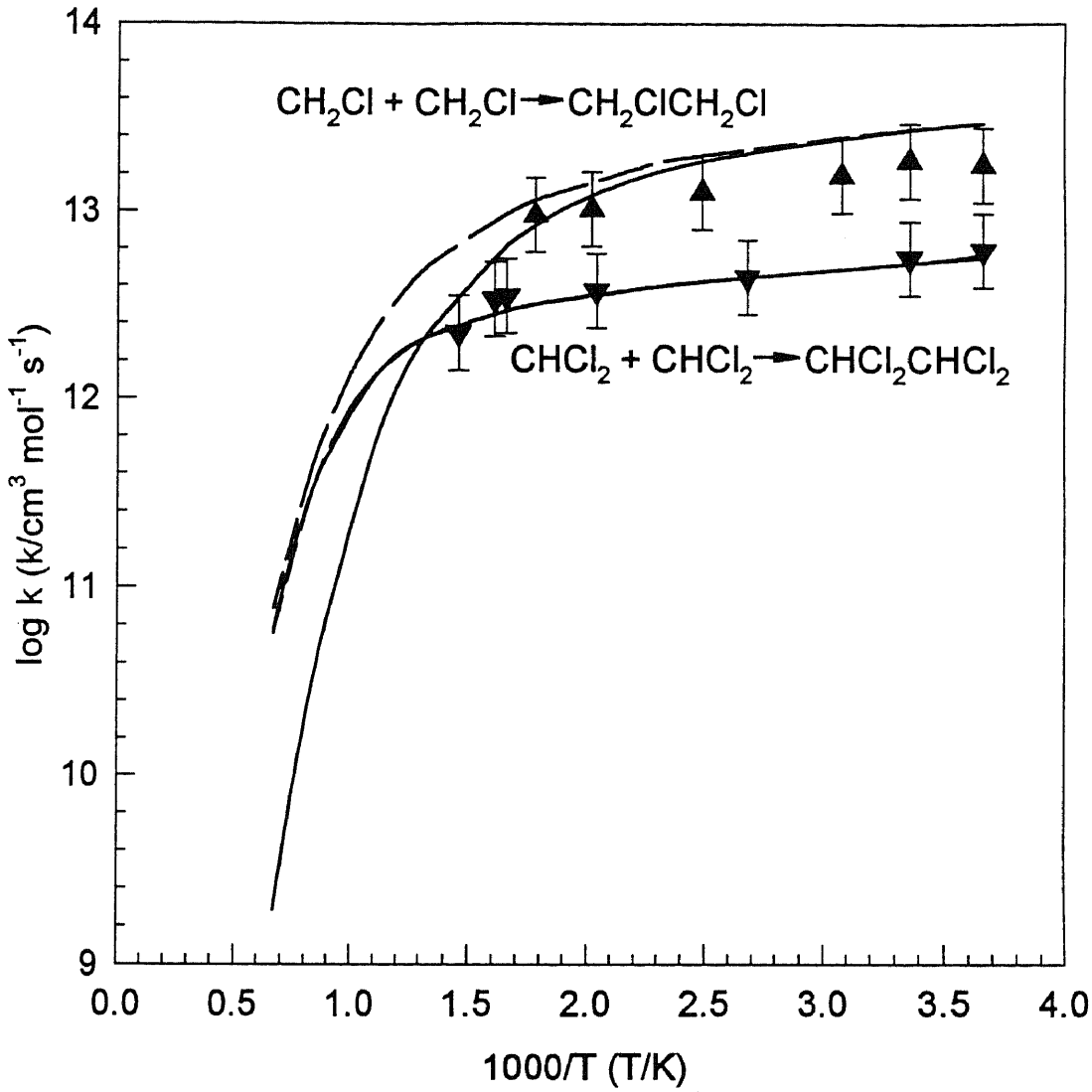

Bath gas : N_2
Symbol: Roussel et al. (1991)
Solid line: Master Eqn. fit
Dash line: CHEMACT fit

Figure D11 Comparison of QRRK and Master Eqn. Calculation to Data of Roussel et al. for CH_2Cl and $CHCl_2$ Self-Combination

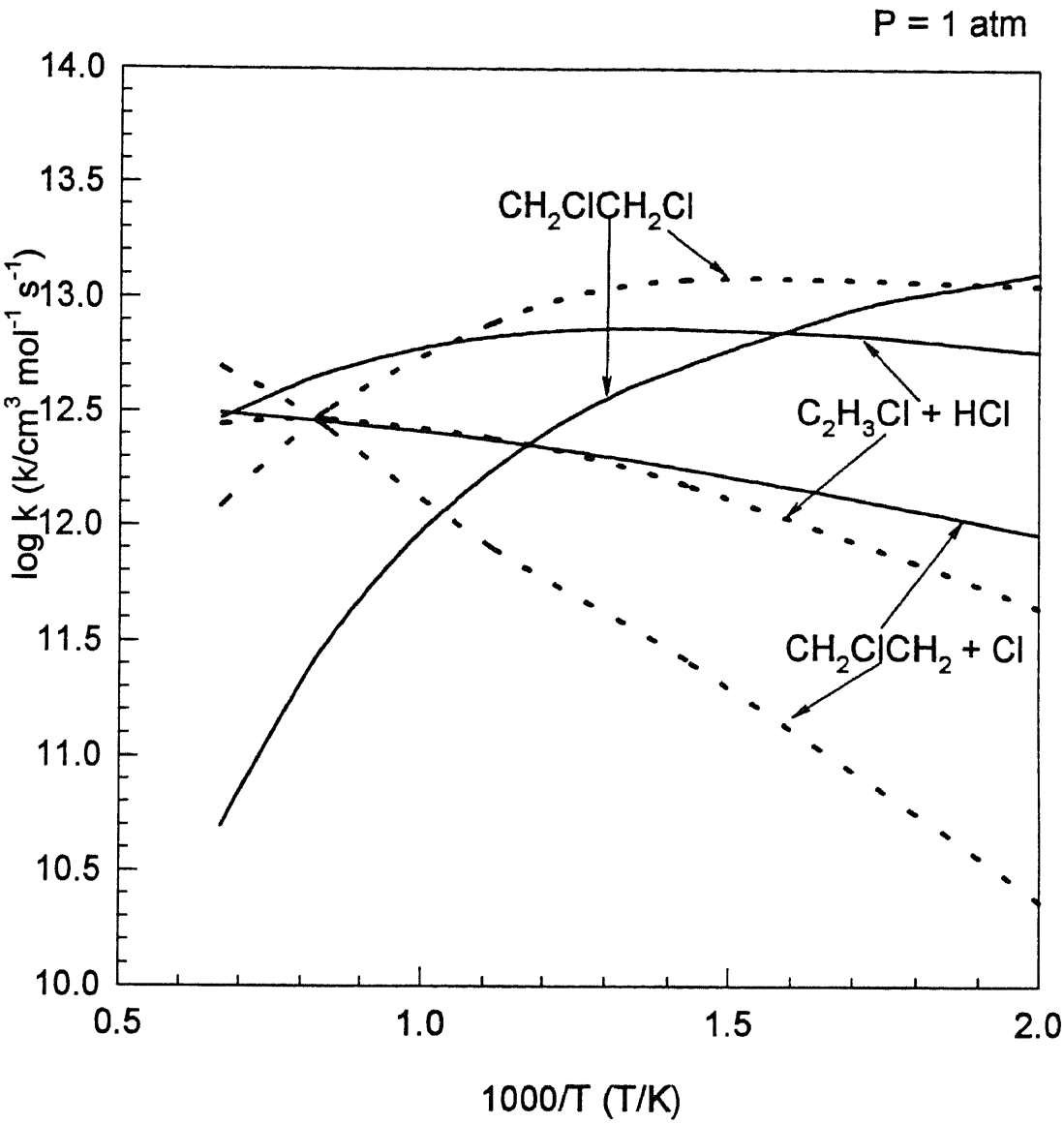

Bath gas : Ar
Dash line : Senkan et al. (1988)
Solid line : this study

Figure D12 Comparison of QRRK Calculation to Calculation of Senkan et al. : $CH_2Cl + CH_2Cl \Leftrightarrow [CH_2ClCH_2Cl]^* \Rightarrow$ Products

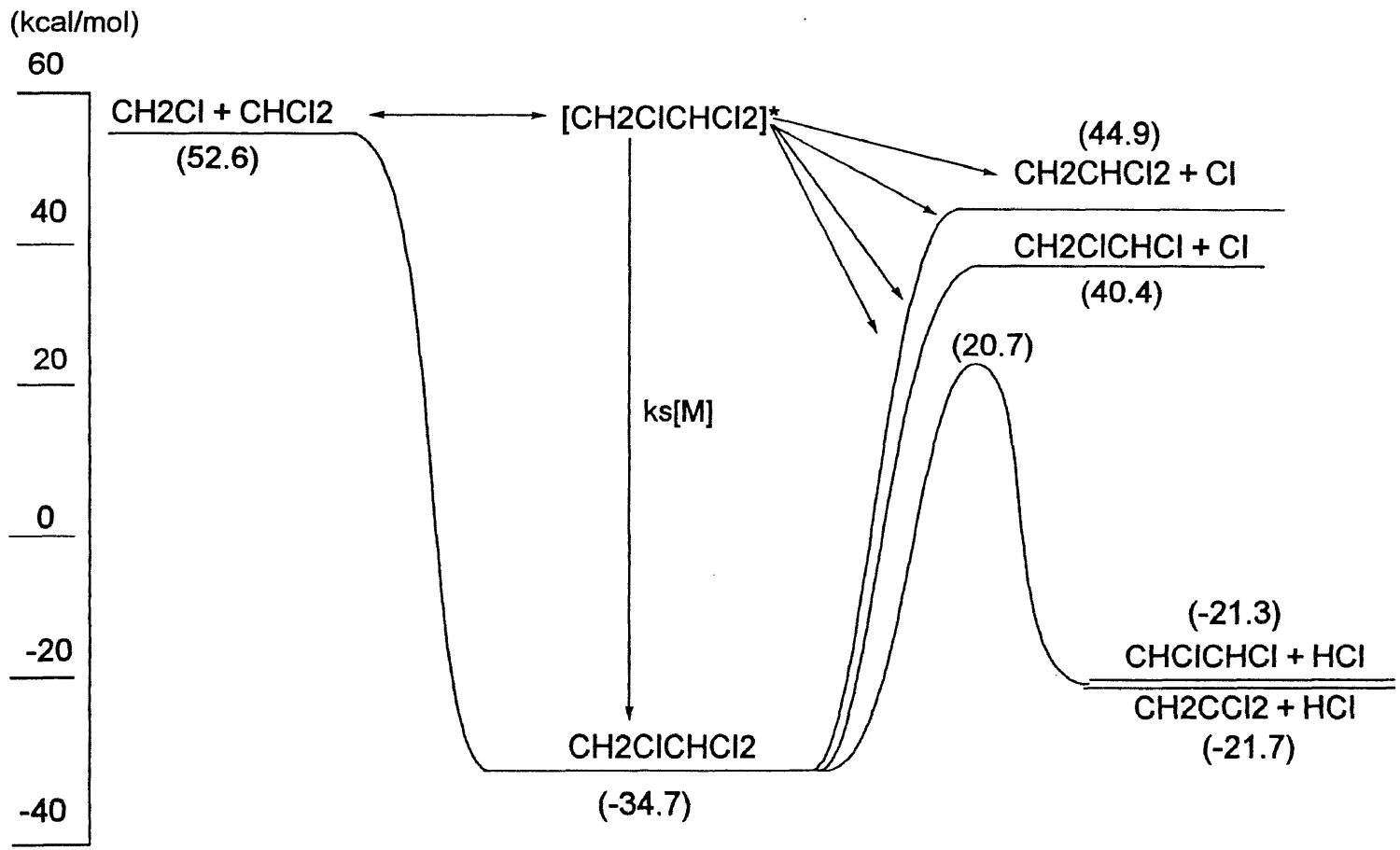

Figure D13 Potential Energy Diagram for
CH2Cl + CHCl2 ⟷ [CH2ClCHCl2]* ⟶ Products

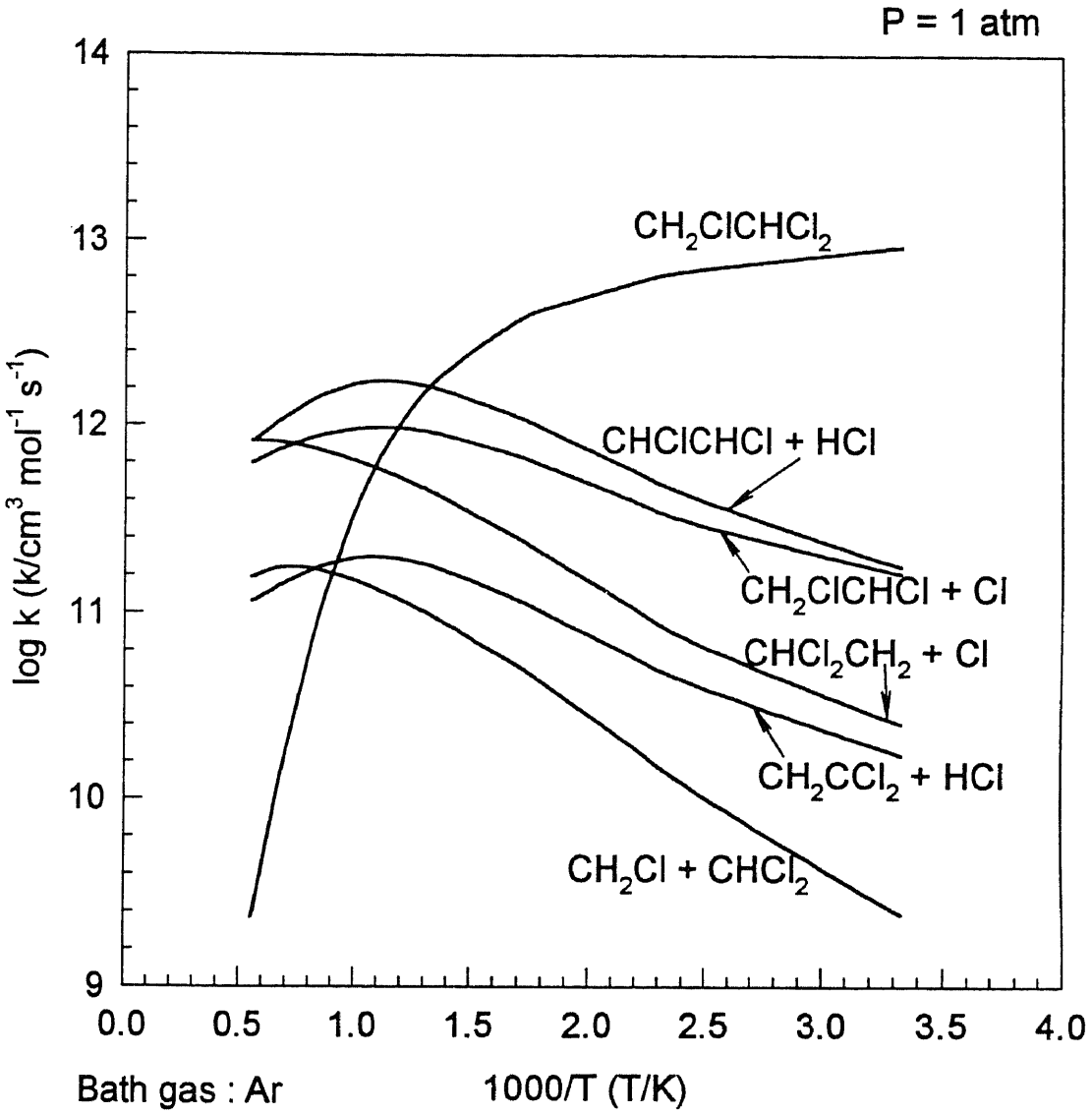

Figure D14 Results of QRRK Analysis
$CH_2Cl + CHCl_2$ <=> $[CH_2ClCHCl_2]^*$ => Products

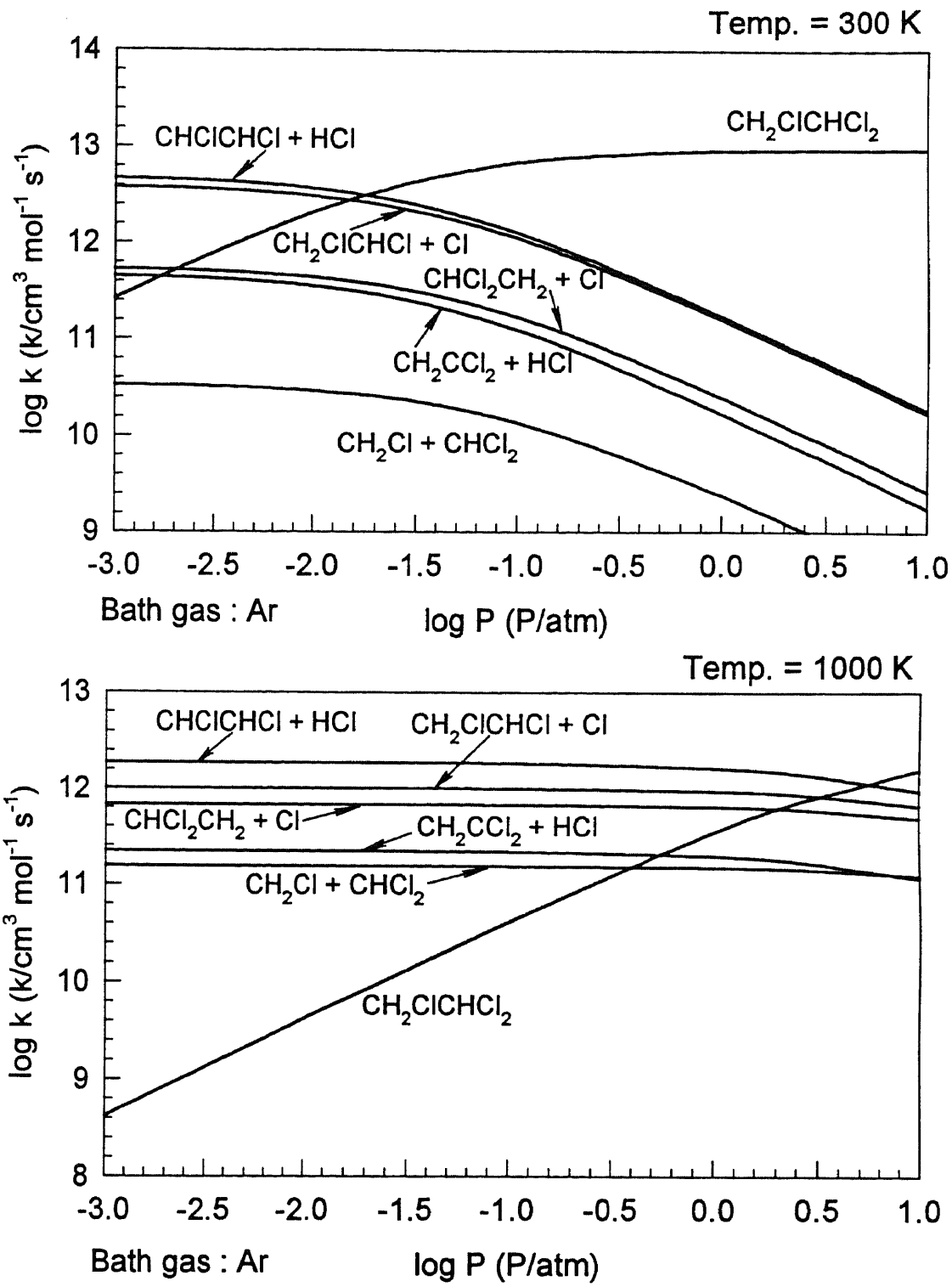

Figure D15 Results of QRRK Analysis
$CH_2Cl + CHCl_2 \Leftrightarrow [CH_2ClCHCl_2]^* \Rightarrow$ Products

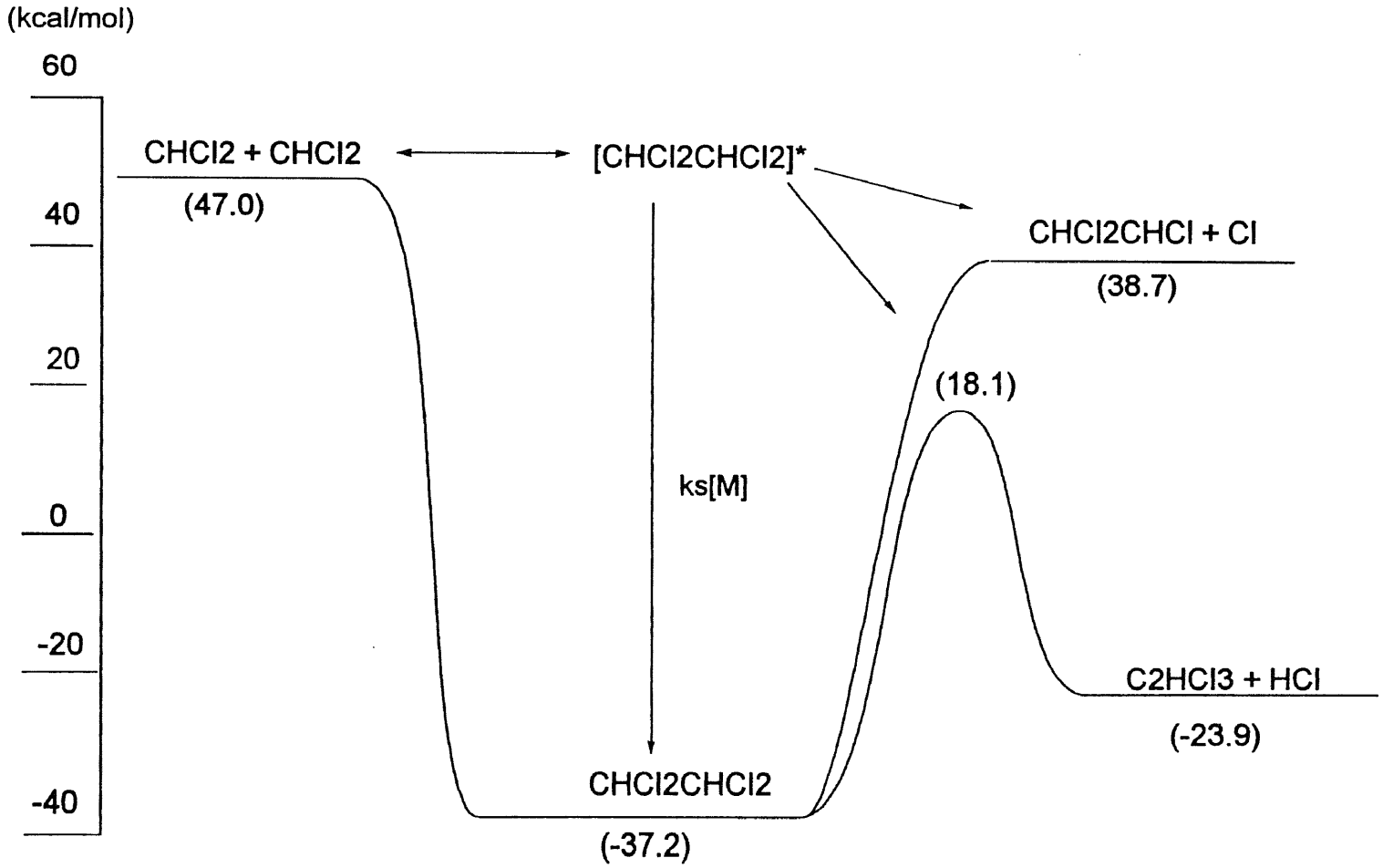

Figure D16 Potential Energy Diagram for
CHCl2 + CHCl2 ⟷ [CHCl2CHCl2]* ⟶ Products

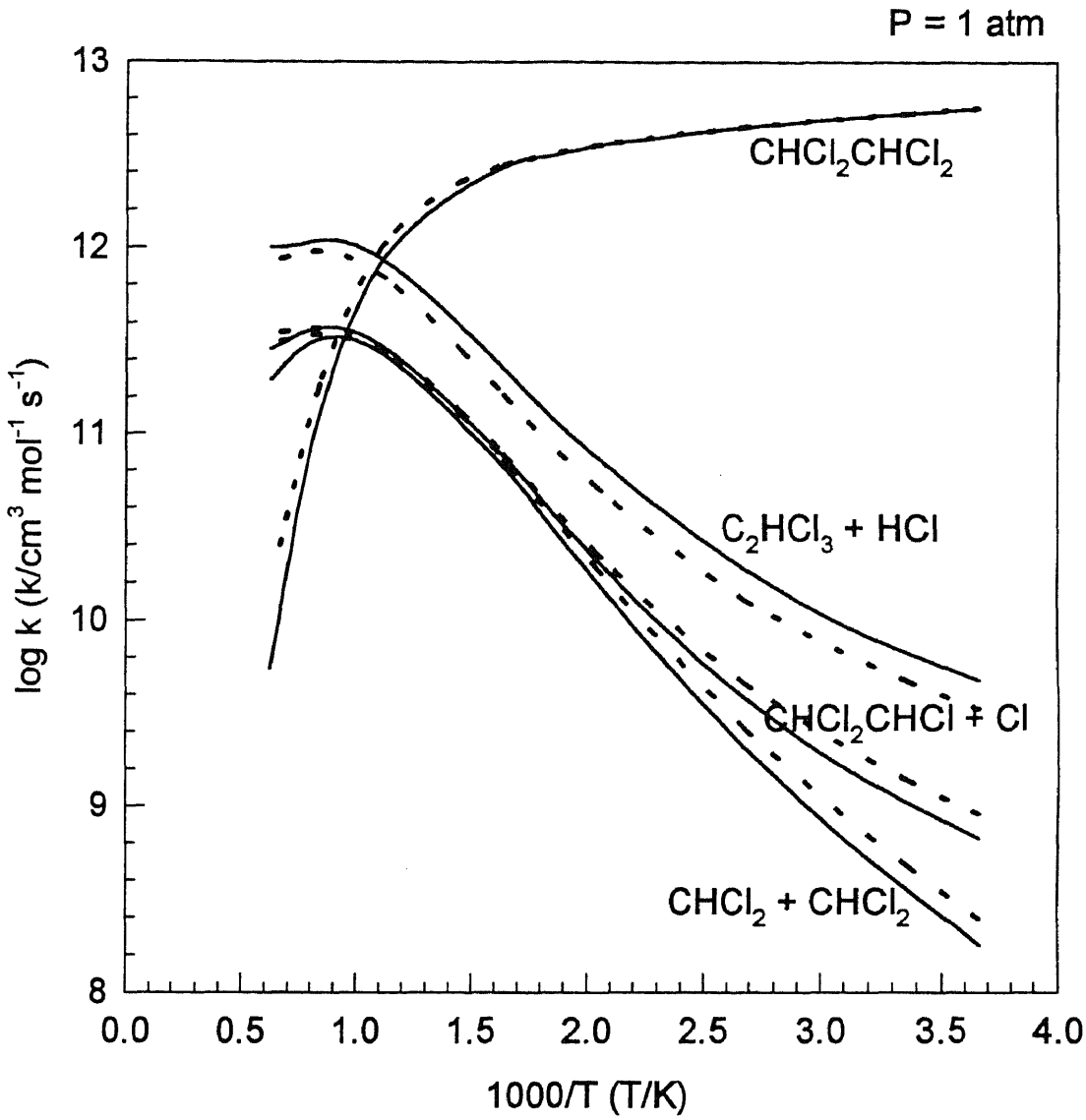

Bath gas : Ar
Solid line: Master Eqn. fit
Dash line: CHEMACT fit

Figure D17 Results of QRRK and Master Eqn. Analysis
$CHCl_2 + CHCl_2$ <=> $[CHCl_2CHCl_2]^*$ => Products

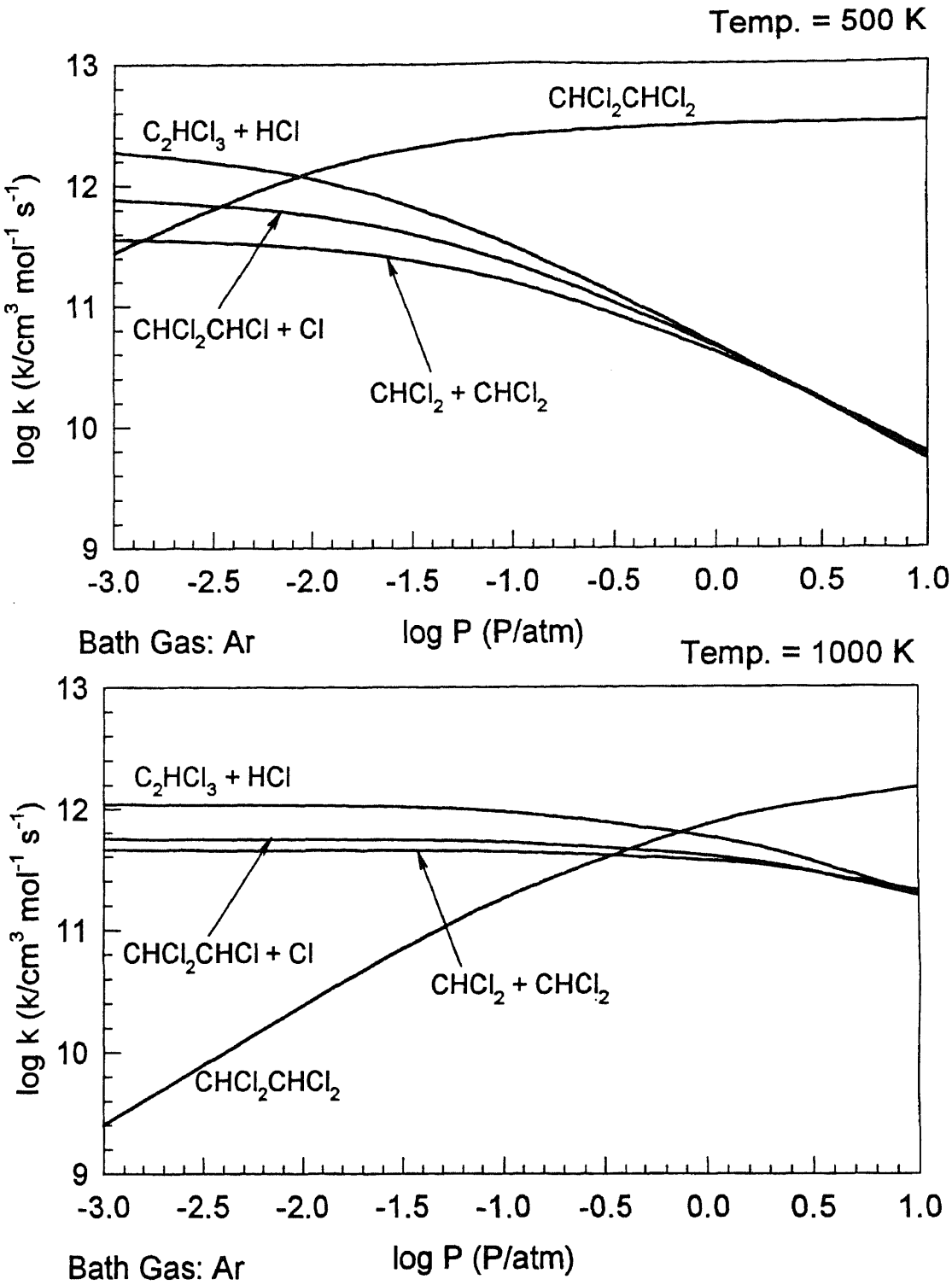

Figure D18 Results of QRRK Analysis
$CHCl_2 + CHCl_2 \Leftrightarrow [CHCl_2CHCl_2]^* \Rightarrow$ Products

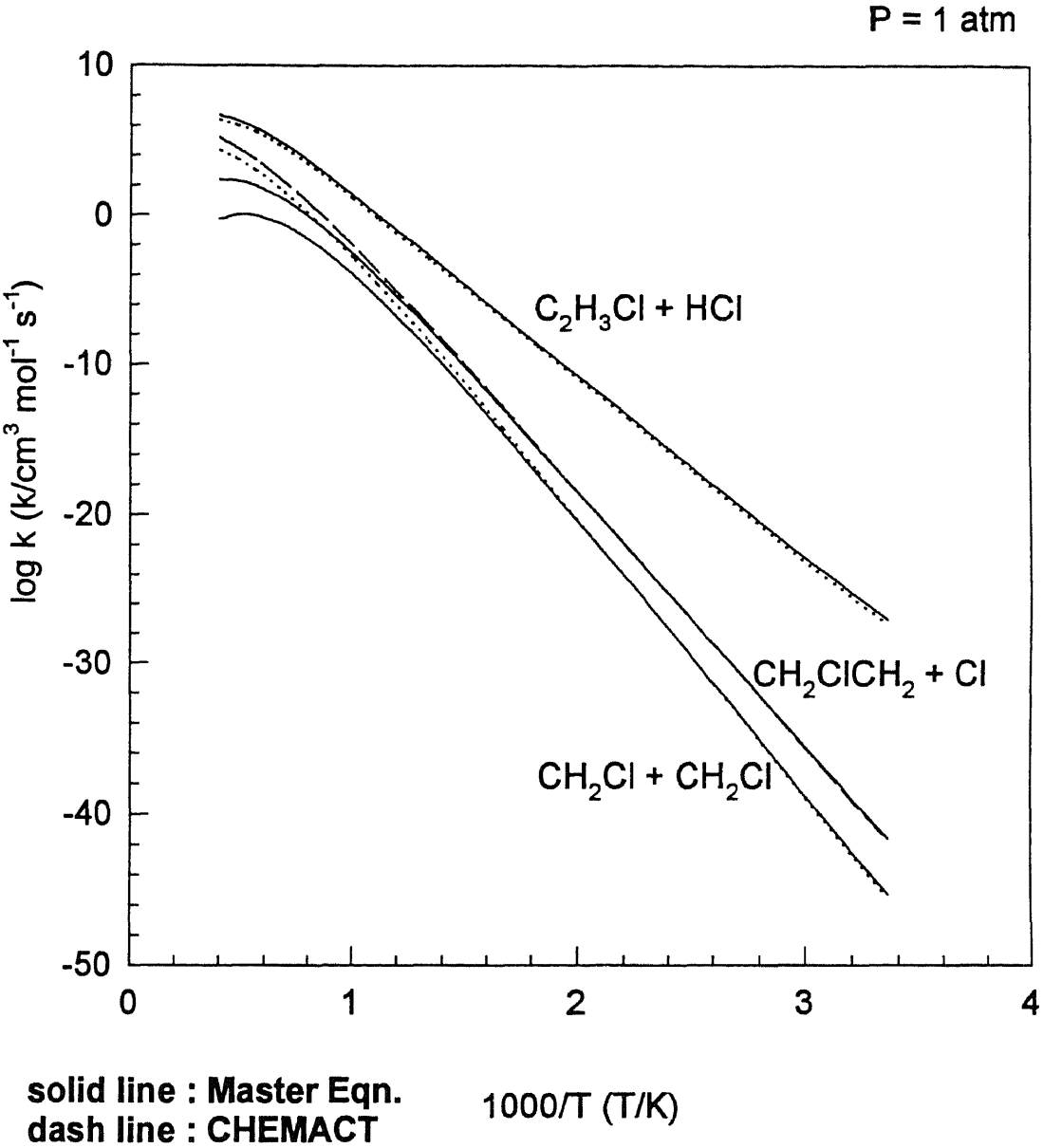

Figure D19 Results of CHEMACT and Master Eqn. CH_2ClCH_2Cl Unimolecular Dissociation

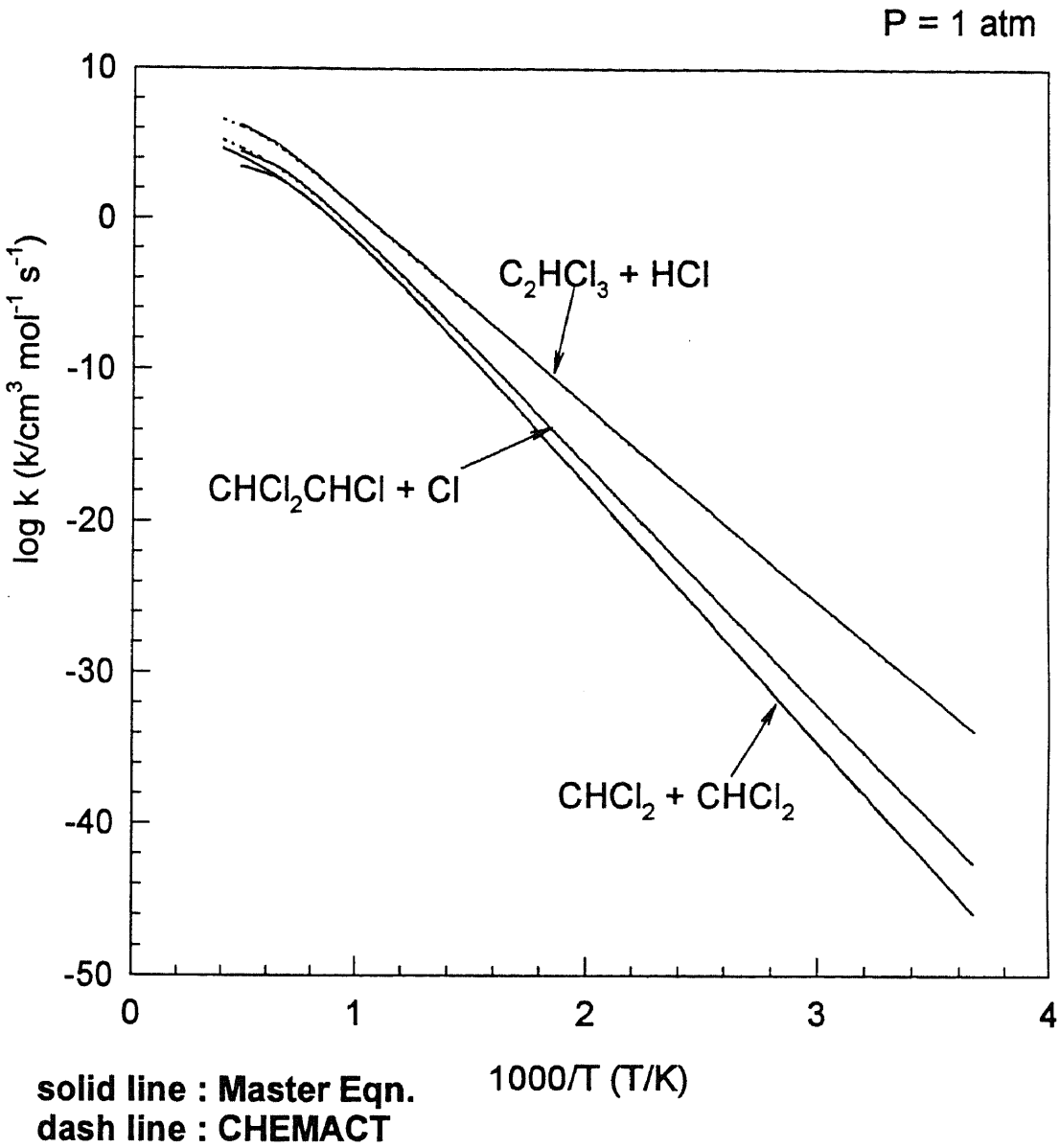

Figure D20 Results of CHEMACT and Master Eqn.
$CHCl_2CHCl_2$ Unimolecular Dissociation

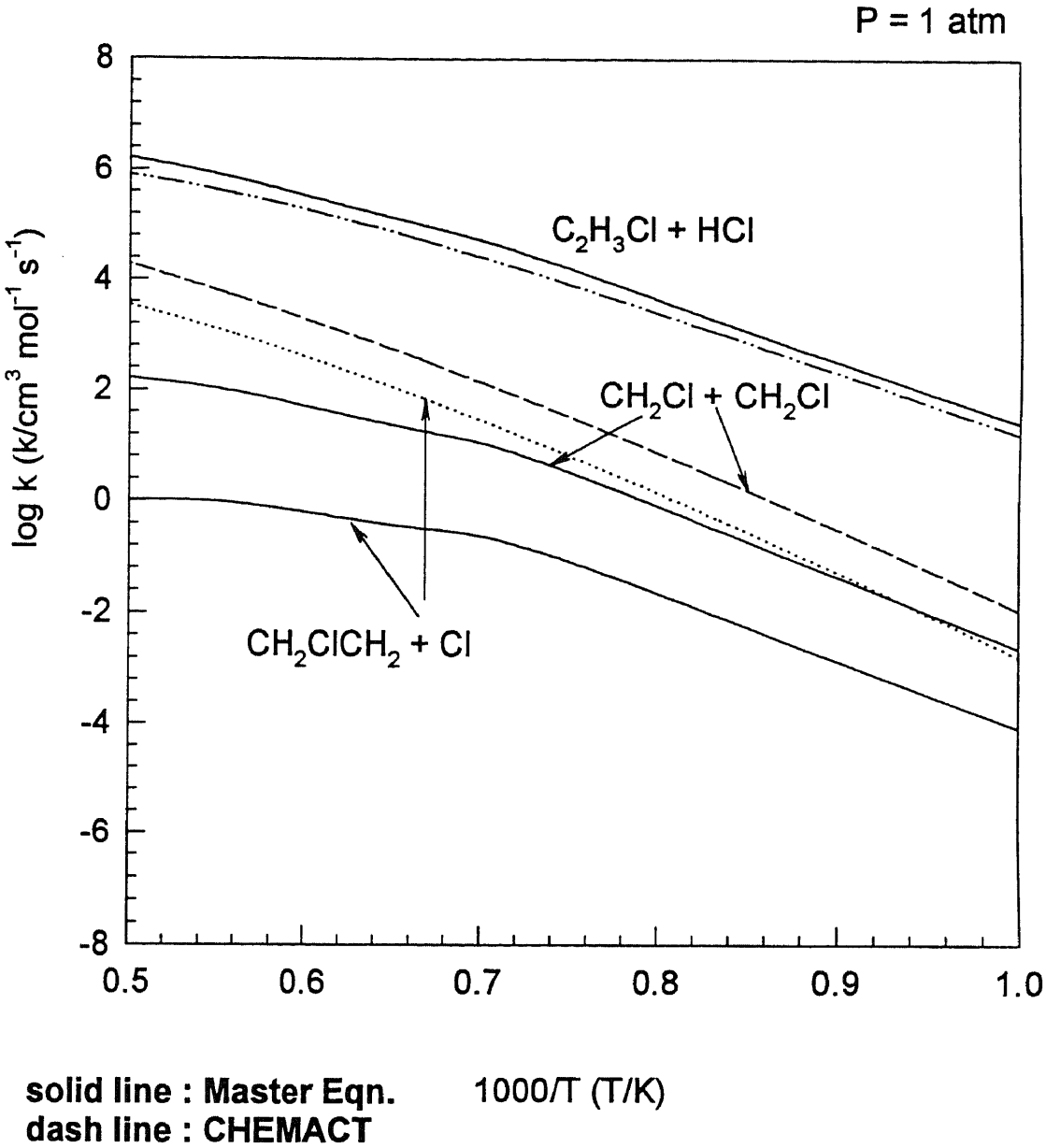

Figure D21 CH_2ClCH_2Cl Unimolecular Dissociation

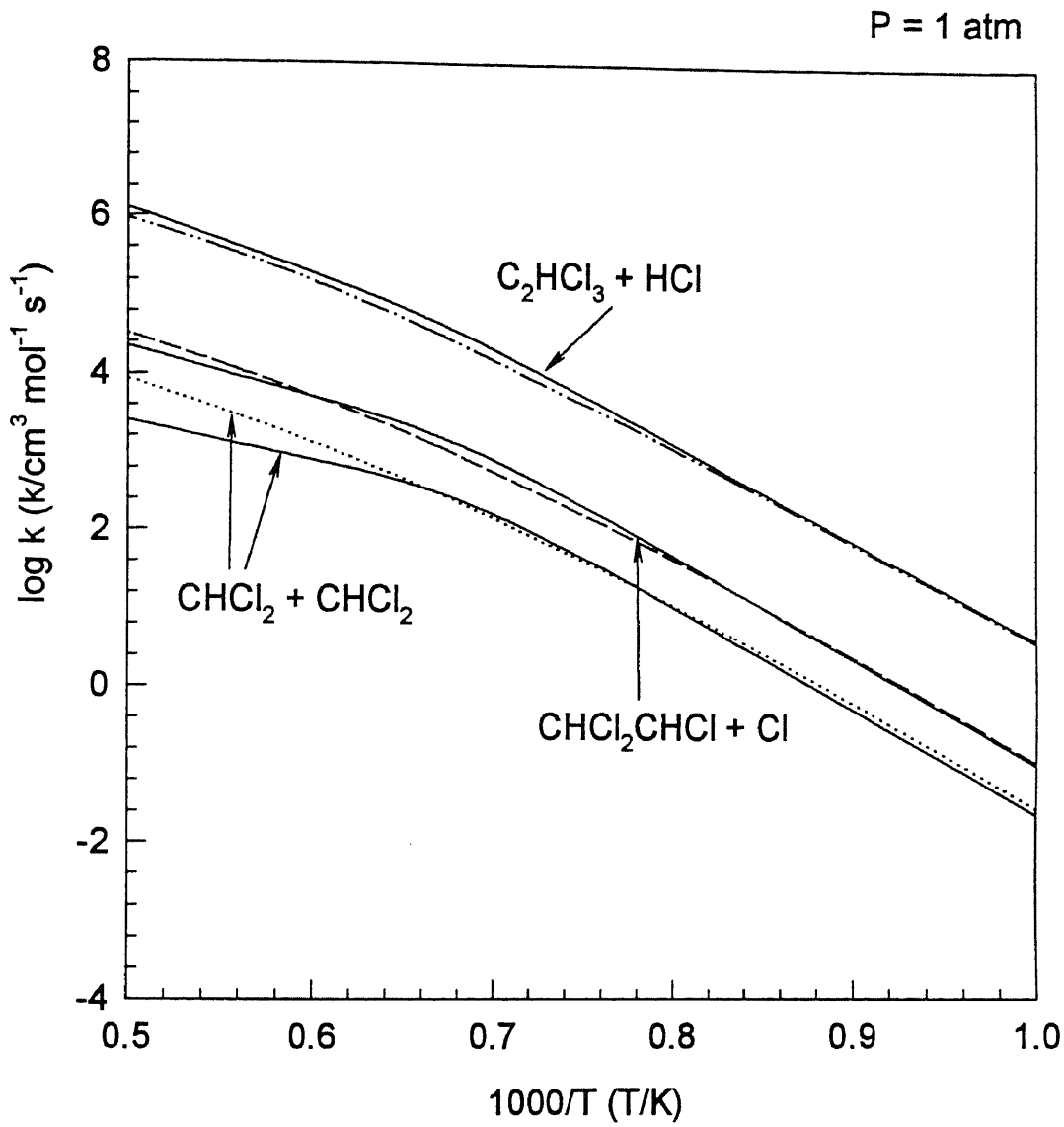

solid line : Master Eqn.
dash line : CHEMACT

Figure D22 $CHCl_2CHCl_2$ Unimolecular Dissociation

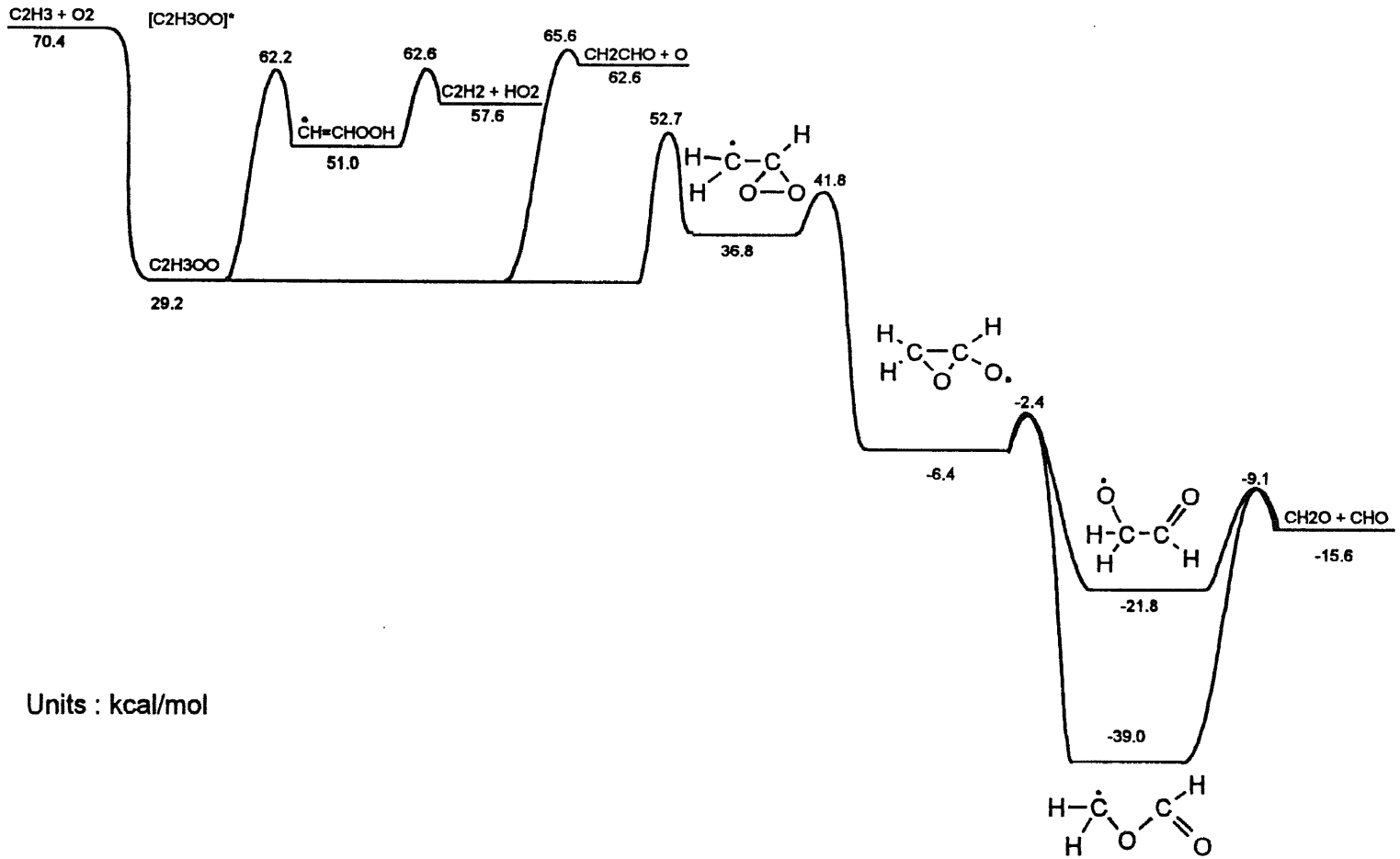

Figure E1 Potential Energy Diagram for
C2H3 + O2 ⟷ [C2H3OO]* ⟶ Products

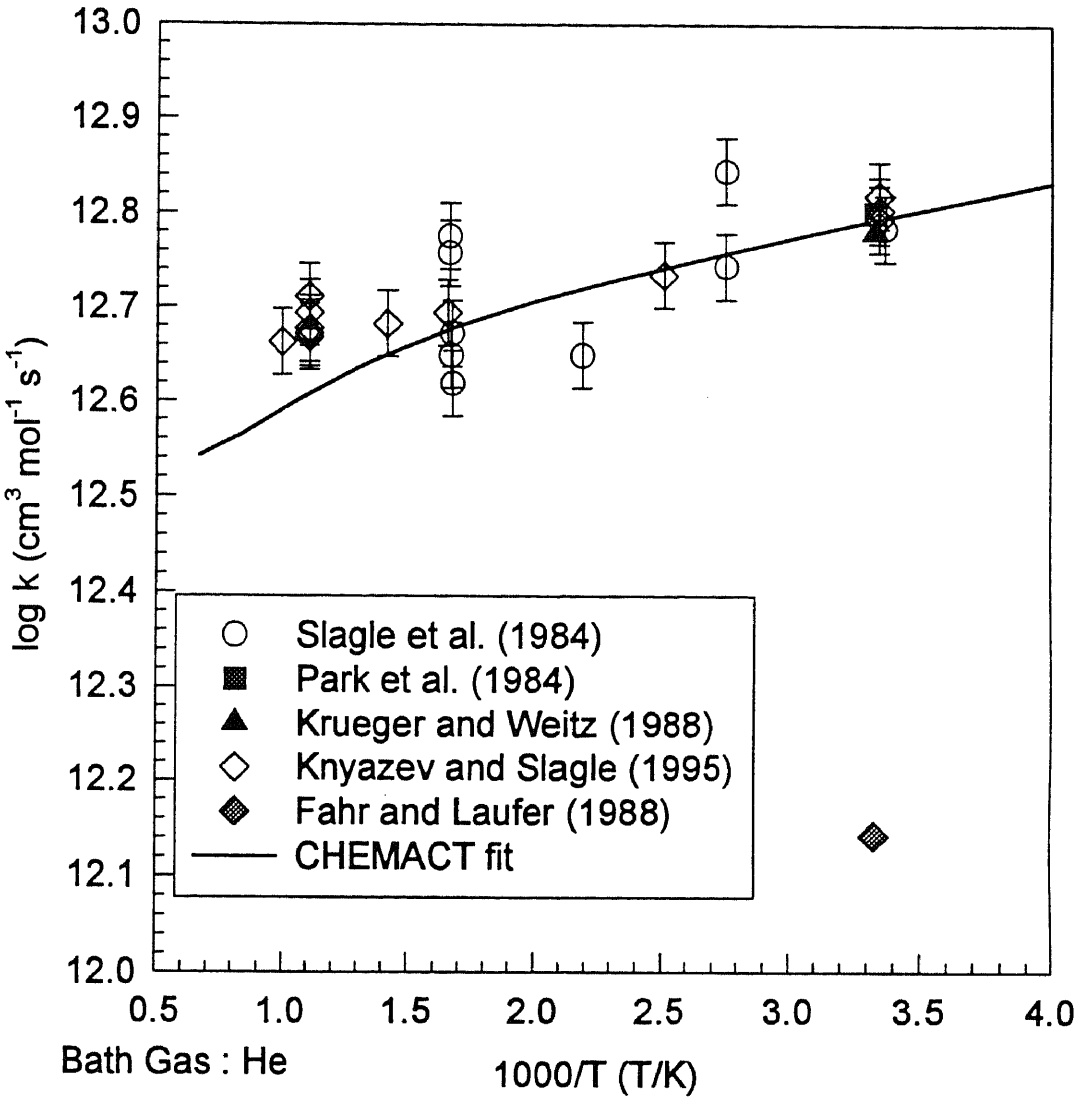

Figure E2 Comparison of Predicted values with Experiments
Vinyl + O_2 $\longrightarrow$ Products

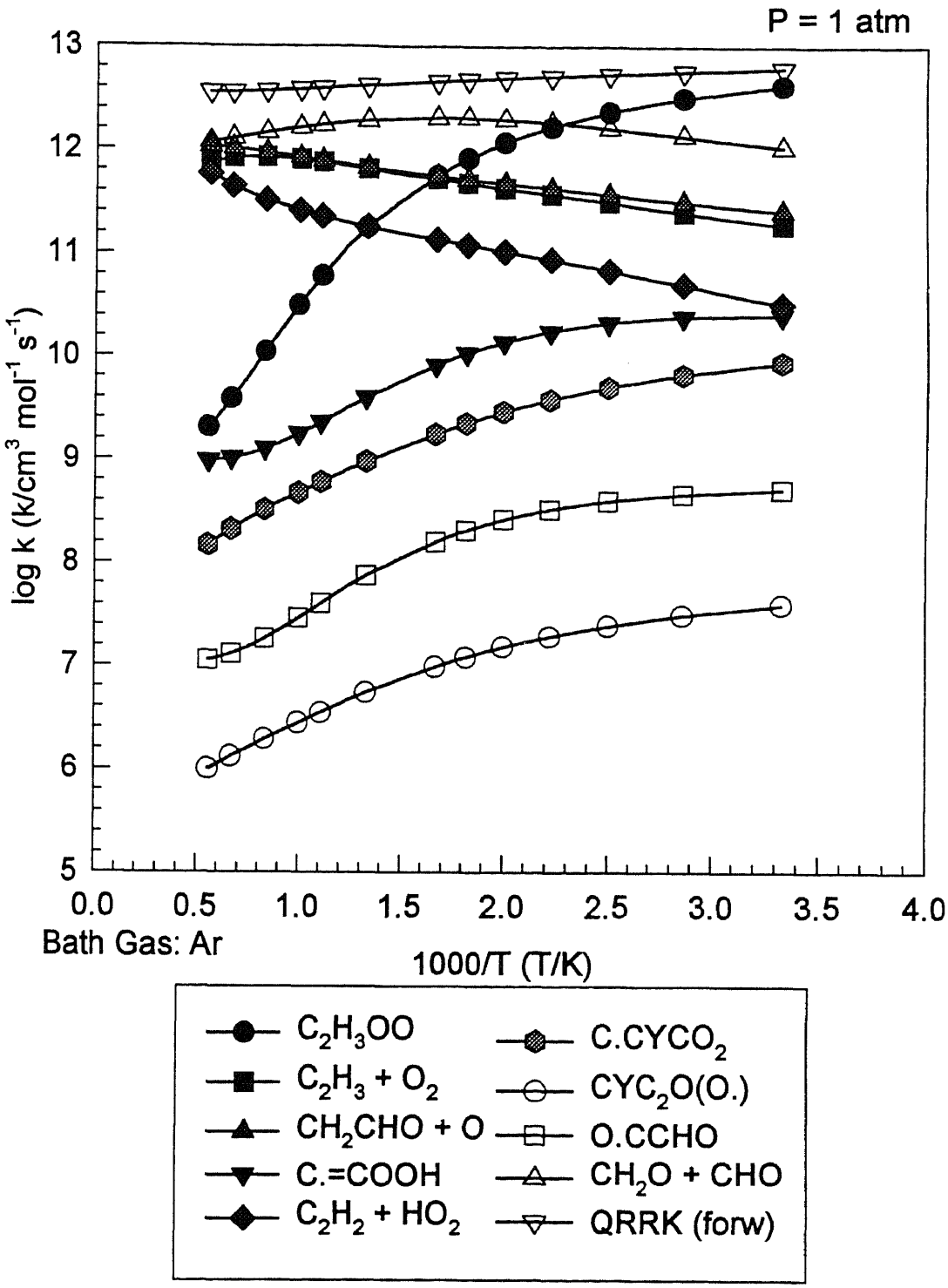

Figure E3 Results of QRRK Calculation for
$C_2H_3 + O_2$ <=> $[C_2H_3OO]^*$ => Products

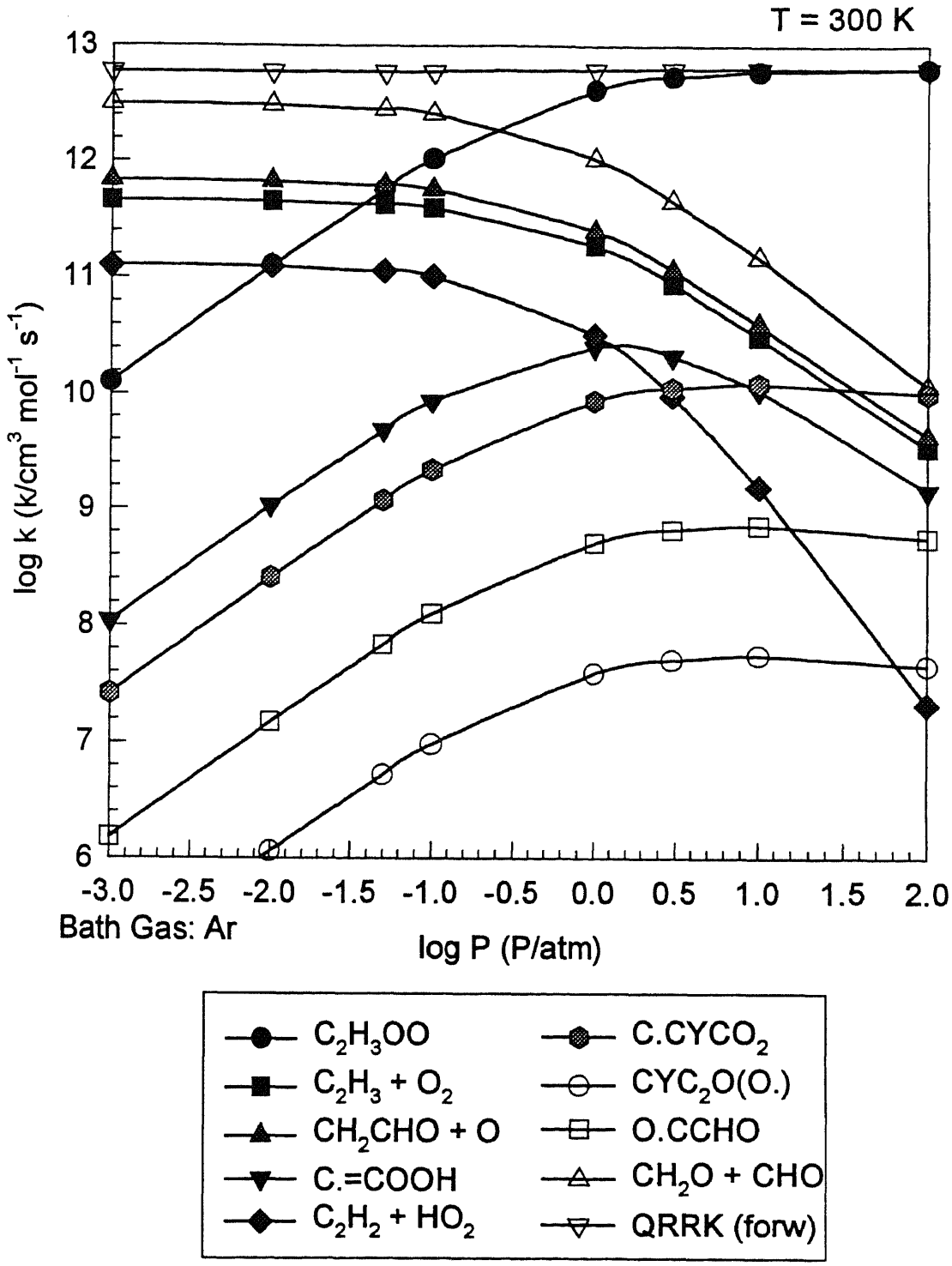

Figure E4 Results of QRRK Calculation for $C_2H_3 + O_2 \Leftrightarrow [C_2H_3OO]^* \Rightarrow$ Products

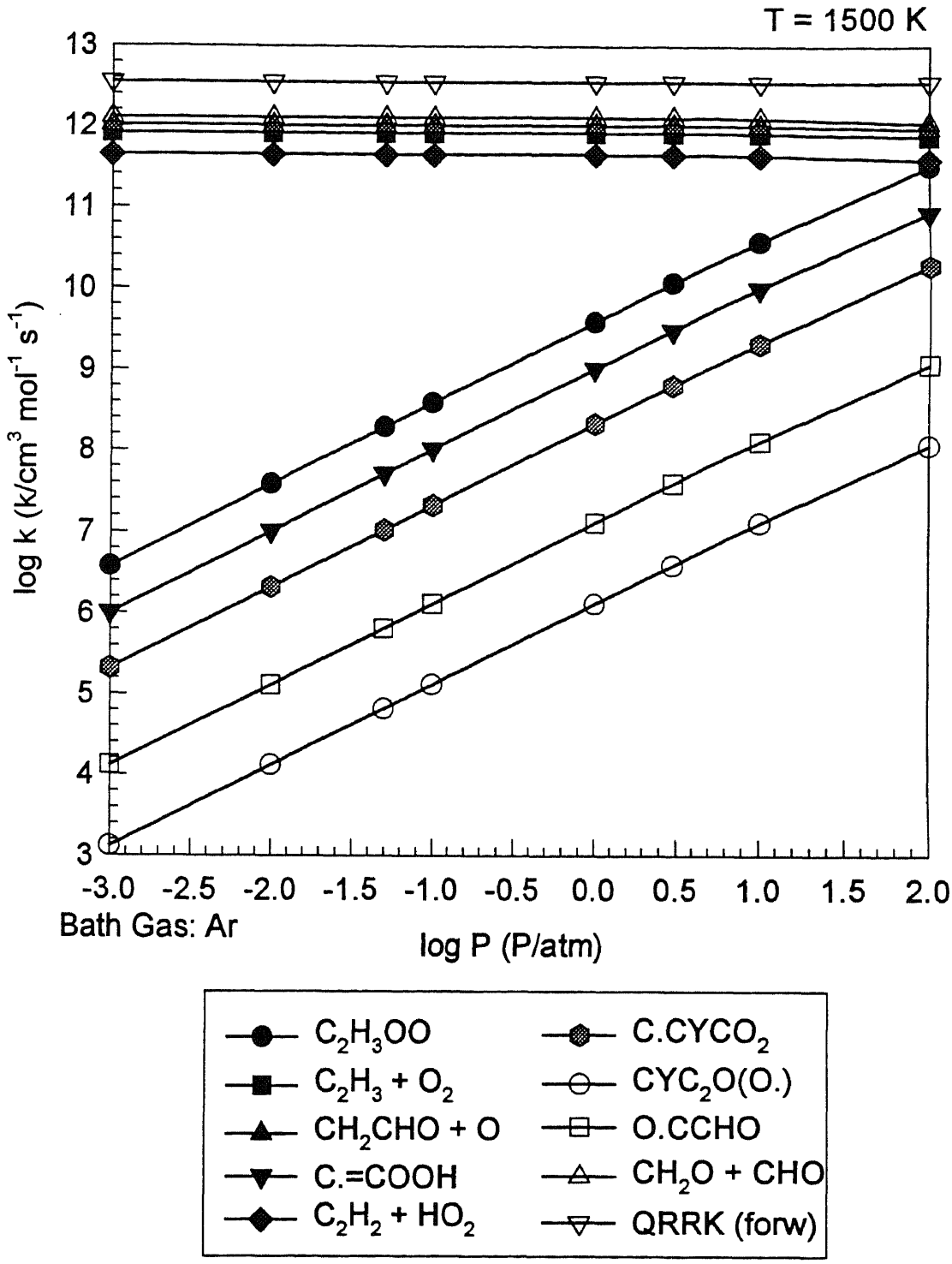

Figure E5 Results of QRRK Calculation for
$C_2H_3 + O_2$ <=> $[C_2H_3OO]^*$ => Products

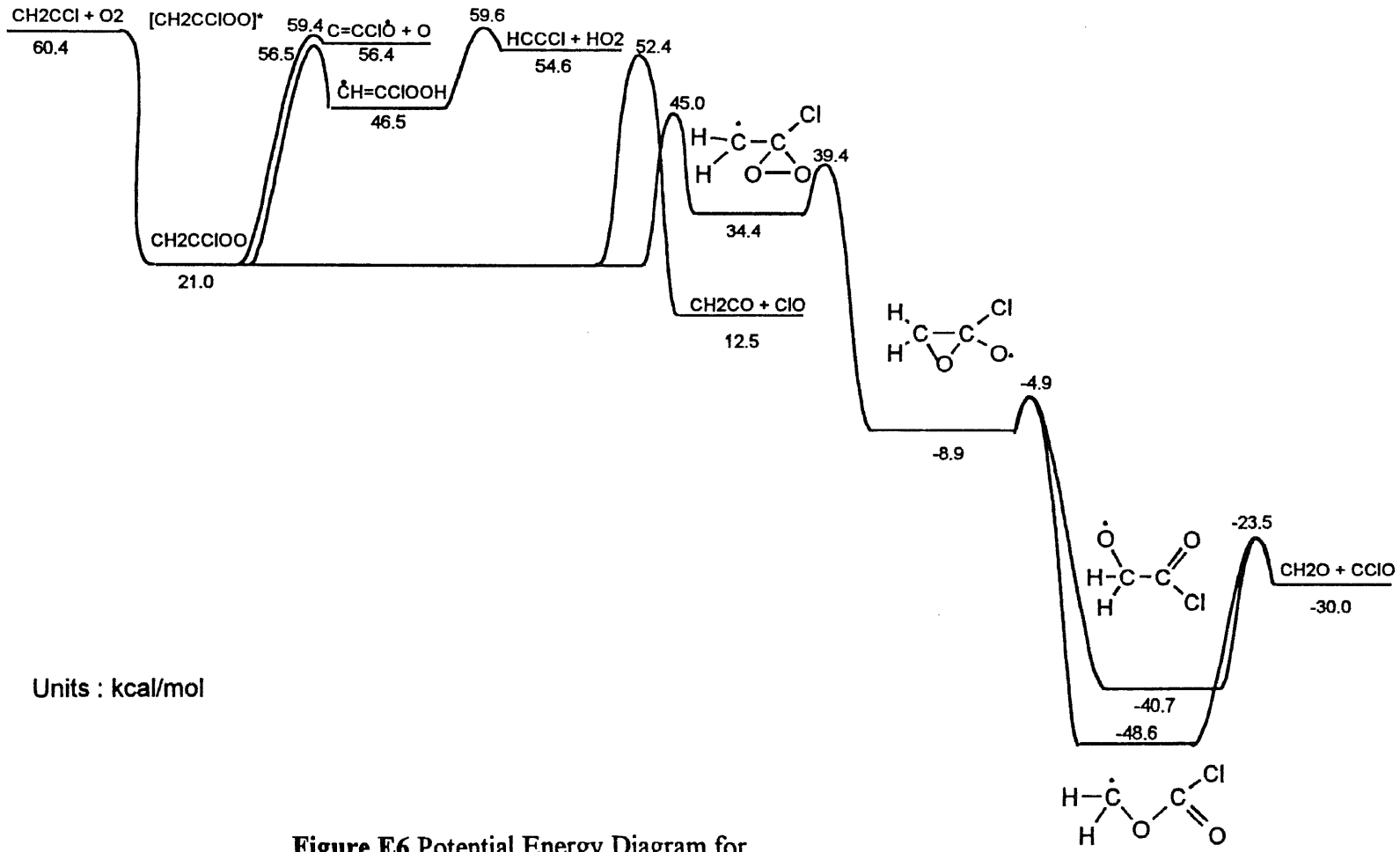

Figure E6 Potential Energy Diagram for
CH2CCl + O2 ⟷ [CH2CClOO]* ⟶ Products

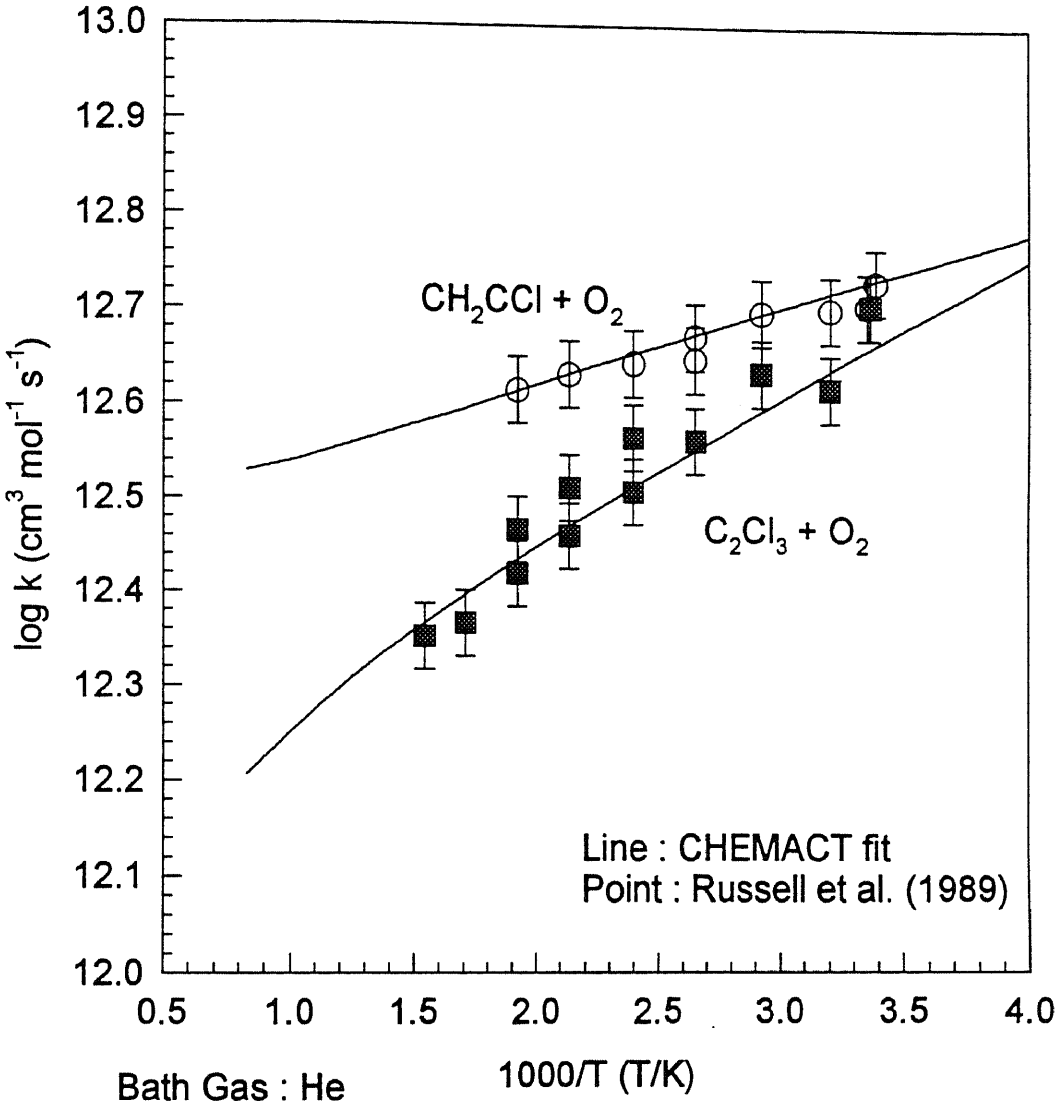

Figure E7 Comparison of Predicted values with Experiments for Chloro Vinyl Radicals + O_2 ⟶ Products

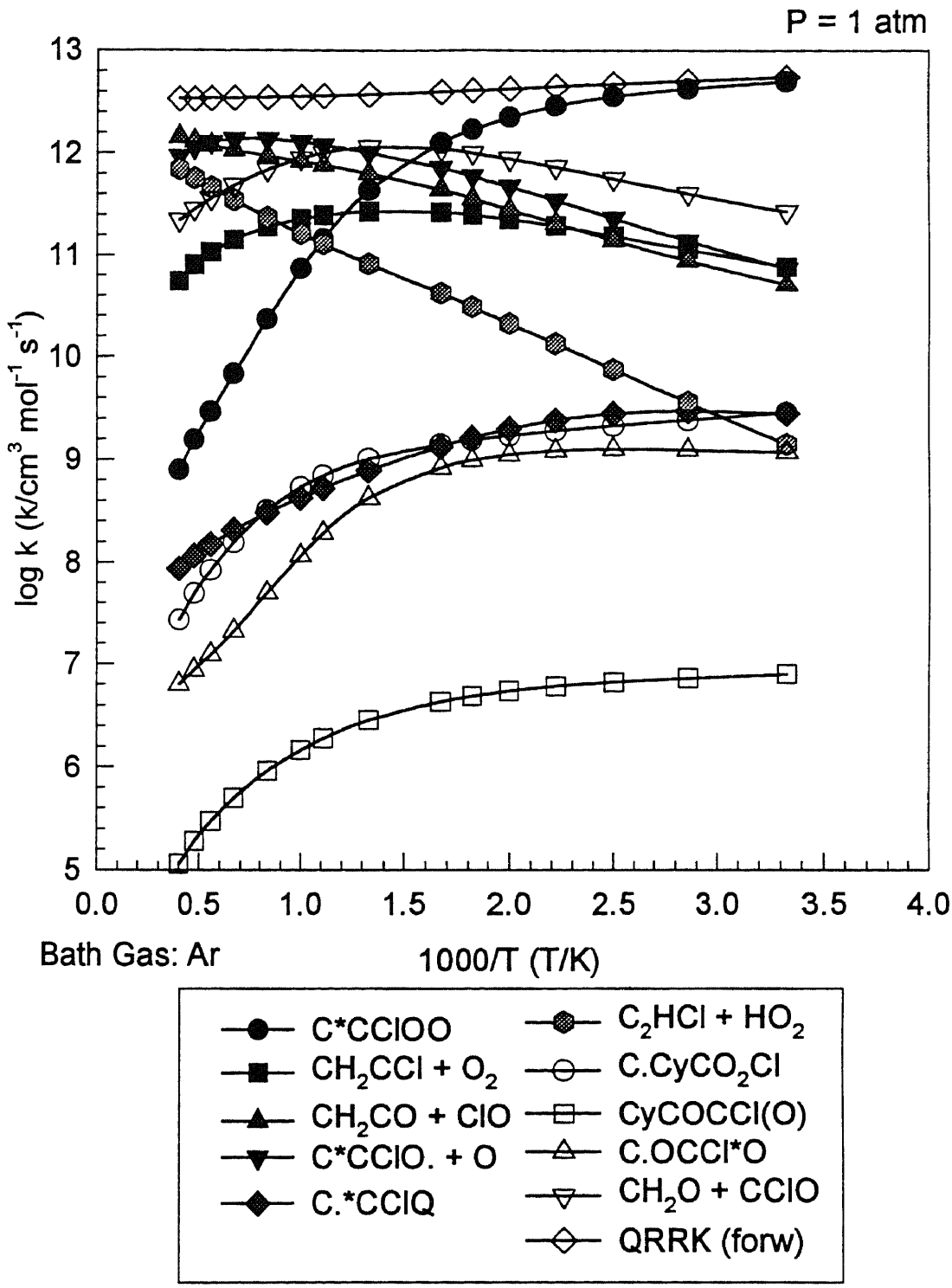

Figure E8 Results of QRRK Calculation for $CH_2CCl + O_2$ <=> [C=CClOO]* => Products

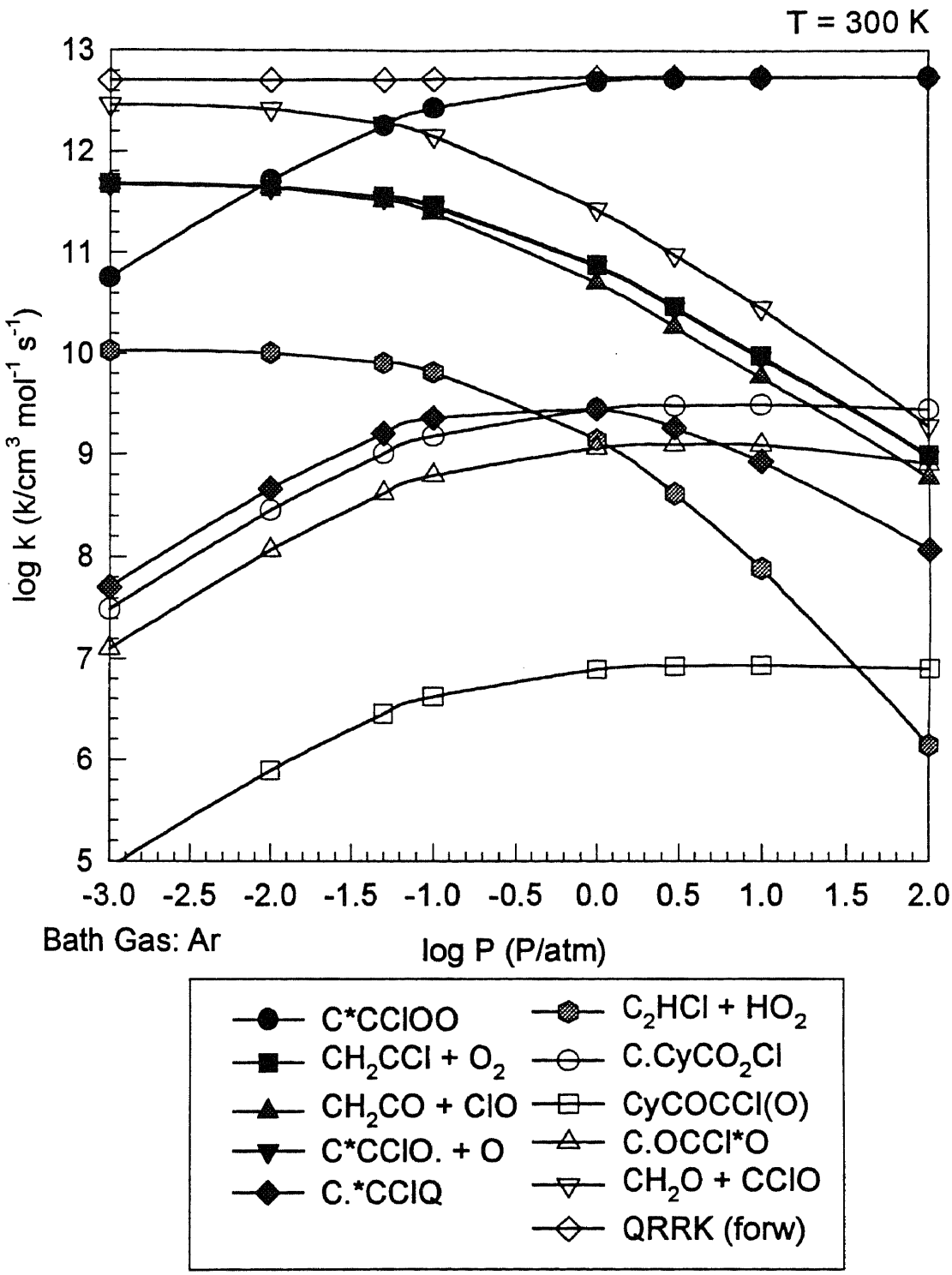

Figure E9 Results of QRRK Calculation for
$CH_2CCl + O_2$ <=> [C=CClOO]* => Products

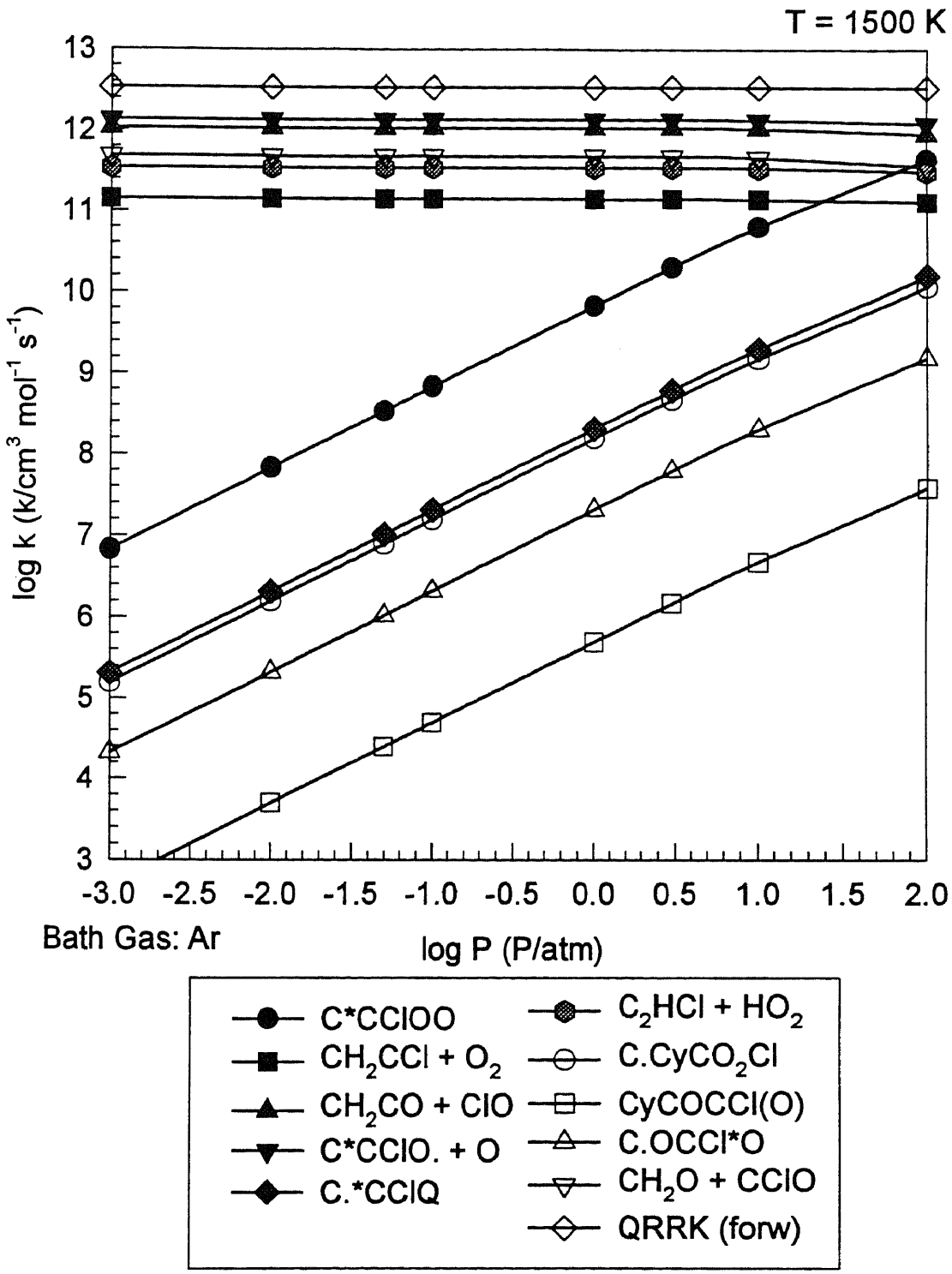

Figure E10 Results of QRRK Calculation for
$CH_2CCl + O_2$ <=> [C=CClOO]* => Products

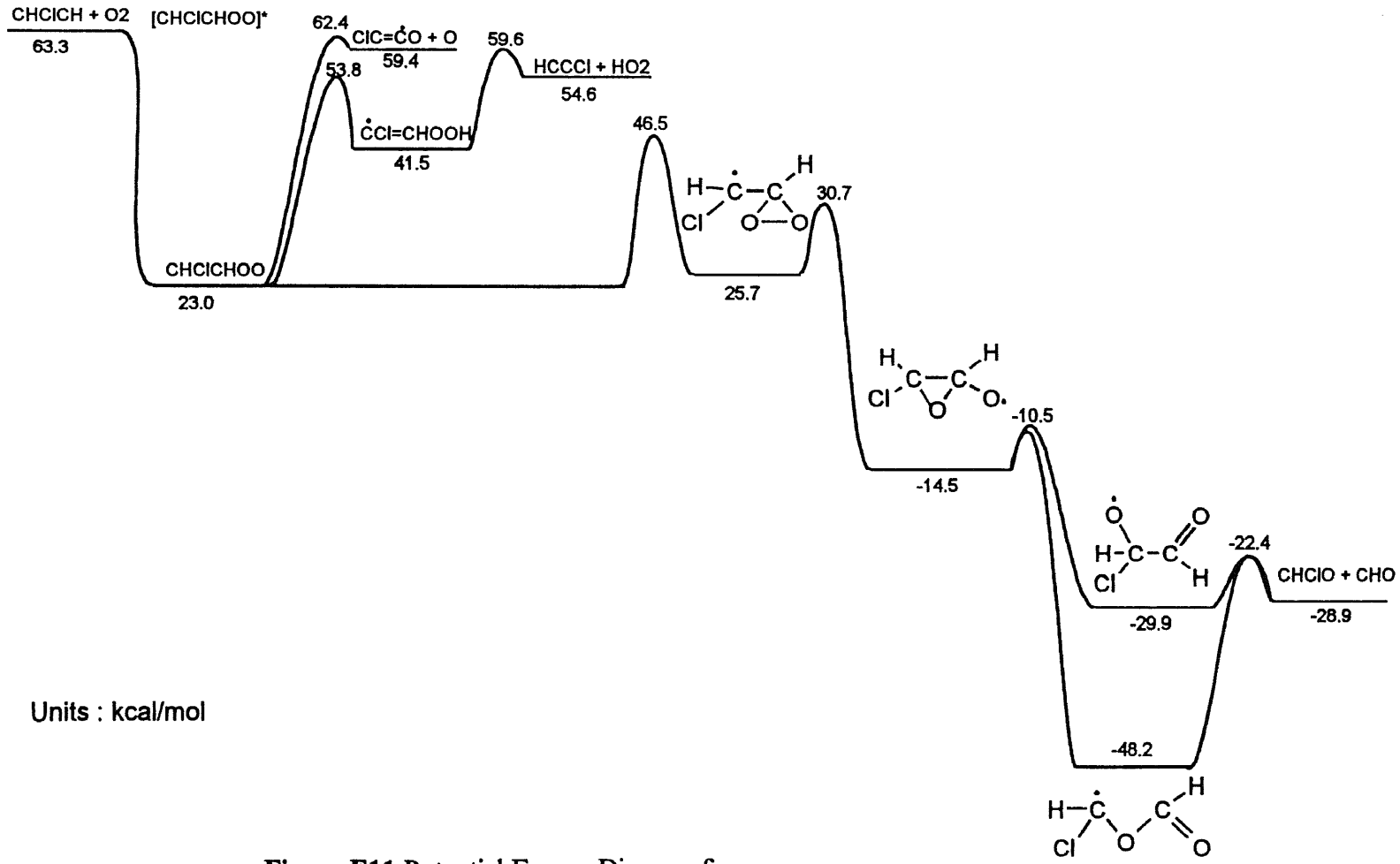

Figure E11 Potential Energy Diagram for
CHClCH + O2 ⟷ [CHClCHOO]* ⟶ Products

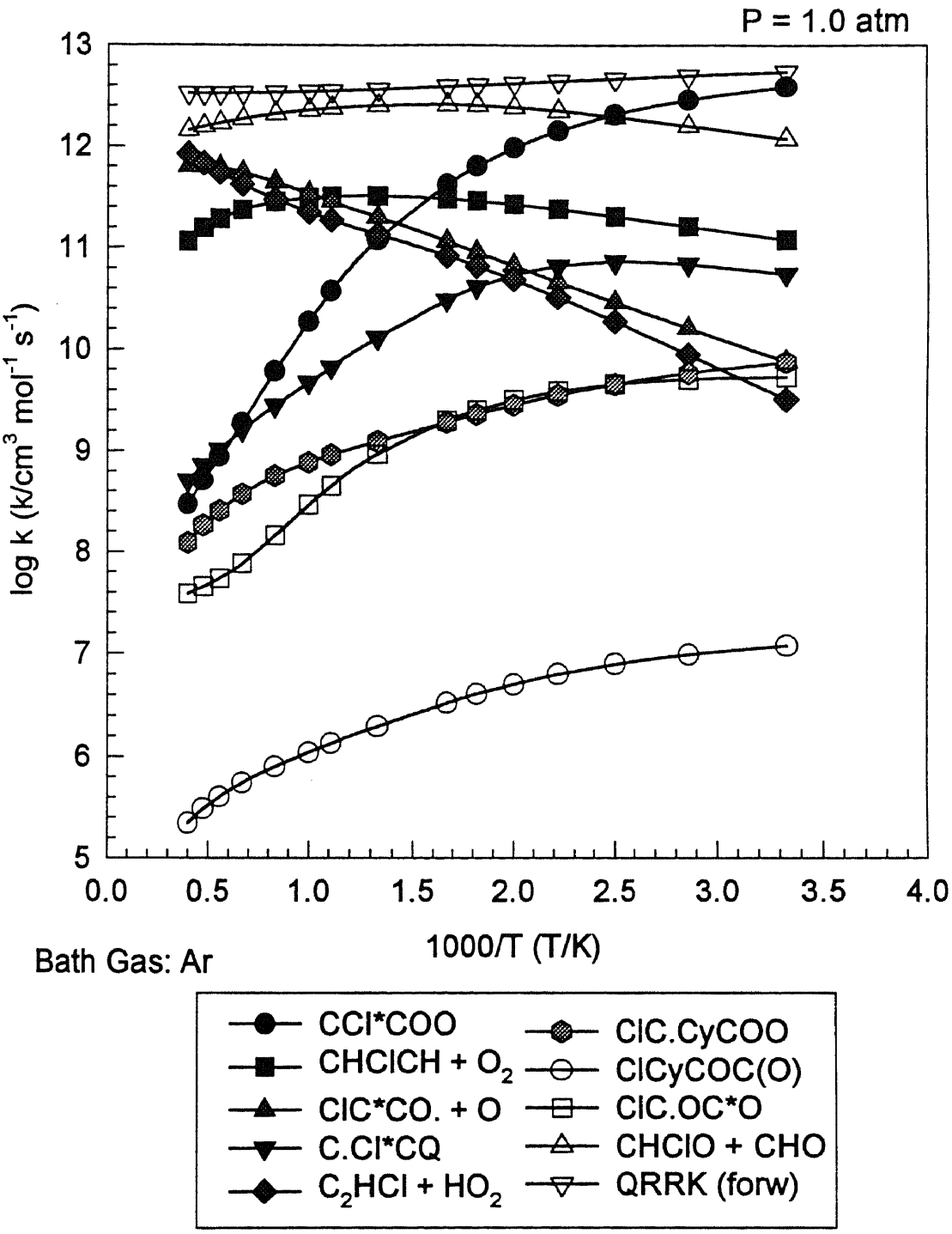

Figure E12 Results of QRRK Calculation for CHClCH + O_2 <=> [CCl=COO]* => Products

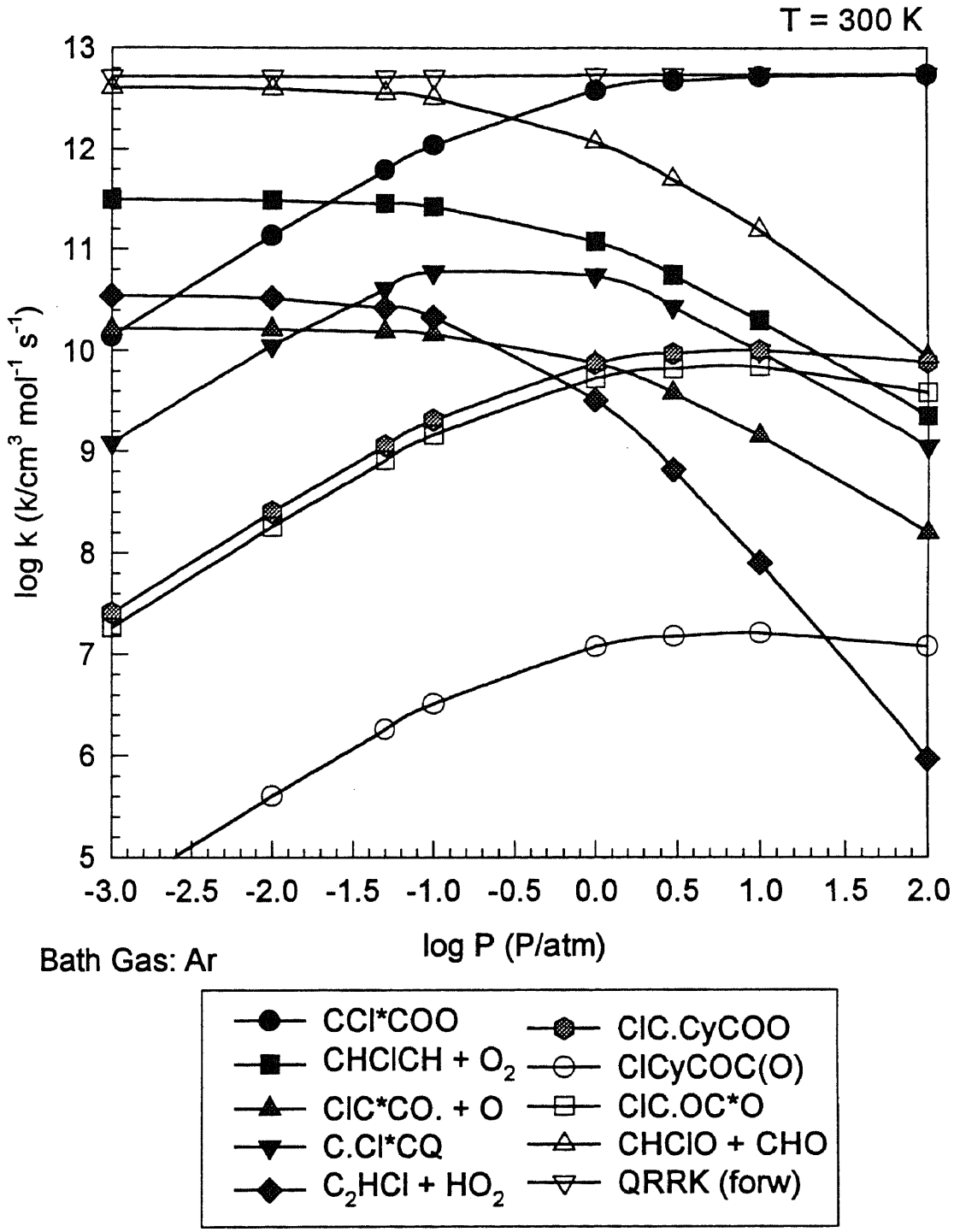

Figure E13 Results of QRRK Calculation for CHClCH + O_2 <=> [CCl=COO]* => Products

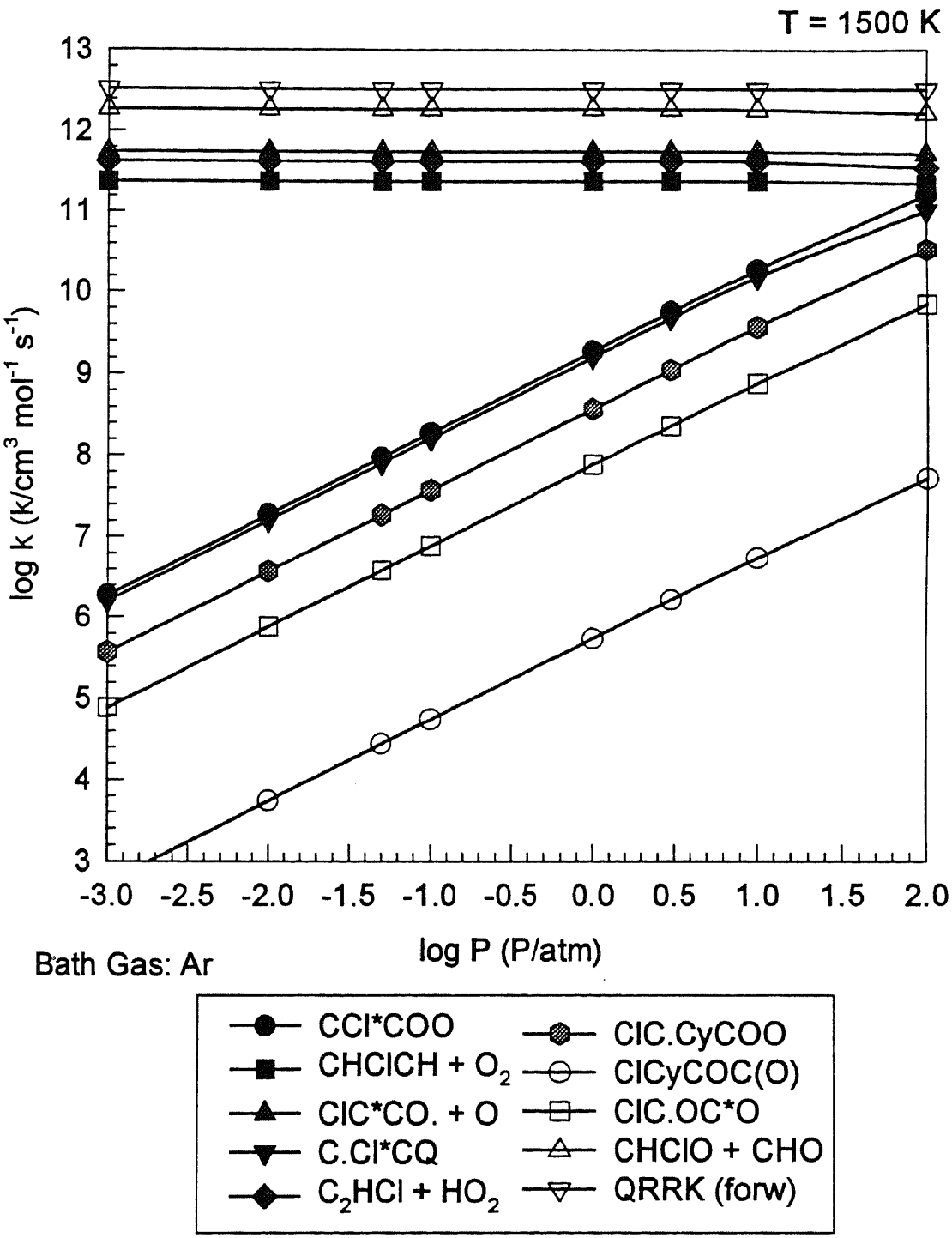

Figure E14 Results of QRRK Calculation for CHClCH + O_2 <=> [CCl=COO]* => Products

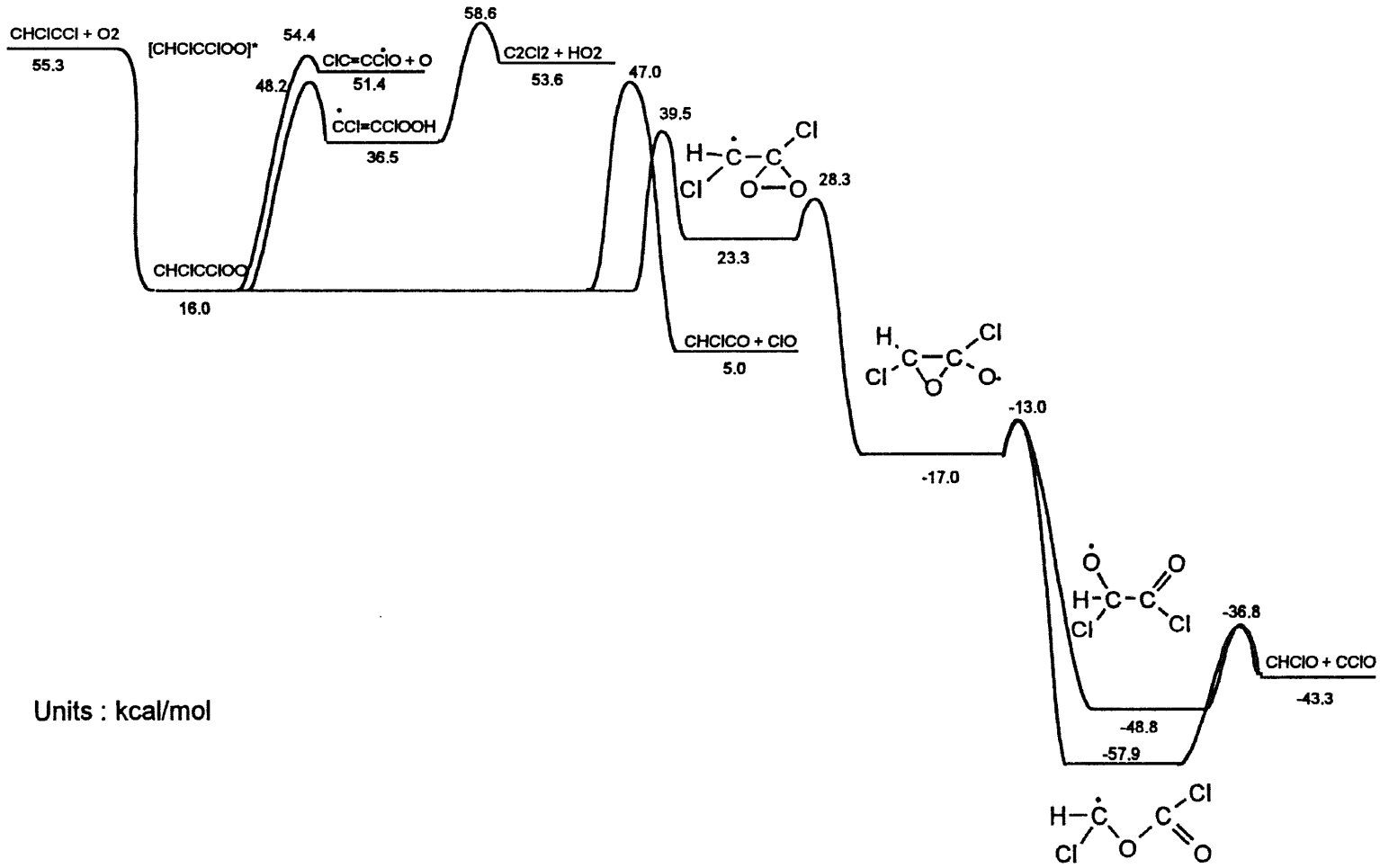

Figure E15 Potential Energy Diagram for
CHClCCl + O2 ⟷ [CHClCClOO]* ⟶ Products

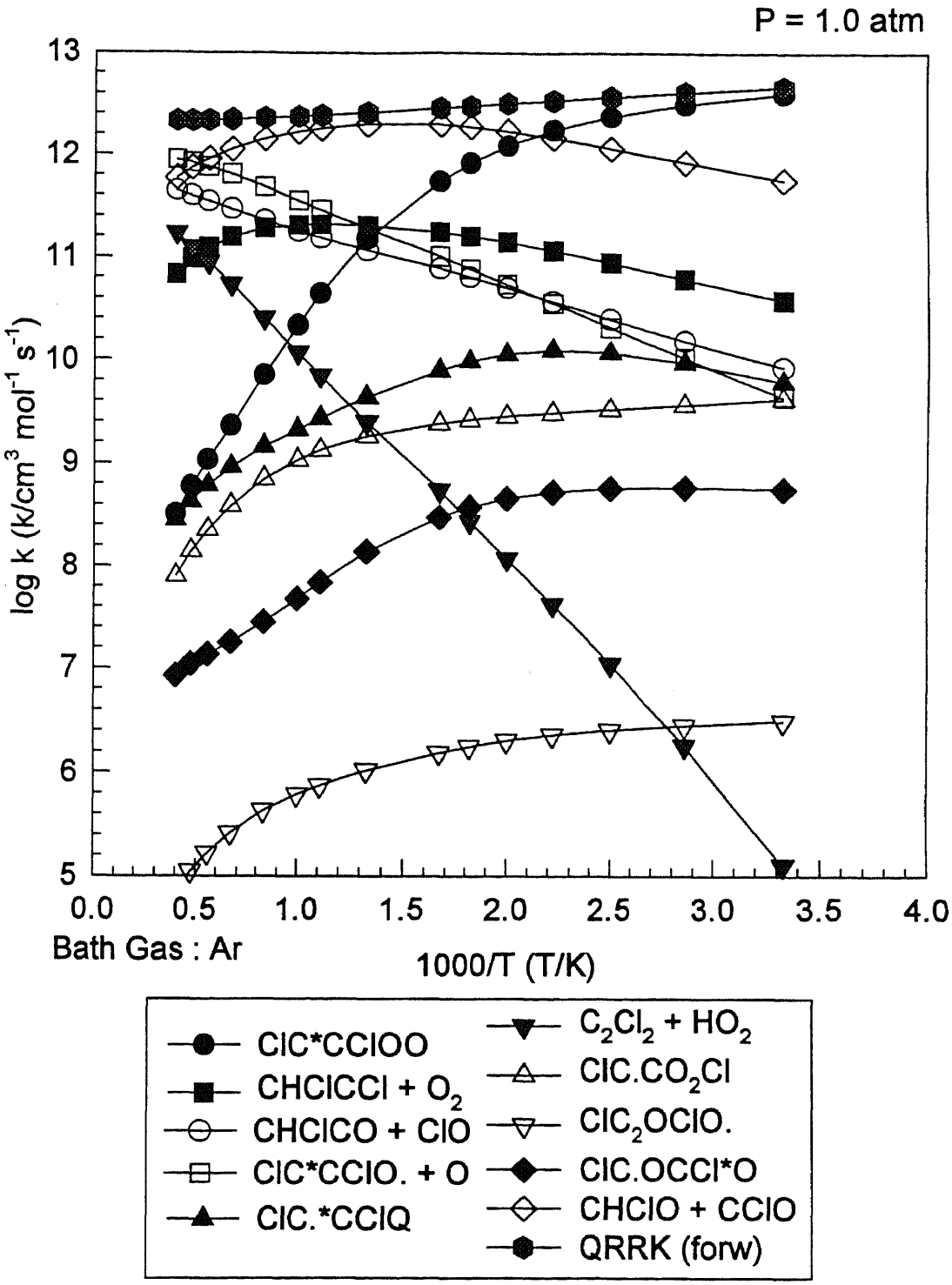

Figure E16 Results of QRRK Calculation for CHClCCl + O_2 <=> [CHClCClOO]* => Products

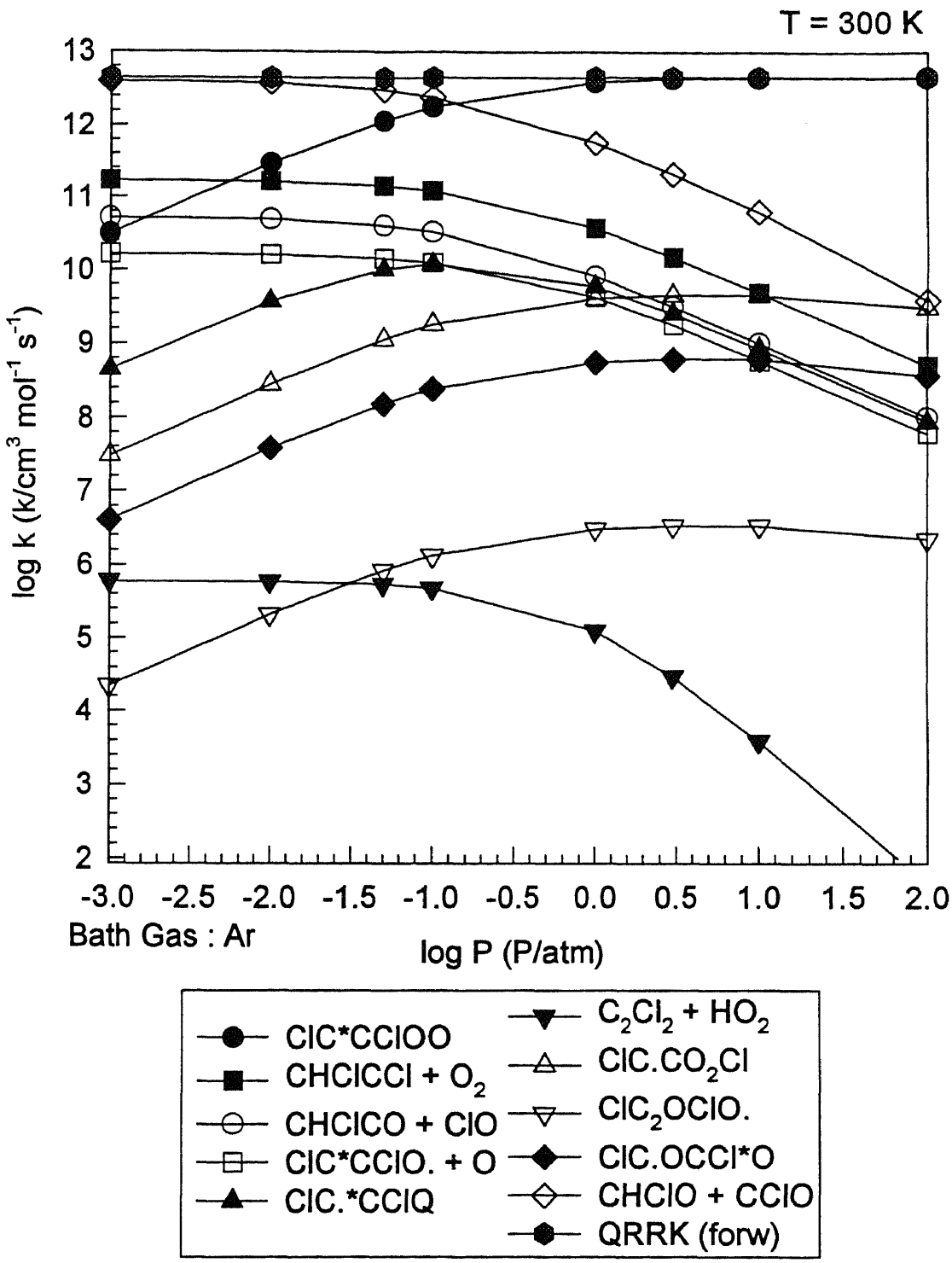

Figure E17 Results of QRRK Calculation for CHClCCl + O_2 <=> [CHClCClOO]* => Products

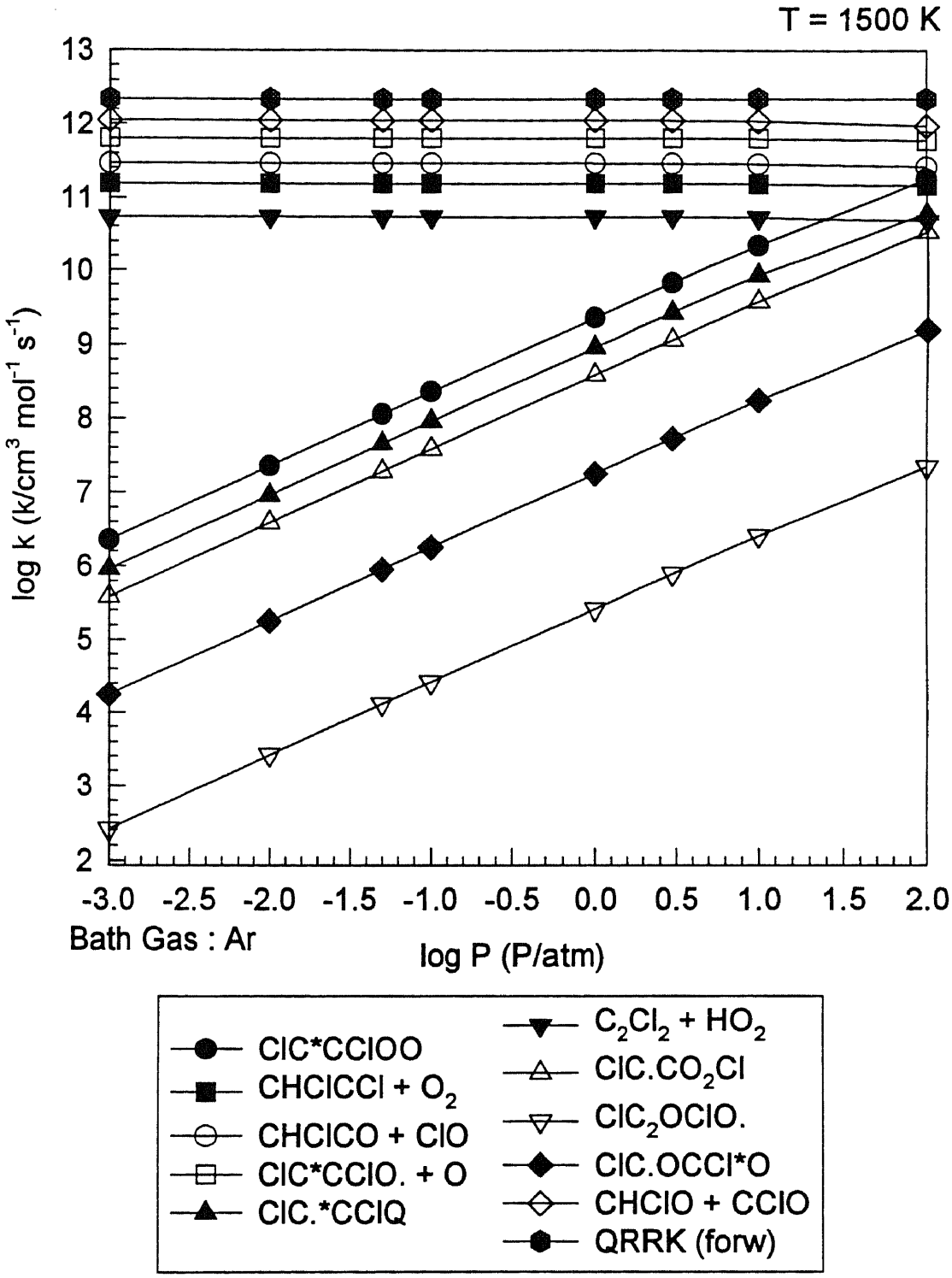

Figure E18 Results of QRRK Calculation for
CHClCCl + O_2 <=> [CHClCClOO]* => Products

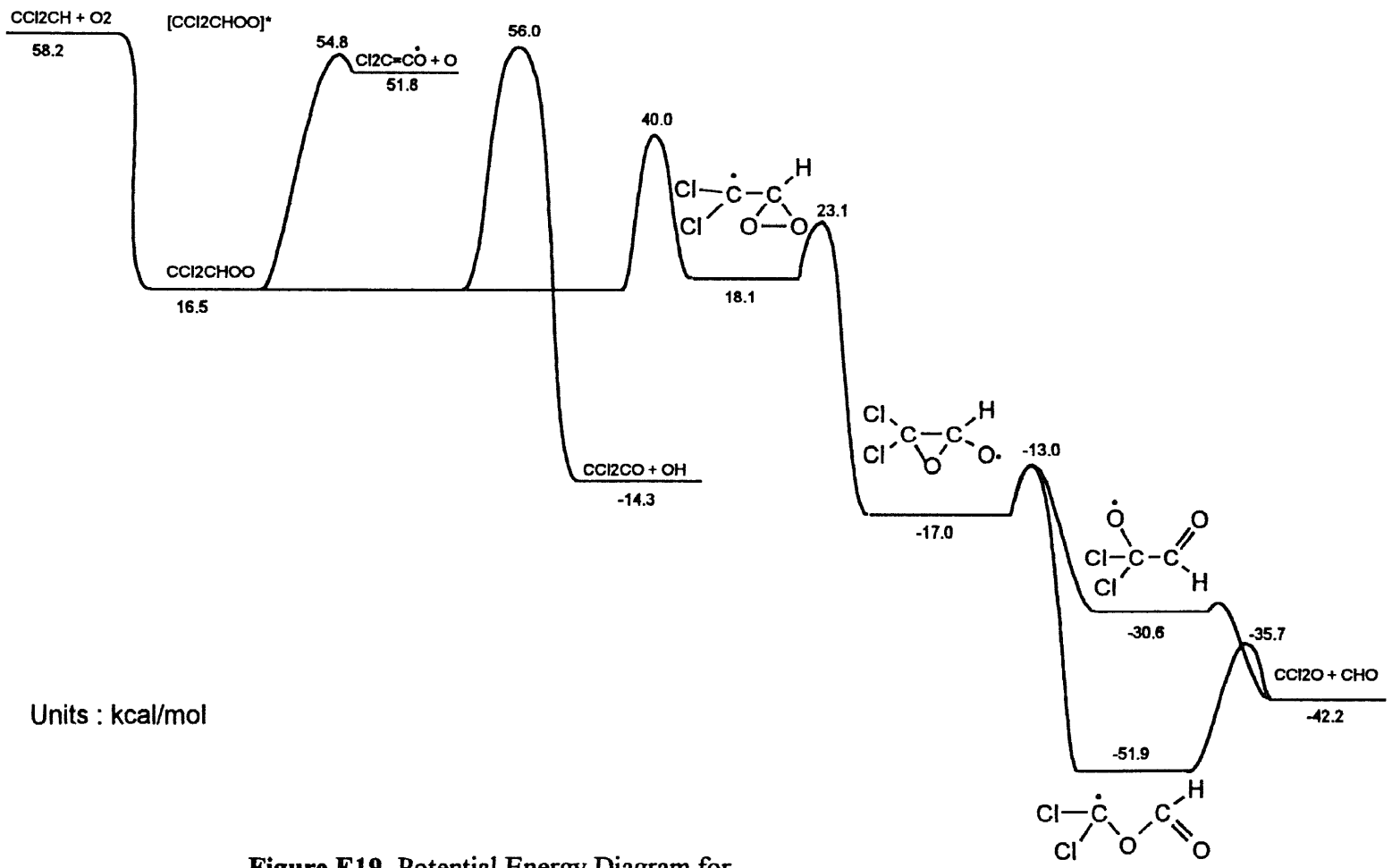

Figure E19 Potential Energy Diagram for
CCl2CH + O2 ⟷ [CCl2CHOO]* ⟶ Products

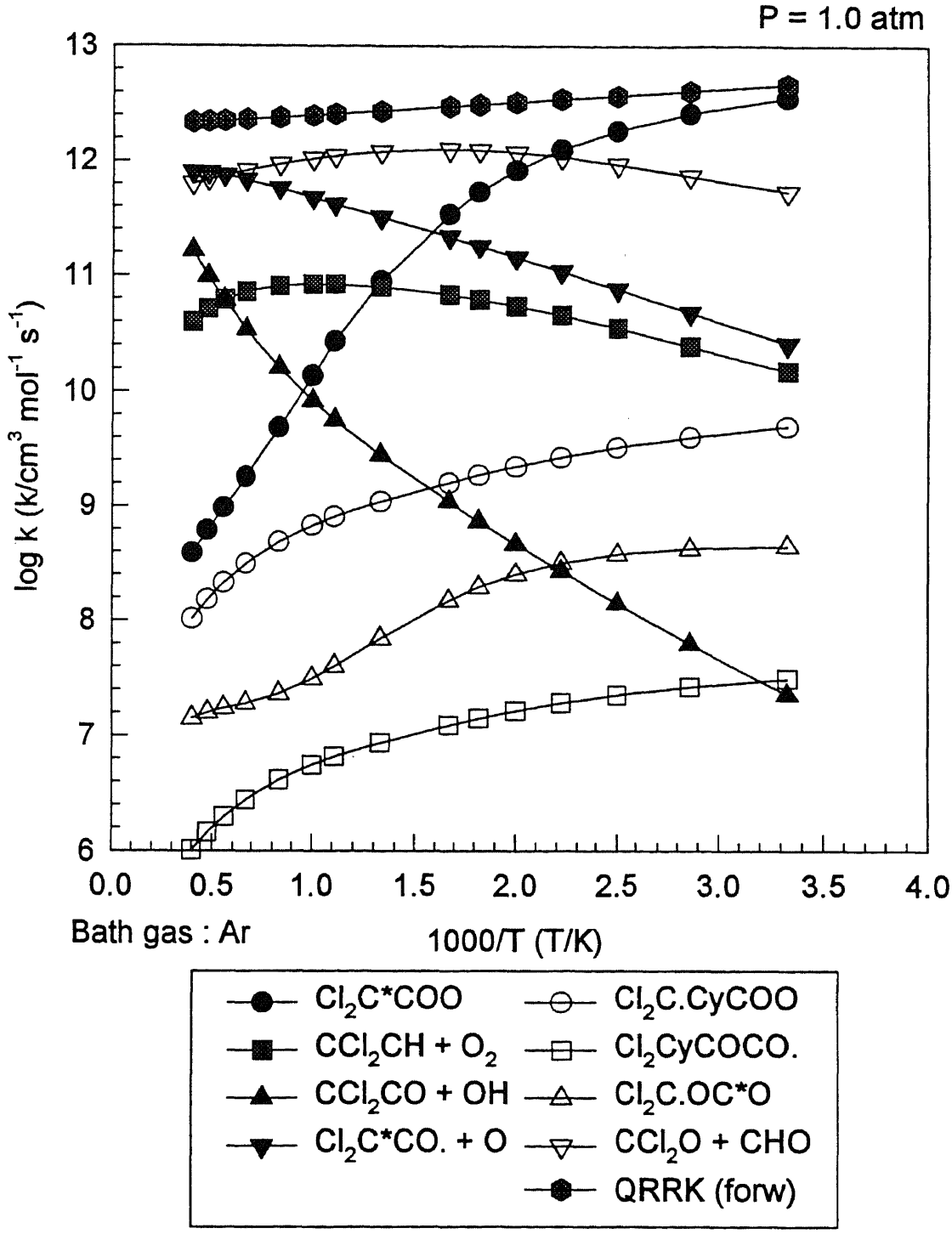

Figure E20 Results of QRRK Calculation for $CCl_2CH + O_2$ <=> $[CCl_2CHOO]^*$ => Products

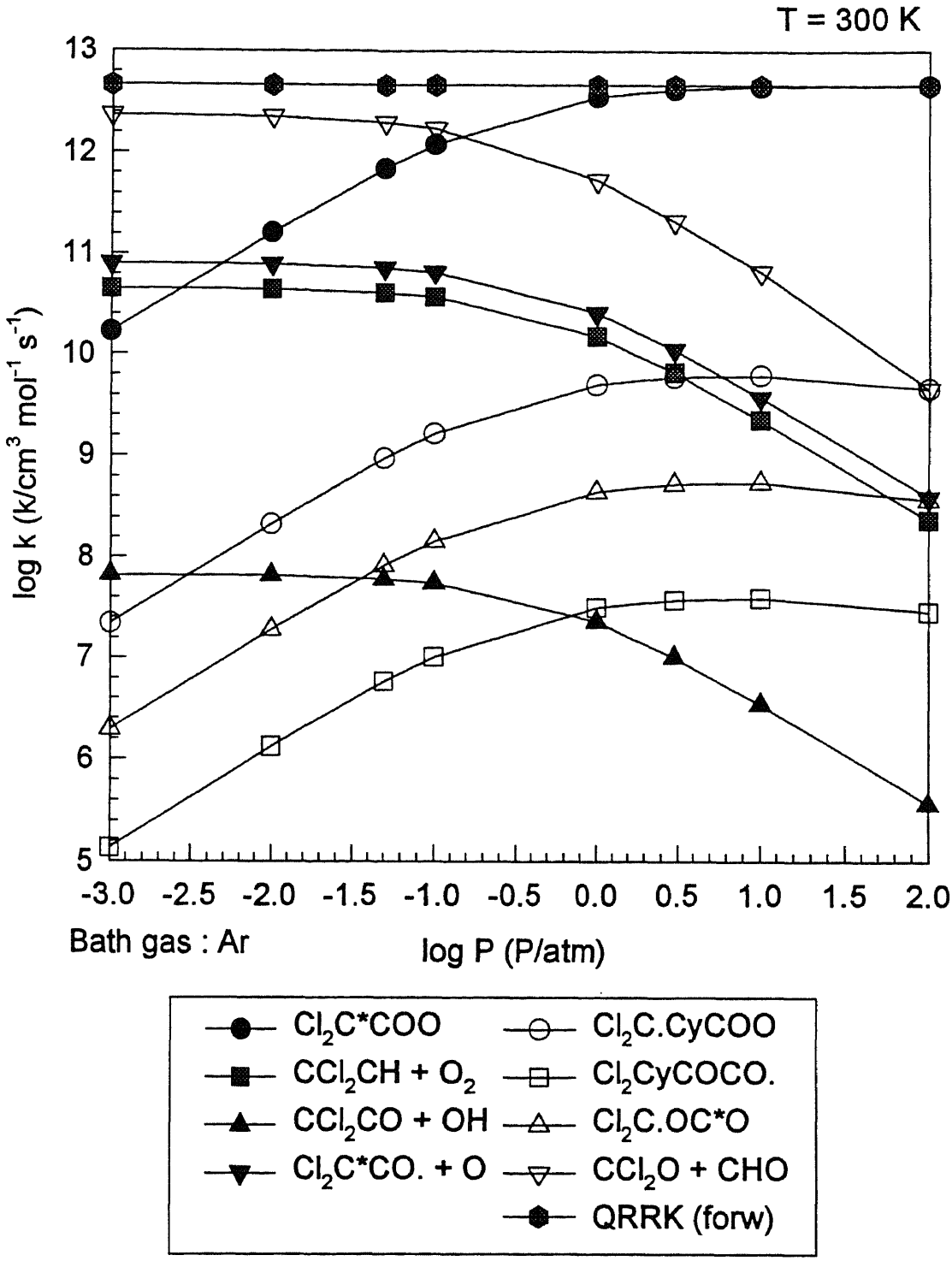

Figure E21 Results of QRRK Calculation for $CCl_2CH + O_2$ <=> $[CCl_2CHOO]^*$ => Products

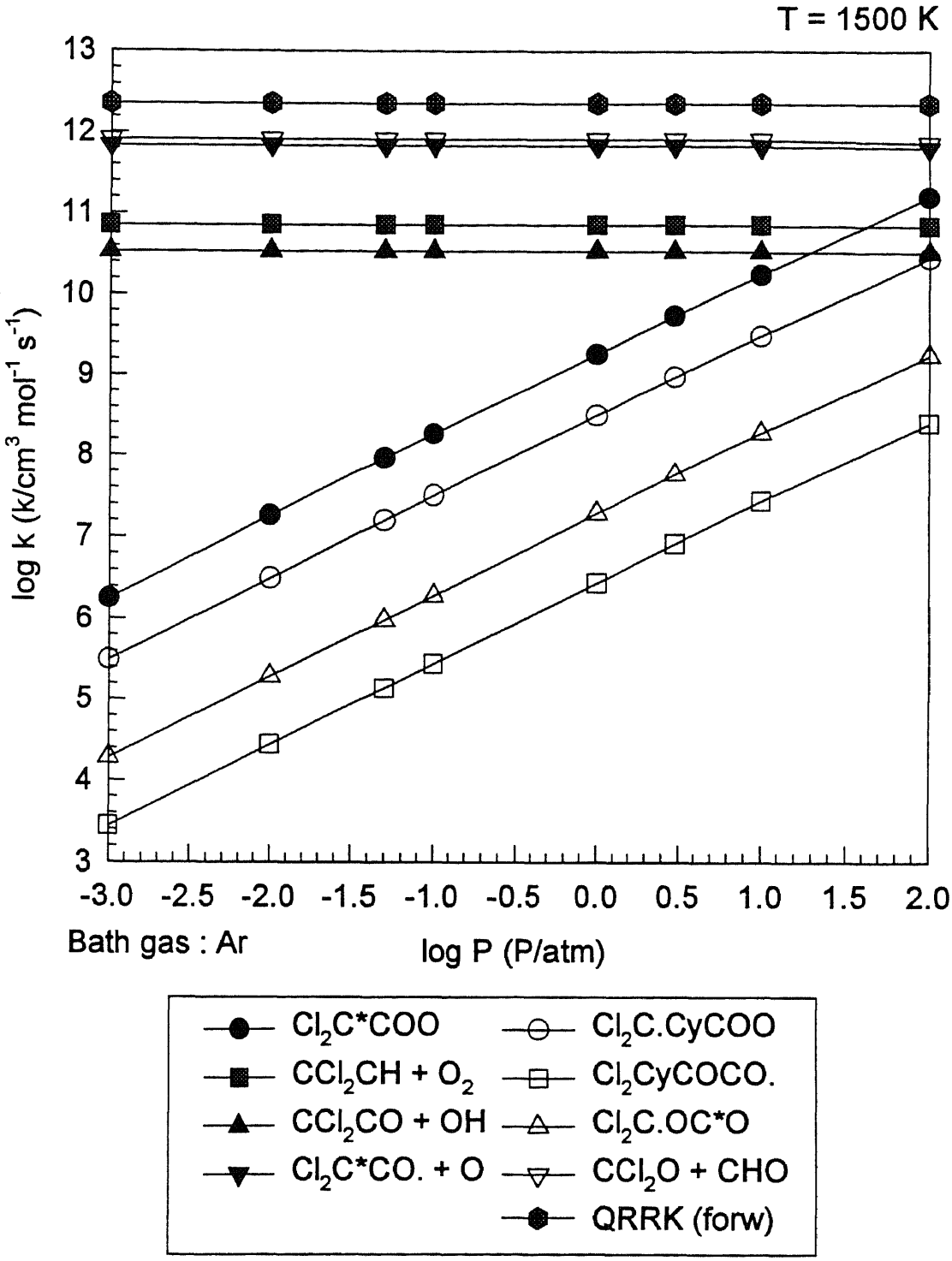

Figure E22 Results of QRRK Calculation for $CCl_2CH + O_2$ <=> $[CCl_2CHOO]^*$ => Products

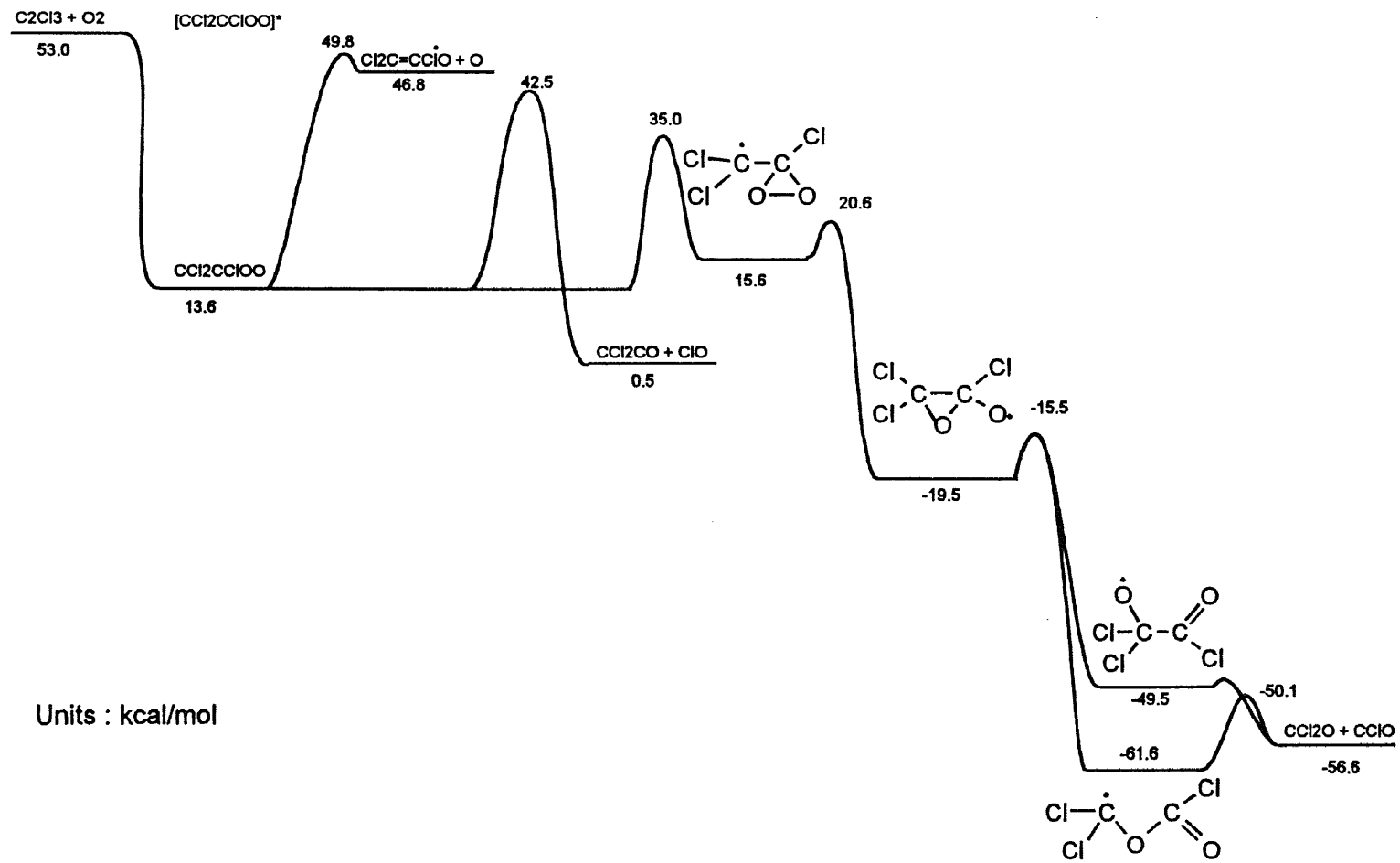

Figure E23 Potential Energy Diagram for
C2Cl3 + O2 ⟷ [C2Cl3OO]* ⟶ Products

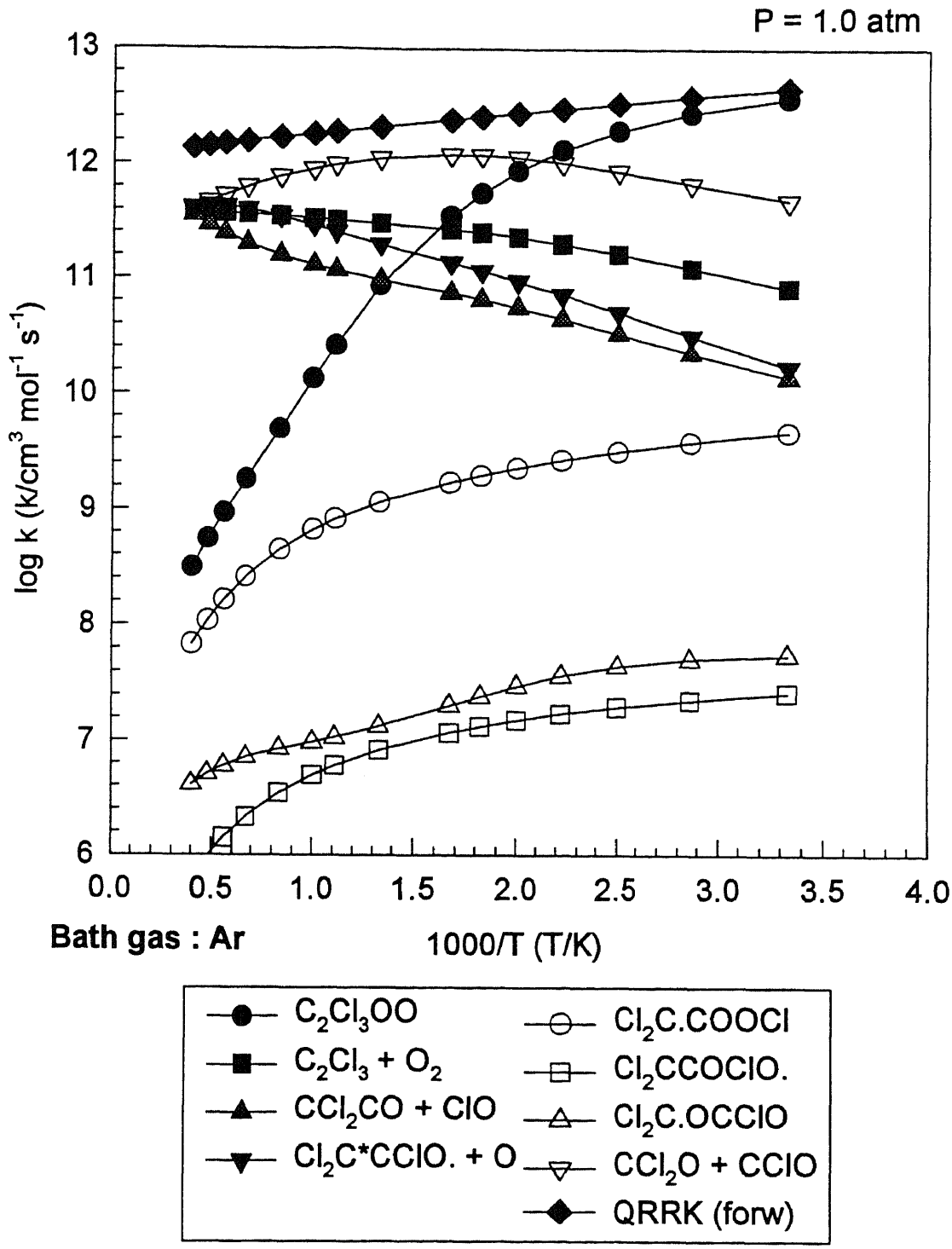

Figure E24 Results of QRRK Calculation for $C_2Cl_3 + O_2$ <=> $[C_2Cl_3OO]^*$ => Products

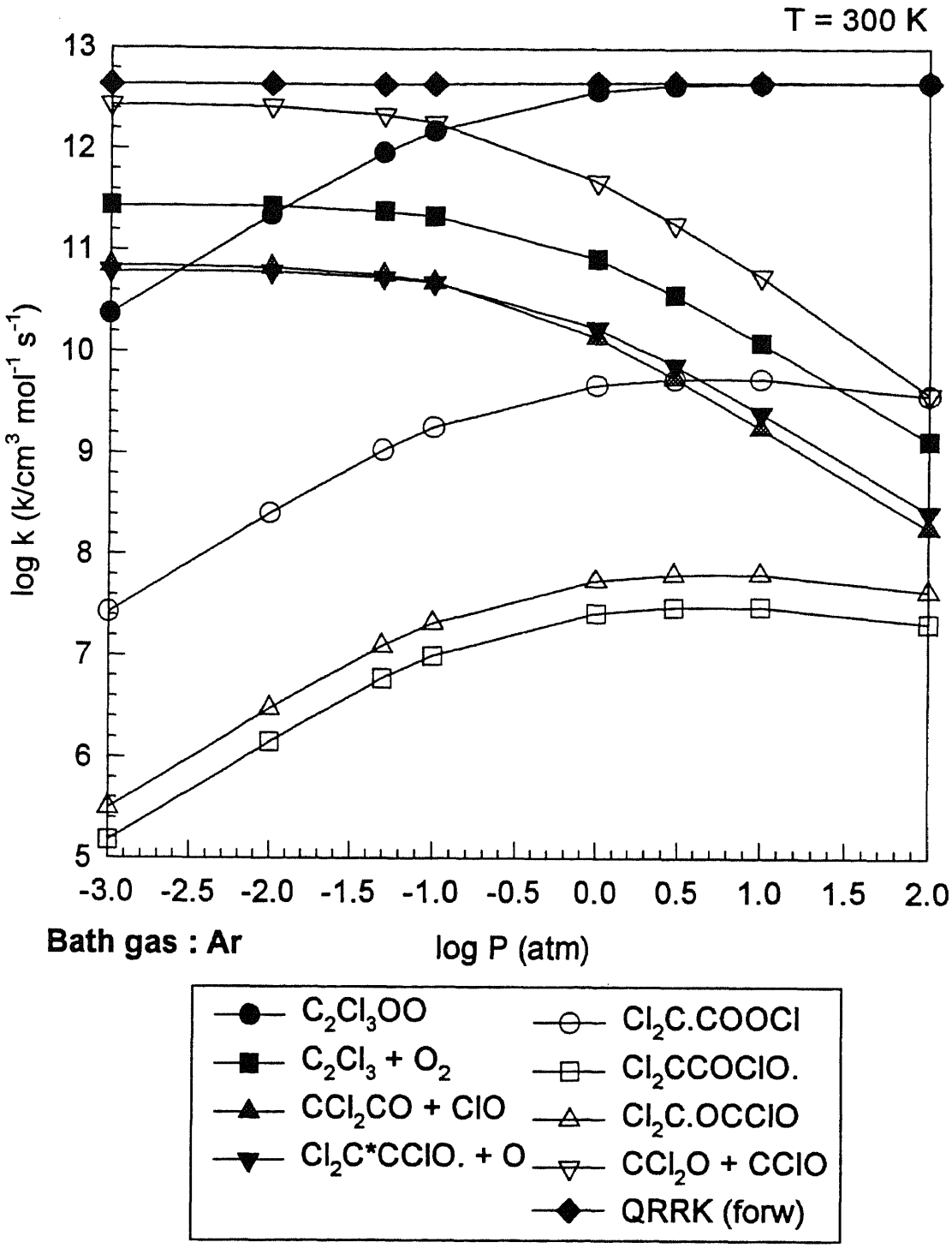

Figure E25 Results of QRRK Calculation for
$C_2Cl_3 + O_2$ <=> $[C_2Cl_3OO]^*$ => Products

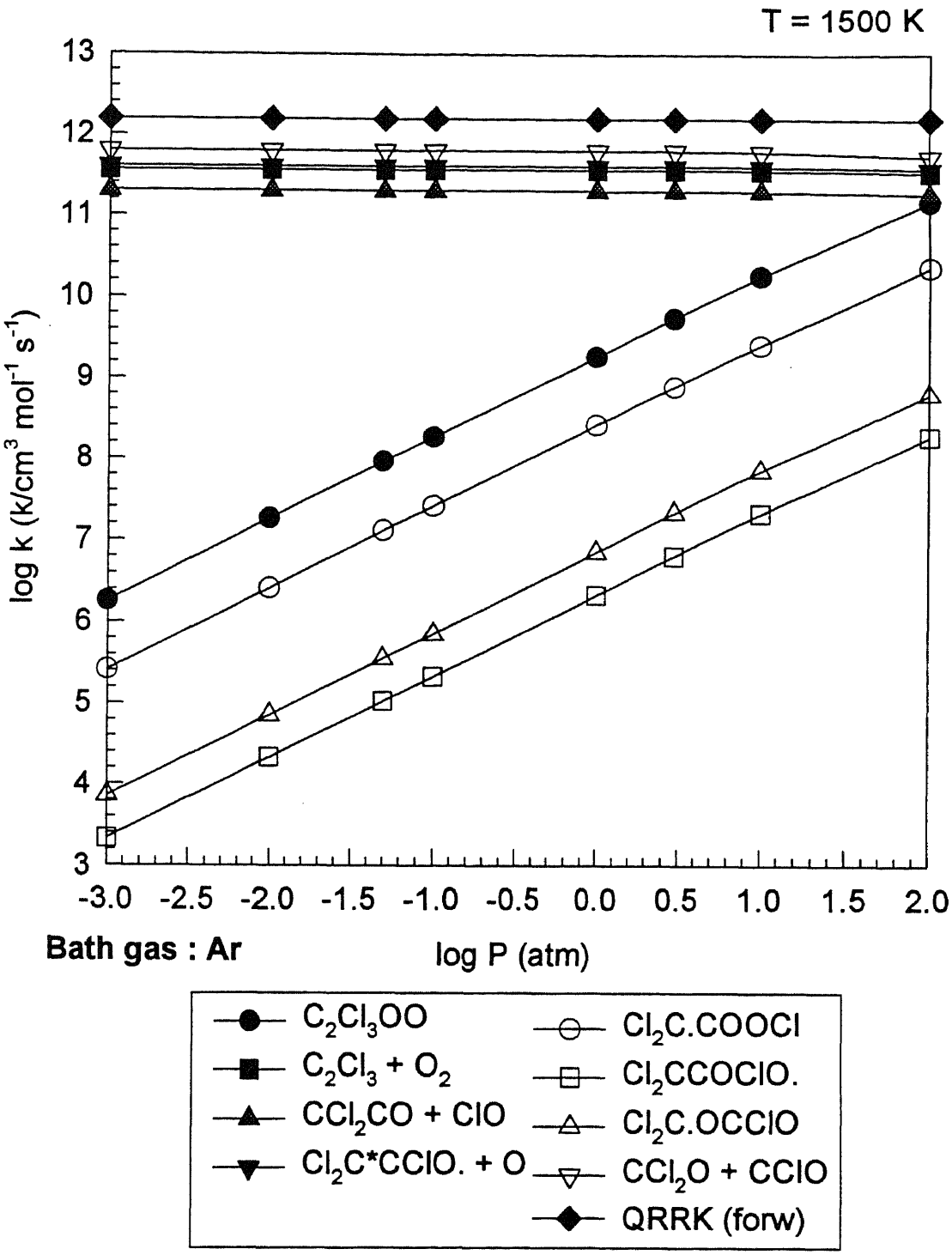

Figure E26 Results of QRRK Calculation for $C_2Cl_3 + O_2 \Leftrightarrow [C_2Cl_3OO]^* \Rightarrow$ Products

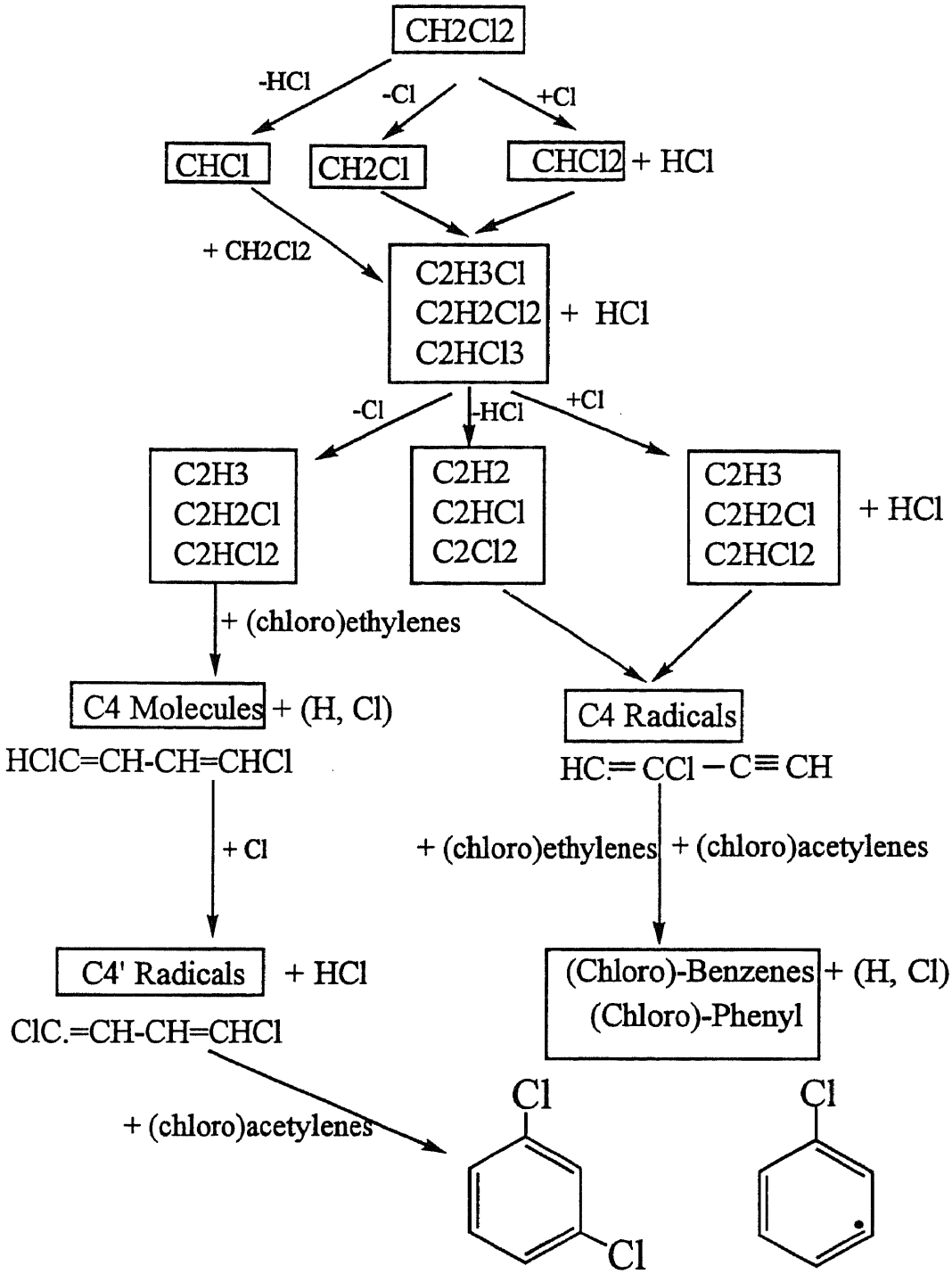

Figure F 1 Reaction Scheme: C1 → C2 → C4 → C6

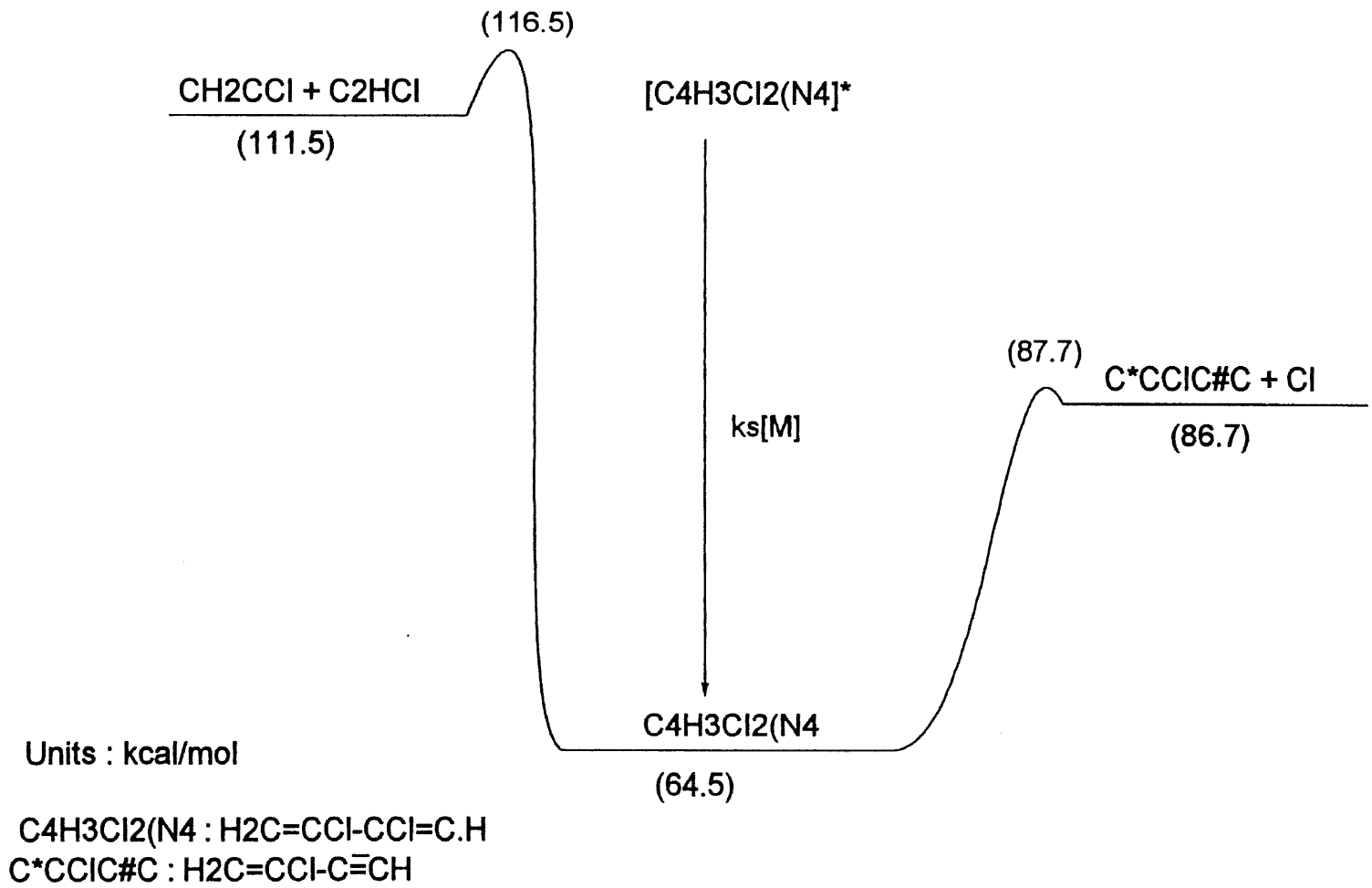

Figure F2 Potential Energy Diagram for
CH2CCl + C2HCl ⟷ [C4H3Cl2(N4]* ⟶ Products

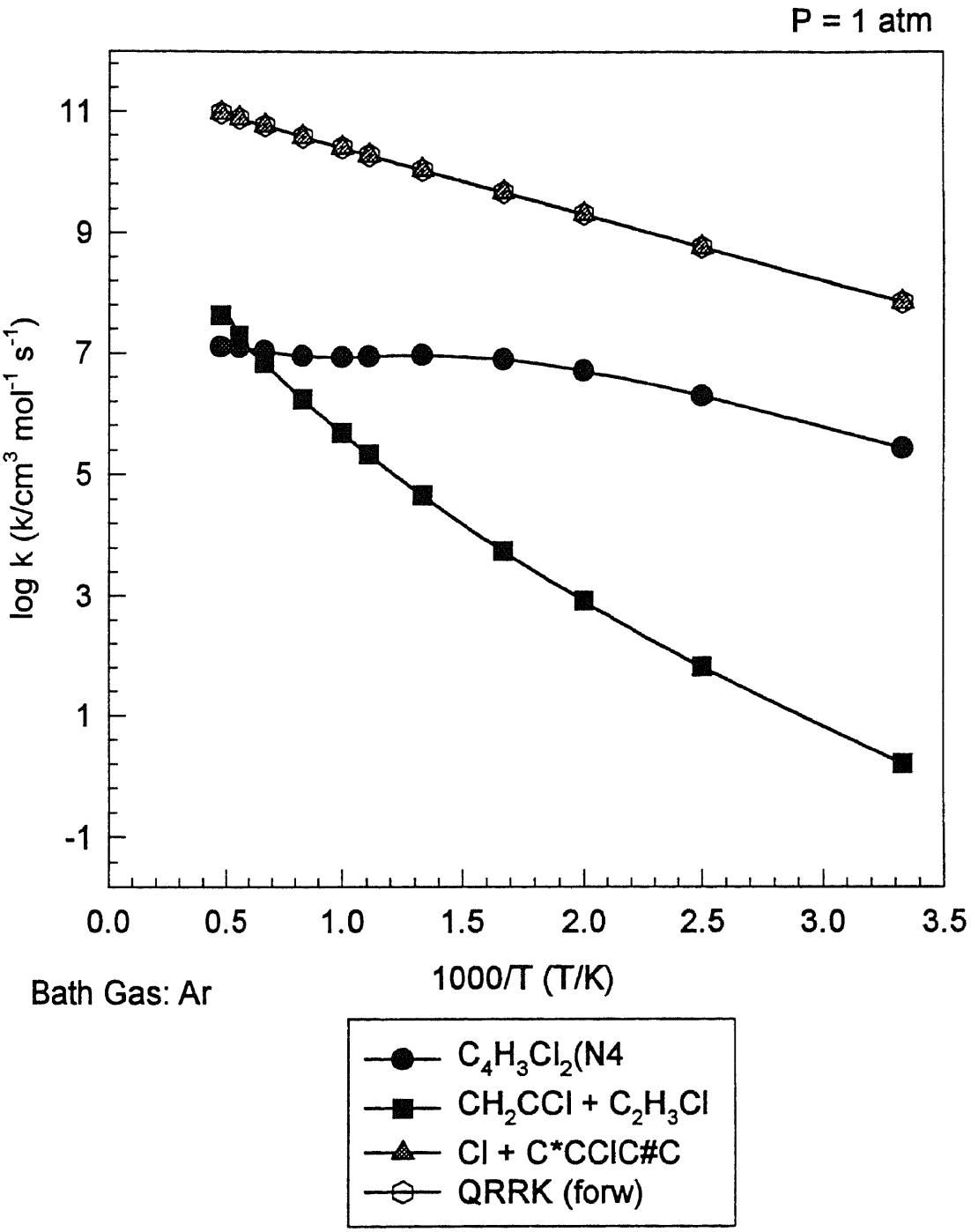

Figure F3 $CH_2CCl + C_2HCl$ <=> $[C_4H_3Cl_2(N4]^*$ => Products

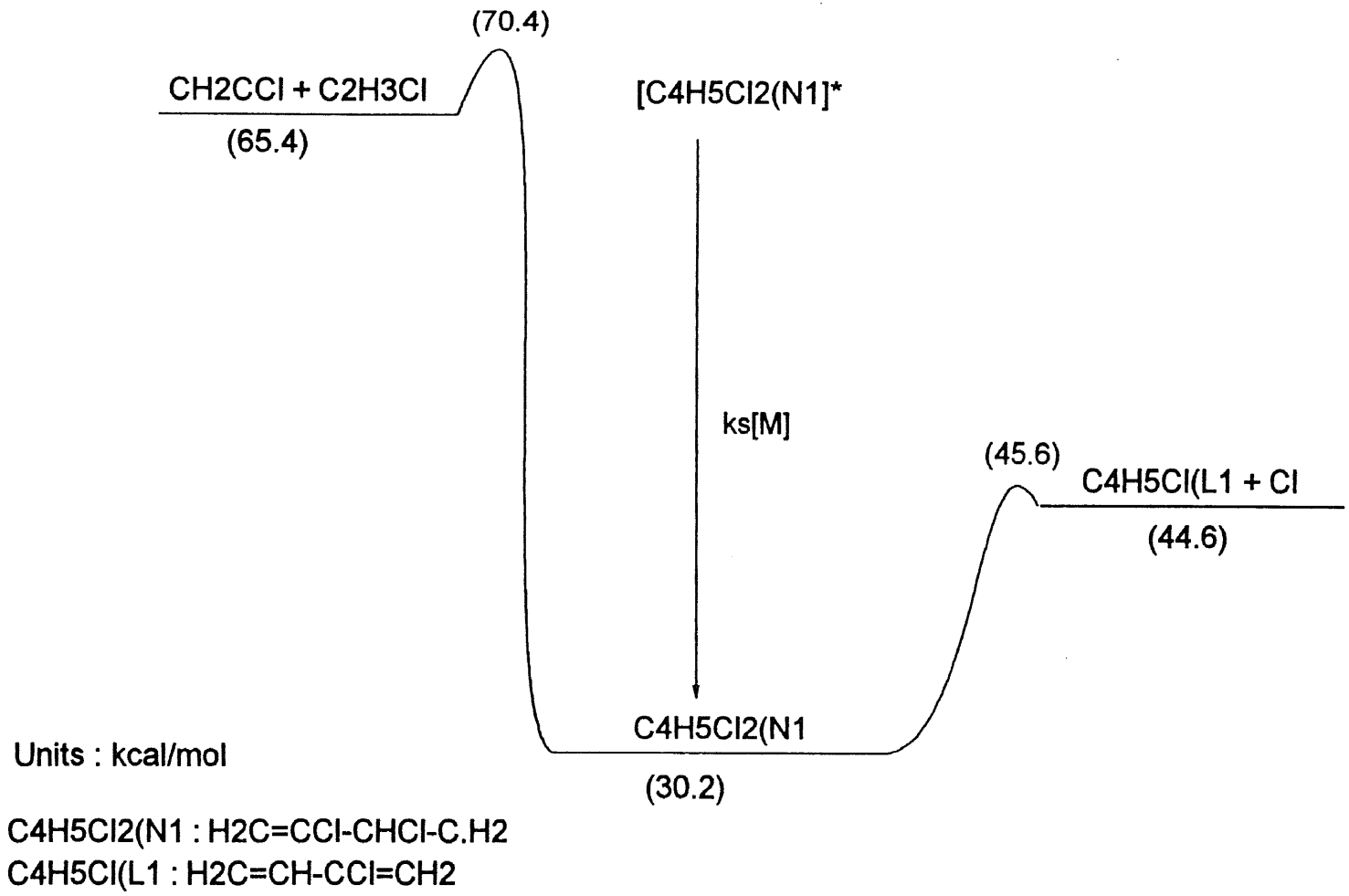

Figure F4 Potential Energy Diagram for
CH2CCl + C2H3Cl ⟷ [C4H5Cl2(N1]* ⟶ Products

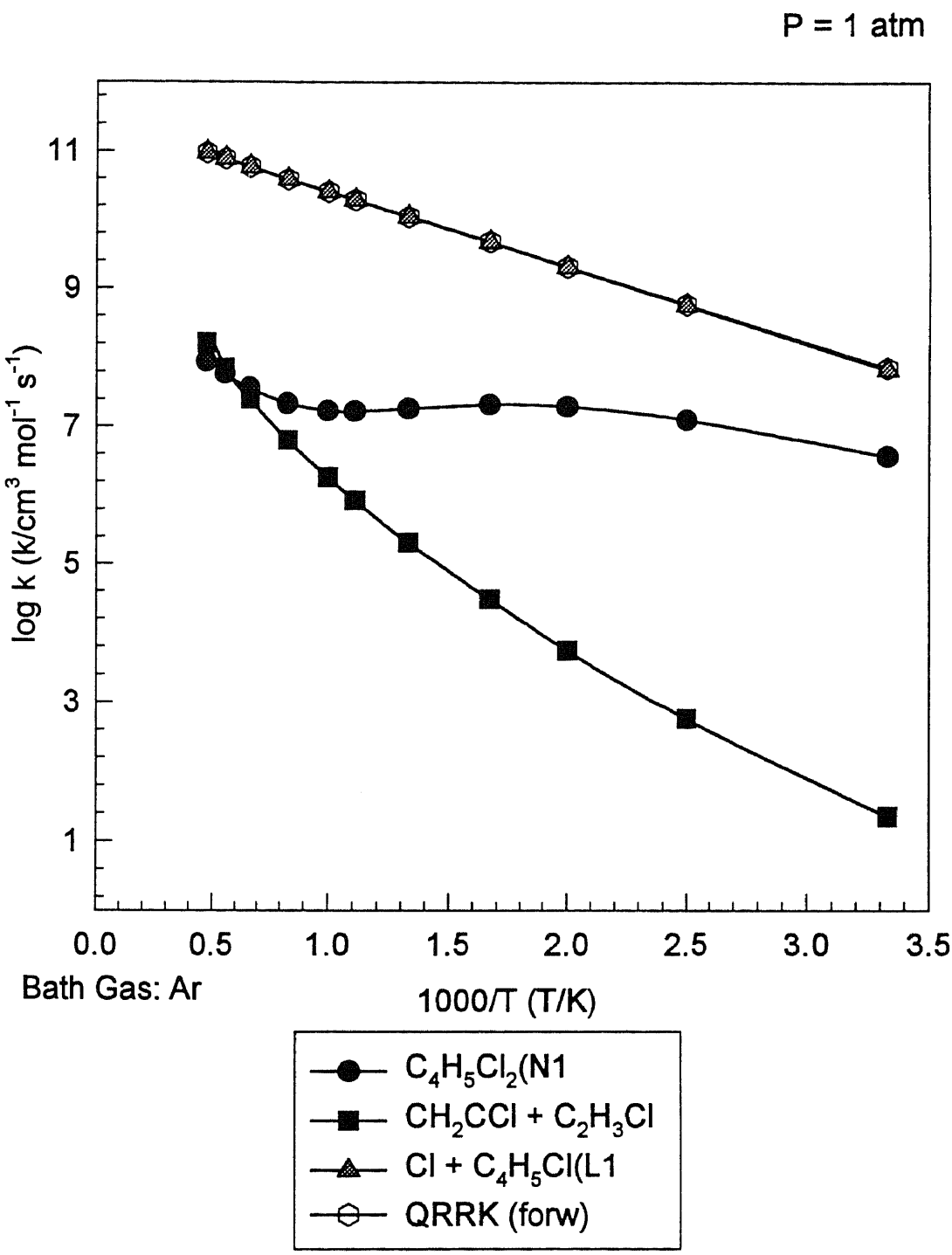

Figure F5 $CH_2CCl + C_2H_3Cl$ <=> $[C_4H_5Cl_2(N1]^*$ => Products

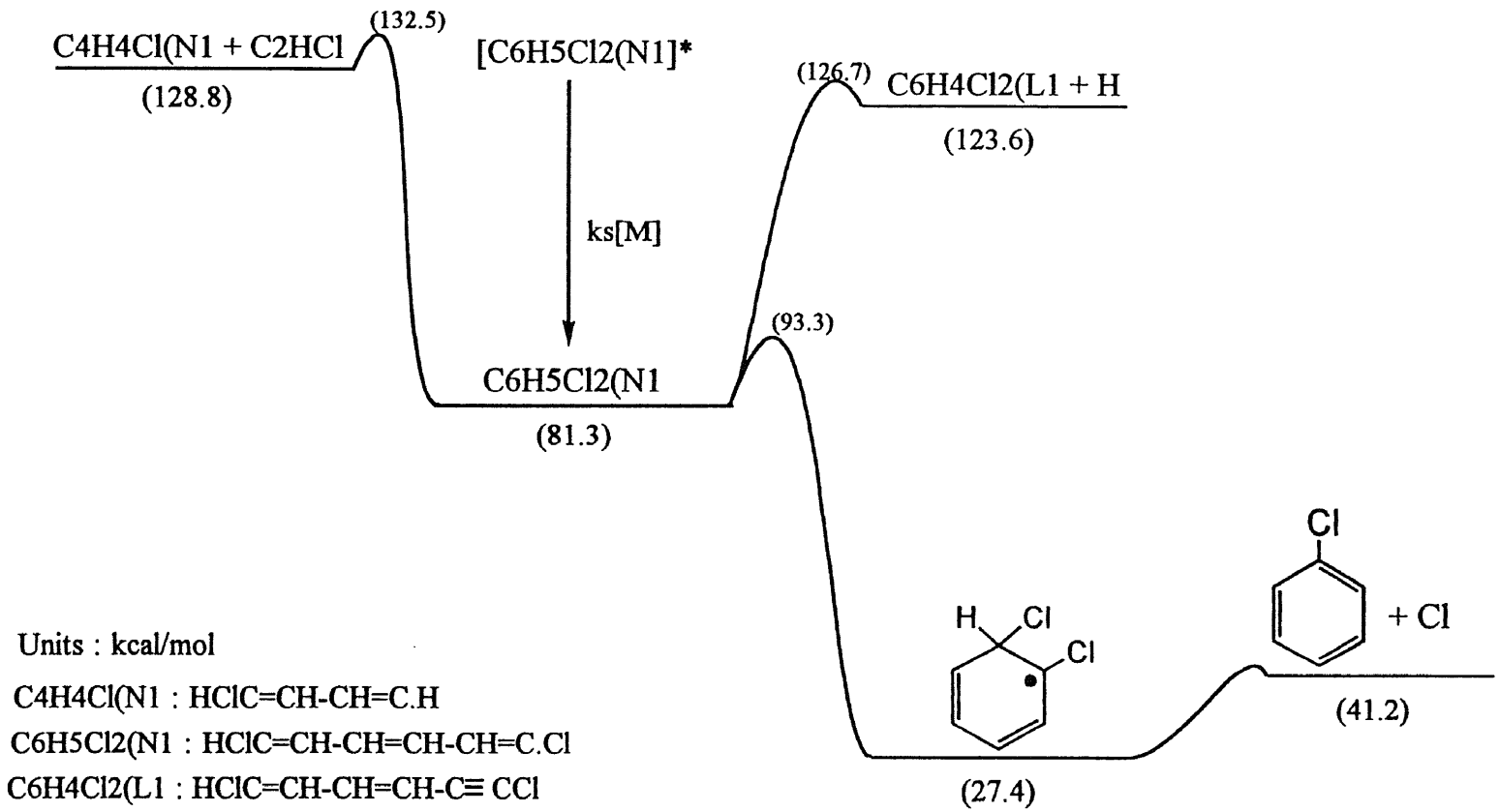

Figure F6 Potential Energy Diagram for
C4H4Cl(N1 + C2HCl ⟷ [C6H5Cl2(N1]* ⟶ Products

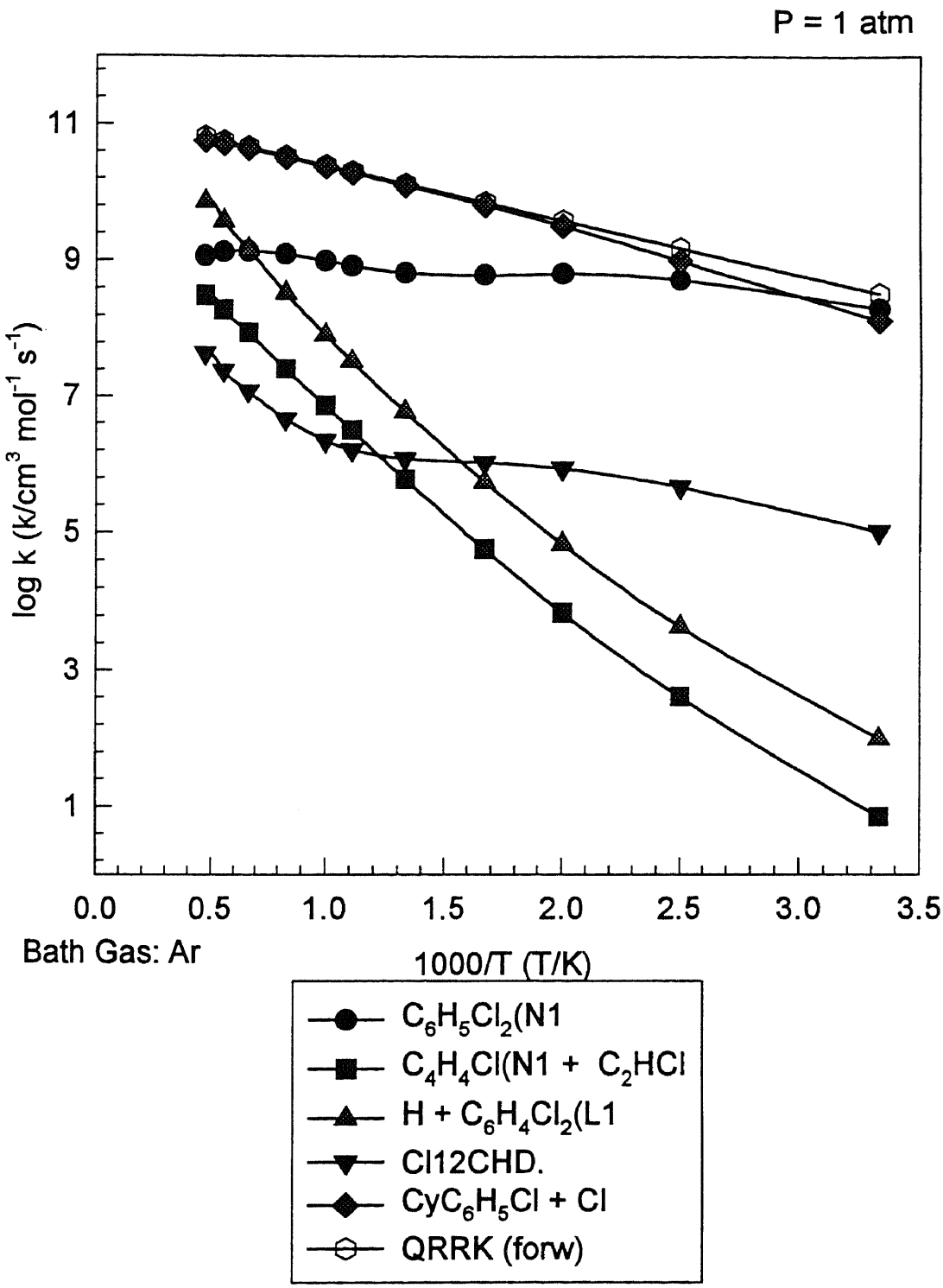

Figure F7 C_4H_4Cl(N1 + C_2HCl <=> [$C_6H_5Cl_2$(N1]* => Products

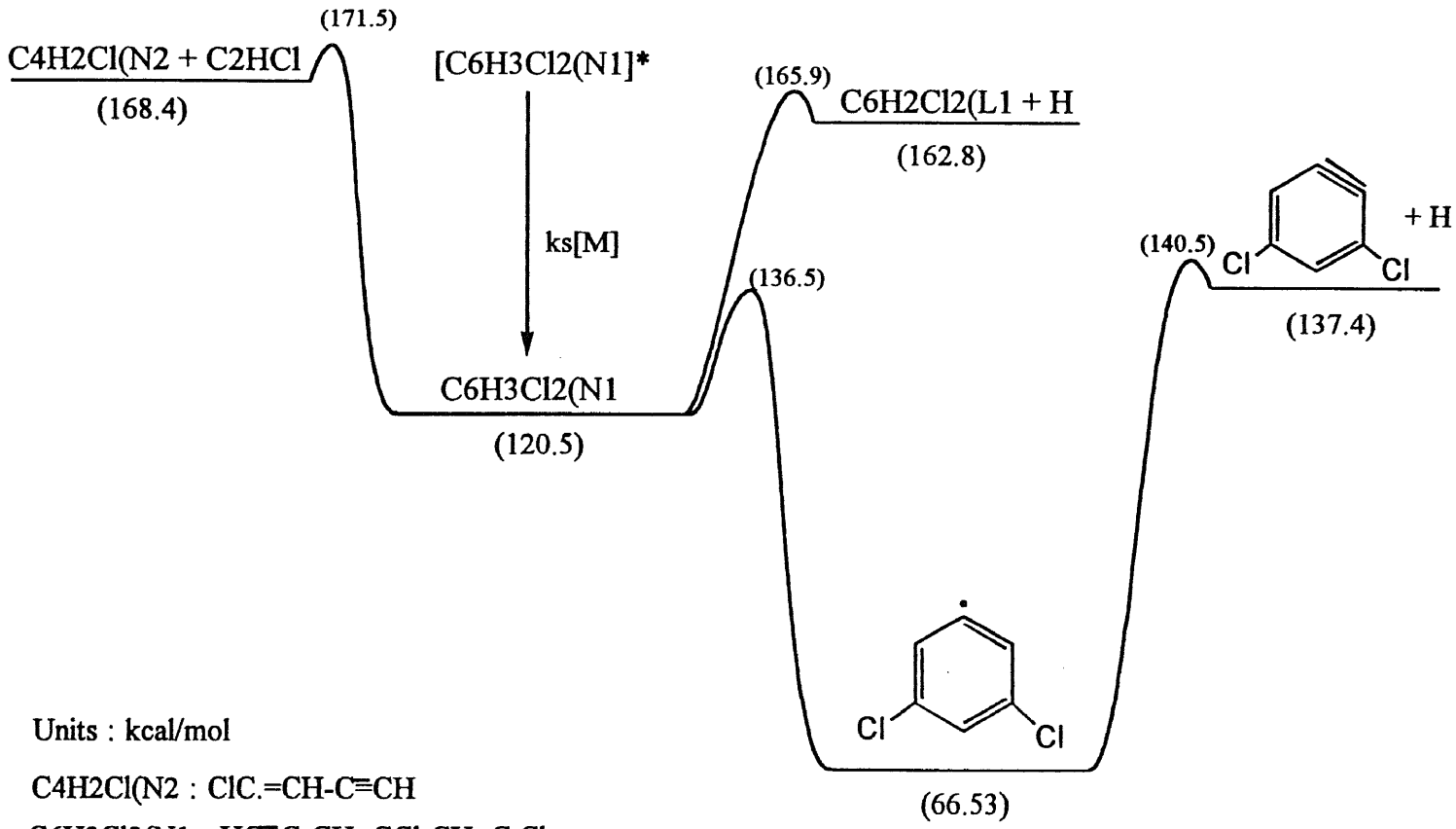

Units : kcal/mol

C4H2Cl(N2 : ClC.=CH-C≡CH

C6H3Cl2(N1 : HC≡C-CH=CCl-CH=C.Cl

C6H2Cl2(L1 : HC≡C-CH=CCl-C≡CCl

Figure F8 Potential Energy Diagram for
C4H2Cl(N2 + C2HCl ⟷ [C6H3Cl2(N1]* ⟶ Products

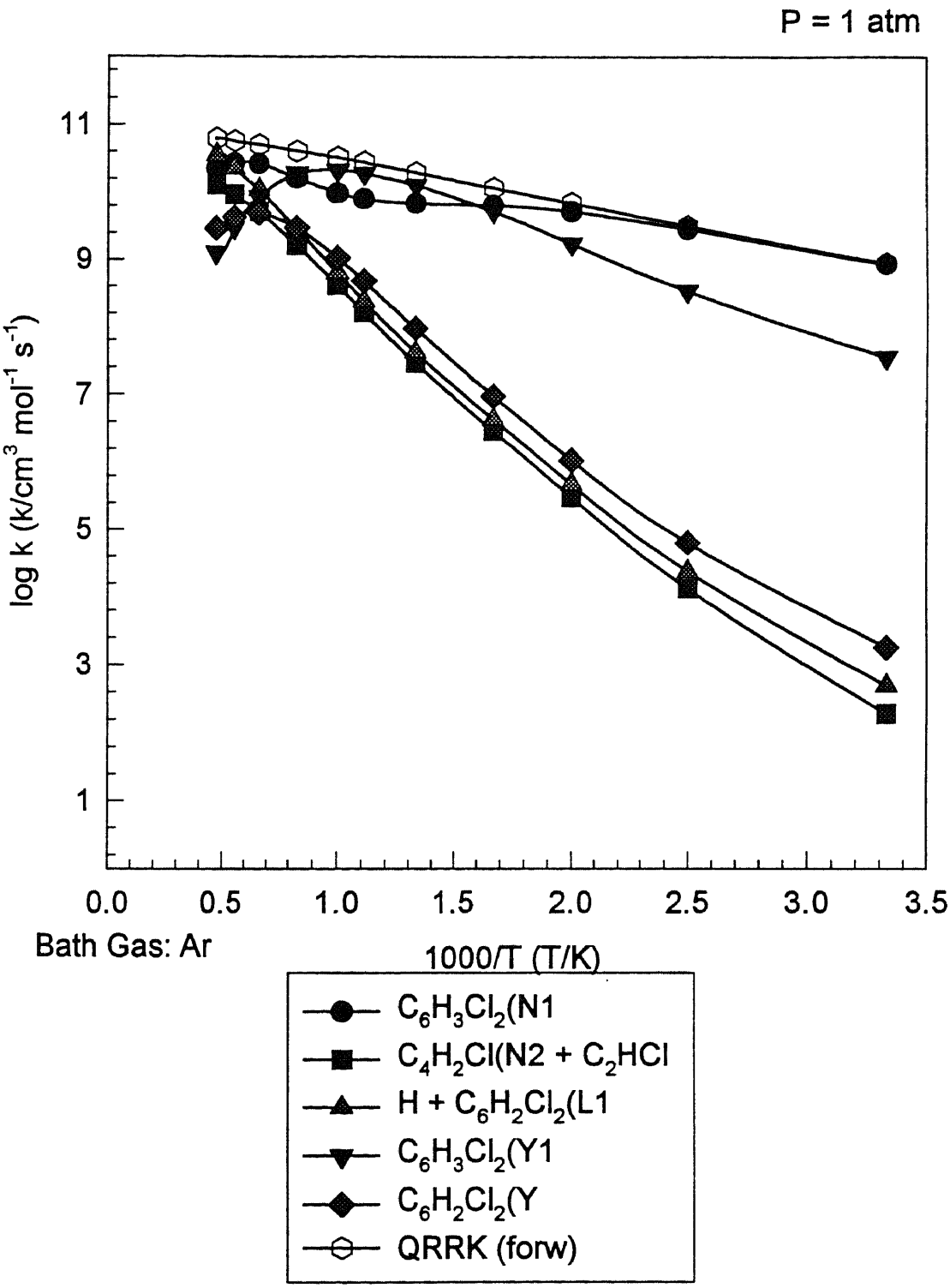

Figure F9 C_4H_2Cl(N2 + C_2HCl <=> [$C_6H_3Cl_2$(N1]* => Products

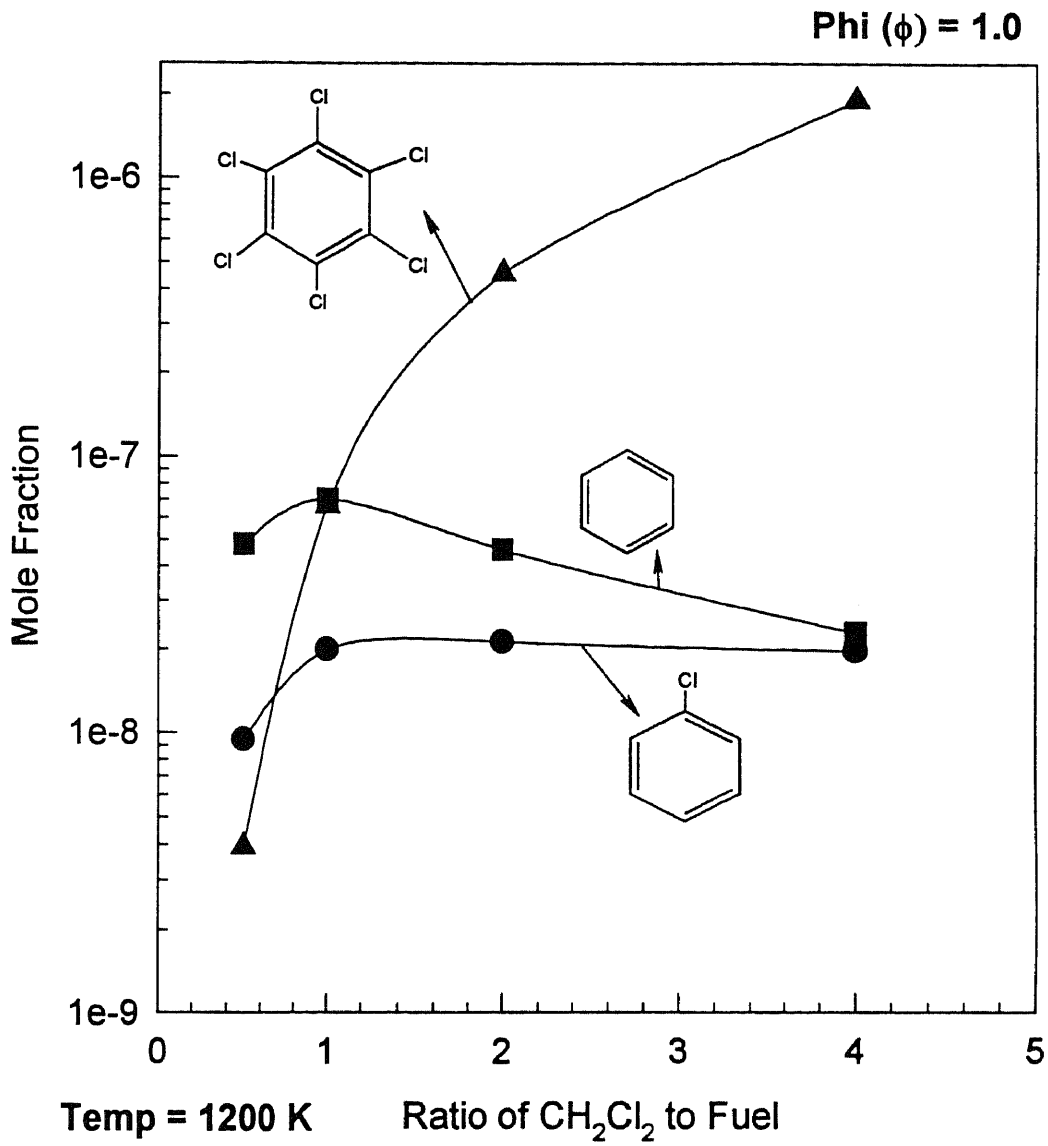

Figure F10 Product Distribution of C_6H_6, CyC_6H_5Cl and C_6Cl_6 vs. Ratio of CH_2Cl_2/Fuel

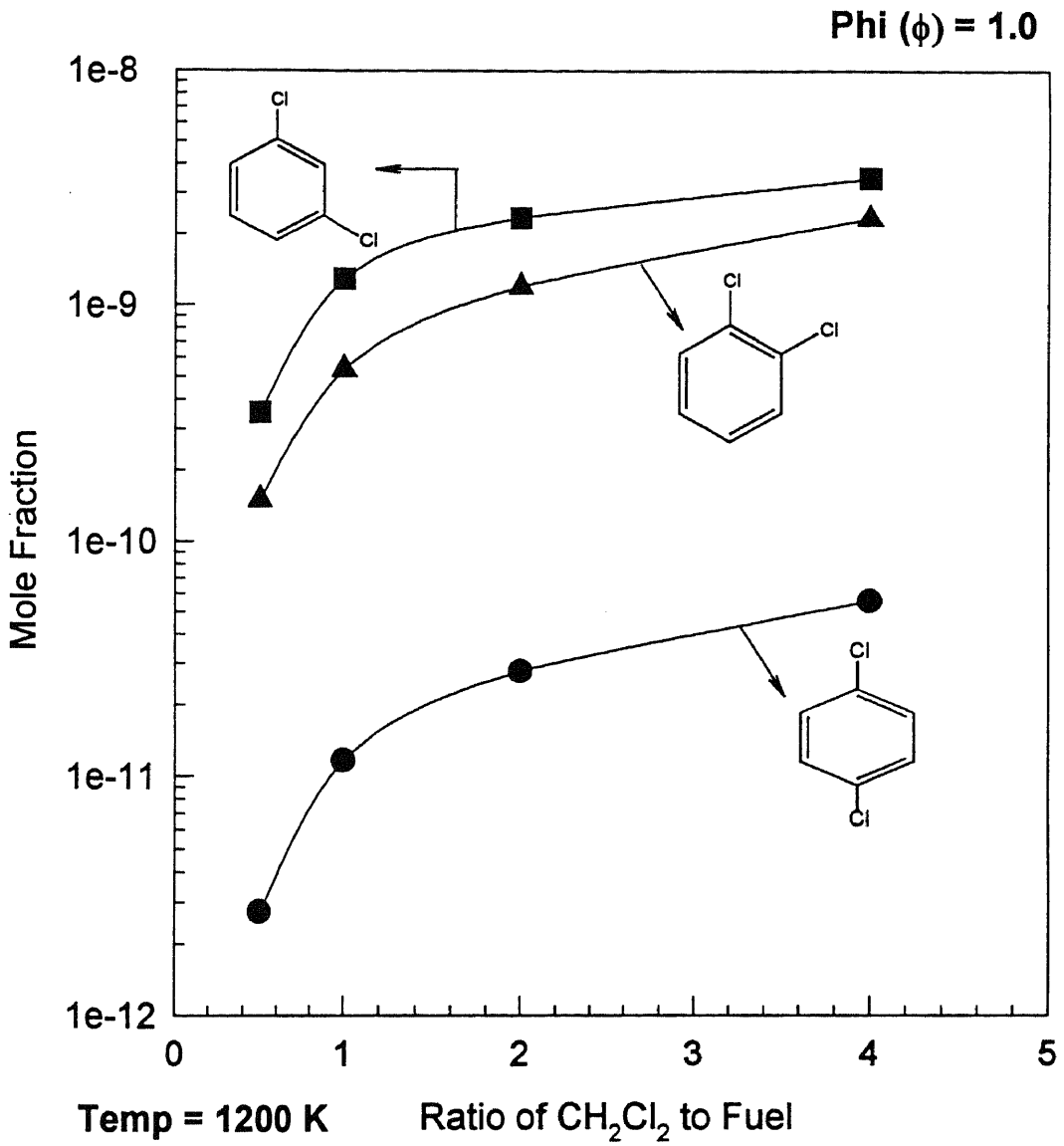

Figure F11 Product Distribution of $CyC_6H_4Cl_2$ vs. Ratio of CH_2Cl_2/Fuel

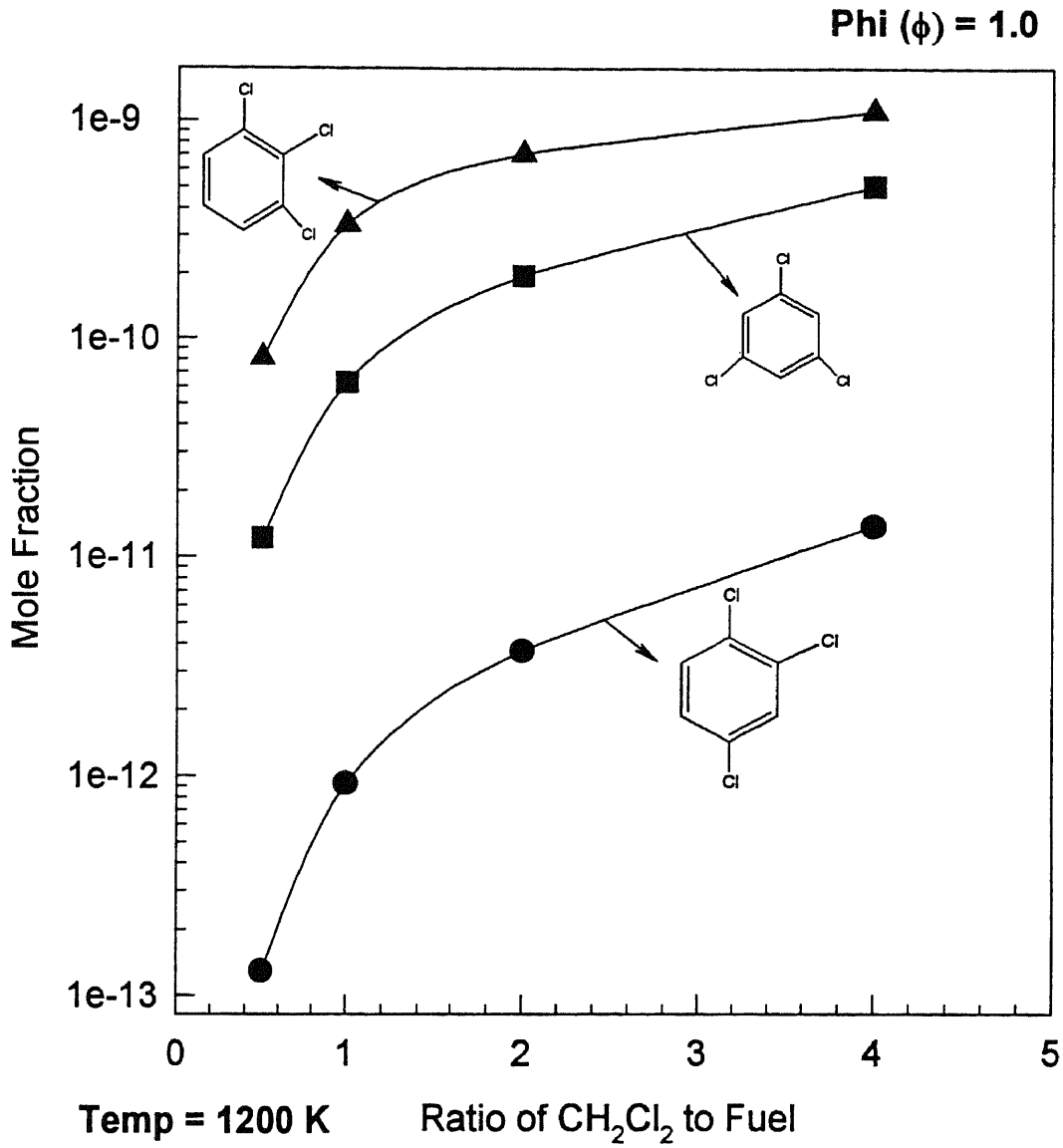

Figure F12 Product Distribution of $CyC_6H_3Cl_3$ vs. Ratio of CH_2Cl_2/Fuel

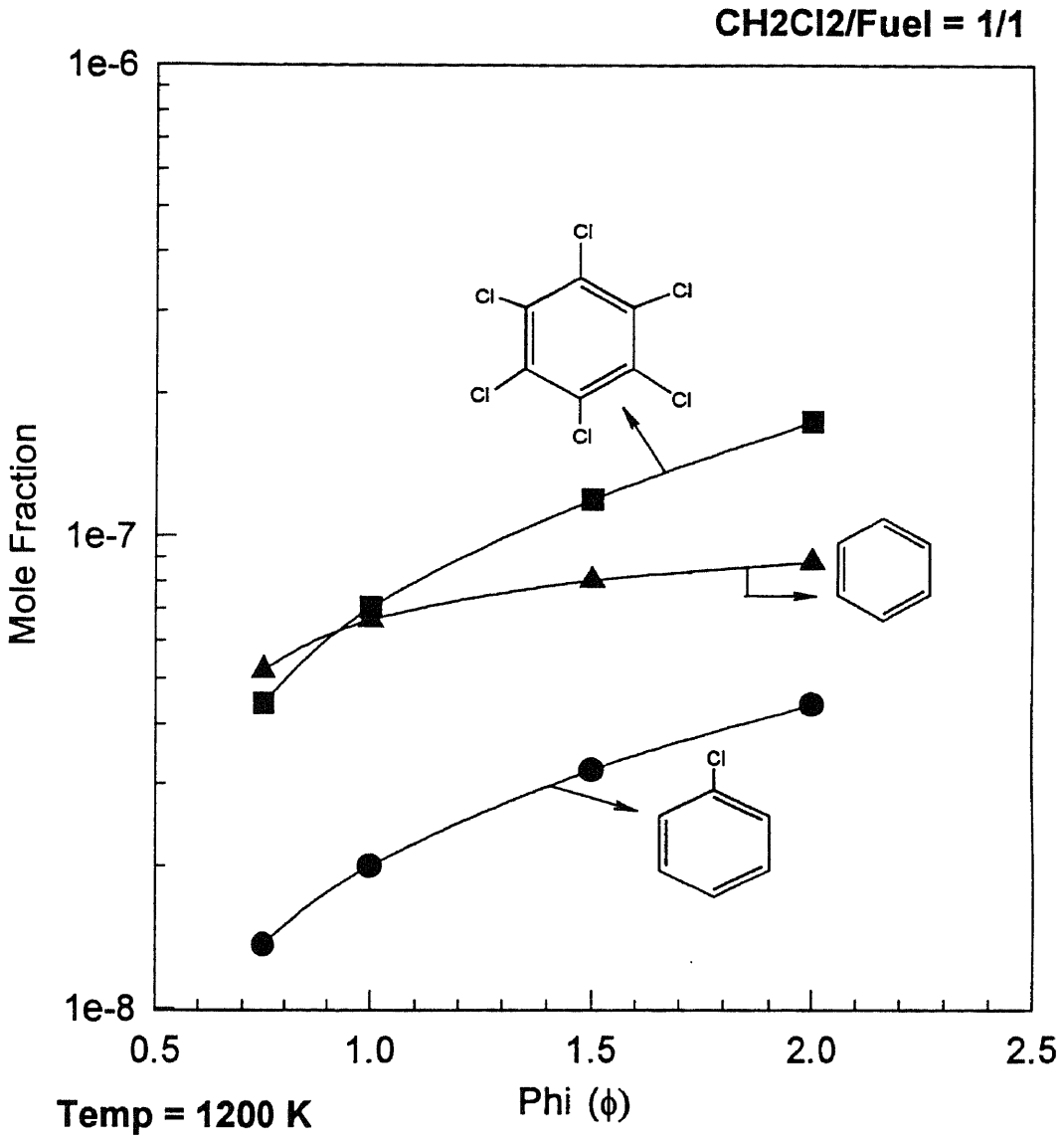

Figure F13 Product Distribution of C_6H_6, CyC_6H_5Cl and C_6Cl_6 vs. Phi (ϕ)

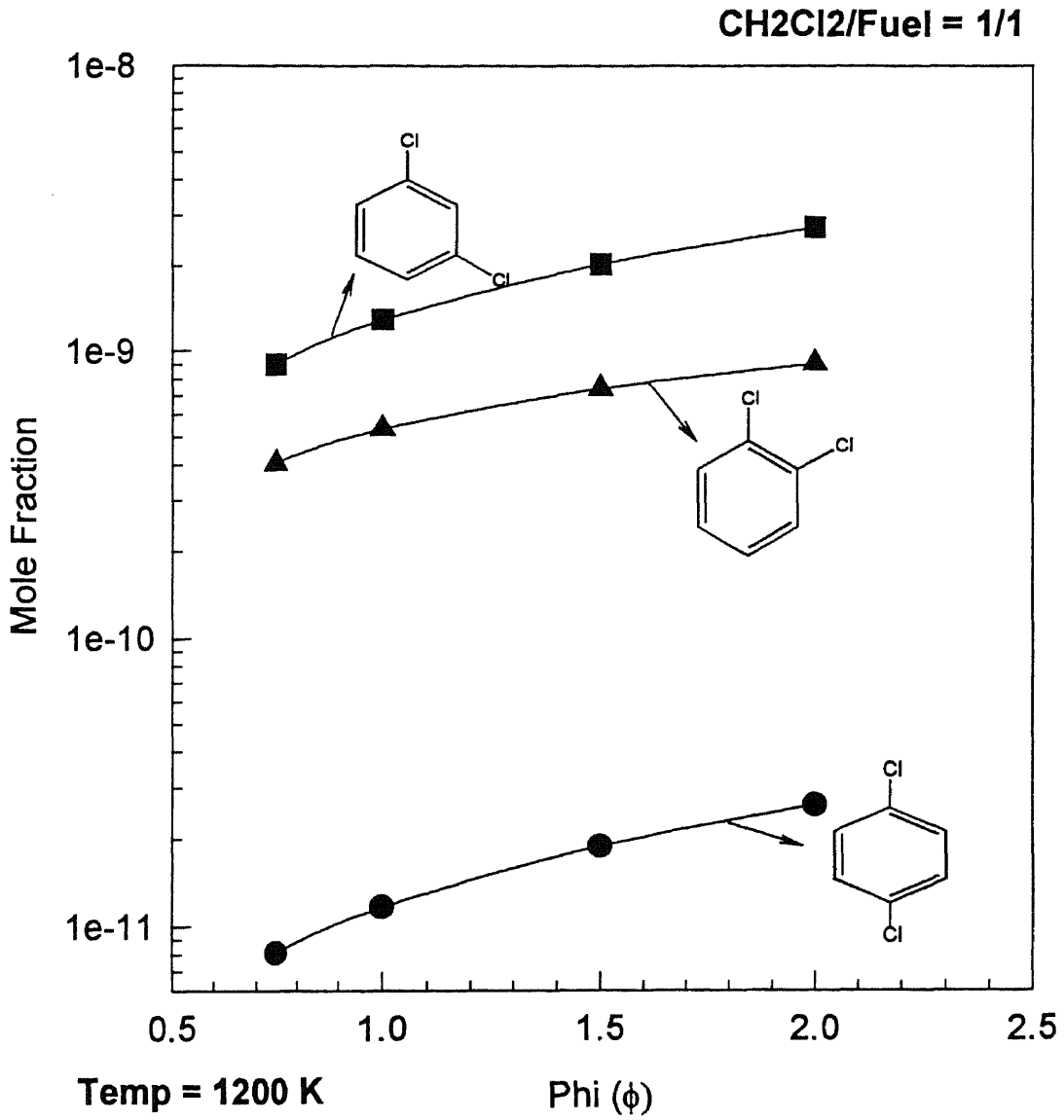

Figure F14 Product Distribution of $CyC_6H_4Cl_2$ vs. Phi (ϕ)

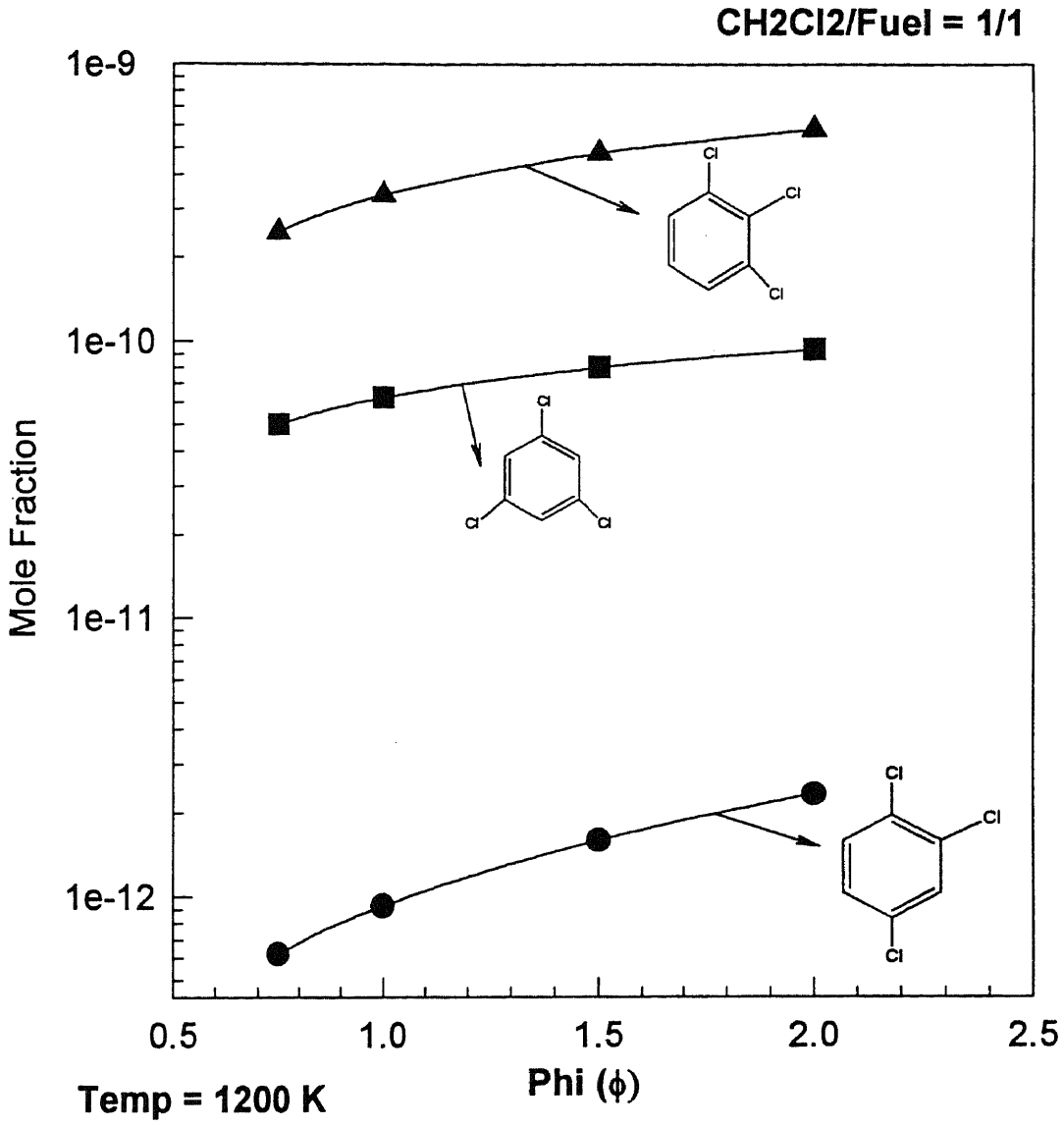

Figure F15 Product Distribution of $CyC_6H_3Cl_3$ vs. Phi (ϕ)

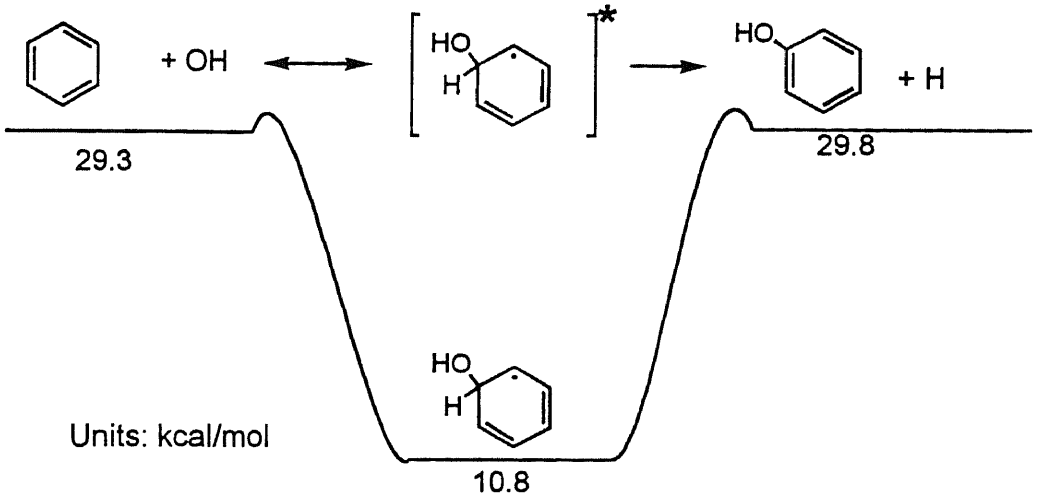

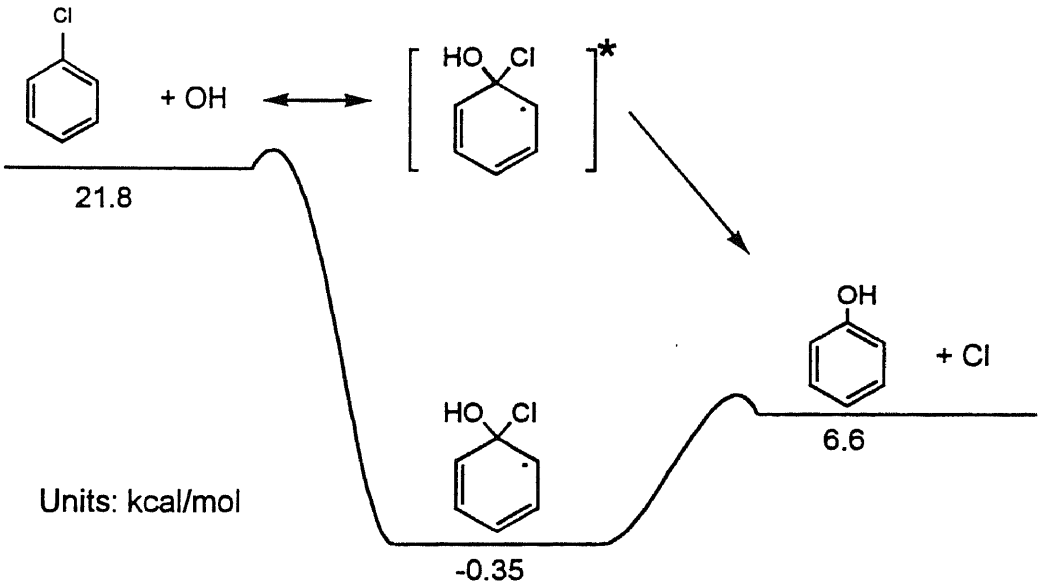

Figure F16 Potential Energy Diagram for CyC6H6 + OH and CyC6H5Cl + OH

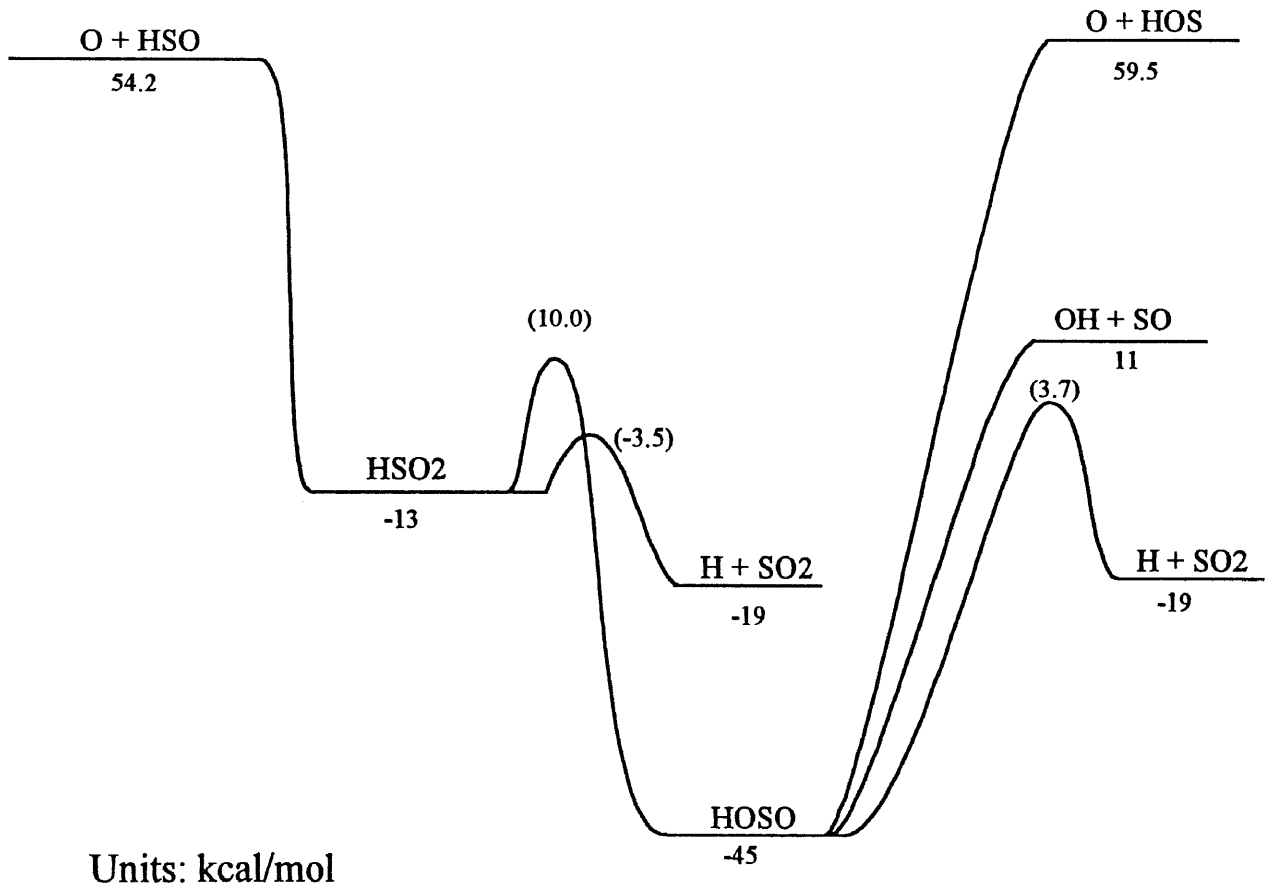

Figure G1 Potential Energy Diagram for

HSO + O ⟷ [HSO2]* ⟶ Products

OH + SO
H + SO2 ⟷ [HOSO]* ⟶ Products

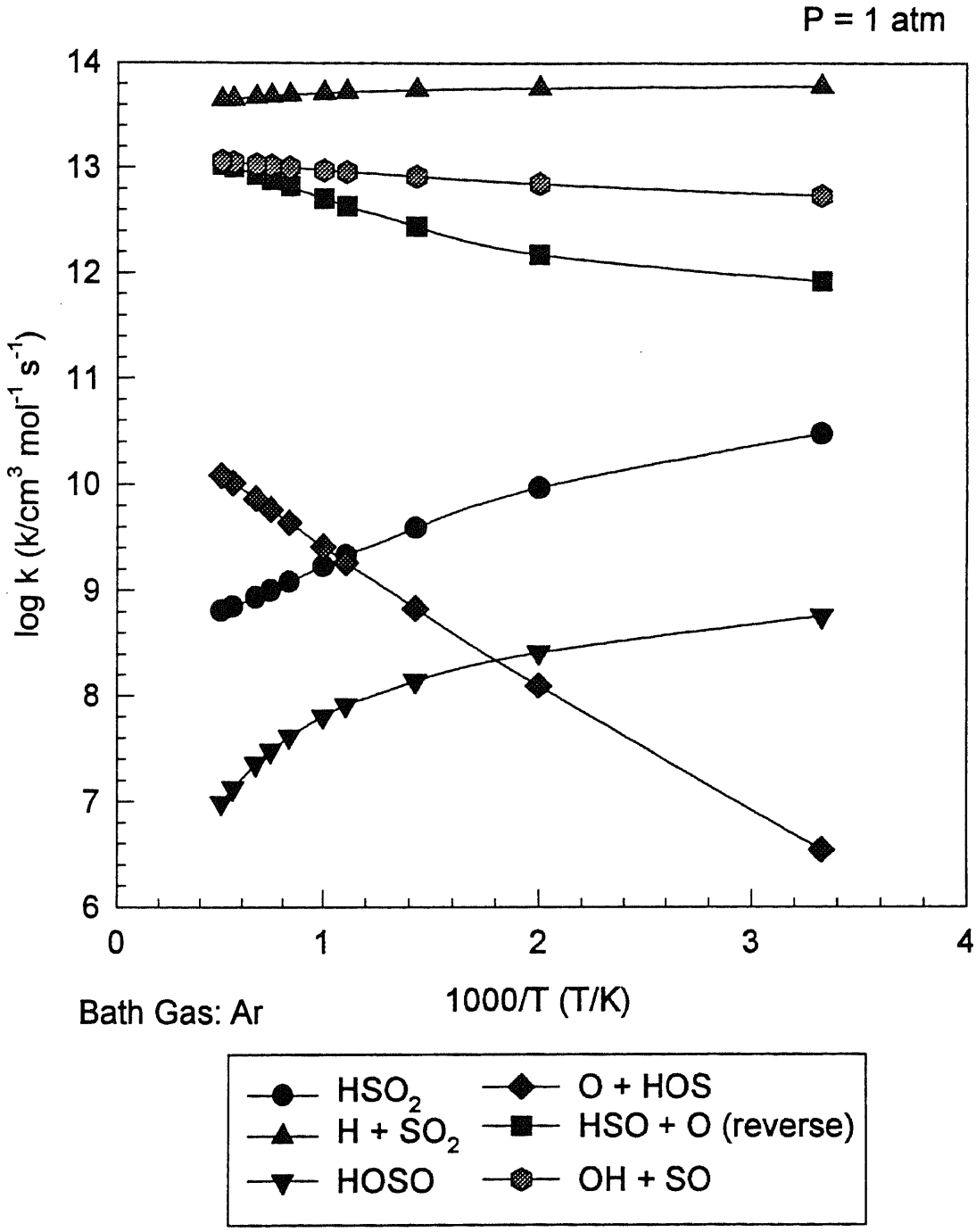

Figure G2 Results of QRRK Calculation for
O + HSO <=> [HSO$_2$]* => Products

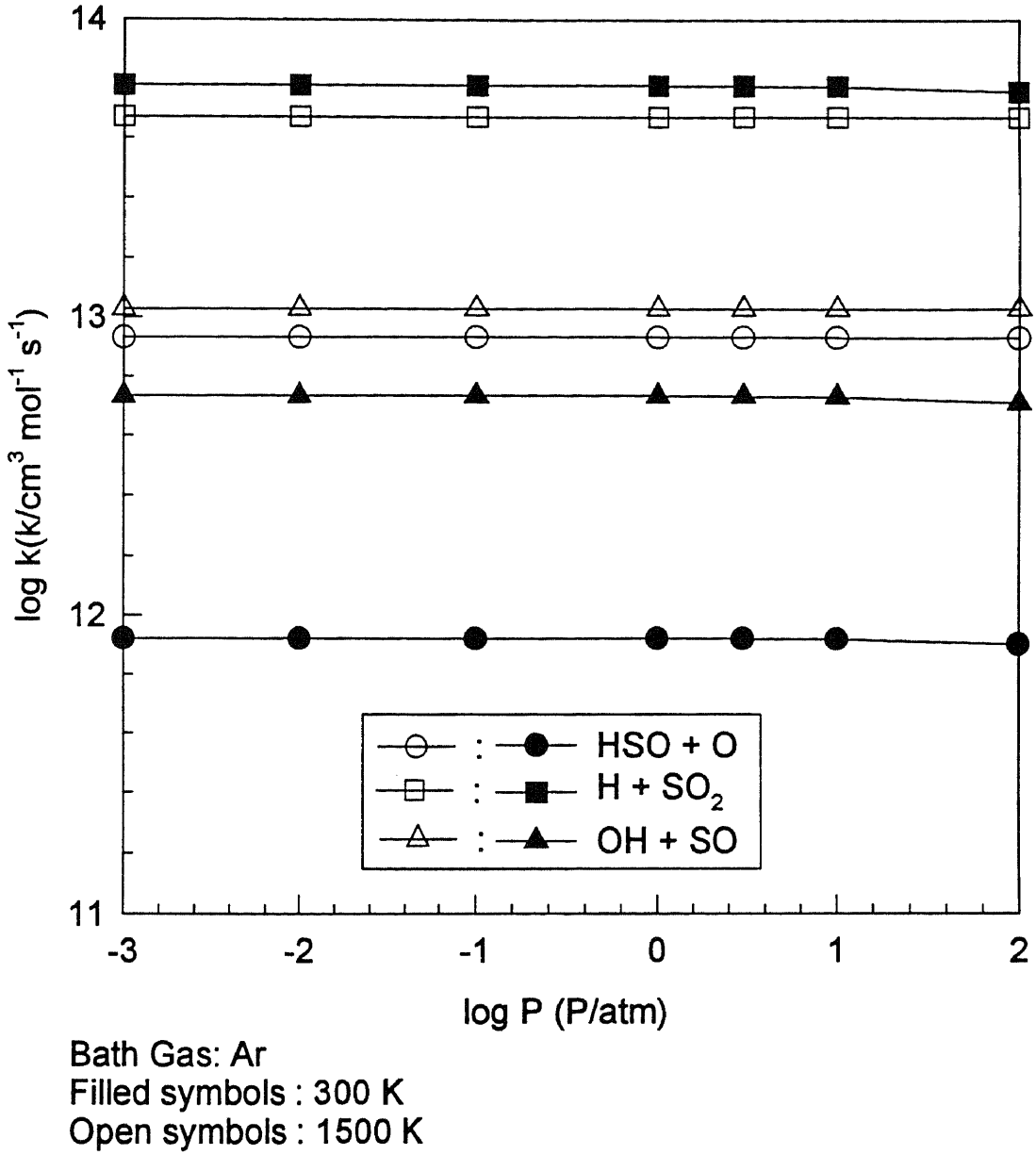

Figure G3 Results of QRRK Calculation for
O + HSO <=> [HSO_2]* => Products

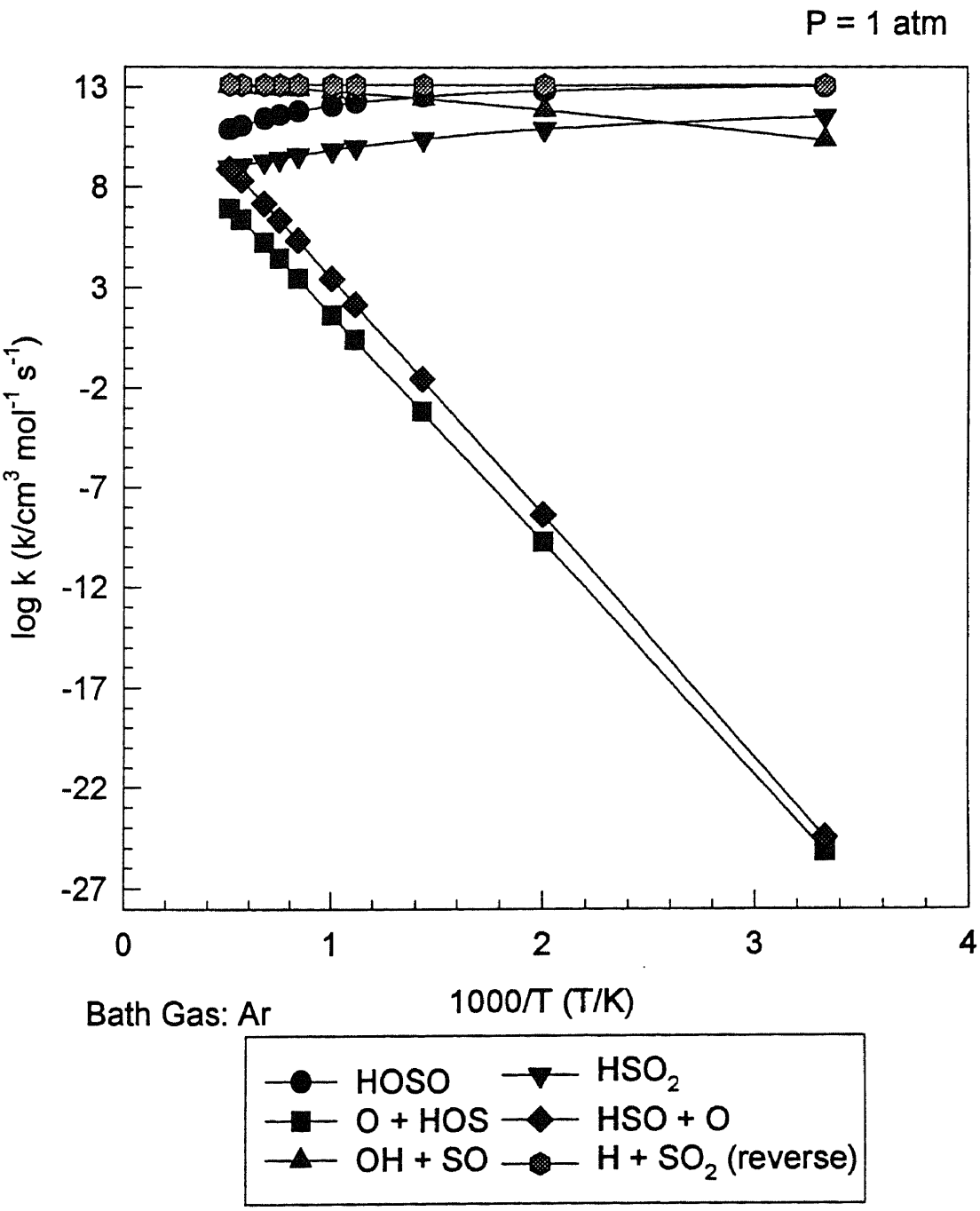

Figure G4 Results of QRRK Calculation

for $H + SO_2 \Leftrightarrow \begin{matrix}[HOSO]^* \\ [HSO_2]^*\end{matrix} \Rightarrow$ Products

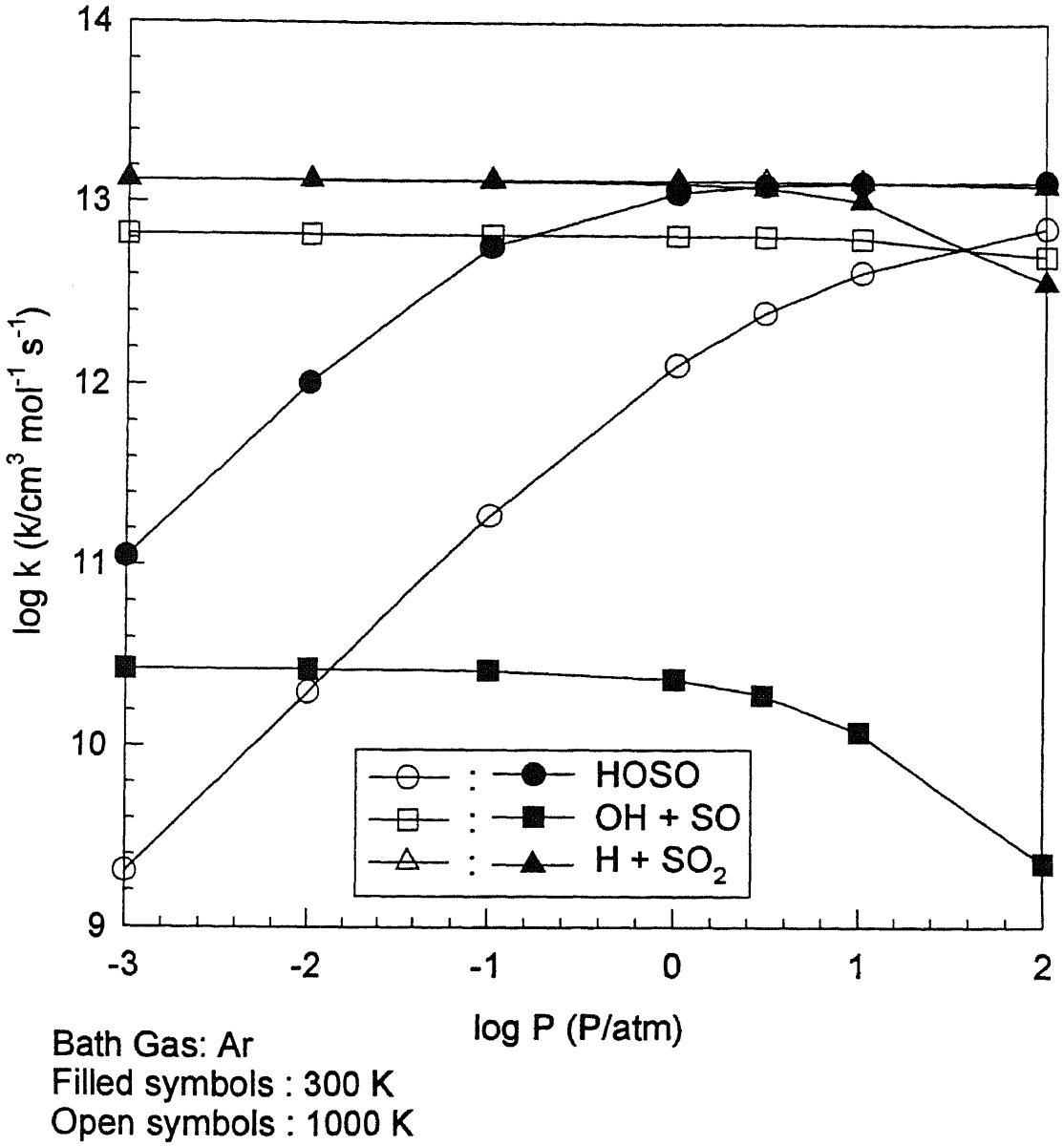

Bath Gas: Ar
Filled symbols : 300 K
Open symbols : 1000 K

Figure G5 Results of QRRK Calculation

for $H + SO_2 \Leftrightarrow \begin{matrix}[HOSO]^* \\ [HSO_2]^*\end{matrix} \Rightarrow$ Products

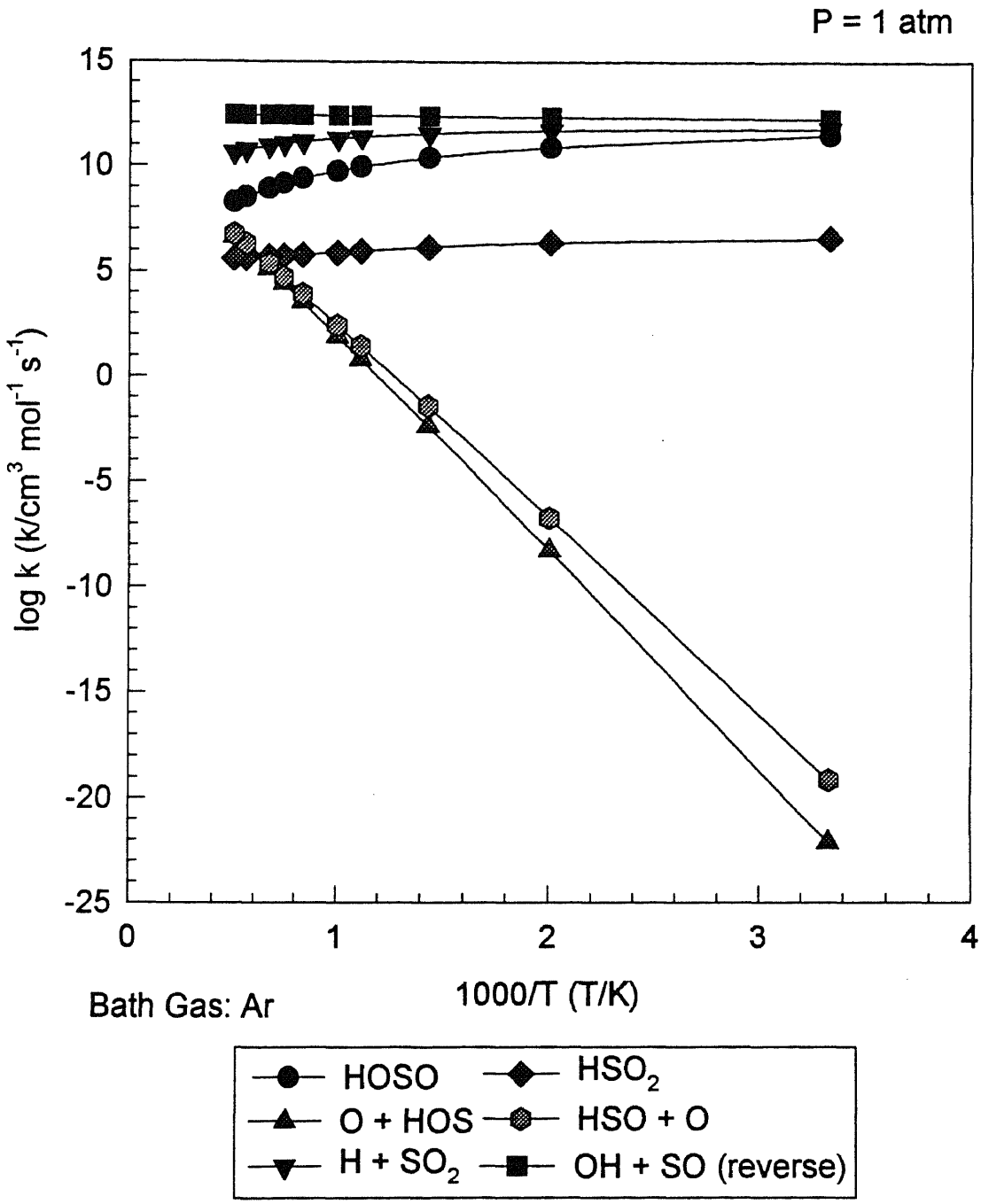

Figure G6 Results of QRRK Calculation for OH + SO <=> [HOSO]* => Products

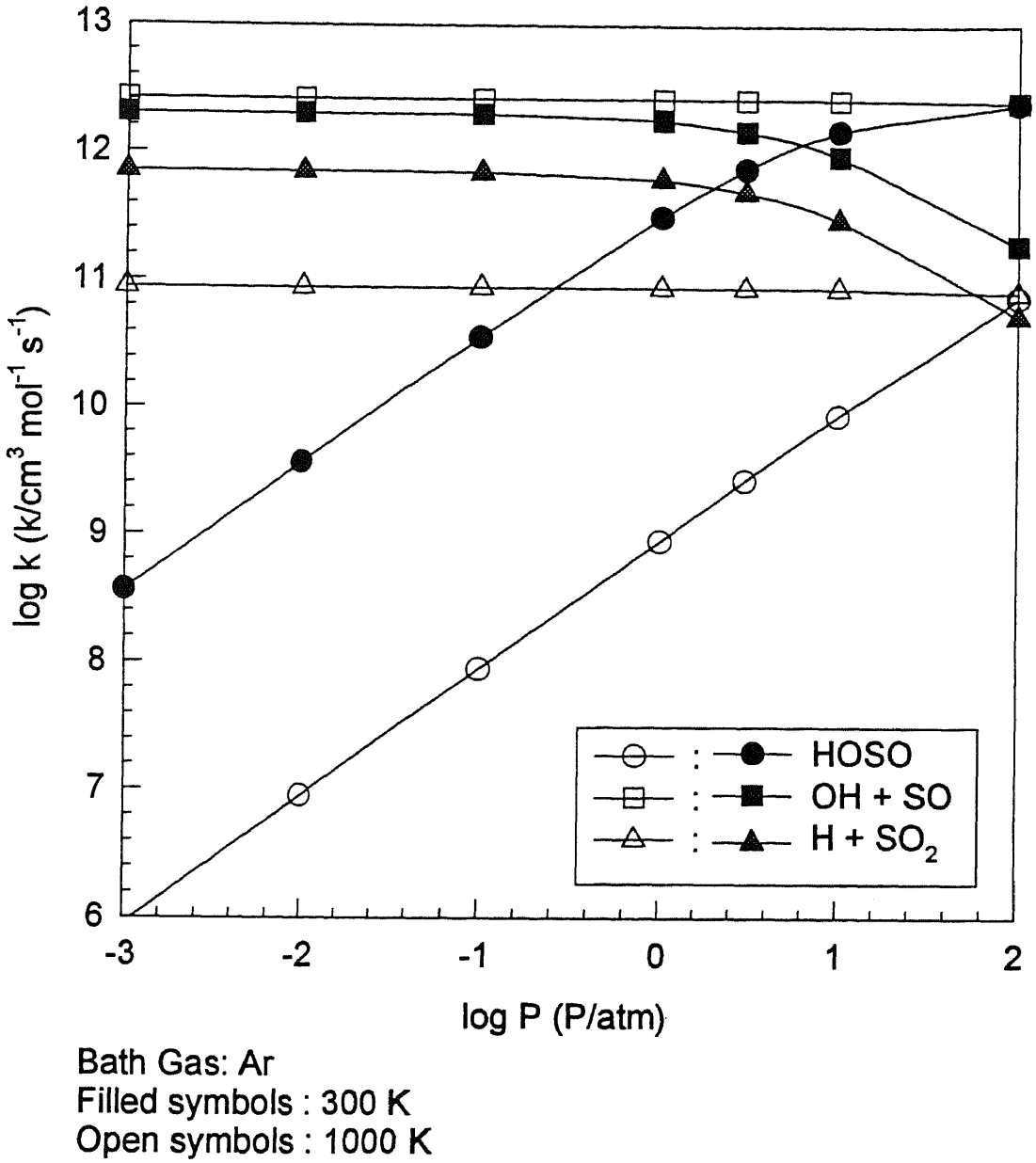

Figure G7 Results of QRRK Calculation
for OH + SO <=> [HOSO]* => Products

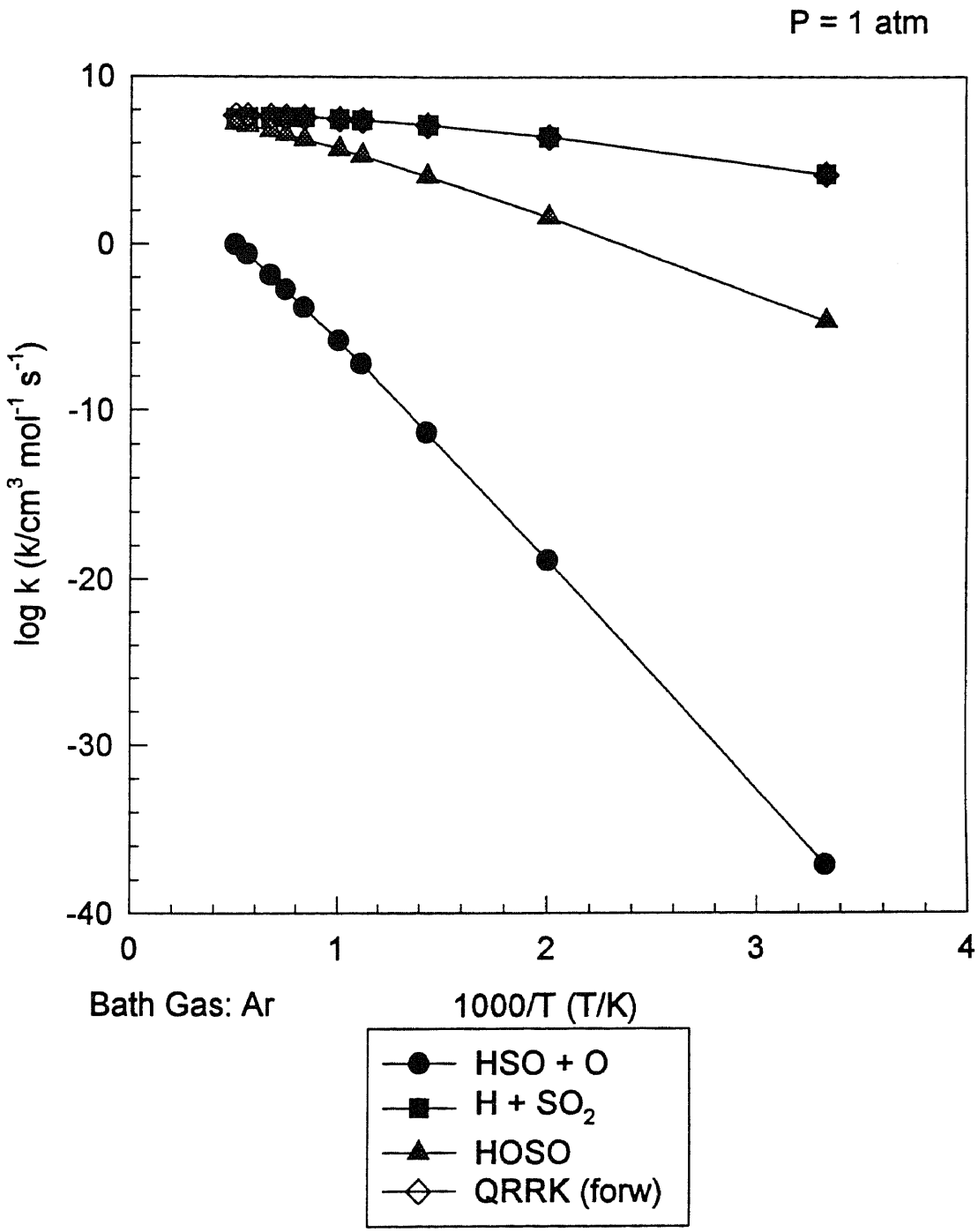

Figure G8 Results of QRRK Calculation for HSO_2 <=> $[HSO_2]^*$ => Products

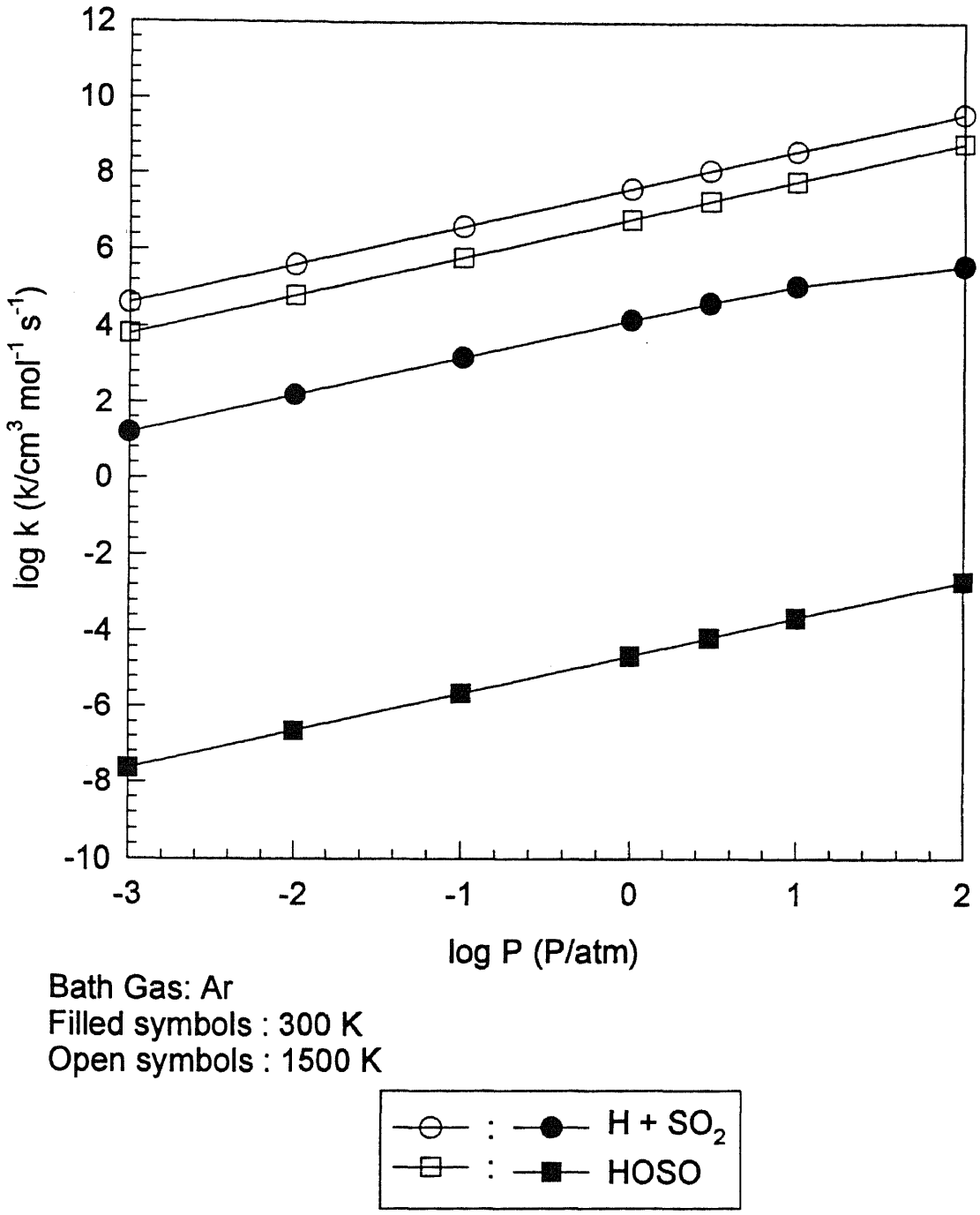

Figure G9 Results of QRRK Calculation for HSO_2 <=> $[HSO_2]^*$ => Products

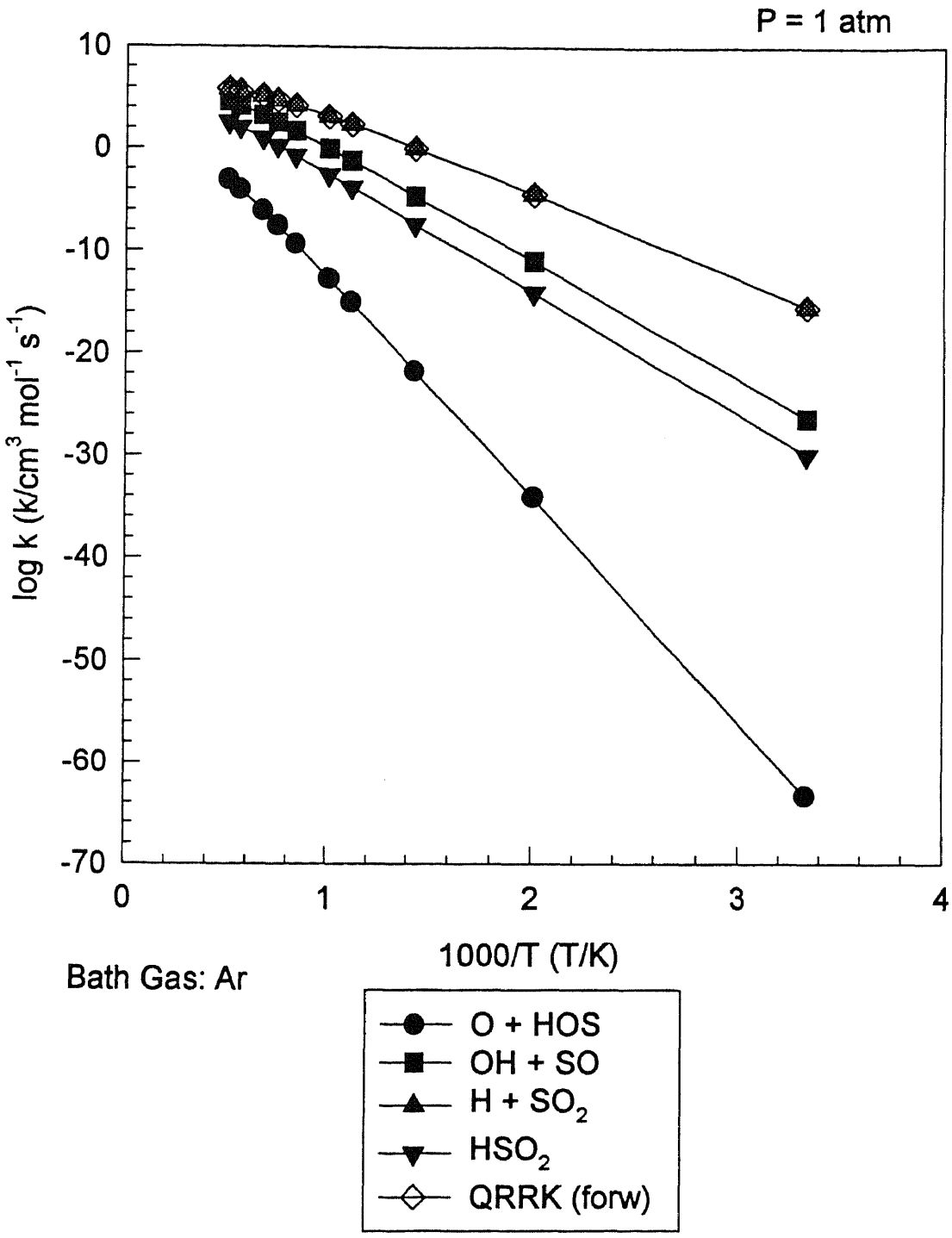

Figure G10 Results of QRRK Calculation for HOSO <=> [HOSO]* => Products

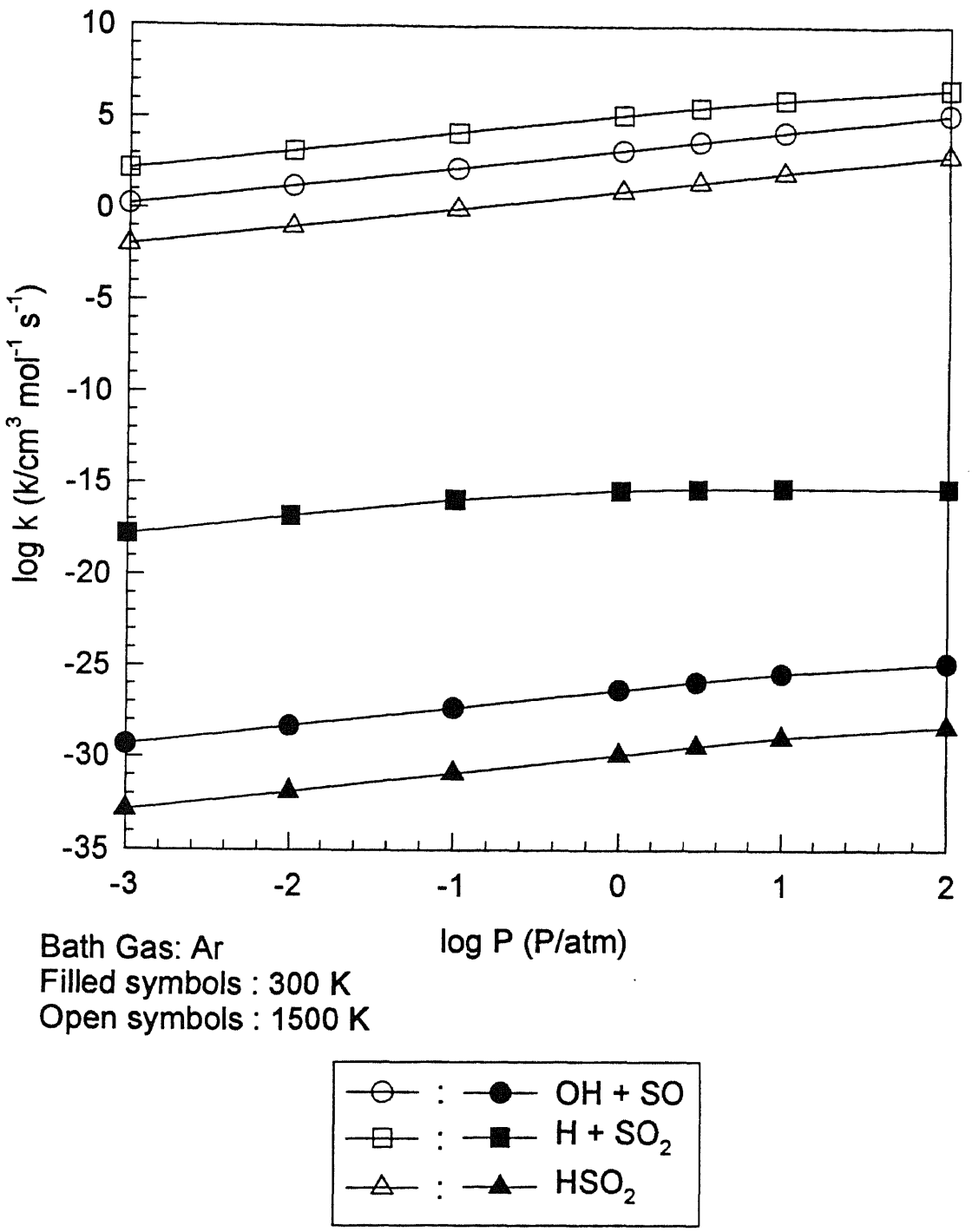

Figure G11 Results of QRRK Calculation for HOSO <=> [HOSO]* => Products

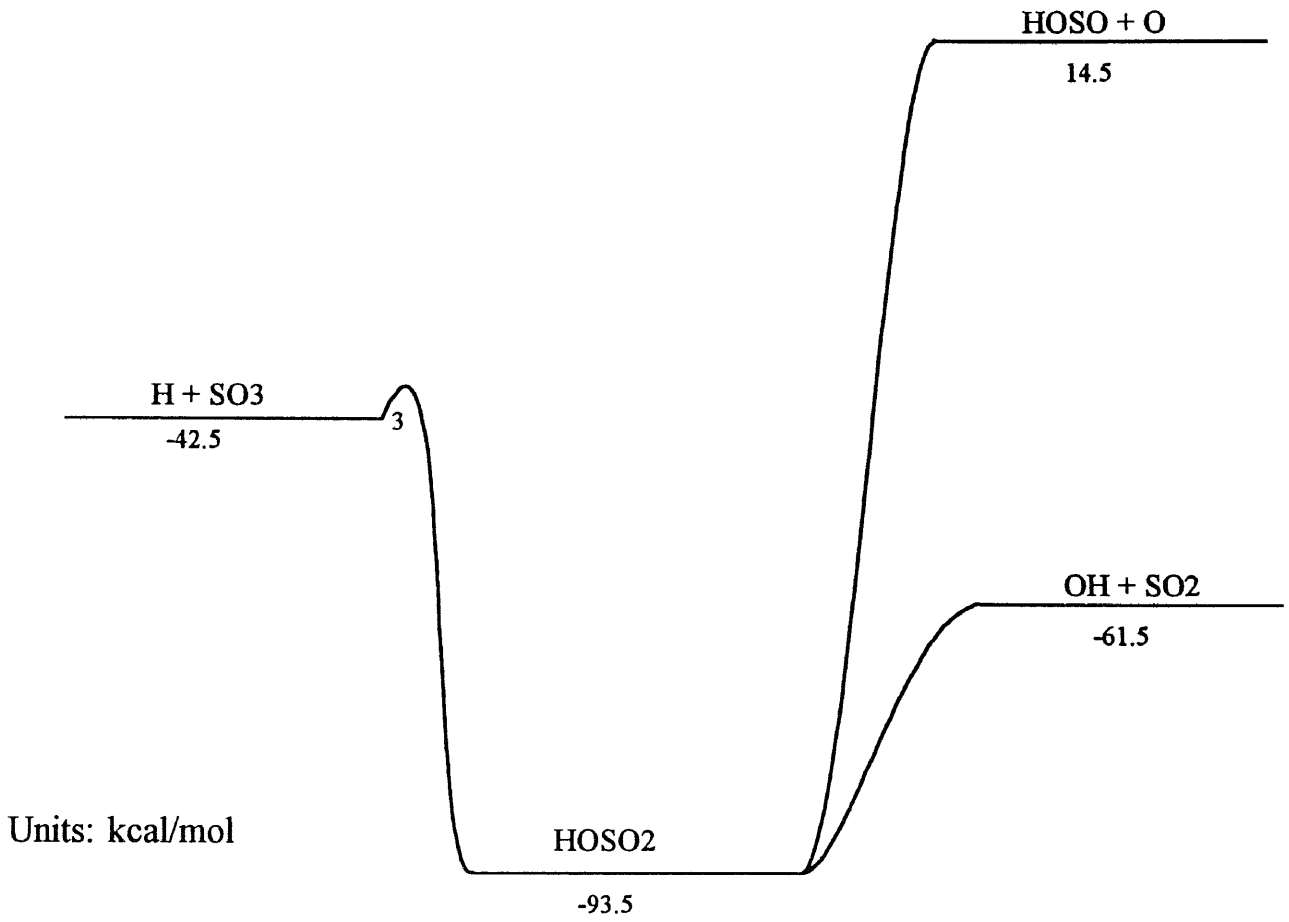

Figure G12 Potential Energy Diagram for

SO3 + H ⟷ [HOSO2]* ⟶ Products

SO2 + OH

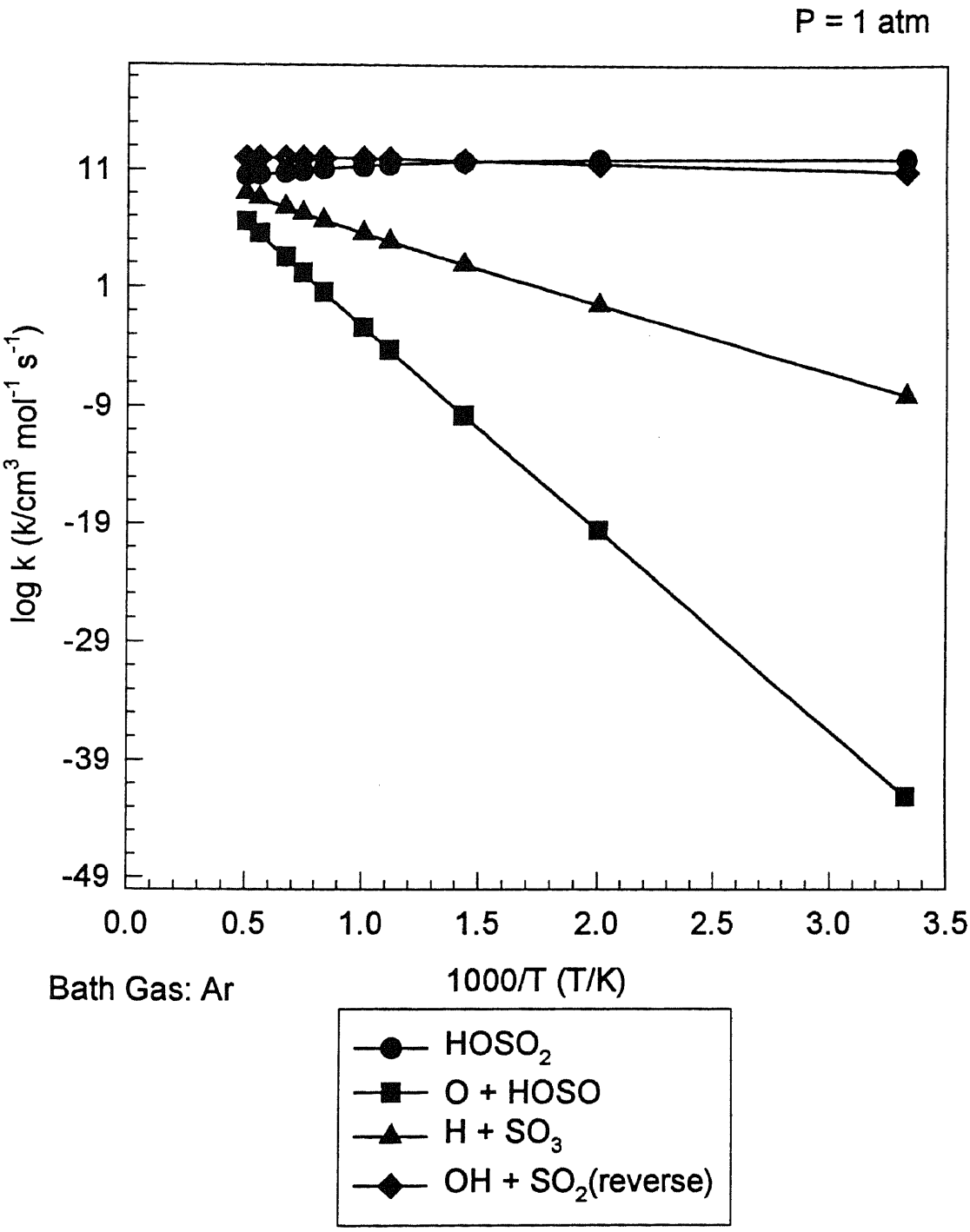

Figure G13 Results of QRRK Calculation for OH + SO_2 <=> $[HOSO_2]^*$ => Products

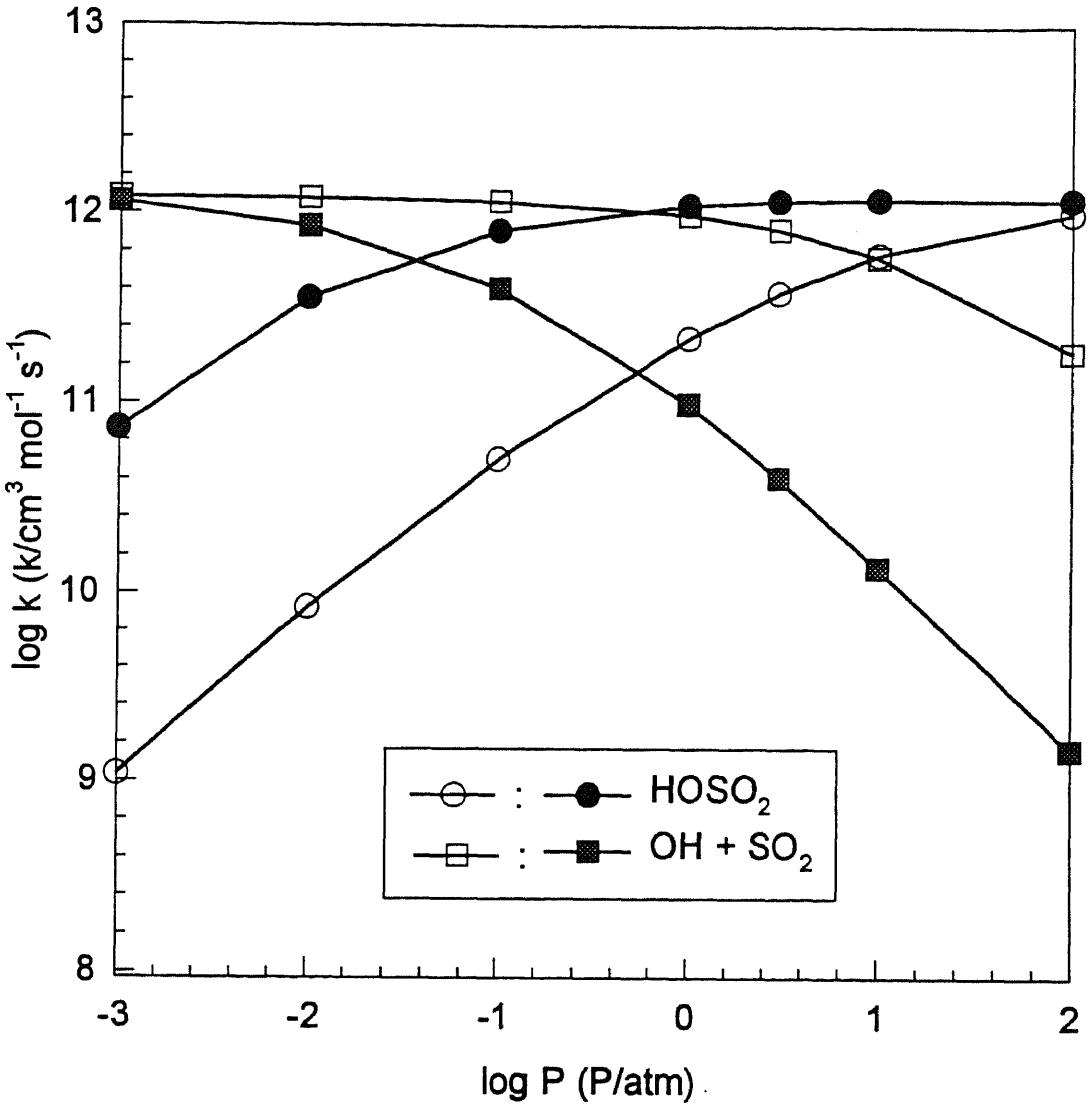

Bath Gas: Ar
Filled symbols : 300 K
Open symbols : 1000 K

Figure G14 Results of QRRK Calculation for OH + SO_2 <=> $[HOSO_2]^*$ => Products

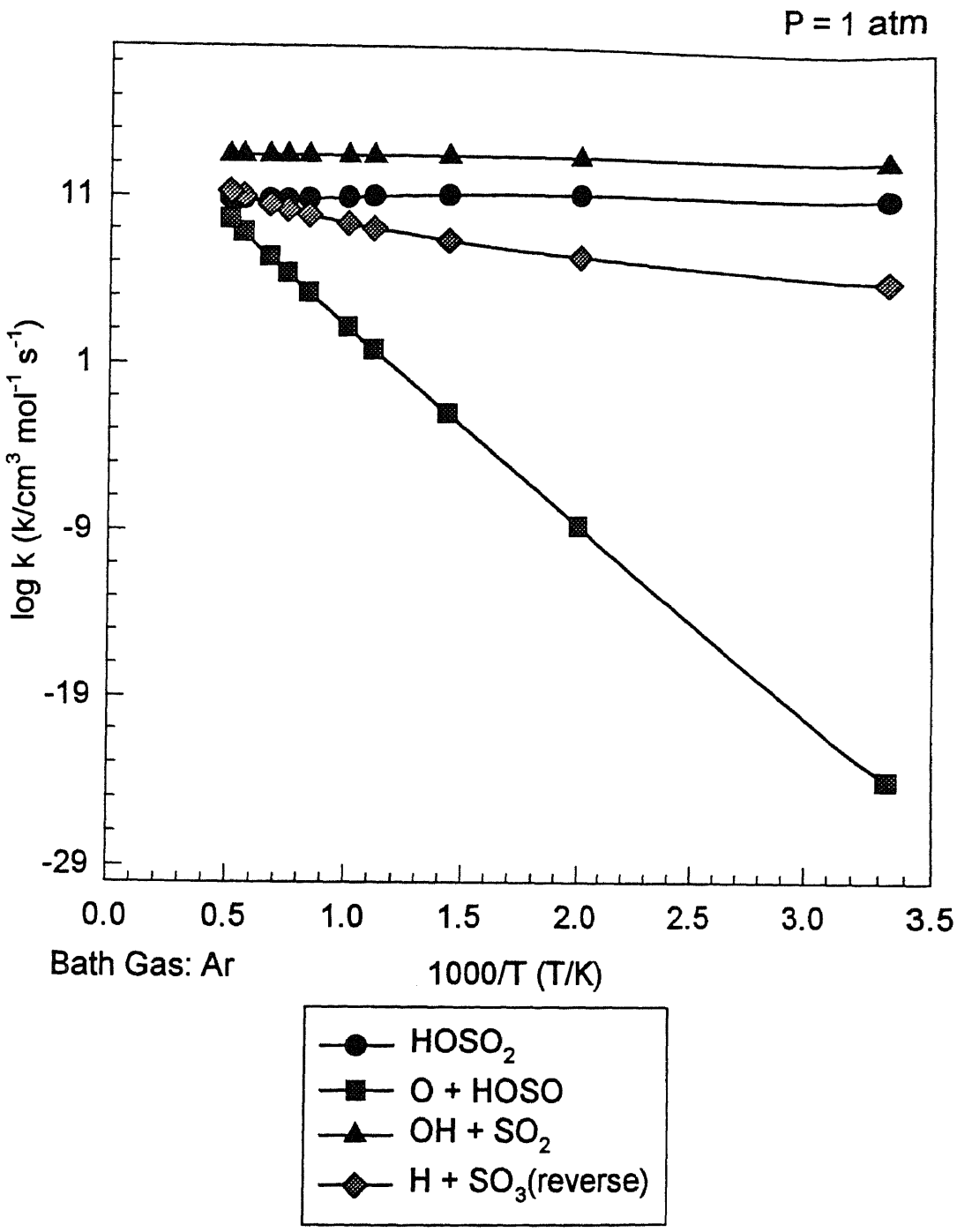

Figure G15 Results of QRRK Calculation for H + SO_3 <=> $[HOSO_2]^*$ => Products

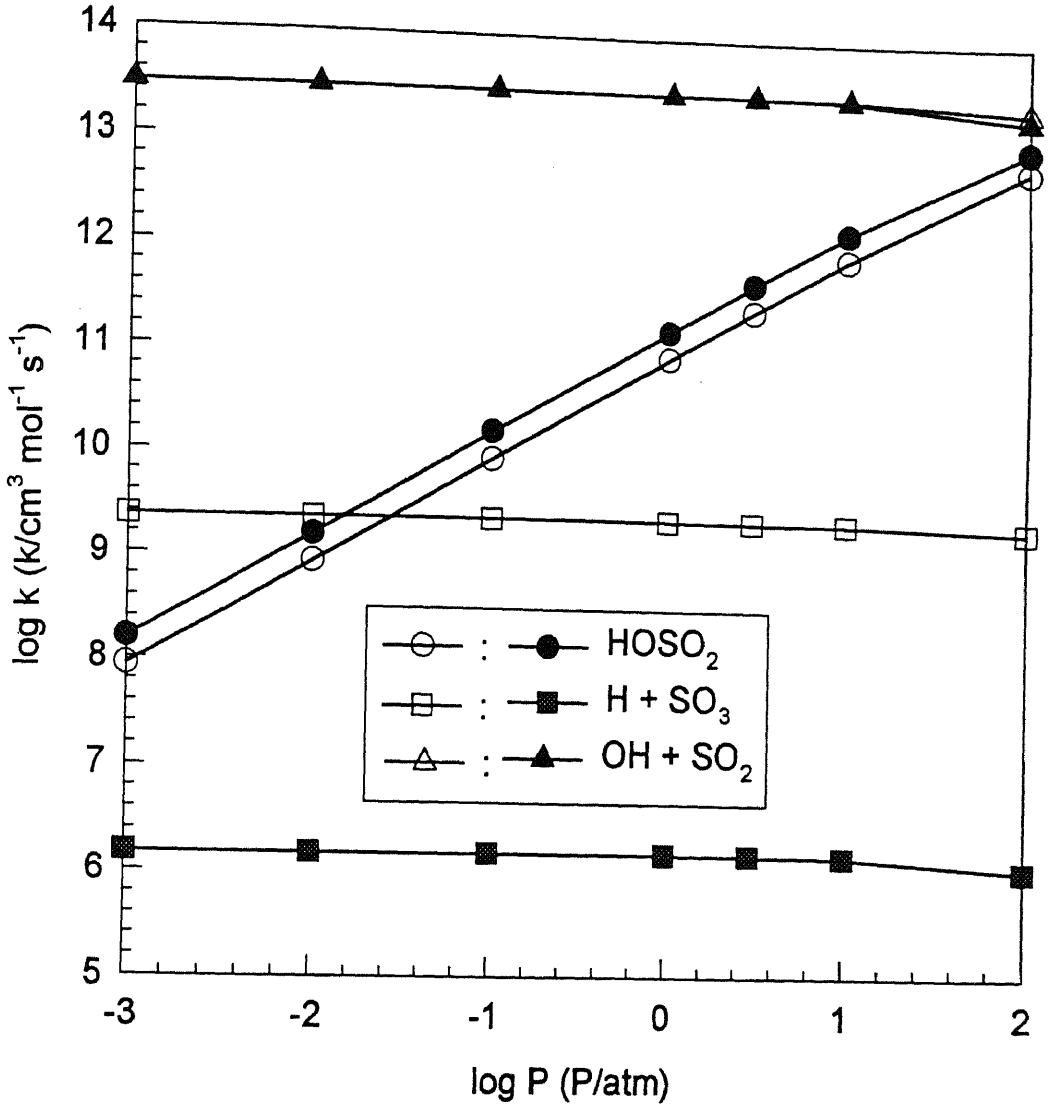

Bath Gas: Ar
Filled symbols : 300 K
Open symbols : 1000 K

Figure G16 Results of QRRK Calculation for H + SO_3 <=> $[HOSO_2]^*$ => Products

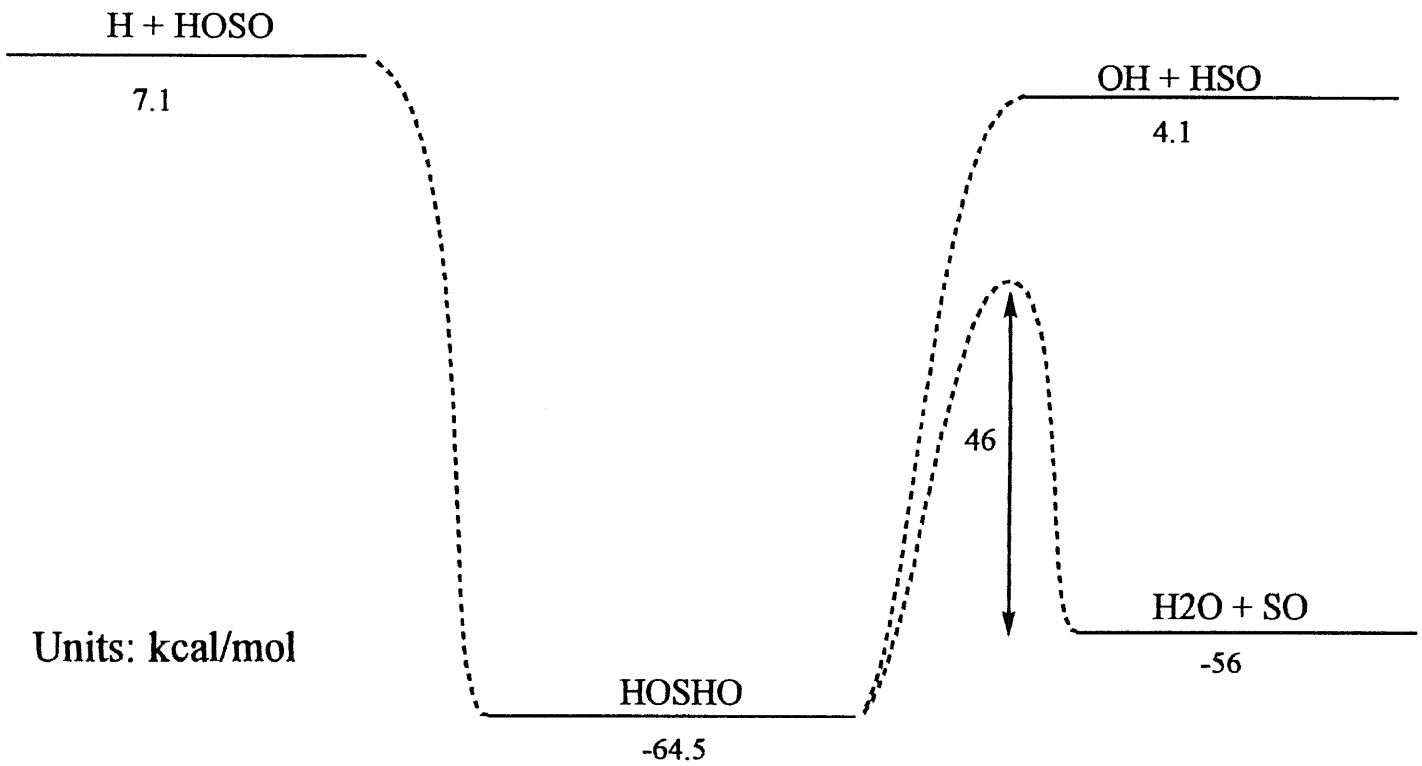

Figure G17 Potential Energy Diagram for

HOSO + H ⟷ [HOSHO]* ⟶ Products

HSO + OH

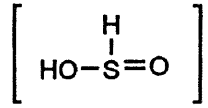

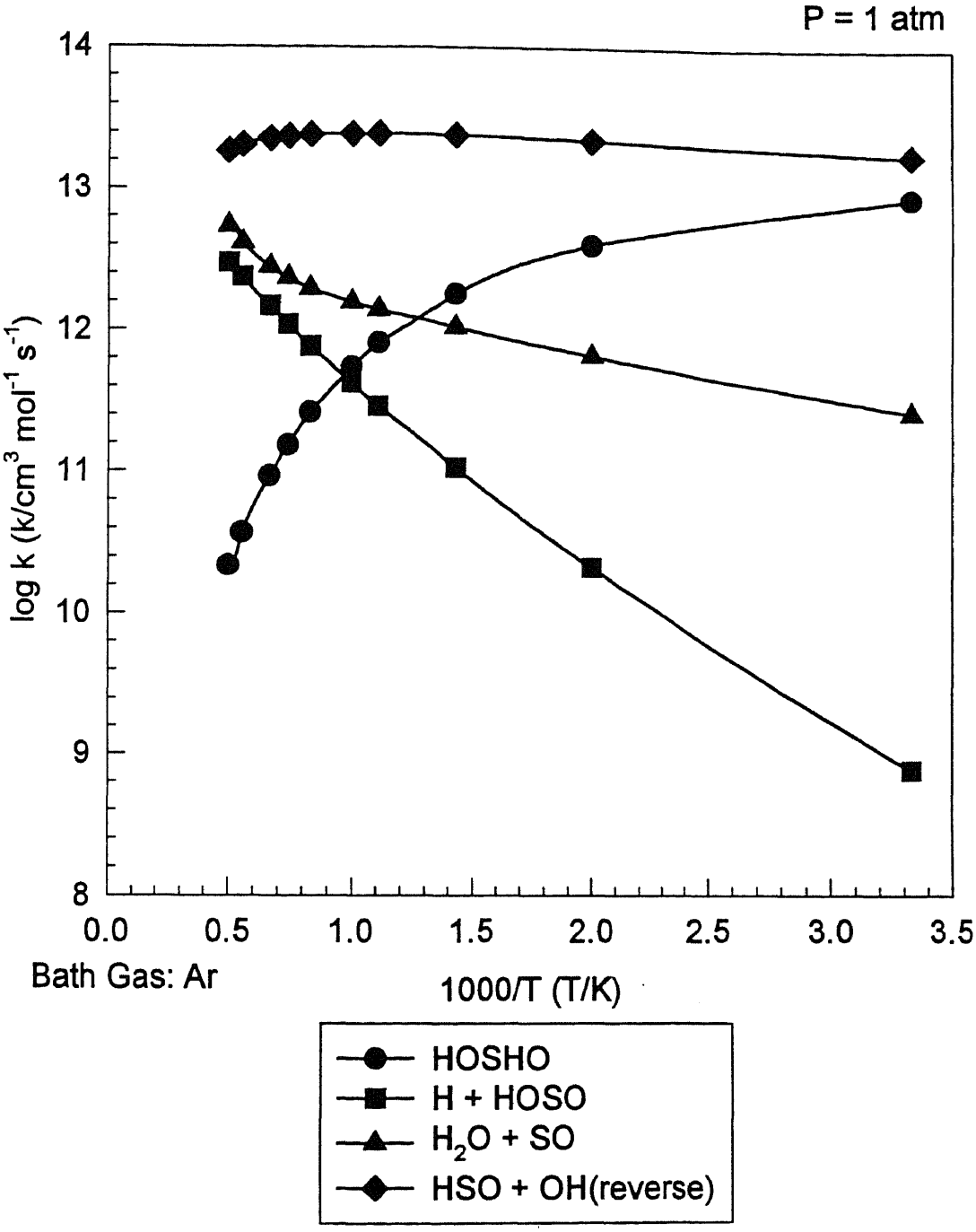

Figure G18 Results of QRRK Calculation for OH + HSO <=> [HOSHO]* => Products

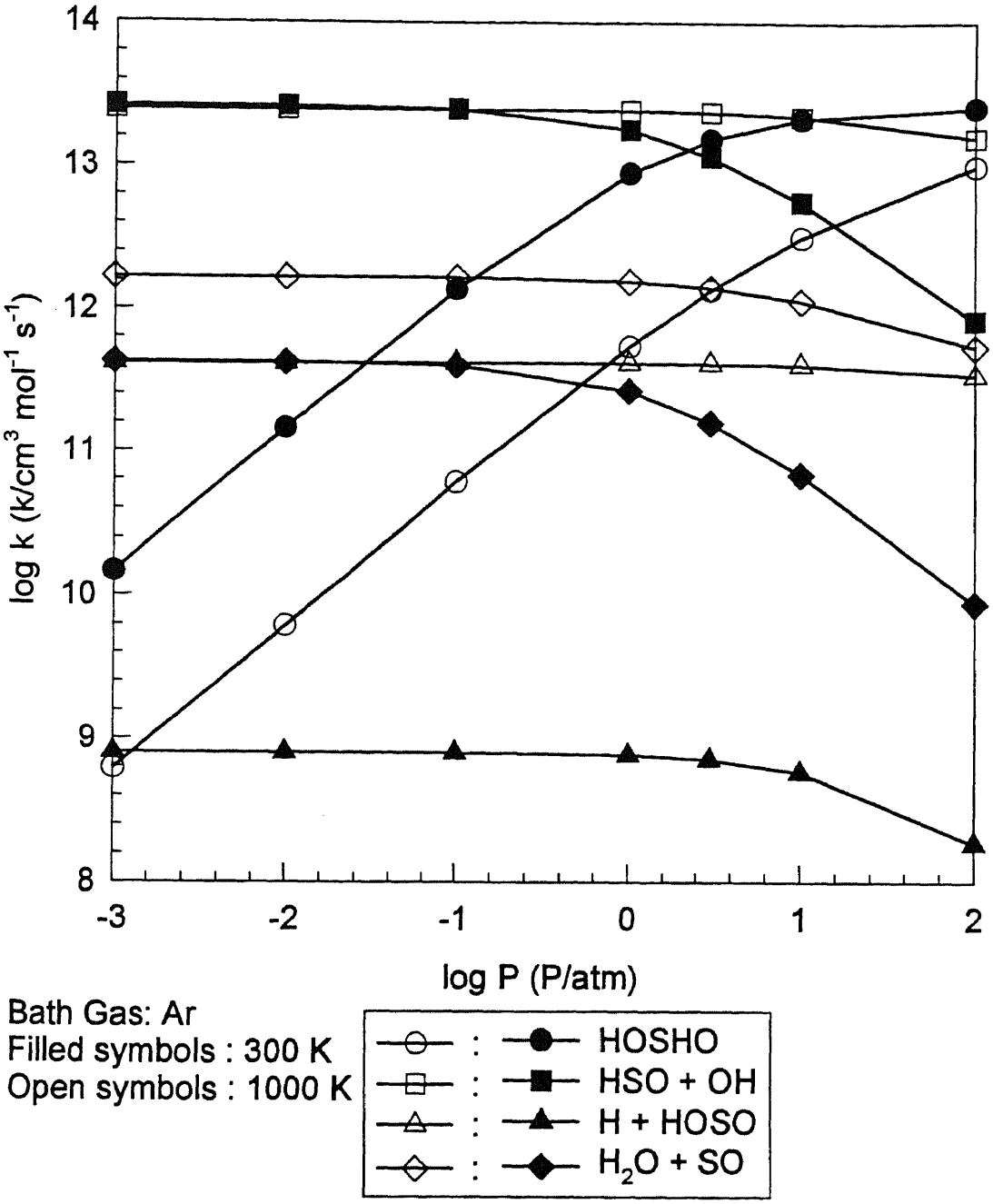

Figure G19 Results of QRRK Calculation for OH + HSO <=> [HOSHO]* => Products

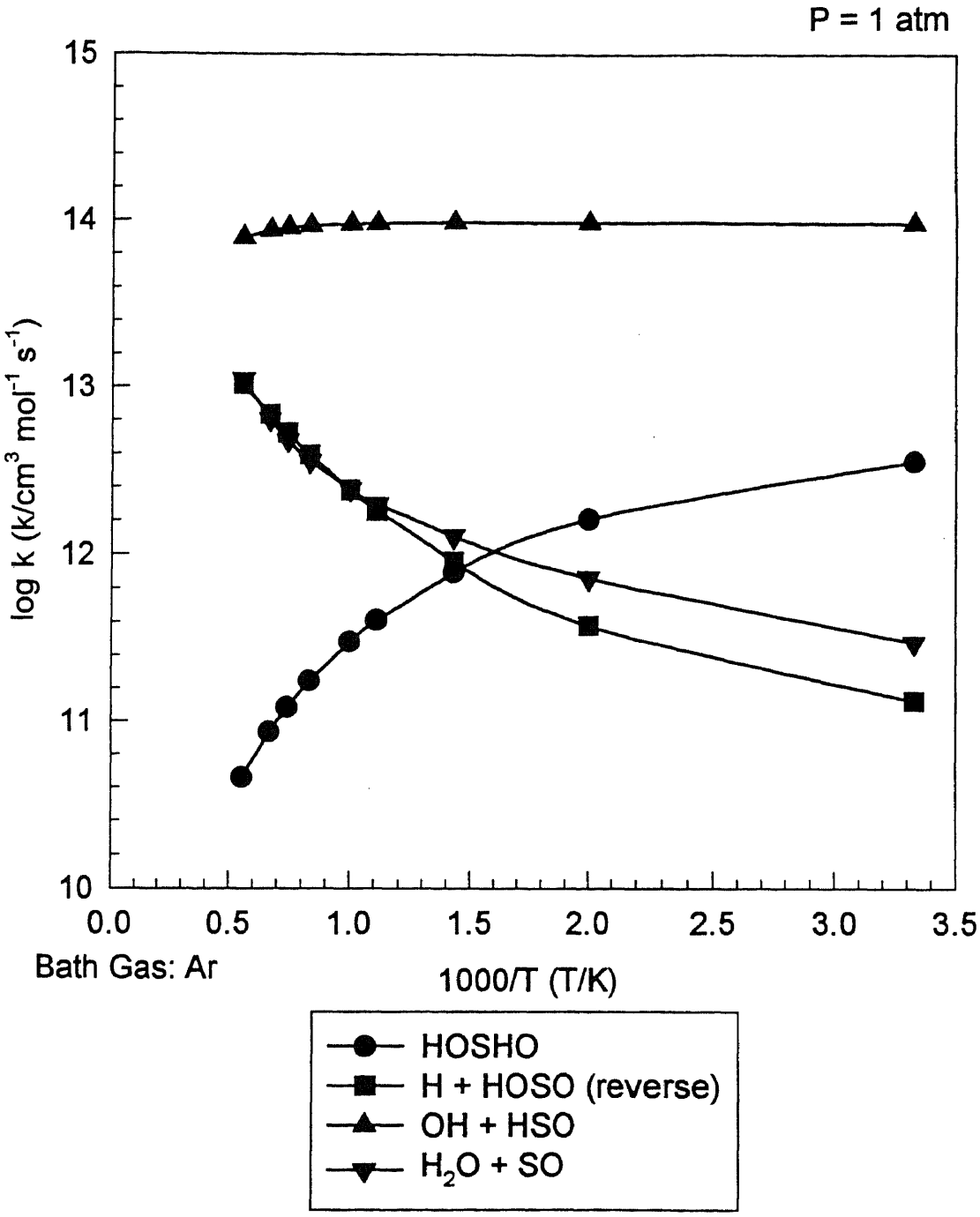

Figure G20 Results of QRRK Calculation for HOSO + H <=> [HOSHO]* => Products

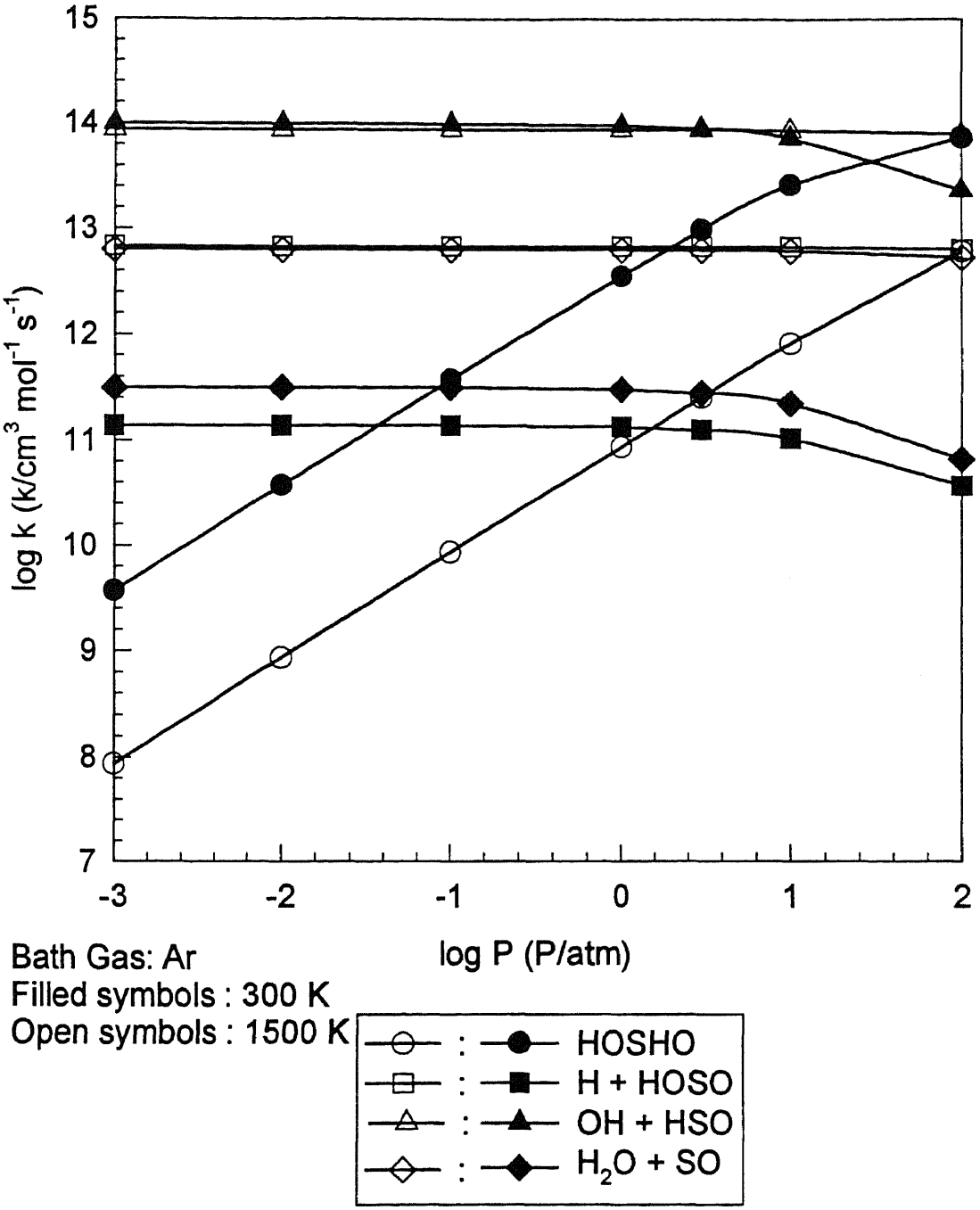

Figure G21 Results of QRRK Calculation for HOSO + H <=> [HOSHO]* => Products

REFERENCES

1 Graham, J. L.; Hall, D. L.; Dellinger, B. *Environ. Sci. Tech.* **1986**, 20, 7.

2 Louw, R.; Dijks, J. H. M.; Mulder, P. *Chemistry and Industry*, **1983**, 759.

3 Chang, W. D.; Karra, S. B.; Senkan, S. M. *Combust. and Flame* **1986**, 49, 107.

4 Karra, S. B.; Gutman, D; Senkan, S. M. *Combust. Sci. and Tech.* **1988**, 60, 45.

5 Rubey, W. A.; Dellinger, B.; Hall, D. L.; Mazer, S. L. *Chemosphere* **1985**, 14, 1483.

6 Fenter, F. F.; Lightfoot, P. D.; Caralp, F.; Lesclaux, R.; Niiranen, J. T.; Gutman, D. *J. Phys. Chem.* **1993**, 97, 4695.

7 Lim, K. P.; Michael, J. V. *Twenty-fifth Symposium (International) on Combustion*; The Combustion Institute: Pittsburgh, **1994**, 809.

8 Frenklach, M; Clary, D. W.; Gardiner, Jr., W. C.; Stein, S. E. *Twentieth Symposium (International) on Combustion*, The Combustion Institute. **1984**, 887.

9 Westmoreland, P. R.; Howard, J. B.; Longwell, J. P. *Twenty-first Symposium (International) on Combustion*. The Combustion Institute. **1986**, 773.

10 Westmoreland, P. R.; Dean, A. M.; Howard, J. B.; Longwell, J. P. *J. Phys. Chem.* **1989**, 93, 8171.

11 Kiefer, J. H.; Sihdu, S. S.; Kern, R. D.; Xie, K.; Chen, H.; Harding, L. B. *Combust. Sci. and Tech.* **1992**, 85, 101.

12 Fahr, A.; Stein, S. E. *Twenty-second Symposium (International) on Combustion*, The Combustion Institute. **1988**, 1023.

13 Wang, H.; Frenklach, M. *J. Phys. Chem.* **1994**, 98, 11465.

14 Shi, Y.; Senkan, S. M. *J. Phys. Chem.* **1991**, 95, 5181.

15 Altwicker, E. A.; Schonberg, J. S.; Konduri, R. K. V. N.; Milligan, M. S. *J. Hazard. Waste Hazard. Mater.* **1990**, 7, 73.

16 Slagle, I. R.; Ratajczak, E.; Gutman, D. *J. Phys. Chem.* **1986**, 90, 402.

17 Hutzinger, O.; Blumich, M. J.; Berg, M. v. d.; Olie, K. *Chemosphere*, **1985**, 14, 581.

18 Jay, K.; Stieglitz, L. *Chemosphere*, **1991**, 22, 987.

19 Bozzelli, J. W.; Wu, Y. P.; Ritter, E. R. *Chemosphere*, **1991**, 23, 1221.

20 Dickson, L. C.; Lenoir, D.; Hutzinger, O. *Eviron. Sci. Technol.* **1992**, 26, 1822.

21 Special Report: EPA's Dioxin Risk Assessment *Eviron. Sci. Technol.* **1995**, 29, 24A.

22 Weissman, M.; Benson, S. W. *Int. J. Chem. Kinet.*, **1984**, 16, 307.

23 Colket, M. B. *Twenty-first Symposium (International) on Combustion*, The Combustion Institute. **1986**, pp.851.

24 Galssman, I. *Twenty-second Symposium (International) on Combustion*, The Combustion Institute. **1988**, pp.295.

25 Benson, S.W. *Thermochemical Kinetics*, 2nd ed., Wiley, New York, **1976**.

26 Spiro, P. A.; Jacob, D. J.; Logan, J. A. *J. Geophys. Res.* **1992**, 97, 6023.

27 Cotton, F. A.; Wilkerson, G. *Advanced Inorganic Chemistry*, 5th ed. Wiley Interscience, **1988**.

28 Houghton, J. T.; Callander B. A.; Varney, S. K. in *Climate Change*, Cambridge University press. **1992**.

29 Black, G. J. *J. Chem. Phys.* **1984**, 80, 1103.

30 Frield, R. R.; Brune, W. H.; Anderson, J. G. *J. Phys. Chem.* **1985**, 89, 5505.

31 Wang, N. S.; Lovejoy E. R.; Howard, C. J. *J. Phys. Chem.* **1987**, 91, 5743.

32 Taylor, P. H.; Dellinger, B. *Eviron. Sci. Technol.* **1988**, 22, 438.

33 Tsang, W. *Combust. Sci. and Tech.* **1990**, 74, 99.

34 Chuang, S. C.; Bozzelli, J. W. *Eviron. Sci. Technol.* **1986**, 20, 568.

35 Chuang, S. C.; Bozzelli, J. W. *Ind. Eng. Chem. Proc. Des.* **1986**, 25, 317.

36 Won, Y. S.; Bozzelli, J. W. *Combust. Sci. and Tech.* **1992**, 85, 345.

37 Mason, L.; Unget, S. U.S. EPA 600/2.79.198, NTIS PB80-131964, **1979**.

38 Senser, D. W.; Morse, J. S.; Cundy, V. A. *Hazard. Waste. and Hazard. Mater.* **1985**, 2, 473.

39 Senser, D. W.; Cundy, V. A.; Morse, J. S. *Combust. Sci. and Tech.* **1987**, 51, 209.

40 Granada, A.; Karra, S. B.; Senkan, S. M. *Ind. Eng. Chem. Res.* **1987**, 26, 1901.

41 Karra, S. B.; Senkan, S. M. *Combust. Sci. and Tech.* **1987**, 54, 333.

42 Taylor, P. H.; Dellinger, B.; Tirey, D. A. *Int. J. Chem. Kinet.*, **1991**, 23, 1051.

43 Huang, S. H. Master Sci. Thesis, NJIT, **1987**.

44 Tsao, H. Master Sci. Thesis, NJIT, **1987**.

45 Tavakoli, J. Ph.D. Dissertation, NJIT, **1988**.

46 Won, Y. S. Master Sci Thesis, NJIT, **1988**.

47 Ho, W. P. Master Sci Thesis, NJIT, **1989**.

48 Won, Y. S. Ph.D. Dissertation, NJIT, **1992**.

49 Yu, Q. R. Master Sci Thesis, NJIT, **1992**.

50 Ho, W. P.; Barat, R. B.; Bozzelli, J. W. *Combust. and Flame* **1992**, 88, 265.

51 Dean, A. M.; Westmoreland, P. R. *Int. J. Chem. Kinet.*, **1987**, 19, 207.

52 Danis, F; Caralp, F; Rayez, M. T.; Lesclaux, R. *J. Phys. Chem.* **1991**, 95, 7300.

53 Kaiser, E. W. *J. Phys. Chem.* **1993**, 97, 11681.

54 Fenter, F. F.; Lightfoot, P. D.; Niiranen, J. T.; Gutman, D. *J. Phys. Chem.* **1993**, 97, 5313.

55 Miller, G. P.; Cundy, V. A.; Lester, T. W.; Bozzelli, J. W. *Combust. Sci. and Tech.* **1994**, 98, 123.

56 Won, Y. S.; Bozzelli, J. W. *Combust. Sci. and Tech.* **1992**, 85, 345.

57 Ho, W. P.; Barat, R. B.; Bozzelli, J. W. *Combust. and Flame* **1992**, 88, 265.

58 Ho, W. P.; Yu, Q. R.; Bozzelli, J. W. *Combust. Sci. and Tech.* **1992**, 85, 23.

59 Chang, W. D.; Karra, S. B.; Senkan, S. M. Central/Western States Section, The Combustion Institute, San Antonio, TX, **1985**.

60 Chang, W. D.; Senkan, S. M. *Combust. Sci. and Tech.* **1988**, 63, 442.

61 Lee, K. Y.; Yang, M. H.; Puri, I. K. *Combust. and Flame* **1993**, 92, 419.

62 Lee, K. Y.; Puri, I. K. *Combust. and Flame* **1993**, 92, 440.

63 Senser, D. W. Ph.D. Dissertation, Lousisiana State University, **1985**.

64 Thomson, M. J.; Lucas, D.; Koshland, C. P.; Sawyer, R. F.; Wu, Y. P.; Bozzelli, J. W. *Combust. and Flame* **1994**, 98, 155.

65 Kee, R. J.; Rupley, F. M.; Miller, J. A. *CHEMKIN-II, A fortran chemical kinetics package for the Analysis of Gas-Phase Chemical Kinetics*, Sandia National Laboratories, Livermore, CA, **1990**.

66 Chen, J. Y. *PFR: Plug Flow Reactor*, Univrsity of California, Berkeley, CA, 1992.

67 Dean, A. M. *J. Phys. Chem.* **1985**, 89, 4600.

68 Dean A. M.; Bozzelli, J. W.; Ritter, E. R. *Combust. Sci. and Tech.* **1991**, 80, 63.

69 Ritter, E. R.; Bozzelli, J. W. *Int. J. Chem. Kinet.* **1991**, 23, 767.

70 Ritter, E. R.; Bozzelli, J. W. The Eastern States Section of The Combuion Institute, Princeton University, New Jersey, **1993**, 459.

71 Lay, T. H. Ph.D. Dissertation, NJIT, Newark, **1995**.

72 Ritter, E. R. Ph.D. Dissertation, NJIT, **1989**.

73 Ritter, E. R. *J. Chem. Inf. Computat. Sci.* **1991**, 31, 400.

74 Chang, A. Y.; Bozzelli, J. W.; Dean, A. M., (To be Published). Personnel Communication.

75 Gilbert, R. G.; Luther, K.; Troe, J. *Ber. Bunsenges. Phys. Chem.* **1983**, 87, 169.

76 Hirschfelder, J. O.; Curtiss, C. F.; Bird, R. B. *Molecular Theory of Gases and Liquids*, 2nd ed., Wiley, London, **1963**.

77 Harrington, R. E.; Rabinovitch, B. S.; Hoare, M. R. *J. Chem. Phys.* **1960**, 33, 744. Kohlmaier, G. H.; Rabinovitch, B. S. *ibid.* **1963**, 38, 1962. Ireton, R. C.; Rabinovitch, B. S. *J. Phys. Chem.* **1974**, 78, 1973.

78 Reid, R. C.; Prusnitz, J. M.; Poling, B. E. *The properties of Gases and Liquids* 3nd ed., McGraw-Hill, Singapore, **1988**.

79 Lay, T. H.; Bozzelli, J. W. The Eastern States Section of The Combustion Institute, Princeton University, New Jersey, **1993**, 449.

80 Stewart, J. J. P. MOPAC 6.0 : A General Molecular Orbital Package, Frank J. Seiler Research Lab., US Air Force Academy, CO 80840, **1990**.

81 Frenklach, M; Hsu, J. P.; Miller, D. L.; Matula, R. A. *Combust. and Flame* **1986**, 64, 141.

82 Minion, J. A.; Louw, R. *Recueil des Travaux Chimiques des pays-Bas*, **1986**, 105/10, 442.

83 Zabel, F. *Int. J. Chem. Kinet.* **1977**, 9, 651.

84 Russell, J. J.; Seetula, J. A.; Gutman, D.; Melius, C. F.; Senkan, S. M. *Twenty-third Symposium (International) on Combustion*; The Combustion Institute: Pittsburgh, **1990**, 163.

85 Russell, J. J.; Seetula, J. A.; Gutman, D.; Senkan, S. M. *J. Phys. Chem.* **1989**, 93, 1934.

86 Cooper, R.; Cumming, J. B.; Gordon, S.; Mulac, W. A. *Radiat. Phys. Chem.* **1980**, 16, 169.

87 Ryan, K. R.; Plumb, I. C. *Int. J. Chem. Kinet.* **1984**, 16, 591.

88 Ho, W. P.; Bozzelli, J. W. *Twenty-fifth Symposium (International) on Combustion*; The Combustion Institute: Pittsburgh, **1992**, 743.

89 Westmoreland, P. R.; Dean, A. M. *AIChE J.* **1986**, 32, 1971.

90 Knyazev, V. D.; Dubinsky, I. A.; Slagle, I. R.; Gutman, D. *J. Phys. Chem.* **1994**, 98, 11099.

91 Hassler, J. C.; Setser, D. W.; Johnson, R. L. *J. Chem. Phys.* **1966**, 45, 3231; 3246.

92 Setser, D. W. communications to the editor, *J. Phys. Chem.* **1971**, 76, 283.

93 Kim, K. C.; Setser, D. W. *J. Phys. Chem.* **1974**, 78, 2166.

94 Hassler, J. C.; Setser, D. W.; Johnson, R. L. *J. Chem. Phys.* **1966**, 45, 3237.

95 Dees, K.; Setser, D. W.; Clark, W. G. *J. Phys. Chem.* **1972**, 75, 2231.

96 Weissman, M.; Benson, S. W. *Int. J. Chem. Kinet.*, **1984**, 16, 941.

97 Tavakoli, J.; Bozzelli, J. W. Collected Papers in Heat Transfer HTD Vol.-104, K.T. Yang, ed., ASME, **1988**, 2, 147.

98 Karra, S. B.; Senkan, S. M. *Ind. Eng. Chem. Res.* **1988**, 27, 447.

99 Roussel, P. B.; Lightfoot, P. D.; Caralp, F.; Catoire, V.; Lesclaux, R.; Forst, W., *J. Chem. Soc. Faraday Trans.* **1991**, 87, 2367.

100 Benson, S. W.; Weissman, M. *Int. J. Chem. Kinet.* **1982**, 14, 1287.

101 Hung, S. L.; Pfefferle, L. D. *Combust. Sci. and Tech.* **1993**, 87, 91.

102 Koshland, C. P.; Fisher, E. M.; Lucas, D. *Combust. Sci. and Tech.* **1992**, 82, 49.

103 Lay, T. H.; Ritter, E. R.; Dean, A. M.; Bozzelli, J. W. in press.

104 Westmoreland, P. R. *Combust. Sci. and Tech.* **1992**, 82, 151.

105 Bozzelli, J. W.; Dean, A. M. *J. Phys. Chem.* **1990**, 94, 3313.

106 Bozzelli, J. W.; Dean, A. M. *J. Phys. Chem.* **1993**, 97, 4427.

107 Bozzelli, J. W.; Chang, A. Y.; Dean, A. M. *Twenty-fifth Symposium International on Combustion*, The Combustion Institute. **1994**, 965.

108 Bozzelli, J. W.; Chang, A. Y.; Dean, A. M. in press.

109 Ben-Amotz, D.; Herschbach, D. *J. Phys. Chem.* **1990**, 94, 3393.

110 Danis, F.; Caralp, F.; Veyret, B.; Loirat, H.; Lesclaux, R. *Intl. J. Chem. Kinet.* **1989**, 21, 715.

111 Cobos, C. J.; Troe, J. *J. Phys. Chem.* **1985**, 83, 1010.

112 Baulch, D. L.; Duxbury, J. *Combust. and Flame* **1980**, 37, 313.

113 Modified from hydrocarbon radical recombination. Allara, D. L.; Shaw, R. *J. Phys. Chem. Ref. Data* **1980**, 9, 523.

114 Wagner, D. M.; Wardlaw, D. W. *J. Phys. Chem.* **1988**, 92, 2462.

115 Huybrechts, G.; Hubin, Y.; Van Mele, B. *Intl. J. Chem. Kinet.* **1992**, 24, 671.

116 Timonen, R.; Lalliorinne, K.; Koskikallio, J. *Acta Chem. Scandinavic* **1986**, 40, 459.

117 Kaiser, E. W.; Rimai, L.; Wallington, T. J. *J. Phys. Chem.* **1989**, 93, 4094.

118 Ellermann, T. *Chem. Phys. Lett.* **1992**, 189, 175.

119 Huybrechts, G.; Meyers, L.; Verbeke, G. *Trans. Faraday Soc.* **1962**, 58, 1128.

120 Slagle, I. R.; Feng, Q.; Gutman, D. *J. Phys. Chem.* **1984**, 88, 3648.

121 McAdam, G. K.; Walker, R. W. *J. Chem. Soc., Faraday Trans. 2,* **1987**, 83, 1509.

122 Gutman, D. *J. Chim. Phys.* **1987**, 84, 409.

123 Kaiser, E. W.; Lorkovic, I. M.; Wallington, T. J. *J. Phys. Chem.* **1989**, 94, 3352.

124 Kaiser, E. W. *J. Phys. Chem.* **1995**, 99, 707.

125 Gulati, S. K.; Walker, R. W. *J. Chem. Soc., Faraday Trans. 2*, **1988**, 84, 401.

126 Cox, R. A.; Cole, J. A. *Combustion and Flame* **1985**, 60, 109.

127 Pitz, W. J.; Westbrook, C. K. *Combustion and Flame* **1986**, 63, 113.

128 Wagner, A. F.; Slagle, I. R.; Sarzynskin, D.; Gutman, D. *J. Phys. Chem.* **1984**, 94, 1853.

129 Slagle, I. R.; Park, J-Y; Heaven, M. C.; Gutman, D. *J. Am. Chem. Soc.* **1984**, 106, 4356.

130 Fahr, A.; Laufer, A. H. *J. Phys. Chem.* **1988**, 92, 7229.

131 Krueger, H.; Weitz, E. *J. Chem. Phys.* **1988**, 88, 1608.

132 Slagle, I. R.; Bernhardt, J. R.; Gutman, D. *Twenty-second Symposium (International) on Combustion*, The Combustion Institute. **1988**, 953.

133 Carpenter, B. K. *J. Am. Chem. Soc.* **1993**, 115, 9806.

134 Knyazev, V. D.; Bencsura, 'A.; Dubinsky, I. A.; Gutman, D.; Melius, C. F.; Senkan, S. M. *J. Phys. Chem.* **1995**, 99, 230.

135 Knyazev, V. D.; Slagle, I. R. submitted to *J. Phys. Chem.* **1995**.

136 Chiang, H. M. Ph.D. Dissertation, NJIT, **1995**.

137 Stieglitz, L; Zwick, G.; Beck, J.; Roth, W.; Vogg, H. *Chemosphere*, **1989**, 18, 1219.

138 Milligan, M. S.; Altwicker, E. R. *Eviron. Sci. Technol.* **1993**, 27, 1595.

139 Addink, R.; Olie, K. submitted to *Eviron. Sci. Technol.* **1995**.

140 Addink, R.; Bakker, W. C. M.; Olie, K. submitted to *Eviron. Sci. Technol.* **1995**.

141 Konduri, R.; Altwicker, E. R. *Chemosphere*, **1994**, 28, 23.

142 Bitter, J. D.; Howard, J. B. *Eighteenth Symposium (International) on Combustion*, The Combustion Institute. **1981**, pp.1105.

143 Bockhorn, H.; Fetting, F.; Wenz, H. W. *Ber. Bunsenges. Phys. Chem.*, **1983**, 87, 1067.

144 Cole, J. A.; Bitter, J. D.; Longwell, J. P.; Howard, J. B. *Combust. and Flame*, **1984**, 56, 51.

145 Stein, S. E.; Walker, J. A.; Suryan, M. M.; Fahr, A. *Twenty-third Symposium (International) on Combustion*, The Combustion Institute. **1990**, 85.

146 Tanzawa, T.; Gardiner, Jr. W. C. *J. Phys. Chem.*, **1980**, 84, 236.

147 Taylor, P. H.; Tirey D. A.; Rubey, W. A.; Dellinger, B. in press.

148 NIST data base, version 5.0, **1992**.

149 Ho, W. P.; Chen, S.; Ritter, E. R.; Bozzelli, J. W. *AICHE* Annual meeting, **1991**, 85f.

150 Air Auality and Stationary Source Emission Control, National Research Council Report, Serial No. 94-4, U.S. Government Printing Office, Washington, D.C. **1975**.

151 Kiefer, J. H.; Kumaran, S. S. *J. Phys. Chem.* **1993**, 97, 414.

152 Cullis, C. F.; Mulcahy, M. F. R. *Combust. and Flame* **1972**, 18, 225.

153 Frenklach, M.; Lee, J. H.; White, J. N.; Gardiner Jr., W. C. *Combust. and Flame* **1981**, 41, 1.

154 Zachariah, M. R.; Smith, O. I. *Combust. and Flame* **1987**, 69, 125.

155 Bradley, J. N.; Dobson, D. C. *J. Chem. Phys.* **1967**, 46, 2872.

156 Fair, D. C.; Thrush, D. C. *Trans. Faraday Soc.* **1969**, 65, 1557.

157 Jourdian, J. L.; Le Bras, G.; Combourueu, J. *Intl. J. of Chem. Kinet.* **1979**, 11, 569.

158 Hynes, A. J.; Wine, P. H. "Kinetics and Mechanisms of the Oxidation of Gaseous Sulfur Compounds" submitted for publication in Combustion Chemistry, 2nd ed., edited by W.C. Gardiner, Springer-Verlag.

159 Webster, P.; Walsh, A. D. *tenth* Symposium *(International) on Combustion*; The Combustion Institute: Pittsburgh **1965**, 463.

160 Fenimore, C. P.; Jones, G. W. *J. Phys. Chem.* **1965**, 69, 3593.

161 Binns, D.; Marshall, P. *J. Chem. Phys.* **1991**, 95, 4940.

162 Wheeler, R. *J. Phys. Chem.* **1968**, 72, 3359.

163 Halstead, C. J.; Jenkins, D. R. *Trans. Faraday Soc.* **1969**, 65, 3013.

164 Durie, R. A.; Johnson, G. M.; Smith, M. Y. *Combust. and Flame* **1971**, 17, 197.

165 Gordon, S.; Mulac, W. A. *Intl. J. Chem. Kinet.* **1975**, symp. 1, 289.

166 David, D. D.; Ravishankara, A. R.; Fisher, S., *Geophys. Res. Lett.* **1979**, 6, 113.

167 Harris, G. W.; Atkinson, R.; Pitts Jr., J. N. *Chem. Phys. Lett.* **1980**, 69, 378.

168 Harris, G. W.; Wayne, R. P. *J. Chem. Soc. Faraday Trans. 1* **1975**, 71, 610.

169 Wine, P. H.; Thompson, R. J.; Ravishankara, A. R.; Semmes, D. H.; Gump, C. A.; Torabi, A.; Nicovich, J. M. *J. Phys. Chem.* **1984**, 88, 2095.

170 Goumri, A.; Rocha, J-D R.; Laakso, D.; Smith, C. E.; Marshall, P. *J. Chem. Phys.* **1994**, 101, 9405.

171 Laakso, D.; Smith, C. E.; Goumri, A.; Rocha, J-D R.; Marshall, P. *Chem. Phys. Lett.* **1994**, 227, 377.

172 Goumri, A.; Laakso, D.; Rocha, J-D R.; Smith, C. E.; Marshall, P. *J. Chem. Phys.* **1995**, 102, 161.

173 Bozzelli, J. W.; Pitz, W. J. *twenty-fifth Symposium (International) on Combustion*, The Combustion Institute.**1994**, 783.

174 Dewar, M. J. S.; Zoebisch, E. G.; Healy, E. F.; Stewart, J. J. P. *J. Am. Chem. Soc.* **1985**, 107, 3902.

175 (1)Stewar, J. J. P. *J. Comput. Chem.* **1989**, 10, 209. (2)*ibid.* 10, 221.

176 Slagle, I. R.; Balocchi, F.; Gutman, D. *J. Phys. Chem.* **1978**, 82, 1333.

177 Benson, S. W. *Chemical Reviews* **1978**, 78, 1.

178 Davidson, F. E.; Clemo, A. R.; Duncan, R. J.; Browett, R. J.; Hobson, J. H.; Grice, R. *Mol. Phys.* **1982**, 46, 33.

179 Luke, B. T.; Mclean, A. D. *J. Phys. Chem.* **1985**, 89, 4592.

180 Melius, C. F. BAC-MP4 heats of formation and free energies unpublished tabulation, **1989**.

181 Xantheas, S. S.; Dunning Jr., T. H. *J. Phys. Chem.* **1993**, 97, 18.

182 Xantheas, S. S.; Dunning Jr., T. H. *J. Phys. Chem.* **1993**, 97, 6616.

183 Balucani, N.; Casavecchia, P.; Stranges, D.; Volpi, G. G. *Chemical Physics Letters*, **1993**, 211, 469.

184 Espinosa-Garcia, J.; Corchado, J. C. *Chemical Physics Letters* **1994**, 218, 128.

185 Plummer, P. L. M. *J. Chem. Phys.* **1990**, 92, 6627.

186 "JANAF Thermochemical Table" 3rd ed., NSRDS-NBS 37, **1987**.

187 Margitan, J. J. *J. Phys. Chem.* **1984**, 88, 3314.

188 Atkinson, R.; Baulch, D. L.; Cox, R. A.; Hampson, R. F.; Kerr, J. A.; Troe, J; *J. Phys. Chem. Ref. Data* **1992**, 21, 1125.

189 Schofield, K. *J. Phys. Chem. Ref. Data* **1973**, 2, 25.

190 Huisken, F.; Krajnovich, D.; Zhang, Z.; Shen, Y. R.; Lee, Y. T. *J. Chem. Phys.* **1983**, 78, 3806.

191 Schmoltner, A. M.; Anex, D. S.; Lee, Y. T. *J. Phys. Chem.* **1992**, 96, 1236.